PROBIOTIC BACTERIA-DERIVED EFFECTOR MOLECULES AND THEIR IMPACT ON THE HOST IN HEALTH AND DISEASE

EDITED BY: Sabina Górska, Corine Sandström, Irma Schabussova, Martin Schwarzer and Anna Magdalena Zawilak-Pawlik

PUBLISHED IN: Frontiers in Microbiology, Frontiers in Nutrition and Frontiers in Immunology

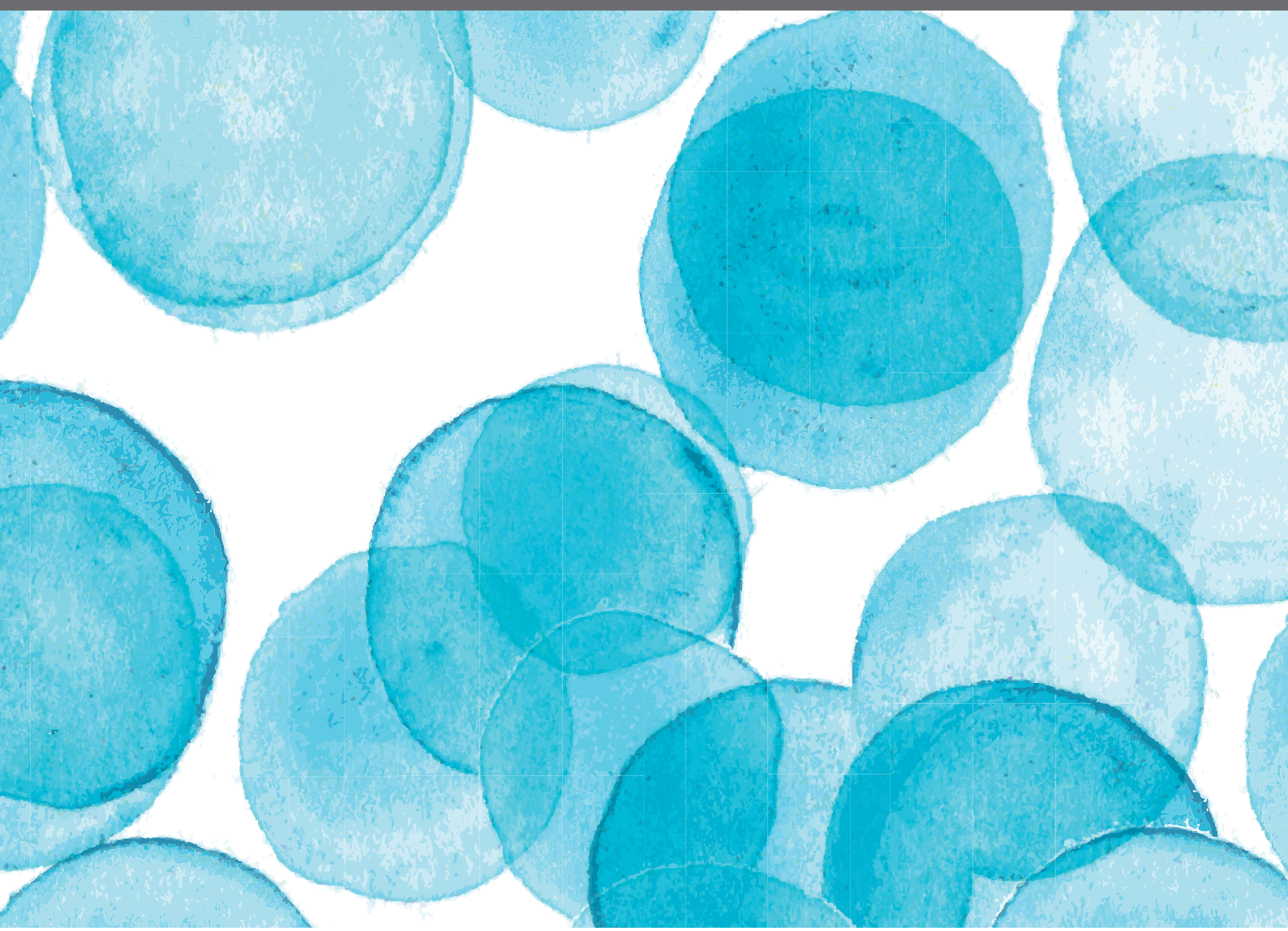

frontiers Research Topics

frontiers

ISSN 1664-8714
ISBN 978-2-83250-504-5
DOI 10.3389/978-2-83250-504-5

About Frontiers

Frontiers is more than just an open-access publisher of scholarly articles: it is a pioneering approach to the world of academia, radically improving the way scholarly research is managed. The grand vision of Frontiers is a world where all people have an equal opportunity to seek, share and generate knowledge. Frontiers provides immediate and permanent online open access to all its publications, but this alone is not enough to realize our grand goals.

Frontiers Journal Series

The Frontiers Journal Series is a multi-tier and interdisciplinary set of open-access, online journals, promising a paradigm shift from the current review, selection and dissemination processes in academic publishing. All Frontiers journals are driven by researchers for researchers; therefore, they constitute a service to the scholarly community. At the same time, the Frontiers Journal Series operates on a revolutionary invention, the tiered publishing system, initially addressing specific communities of scholars, and gradually climbing up to broader public understanding, thus serving the interests of the lay society, too.

Dedication to Quality

Each Frontiers article is a landmark of the highest quality, thanks to genuinely collaborative interactions between authors and review editors, who include some of the world's best academicians. Research must be certified by peers before entering a stream of knowledge that may eventually reach the public - and shape society; therefore, Frontiers only applies the most rigorous and unbiased reviews.
Frontiers revolutionizes research publishing by freely delivering the most outstanding research, evaluated with no bias from both the academic and social point of view. By applying the most advanced information technologies, Frontiers is catapulting scholarly publishing into a new generation.

What are Frontiers Research Topics?

Frontiers Research Topics are very popular trademarks of the Frontiers Journals Series: they are collections of at least ten articles, all centered on a particular subject. With their unique mix of varied contributions from Original Research to Review Articles, Frontiers Research Topics unify the most influential researchers, the latest key findings and historical advances in a hot research area! Find out more on how to host your own Frontiers Research Topic or contribute to one as an author by contacting the Frontiers Editorial Office: frontiersin.org/about/contact

PROBIOTIC BACTERIA-DERIVED EFFECTOR MOLECULES AND THEIR IMPACT ON THE HOST IN HEALTH AND DISEASE

Topic Editors:
Sabina Górska, Hirszfeld Institute of Immunology and Experimental Therapy, Polish Academy of Sciences, Poland
Corine Sandström, Swedish University of Agricultural Sciences, Sweden
Irma Schabussova, Medical University Vienna, Austria
Martin Schwarzer, Institute of Microbiology, Academy of Sciences of the Czech Republic (ASCR), Czechia
Anna Magdalena Zawilak-Pawlik, Hirszfeld Institute of Immunology and Experimental Therapy, Polish Academy of Sciences, Poland

Citation: Górska, S., Sandström, C., Schabussova, I., Schwarzer, M., Zawilak-Pawlik, A. M., eds. (2022). Probiotic Bacteria-derived Effector Molecules and Their Impact on the Host in Health and Disease. Lausanne: Frontiers Media SA. doi: 10.3389/978-2-83250-504-5

Table of Contents

frontiers | Frontiers in Microbiology

TYPE Editorial
PUBLISHED 29 November 2022
DOI 10.3389/fmicb.2022.1089461

OPEN ACCESS

EDITED AND REVIEWED BY
Giovanna Suzzi,
University of Teramo, Italy

*CORRESPONDENCE
Sabina Górska
sabina.gorska@hirszfeld.pl
Martin Schwarzer
schwarzer@biomed.cas.cz

SPECIALTY SECTION
This article was submitted to Food Microbiology, a section of the journal Frontiers in Microbiology

RECEIVED 04 November 2022
ACCEPTED 14 November 2022
PUBLISHED 29 November 2022

CITATION
Górska S, Schwarzer M, Schabussova I, Zawilak-Pawlik AM and Sandström C (2022) Editorial: Probiotic bacteria-derived effector molecules and their impact on the host in health and disease.
Front. Microbiol. 13:1089461.
doi: 10.3389/fmicb.2022.1089461

Editorial: Probiotic bacteria-derived effector molecules and their impact on the host in health and disease

Sabina Górska[1]*, Martin Schwarzer[2]*, Irma Schabussova[3], Anna Magdalena Zawilak-Pawlik[4] and Corine Sandström[5]

[1]Laboratory of Microbiome Immunobiology, Hirszfeld Institute of Immunology and Experimental Therapy, Polish Academy of Sciences, Wroclaw, Poland, [2]Laboratory of Gnotobiology, Institute of Microbiology of the Czech Academy of Sciences, Prague, Czechia, [3]Institute of Specific Prophylaxis and Tropical Medicine, Medical University of Vienna, Vienna, Austria, [4]Laboratory of Molecular Biology of Microorganisms, Hirszfeld Institute of Immunology and Experimental Therapy, Polish Academy of Sciences, Wrocław, Poland, [5]Department of Molecular Sciences, Swedish University of Agricultural Sciences, Uppsala, Sweden

KEYWORDS

***Bifidobacterium, Lactobacillus*, probiotics, post-biotics, vesicles, exopolysaccharides, peptidoglycan**

Editorial on the Research Topic
Probiotic bacteria-derived effector molecules and their impact on the host in health and disease

Bacteria are one of the main modulators of the physiology and the immune system of the host organism (Tlaskalova-Hogenova et al., 2011). Changes in the composition and abundance of bacterial communities, especially, but not exclusively, in the gastrointestinal tract are believed to be a key factor in the host's susceptibility to various diseases (e.g., allergy, inflammatory bowel disease, irritable bowel syndrome, or necrotizing enterocolitis). It is not surprising that prophylactic/therapeutic approaches to modulate the microbiota composition, for example by probiotic bacteria, are being pursued. Along these lines, the history and diversity of probiotics, as well as outlines of conventional *in vitro* assays and *in vivo* models, have been in-depth reviewed by Milner et al. Despite the interest in probiotics as food or supplement use in the clinic, there are huge discrepancies observed in the outcomes of such studies. Duboux et al. suggest that these differences, besides being attributed to variations in the bacterial species and clinical trial protocols, target population, probiotic dosage, or outcome parameters measured, may stem from the methods used to produce the live bioactive ingredients. In their review, the authors suggest that the implementation of molecular level quality controls based on validated probiotic niche factors and effector molecules could improve the functional reliability of probiotic products.

Experimental and clinical data indicate that the efficacy of probiotics differs from strain to strain and therefore, in the screening for new probiotic bacterial products, it is necessary to compare and analyze the characteristics and safety at the strain level. The members of *Enterococcus*, the symbiotic bacteria in the intestine, exhibit dual

characteristics of probiotic function and potential pathogenicity. Zhou et al. characterized *Enterococcus durans* A8-1 isolated from a fecal sample of a healthy Chinese infant. Strain A8-1 was able to tolerate and survive the simulated gastric and intestinal juices and showed the potential to colonize the intestinal epithelial cells and competitively exclude enteropathogens with the ability to downregulate the levels of inflammatory cytokines. Zebrafish model was used by Huang et al. to screen forty probiotic bacterial strains for the prevention of inflammatory bowel disease. One candidate, *Bacillus smithii* XY1, restored the intestinal epithelial cell integrity after dextran sodium sulfate (DSS)-induced damage, as well as regulated the expression of inflammation-related genes. Subclinical enteritis poses a significant threat to the chicken industry, severely hampering the growth performance of broilers. Wang et al. showed that treatment of broiler chicks with *Bacillus subtilis* DSM29784 improved the composition and metabolism of the intestinal microbiota, and the intestinal structure, and reduced inflammation and apoptosis in *Clostridium perfringens*-induced intestinal inflammation resulting in improved growth performance.

Probiotics can act at different levels of the host immune system e.g., physical barrier, innate immunity, and adaptive immunity. Kim et al. demonstrated that *Bifidobacterium animalis* ssp. *lactic* HY8002 enhanced the intestinal epithelial cells' barrier integrity by restoring the expression of tight junction proteins, kanamycin-induced reduction in Peyer's patch cell number, and serum and fecal IgA levels in the mouse small intestine. Next, Won et al. studied the effect of oral administration of *Latilactobacillus sakei* ADM14 on obesity and fatty liver in a high-fat diet mouse model. Authors have demonstrated the regulatory activity of strain ADM14 on host lipid metabolism and composition of fecal microbiota that led to decreased body weight gain, fat tissue mass, and liver weight in treated mice. Lee et al. showed that administration of *Lactobacillus rhamnosus* TWK10 enhanced muscle strength in young mice and prevented loss of muscle strength or bone mass in aged mice. Furthermore, learning and memory abilities were improved. Administration of TWK10 had also an influence on gut microbial composition decreasing the aging-associated accumulation of pathogenic bacterial taxa and increasing bacteria-producing short-chain fatty acids (SCFA). Lin et al. compared the effect of dietary fiber supplementation vs. butyrate/probiotic supplementation on semen quality and intestinal microbiome in a boar model. The findings of this study indicate that dietary fiber supplementation improves gut microbiota and promotes SCFA production, which is linked to enhanced spermatogenesis and semen quality. Moreover, the effects of dietary fiber were superior to those of derived metabolites and probiotic supplementation. Finally, Kang and Cai commented on the ability of *Lactobacillus plantarum* GUANKE to boost severe acute respiratory syndrome coronavirus 2 (SARS-CoV-2)-vaccine-induced effective memory immune response by enhancing interferon signaling and suppressing apoptotic and inflammatory pathways. They suggest that using probiotics to boost vaccine efficacy is an inspiration for future research directions.

Recent research indicates that live and proliferating bacteria are not the prerequisite for obtaining health-promoting effects. In experimental studies, the beneficial effects are also achieved by inactivated bacteria or bacteria-secreted extracellular vesicles or certain effector molecules located on the bacterial surface (e.g., peptidoglycan and polysaccharides), secreted by bacteria (e.g., antibacterial peptides) or released after bacterial lysis (e.g., proteins, exopolysaccharides, and DNA) (Lebeer et al., 2018; Pyclik et al., 2020). In this regard, some studies have demonstrated the potential of inactivated microbes. Jhong et al. evaluated the antiosteoporotic effects of heat-killed *Lacticaseibacillus paracasei* GMNL-653 in ovariectomized (OVX) mice. The GMNL-653 exerts anti-inflammatory activity which restored gut microbiota dysbiosis and maintained intestinal barrier integrity in the OVX mice. However, Pyclik et al. showed that both live and heat-killed *Bifidobacterium longum ssp. longum* CCM 7952 are able to alleviate the allergy symptomes in mouse OVA-induced allergy model, albeit in a different manner. Studies performed by Pyclik et al. indicated that research on bacterial effector molecules is warranted to elucidate the mechanism of beneficial effects of probiotics.

The effector molecules presented on the bacterial surface, including cell components or metabolic products secreted into the environment, may impart an array of health-promoting properties. One of them are exopolysaccharides (EPS). The EPS have received a lot of attention due to their industrial and therapeutic applications. Brdarić et al. investigated the capacity of eight EPS-producing lactobacilli to adsorb Cd, one of the most significant toxic elements. The most promising EPS turned out to be produced by strain BGAN8 which exhibited a high Cd-binding capacity and prevented Cd-mediated toxicity in intestinal epithelial Caco-2 cells. Khalil et al. isolated and characterized EPS from different Lactic Acid Bacteria and *Bifidobacterium* strains in terms of their antioxidant, antitumor, and periodontal regeneration properties. The antioxidant capacity of EPS varied significantly among tested strains indicating that certain chemical structures provide a beneficial effect. The EPS_5, composed mainly of galactose, showed the highest cytotoxicity against human cancer lines. Moreover, EPS_5 treatment selectively regulated the expression of some apoptotic genes expression. Recently, other probiotic molecules i.e., extracellular vesicles have fascinated many scientific groups. Rubio et al. reviewed the EVs derived from Gram-positive and Gram-negative probiotic bacteria in interaction with the host. Novel EV-based technologies are promising for the design of therapies and/or vaccines against infections.

With this topic, we have assembled a set of 15 research articles that bring new insights into active probiotic and post-biotic research areas. These studies highlighted the need for rigorous probiotic selection and the exciting possibility of using inactivated probiotics or bacteria-derived molecules to confer health benefits to the host.

Author contributions

All authors listed have made a substantial, direct, and intellectual contribution to the work and approved it for publication.

Funding

This work was supported by grant 19-02261S of the Czech Science Foundation and 8J20AT011 of the Ministry of Education, Youth and Sports of the Czech Republic. This work was supported by grant co-founded by the National Science Centre of Poland under grant decision number UMO-2017/26/E/NZ7/01202 and by the Polish National Agency for Academic Exchange under grant decision number PPN/BIL/2018/1/00005. IS: OEAD PL 03/2022 and CZ 06/2020 and Danube Allergy Research Cluster.

Conflict of interest

The authors declare that the research was conducted in the absence of any commercial or financial relationships that could be construed as a potential conflict of interest.

Publisher's note

References

Lebeer, S., Bron, P. A., Marco, M. L., Van Pijkeren, J. P., O'Connell Motherway, M., Hiil, C., et al. (2018). Identification of probiotic effector molecules: present state and future perspectives. *Curr. Opin. Biotechnol.* 49, 217–223. doi: 10.1016/j.copbio.2017.10.007

Pyclik, M., Srutkova, D., Schwarzer, M., and Gorska, S. (2020). Bifidobacteria cell wall-derived exo-polysaccharides, lipoteichoic acids, peptidoglycans, polar lipids, and proteins - their chemical structure and biological attributes. *Int. J. Biol. Macromol.* 147, 333–349. doi: 10.1016/j.ijbiomac.2019.12.227

Tlaskalova-Hogenova, H., Stěpánková, R., Kozáková, H., Hudcovic, T., Vannucci, L., Tučková, L., et al. (2011). The role of gut microbiota (commensal bacteria) and the mucosal barrier in the pathogenesis of inflammatory and autoimmune diseases and cancer: contribution of germ-free and gnotobiotic animal models of human diseases. *Cell. Mol. Immunol.* 8, 110–120. doi: 10.1038/cmi.2010.67

frontiers in Immunology

ORIGINAL RESEARCH
published: 20 July 2021
doi: 10.3389/fimmu.2021.707728

Viability Status-Dependent Effect of *Bifidobacterium longum* ssp. *longum* CCM 7952 on Prevention of Allergic Inflammation in Mouse Model

Marcelina Joanna Pyclik[1], Dagmar Srutkova[2], Agnieszka Razim[1], Petra Hermanova[2], Tereza Svabova[2], Katarzyna Pacyga[1], Martin Schwarzer[2†] and Sabina Górska[1*†]*

[1] Laboratory of Microbiome Immunobiology, Hirszfeld Institute of Immunology and Experimental Therapy, Polish Academy of Sciences, Wroclaw, Poland, [2] Laboratory of Gnotobiology, Institute of Microbiology, Czech Academy of Sciences, Novy Hradek, Czechia

OPEN ACCESS

Edited by:
Julio Villena,
CONICET Centro de Referencia para Lactobacilos (CERELA), Argentina

Reviewed by:
María Fernanda Raya Tonetti, Consejo Nacional de Investigaciones Científicas y Técnicas (CONICET), Argentina
Jun-Song Wang, Nanjing University of Science and Technology, China

***Correspondence:**
Dagmar Srutkova
srutkova@biomed.cas.cz
Sabina Górska
sabina.gorska@hirszfeld.pl

†These authors share senior authorship

Specialty section:
This article was submitted to Nutritional Immunology, a section of the journal Frontiers in Immunology

Received: 10 May 2021
Accepted: 28 June 2021
Published: 20 July 2021

Citation:
Pyclik MJ, Srutkova D, Razim A, Hermanova P, Svabova T, Pacyga K, Schwarzer M and Górska S (2021) Viability Status-Dependent Effect of Bifidobacterium longum ssp. longum CCM 7952 on Prevention of Allergic Inflammation in Mouse Model. Front. Immunol. 12:707728. doi: 10.3389/fimmu.2021.707728

The classical definition of probiotics states that bacteria must be alive to be beneficial for human organism. However, recent reports show that inactivated bacteria or their effector molecules can also possess such properties. In this study, we investigated the physical and immunomodulatory properties of four *Bifidobacterium* strains in the heat-treated (HT) and untreated (UN) forms. We showed that temperature treatment of bacteria changes their size and charge, which affects their interaction with epithelial and immune cells. Based on the *in vitro* assays, we observed that all tested strains reduced the level of OVA-induced IL-4, IL-5, and IL-13 in the spleen culture of OVA-sensitized mice. We selected *Bifidobacterium longum* ssp. *longum* CCM 7952 (Bl 7952) for further analysis. *In vivo* experiments confirmed that untreated Bl 7952 exhibited allergy-reducing properties when administered intranasally to OVA-sensitized mice, which manifested in significant suppression of airway inflammation. Untreated Bl 7952 decreased local and systemic levels of Th2 related cytokines, OVA-specific IgE antibodies and simultaneously inhibited airway eosinophilia. In contrast, heat-treated Bl 7952 was only able to reduce IL-4 levels in the lungs and eosinophils in bronchoalveolar lavage, but increased neutrophil and macrophage numbers. We demonstrated that the viability status of Bl 7952 is a prerequisite for the beneficial effects of bacteria, and that heat treatment reduces but does not completely abolish these properties. Further research on bacterial effector molecules to elucidate the beneficial effects of probiotics in the prevention of allergic diseases is warranted.

Keywords: probiotic, heat inactivation, intranasal administration, *Bifidobacterium*, Ovalbumin sensitization, allergy

INTRODUCTION

Food and respiratory allergies have become a significant health burden in both developed and developing countries. Recent data indicate that the percentage of people demonstrating symptoms of allergy reaches up to 40% of the world population (1, 2). Allergies are characterized by an abnormal reaction of the body to a commonly harmless substance. Hypersensitivity type I reaction

is associated with Th2 polarized lymphocyte response and involves production of IL-4, IL-5, and IL-13 cytokines and allergen-specific IgE antibodies. In particular, IL-4 and IL-13 regulate many aspects of allergic response, *i.e.*, in B cells prompt the immunoglobulin switch to IgG1 and IgE, activate and recruit eosinophils and induce mucus hypersecretion in lung tissue (3). In respiratory allergies, nasal and lung epithelial cells are the first cells encountering allergen, such as house-dust mite faeces, fungal spores or plant pollen. Besides being a physical barrier separating the internal milieu from the external environment, epithelial cells also play an important role in initial recognition of antigens and regulation of the immune responses to them (4). Moreover, epithelial cells are able to secrete a large number of cytokines and chemokines that regulate the activation of T and/or B lymphocytes, eosinophils, mast cells, and ILC2 cells (5, 6).

Growing evidence suggests that probiotics could be a promising strategy in the prevention/treatment of allergy diseases (7). Recently, several studies have shown that prophylactic administration of probiotics attenuates the production of pro-inflammatory responses in house dust mite-induced asthma model (8, 9). Along with these results, it has been shown that intranasal administration could be more effective compared to standard intragastric route (10). It has been also noticed, that probiotics interaction with mucosa of the respiratory tract leads to the activation of both local and systemic immune responses (11, 12).

While probiotics are generally regarded as safe, the administration of live bacteria to certain groups of patients could cause bacteremia (13). This especially concerns people with weakened immune system *e.g.*, new-borns or elderly people (14, 15). Until recently, it was considered that probiotics should be administered alive in order to exert their beneficial properties (16, 17). However, there is an accumulating evidence showing that even administration of inactivated bacterial strains and bacteria-derived molecules is able to ameliorate the development of airway allergy (18–21). For example, it has been shown that administration of thermally inactivated *Enterococcus feacalis* reduced nasal mucosa swelling and decreased eosinophil level in a mouse model of allergic rhinitis (22). Similarly, thermally inactivated *Lactobacillus* (*L.*) *casei* Shirota inhibits the production of IgE in mouse model of allergy, which may indicate a protective role in allergy modulation (23). Even so, depending on the bacterial species or bacterial strain, desired probiotic properties may be retained only partially or lost completely during heat inactivation (24).

In this study we characterized the viability status-dependent physical and immunomodulatory properties of four strains belonging to different *Bifidobacterium* species. On the basis of the potential to downregulate the allergic and inflammatory cytokine response, we selected *Bifidobacterium longum* ssp. *longum* CCM 7952 (Bl 7952) strain to further investigate the impact of thermal inactivation on prevention and modulation of allergic immune response to ovalbumin (OVA) in a mouse model of allergy. We found that intranasal administration of untreated Bl 7952 strain prevented the development of allergic lung inflammation and modulated both local and systemic OVA-specific immune responses. These immunomodulatory properties were partially lost when heat-treated Bl 7952 was used.

MATERIALS AND METHODS

Cultivation and Inactivation of Bacterial Strains

Four *Bifidobacterium* strains: *B. longum* ssp. *longum* CCM 7952 (Bl 7952), *B. longum* ssp. *infantis* CCDM 369 (Bin 369), *B. animalis* CCDM 218 (Ban 218), and *B. adolescentis* CCDM 373 (Bad 373) were obtained from the Collection of Dairy Microorganisms (Laktoflora, Milcom, Tábor, Czech Republic). They were isolated from fecal samples of healthy adults or breast-fed infants. Stocks of strains were kept at −80°C in MRS (De Man, Rogosa and Sharpe medium, Sigma Aldrich, USA) with 0.05% L-cysteine (Sigma Aldrich, USA) and 20% glycerol. The isolates were cultivated for 48 or 72 h in MRS broth (Sigma Aldrich, USA) with 0.05% L-cysteine (Merck Millipore, Massachusetts, USA) at 37°C in anaerobic conditions (80% N_2, 10% CO_2, 10% H_2). They were centrifuged (4,500 × g, 15 min, 4°C) and washed with sterile phosphate-buffered saline (PBS). The number of cells was determined by CFU counting on MRS agar plates with 0.05% L-cysteine after 48 h of anaerobic incubation or by QuantomTx Microbial Cell Counter (Logos Biosystems, South Korea) and associated with the values obtained during the measurement of OD_{600}. Bacterial survival in PBS (HIIET PAS, Poland) after 72 h at 4°C was checked by plate culture and CFU counting. Heat inactivation was performed at 65°C for 1 h, and samples were stored at 4°C until use. Loss of viability was examined by culture on MRS agar plates supplemented with L-cysteine in anaerobic conditions.

Scanning Electron Microscopy at Low Voltage

The untreated bacteria (10^7 CFU/ml) were plated onto an MRS Agar plate and after 48 h of incubation were pressed against a silicon chip (7 × 7 mm), while the heat-treated bacteria were prepared in a volume of 1 ml in an Eppendorf in which a silicon chip was placed. In both cases, a 2 min incubation was performed, and then the chip was removed for further preparation steps for imaging. The bacteria-containing chip was rinsed with PBS (HIIET PAS, Poland) at room temperature and immersed in 2.5% glutaraldehyde (Sigma Aldrich) in 0.1 M cacodylate buffer. Fixation was continued for 30 min, followed by washing (5 × 30 min, 4°C) with 0.1 M cacodylate buffer and dehydration in serial concentrations of ice-cold methanol (25, 40, 60, 80, and 100%). All samples designed for imaging at room temperature underwent critical point drying with 100% methanol exchanged for liquid CO_2 in an automated manner (CPD300 AUTO, Leica Microsystems, Germany) and were imaged under a cross-beam scanning electron microscope equipped with a Schottky field-emission cathode (Auriga 60, Carl Zeiss) at 1.2 kV accelerating voltage.

Physical Measurements of Untreated and Heat-Treated Bifidobacteria

Two samples of each *Bifidobacterium* strain at a density of 10^7 CFU/ml were prepared in 300 µl of PBS. Inactivation was performed by heat treatment at 65°C for 1 h. After cooling to room temperature (25°C), both untreated (UN) and heat-treated

(HT) were transferred to the measuring cuvette and analyzed in terms of their size (Dynamic Light Scattering, DLS) and zeta potential (Electrophoretic Light Scattering, ELS) using Zetasizer Nano ZS (Malvern Panalytical, UK). Measurements were made in milli-Q water in a Folded Capillary Cell (DTS1070, Malvern Panalytical). Each probe was measured five times at 25°C (at least 15 runs, voltage adjusted automatically by the software). To perform calculation dispersant RI 1.333 and viscosity (Cp) as 0.87 were used.

Cell Lines and Culture Conditions

A cancerous epithelial line TC-1 (ATCC CRL-2785) isolated from murine lungs immortalized with human papillomavirus 16 (HPV-16) E6/E7 and c-Ha-Ras cotransformed was maintained in Dulbecco's Modified Eagle Medium (DMEM, Gibco, Thermo Fisher Scientific, USA) with 10% fetal bovine serum (FBS, Gibco, Thermo Fisher Scientific), 100 U/ml penicillin, 100 µg/ml streptomycin and 2 mM L-glutamine (Gibco).

JAWS II cell line (ATCC CRL-11904) was established from bone marrow-derived dendritic cells of C57BL/6 mouse and was maintained in Alpha Minimum Essential Medium Eagle (Alpha MEM, Gibco) with 10% FBS, 100 U/ml penicillin, 100 µg/ml streptomycin, 2 mM L-glutamine, 1 mM sodium pyruvate (Sigma Aldrich), and 5 ng/ml granulocyte-macrophage colony-stimulating factor (GM-CSF, Invitrogen, Thermo Fisher Scientific).

Both cell lines were cultivated in an incubator at 37°C, 5% CO_2. Culture media were changed every two to three days, and the cell lines were trypsinized with 0.25% trypsin-EDTA pH 7.2 solution when 80% confluency was reached.

Bifidobacterium Engulfment by Epithelial Cells

TC-1 cells were seeded at density of 0.4×10^6 cells/ml on 24-well plate in medium without antibiotics (DMEM, 10% FBS) and left for 5 h to adhere at 37°C, 5% CO_2. Next, UN and HT bifidobacteria were stained as in the manufacturer protocol with SYTO™ 9 (Thermo Fisher Scientific) and were added to the epithelial cells in the ratio of 1:10 (TC-1:bacteria) in antibiotic-free medium. Bacteria were counted with QuantomTx Microbial Cell Counter (Labos Biosystem). Samples were incubated overnight and the next day, TC-1 cells were washed twice with pre-warmed PBS. Cells were detached from the plate with trypsin and analyzed by the BD FACSCalibur Flow Cytometry System (BD Biosciences, USA) in terms of green fluorescence. TC-1 cells mixed with PBS were used as negative control. Each experiment was repeated three times.

Bifidobacterium Transfer Between Epithelial and Dendritic Cells

TC-1 cells were grown and loaded with stained bacteria as described above. Simultaneously, JAWS II cells were cultivated and stained with red fluorescent dye PKH26 (Sigma Aldrich). Next, they were added to the TC-1 cells in an approximate ratio of 1:1 in JAWS II complete medium. Cells were co-cultured for 4 h in the incubator (37°C, 5% CO_2). Cells were detached from the plate with trypsin and analyzed by the BD FACSCalibur Flow Cytometry System in terms of green and red fluorescence. Each experiment was repeated three times.

TC-1 Cell Stimulation With Bifidobacteria

TC-1 cells were seeded at density of 2×10^6 cells/ml on 96-well plate in medium without antibiotics (DMEM, 10% FBS) and stimulated with UN or HT bifidobacteria strains in the ratio of 1:10 (TC-1:bacteria). TC-1 cells stimulated with PBS were used as controls. The supernatants were collected after 20 h of incubation at 37°C, 5% CO_2. The levels of IL-6 and MCP-1 were quantified using enzyme-linked immunosorbent assay (ELISA) detection kits (Invitrogen or BD OptEIA Pharmingen, USA) according to the instructions of the manufacturer. Each experiment was repeated three times.

Bone Marrow-Derived Dendritic Cell Isolation and Stimulation

The mouse bone marrow precursors were isolated from femurs and tibias of BALB/c mice (8-weeks old). Cells were cultured at density of 4×10^6 cells/ml on Petri dishes in 10 ml of Roswell Park Memorial Institute (RPMI 1640, Sigma Aldrich) culture medium containing 10% FBS, 150 µg/ml gentamycin (Sigma Aldrich) and 20 ng/ml GM-CSF (Invitrogen). Fresh medium was added at days 3 and 6, and BMDCs were used for experiments on day 7 of culture. BMDCs (0.5×10^6 cells/ml) were stimulated with UN or HT bacteria in ratio of 1:10 (BMDCs:bacteria) for 20 h. Control BMDCs were stimulated with PBS. Levels of IL-10 and IL-12p70 in culture supernatants were determined by ELISA Ready-Set-Go! kits (eBioscience, Germany, San Diego, CA, USA) according to the instructions of the manufacturer. Each experiment was repeated twice.

Stimulation of TLR2, TLR4, NOD2, and NOD1 Receptors

The human embryonic kidney cell line HEK293 stably transfected with a plasmid carrying the human (h) TLR2/CD14 gene was kindly provided by M. Yazdanbakhsh (Leiden, The Netherlands), and hTLR4/MD2/CD14 by B. Bohle (Vienna, Austria). Cells transfected with hNOD2 and hNOD1 were purchased from InvivoGen (InvivoGen, USA). The cells were stimulated for 20 h with UN and HT bifidobacteria at concentrations of approximately 1×10^7 CFU/ml in 96-well plates. TLR2 ligand Pam3CSK4 (1 µg/ml, InvivoGen), NOD2 ligand muramyl dipeptide (MDP; 100 ng/ml; InvivoGen), TLR4 ligand ultrapure LPS-EB (1 µg/ml, Sigma Aldrich), and NOD1 ligand acylated derivative of the iE-DAP dipeptide (C12-iE-DAP; 100 ng/ml; InvivoGen) were used as positive controls. Culture supernatants were harvested and human IL-8 concentrations, as level of respective receptor activation, were analyzed by ELISA (Invitrogen, Thermo Fisher Scientific) according to the instructions of the manufacturer. Each experiment was repeated three times.

Stimulation of Splenocytes From OVA-Sensitized Mice With UN and HT *Bifidobacterium* Strains

Immunomodulatory potential of *Bifidobacterium* strains was tested *ex vivo* on splenocytes derived from ovalbumin (OVA)-

sensitized BALB/c mice (8–12 weeks of age; n = 3) in four independent experiments. Female mice were sensitized by two intraperitoneal (i.p.) injections of 10 μg of OVA (Sigma Aldrich, grade V) mixed with 0.65 mg/100 μl of Alum (Serva, Germany) in final volume of 200 μl in a two-week interval. Seven days after the second immunization, mice were anesthetized by 3% isoflurane and euthanized by cervical dislocation. Spleens were aseptically removed and prepared by disruption of the tissues through a 70 μm cell strainer into culture medium RPMI 1640 with 10% FBS, 100 U/ml of penicillin, 100 μg/ml streptomycin, and 10 mM HEPES. Splenocytes (5×10^6 cells/ml) were re-stimulated in 96-well flat-bottom plates with OVA (500 μg/ml, Worthington, USA) together with UN/HT bifidobacteria in a ratio of 1:10 (cells:bacteria) for 72 h. Splenocytes stimulated only with OVA were used as baseline of cytokine response to OVA re-stimulation. Unstimulated splenocytes were used as a negative control. Concentration of cytokines was measured in supernatants by the Milliplex Map Mouse Cytokine/Chemokine Panel (IL-4, IL-5, IL-13, and IFN-γ) according to the instructions of the manufacturer and analyzed with Luminex 2000 System (Bio-Rad Laboratories, CA, USA).

In Vivo Effect of UN and HT *B. longum* ssp. *longum* CCM 7952 (Bl 7952) in Mouse Model of OVA-Induced Allergy

Animals

Pathogen-free female BALB/c mice (6–8 weeks of age) were maintained in individually ventilated cages (IVC, Tecniplast, Italy) with a 12:12-h light–dark cycle and free access to water and sterile irradiated diet (Altromin Spezialfutter GmbH & Co. KG, Lage, Germany). The animal experiments were approved by the committee for the protection and use of experimental animals of the Institute of Microbiology, The Czech Academy of Sciences (no. 91/2019).

Experimental Design

Mice (n = 6–8 per group) were divided into three experimental groups: PBS/OVA, untreated (UN) Bl 7952/OVA or heat-treated (HT) Bl 7952/OVA. Mice were sensitized by i.p. injections of 10 μg of OVA (Sigma Aldrich, grade V) mixed with PBS and adsorbed on 0.65 mg of Alum (Serva) in a final volume of 200 μl, on days 1 and 14. Third boosting immunization (i.p.) was performed one week after the second injection by 15 μg OVA (Sigma Aldrich, grade V) in PBS mixed with Alum (0.65 mg per dose) (200 μl). Seven days after the third immunization, mice were anesthetized by 3% isoflurane and challenged by intranasal administration of 100 μg of OVA in PBS in a dose of 30 μl. The procedure was repeated each day for 4 consecutive days. Four hours before each sensitization and OVA-challenge application, mice were anesthetized by 3% isoflurane and PBS; untreated or heat-treated Bl 7952 (1×10^7 CFU/30 μl) were applied intranasally (i.n.). Mice were anesthetized by 3% isoflurane and euthanized on the day following the fourth challenge and samples [serum, spleen, bronchoalveolar lavage (BAL), lung lobes] were collected (**Figure 1**). The experiment was repeated twice yielding similar results; data from a representative experiment are shown.

Quantification of Cytokine Production by Splenocytes

Spleen cell suspensions (5×10^6 cells/ml) were cultured on 96-well flat-bottom plates in 200 μl of complete RPMI 1640. Cells were re-stimulated with OVA (500 μg/ml; Worthington, USA) or left unstimulated and cultured at 37°C, 5% CO_2 for 72 h. Supernatants were collected and stored at −40°C until further analysis. The levels of IL-4, IL-5, IL-10, and IL-13 were determined using a Mouse Cytokine/Chemokine Multiplex Immunoassay (Millipore) and analyzed with a Luminex 200 System (Bio-Rad Laboratories). IFN-γ was assessed by ELISA kit (R&D Duo set System, USA) according to the instructions of the manufacturer.

Histopathological Evaluation of Lung Inflammation

Small lung lobes were fixed in 4% paraformaldehyde for 24 h and stored in 80% ethanol. After embedding in paraffin, 5 μm-thick sections were treated with periodic acid-Schiff (PAS) staining. Histological pathology scoring was evaluated using light microscopy (×100 magnification) according to Drinić et al. (25) and expressed as: (i) perivascular and peribronchiolar inflammation (grade: 0 = no changes; 1 = few perivascular and peribronchiolar inflammatory cells; 2 = moderate numbers of cell infiltrations on several perivascular and peribronchiolar sites; 3 = large number of diffuse infiltrated cell cuffs), (ii) the presence of leukocytes in alveolar spaces (grade: 0 = no cells; 1 = 2–4 cells; 3 = 4–10 cells; 3 = more than 10 cells), and (iii) number of PAS positive cells per 50 counted bronchoalveolar epithelial cells (0 = no cells; 1 = <12; 2 =12–25; 3 = >25). The histopathological score is expressed as a sum of single scores divided by 3.

Analysis of Bronchoalveolar Lavage

BAL fluid (BALF) was collected from each animal *via* cannulation of the exposed trachea and gentle flushing of the lungs with 2 × 0.5 ml of sterile Dulbecco's Phosphate Buffered Saline (D-PBS, Gibco). BALF was centrifuged (400 × g, 7 min, 4°C), and the supernatant was collected and stored at −40°C. Cell pellet was recovered for cellular analysis by 200 μl of RPMI medium. After cell counting, cells were spun down onto microscope slide, fixed with methanol and stained by Dip-Quick-stain kit according to instruction of the manufacturer (Medical products, Czech Republic). Cytospin preparations were differentiated according to standard morphologic criteria by counting 200 cells *via* light microscopy (26). The levels of IL-4, IL-5, IL-10, and IFN-γ were determined using a Mouse Cytokine/Chemokine Multiplex Immunoassay (Millipore) or ELISA kit (R&D Duoset System, Minneapolis, MN, USA) according to the instructions of the manufacturer.

Humoral Immune Response in Serum and BALF

Levels of OVA-specific IgG1, IgG2a, and IgA in serum or BALF were determined by ELISA as previously described (27). Briefly, the 96-well microtiter plates (Nunc MaxiSorp, Thermo Fisher Scientific) were coated with OVA (5 μg/ml), and mouse serum samples were diluted 1:10,000 for IgG1, 1:100 for IgG2a, and 1:10

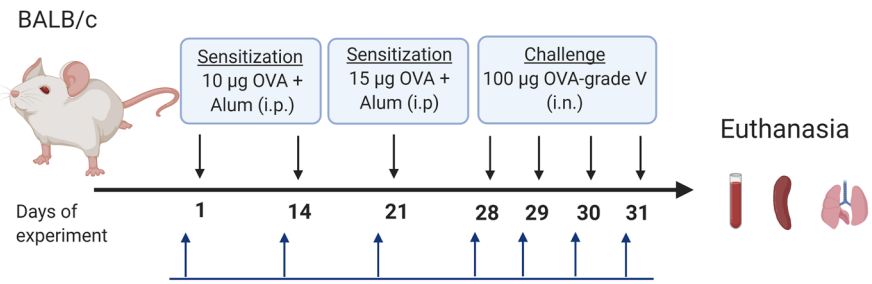

Groups	4 hours before OVA administration
PBS/OVA	PBS (30 µl, i.n.)
UN Bl 7952/OVA	Untreated Bl 7952 (10^7 CFU, 30 µl, i.n.)
HT Bl 7952/OVA	Heat-treated Bl 7952 (10^7 CFU, 30 µl, i.n.)

FIGURE 1 | Experimental design—bacterial administration and systemic sensitization and challenge of BALB/c mice to OVA. Female BALB/c mice 6–8-week-old (n = 6 to 8) were i.p. sensitized with 10 µg of OVA + Alum on days 1 and 14 of experiment, boosting dose of 15 µg of OVA + Alum was administrated on day 21. Seven days after third immunization, the challenge with 100 µg of OVA was performed for 4 consecutive days. Untreated (UN Bl 7952) or heat-treated (HT Bl 7952) bifidobacteria in dose 1×10^7 CFU/30 µl or PBS were administered intranasally 4 h before each sensitization and challenge. Mice were euthanized on day 32, and samples were collected (Created with BioRender.com).

for IgA quantification. Rat anti-mouse IgG1, IgG2a and IgA antibodies (1:500; Pharmingen, BD Biosciences, USA) were applied, followed by peroxidase-conjugated mouse anti-rat IgG antibodies (1:2,000; Jackson Immuno Labs, USA). Antibody levels were reported as optical density (OD) at wavelength λ = 405 nm.

The activity of OVA-specific IgE in serum (diluted 1:810) and BALF (undiluted) was measured by rat basophil leukemia (RBL-2H3) cells degranulation assay as described previously (28). The level of total IgA was measured in BALF (diluted 1:20) by ELISA quantification kit (Bethyl, USA) according to the instructions of the manufacturer.

The whole-bacterial cell enzyme-linked immunosorbent assay was used to determine the level of untreated and heat-treated Bl 7952-specific IgA (29). The 96-well microtiter plates were coated by 25 µg of dry mass of bacteria UN or HT in PBS per well and fixed by 0.1% glutaraldehyde for 30 min. Plate was incubated in 0.1% bovine serum albumin (BSA, Sigma Aldrich) with 0.1 M glycine for 2 h. Wells were aspirated, and plate was incubated overnight at 4°C with 0.25% BSA and magnesium chloride (Sigma Aldrich). Samples of BALF (diluted 1:1) were added and after 3-h incubation, the bacteria-specific IgA was detected using horse-radish peroxidase-conjugated IgA antibody (1:10,000; Bethyl, USA) according to the instructions of the manufacturer.

Statistical Analysis

Data are expressed as mean ± standard deviation (SD). For *in vitro* experiments, the significance of data obtained for UN/HT bacteria treatment was analyzed by unpaired Student's t-test. Comparison between OVA group and bacteria groups in OVA-sensitized splenocytes was analyzed by one-way ANOVA with Dunnett's multiple comparison test. In *in vivo* experiment for comparisons between PBS/OVA and bacteria-treated experimental groups, one-way ANOVA with Dunnett's multiple comparison test was used. A significant difference was considered to exist when the *p-value* was <0.05. Statistical analysis was performed using GraphPad Prism 8.1 Software (San Diego, CA, USA). ****p < 0.0001, ***p < 0.001, **p < 0.01, *p < 0.05; ns, no significance.

RESULTS

Heat Treatment Alters Bacterial Surface, Size and Zeta Potential

In order to evaluate the morphological differences in *Bifidobacterium* strains resulting from heat treatment, scanning electron microscopy at low voltage, DLS, and ELS analysis were performed. Heat inactivation of bacteria for 1 h at 65°C induced slight morphological cellular changes (**Supplementary Figure S1**). UN bacteria were characterized by smooth surface in all examined strains, whereas surface of HT bacteria was more porous and irregular. Images of HT bacteria cells revealed no lysis or decomposition of bacterial cells (**Supplementary Figure S1**). DLS analysis showed that the size of UN bifidobacterial strains varies between 2.417 µm (SD ± 0.277) for Bl 7952 strain and 2.979 µm (SD ± 0.234) for Bad 373 strain (**Figure 2A**). After the heat treatment, the bacterial cell size of Bl 7952 and Ban 218 decreased. Contrarily, the cell size of Bad 373 increased and that of Bin 369 remained unchanged. Changes in size did not correspond with changes in bacteria zeta potential (**Figure 2B**) since only two strains, Bin 369 and Bad 373, have significantly lower zeta potential after heat inactivation.

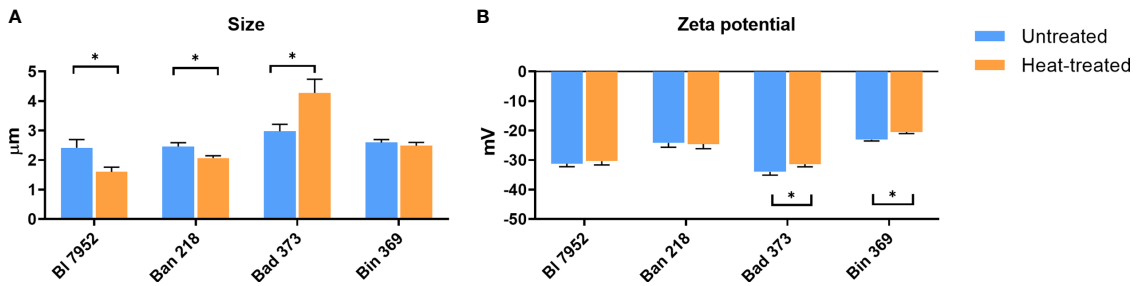

FIGURE 2 | Physicochemical differences between untreated and heat-treated bifidobacteria. **(A)** Size (µm) and **(B)** zeta potential measurements (mV) of untreated (UN, blue bars) and heat-treated (HT, orange bars) bifidobacteria strains were performed using Zetasizer Nano ZS. Data are shown as mean ± SD of five measurements; statistical differences were analyzed by multiple t-tests between UN and HT, *p < 0.05 statistically significant difference.

Heat Treatment Affects Bifidobacteria Engulfment and Cytokine Induction in Epithelial Cells Along With Transfer Capacity Between Epithelial and Dendritic Cells

We assessed whether the observed heat treatment induced changes on bacterial surface properties have an effect on further bacteria processing by epithelial TC-1 cells. We observed a trend towards decreased engulfment of HT bacteria compared to UN bacteria, with a statistically significant decrease for Bin 369 and Bad 373 strains (**Figure 3A**). Next, we focused on bacterial transfer between TC-1 epithelial and antigen presenting cells (JAWS II). In agreement with lower engulfment of HT bacteria, the transfer of these bacteria to the dendritic cells was also lower (**Figure 3B**). In particular, significant decrease was observed for Bin 369 and Bad 373 strains, which are in line with the results of the engulfment experiments (**Figure 3A**). Epithelial and antigen presenting cells were able to produce cytokines and chemokines following the antigen exposure. Upon exposure to UN bifidobacteria, TC-1 cells produced the chemokine MCP-1 and cytokine IL-6 (**Figures 3C, D**); however cytokines such as IL-10, IL-12p70, IFN-γ, TGF-β, and TNF-α were undetectable (data not shown). Stimulation with HT bacteria was associated with a decrease in both MCP-1 and IL-6 levels compared to UN bifidobacteria. Both UN and HT bacteria triggered cytokine production and maturation of bone-marrow dendritic cells in a species dependent manner (**Figures 3E, F**). The untreated and heat-treated Bl 7952 and Ban 218 strains induced higher levels of IL-10 compared to Bad 373 and Bin 369. On the other hand, stimulation of BMDCs with Bin 369 strain led to the induction of higher levels of IL-12p70 compared to Ban 218. Surprisingly, all bacteria induced the same levels of IL-10 (**Figure 3E**) and IL-12p70 (**Figure 3F**) independently of their viability status. Only in the case of strain Ban 218 that the temperature treatment caused a significant increase of IL-12p70 with no changes in IL-10 levels.

In order to investigate the role of TLR and NOD receptors in bifidobacteria recognition, we examined HEK293 cells stably transfected with hTLR2, hTLR4, hNOD2, and hNOD1 stimulated with both UN and HT bacteria. Bifidobacteria strains were recognized mostly *via* hTLR2 (**Figure 3G**) and only slightly by hNOD2 receptors (**Figure 3H**). No signaling was observed in the case of hTLR4 and hNOD1 (data not shown). The temperature treatment did not change the general recognition of bacteria. In the HEK293-hTLR2 cell line, we observed that in the majority of tested strains, inactivated bacteria showed a stronger receptor activation (**Figure 3G**). In turn, in the HEK293-hNOD2 cell line, no significant differences between UN and HT strains were observed (**Figure 3H**).

Impact of Bifidobacteria on OVA-Induced Cytokine Production in Splenocyte Cultures From OVA-Sensitized Mice

We assessed the immunomodulatory potential of UN and HT bifidobacteria on recall OVA-induced cytokines from OVA-sensitized mouse splenocytes. As expected, OVA stimulation induced production of pro-allergic Th2-related cytokines IL-5 (**Figure 4A**), IL-4 (**Figure 4B**), and IL-13 (**Figure 4C**) and no Th1 related IFN-γ (**Figure 4D**). Regardless of bacteria viability status, all bifidobacterial strains were able to significantly downregulate the OVA-induced Th2 cytokines. However, in the case of Bl 7952, we observed that HT bacteria caused a weaker IL-4 suppression compared to UN bacteria (**Figure 4B**). Interestingly, the induction of IFN-$\gamma$was strain dependent (**Figure 4D**). Ban 218 and Bin 369, independently of the viability status, were the most robust inducers of this pro-inflammatory cytokine. On the other hand, Bl 7952 induced negligible level of IFN-γ suggesting regulatory, rather than Th1 inducing properties for these bacteria as compared to other tested species.

Intranasal Administration of Untreated and Heat-Treated Bl 7952 at the Time of Sensitization and Challenge Differently Attenuates the OVA-Induced Cellular and Humoral Immune Responses

In our previous study, Bl 7952 has been shown to prevent allergic sensitization in mono-colonized associated gnotobiotic mice

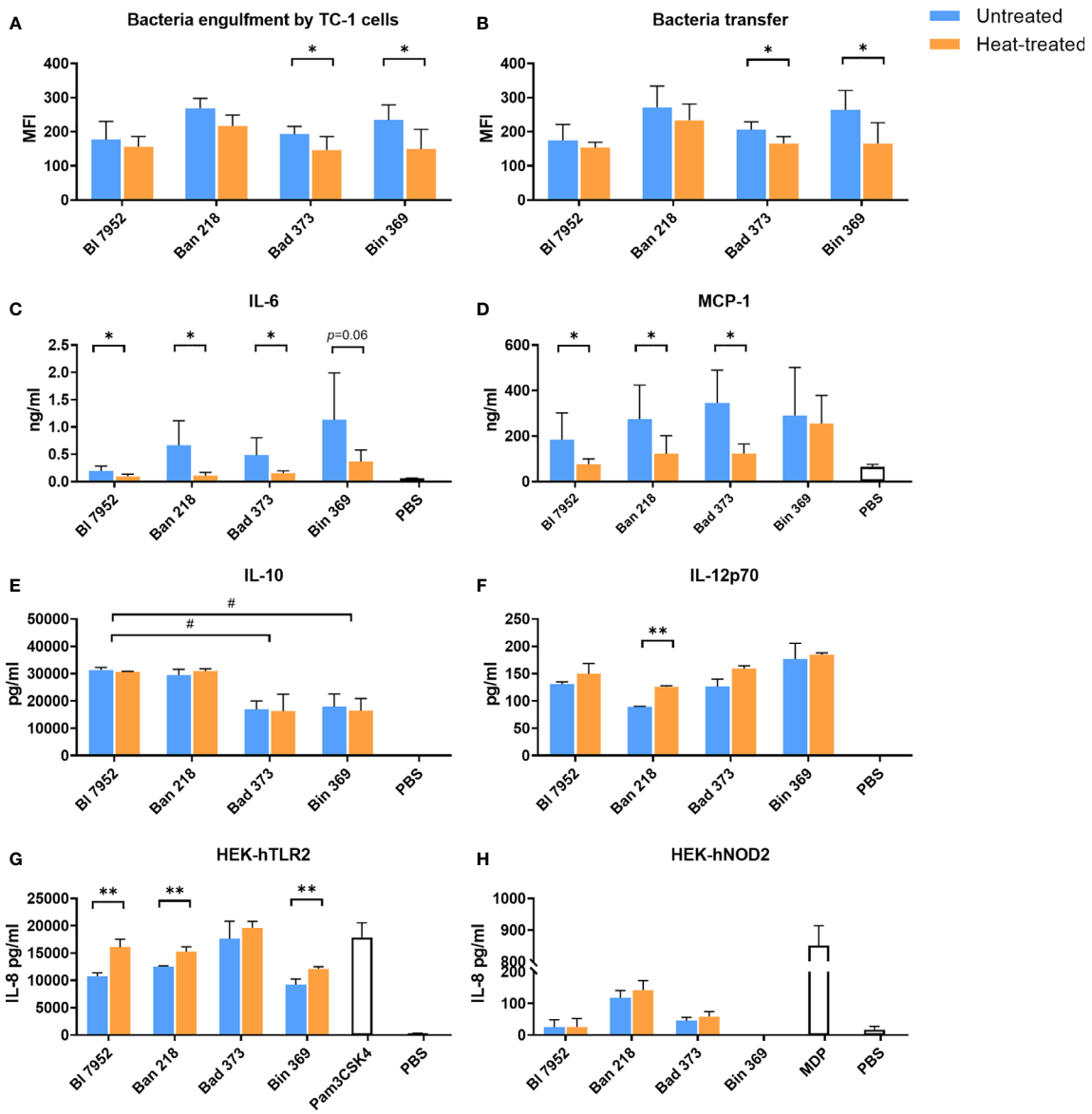

FIGURE 3 | Untreated and heat-treated bifidobacteria strains differently interact with epithelial and immune cells *in vitro*. **(A)** Engulfment by airway epithelial cells and **(B)** transfer between airway epithelial cells and dendritic cells of untreated (UN, blue bars) and heat-treated (HT, orange bars) bifidobacteria. Epithelial cells (TC-1 cells) were incubated overnight with SYTO™ 9-stained bacteria cells. After washing of bacteria, epithelial cells were co-cultured with PKH26-stained JAWS II cells for 4 h. Fluorescence of double stained dendritic cells was analyzed by FACS and expressed as mean fluorescence units (MFI). The level of **(C)** MCP-1 and **(D)** IL-6 cytokine production from TC-1 cells was measured by ELISA in culture supernatants after 24-h stimulation with bifidobacteria (UN or HT) or PBS. The level of **(E)** IL-10 and **(F)** IL-12p70 cytokine production was determined in supernatants of BMDCs after 20-h stimulation with UN or HT bifidobacteria or PBS. Activation of **(G)** TLR2 and **(H)** NOD2 receptors was determined using human embryonic kidney cells (HEK293) stably transfected with human TLR2 or NOD2 expressing vectors and expressed as production of IL-8 cytokine after 20-h stimulation by UN or HT bifidobacteria strains. TLR2 ligand Pam3CSK4 (1 μg/ml) and NOD2 ligand muramyl dipeptide (MDP; 100 ng/ml) were used as positive controls. Cells treated with PBS were used as negative control. Data are collected from three independent experiments. Data are shown as mean ± SD and analyzed with unpaired Student's t-test between untreated and heat-treated bacteria. *$p < 0.05$, **$p < 0.01$ statistically significant difference. Comparison between bifidobacterial strains was calculated by one-way ANOVA Dunett's multiple comparison test. #$p < 0.05$.

(30). Here we have shown the ability of Bl 7952 to supress OVA-induced Th2 cytokine in conventional mice without inducing Th1 cytokine production in splenocyte cultures from OVA-sensitized mice. It has been suggested that regulatory immune response rather than strongly inducing Th1 response could be more effective in prevention of allergies (31, 32). Therefore, we selected Bl 7952 for further *in vivo* experiments. Bl 7952, either as UN or HT was applied intranasally and impact on the systemic as well as local immune responses was evaluated in mouse model of OVA-induced airway allergy.

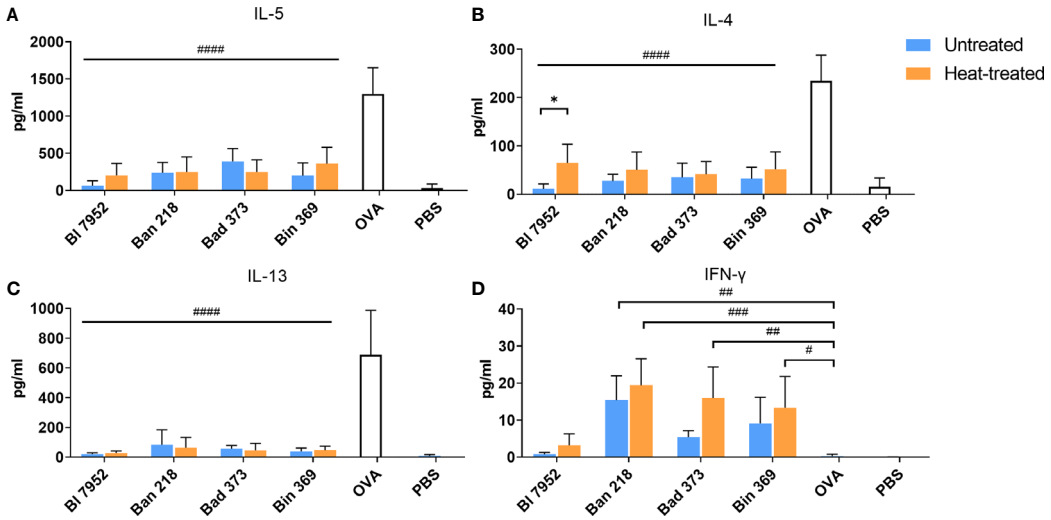

FIGURE 4 | Untreated and heat-treated bifidobacteria strains influence the OVA-induced cytokine production in splenocyte cultures from OVA-sensitized mice. Effect of untreated (UN, blue bars) and heat-treated (HT, orange bars) bifidobacteria strains on cytokine production: **(A)** IL-5, **(B)** IL-4, **(C)** IL-13, and **(D)** IFN-γ was measured in supernatants after 72 h cultivation of splenocytes isolated from OVA-sensitized mice and re-stimulated by OVA with or without bifidobacteria strains. Cells stimulated by PBS only served as negative control. Values are pooled from two independent experiments. Significant difference between UN and HT bacteria was estimated by unpaired Student's t-test (*p <.0.05). Comparison between OVA-stimulated and bifidobacteria + OVA-stimulated groups was calculated by one-way ANOVA Dunett's multiple comparison test. OVA group was used as control, $^{\#}p < 0.05$, $^{\#\#}p < 0.01$, $^{\#\#\#}p < 0.001$, $^{\#\#\#\#}p < 0.0001$.

To assess the effect of the Bl 7952 (untreated and heat-treated) treatment on the systemic allergic response of mice we measured the cytokine production from OVA stimulated splenocytes. Administration of untreated Bl 7952 downregulated the Th2-related cytokines IL-4 and IL-5, whereas heat-treated Bl 7952 significantly reduced only the production of IL-5 compared to PBS/OVA group (**Figures 5A, B**). There was no significant difference among the bacteria-treated and PBS/OVA groups in the levels of OVA-induced IL-10 and INF-γ cytokines (**Figures 5C, D**). The application of untreated Bl 7952 significantly reduced the serum levels of Th2-related OVA-specific IgE and Th1-related IgG2a antibodies compared to the PBS/OVA group (**Figures 5E, G**). We did not observe this effect after administration of heat-treated Bl 7952. Furthermore, Th2-related OVA-specific IgG1 antibodies (**Figure 5F**) were significantly reduced by both groups of Bl 7952 when compared to PBS/OVA group. There were no differences among the groups in the levels of OVA-specific and total IgA antibody (**Figures 5H, I**).

Intranasal Administration of Untreated and Heat-Treated Bl 7952 at the Time of Sensitization and Challenge Differently Reduces Allergic Inflammation in Lungs of OVA-Sensitized Mice

Lung histological analysis showed a reduction of cell infiltration, a lower percentage of mucus-producing cells, decreased perivascular and peribronchiolar inflammation together with lower presence of leukocytes in alveolar spaces in both Bl 7952/OVA groups as compared to control PBS/OVA group (**Figures 6A, B**). The reduced lung allergic inflammation was further confirmed by cellular differential count showing significant decrease in the number of eosinophils in the bronchoalveolar lavage (BAL) of both Bl 7952/OVA groups when compared to the PBS/OVA group. However, the intranasal administration of heat-treated Bl 7952 led to increased amount of neutrophils and macrophages, and no decrease in counts of total cell number in BAL compared to PBS/OVA group (**Figure 6C**). The results of BAL cytokine analysis showed that administration of untreated Bl 7952 significantly decreased the level of IL-4 and IL-5 and increased the level of regulatory cytokine IL-10 compared to the PBS/OVA group (**Figures 6D–F**). The heat-treated Bl 7952 also significantly decreased IL-4, but the levels of IL-5 and IL-10 remained unchanged compared to the PBS/OVA group. We did not observe any changes in the levels of IFN-γ among tested groups (**Figure 6G**).

Next, we measured the humoral immune response in the BAL. Results showed that only untreated Bl 7952 was able to reduce the levels of OVA-specific IgE antibodies as shown by IgE-dependant basophil degranulation assay (**Figure 6H**). Moreover, only untreated Bl 7952 significantly increased the levels of total IgA in BAL compared to PBS/OVA (**Figure 6I**). Surprisingly, OVA-specific IgA levels were not significantly different among the groups (**Figure 6J**). This prompted us to assess the bacteria specific IgA levels. When the plate was coated with bacterial mass of untreated Bl 7952, we observed significantly higher levels of specific IgA in BAL of untreated Bl 7952/OVA group compared to PBS/OVA. Heat-treated Bl 7952/OVA group showed higher levels of specific IgA in BAL

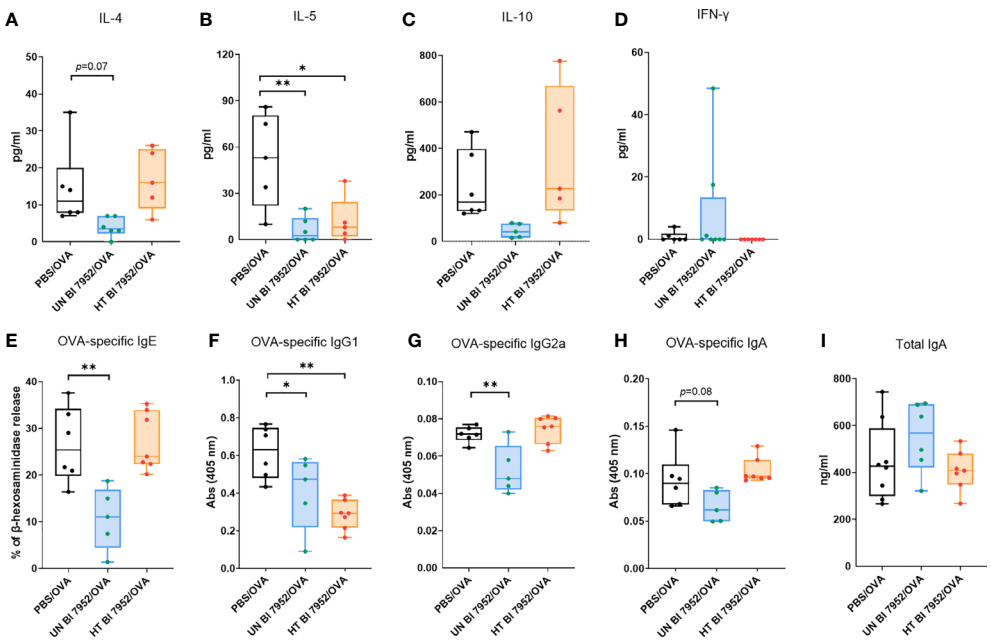

FIGURE 5 | Intranasal administration of untreated and heat-treated Bl 7952 differently attenuates the OVA-induced cellular and humoral immune responses. Effect of PBS (PBS/OVA, black box), untreated Bl 7952 (UN Bl 7952/OVA, blue box) and heat-treated Bl 7952 (HT Bl 7952/OVA, orange box) strain on cytokine production was determined in supernatants of OVA-stimulated splenocytes isolated from bacteria or PBS pre-treated and OVA-sensitized and challenged mice. **(A)** IL-4, **(B)** IL-5, **(C)** IL-10 and **(D)** IFN-γ cytokines are expressed as pg/ml. Levels of OVA-specific **(E)** IgE as % of β-hexosaminidase release by RBL assay, **(F)** IgG1, **(G)** IgG2a, **(H)** IgA and **(I)** total IgA antibodies were measured in sera of experimental mice. Values are expressed as boxplot with mean and min to max value bars; each dot represents a single mouse. Significant difference between PBS/OVA and bifidobacteria-treated/OVA experimental groups was calculated by one-way ANOVA with Dunnett's multiple comparison test *p <.0.05. **p < 0.01.

when compared to OVA/PBS group (**Figure 6K**). Contrary, when the plate was coated with dry mass of heat-treated Bl 7952, level of specific IgA antibodies in BAL did not differ between studied groups and remained low.

DISCUSSION

In the current study we compared four *Bifidobacterium* strains in order to evaluate the impact of heat inactivation (treatment) on their physical and immunomodulatory properties. We selected the strain *Bifidobacterium longum* ssp. *longum* CCM 7952 (Bl 7952) to investigate *in vivo* the influence of its viability status on the prevention and modulation of the allergic immune response to OVA in a mouse model of allergy.

The classical definition of probiotics states that bacteria must be alive in order to be beneficial for human organism, but recent research suggests that inactivated bacteria are able to maintain the desired beneficial properties (33, 34). The use of inactivated microorganisms expands the possibility of using probiotics in the elderly, neonates, or people with compromised immune system (35, 36). Here, we have shown that mild heat treatment inactivates the bacteria without disruption of the cells, which Taddese et al. considered to be the most important factor in choosing the optimal inactivation method (37). Other inactivation methods such as chemical treatment (38), ultraviolet rays (39), and sonication (40) may be associated with bacterial cell wall damage. Nevertheless, heat treatment induced changes in the structure of the cell wall of all bifidobacterial species tested, resulting in a more irregular and porous appearance compared to untreated bacteria as documented by electron microscopy.

Our subsequent studies of cell size and zeta potential of *Bifidobacterium* show significant physical differences after heat treatment. Similar changes were reported by Baatout at al. who observed that increased temperature leads to an increase in cell size of *E. coli* and, on the contrary, to a decrease in cell size of *Shewanella oneidensis* (41). Such changes may lead to alteration of surface structure and membrane permeability of bacteria. Some proteins might undergo structural changes, denaturation or aggregation, and thus lose their active structure (42). Consequently, important epitopes recognized by the immune system may be hidden or revealed. Finally, the use of high temperatures can lead to the loss of D-alanine in teichoic acids (43), resulting in chelation of magnesium ions in the cell wall, thus altering the surface charge of bacteria.

Interestingly, we have shown that the changes in size of the bacterial strains upon thermal treatment have no significant effect on the degree of their engulfment and transfer into immune cells, in contrast to the changes in zeta potential. The

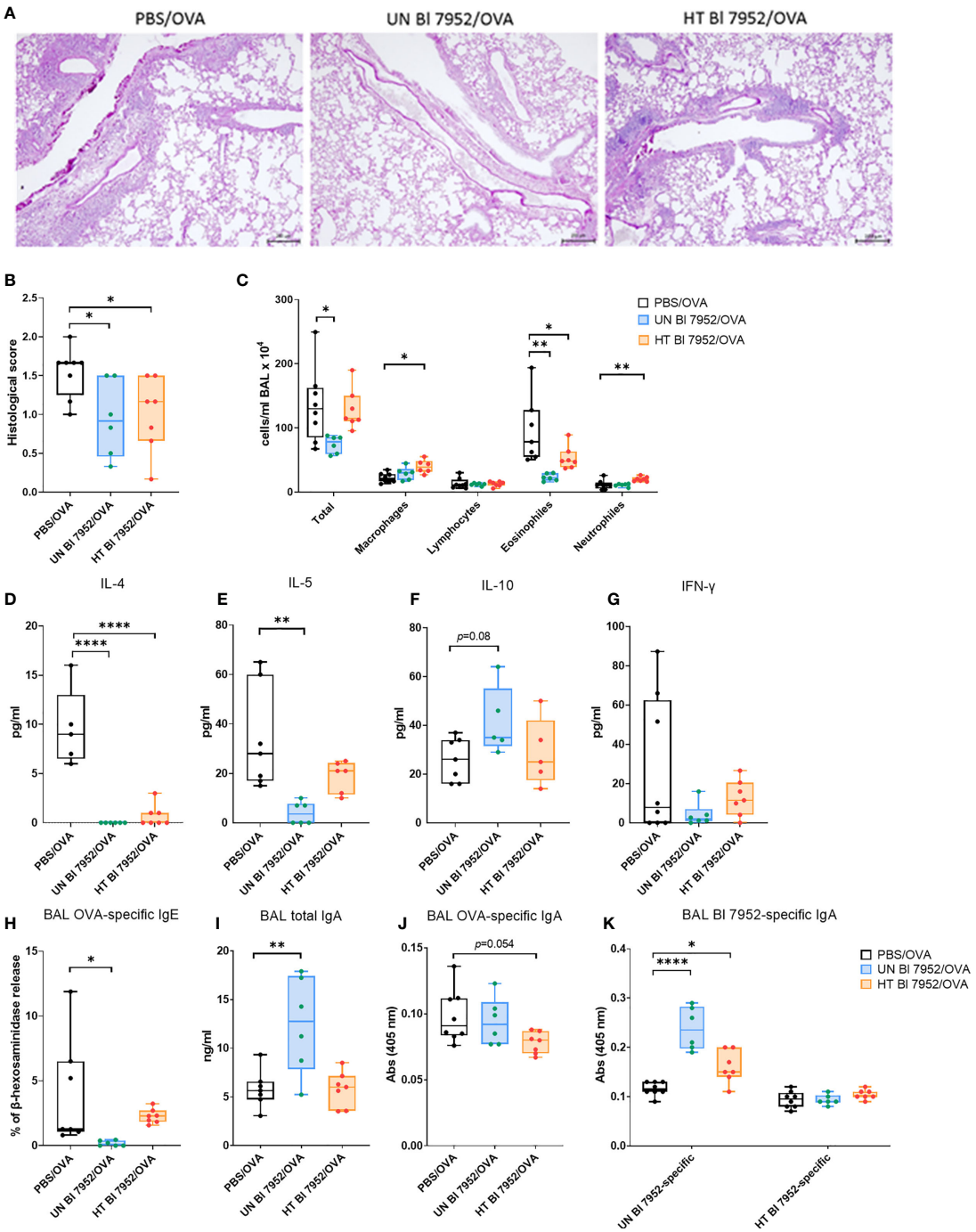

FIGURE 6 | Intranasal administration of untreated and heat-treated BI 7952 differently reduces allergic inflammation in lungs of OVA-sensitized mice **(A)** Representative tissue section Periodic Acid-Schiff staining of the lungs from OVA-sensitized and challenged mice pre-treated with PBS (PBS/OVA, black box), untreated BI 7952 (UN BI 7952/OVA, blue box) and heat-treated BI 7952 (HT BI 7952/OVA, orange box) strain. Scale (200 μm) applies to all presented images, magnification ×100. **(B)** Inflammatory score of the lungs was determined by histopathological analysis. **(C)** Total and differential cell counts were determined in bronchoalveolar lavage (BAL). Levels of spontaneous cytokine production from BAL fluid **(D)** IL-4, **(E)** IL-5, **(F)** IL-10 and **(G)** IFN-γ were expressed as pg/ml. **(H)** OVA-specific IgE was determined in BAL fluid as % of β-hexosaminidase release assay. **(I)** Total IgA in BAL fluid was measured by ELISA and expressed as ng/ml. **(J)** OVA-specific IgA and **(K)** untreated or heat-treated BI 7952-specific IgA were determined in BAL fluid as optical density (λ = 405 nm). Results are shown as boxplot means and min to max value bars; each dot represents a single mouse. Significant difference between PBS/OVA and bifidobacteria-treated/OVA experimental groups was calculated by one-way ANOVA with Dunnett's multiple comparison test *p <.0.05. **p < 0.01, ****p < 0.0001.

surface electric charge of the two out of the four tested strains dropped significantly after thermal inactivation compared to untreated bacteria. At the same time, we observed marked decrease in their engulfment by epithelial cell line and, as a possible consequence, a decrease in bacterial engulfment by immune cells. Our results are consistent with a study by Galdeano et al. who conducted similar research with live and heat-treated *Lactobacillus* strains. After feeding the bacteria to mice they showed that live bacteria have higher impact on immune cells and live and inactivated bacteria may have different affinity to bind to immune cells (44).

Usually, the probiotic bacteria are administered *via* the oral route. However, recent studies indicate the niche-specific effect of nasal administration of probiotics (10, 11) and the interaction with the immune system and the epithelium of the upper and lower airways. Therefore, we investigated the immunomodulatory properties of tested bacteria on the mouse lung epithelial cell line (TC-1). Interestingly, UN and HT bacteria elicit different levels of IL-6 and MCP-1. These cytokines are involved in macrophage recruitment and activation, which are associated with regulation of the airway inflammation (45). In contrast, bacteria-stimulated dendritic cells showed no changes in maturation and cytokine induction between UN and HT bacteria. It is well established that high IL-12 production by DC, matured by microbial stimuli, leads to Th1 polarization (46) and conversely, high IL-10 production leads to Treg or Tr1 polarization (47). In agreement with Weiss et al., our data showed that analyzed bifidobacteria strains induce low levels of IL-12p70 cytokine and high levels of IL-10 when added to BMDCs. The ability to induce cytokines appears to be specific to each bifidobacterial strain, but is not dependent on viability status, with the exception of strain Ban 218. These results prompted us to ask about differences in the activation of pattern recognition receptors by UN and HT bifidobacterial strains.

We showed that all tested bifidobacterial strains strongly activate the TLR2 receptor. Activation of this receptor is desirable when evaluating bacteria with probiotic properties, as TLR2 activation has been associated with the induction of immunomodulatory and anti-inflammatory effects (48). In addition, it is well documented that TLR2 ligands present on live or killed bacteria in bacterial extracts or surface components, are able to inhibit the allergic response (49, 50). Interestingly, we observed a significant increase in the activation of TLR2 after heat treatment of most tested *Bifidobacterium* strains. This could be due to changes in the structure of the cell wall that facilitate the access of the binding molecule to the receptor (51).

We further focused on the effect of thermal inactivation on the ability of tested *Bifidobacterium* strains to downregulate the cellular recall immune response to allergen in splenocytes from mice sensitized with OVA. Our data show that all strains suppressed the production of the pro-allergic cytokines IL-4, IL-5, and IL-13, but only strain Bl 7952 did not upregulate the pro-inflammatory IFN-γ. Next, we observed that although the general profile of immunomodulation was similar between both UN and HT bacteria, significant differences emerged for some strains depending on viability status. In this context, Lopez et al. found that both live and UV-inactivated *Lactobacillus rhamnosus* GG induced the same reduction in the pro-inflammatory cytokine IL-8 upon flagellin induction in Caco-2 cells, but through activation of different signaling pathways (20). Interestingly, inactivation with subsequent loss of viability and cell lysis may induce further and more complex immunomodulation than expected (52).

In our previous studies, we have shown that neonatal mono-colonization with Bl 7952 reduces allergic sensitization, likely through activation of regulatory responses *via* TLR2, MyD88, and MAPK signaling pathways (30). In addition, Bl 7952 administration also protects epithelial barrier integrity during intestinal inflammation (53). Based on these studies and results from *in vitro* experiments we selected Bl 7952 to test its ability to prevent the development of allergic inflammation in a mouse model of airway allergy. Intranasal administration of strain Bl 7952 prior to allergen sensitization and challenge significantly suppressed the allergic immune response in viability status-dependent manner. We showed that intranasal administration of UN bacteria was able to significantly decrease the level of allergen-specific IgE, IgG1, and IgG2a antibodies in sera. On the other hand, heat-treated Bl 7952 markedly reduced only the level of OVA-specific IgG1. Decrease in allergic sensitization should be associated with significant decrease of allergen-specific antibody; however studies have shown that the beneficial effect of probiotic treatment may also occur in the absence of specific antibodies reduction (54).

At the local level, we observed that Bl 7952, depending on viability, significantly decreased the number of pulmonary eosinophils, with or without an increase in neutrophil and macrophage numbers. These results are consistent with the properties of *B. breve* MRx0004, whose therapeutic and prophylactic administration reduced the level of eosinophils and increased the number of macrophages in the mouse asthma model (8). At the same time, we observed a significant reduction in IL-4 and IL-5 in BAL of both Bl 7952 treated groups. IL-5 reduction in BAL fluids was previously shown to correspond with reduced lung inflammation in a mouse model of allergic polysensitization (32). Surprisingly, we observed that UN bacteria have a different ability to induce IL-10 compared to HT bacteria in BAL. IL-10 has a potent immunosuppressive capacity and essentially contributes to allergen tolerance (55).

Along with decreased Th-2 cytokine levels, we observed also a decrease in OVA-specific IgE in BAL both UN and HT Bl 7952-treated groups. This was accompanied by an increase in total IgA in the UN Bl 7952-treated group. Surprisingly, there was little difference in OVA-specific IgA in BAL among the groups. This prompted us to test the UN and HT bacteria-specific IgA antibodies. Interestingly, we observed a significant increase in the level of bacteria-specific IgA antibodies in BAL of mice treated with UN Bl 7952, while we did not see any bacteria-specific IgA production in HT Bl 7952 treated group.

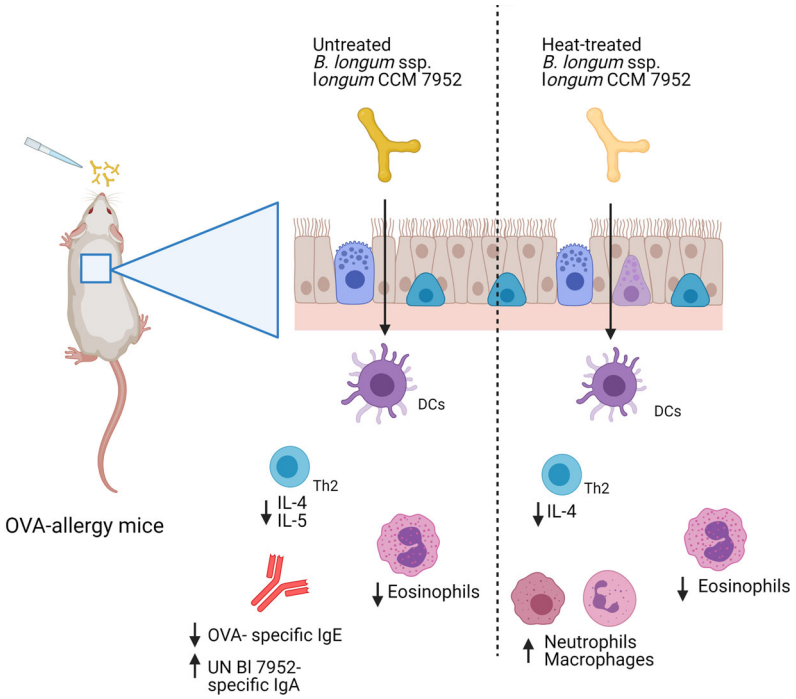

FIGURE 7 | Graphical representation of results. Intranasal administration of Bl 7952 to OVA-sensitized mice suppresses allergic inflammation. However, thermal inactivation of Bl 7952 modifies the immunomodulatory properties of this strain (Created with BioRender.com).

These data suggest that the heat-sensitive conformational epitopes of cell wall antigens specific for induction of IgA response were altered. Secretory IgA plays a critical role in tolerance induction and maintenance of mucosal homeostasis in the host by opsonizing and neutralizing pathogens and toxins, resulting in immune exclusion and reducing the antigenic burden on the mucosal immune system. Its protective role has also been widely documented in the management of allergic immune response (9, 56–58). Concomitantly, the decrease in IgA level has been associated with a higher likelihood of developing allergies or asthma (59–61). Nevertheless, not all bacterial strains have the ability to stimulate IgA production. Li et al. showed that only three out of five tested probiotic strains of *L. casei* induced IgA production in mice with house dust mite-induced asthma, indicating that the activity to stimulate IgA production is strain-dependent (9).

Collectively, we have shown that heat treatment of strain Bl 7952 did result in a decreased ability of this bacterium to prevent and modulate the allergic immune response to ovalbumin in a mouse model of allergy (**Figure 7**). These results were surprising given the observed moderate effect of heat treatment on the immunomodulatory properties of the bacterium in *in vitro* assays. Our results caution against the extrapolating *in vitro* results obtained with inactivated bacteria to the general biological effect of bacteria, and advocated testing the activity of both live and inactivated bacteria in *in vivo* experimental animal models. Further research is warranted to elucidate the immunomodulatory molecules isolated from bacterial strains and their potential use in the prevention of airway allergy diseases.

DATA AVAILABILITY STATEMENT

The raw data supporting the conclusions of this article will be made available by the authors, without undue reservation.

ETHICS STATEMENT

The animal study was reviewed and approved by Institute of Microbiology, The Czech Academy of Sciences (no. 91/2019).

AUTHOR CONTRIBUTIONS

MP prepared the bacteria, performed the *in vitro* experiments, cultivated and stimulated the SPL and TC-1 cell lines, measured the OVA-specific antibody, analyzed the results and drafted the manuscript. MS and DS designed the *in vivo* experiments on mice. DS performed the *in vivo* experiments, histology analysis and BALF cell count, drafted the manuscript. AR performed the DLS and ELS measurement, engulfment and transfer research. PH cultivate the SPL and HEK cell line, KP performed the SPL stimulation, TS performed the RBL test and Bl 7952-specific IgA

ELISA. MS coordinate and conceived the study, wrote the manuscript. SG was a supervisor of MP and KP, designed, coordinate and conceived of the study, wrote the manuscript. All authors contributed to the article and approved the submitted version.

FUNDING

This work was supported by grant co-founded by the National Science Centre of Poland under grant decision number UMO-2017/26/E/NZ7/01202; by the Polish National Agency for Academic Exchange under grant decision number PPN/BIL/2018/1/00005, by grants 19-02261S and 21-19640M of the Czech Science Foundation and 8JPL19046 of the Ministry of Education, Youth and Sports of the Czech Republic. The group of MS is supported by EMBO Installation Grant.

ACKNOWLEDGMENTS

We would like to thank Marek Drab for performing SEM image of bacteria and Jaroslava Valterová and Šárka Maisnerová for excellent technical assistance.

SUPPLEMENTARY MATERIAL

The Supplementary Material for this article can be found online at: https://www.frontiersin.org/articles/10.3389/fimmu.2021.707728/full#supplementary-material

REFERENCES

1. Loh W, Tang MLK. The Epidemiology of Food Allergy in the Global Context. *Int J Environ Res Public Health* (2018) 15(9):2043. doi: 10.3390/ijerph15092043
2. https://www.who.int/en/news-room/fact-sheets/detail/asthma, date: 11.03.2021, 12 am.
3. Jordakieva G, Jensen-Jarolim E. The Impact of Allergen Exposure and Specific Immunotherapy on Circulating Blood Cells in Allergic Rhinitis. *World Allergy Organ J* (2018) 11:1–13. doi: 10.1186/s40413-018-0197-0
4. Roan F, Obata-Ninomiya K, Ziegler SF. Epithelial Cell–Derived Cytokines: More Than Just Signaling the Alarm. *J Clin Invest* (2019) 129:1441–51. doi: 10.1172/JCI124606
5. Chan BCL, Lam CWK, Tam LS, Wong CK. IL33: Roles in Allergic Inflammation and Therapeutic Perspectives. *Front Immunol* (2019) 10:364. doi: 10.3389/fimmu.2019.00364
6. Halim TYF, Steer CA, Mathä L, Gold MJ, Martinez-Gonzalez I, McNagny KM, et al. Group 2 Innate Lymphoid Cells are Critical for the Initiation of Adaptive T Helper 2 Cell-Mediated Allergic Lung Inflammation. *Immunity* (2014) 40:425–35. doi: 10.1016/j.immuni.2014.01.011
7. Tashiro H, Shore SA. The Gut Microbiome and Ozone-Induced Airway Hyperresponsiveness: Mechanisms and Therapeutic Prospects. *Am J Respir Cell Mol Biol* (2020) 64(3):1–46. doi: 10.1165/rcmb.2020-0288tr
8. Raftis EJ, Delday MI, Cowie P, McCluskey SM, Singh MD, Ettorre A, et al. Bifidobacterium Breve MRx0004 Protects Against Airway Inflammation in a Severe Asthma Model by Suppressing Both Neutrophil and Eosinophil Lung Infiltration. *Sci Rep* (2018) 8:1–13. doi: 10.1038/s41598-018-30448-z
9. Li L, Fang Z, Lee YK, Zhao J, Zhang H, Lu W, et al. Prophylactic Effects of Oral Administration of: Lactobacillus Casei on House Dust Mite-Induced Asthma in Mice. *Food Funct* (2020) 11:9272–84. doi: 10.1039/d0fo01363c
10. Pellaton C, Nutten S, Thierry AC, Boudousquié C, Barbier N, Blanchard C, et al. Intragastric and Intranasal Administration of Lactobacillus Paracasei NCC2461 Modulates Allergic Airway Inflammation in Mice. *Int J Inflam* (2012) 2012:1–8. doi: 10.1155/2012/686739
11. Spacova I, Petrova MI, Fremau A, Pollaris L, Vanoirbeek J, Ceuppens JL, et al. Intranasal Administration of Probiotic Lactobacillus Rhamnosus GG Prevents Birch Pollen-Induced Allergic Asthma in a Murine Model. *Allergy Eur J Allergy Clin Immunol* (2019) 74:100–10. doi: 10.1111/all.13502
12. De Boeck I, Spacova I, Vanderveken OM, Lebeer S. Lactic Acid Bacteria as Probiotics for the Nose? *Microb Biotechnol* (2021) 0:1–11. doi: 10.1111/1751-7915.13759
13. Yelin I, Flett KB, Merakou C, Mehrotra P, Stam J, Snesrud E, et al. Genomic and Epidemiological Evidence of Bacterial Transmission From Probiotic Capsule to Blood in ICU Patients. *Nat Med* (2019) 25:1728–32. doi: 10.1038/s41591-019-0626-9
14. Avcin SL, Pokorn M, Kitanovski L, Premru MM, Jazbec J. Bifidobacterium Breve Sepsis in Child With High-Risk Acute Lymphoblastic Leukemia. *Emerg Infect Dis* (2015) 21:1674–5. doi: 10.3201/eid2109.150097
15. Esaiassen E, Hjerde E, Cavanagh JP, Simonsen GS, Klingenberg C. Bifidobacterium Bacteremia: Clinical Characteristics and a Genomic Approach to Assess Pathogenicity. *J Clin Microbiol* (2017) 55:2234–48. doi: 10.1128/JCM.00150-17
16. Williams N. Probiotics. *Am J Heal Syst Pharm* (2010) 67:449–58. doi: 10.2146/ajhp090168
17. Hill C, Guarner F, Reid G, Gibson GR, Merenstein DJ, Pot B, et al. The International Scientific Association for Probiotics and Prebiotics Consensus Statement on the Scope and Appropriate Use of the Term Probiotic. *Nat Rev Gastroenterol Hepatol* (2014) 11:506–14. doi: 10.1038/nrgastro.2014.66
18. Aguilar-Toalá JE, Garcia-Varela R, Garcia HS, Mata-Haro V, González-Córdova AF, Vallejo-Cordoba B, et al. Postbiotics: An Evolving Term Within the Functional Foods Field. *Trends Food Sci Technol* (2018) 75:105–14. doi: 10.1016/J.TIFS.2018.03.009
19. Kumpu M, Kekkonen RA, Korpela R, Tynkkynen S, Järvenpää S, Kautiainen H, et al. Effect of Live and Inactivated Lactobacillus Rhamnosus GG on Experimentally Induced Rhinovirus Colds: Randomised, Double Blind, Placebo-Controlled Pilot Trial. *Benef Microbes* (2015) 6:631–9. doi: 10.3920/BM2014.0164
20. Lopez M, Li N, Kataria J, Russell M, Neu J. Live and Ultraviolet-Inactivated Lactobacillus Rhamnosus GG Decrease Flagellin-Induced Interleukin-8 Production in Caco-2 Cells. *J Nutr* (2008) 138:2264–8. doi: 10.3945/jn.108.093658
21. Pyclik M, Srutkova D, Schwarzer M, Górska S. Bifidobacteria Cell Wall-Derived Exo-Polysaccharides, Lipoteichoic Acids, Peptidoglycans, Polar Lipids and Proteins – Their Chemical Structure and Biological Attributes. *Int J Biol Macromol* (2020) 147:333–49. doi: 10.1016/j.ijbiomac.2019.12.227
22. Zhu L, Shimada T, Chen R, Lu M, Zhang Q, Lu W, et al. Effects of Lysed Enterococcus Faecalis FK-23 on Experimental Allergic Rhinitis in a Murine Model. *J BioMed Res* (2012) 26:226–34. doi: 10.7555/JBR.26.20120023
23. Lim LH, Li HY, Huang CH, Lee BW, Lee YK, Chua KY. The Effects of Heat-Killed Wild-Type Lactobacillus Casei Shirota on Allergic Immune Responses in an Allergy Mouse Model. *Int Arch Allergy Immunol* (2009) 148:297–304. doi: 10.1159/000170383
24. Piqué N, Berlanga M, Miñana-Galbis D. Health Benefits of Heat-Killed (Tyndallized) Probiotics: An Overview. *Int J Mol Sci* (2019) 20(10):2534. doi: 10.3390/ijms20102534
25. Drinić M, Wagner A, Sarate P, Zwicker C, Korb E, Loupal G, et al. Toxoplasma Gondii Tachyzoite-Extract Acts as a Potent Immunomodulator Against Allergic Sensitization and Airway Inflammation. *Sci Rep* (2017) 7:1–12. doi: 10.1038/s41598-017-15663-4
26. Sarate PJ, Srutkova D, Geissler N, Schwarzer M, Schabussova I, Inic-Kanada A, et al. Pre- and Neonatal Imprinting on Immunological Homeostasis and Epithelial Barrier Integrity by Escherichia Coli Nissle 1917 Prevents Allergic Poly-Sensitization in Mice. *Front Immunol* (2021) 11:612775. doi: 10.3389/fimmu.2020.612775

27. Schwarzer M, Hermanova P, Srutkova D, Golias J, Hudcovic T, Zwicker C, et al. Germ-Free Mice Exhibit Mast Cells With Impaired Functionality and Gut Homing and do Not Develop Food Allergy. *Front Immunol* (2019) 10:205. doi: 10.3389/fimmu.2019.00205
28. Górska S, Schwarzer M, Srutkova D, Hermanova P, Brzozowska E, Kozakova H, et al. Polysaccharides L900/2 and L900/3 Isolated From Lactobacillus Rhamnosus LOCK 0900 Modulate Allergic Sensitization to Ovalbumin in a Mouse Model. *Microb Biotechnol* (2017) 10:586–93. doi: 10.1111/1751-7915.12606
29. Koba M, Śmietana M, Brzozowska E, Ǵorska S, Janik M, Mikulic P, et al. Bacteriophage Adhesin-Coated Long-Period Grating-Based Sensor: Bacteria Detection Specificity. *J Light Technol* (2016) 34:4531–6. doi: 10.1109/JLT.2016.2532466
30. Schwarzer M, Srutkova D, Schabussova I, Hudcovic T, Akgün J, Wiedermann U, et al. Neonatal Colonization of Germ-Free Mice With Bifidobacterium Longum Prevents Allergic Sensitization to Major Birch Pollen Allergen Bet V 1. *Vaccine* (2013) 31:5405–12. doi: 10.1016/j.vaccine.2013.09.014
31. Abdel-Gadir A, Stephen-Victor E, Gerber GK, Noval Rivas M, Wang S, Harb H, et al. Microbiota Therapy Acts via a Regulatory T Cell Myd88/Rorγt Pathway to Suppress Food Allergy. *Nat Med* (2019) 25:1164–74. doi: 10.1038/s41591-019-0461-z
32. Schabussova I, Hufnagl K, Wild C, Nutten S, Zuercher AW, Mercenier A, et al. Distinctive Anti-Allergy Properties of Two Probiotic Bacterial Strains in a Mouse Model of Allergic Poly-Sensitization. *Vaccine* (2011) 29:1981–90. doi: 10.1016/j.vaccine.2010.12.101
33. de Almada CN, Almada CN, Martinez RCR, Sant'Ana AS. Paraprobiotics: Evidences on Their Ability to Modify Biological Responses, Inactivation Methods and Perspectives on Their Application in Foods. *Trends Food Sci Technol* (2016) 58:96–114. doi: 10.1016/J.TIFS.2016.09.011
34. Zendeboodi F, Khorshidian N, Mortazavian AM, da Cruz AG. Probiotic: Conceptualization From a New Approach. *Curr Opin Food Sci* (2020) 32:103–23. doi: 10.1016/j.cofs.2020.03.009
35. Doron S, Snydman DR. Risk and Safety of Probiotics. *Clin Infect Dis* (2015) 60:129–34. doi: 10.1093/cid/civ085
36. Bertelli C, Pillonel T, Torregrossa A, Prod'hom G, Julie Fischer C, Greub G, et al. Bifidobacterium Longum Bacteremia in Preterm Infants Receiving Probiotics. *Clin Infect Dis* (2015) 60:924–7. doi: 10.1093/cid/ciu946
37. Taddese R, Belzer C, Aalvink S, de Jonge MI Nagtegaal ID, Dutilh BE, et al. Bacterial Zombies And Ghosts: Production Of Inactivated Gram-Positive And Gram-Negative Species With Preserved Cellular Morphology And Cytoplasmic Content. *bioRxiv* (2018) 458158. doi: 10.1101/458158
38. Otzen DE, Sehgal P, Nesgaard LW. Alternative Membrane Protein Conformations in Alcohols. *Biochemistry* (2007) 46:4348–59. doi: 10.1021/bi700091r
39. Tomb RM, White TA, Coia JE, Anderson JG, MacGregor SJ, Maclean M. Review of the Comparative Susceptibility of Microbial Species to Photoinactivation Using 380-480 Nm Violet-Blue Light. *Photochem Photobiol* (2018) 94:445–58. doi: 10.1111/php.12883
40. Piyasena P, Mohareb E, McKellar RC. Inactivation of Microbes Using Ultrasound: A Review. *Int J Food Microbiol* (2003) 87:207–16. doi: 10.1016/S0168-1605(03)00075-8
41. Baatout S, De Boever P, Mergeay M. Temperature-Induced Changes in Bacterial Physiology as Determined by Flow Cytometry. *Ann Microbiol* (2005) 55:73–80.
42. Laskowska E, Bohdanowicz J, Kuczyńska-Wiśnik D, Matuszewska E, Kędzierska S, Taylor A. Aggregation of Heat-Shock-Denatured, Endogenous Proteins and Distribution of the IbpA/B and Fda Marker-Proteins in Escherichia Coli WT and Grpe280 Cells. *Microbiology* (2004) 150:247–59. doi: 10.1099/mic.0.26470-0
43. Mackey B. Injured Bacteria. In: M Lund, TC Baird-Parker, GW Gould, editors. *The Microbiological Safety, and Quality of Food*. Gaithersburg, Md.: Aspen Publisher (2000). p. 315–41.
44. Galdeano CM, Perdigón G. Role of Viability of Probiotic Strains in Their Persistence in the Gut and in Mucosal Immune Stimulation. *J Appl Microbiol* (2004) 97:673–81. doi: 10.1111/j.1365-2672.2004.02353.x
45. Liu C, Zhang X, Xiang Y, Qu X, Liu H, Liu C, et al. Role of Epithelial Chemokines in the Pathogenesis of Airway Inflammation in Asthma (Review). *Mol Med Rep* (2018) 17:6935–41. doi: 10.3892/mmr.2018.8739
46. Weiss G, Christensen HR, Zeuthen LH, Vogensen FK, Jakobsen M, Frøkiær H. Lactobacilli and Bifidobacteria Induce Differential Interferon-β Profiles in Dendritic Cells. *Cytokine* (2011) 56:520–30. doi: 10.1016/j.cyto.2011.07.024
47. Schülke S. Induction of Interleukin-10 Producing Dendritic Cells as a Tool to Suppress Allergen-Specific T Helper 2 Responses. *Front Immunol* (2018) 9:455. doi: 10.3389/fimmu.2018.00455
48. Bermúdez-Brito M, Plaza-Díaz J, Muñoz-Quezada S, Gómez-Llorente C, Gil A. Probiotic Mechanisms of Action. *Ann Nutr Metab* (2012) 61:160–74. doi: 10.1159/000342079
49. Fuchs B, Braun A. Modulation of Asthma and Allergy by Addressing Toll-Like Receptor 2. *J Occup Med Toxicol* (2008) 3:2–5. doi: 10.1186/1745-6673-3-S1-S5
50. Taylor RC, Richmond P, Upham JW. Toll-Like Receptor 2 Ligands Inhibit T H2 Responses to Mite Allergen. *J Allergy Clin Immunol* (2006) 117:1148–54. doi: 10.1016/j.jaci.2006.02.014
51. Oliveira-Nascimento L, Massari P, Wetzler LM. The Role of TLR2 Ininfection and Immunity. *Front Immunol* (2012) 3:79. doi: 10.3389/fimmu.2012.00079
52. Taverniti V, Guglielmetti S. The Immunomodulatory Properties of Probiotic Microorganisms Beyond Their Viability (Ghost Probiotics: Proposal of Paraprobiotic Concept). *Genes Nutr* (2011) 6:261–74. doi: 10.1007/s12263-011-0218-x
53. Srutkova D, Schwarzer M, Hudcovic T, Zakostelska Z, Drab V, Spanova A, et al. Bifidobacterium Longum CCM 7952 Promotes Epithelial Barrier Function and Prevents Acute DSS-Induced Colitis in Strictly Strain-Specific Manner. *PloS One* (2015) 10(7):134050. doi: 10.1371/journal.pone.0134050
54. Spacova I, Van Beeck W, Seys S, Devos F, Vanoirbeek J, Vanderleyden J, et al. Lactobacillus Rhamnosus Probiotic Prevents Airway Function Deterioration and Promotes Gut Microbiome Resilience in a Murine Asthma Model. *Gut Microbes* (2020) 11:1729–44. doi: 10.1080/19490976.2020.1766345
55. Akdis CA, Akdis M. Mechanisms of Immune Tolerance to Allergens: Role of IL-10 and Tregs. *J Clin Invest* (2014) 124:4678–80. doi: 10.1172/JCI78891
56. Corthésy B. Multi-Faceted Functions of Secretory IgA at Mucosal Surfaces. *Front Immunol* (2013) 4:185. doi: 10.3389/fimmu.2013.00185
57. Smeekens JM, Johnson-Weaver BT, Hinton AL, Azcarate-Peril MA, Moran TP, Immormino RM, et al. Fecal IgA, Antigen Absorption, and Gut Microbiome Composition Are Associated With Food Antigen Sensitization in Genetically Susceptible Mice. *Front Immunol* (2021) 11:599637. doi: 10.3389/fimmu.2020.599637
58. Gloudemans AK, Lambrecht BN, Smits HH. Potential of Immunoglobulin A to Prevent Allergic Asthma Information. *Clin Dev Immunol* (2013) 2013:542091. doi: 10.1155/2013/542091
59. Kim WJ, Choi IS, Kim CS, Lee JH, Kang HW. Relationship Between Serum IgA Level and Allergy/Asthma. *Korean J Intern Med* (2017) 32:137–45. doi: 10.3904/kjim.2014.160
60. Dzidic M, Abrahamsson TR, Artacho A, Björkstén B, Collado MC, Mira A, et al. Aberrant IgA Responses to the Gut Microbiota During Infancy Precede Asthma and Allergy Development. *J Allergy Clin Immunol* (2017) 139:1017–1025.e14. doi: 10.1016/j.jaci.2016.06.047
61. Frossard CP, Hauser C, Eigenmann PA. Antigen-Specific Secretory IgA Antibodies in the Gut are Decreased in a Mouse Model of Food Allergy. *J Allergy Clin Immunol* (2004) 114:377–82. doi: 10.1016/j.jaci.2004.03.040

Conflict of Interest: The authors declare that the research was conducted in the absence of any commercial or financial relationships that could be construed as a potential conflict of interest.

frontiers in Microbiology

REVIEW
published: 09 August 2021
doi: 10.3389/fmicb.2021.689958

Utilizing Probiotics for the Prevention and Treatment of Gastrointestinal Diseases

Erin Milner[1,2], Benjamin Stevens[1], Martino An[1], Victoria Lam[1], Michael Ainsworth[1], Preston Dihle[1], Jocelyn Stearns[1], Andrew Dombrowski[1], Daniel Rego[1] and Katharine Segars[1]*

[1] Department of Chemistry and Life Science, United States Military Academy, West Point, NY, United States, [2] Department of Medicine, Uniformed Services University of the Health Sciences, Bethesda, MD, United States

Probiotics are heavily advertised to promote a healthy gastrointestinal tract and boost the immune system. This review article summarizes the history and diversity of probiotics, outlines conventional *in vitro* assays and *in vivo* models, assesses the pharmacologic effects of probiotic and pharmaceutical co-administration, and the broad impact of clinical probiotic utilization for gastrointestinal disease indications.

Keywords: probiotics, probiotic cultures, probiotic microbiology, food microbiology, probiotic pharmacology, probiotic treatment of gastrointestinal disease

OPEN ACCESS

Edited by:
Irma Schabussova, Medical University Vienna, Austria

Reviewed by:
Robert J. Moore, RMIT University, Australia
Carolina Maldonado-Galdeano, CONICET Centro de Referencia para Lactobacilos (CERELA), Argentina

****Correspondence:***
Erin Milner
erin.milner@westpoint.edu

Specialty section:
This article was submitted to Food Microbiology, a section of the journal Frontiers in Microbiology

Received: *01 April 2021*
Accepted: *05 July 2021*
Published: *09 August 2021*

Citation:
Milner E, Stevens B, An M, Lam V, Ainsworth M, Dihle P, Stearns J, Dombrowski A, Rego D and Segars K (2021) Utilizing Probiotics for the Prevention and Treatment of Gastrointestinal Diseases. Front. Microbiol. 12:689958. doi: 10.3389/fmicb.2021.689958

INTRODUCTION

Probiotic supplement utilization has been steadily increasing based upon the perceived health benefits associated with replenishing the gut microbiome (Saxelin, 2008; Vanderhoof and Young, 2008). A variety of probiotic strains are undergoing clinical trials to treat complex gastrointestinal and inflammatory diseases, but the traditional drug development paradigm associated with preclinical and clinical studies is lacking. In addition, the myriad of probiotic strains and formulations, coupled with a lack of regulatory and quality control associated with commercially available products, has confounded their utilization in patients. Considering these issues, this manuscript focuses on highlighting the history and taxonomy of select probiotics, outlining the data associated with preclinical *in vitro* assays and *in vivo* animal models, and evidence for clinical efficacy and safety for several gastrointestinal disease indications.

HISTORY AND TAXONOMY OF SELECT PROBIOTICS

Defining Probiotics

Understanding the complex relationship of microbes within the host gastrointestinal (GI) system has long been an elusive and evolving narrative. While Hippocrates ruminated that "death sits in the bowels," Nobel Laureate Elie Metchnikoff, who studied immune response, indicated "*lactobacilli* as probiotics ('probios,' conducive to life of the host as opposed to antibiotics)" and advocated for the consumption of lactic acid-producing bacteria (Gasbarrini et al., 2016). The World Health Organization (WHO) and the Food and Agriculture Organization (FAO) of the United States adopted a broader definition of probiotic as "live microorganisms which when administered in adequate amounts confer a health benefit on the host organism" (Joint Food and Agriculture Organization World Health Organization Working Group, 2002).

History of Probiotics

Historical references that date back to 7000 BCE in the Neolithic villages of China and 5000 BCE in Mesopotamia often mention the use of food fermentation techniques (Gasbarrini et al., 2016). Fermentation remained a primary beneficial use of microbes until the late 1800s with the modern concept of the microbiome, which continued to be developed into the early 1900s (Farré-Maduell and Casals-Pascual, 2019). Conducting research at the Pasteur Institute, Metchnikoff studied the benefits of microbes on human health and proposed a theory that, "the dependence of the intestinal microbes on the food makes it possible to adopt measures to modify the flora in our bodies and to replace the harmful microbes by useful microbes" (Metchnikoff, 1907; Gasbarrini et al., 2016). Recognizing health benefits from Bulgarian yogurt and fermented foods, his approach to microbial-treated nutrition revolutionized the dairy industry and promoted a new food industry (Gasbarrini et al., 2016; Farré-Maduell and Casals-Pascual, 2019). A contemporary of Metchnikoff, Dr. Alfred Nissle is credited with identifying *Escherichia coli* strain Nissle 1917 from a soldier who had shown resistance to diarrheal diseases afflicting other soldiers. Dr. Nissle patented the discovery with the trade name "Mutaflor," a probiotic product that remains currently available (Sonnenborn, 2016; Farré-Maduell and Casals-Pascual, 2019). The probiotic industry continues to flourish due to high consumer demand and the United States market may encompass $77.9 billion by 2025 (Grandview Research, 2019). Probiotics are heavily marketed as part of a preventative healthcare diet, which may appeal to health-oriented consumers. Currently the industry is developing new probiotic supplements such as drops, tablets, and capsules for the rapidly expanding market (Probiotics Market Size Share and Trends Analysis Report By Product, 2019).

Diversity of Probiotic Strains

The evolving history of human interactions with beneficial microbes has generated a diverse panel of probiotic organisms currently marketed for public consumption. Available probiotics encompass a range of microorganisms as outlined in **Table 1**, including yeast such as *Saccharomyces* species, as well as bacteria from notably different genera (National Institutes of Health, 2019). A study of over 170 species of *Lactobacillus* concluded that there are significant differences among genomes, phenotypes, and biological effects in experimental models, which leads to variability and inconsistencies when comparing study outcomes (Azaïs-Braesco et al., 2010). Different phenotypic traits (**Table 1**) exhibited by the diverse organisms may contribute to their utility as probiotic supplements. For example, acid tolerance is likely correlated to probiotic survival as they encounter acidic environments during digestion. *Bifidobacterium animalis* subsp. *lactis* BB-12 is considered to have a high tolerance for acidic conditions and produces bile salt hydrolase enzymes, limiting harm from bile salt exposure in the intestines (Jungersen et al., 2014). Similarly, oxygen tolerance is an important feature of probiotic organisms. Although many gastrointestinal microbes are anaerobic, traditional probiotic bacteria survive in aerobic environments prior to ingestion (Talwalkar et al., 2001). Talwalkar et al. (2001) have reported high oxygen tolerance for several strains of *Lactobacillus acidophilus*, a species commonly used for probiotics. Spore formation may afford an additional benefit for probiotic organisms, supporting their ability to endure sometimes harsh preparation and storage conditions (Cutting, 2011). *Saccharomyces cerevisiae* is a commonly used yeast for fermentation and biofuels (Belda et al., 2019) and *Bacillus subtilis* is a widely studied probiotic species with dormant spores that survive in extreme conditions and a variety of environments (Kovács, 2019).

PRECLINICAL *IN VITRO* ASSAYS AND *IN VIVO* ANIMAL MODELS

In vitro Antimicrobial Activity

In vitro assays have demonstrated several bacterial and yeast species inhibit the growth of pathogenic species (Fijan et al., 2018) or reduce pathogen adhesion to gut epithelial cells (Collado, 2006). In particular, *B. animalis* subsp. *lactis* BB-12 and *Lactobacillus reuteri DSM 17938* inhibited the growth of *E. coli* (Fijan et al., 2018). The concept of employing probiotic species in conjunction with phage treatment to reduce the cytotoxicity of pathogenic *E. coli* was found to be effective at controlling hemorrhagic *E. coli* and ameliorating its cytotoxic effects (Mohsin et al., 2015; Dini et al., 2016). *Lactobacillus paracasei* FJ861111.1 has demonstrated significant inhibition against several common intestinal pathogens including *Shigella dysenteriae*, *E. coli*, and *Candida albicans* via agar diffusion assay models (Deng et al., 2015). A significant decrease in adherence of food-borne pathogens to HT-29 cells (human colon adenocarcinoma cell line) in the presence of *L. paracasei* was also demonstrated (Deng et al., 2015).

Clostridioides difficile growth was inhibited in a pH-dependent manner when co-cultured with commercial *Bifidobacterium* and *Lactobacillus* strains (Fredua-Agyeman et al., 2017). The same study also demonstrated inhibition by neutralized cell free supernatant by both strains, although the *Bifidobacterium* strain showed greater inhibition than the *Lactobacillus* strain. In addition, probiotic mixtures have demonstrated effectiveness against *C. difficile* (Deng et al., 2015).

Listeria monocytogenes, a common foodborne pathogen, was inhibited by strains of *Lactobacillus plantarum* B7 and *Lactobacillus rhamnosus* D1, demonstrated using spot-on-lawn antagonism (Valente et al., 2019). Probiotic formulations of *L. rhamnosus*, *B. lactis*, and *Bifidobacterium longum* have been shown to reduce proinflammatory cytokines *in vitro* (Sichetti et al., 2018). A Caco-2 cell monolayer *in vitro* assay has been developed to probe the expression of genes involved in the tight junction signaling as a possible mechanism probiotic species utilize to improve intestinal barrier function (Anderson, 2010). Researchers are beginning to elucidate the anti-inflammatory mechanisms associated with *Saccharomyces boulardii* relating to the modulation of protein kinase activity, expression of peroxisome proliferator-activated receptor-gamma, and inhibition of proinflammatory cytokine production (Pothoulakis, 2009). *S. boulardii* has also demonstrated growth inhibition of intestinal pathogens such as *C. albicans, Yersinia enterocolitica,*

TABLE 1 | Selected probiotic products used in the commercial market.

Probiotic (Genus, Species, strain)	Eukaryotic vs Prokaryotic	Gram stain (−/+)	Spore-Forming	Oxygen Tolerance	Formulation	References
Bacillus coagulans Nr	Prokaryotic	+	Yes	Aerobic[a]	Capsules	Holt et al., 2000; Sniffen et al., 2018
Bifidobacterium lactis (*Animalis*) Dn-173010 (Cncm I-2494)	Prokaryotic	+	No	0.88 (Tolerant via RBGR study)	Yogurt	Holt et al., 2000; Sniffen et al., 2018; Talwalkar et al., 2001
Bifidobacterium animalis Lactis Bb-12 (Cncm I-3446)	Prokaryotic	+	No	0.02	Capsules, Powder, Fermented Milk	Holt et al., 2000; Jungersen et al., 2014; Sniffen et al., 2018; Talwalkar et al., 2001
Escherichia coli Nissle 1917	Prokaryotic	−	No	Facultative anaerobe[a]	Capsules, Suspension	Holt et al., 2000; Madigan, 2018; Sniffen et al., 2018
Lactobacillus acidophilus (multiple strains)	Prokaryotic	+	No	RBGR values ranged from 0.43 to 0.70 among strains tested.	Satchet, Capsules	Holt et al., 2000; Sniffen et al., 2018; Talwalkar et al., 2001
Lactobacillus casei Dn-114001 (Cncm I-1518)	Prokaryotic	+	No	0.84 (Tolerant via RBGR study)	Fermented Drink, Yogurt	Holt et al., 2000; Talwalkar et al., 2001
Lactobacillus rhamnosus GG (ATCC 53013)	Prokaryotic	+	No	Facultative anaerobe[a]	Yogurt, Capsules	Holt et al., 2000; Sniffen et al., 2018
Saccharomyces boulardii Cncm I-745 (ATCC 74012)	Eukaryotic	N/A	No	Facultative anaerobe[a]	Capsules, Sachets	Koutsokali and Valahas, 2020; McCullough et al., 1998; Sniffen et al., 2018; McFarland, 1998; McCullough et al., 1998; McFarland, 1996; Sniffen et al., 2018

Relative Bacterial Growth Ratio (RBGR) is a quantitative method for assessing oxygen tolerance (Talwalkar et al., 2001). RBGR values are provided in the table for bacteria that were included in the study (Talwalkar et al., 2001). [a]*Not included in the Talwalkar et al. RBGR study.*

Aeromonas hemolysin, Salmonella Typhimurium (Ducluzeau and Bensaada, 1982; Altwegg et al., 1995; Zbinden, 1999).

In vivo Animal Models

Several animal models are commonly used for the preliminary assessment of efficacy and safety of probiotics, including mice, zebrafish, and *Drosophila* (fruit fly), which have grown in popularity as cost-effective and simplified models to investigate host-microbiota interactions (Trinder, 2017). While there are limitations associated with preclinical models to study probiotics and host-specific microbiota interactions, these species provide an avenue for investigating the diverse microbiota ecosystem and unraveling the complex interactions prior to costly and logistically burdensome clinical trials.

The differences in gastrointestinal anatomy, physiology, and microbiotas are evident, yet the reduced expense and ease of maintaining zebrafish and *Drosophila* colonies under germ-free (GF) conditions has led to their utilization albeit with limitations (Kamareddine et al., 2020). While human microbiota consists of Actinobacteria, Bacteroidetes, Firmicutes, Proteobacteria, and Verrucomicrobia, *Drosophila* are conventionally populated with Proteobacteria and Firmicutes and zebrafish with Bacteroidetes, Firmicutes, Fusobacteria, and Proteobacteria (Blum, 2013; Xiao, 2015; Kamareddine et al., 2020). In addition to bacterial species, *Drosophila* provide the opportunity to study several yeasts (e.g., Candida and Pichia) (Chandler, 2012; Stamps, 2012). *Drosophila* and Zebrafish models can be employed with conventional microbiota or GF with subsequent selective colonization (Kamareddine et al., 2020). As with all GF models, limitations exist regarding food sources that may contain autoclave-resistant microbial products (Hyun, 1983). While zebrafish are maintained at 28°C in an aquatic environment, which limits the colonization of microbes and confounds the correlation of results to land-based species, they may be colonized by several probiotic bacterial species of interest to humans (to include *Bifidobacterium* and *Lactobacilli*). The simplicity of the zebrafish model allowed researchers to develop an intestinal motility model to assess three strains of peristalsis-promoting probiotics (*Lactobacillus acidophilium*, *L. rhamnosus*, and *B. animalis lactis*) at varying concentrations utilizing a fluorescent dye and image analysis (Lu, 2019) (Wang, 2020). *Drosophila* have been employed as a model to study host-microbiota interactions as a simplified and affordable alternative to mammalian animal models for high-throughput screening of probiotics and to further elucidate host defensive mechanisms against GI pathogens. Zebrafish and *Drosophila* models mimicking gastrointestinal inflammatory conditions have been developed to study host and microbiota interactions and quantify inflammatory biomarker response (Jiang, 2009; Oehlers, 2011; He, 2013).

Murine models have been utilized to study gut microbiota due to their mammalian physiology, but cost is a consideration, especially GF varieties requiring maintenance in special facilities, routine monitoring, and trained personnel. GF mice function as a sterile control or host for selective colonization, but limitations exist based upon their immature intestinal immune system (Laukens et al., 2016). A subset of GF humanized mice has allowed for the replication of a humanized biome with mixed results indicating host-specific interactions that are challenging to replicate (Laukens et al., 2016). Strain, genotype, phenotype, and gender differences further confound the extrapolation of results and have led to the development of guidelines to control murine microbiota model variability (Laukens et al., 2016).

Germ-free mice were utilized to study the involvement of microbiota in gastrointestinal diseases such as inflammatory

bowel disease and colitis, and subsequent prophylactic and treatment modalities of probiotics. For example, Lactic acid bacteria (LAB) were investigated to prevent chronic inflammation. *L. plantarum* persisted in the digestive tracts of mice with TNBS-induced colitis for up to ten days after treatment without harmful effects exhibited. Overall, intestinal inflammation decreased and there was no incidence of bacterial dissemination (Pavan et al., 2003; Hu et al., 2019). *L. reuteri* has been shown to reduce *C. difficile* infection in mice. Based on a recent study, a single dose of *L. reuteri* biofilm is efficacious in the prevention of *C. difficile* colitis. When administered either therapeutically or prophylactically, it can reduce the frequency and prevalence of the infection (Shelby et al., 2020). Researchers have also combined conventional and GF mice and zebrafish models to investigate how host-specific interactions modify microbiota communities (Rawls, 2006). Zebrafish were colonized with mouse gut microbiota and mice were colonized with zebrafish microbiota, which allowed for comparison of the host and transplanted communities at the phylogenetic level. Their results indicated the host gut altered the microbiome after transplantation between these species, which further indicates the limitations of extrapolating data across species.

REGULATION, CLINICAL EFFICACY, AND SAFETY

Probiotics in the United States could be regulated by the Food and Drug Administration (FDA) as drugs, biologics, or dietary supplements based on the intended use (U.S. Food and Drug Administration National Institute of Health National Institute of Allergy and Infectious Diseases, 2018; National Institutes of Health National Center for Complementary and Integrative Health, 2021). These products are under the purview of different centers within the FDA, often covered by different laws. As such, it may not always be clear to end-users how a commercially available probiotic is marketed. When considered dietary supplements, probiotics are regulated according to the Dietary Supplement Health and Education Act of 1994 (DSHEA) and the requirements tend to be more in line with food safety expectations rather than drug or biologics (U.S. Food and Drug Administration National Institute of Health National Institute of Allergy and Infectious Diseases, 2018; Venugopalan et al., 2010; U.S. Food and Drug Administration, 2019). A key difference between dietary supplement and drug/biologic regulation lies in the requirements that manufacturers must meet before marketing their products. The FDA typically requires thorough review of *in vitro, in vivo*, and clinical studies before drug approval or biologic licensing, which may be submitted in the form of detailed applications designed to evaluate safety and effectiveness (U.S. Food and Drug Administration, 2014, 2017). As dietary supplements, probiotics are primarily subjected to FDA premarket review only when they are comprised of a "new dietary ingredient," which DSHEA describes as "dietary ingredient that was not marketed in the United States before October 15, 1994" (National Institutes of Health Office of Dietary Supplements, 1994). For dietary supplements, it is left to the manufacturers discretion to establish whether their ingredient is new (U.S. Food and Drug Administration, 2020), which could potentially cause inconsistencies in which probiotics are reviewed by the FDA. Manufacturers of dietary supplements with new dietary ingredients are expected to submit a premarket notification to the FDA, which differs from drug approval or biologics licensing in the degree of safety/efficacy evaluation and resulting regulatory decision (U.S. Food and Drug Administration National Institute of Health National Institute of Allergy and Infectious Diseases, 2018). If the manufacturer does not deem their dietary ingredient to be "new," the FDA generally relies on the companies to ensure that their products meet marketing and labeling requirements. Consequently, the same probiotic product could have very different testing requirements and regulatory processes according to how it will be labeled for use.

Once marketed, labeling and health claims are also a potential complicating factor in probiotic usage. According to DSHEA, dietary supplement labeling "may not claim to diagnose, mitigate, treat, cure, or prevent a specific disease or class of diseases (National Institutes of Health Office of Dietary Supplements, 1994)." It is relevant to note that per DSHEA, labeling statements are allowable if "the statement claims a benefit related to a classical nutrient deficiency disease and discloses the prevalence of such disease in the United States, describes the role of a nutrient or dietary ingredient intended to affect the structure or function in humans, characterizes the documented mechanism by which a nutrient or dietary ingredient acts to maintain such structure or function, or describes general well-being from consumption of a nutrient or dietary ingredient. . ." (National Institutes of Health Office of Dietary Supplements, 1994). This distinction in acceptable labeling could result in ambiguous claims concerning probiotic health benefits, which may not be easily interpreted by the public. Dietary supplement advertising falls under the regulatory purview of the Federal Trade Commission rather than the FDA (U.S. Food and Drug Administration, 2019) and shared federal jurisdiction increases the complexity of monitoring product claims marketed to consumers. Further, the National Institutes of Health has noted reports of probiotics with potentially dangerous contents that did not match the labeling (National Institutes of Health National Center for Complementary and Integrative Health, 2021). The Council for Responsible Nutrition and International Probiotics Association offers labeling guidance to probiotic manufacturers that includes specifying detailed information at the strain level concerning the type, quantity, and storage conditions of the organisms; however, these parameters are presented as recommendations rather than requirements (International Probiotics Association, 2017). Historically, many studies have noted that laboratory testing does not always corroborate the presence of microorganisms claimed in probiotic labeling (Yeung, 2012). More recently, Metras et al. (2021) conducted a study to compare labeling information with the actual microbial content of five commercially available fermented kefir products regulated as dietary supplements. Their results demonstrated inconsistencies between the information claimed on the labeling and the actual species and quantified colonies that were present under the conditions tested (Metras, 2020).

Due to lack of probiotic prescribing information, healthcare providers do not have succinct resources outlining the indications, dosage and administration, contraindications, warnings and precautions, adverse reactions, drug interactions, and use in specific populations (Reid et al., 2019). Consequently, much of the knowledge concerning safety and efficacy is derived from a patchwork of literature, which must be reviewed and interpreted by people interested in clinical applications for probiotics. A more standardized approach to probiotic regulation, testing, and labeling processes would be beneficial to reduce the variability and inconsistency that currently exists in the literature. For example, consistent *in vivo* testing requirements could generate a more robust body of literature concerning whether a given strain is effective against a specific condition and how formulation may affect delivery and disease outcome, information that is generally lacking at present (Sniffen et al., 2018).

Microbiota and Gastrointestinal Pathology and Pathophysiology

The dynamic mix of host cells and microorganisms have evolved (Bäckhed et al., 2005; Ley, 2006) and integrated into critical physiological functions such as shaping the intestinal epithelium (Natividad and Verdu, 2013), digestion (Chang and Martinez-Guryn, 2019), regulating host immunity (Gensollen et al., 2016), and protecting against pathogens (Bäumler and Sperandio, 2016). The microbiota contributes to carbohydrate, lipid, protein metabolism and digestion (simple sugars, fatty acids, and amino acids) via the principal absorption sites of the major nutrients. The small intestine has two primary functions, digestion and absorption, that are affected by the GI microbiota. Segmental movements of the small intestine mix ingested materials with pancreatic, hepatobiliary, and intestinal secretions along with microbiota enzymes. Metabolomic advances are beginning to elucidate the interwoven relationship between healthy and diseased mucosa-associated microbiota, which are strongly correlated to dietary sources (Eetemadi et al., 2020).

As shown in **Figure 1**, the villus consists of a central lymph channel (lacteal) surrounded by a network of blood capillaries within lymph tissue bordered by epithelial cells (Noah et al., 2011). Surrounding each villus are small pits called the crypts of Lieberkuhn, which contain undifferentiated cells that proliferate rapidly and migrate toward the tip of the villus and are shed into the intestinal lumen (Noah et al., 2011). Maturation and migration from the crypts to the tip of the villus requires 5–7 days and approximately 20–50 million epithelial cells are extruded into the intestinal lumen each minute (Gehart and Clevers, 2019). The cellular composition within the gastrointestinal tracks was recently estimated at 3×10^{13} host cells along with 4×10^{13} microbiota cells (Sender et al., 2016), whereby colonization and microbial diversity occurs in parallel with the development of the mucosal absorption and immune system response (Aidy et al., 2013). Both metabolic processes and signal transduction pathways between the host and microbiota are intimately linked and alterations within the gastrointestinal environment can lead to pathophysiological consequences (Bermudez-Brito et al., 2012; Zhang, 2019).

Although not fully elucidated, the enhanced mucosal barrier function, inhibition of pathogen adhesion, and competitive exclusion of pathogenic microorganisms are also mediated by gut microbiota and probiotic administration (Bermudez-Brito et al., 2012; Cornick et al., 2015). The villous epithelium consists of mucus producing goblet cells and absorptive cells, which are responsible for the absorption of nutrients and medications. Pathogenic microbes and microbial toxins can disrupt goblet cell function and disrupt the integrity of the mucus barrier, leading to chronic inflammatory diseases (Cornick et al., 2015). Probiotics, such as *L. rhamnosis* and *L. plantarum*, have been shown to enhance the mucus barrier (Wang et al., 2014), regulate epithelial cell function (Ohland and Macnaughton, 2010), suppress oxidative stress (Ciorba et al., 2012), and mitigate

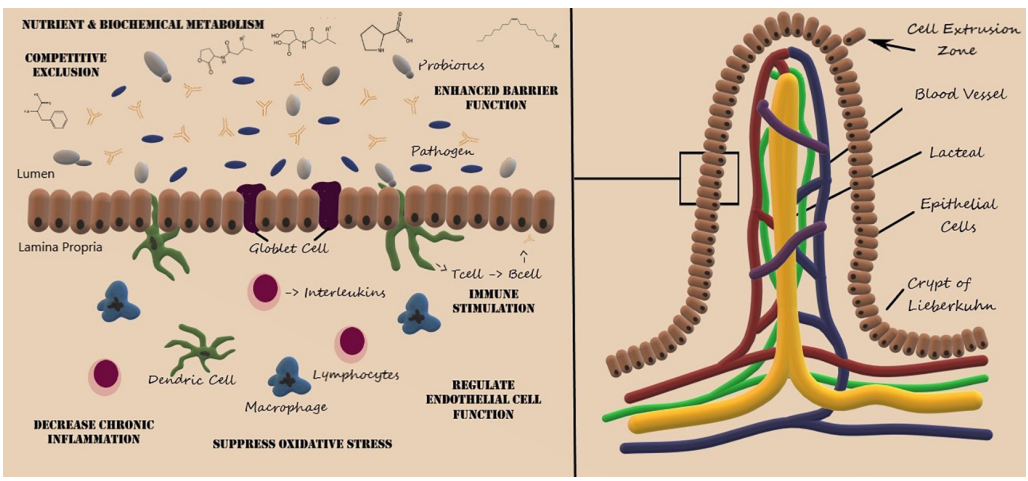

FIGURE 1 | Structure of the villus of the small intestine and representative probiotic mechanisms of action. Artwork by Audrey Milner.

immune response thereby decreasing chronic inflammation (Mann et al., 2013).

Effect of Antibiotics on the Gut Microbiota

It is important to acknowledge the complicated relationship between gastrointestinal disease, gut microbiota, probiotics, and antibiotics. Maintaining the appropriate gut microbiota ecosystem in the age of antibiotic treatments (Gibson et al., 2015) and resistance (Schaik, 2015) is of particular importance. Common pathogenic strains that contribute to GI diseases are *Campylobacter*, *C. difficile, E. coli, Helicobacter pylori, Salmonella* species*, Shigella, Staphylococcus aureus, Clostridium perfringens, Listeria monocytogenes, Bacillus cereus,* and *Y. enterocolitica* (Alby and Nachamkin, 2016; Harmon, 2017; Sandra and Tallent, 2020). Symptoms include diarrhea, vomiting, abdominal pain, and heartburn (Alby and Nachamkin, 2016). However, elders and immunocompromised individuals can have serious complications from GI diseases due to potentially weakened immune systems. Oftentimes GI infections are treated with antibiotics, however, the rise of antibiotic resistant bacterial strains is yielding mixed results. Thus, researchers are looking for new alternatives to combat GI infections, for example, the use of probiotics and fecal transplant.

The introduction of antibiotics alters the microbial ecosystem, which can lead to a limited gut microbial diversity (Fjalstad et al., 2018) and the reestablishment of pathogenic infections (Yoon and Yoon, 2018). The necessity to limit antibiotic treatment in neonates is prominent due to potentially disease-promoting microbiota alterations. Antibiotic exposure in infants and young children may have significant impacts on the microbiota during critical periods of development (Silverman et al., 2017). Antibiotic treatments can cause reduced colonization rates and increased risk of multi-drug resistant (MDR) strains (Fjalstad et al., 2018). Conversely, the natural microbiome recovery post antibiotic administration has been explored in murine models (Ng, 2019) and documented in human studies with varied microbiome population effects given the heterogeneity associated with antibiotic treatment regimens (MacPherson, 2018; Elvers, 2020).

Antibiotic-Associated Diarrhea

Antibiotic-associated diarrhea (AAD) is a common side effect of antibiotic usage, which affects up to 30% of patients administered antibiotics (McFarland, 2007). There are believed to be several ways by which antibiotics cause diarrhea, including killing beneficial microbes and influencing metabolic processes (McFarland, 1998; Silverman et al., 2017). Some antibiotics, such as amoxicillin-clavulanate, ampicillin, cephalosporin and clindamycin may cause AAD with increased incidence (McFarland, 1998; Silverman et al., 2017). In addition to the type of antibiotics used, individual patient susceptibility may also influence the development of AAD (Barbut and Meynard, 2002).

Probiotics are a common choice for patients suffering from AAD and have been widely advocated as a safe and effective way to reduce adverse side effects of antibiotics on gastrointestinal function (Mills, 2018). *C. difficile* infection can occur following the antibiotic-associated loss of intestinal flora, potentially increasing serious diarrheal disease (Silverman et al., 2017), and is one of the principal causes of AAD (Young et al., 2018). *C. difficile* infection has an incidence of approximately 500,000 infections per year in the United States and approximately 30,000 cases resulting in fatality within 30 days (Mada and Alam, 2020). A meta-analysis of 25 randomized controlled trials indicated probiotics reduced the relative risk of ADD (RR = 0.43, 95% CI 0.31, 0.58, $p < 0.001$) and the analysis of six randomized trials led to statistically significant reduction in *C. difficile* (RR = 0.59, 95% CI 0.41, 0.85, $p < 0.005$) (McFarland, 2006). In particular, *L. rhamnosus* GG *and S. boulardii,* were identified as effective for treating AAD and *S. boulardii* was particularly effective for reducing *C. difficile* infection.

Lactobacillus rhamnosus GG and *S. boulardii,* have been proposed to maintain the gut microbiota and production of energy via fermentation as well as competition with pathogen binding sites (Hickson, 2011; Vecchio et al., 2015). However, the mechanisms of action are still unknown (Hickson, 2011). When investigating the efficacy in reducing AAD, *S. boulardii* resulted in a relative risk of 0.47 [95% confidence interval (CI) = 0.35, 0.63; $p < 0.001$] and 0.31 (95% CI = 0.13, 0.72; $p = 0.006$) for *L. rhamnosus* (Hickson, 2011). A recent study demonstrated that *S. boulardii* acts to reduce toxin A-receptor binding by releasing a protease that cleaves toxin A, an exotoxin released by *C. difficile* (Castagliuolo et al., 1996; Pothoulakis, 2009). A controlled clinical trial focusing on the prevention of *C. difficile* infection with *S. boulardii* indicated a reduction of *C. difficile* relapse in the recurrent treatment group of patients receiving high-dose vancomycin ($p = 0.05$), furthering support for usage (Surawicz et al., 2000). However, two studies examining *S. boulardii* found that the probiotic had no significant effect in treating *C. difficile* associated diarrhea (AD; Surawicz et al., 1989; Kotowska et al., 2005). *L. rhamnosus* is reported to increase the production of gut mucin, which functions as a barrier defense for the epithelium thereby reducing the effects of *C. difficile* AD (Mack et al., 1999).

A study investigating 29 probiotics found that Bio-K+ (a probiotic cocktail comprised of *L. acidophilus, Lactobacillus casei, and L. rhamnosus*) survived the GI environment inhibiting growth and toxin neutralization (Auclair et al., 2015). BIO-K+ also decreased the production of methicillin-resistant *S. aureus* by 99%, providing evidence for growth inhibition (Karska-Wysocki et al., 2010). Furthermore, in terms of toxin neutralization, Bio-K+ demonstrated anticytotoxic effects in a toxin neutralization assay that tested 13 strains (Auclair et al., 2015). *B. bifidum* and *Streptococcus thermophilus* were supplemented into an infant's diet and showed decreased occurrence of diarrheal symptoms (Saavedra et al., 1994). Regarding safety concerns, a report investigated the production of putrescine via *B. bifidum*, but determined the concentrations were consistent with safe food sources (Kim et al., 2018).

Helicobacter pylori Infection

Helicobacter pylori infection (HPI) occurs in roughly 60% of the world's population and can cause various gastroenterological disorders including conditions associated with dyspepsia, peptic ulcer, and stomach cancers (Chey et al., 2017; Hooi,

2017). Available treatment methods for HPI usually involve combinations of two or three antibiotics with a proton pump inhibitor, referred to as "triple therapy" or "quadruple therapy," respectively (Ables et al., 2007; Chey et al., 2017). Total eradication is rare, as the efficacy of these treatments tend to vary and are impacted by antibiotic resistant strains (Higuchi et al., 2006; Sun et al., 2010). Studies have shown that using probiotics in conjunction with other treatments may aid in eradication of *H. pylori*. When combined with a triple therapy of omeprazol, clarithromycin, and amoxicillin, pre-treatment of patients with *L. acidophilus, S. faecalis*, and *B. subtilis* for two-weeks improved the eradication rate by 18.7% compared to the control (Du et al., 2012). A 24-month clinical trial involving nearly 500 subjects found similar results with a combination of probiotic treatment and triple therapy increasing eradication rate by 7% (Rieko et al., 2020). It is proposed that this colonization reduction may be due to a decrease in the biotic load despite *H. pylori* antimicrobial resistance (Du et al., 2012). In the afore mentioned studies, research was performed with pretreatment of probiotics, but not with concurrent treatment alongside the triple therapy. Although some studies have shown successful *H. pylori* eradication with additional probiotic treatment, a meta-analysis performed by Lu et al. (2016) suggests that probiotic use provided little benefit over a placebo. Additionally, Cindoruk et al. (2007) reported that using *S. boulardii* along with an antibiotic triple therapy did not result in a statistically significant eradication increase but did reduce symptoms associated with treatment when compared to a placebo (Cindoruk et al., 2007). Overall, additional studies are required to elucidate the effectiveness of probiotics with HPI (Chey et al., 2017) and the effect of antibiotic treatments on the survival of probiotics (Rieko et al., 2020).

Blastocystis

Blastocystis species are anaerobic intestinal protozoans, typically considered to be pathogenic although there is increasing evidence that they should be considered a commensal (Sinclair, 2016; Deng, 2021). Infections may be present in both asymptomatic and symptomatic individuals, potentially demonstrating generalized gastrointestinal symptoms (Coyle et al., 2012; Wawrzyniak et al., 2013). There are medications available for *Blastocystis* infections, including the commonly used metronidazole or trimethoprimsulfamethoxazole; however, clinical indications for when to treat remain somewhat ambiguous (Coyle et al., 2012; Sekar and Shanthi, 2013; Wawrzyniak et al., 2013). Further, there have been case reports of treatment that did not eradicate *Blastocystis* (Roberts et al., 2014), and emerging resistance to metronidazole has been reported (Sekar and Shanthi, 2013). Despite the apparent need for clarity regarding effective treatment of *Blastocystis* infections, limited clinical data is available investigating probiotics to support treatment of *Blastocystis*. One trial examined the use of *S. boulardii* in lieu of metronidazole in symptomatic children with *Blastocystis hominis* positive stools. After one month, those treated with doses of *S. boulardii* had a 94.4% clinical cure rate and 73.3% clinical cure rate was reported for those who received the standard metronidazole treatment; whereas the parasitological cure rate was similar between each group (Dinleyici et al., 2010). While *S. boulardii* efficacy against *B. hominis* has not been thoroughly characterized, it has been suggested that probiotics may displace protozoan pathogens in the gastrointestinal tract and potentially alter the patient's immune response, thus improving the clinical outcome (Vitetta et al., 2016). An *in vitro* study evaluated the use of some probiotic bacteria and demonstrated that *L. rhamnosus*, *L. lactis*, and *Enterococcus faecium* reduced *Blastocystis* under the culture conditions tested (Lepczyńska and Dzika, 2019). In addition, a similar study which examined the interactions between Blastocystis subtype 7 (ST7) and various gut bacteria, found that *Blastocystis* ST7 reduced beneficial *Bifidobacterium* and *Lactobacillus* species in mice (Yason, 2019).

Acute Gastroenteritis

Acute gastroenteritis (AG) refers to inflammation within the gastrointestinal track, most often accompanied by an infection and characterized by sudden emergence of symptoms including nausea, vomiting, watery stool, and abdominal discomfort (Graves, 2013; Hartman et al., 2019). Symptomatic treatment, anti-infective therapy, and addressing dehydration are the primary clinical focus (Zollner-Schwetz and Krause, 2015; Hartman et al., 2019). An estimated 1.5–2.5 million children die each year from infectious gastroenteritis. Molecular, immunoassay and culture methods are utilized to diagnose the diverse bacterial and viral pathogens leading to the etiology (Humphries, 2015; Tarr, 2019). Probiotic products may also be useful for AG, in part by modifying the gastrointestinal microbiome, as well as exerting effects on physiology, such as anti-inflammatory responses and fortification of epithelial cell tight junctions (Kluijfhout et al., 2020). The probiotics *lactobacilli* and *S. boulardii* are the most researched in treating this disease (Kluijfhout et al., 2020). *S. boulardii* produced a significant decrease in diarrhea (14.0% day 1; 13.1% day 2) when administered to treat AG (Kluijfhout et al., 2020). In terms of the mechanism of action, *S. boulardii* has been shown to disrupt the production of proinflammatory cytokines and interfere with inflammation nuclear factors (Sougioultzis et al., 2006). Conversely, another study found that *L. rhamnosus* and *Lactobacillus helveticus* did not demonstrate a decrease in presence or symptoms associated with viral infection (Freedman et al., 2020).

Necrotizing Enterocolitis

Necrotizing enterocolitis (NEC) is the leading cause of neonatal morbidity and mortality (Neu and Walker, 2011). Although the etiology of NEC is not clear, immature immune function and alteration of the intestinal microbiome post antibiotic treatment may be contributing factors (Xiong et al., 2020). Common symptoms include feeding intolerance, lethargy, bloating, and bloody stools. Treatment focuses upon fluid replacement, nutrition, anti-infective therapy, and surgery. There have been several meta-analyses indicating probiotics prevent NEC. A meta-analysis of 24 randomized controlled trials demonstrated clinical efficacy (RR 0.65, 95% CI 0.52–0.81; 17 studies, 5,112 infants) in reducing the incidence of NEC

utilizing *Lactobacillus* monotherapy or co-administration with *Bifidobacterium* (AlFaleh and Anabrees, 2014), which are present in the microbiomes of healthy infants (Eugenia Bezirtzoglou, 2011). Another meta-analysis (RR 0.36, 95% CI, 0.24–0.53, n = 7345 infants) showed prophylactic efficacy of developing NEC in probiotic-treated infants (Chang, 2017). Although, a 2015 study involving 1,315 infants indicated no evidence of the benefit of using *Bifidobacterium breve* BBG-001 for the prevention of NEC in preterm infants, underscoring the species variability relative to clinical outcomes (Costeloe et al., 2016).

Irritable Bowel Syndrome and Functional Bowel Disorders

Irritable Bowel Syndrome (IBS) occurs on a spectrum from mild to severe and includes recurrent abdominal discomfort and pain, bloating, and stool alterations varying between constipation and diarrhea (Defrees, 2017). The etiology of IBS remains unclear and the symptoms are often associated with differential diagnoses (Aziz and Simrén, 2021). Studies involving probiotics have shown clinical benefits in treating IBS patients such as fecal consistency, flatulence, bloating, the number of symptoms present, appetite, bowel frequency, and nourishment (Harris and Baffy, 2017). Recent clinical data has supported utilizing probiotics to modify the microflora within the gut to reduce inflammation (Boirivant and Strober, 2007).

In the case of a clinical study conducted to determine the ability for *L. acidophilus* and *B. animalis* subsp. *lactis* to treat bowel disorders, the difference between the test and placebo groups were not statistically significant for the primary endpoints of GI relief and satisfaction. However, several of the symptoms studied significantly improved when compared to the control group. Abdominal bloat showed statistically significant improvement when compared to the control group with a p-value of 0.009 after 4 weeks and a value of 0.06 after 8 weeks (Ringel-Kulka et al., 2015). Additionally, there were no significant changes in standard blood test ranges and fecal samples as safety indicators (Ringel-Kulka et al., 2015).

Lactobacillus acidophilus CL1285, *L. casei* LBC80R and *L. rhamnosus* CLR2 have been identified as potential treatments to relieve the symptoms associated with IBS (Preston et al., 2018). This combination of probiotics demonstrated endpoint improvement including abdominal pain, days in pain, buildup of gas within the stomach, and stool habits. Primarily mild to moderate safety concerns were reported in some treatment and placebo participants; however, the authors concluded the concerns could not be definitively linked to the intervention (Preston et al., 2018). Additionally, a small study was conducted to evaluate the safety of *L. casei* shirota when treating diarrhea occurring in critically ill children, in which no safety signals were observed (Srinivasan et al., 2006).

HIV/AIDS-Associated Diarrhea

Gastrointestinal diseases are a common disorder in patients suffering from human immunodeficiency virus (HIV) and/or acquired immunodeficiency disorder (AIDS), with roughly 40% of HIV/AIDS patients suffering from GI related hyponatremia in certain areas of the world (Shu et al., 2018). Diarrhea in HIV/AIDS affected individuals can be caused by a variety of opportunistic infections or noninfectious causes linked to treatment regimens (Dikman et al., 2015). Current treatment for patients suffering from AIDS-AD involve antisecretory agents and/or fecal microbiota transplantation therapy (Dikman et al., 2015; Ouyang, 2020). Several promising studies have provided insight into utilizing probiotics as an affordable and accessible option to combat diarrhea in patients with HIV/AIDS induced diarrhea. Probiotic yogurts have been historically utilized in Africa to ease HIV/AIDS AD (Reid, 2010; Whaling, 2012). In a 2008 study conducted in Nigeria, yogurt with probiotics *Lactobacillus delbruekii* subsp. *bulgaricus* and *S. thermophilus*, or *L. rhamnosus GR-1* and *L. reuteri RC-14* resolved diarrheal symptoms in 12/12 patients after 15 days of consumption compared to 2/12 in the control group (Anukam et al., 2008). However, Salminen et al. (2004) study demonstrated little to no difference between experimental and control groups (Salminen et al., 2004). A double-blinded, randomized, placebo-controlled trial involving 44 patients over 12 weeks utilizing molecular sequencing techniques to analyze changes in the gut microbiome following *S. boulardii* administration demonstrated a significant reduction in pathogenic bacterial species of the Clostridiaceae family and a reduction in inflammatory biomarkers (Villar-García, 2017).

Drug Interactions

The co-administration of probiotics with orally administered drugs warrants further investigation. Although oral administration of drugs is the most convenient, economical, and common route of administration, subsequent interactions with food, co-administered drugs, or microbiota may influence absorption and bioavailability. Gut microbiota are known to produce a diverse array of enzymes capable of metabolizing nutrients and drugs (Claus et al., 2011), which could alter the structure of the parent compound and subsequent membrane diffusion, active transport into the bloodstream, and/or efficacy. The therapeutic activity of lactulose depends on the metabolism by intestinal bacteria such as *Lactobacillus* (Sahota et al., 1982), which are also employed as probiotics. Interestingly, *Lactobacillus* metabolites have also been shown to compete for hepatic uptake of drugs such as simvastain, thereby altering the pharmacodynamics (Kaddurah-Daouk et al., 2011). While significant data outlining the relationship between gut microbiota and drug pharmacokinetics and pharmacodynamics (PK/PD) has been reported (Yoo et al., 2014; Swansan, 2015; Zhang et al., 2018), insufficient studies have been conducted to determine the drug interactions associated with the co-administration of probiotics. One animal study determined the administration of *E. coli* Nissle 1917 (ATCC 25922) altered the PK of amidarone absorption in rats and led to a 43% increase in exposure (Matuskova et al., 2014).

CONCLUSION

Natural microbial colonization occurs after birth and may vary significantly based upon environmental factors and antibiotic

administration (Conlon and Bird, 2014). The gut microbiota has gained interest in recent years with respect to probiotic dietary interventions and the regulation of intestinal homeostasis. The metabolic importance of the gut microbiota to nutrient and drug pharmacokinetics underscores the potential of probiotic use for preventive or therapeutic applications in various gastrointestinal disorders. From a mechanistic perspective, probiotics have been shown to strengthen the gut epithelial barrier and reduce inflammation.

Although promising results have been demonstrated for a variety of probiotics undergoing clinical trials to treat complex gastrointestinal and inflammatory diseases, the traditional drug development paradigm associated with preclinical and clinical studies is lacking. Since probiotics are not typically under premarket evaluation by the FDA, the formulation, dosing regimen, mechanism(s) of action, and clinical pharmacology are not readily available in a package insert for healthcare providers. Despite the variability, safety considerations will generally favor a commercially available probiotic approach over the administration of fecal transplantation. An increasing number of clinical trials have indicated improved patient outcomes relative to probiotic use to treat IBS, NEC, antibiotic and HIV AD, and AG. To date, well-controlled clinical studies to clearly document the prophylactic and therapeutic effects of probiotics are limited, which illustrates the numerous gaps relative to the systematic evaluation of species, formulations, and dosing relative to disease indication.

Despite the drawbacks, clinicians recognize the importance of gut microbiota in disruption of several diseases and have been exploring the use of probiotics to restore a 'healthy' microbiome. Often patients either self-administer or a healthcare provider indicates probiotic use to restore gut microbiota, but the clinical outcomes are challenging to extrapolate given the heterogeneity of probiotics relative to species, strain(s), purity, formulation, and manufacturer. The concomitant use of probiotics, antibiotics, and other drug classes further alters the pharmacokinetic and pharmacodynamic profile of treatment regimens, while introducing the potential for drug-drug interactions and should be considered relative to patient polypharmacy (Zhang et al., 2018). The myriad of descriptive and observational studies reviewed underscore the need for randomized controlled trials with clearly defined formulations, species, strain(s), dosing regimens, pharmacodynamic endpoints, clinical outcomes and biostatistical analyses.

AUTHOR CONTRIBUTIONS

DR is a student of Newburgh Free Academy, Newburgh, New York who participated in a student research program at the United States Military Academy. All authors contributed to manuscript drafts and revisions, read, and approved the submitted version.

FUNDING

The faculty and cadets are honored for the support of the United States Military Academy.

ACKNOWLEDGMENTS

The authors would like to acknowledge Audrey Milner, who created **Figure 1**.

REFERENCES

Ables, A., Simon, I., and Melton, E. (2007). Update on *Helicobacter pylori* treatment. *Am. Fam. Physician.* 75, 351–358.

Aidy, S. E., Hooiveld, G., Tremaroli, V., Backhed, F., and Kleerebezem, M. (2013). The gut microbiota and mucosal homeostasis: colonized at birth or at adulthood, does it matter? *Gut Microbes* 4, 118–124. doi: 10.4161/gmic.23362

Alby, K., and Nachamkin, I. (2016). Gastrointestinal infections. *Microbiol. Spectr.* 4, doi: 10.1128/microbiolspec.DMIH2-0005-2015

AlFaleh, K., and Anabrees, J. (2014). Probiotics for prevention of necrotizing enterocolitis in preterm infants. *Evid.Based Child Health* 9, 584–671. doi: 10.1002/ebch.1976

Altwegg, M., Schnack, J., and Zbinden, R. (1995). Influence of Saccharomyces boulardii on Aeromonas hemolysin. *Med. Microbiol. Lett.* 4, 417–425.

Anderson, R. C. (2010). Lactobacillus plantarum MB452 enhances the function of the intestinal barrier by increasing the expression levels of genes involved in tight junction formation. *BMC Microbiol.* 10:316. doi: 10.1186/1471-2180-10-316

Anukam, K., Osazuwa, E., Osadolor, H., Bruce, A., and Reid, G. (2008). Yogurt containing probiotic Lactobacillus rhamnosus GR-1 and L. reuteri RC-14 helps resolve moderate diarrhea and increases CD4 count in HIV/AIDS patients. *J. Clin. Gastroenterol.* 42, 239–243.

Auclair, J., Frappier, M., and Millette, M. (2015). Lactobacillus acidophilus CL1285, Lactobacillus casei LBC80R, and Lactobacillus rhamnosus CLR2 (Bio-K+): characterization, manufacture, mechanisms of action, and quality control of a specific probiotic combination for primary prevention of clostridium dif. *Clin. Infect. Dis.* 60(suppl_2), S135–S143. doi: 10.1093/cid/civ179

Azaïs-Braesco, V., Bresson, J., Guarner, F., and Corthier, G. (2010). Not all lactic acid bacteria are probiotics, . but some are. *Br. J. Nutr.* 103, 1079–1081. doi: 10.1017/S0007114510000723

Aziz, I., and Simrén, M. (2021). The overlap between irritable bowel syndrome and organic gastrointestinal diseases. *Lancet Gastroenterol. Hepatol.* 6, 139–148. doi: 10.1016/S2468-1253(20)30212-0

Bäckhed, F., Ley, R., Sonnenburg, J., Peterson, D., and Gordon, J. (2005). Host-bacterial mutualism in the human intestine. *Science* 307, 1915–1920. doi: 10.1126/science.1104816

Barbut, F., and Meynard, J. (2002). Managing antibiotic associated diarrhoea. *Br. Med. J.* 324, 1345–1346. doi: 10.1136/bmj.324.7350.1345

Bäumler, A. J., and Sperandio, V. (2016). Interactions between the microbiota and pathogenic bacteria in the gut. *Nature* 535, 85–93. doi: 10.1038/nature18849

Belda, I., Ruiz, J., Santos, A., Van Wyk, N., and Pretorius, I. S. (2019). Saccharomyces cerevisiae. *Trends Gemet.* 35, 956–957. doi: 10.1015/j.tig.2019.08.009

Bermudez-Brito, M., Plaza-Díaz, J., Muñoz-Quezada, S., Gómez-Llorente, C., and Gil, A. (2012). Probiotic mechanisms of action. *Ann. Nutr. Metab.* 61, 160–174. doi: 10.1159/000342079

Blum, J. E. (2013). Frequent replenishment sustains the beneficial microbiome of Drosophila melanogaster. *mBio* 4:e860–13. doi: 10.1128/mBio.00860-13

Boirivant, M., and Strober, W. (2007). The mechanism of action of probiotics. *Curr. Opin. Gastroenterol.* 23, 679–692. doi: 10.1097/MOG.0b013e3282f0cffc

Castagliuolo, I., Lamont, J. T., Nikulasson, S. T., and Pothoulakis, C. (1996). Saccharomyces boulardii protease inhibits Clostridium difficile toxin A effects in the rat ileum. *Infect. Immun.* 64, 5225–5232. doi: 10.1128/IAI.64.12.5225-5232.1996

Chandler, J. A. (2012). Yeast communities of diverse *Drosophila* species: comparison of two symbiont groups in the same hosts. *Appl. Environ. Microbiol.* 78, 7327–7336.

Chang, E. B., and Martinez-Guryn, K. (2019). Small intestinal microbiota: the neglected stepchild needed for fat digestion and absorption. *Gut Microb.* 10, 235–240. doi: 10.1080/19490976.2018.1502539

Chang, H. Y. (2017). Multiple strains probiotics appear to be the most effective probiotics in the prevention of necrotizing enterocolitis and mortality: An updated meta-analysis. *PLoS One* 12:e0171579. doi: 10.1371/journal.pone.0171579

Chey, W. D., Leontidis, G. I., Howden, C. W., and Moss, S. F. (2017). ACG clinical guideline: treatment of *Helicobacter* pylori infection. *Am. J. Gastroenterol.* 112, 212–238. doi: 10.1038/ajg.2016.563

Cindoruk, M., Erkan, G., Karakan, T., Dursun, A., and Unal, S. (2007). Efficacy and Safety of Saccharomyces boulardii in the 14-day Triple Anti-*Helicobacter* pylori therapy: a prospective randomized placebo-controlled double-blind study. *Helicobacter* 12, 309–316. doi: 10.1111/j.1523-5378.2007.00516.x

Ciorba, M. A., Riehl, T. E., Rao, M. S., Moon, C., Ee, X., Nava, G. M., et al. (2012). Lactobacillus probiotic protects intestinal epithelium from radiation injury in a TLR-2/cyclo-oxygenase-2-dependent manner. *Gut* 61, 829–838. doi: 10.1136/gutjnl-2011-300367

Claus, S. P., Ellero, S. L., Berger, B., Krause, L., Bruttin, A., Molina, J., et al. (2011). Colonization-induced host-gut microbial metabolic interaction. *mBio* 2:e271–10. doi: 10.1128/mBio.00271-10

Collado, M. C. (2006). Protection mechanism of probiotic combination against human pathogens: *in vitro* adhesion to human intestinal mucus. *Asia Pac. J. Clin. Nutr.* 15, 570–575.

Conlon, M., and Bird, A. (2014). The impact of diet and lifestyle on gut microbiota and human health. *Nutrients* 7, 17–44. doi: 10.3390/nu7010017

Cornick, S., Tawiah, A., and Chadee, K. (2015). Roles and regulation of the mucus barrier in the gut. *Tissue Barriers* 3:e982426.

Costeloe, K., Hardy, P., Juszczak, E., Wilks, M., and Millar, M. R. (2016). Bifidobacterium breve BBG-001 in very preterm infants: a randomised controlled phase 3 trial. *Lancet* 387, 649–660. doi: 10.1016/S0140-6736(15)01027-2

Coyle, C. M., Varughese, J., Weiss, L. M., and Tanowitz, H. B. (2012). Blastocystis: to treat or not to treat. *Clin. Infect. Dis.* 54, 105–110. doi: 10.1093/cid/cir810

Cutting, S. M. (2011). Bacillus probiotics. *Food Microbiol.* 28, 214–220. doi: 10.1016/j.fm.2010.03.007

Defrees, D. N. (2017). Irritable bowel syndrome: epidemiology, pathophysiology, diagnosis, and treatment. *Primary Care* 44, 655–671. doi: 10.1016/j.pop.2017.07.009

Deng, K., Chen, T., Wu, Q., Xin, H., Wei, Q., Hu, P., et al. (2015). *In vitro* and *in vivo* examination of anticolonization of pathogens by Lactobacillus paracasei FJ861111.1. *J. Dairy Sci.* 98, 6759–6766. doi: 10.3168/jds.2015-9761

Deng, L. W. (2021). New insights into the interactions between Blastocystis, the gut microbiota, and host immunity. *PLoS Pathog.* 17:e100925. doi: 10.1371/journal.ppat.1009253

Dikman, A., Schonfeld, E., Srisarajivakul, N., and Poles, M. (2015). Human immunodeficiency virus-associated diarrhea: still an issue in the era of antiretroviral therapy. *Dig. Dis. Sci.* 60, 2236–2245.

Dini, C., Bolla, P., and de Urraza, P. (2016). Treatment of in vitro enterohemorrhagic *Escherichia coli* infection using phage and probiotics. *J. Appl. Microbiol.* 121, 78–88. doi: 10.1111/jam.13124

Dinleyici, E. C., Eren, M., Dogan, N., Reyhanioglu, S., Yargic, Z. A., and Vandenplas, Y. (2010). Clinical efficacy of Saccharomyces boulardii or metronidazole in symptomatic children with Blastocystis hominis infection. *Nat. Library Med.* 108, 541–545. doi: 10.1007/s00436-010-2095-4

Du, Y., Su, T., Fan, J., Lu, Y., Zheng, P., Li, X., et al. (2012). Adjuvant probiotics improve the eradication effect of triple therapy for *Helicobacter* pylori infection. *World J. Gastroenterol.* 18, 6302–6307.

Ducluzeau, R., and Bensaada, M. (1982). [Comparative effect of a single or continuous administration of "Saccharomyces boulardii" on the establishment of various strains of "candida" in the digestive tract of gnotobiotic mice]. *Ann. Microbiol. (Paris)* 133, 491–501.

Eetemadi, A., Rai, N., Pereira, B. M., Kim, M., Schmitz, H., and Tagkopoulos, I. (2020). The computational diet: a review of computational methods across diet. Microbiome, and Health. *Front. Microbiol.* 11:393. doi: 10.3389/fmicb.2020.00393

Elvers, K. T. (2020). Antibiotic-induced changes in the human gut microbiota for the most commonly prescribed antibiotics in primary care in the UK: a systematic review. *BMJ Open* 10:e035677. doi: 10.1136/bmjopen-2019-035677

Eugenia Bezirtzoglou, E. S. (2011). Immunology and probiotic impact of the newborn and young children intestinal microflora. *Anaerobe* 17, 369–374. doi: 10.1016/j.anaerobe.2011.03.010

Farré-Maduell, E., and Casals-Pascual, C. (2019). The origins of gut microbiome research in Europe: from Escherich to Nissle. *Hum. Microb. J.* 14:100065. doi: 10.1016/j.humic.2019.100065

Fijan, S., Sulc, D., and Steyer, A. (2018). Study of the *In Vitro* antagonistic activity of various single-strain and multi-strain probiotics against *Escherichia coli*. *Int. J. Environ. Res. Public Health* 15:1539. doi: 10.3390/ijerph15071539

Fjalstad, J., Esaiassen, E., Juvet, L. K., van den Anker, J. N., and Klingenberg, C. (2018). Antibiotic therapy in neonates and impact on gut microbiota and antibiotic resistance development: a systematic review. *J. Antimicrob. Chemother.* 73, 569–580. doi: 10.1093/jac/dkx426

Fredua-Agyeman, M., Stapleton, P., Basit, A., Beezer, A., and Gaisford, S. (2017). In vitro inhibition of Clostridium difficile by commercial probiotics: a microcalorimetric study. *Int. J. Pharm.* 517, 96–103. doi: 10.1016/j.ijpharm.2016.12.005

Freedman, S. B., Xie, J., Nettel-Aguirre, A., Pang, X.-L., Chui, L., Williamson-Urquhart, S., et al. (2020). A randomized trial evaluating virus-specific effects of a combination probiotic in children with acute gastroenteritis. *Nat. Commun.* 11:2533. doi: 10.1038/s41467-020-16308-3

Gasbarrini, G., Bonvicini, F., and Gramenzi, A. (2016). Probiotics history. *J. Clin. Gastroenterol.* 50(Suppl. 2), S116–S119. doi: 10.1097/MCG.0000000000000697

Gehart, H., and Clevers, H. (2019). Tales from the crypt: new insights into intestinal stem cells. *Nat. Rev. Gastroenterol. Hepatol.* 16, 19–34. doi: 10.1038/s41575-018-0081-y

Gensollen, T., Iyer, S. S., Kasper, D. L., and Blumberg, R. S. (2016). How colonization by microbiota in early life shapes the immune system. *Science* 352, 539–544. doi: 10.1126/science.aad9378

Gibson, M. K., Crofts, T. S., and Dantas, G. (2015). Antibiotics and the developing infant gut microbiota and resistome. *Curr. Opin. Microbiol.* 27, 51–56. doi: 10.1016/j.mib.2015.07.007

Grandview Research (2019). *Probiotics Market Size, Share & Trends Analysis Report By Product (Food & Beverages, Dietary Supplements), By Ingredient (Bacteria, Yeast), By End Use, By Distribution Channel, And Segment Forecasts, 2019 - 2025*. Available online at: https://www.grandviewresearch.com/industry-analysis/probiotics-market (accessed June 05, 2021)

Graves, N. S. (2013). Acute gastroenteritis. *Natl. Library Med.* 40, 727–741. doi: 10.1016/j.pop.2013.05.006

Harmon, E. J. (2017). *Bacteriological Analytical Manual (BAM) Chapter 16: Clostridium Perfringens*. Silver Spring, MD: Food and Drug Administration.

Harris, L., and Baffy, N. (2017). Modulation of the gut microbiota: a focus on treatments for irritable bowel syndrome. *Postgrad Med.* 129, 872–888.

Hartman, S., Brown, E., Loomis, E., and Russell, H. A. (2019). Gastroenteritis in children. *Am. Family Phys.* 99, 159–165.

He, Q. W. (2013). Microbial fingerprinting detects intestinal microbiota dysbiosis in Zebrafish models with chemically-induced enterocolitis. *BMC Microbiol.* 13:289. doi: 10.1186/1471-2180-13-289

Hickson, M. (2011). Probiotics in the prevention of antibiotic-associated diarrhoea and Clostridium difficile infection. *Therapeutic Adv. Gastroenterol.* 4, 185–197. doi: 10.1177/1756283X11399115

Higuchi, K., Maekawa, T., Nakagawa, K., Chouno, S., Hayakumo, T., Tomono, N., et al. (2006). Efficacy and safety of *Helicobacter* pylori eradication therapy with omeprazole, amoxicillin and high- and low-dose clarithromycin in Japanese patients: a randomised, double-blind, multicentre study. *Clin. Drug Investig.* 26, 403–414.

Holt, J. G., Krieg, N. A., Sneath, P. H., Staley, J. T., and Williams, S. T. (2000). *Bergey's Manual of Determinative Bacteriology*, 9th Edn. Philadelphia, PA: Williams & Wilkins.

Hooi, J. L. (2017). Global Prevalence of *Helicobacter* pylori infection: systematic review and meta-analysis. *Gastroenterology* 153, 420–429. doi: 10.1053/j.gastro.2017.04.022

Hu, L., Zhou, M., Young, A., Zhao, W., and Yan, Z. (2019). In vivo effectiveness and safety of probiotics on prophylaxis and treatment of oral candidiasis: a systematic review and meta-analysis. *BMC Oral Health* 19:140. doi: 10.1186/s12903-019-0841-2

Humphries, R. M. (2015). Practical guidance for clinical microbiology laboratories: diagnosis of bacterial gastroenteritis. *Clin. Microbiol. Rev.* 28, 3–31. doi: 10.1128/CMR.00073-14

Hyun, H. H. (1983). Ultrastructure and extreme heat resistance of spores from thermophilic Clostridium species. *J. Bacteriol.* 156, 1332–1337. doi: 10.1128/JB.156.3.1332-1337.1983

International Probiotics Association (2017). *Council for Responsible Nutrition*. Available online at: https://www.crnusa.org/sites/default/files/pdfs/CRN-IPA-Best-Practices-Guidelines-for-Probiotics.pdf (accessed May 10, 2021)

Jiang, H. P. (2009). Cytokine/Jak/Stat signaling mediates regeneration and homeostasis in the *Drosophila* midgut. *Cell* 137, 1343–1355. doi: 10.1016/j.cell.2009.05.014

Joint Food and Agriculture Organization/ World Health Organization Working Group (2002). *Joint FAO/WHO Working Group Report on Drafting Guidelines for the Evaluation of Probiotics in Food*. Geneva: World Health Organization.

Jungersen, M., Wind, A., Johansen, E., Christensen, J. E., Stuer-Lauridsen, B., and Eskesen, D. (2014). The science behind the probiotic strain Bifidobacterium animalis subsp. lactis BB-12. *Microorganisms* 2, 92–110. doi: 10.3390/microorganisms2020092

Kaddurah-Daouk, R., Baillie, R., Zhu, H., Zeng, Z., Wiest, M., Nguyen, U., et al. (2011). Enteric microbiome metabolites correlate with response to simvastatin treatment. *PLoS One* 6:e25482. doi: 10.1371/journal.pone.0025482

Kamareddine, L., Najjar, H., Umar Sohail, M., Abdulkader, H., and Al-Asmakh, M. (2020). The microbiota and gut-related disorders: insights from animal models. *Cells* 9:2401. doi: 10.3390/cells9112401

Karska-Wysocki, B., Bazo, M., and Smoragiewicz, W. (2010). Antibacterial activity of Lactobacillus acidophilus and Lactobacillus casei against methicillin-resistant Staphylococcus aureus (MRSA). *Microbiol. Res.* 165, 674–686. doi: 10.1016/j.micres.2009.11.008

Kim, M. J., Ku, S., Kim, S. Y., Lee, H. H., Jin, H., Kang, S., et al. (2018). Safety Evaluations of Bifidobacterium bifidum BGN4 and Bifidobacterium longum BORI. *Int. J. Mol. Sci.* 19:1422. doi: 10.3390/ijms19051422

Kluijfhout, S., Trieu, T., and Vandenplas, Y. (2020). Efficacy of the probiotic probiotical confirmed in acute gastroenteritis. *Pediatr. Gastroenterol. Hepatol. Nutr.* 23, 464–471. doi: 10.5223/pghn.2020.23.5.464

Kotowska, M., Albrecht, P., and Szajewska, H. (2005). Saccharomyces boulardii in the prevention of antibiotic-associated diarrhoea in children: a randomized double-blind placebo-controlled trial. *Alimentary Pharmacol. Therapeutics* 21, 583–590. doi: 10.1111/j.1365-2036.2005.02356.x

Koutsokali, M., and Valahas, M. (2020). Anaerobic and aerobic respiration in yeast: small-scale variations on a classic laboratory activity. *J. Chem. Educ.* 97, 1041–1047. doi: 10.1021/acs.jchemed.9b00994

Kovács, ÁT. (2019). Bacillus subtilis. *Trends Microbiol.* 27, 724–725. doi: 10.1016/j.tim.2019.03.008

Laukens, D., Brinkman, B. M., Raes, J., De Vos, M., and Vandenabeele, P. (2016). Heterogeneity of the gut microbiome in mice: guidelines for optimizing experimental design. *FEMS Microbiol. Rev.* 40, 117–132. doi: 10.1093/femsre/fuv036

Lepczyńska, M., and Dzika, E. (2019). The influence of probiotic bacteria and human gut microorganisms causing opportunistic infections on Blastocystis ST3. *Gut Pathogens* 11, 2–11. doi: 10.1186/s13099-019-0287-8

Ley, R. E. (2006). Ecological and evolutionary forces shaping microbial diversity in the human intestine. *Cell* 124, 837–848. doi: 10.1016/j.cell.2006.02.017

Lu, C., Sang, J., He, H., Wan, X. W., Lin, Y., Li, L., et al. (2016). Probiotic supplementation does not improve eradication rate of *Helicobacter pylori* infection compared to placebo based on standard therapy: a meta-analysis. *Nat. Sci. Rep.* 6:23522. doi: 10.1038/srep23522

Lu, Y. Z. (2019). Screening of intestinal peristalsis-promoting probiotics based on a zebrafish model. *Food Funct.* 10, 2075–2082. doi: 10.1039/c8fo02523a

Mack, D. R., Michail, S., Wei, S., McDougall, L., and Hollingsworth, M. A. (1999). Probiotics inhibit enteropathogenic E. coli adherence *in vitro* by inducing intestinal mucin gene expression. *Am. J. Physiol.* 276, G941–G950. doi: 10.1152/ajpgi.1999.276.4.G941

MacPherson, C. W. (2018). Gut bacterial microbiota and its resistome rapidly recover to basal state levels after short-term amoxicillin-clavulanic acid treatment in healthy adults. *Sci. Rep.* 8:11192. doi: 10.1038/s41598-018-29229-5

Mada, P. K., and Alam, M. U. (2020). *Clostridium Difficile*. Available online at: https://www.ncbi.nlm.nih.gov/books/NBK431054 (accessed December 15, 2020)

Madigan, M. T. (2018). *Brock Biology of Microorganisms*. London: Pearson.

Mann, E. R., Landy, J. D., Bernardo, D., Peake, S. T., Hart, A. L., Al-Hassi, H. O., et al. (2013). Intestinal dendritic cells: their role in intestinal inflammation, manipulation by the gut microbiota and differences between mice and men. *Immunol. Lett.* 150, 30–40. doi: 10.1016/j.imlet.2013.01.007

Matuskova, Z., Anzenbacherova, E., Vecera, R., Tlaskalova-Hogenova, H., Kolar, M., and Anzenbacher, P. (2014). Administration of a probiotic can change drug pharmacokinetics: effect of E. coli Nissle 1917 on amidarone absorption in rats. *PLoS One* 9:e87150. doi: 10.1371/journal.pone.0087150

McCullough, M. J., Clemons, K. V., McCusker, J. H., and Stevens, D. A. (1998). Species identification and virulence attributes of Saccharomyces boulardii (nom. inval.). *J. Clin. Microbiol.* 36, 2613–2617. doi: 10.1128/JCM.36.9.2613-2617.1998

McFarland, L. (1996). Saccharomyces boulardiiIs Not Saccharomyces cerevisiae. *Clin. Infect. Dis.* 22, 200–201. doi: 10.1093/clinids/22.1.200

McFarland, L. (1998). Epidemiology, risk factors and treatments for antibiotic-associated diarrhea. *Dig. Dis.* 16, 292–307. doi: 10.1159/000016879

McFarland, L. V. (2006). Meta-analysis of probiotics for the prevention of antibiotic associated diarrhea and the treatment of Clostridium difficile disease. *Am. J. Gastroenterol.* 101, 812–822. doi: 10.1111/j.1572-0241.2006.00465.x

McFarland, L. V. (2007). Diarrhoea associated with antibiotic use. *BMJ (Clin. Res. ed.)* 335, 54–55. doi: 10.1136/bmj.39255.829120.47

Metchnikoff, É (1907). *The Prolongation of Life: Optimistic Studies. (P. Chalmers Mitchell, Trans.)*. New York, NY: Springer.

Metras, B. N. (2020). Assessment of commercial companion animal kefir products for label accuracy of microbial composition and quantity. *J. Anim. Sci.* 98:skaa301. doi: 10.1093/jas/skaa301

Metras, B. N., Holle, M. J., Parker, V. J., Miller, M. J., and Swanson, K. S. (2021). Commercial kefir products assessed for label accuracy of microbial composition and density. *JDS Comms.* 2, 87–91. doi: 10.3168/jdsc.2020-0056

Mills, J. P. (2018). Probiotics for prevention of Clostridium difficile infection. *Curr. Opin. Gastroenterol.* 34, 3–10. doi: 10.1097/MOG.0000000000000410

Mohsin, M., Guenther, S., Schierack, P., Tedin, K., and Wieler, L. H. (2015). Probiotic *Escherichia coli* Nissle 1917 reduces growth, Shiga toxin expression, release and thus cytotoxicity of enterohemorrhagic *Escherichia coli*. *Int. J. Med. Microbiol.* 305, 20–26. doi: 10.1016/j.ijmm.2014.10.003

National Institutes of Health, National Center for Complementary and Integrative Health (2021). *Probiotics: What You Need To Know*. Bethesda, MD: National Institutes of Health.

National Institutes of Health (2019). *Probiotics Fact Sheet for Consumer*. Bethesda, MD: National Institutes of Health.

National Institutes of Health, Office of Dietary Supplements (1994). *Dietary Supplement Health and Education Act of 1994 Public Law 103-417 103rd Congress*. Available online at: https://ods.od.nih.gov/about/dshea_wording.aspx#sec3 (accessed May 7, 2021).

Natividad, J. M., and Verdu, E. F. (2013). Modulation of intestinal barrier by intestinal microbiota: pathological and therapeutic implications. *Pharmacol. Res.* 69, 42–51. doi: 10.1016/j.phrs.2012.10.007

Neu, J., and Walker, W. A. (2011). Necrotizing enterocolitis. *N. Engl. J. Med.* 364, 255–264. doi: 10.1056/NEJMra1005408

Ng, K. M.-D. (2019). Recovery of the gut microbiota after antibiotics depends on host diet, community context, and environmental reservoirs. *Cell Host Microbe* 26, 650–665.e4. doi: 10.1016/j.chom.2019.10.011

Noah, T. K., Donahue, B., and Shroyer, N. F. (2011). Intestinal development and differentiation. *Exp. Cell Res.* 317, 2702–2710. doi: 10.1016/j.yexcr.2011.09.006

Oehlers, S. H. (2011). A chemical enterocolitis model in zebrafish larvae that is dependent on microbiota and responsive to pharmacological agents. *Dev. Dyn.* 240, 288–298. doi: 10.1002/dvdy.22519

Ohland, C. L., and Macnaughton, W. K. (2010). Probiotic bacteria and intestinal epithelial barrier function. *Am. J. Physiol. Gastrointest Liver Physiol.* 298, G807–G819.

Ouyang, J. I. (2020). Treating From the Inside Out: Relevance of Fecal Microbiota Transplantation to Counteract Gut Damage in GVHD and HIV Infection. *Front. Med. (Lausanne)* 7:421. doi: 10.3389/fmed.2020.00421

Pavan, S., Desreumaux, P., and Mercenier, A. (2003). Use of mouse models to evaluate the persistence, safety, and immune modulation capacities of lactic acid bacteria. *Clin. Diagn Lab Immunol.* 10, 696–701. doi: 10.1128/cdli.10.4.696-701.2003

Pothoulakis, C. (2009). Review article: anti-inflammatory mechanisms of action of Saccharomyces boulardii. *Alimentary Pharmacol. Therapeutics* 30, 826–833. doi: 10.1111/j.1365-2036.2009.04102.x

Preston, K., Krumian, R., Hattner, J., Montigny, D., Stewart, M., and Gaddam, S. (2018). Lactobacillus acidophilus CL1285, Lactobacillus casei LBC80R and Lactobacillus rhamnosus CLR2 improve quality-of-life and IBS symptoms: a double-blind, randomised, placebo-controlled study. *Benef. Microbes* 9, 697–706.

Probiotics Market Size Share and Trends Analysis Report By Product (2019). *Grand View Research*. Available online at: https://www.grandviewresearch.com/press-release/global-probiotics-market (accessed January 21, 2021)

Rawls, J. F. (2006). Reciprocal gut microbiota transplants from zebrafish and mice to germ-free recipients reveal host habitat selection. *Cell* 127, 423–433. doi: 10.1016/j.cell.2006.08.043

Reid, G. (2010). The potential role for probiotic yogurt for people living with HIV/AIDS. *Gut Microbes* 1, 411–414. doi: 10.4161/gmic.1.6.14079

Reid, G., Gadir, A., and Dhir, R. (2019). Probiotics: reiterating what they are and what they are not. *Front. Microbiol.* 10:424. doi: 10.3389/fmicb.2019.00424

Rieko, M., Osamu, H., Yosuke, S., Atsushi, M., and Yuji, N. (2020). Effectiveness of including probiotics to *Helicobacter* pylori eradication therapies. *J. Clin. Biochem. Nutr.* 67, 102–104.

Ringel-Kulka, T., Palsson, O., Maier, D., Carroll, I., Galanko, J., Leyer, G., et al. (2015). *Clinical trial: Probiotic Bacteria Lactobacillus acidophilus NCFM and Bifidobacterium lactis Bi-07 Versus Placebo for the Symptoms of Bloating in Patients with Functional Bowel Disorders*. Bethesda, MD: National Center for Biotechnology Information.

Roberts, T., Ellis, J., Harkness, J., Marriott, D., and Stark, D. (2014). Treatment failure in patients with chronic Blastocystis infection. *J. Med. Microbiol.* 63, 252–257. doi: 10.1099/jmm.0.065508-0

Saavedra, J. M., Bauman, N. A., Perman, J. A., Yolken, R. H., and Oung, I. (1994). Feeding of Bifidobacterium bifidum and Streptococcus thermophilus to infants in hospital for prevention of diarrhoea and shedding of rotavirus. *Lancet* 344, 1046–1049. doi: 10.1016/s0140-6736(94)91708-6

Sahota, S. S., Bramley, P. M., and Menzies, I. S. (1982). The fermentation of lactulose by colonic bacteria. *J. Gen. Microbiol.* 128, 319–325. doi: 10.1099/00221287-128-2-319

Salminen, M., Tynkkynen, S., Rautelin, H., Poussa, T., Saxelin, M., Ristola, M., et al. (2004). The efficacy and safety of probiotic Lactobacillus rhamnosus GG on prolonged, noninfectious diarrhea in HIV Patients on antiretroviral therapy: a randomized, placebo-controlled, crossover study. *HIV Clin. Trials* 5, 183–191.

Sandra, M., and Tallent, A. K. (2020). *Bacteriological Analytical Manual (BAM) Chapter 14: Bacillus Cereus*. Silver Spring, MA: Food and Drug Administration.

Saxelin, M. (2008). Probiotic formulations and applications, the current probiotics market, and changes in the marketplace: a European perspective. *Clin. Infect. Dis.* 46, S144–S151. doi: 10.1086/523337

Schaik, W. V. (2015). The human gut resistome. *Philos Trans. R. Soc. Lond B Biol. Sci.* 370, e1–e9. doi: 10.1098/rstb.2014.0087

Sekar, U., and Shanthi, M. (2013). Blastocystis: consensus of treatment and controversies. *Trop. Parasitol.* 3, 35–39. doi: 10.4103/2229-5070.113901

Sender, R., Fuchs, S., and Milo, R. (2016). Are we really vastly outnumbered? Revisiting the ratio of bacterial to host cells in humans. *Cell* 164, 337–340. doi: 10.1016/j.cell.2016.01.013

Shelby, R., Janzow, G., Mashburn-Warren, L., Galley, J., Tengberg, N., Navarro, J., et al. (2020). A novel probiotic therapeutic in a murine model of Clostridioides difficile colitis. *Gut Microbes* 12:1814119. doi: 10.1080/19490976.2020

Shu, Z., Tian, Z., Chen, J., Ma, J., Abudureyimu, A., Qian, Q., et al. (2018). HIV/AIDS-related hyponatremia: an old but still serious problem. *Ren. Fail.* 40, 68–74.

Sichetti, M., Marco, S. D., Pagiotti, R., Traina, G., and Pietrella, D. (2018). Anti-inflammatory effect of multistrain probiotic formulation (L. rhamnosus. B. lactis, and B. longum). *Nutrition* 53, 95–102. doi: 10.1016/j.nut.2018.02.005

Silverman, M. A., Konnikova, L., and Gerber, J. S. (2017). Impact of antibiotics on necrotizing enterocolitis and antibiotic-associated diarrhea. *Gastroenterol. Clin. North Am.* 46, 61–76.

Sinclair, J. B. (2016). Blastocystis hominis: the fascinating enigma. *Aust. J. Med. Sci.* 37, 3–4.

Sniffen, J. C., McFarland, L. V., Evans, C. T., and Goldstein, E. J. (2018). Choosing an appropriate probiotic product for your patient: an evidence-based practical guide. *PLoS One* 13:e0209205. doi: 10.1371/journal.pone.0209205

Sonnenborn, U. (2016). *Escherichia coli* strain Nissle 1917-from bench to bedside and back: history of a special *Escherichia coli* strain with probiotic properties. *FEMS Microbiol. Lett.* 363:fnw212. doi: 10.1093/femsle/fnw212

Sougioultzis, S., Simeonidis, S., Bhaskar, K., Chen, X., Anton, P., Keates, S., et al. (2006). Saccharomyces boulardii produces a soluble anti-inflammatory factor that inhibits NF-kappaB-mediated IL-8 gene expression. *Natl. Library Med.* 343, 69–76. doi: 10.1016/j.bbrc.2006.02.080

Srinivasan, R., Meyer, R., Padmanabhan, R., and Britto, J. (2006). Clinical safety of Lactobacillus casei shirota as a probiotic in critically ill children. *J. Pediatr. Gastroenterol. Nutr.* 42, 171–173.

Stamps, J. A.-M. (2012). *Drosophila* regulate yeast density and increase yeast community similarity in a natural substrate. *PLoS One* 7:e42238. doi: 10.1371/journal.pone.0042238

Sun, Q., Liang, X., Zheng, Q., Gu, W., Liu, W., Xiao, S., et al. (2010). Resistance of *Helicobacter* pylori to antibiotics from 2000 to 2009 in Shanghai. *World J. Gastroenterol.* 16, 5118–5121.

Surawicz, C., McFarland, L., Greenberg, R., Rubin, M., Fekety, R., Mulligan, M., et al. (2000). The search for a better treatment for recurrent Clostridium difficile disease: use of high-dose vancomycin combined with Saccharomyces boulardii. *Clin. Infect. Dis.* 31, 1012–1017. doi: 10.1086/318130

Surawicz, C. M., Elmer, G. W., Speelmen, P., McFarland, L. V., Chinn, J., and Van Belle, G. (1989). Prevention of antibiotic-associated diarrhea by Saccharomyces boulardii: a prospective study. *Gastroenterology* 96, 981–988. doi: 10.1016/0016-5085(89)91613-2

Swansan, H. (2015). Drug metabolism by the host and gut microbiota: a partnership. *Drug Metab. Dispos.* 43, 1499–1504. doi: 10.1124/dmd.115.065714

Talwalkar, A., Kailasapathy, K., Peiris, P., and Arumungaswamy, R. (2001). Application of RBGR - a simple way for screening of oxygen tolerance in probiotic bacteria. *Int. J. Food Microbiol.* 71, 245–248. doi: 10.1016/S0168-1605(01)00563-3

Tarr, G. C.-A. (2019). Performance of stool-testing recommendations for acute gastroenteritis when used to identify children with 9 potential bacterial enteropathogens. *Clin. Infect. Dis. Official Publ. Infect. Dis. Soc. Am.* 69, 1173–1182. doi: 10.1093/cid/ciy1021

Trinder, M. D. (2017). Drosophila melanogaster as a high-throughput model for host-microbiota interactions. *Front. Microbiol.* 8:751. doi: 10.3389/fmicb.2017.00751

U.S. Food and Drug Administration (2014). *Types of Applications*. Silver Spring, MD: Food and Drug Administration.

U.S. Food and Drug Administration (2017). *The FDA's Drug Review Process: Ensuring Drugs Are Safe and Effective*. Silver Spring, MD: Food and Drug Administration.

U.S. Food and Drug Administration (2019). *Questions and Answers on Dietary Supplements*. Silver Spring, MD: Food and Drug Administration.

U.S. Food and Drug Administration (2020). *New Dietary Ingredients in Dietary Supplements - Background for Industry*. Silver Spring, MD: Food and Drug Administration.

U.S. Food and Drug Administration; National Institute of Health, National Institute of Allergy and Infectious Diseases (2018). *Science and Regulation of Live Microbiome-based Products used to Prevent, Treat, and Cure Disease in Humans*. Available online at: https://www.fda.gov/media/128302/download (accessed May 7, 2021)

Valente, G., Acurcio, L., Freitas, L., Nicoli, J., Silva, A., Souza, M., et al. (2019). Short communication: *In vitro* and *in vivo* probiotic potential of Lactobacillus

plantarum B7 and Lactobacillus rhamnosus D1 isolated from Minas artisanal cheese. *J. Dairy Sci.* 102, 5957–5961. doi: 10.3168/jds.2018-15938

Vanderhoof, J. A., and Young, R. (2008). Probiotics in the United States. *Clin. Infect. Dis.* 46(Suppl 2:S67-72), S144–S151. doi: 10.1086/523339

Vecchio, A. L., Guandalini, S., and Guarino, A. (2015). Probiotics for prevention and treatment of diarrhea. *J. Clin. Gastroenterol.* 49, S37–S45. doi: 10.1097/MCG.0000000000000349

Venugopalan, V., Shriner, K. A., and Wong-Beringer, A. (2010). Regulatory oversight and safety of probiotic use. *Emerg. Infect. Dis.* 16, 1661–1665. doi: 10.3201/eid1611.100574

Villar-García, J. G.-F. (2017). Impact of probiotic Saccharomyces boulardii on the gut microbiome composition in HIV-treated patients: a double-blind, randomised, placebo-controlled trial. *PLoS One* 12:e0173802. doi: 10.1371/journal.pone.0173802

Vitetta, L., Saltzman, E. T., Nikov, T., Ibrahim, I., and Hall, S. (2016). Modulating the gut micro-environment in the treatment of intestinal parasites. *J. Clin. Med.* 5:102. doi: 10.3390/jcm5110102

Wang, L., Cao, H., Liu, L., Wang, B., Walker, W. A., Acra, S. A., et al. (2014). Activation of epidermal growth factor receptor mediates mucin production stimulated by p40, a lactobacillus rhamnosus GG-derived Protein. *J. Bio. Chem.* 289, 20234–20244. doi: 10.1074/jbc.M114.553800

Wang, T. D. (2020). Probiotics modulate intestinal motility and inflammation in Zebrafish models. *Zebrafish* 17, 382–393. doi: 10.1089/zeb.2020.1877

Wawrzyniak, I., Poirier, P., Viscogliosi, E., Dionigia, M., Texier, C., Delbac, F., et al. (2013). Blastocystis, an unrecognized parasite: an overview of pathogenesis and diagnosis. *Therapeutic Adv. Infect. Dis.* 1, 167–178. doi: 10.1177/2049936113504754

Whaling, M. A. (2012). Perceptions about probiotic yogurt for health and nutrition in the context of HIV/AIDS in Mwanza, Tanzania. *J. Health Popul. Nutr.* 30, 31–40. doi: 10.3329/jhpn.v30i1.11273

Xiao, L. F. (2015). A catalog of the mouse gut metagenome. *Nat. Biotechnol.* 33, 1103–1108. doi: 10.1038/nbt.3353

Xiong, T., Maheshwari, A., Neu, J., Ei-Saie, A., and Pammi, M. (2020). An overview of systematic reviews of randomized-controlled trials for preventing necrotizing enterocolitis in preterm infants. *Neonatology* 117, 46–56. doi: 10.1159/000504371

Yason, J. A. (2019). Interactions between a pathogenic Blastocystis subtype and gut microbiota: *in vitro* and *in vivo* studies. *Microbiome* 7:30. doi: 10.1186/s40168-019-0644-3

Yeung, P. S. (2012). Species-specific identification of commercial probiotic strains. *J. Dairy Sci.* 85, 1039–1051. doi: 10.3168/jds.S0022-0302(02)74164-7

Yoo, D., Kim, I., Van Le, T., Jung, I., Yoo, H., and Kim, D. (2014). Gut microbiota-mediated drug interactions between lovastatin and antibiotics. *Drug Metab. Dispos.* 42, 1508–1513. doi: 10.1124/dmd.114.058354

Yoon, M. Y., and Yoon, S. S. (2018). Disruption of the gut ecosystem by antibiotics. *Yonsei Med. J.* 59, 4–12.

Young, V. B., Dieterle, M. G., and Rao, K. (2018). Novel therapies and preventative strategies for primary and recurrent Clostridium difficile infections. *Ann. N. Y. Acad. Sci.* 1435, 110–138. doi: 10.1111/nyas.13958

Zbinden, R. (1999). Inhibition of Saccharomyces boulardii (nom. inval.) on cell invasion of *Salmonella* typhimurium and Yersinia enterocolitica. *Micro Ecol. Health* 44, 158–162. doi: 10.1080/089106099435736

Zhang, J., Zhang, J., and Wang, R. (2018). Gut microbiota modulates drug pharmacokinetics. *Drug Metab. Rev.* 50, 357–368. doi: 10.1080/03602532.2018.1497647

Zhang, Z. T. (2019). emystifying the manipulation of host immunity, metabolism, and extraintestinal tumors by the gut microbiome. *Signal Transduct Target Ther.* 4:41. doi: 10.1038/s41392-019-0074-5

Zollner-Schwetz, I., and Krause, R. (2015). Therapy of acute gastroenteritis: role of antibiotics. *Clin. Microbiol. Infect.* 21, 744–749. doi: 10.1016/j.cmi.2015.03.002

Author Disclaimer: The views expressed herein are those of the authors and do not reflect the position of the United States Military Academy, the Department of the Army, or the Department of Defense.

Conflict of Interest: The authors declare that the research was conducted in the absence of any commercial or financial relationships that could be construed as a potential conflict of interest.

Publisher's Note: All claims expressed in this article are solely those of the authors and do not necessarily represent those of their affiliated organizations, or those of the publisher, the editors and the reviewers. Any product that may be evaluated in this article, or claim that may be made by its manufacturer, is not guaranteed or endorsed by the publisher.

frontiers in Microbiology

ORIGINAL RESEARCH
published: 16 September 2021
doi: 10.3389/fmicb.2021.723187

Bacillus subtilis DSM29784 Alleviates Negative Effects on Growth Performance in Broilers by Improving the Intestinal Health Under Necrotic Enteritis Challenge

Yuanyuan Wang[1], Yibin Xu[1], Shengliang Xu[2], Jinyong Yang[3], Kaiying Wang[1]* and Xiuan Zhan[1]**

[1]Institute of Feed Science, College of Animal Sciences, Zhejiang University, Hangzhou, China, [2]Haiyan Animal Husbandry and Veterinary Bureau, Haiyan, China, [3]Zhejiang Animal Husbandry Technology Extension and Livestock and Poultry Monitoring Station, Hangzhou, China

OPEN ACCESS

Edited by:
Corine Sandström, Swedish University of Agricultural Sciences, Sweden

Reviewed by:
Shiyu Tao, Huazhong Agricultural University, China
Tarique Hussain, Nuclear Institute for Agriculture and Biology, Pakistan

***Correspondence:**
Xiuan Zhan
xazan@zju.edu.cn
Jinyong Yang
vineus425@hotmail.com
Kaiying Wang
zjuwky@zjuedn.cn

Specialty section:
This article was submitted to Food Microbiology, a section of the journal Frontiers in Microbiology

Received: 10 June 2021
Accepted: 05 August 2021
Published: 16 September 2021

Citation:
Wang Y, Xu Y, Xu S, Yang J, Wang K and Zhan X (2021) Bacillus subtilis DSM29784 Alleviates Negative Effects on Growth Performance in Broilers by Improving the Intestinal Health Under Necrotic Enteritis Challenge. Front. Microbiol. 12:723187. doi: 10.3389/fmicb.2021.723187

Along with banning antibiotics, necrotic enteritis (NE), especially subclinical enteritis (SNE), poses a significant threat to the chicken industry; however, probiotics are a potentially promising intervention. We aimed to investigate the beneficial effects of *Bacillus subtilis* DSM29784 (BS) on the treatment of *Clostridium perfringens* (CP)-induced SNE in broilers. A total of 360 1-day-old broiler chicks were divided into three treatment groups, namely control (Ctr), SNE, and BS treatment (BST) groups, all of which were fed with a basal died for 21 days, and then from day 22 onward, only the BST group had a BS supplemented diet (1×10^9 colony-forming units BS/kg). On day 15, all chicks, except the Ctr group, were challenged with a 20-fold dose coccidiosis vaccine and 1 ml CP (2×10^8) on days 18–21 for SNE induction. Beneficial effects were observed on growth performance in BST compared to SNE broilers. BST treatment alleviated intestinal lesions and increased the villus height/crypt depth ratio. Further, BST broilers showed increased maltase activity in the duodenum compared with SNE chicks, and a significantly decreased caspase-3 protein expression in the jejunum mucosa. Moreover, an increased abundance of *Ruminococcaceae* and *Bifidobacterium* beneficial gut bacteria and an altered gut metabolome were observed. Taken together, we demonstrate that the manipulation of microbial gut composition using probiotics may be a promising prevention strategy for SNE by improving the composition and metabolism of the intestinal microbiota, intestinal structure, and reducing inflammation and apoptosis. Hence, BS potentially has active ingredients that may be used as antibiotic substitutes and effectively reduces the economic losses caused by SNE. The findings of this study provide a scientific foundation for BS application in broiler feed in the future.

Keywords: performance, broilers, subclinical necrotic enteritis, *Bacillus subtilis* DSM29784, microbiota, metabolome

INTRODUCTION

Necrotic enteritis (NE) is an enteric disease with a significant economic burden, in terms of mortality and welfare, on the poultry industry, especially in broiler chickens in China (Wu et al., 2012; Gu et al., 2019; Khan et al., 2021). The causative agent of NE is *Clostridium perfringens* (CP), a ubiquitous Gram-positive bacterium that produces spores and highly potent toxins (Gohari et al., 2021). Clinical NE is characterized by high mortality in poultry, while subclinical NE (SNE), which is becoming more prevalent, is mainly characterized by intestinal mucosal damage without clinical signs or mortality (Rajput et al., 2020). In addition, SNE causes wet litter (Williams, 2005) and possible contamination of poultry products for human consumption (Villagran-de la Mora et al., 2020). Gastrointestinal tract infections are believed to cause annual losses of 2–6 billion USD to the global poultry industry (Dahiya et al., 2006). However, microbial-based therapy improved the economic benefit of broilers with NE (Sallam et al., 2021).

Antibiotics are commonly used as growth promoters and for prophylaxis of SNE (Prescott et al., 2016). Residues of these antibiotics in poultry products have harmful effects on human health, such as antibiotic resistance (Bani-Asadi et al., 2021). However, antibiotics have been banned as feed additives in China and many other regions; in the absence of antibiotics alternatives, chickens raised under current intensive production systems face a higher risk of enteric pathogen infection (Lee et al., 2015). Clostridial diseases in poultry, such as NE, have once again become a disease of worldwide economic importance, and hence identifying antibiotic alternatives for disease control in poultry remains essential.

Currently, probiotics are the most extensively used alternatives to enhance growth and improve health in poultry production (Hofacre et al., 2018; Rodrigues et al., 2018). Probiotics are live microbial supplements that confer health benefits to the host when administered in adequate amounts (Alagawany et al., 2018). Studies have shown that probiotics favor intestinal health and the production performance of broilers by exerting beneficial effects on intestinal morphology, microflora, nutrient absorption, antioxidative capacity, and immune response (Wang et al., 2017b; Chen et al., 2018; Rodjan et al., 2018; Wu et al., 2019). Therefore, management of poultry gut health is an important strategy for maintaining productivity in the post-antibiotic era. The use of probiotics is one such strategy that has gained attention over recent years (Shini and Bryden, 2021) with accumulating evidence showing that probiotics have a significant effect in preventing NE (Caly et al., 2015; Li et al., 2017b; Khalique et al., 2020; Zhao et al., 2020). Among the various bacterial species used as probiotics, *Bacillus* spp. strains are the most promising feed supplements for poultry due to their spores exhibiting health-promoting benefits, as well as having the capacity to survive harsh environmental conditions, such as the high temperatures used in the pelleting process and the low pH in the gastrointestinal tract (Shivaramaiah et al., 2011). *Bacillus* spores improve gut health by competitive exclusion, production of antimicrobial peptides and beneficial metabolites, and stimulation of the intestinal immune system (Hayashi et al., 2018). *B. subtilis*, which has a broad activity against Clostridium spp., and improves overall performance in broilers (Jayaraman et al., 2013).

The interface of the immune system and metabolism is an emerging field of research (Liu et al., 2021). Metabolomics is an effective method for describing the global metabolism of living organisms and capturing the metabolic changes associated with external stimuli (Zhang et al., 2017). Generally, host and their intestinal microorganisms form the host–microbial–metabolic axis, whereas the normal microflora in the gut can metabolize ingested and endogenous macromolecular carbohydrates such as proteins and fatty acids. In addition, microorganisms interact with the metabolism of organisms to produce various metabolites such as short-chain fatty acids, amino acids, and peptides. These metabolites play a vital role in the immune homeostasis of intestinal tissues, and even the whole body (Li et al., 2011; Duca et al., 2014). Therefore, an integrated immuno-metabolic approach can identify potential therapeutic targets. Previous studies have demonstrated that *B. subtilis* DSM29784 (BS) can improve the growth performance and gut health in turkeys (Mohammadigheisar et al., 2019). We have previously reported that supplementary probiotic BS could be used as an alternative to antibiotics for broiler chickens, by decreasing the feed conversion rate and improving intestinal health (Wang et al., 2021). However, reports on the effects of BS supplementation on the treatment of SNE broilers are scarce. Therefore, the aims of this study were to investigate the effects of BS supplementation as a treatment on the growth performance and the composition, and metabolism, of the intestinal microbiota, intestinal structure of broiler chickens following CP challenge, and determine whether BS supplementation reduces poor growth performance caused by CP in broiler chickens.

Abbreviations: ABC, ATP-binding cassette; ADFI, Average daily feed intake; ADG, Average daily gain; BCA, Bicinchoninic acid; BS, *Bacillus subtilis* DSM 29784; BST, BS treatments groups; BW, Body weight; CAT, Catalase; cfu, Colony-forming units; CP, *Clostridium perfringens*; ELISA, Enzyme-linked immunosorbent assay; F:G, Feed: gain ratio; GSH-Px, Glutathione peroxidase; H&E, Haematoxylin and eosin; HRP, Horse radish peroxidase; IFN-γ, Interferon-gamma; IgG, Immunoglobulin G; IL, Interleukin; KEGG, Kyoto Encyclopedia of Genes and Genomes; LDA, Linear discriminant analysis; MDA, Malondialdehyde; MUC2, Mucin 2; NE, Necrotic enteritis; PBS, Phosphate-buffered saline; PBST, Phosphate-Buffered Saline Tween; PCA, Principal component analysis; PCR, Polymerase chain reaction; SEM, Scanning electron microscopy; sIgA, Secretory immunoglobulin A; SNE, Subclinical necrotic enteritis; SOD, Superoxide dismutase; SPSS, Statistical Product and Service Solutions; TEM, Transmission electron microscopy; TMB, Tetramethy1 benzidine; TNF-α, Tumor necrosis factor α; VIP, Variable importance in projection.

MATERIALS AND METHODS

All procedures herein were conducted in accordance with the Chinese Guidelines for Animal Welfare and approved by the Zhejiang University Institutional Animal Care and Use Committee (Permission number: ZJU2019-480-12).

Probiotic Bacterial Culture and Powder Preparation

The probiotic *B. subtilis* DSM29784 strain (BS) used in this study was presented by the Chinese Academy of Sciences

(Beijing, China). Bacteria were cultured overnight in Luria–Bertani broth (Solarbio, No. L1010, Beijing, China) at 180 rpm in a shaking incubator (Jiecheng, Shanghai, China) at 37°C and were then pelleted by centrifugation at 5,000 × *g* for 10 min at 4°C. The pellets were then washed twice with sterile phosphate buffer saline (PBS; pH 7.3; Aladdin, Shanghai, China), resuspended in skim milk powder (Devondale, Australia), and diluted to the final concentration of 2×10^9 cfu/g.

Experimental Design and Bird Husbandry

A total of 360 1-day-old Lingnan Yellow broiler chicks with similar body weight were purchased from Xingjian hatchery (Jiaxing, China). Chicks were weighted and divided into 3 treatment groups. Each group consisted of 6 replicates with 20 birds (10 males and 10 females) per replicate with a total of 18 floor pens (area of 2 m × 4 m) covered with fresh wood shavings. The temperature was maintained at 32–34°C for the first 3 days and then reduced by 2–3°C per week, to a final temperature of 26°C with a humidity of 60–65%. Birds were given *ad libitum* access to water and food throughout the experiment (63 days) and were kept under full light for the first 3 days, and then changed to light–dark (2 Light–Dark) cycle. Chicks were fed with diets in pellet form as follows: negative control group (Ctr), positive control group (SNE), and BS treatment group (BST) fed with a basal died for 21 days and then, from day 22 onward, only the BST group had a BS (1×10^9 colony-forming units BS/kg) supplemented diet. The composition and nutrient concentration of the basal diet are listed in **Table 1**.

TABLE 1 | Composition and nutrient level of the basal diet used in different phases of trial (% as fed basis).

Ingredients, %	Starter (1–21 days)	Grower (22–42 days)	Finisher (43–63 days)
Corn	62.50	67.50	75.00
Soybean meal	31.00	23.50	14.50
CPM[c]	2.00	4.00	5.00
Soybean oil	0.50	1.00	1.50
NaCl	0.30	0.30	0.30
$CaHPO_4$	1.20	1.00	0.80
Limestone	1.50	1.30	1.20
Zeolite	-	0.40	0.70
Premix[a]	1.00	1.00	1.00
Total	100.00	100.00	100.00
Nutrient levels[b] (%)			
ME (MJ/kg)	12.22	12.59	12.97
CP	21.09	19.16	16.07
Lys	1.09	0.99	0.87
Met	0.49	0.38	0.35
Met+Cys	0.87	0.73	0.65
Calcium	0.90	0.85	0.69
Total phosphorus	0.58	0.52	0.45

[a]*The Premix provides per kg of diet: Fe 80 mg, Cu 8 mg, Zn 60 mg, Mn 80 mg, I 0.35 mg, Se 0.15 mg, V_A 9,600 IU, V_{D3} 1,500 IU, V_E 20 mg, V_{k3} 1 mg, V_{B1} 2.2 mg, V_{B2} 4.2 mg, V_{B6} 4.2 mg, V_{B12} 0.012 mg, nicotinamide 42 mg, D-calcium pantothenate 12 mg, folic acid 1.0 mg, D-biotin 0.18 mg, and choline 800 mg.*

[b]*ME is a calculated value; other nutrient levels are measured values.*

[c]*CPM is corn gluten meal.*

Clostridium perfringens Culture and Coccidiosis Vaccine

The *C. perfringens* type-A strain (American Type Culture Collection 13124) was obtained from the Guangdong Microbial Culture Collection Center (Guangzhou, China). The strain was aseptically inoculated into Reinforced Clostridial Medium (Guangdong HuanKai Microbial Sci. & Tech. Co., Ltd., Guangdong, China) overnight at 37°C in an anaerobic environment before being used for the challenge. The live coccidiosis quadrivalent vaccine for chickens (Eimeria tenella strain PTMZ, E. necatrix strain PNHZ, E. maxima strain PMHY, and E. acervulina strain PAHY) was provided by Foshan Zhengdian Biotechnology Co., Ltd. (Guangdong, China).

Subclinical Necrotic Enteritis Broiler Model

SNE was induced in broilers as previously described (Wu et al., 2018) with minor modifications. Briefly, prior to SNE challenge (day 14), birds were given sufficient water, but no food was provided overnight. On day 15, the SNE-challenged and BST groups received 20 times more concentrated than usual per bird by oral gavage. The birds in each group were then gavaged with 1 ml of *C. perfringens* (2×10^8 cfu/ml) on days 18–21, and the food was cut off overnight but water was provided before each challenge. Meanwhile, the birds in the Ctr group received equivalent sterile PBS instead at day 15, and 1 ml of sterile Reinforced Clostridium Medium (Guangdong HuanKai Microbial Sci. &Tech. Co., Ltd.) was administered daily on days 18–21. Samples were harvested on days 28 and 35.

Measurement of Growth Performance and Harvesting Samples

Feed intake and body weight (BW) of broilers was measured per replicate as the unit on days 1, 21, 42, and 63. Mortality was monitored daily; dead birds were recorded and weighed to adjust the estimates of gain, intake, and feed conversion ratios as appropriate. The average daily gain, average daily feed intake (ADFI), and feed: gain ratio (F:G) were calculated.

On days 28 and 35, 12 birds (2 birds per replicate) from each group were randomly selected and weighed after withdrawing feed, but still providing fresh water, for 12 h. The chicks were electrically stunned, exsanguinated, and dissected by a trained team who harvested tissue samples. First, the small intestine from each bird was removed, opened, and scored for intestinal lesions, by the same trained observer, using the following scale: 0, no gross lesions; 1, thin, friable small intestine; 2, focal necrosis, ulceration, or both; 3, patchy necrosis; and 4, severe, extensive mucosal necrosis (Johnson and Reid, 1970). The average score was computed per pen, and the pen was the experimental unit for lesion scoring. Following this, 0.5 cm of the upper jejunum wall was fixed in 25% glutaraldehyde (pH 74; Aladdin, Shanghai, China) and 4% paraformaldehyde (Aladdin, Shanghai, China), respectively, and the mucosa of the remaining jejunum, and the middle segments of the duodenum were gently scraped. The upper portion of the cecum was then tied with a string and snap-frozen in liquid nitrogen. In addition, the contents of the cecum were gently scraped with a blade and stored at – 80°C until analysis.

Duodenal and jejunal mucosa samples (1 g) were homogenized in 9 ml of 0.9% sterile saline (Aladdin, Shanghai, China) on ice and centrifuged at 3,000 × *g* for 15 min at 4°C. The total protein concentration of the supernatant was measured using a Pierce™ bicinchoninic acid (BCA, No. A045-4-2) Protein Assay Kit, according to the manufacturer's protocol (Thermo Fisher Scientific). The prepared supernatant was stored at –80°C and used for test.

Jejunum Morphology

At necropsy, jejunal tissue samples were harvested and fixed in 4% paraformaldehyde (No. BL539A, Biosharp, Beijing, China), dehydrated, and processed into paraffin sections according to a standard procedure (Wu et al., 2019). Paraffin sections were then subjected to hematoxylin and eosin staining (H&E; Google Bio, Wuhan, China) staining for histopathological analysis (Xu et al., 2018) Transmission electron microscopy (Wang et al., 2018) and scanning electron microscopy (SEM; Hu et al., 2018) of the jejunal tissue were conducted according to previous studies.

Histomorphological Measurements of the Jejunum

Morphometric measurements of jejunal villi were performed at 40× magnification using a light microscope (Precise, Beijing, China). The criterion for villus selection was based on the presence of an intact lamina propria. Villi length was measured from the tip of the villus to the villus-crypt junction; whereas crypt depth was defined as the depth of the invagination between adjacent villi (Awad et al., 2009).

Total RNA Extraction and Quantitative Real-Time PCR

Based on a previously described methods (Wang et al., 2019), RNA was extracted from the intestinal mucosa using RNAiso Plus reagent (No. RR047A, TaKaRa Bio, Kusatsu, Japan) according to the manufacturer's instructions. Complementary DNA (cDNA) was synthesized from 1 μg of total RNA using M-MLV reverse transcriptase (No. RR420A, TaKaRa Bio) according to the manufacturer's instructions. Transcriptional changes were then identified by quantitative PCR (qPCR), using SYBR® Green Premix Ex Taq™ (TaKaRa) and the ABI 7500 Fast Real-Time PCR system (Applied Biosystems, Carlsbad, CA, United States). Thermocycling was as follows: 95°C for 30 s, followed by 40 cycles of 95°C for 5 s and 60°C for 34 s, and finally a melting curve analysis to monitor the purity of the PCR product. Primer sequences are shown in **Table 2**. The $2^{-\Delta\Delta CT}$ method was used to estimate mRNA abundance. ΔCt is Ct, target−Ct, reference, and ΔΔCt is ΔCt, treatment−ΔCt, control. Relative gene expression levels were normalized to those of the eukaryotic reference gene, β-actin.

Biochemical Determinations

The enzymatic activities of sucrase (No. A082-2-1), amylase (No. C016-1-1), and maltase (No. A082-3-1) in the duodenal mucosa were determined using colorimetric methods and measured with a spectrophotometer (BioMate 5; Thermo Electron Corporation, Hemel Hempstead, United Kingdom). The assays were conducted using assay kits according to the manufacturer's instructions (Nanjing Jiancheng Bioengineering Institute, Nanjing, China). Absorbance was measured using an Infinite M200 Pro NanoQuant™ (Tecan, Mannedorf, Switzerland).

TABLE 2 | Sequences of real-time PCR primers.

Gene name	Primers (5'-3')	Products	GenBank
Claudin-1	F: TGGCCACGTCATGGTATGG R: AACGGGTGTGAAAGGGTCATAG	62	NM_001013611
Occluding	F: GAGCCCAGACTACCAAAGCAA R: GCTTGATGTGGAAGAGCTTGTTG	68	NM_205128
Muc-2	F: GCCTGCCCAGGAAATCAAG R: CGACAAGTTTGCTGGCACAT	59	NM_001318434
β -actin	F: GAGAAATTGTGCGTGACATCA R: CCTGAACCTCTCATTGCCA	152	NM_205518

Muc-2, Mucin-2.

ELISA Determinations

Levels of secretory immunoglobulin A (sIgA, No. H108-2), immunoglobulin G (IgG, No. H106), interleukin (IL)-6 (No. H007-1-2), IL-1β (No. H002), tumor necrosis factor α (TNF-α, No. H052-1), interferon-gamma (IFN-γ, No. H025), Bcl-2 (No. H073), Bax (No. H379-1), and caspase-3 (No. H076) in the jejunal mucosa were determined by ELISA (Nanjing Jiancheng Institute of Bioengineering) according to the manufacturer's instructions. Briefly, supernatant from jejunal mucosal samples were pipetted into enzyme wells, which has been pre-coated with antibodies specific for sIgA, IgG, IL-1β, TNF-α, IFN-γ, IL-6, Bcl-2, Bax, and caspase-3, then add recognition antigen labeled by horse radish peroxidase (HRP); after been incubated 30 min at 37°C, both compete with solid phase antigen and formed immune complex; after been washing by Phosphate Buffered Saline Tween (PBST), the combined HRP catalyzes Tetramethy1 benzidine (TMB) into blue, and turns into yellow by the action of acid; it has absorption peak under 540 nm wavelength, and the absorbance of each well was determined using a SpectraMax M5 (Molecular Devices, San Jose, CA, United States; Li et al., 2017a).

Cecal DNA Extraction and 16S rRNA Gene Sequencing

Microbial genomic DNA was extracted from freeze-dried cecal content samples using a commercial magnetic bead DNA isolation kit purchased from Hangzhou Foreal Nanotechnology (Hangzhou, China). The V3–V4 region of the bacterial 16S rRNA gene was amplified using the 341F/806R primer pair combined with adapter and barcode sequences. PCR products were quantified using Quant-iT dsDNA HS Reagent (Thermo Fisher Scientific, Suzhou, China) and pooled. High-throughput sequencing analysis of bacterial rRNA genes was performed using the Illumina HiSeq 2,500 platform (2 × 250 paired ends; Illumina, San Diego, CA, United States) at Biomarker

Technologies Corporation (Beijing, China). Raw high-throughput sequence data were deposited in the NCBI database with the BioProject ID PRJNA713493.[1]

The QIIME (version 1.9.1) data analysis package was used for 16S rRNA data analysis.[2] The original sequence data were spliced using FLASH (version 1.2.11; Magoc and Salzberg, 2011) and then subjected to mass filtering with Trimmomatic (version 0.33; Bolger et al., 2014). The effective sequences were grouped into operational taxonomic units (OTUs) using the clustering program USEARCH (version 10.0; Edgar, 2013), against the Silva 119 database, preclustered at 97% sequence identity. The OTUs were further subjected to taxonomy-based analysis using the Remove Data Processor algorithm, and α diversity and β diversity were analyzed. Linear discriminant analysis, Effect Size (LEfSe; version 1.0) analysis, and linear discriminant analysis (LDA) were performed using an online LEfSe tool.[3]

Measurement of Cecal Metabolites

Based on a previously described method (Sun et al., 2020), frozen cecal digesta (0.5 g) were lyophilized for 24 h and transferred into a 1-ml polyethylene tube. The digesta was combined with 100 µl of methoxyamine hydrochloride in pyridine (20 mg/ml) and vigorously vortexed for 30 s. The samples were heated in a water bath at 37°C for 90 min, followed by the addition of 200 µl of bis (trimethylsilyl)-trifluoroacetamide in 1% trimethylchlorosilane. The samples were then heated at 70°C for 60 min, removed, and allowed to remain at room temperature for 30 min. Subsequently, the samples were centrifuged at 10,000 × g at 4°C for 10 min, and 100 µl of the supernatant from each sample was transferred into a Gas Chromatography vial. Following the addition of 400–500 µl of n-hexane, the samples were used for Gas Chromatography–Mass Spectrometry (GC–MS) in the automatic sampling mode.

Each 1 µl sample was injected into the Agilent 6890/5973 system equipped with a fused silica capillary column (30.0 m × 0.25 mm i.d.) packed with 0.25 µm HP-5MS (Agilent, Santa Clare, CA, United States). Helium was used as the carrier at a constant flow rate of 1.0 ml/min. The column temperature was maintained at 70°C for 2 min, increased to 200°C at a rate of 10°C/min, followed by an increase to 280°C at a rate of 5°C/min, which was maintained for 6 min. The full scanning mode was adopted for mass spectrometry detection with a detection range of 50–650 (m/Z).

Statistical Analysis

The metabolic profile data were processed using Soft Independent Modeling of Class Analogy software (version 13.0; Sartorius Stedim Data Analytics AB, Umea, Sweden). Principal component analysis (PCA), projections to latent structures-discriminant analysis (PLS-DA), and orthogonal partial least squares discriminant analysis (OPLS-DA) were used to process the cecum metabolomic data. Variable importance in projection (VIP > 1) and Welch's *t*-test ($p < 0.05$) values were compared to obtain the profile of each metabolite. Kyoto Encyclopedia of Genes and Genomes (KEGG) enrichment analysis was used, and all qualitative metabolites were taken as the background. The Fisher's exact test was used to analyze and calculate the degree of enrichment of the metabolites in each pathway. Spearman correlation analysis was performed for cecal metabolites and microbiota.

Other data were analyzed with a one-way ANOVA followed by Tukey's multiple comparison test using Statistical Product and Service Solutions (SPSS) software (version 22.0; SPSS Inc., Chicago, IL, United States). Statistical significance was set at $p < 0.05$. The data were expressed as mean ± SEM, and graphs were generated using GraphPad Prism software (version 5.0; San Diego, CA, United States).

RESULTS

Growth Performance of Broilers

Growth performance results are presented in **Table 3**. During the starter phase from days 1–42, there was no significant effect on BW, Average Daily Gain (ADG), ADFI, and F:G because of BS supplementation when compared with SNE group ($p > 0.05$). In contrast, from days 43–63, treatment with BS improved the BW of broilers. Moreover, considering the entire growth period from days 1 to 63, the ADG of broilers in the BST group was

TABLE 3 | Effects of *Bacillus subtilis* DSM29784 treatment group on the growth performance of subclinical enteritis (SNE) broilers.

Items	Ctr	SNE	*Bacillus subtilis* treatment (BST)	SEM	*p*
Starter phase (days 1–21)					
BW at day 21 (g)	555.80^{a}	528.97^{b}	525.33^{b}	11.76	0.040
ADG (g/d)	24.34^{a}	23.06^{b}	22.87^{b}	0.567	0.042
ADFI (g/d)	42.04	42.53	41.89	0.954	0.785
F:G	1.73^{b}	1.85^{a}	1.83^{a}	0.029	0.002
Grower phase (days 22 ~ 42d)					
BW at day 42 (g)	1615.01^{a}	1374.69^{b}	1407.67^{b}	32.885	<0.001
ADG (g/d)	50.44^{a}	40.27^{b}	42.02^{b}	1.513	<0.001
ADFI (g/d)	122.15	111.41	109.37	6.069	0.111
F:G	2.42^{b}	2.76^{a}	2.61^{ab}	0.102	0.017
Finisher phase (days 43 ~ 63d)					
BW at day 63 (g)	2683.55^{a}	2221.81^{c}	2312.58^{b}	36.193	<0.001
ADG (g/d)	50.88^{a}	40.34^{b}	43.09^{b}	1.398	<0.001
ADFI (g/d)	153.74	140.78	144.33	7.045	0.198
F:G	3.02^{b}	3.49^{a}	3.36^{a}	0.148	0.016
Whole phase (days 1 ~ 63d)					
ADG (g/d)	41.89^{a}	34.56^{c}	35.99^{b}	0.576	<0.001
ADFI (g/d)	101.84^{a}	90.72^{b}	94.90^{b}	2.840	0.005
F:G	2.43^{b}	2.63^{a}	2.59^{a}	0.066	0.023

^{a,b}*Mean values within a row with no common superscript differ significantly ($p < 0.05$). Ctr group, basal diet in control group; SNE group, basal diet + SNE (20-fold dose coccidiosis vaccine) + 1 ml of Clostridium perfringens (2×10^{8} cfu/ml coinfection); BST group, basal diet (days 1–21) + 1×10^{9} colony-forming units (cfu)/kg BS diet (days 22–63) + SNE. SEM, standard error of mean; BW, body weight; ADG, average daily gain; ADFI, average daily feed intake; and F:G, feed conversion ratio.*

[1]https://www.ncbi.nlm.nih.gov/sra
[2]http://qiime.org/
[3]http://huttenhower.sph.harvard.edu/lefse/

enhanced when compared with the SNE group ($p < 0.05$). Furthermore, the SNE group had a lower BW in the final phase from days 43 to 63 and lower ADG during the whole experiment than the other two groups ($p < 0.05$). However, the Ctr group showed significantly higher BW and ADG, and lower F/G in each period compared to the SNE group ($p < 0.05$).

Intestinal Lesion Scores

Intestinal lesion scores in the small intestines harvested on days 28 and 35 are presented in **Table 4**. Birds in all treatment groups had low lesion scores, indicating that the *C. perfringens* infection was subclinical. Higher lesion scores were observed in the SNE group in comparison to other groups, and a significant difference was observed on day 28 ($p < 0.05$), which indicating that the infection was worsen in these birds. Interestingly, lesion scores in the BST group were not significantly different from those in the Ctr group ($p > 0.05$).

Histological Observation

H&E staining showed that the Ctr group exhibited an integrated structure of the jejunal mucosa, ordered intestinal villi, deep crypts, and a clear and complete gland structure (**Figure 1A**). However, tissues harvested from the SNE group showed that the structure of the jejunal mucosa was incomplete, villi were sparse and shorter, and the crypts were shallow with a sporadic distribution. The intestinal mucosal structure in chicks treated with BST was markedly improved, and the intestinal villi showed a longer and denser arrangement. Furthermore, BST significantly increased the villus height/crypt depth ratio compared with that observed in the SNE group, similar results were observed in the Ctr group (**Table 4**). SEM imaging showed that the Ctr group had complete jejunum villi structure, which formed full and closely arranged structures. In contrast, the jejunum villi structure in the SNE group was severely damaged, while those in the BST group showed an improvement (**Figure 1B**). These observations were also observed in by TEM imaging of the jejunum (**Figure 1C**).

TABLE 4 | The jejunum histomorphology of broilers infected with *Clostridium perfringens*.

Items	Ctr	SNE	BST	SEM	*p*
Villus height (μm)	1437.22^{a}	1047.27^{b}	1128.68^{b}	46.29	<0.001
Crypt depth (μm)	208.40^{a}	188.85^{a}	160.65^{b}	9.29	<0.001
Villus/Crypt ratio	6.95^{a}	5.55^{b}	7.19^{a}	0.43	0.001
Lesion score					
Day 28	0.50^{b}	1.33^{a}	0.83^{ab}	0.22	0.002
Day 35	0.58	1.67	0.83	0.46	0.059

^{a,b}*Mean values within a row with no common superscript differ significantly ($p < 0.05$). Ctr group, basal diet in control group; SNE group, basal diet + SNE (20-fold dose coccidiosis vaccine) + 1 ml of Clostridium perfringens (2×10^8 cfu/ml coinfection); BST group, basal diet (days 1–21) + 1×10^9 colony-forming units (cfu)/kg BS diet (days 22–63) + SNE. SEM, standard error of mean. 0, no gross lesions, normal intestinal appearance; 1, thin walled or friable and few whitish plaques in the serosal surface (mild); 2, thin-walled, focal necrosis or ulceration, and small amounts of gas production (moderate); 3, thin-walled, large patches of necrosis, gas-filled intestine, and small flecks of blood (marked or severe); 4, severe extensive necrosis, marked haemorrhage, and excessive amounts of gas in the intestine (very severe).*

Expression of Genes Related to Intestinal Tight Junctions

As shown in **Figure 2**, expression levels of claudin-1 and occludin transcripts in the jejunum were significantly decreased in the SNE group ($p < 0.05$), compared to the Ctr group. However, no significant differences ($p > 0.05$) in claudin-1 and occludin expression were observed between the BST and Ctr groups. Notably, the relative expression of Muc-2 in the SNE group was markedly upregulated (82.73% and 120.35%) compared to the Ctr and BST groups, respectively.

Biochemical Indices in the Duodenum

Table 5 summarizes the effect of BS treatment on sucrase, amylase, and maltase enzymatic activity in the duodenal mucosa. Compared to the Ctr group, SNE significantly decreased ($p < 0.05$) sucrase and maltase activity in the duodenum, whereas no significant difference was observed in BST group ($p > 0.05$), except for maltase activity. In addition, no significant difference was observed for amylase activity in each treatment groups ($p > 0.05$).

Immune Response in Jejunal Mucosa

Cytokine secretion in the jejunal mucosa is shown in **Figure 3**. The expression levels of sIgA and IgG were significantly lower in the SNE group than in the Ctr group ($p < 0.05$), however no significant difference in sIgA secretion was noted between the BST and Ctr groups ($p > 0.05$; **Figures 3A,B**). Furthermore, the secretion levels of IL-1β, TNF-α, INF-γ, and IL-6 were significantly upregulated in the SNE group, compared with those in the Ctr group. There were no significant differences between the BST and Ctr groups for these parameters except for the TNF-α and INF-γ ($p > 0.05$; **Figures 3C–F**).

Apoptosis-Related Proteins in the Jejunum

Figure 4 summarizes the levels of apoptosis-related proteins in the jejunum. Caspase-3 secretion in the jejunal mucosa of the SNE group was higher than both the Ctr and BST groups ($p < 0.05$). In addition, no significant changes were observed in Bax and Bcl-2 levels among the three treatment groups ($p > 0.05$).

Microbial Community Structure of the Ceca

Rarefaction curve analysis of OTUs in all samples approached a plateau (**Figure 5A**), indicating that the sampling depths were sufficient to capture the overall microbial diversity in all harvested samples. **Figure 5B** shows a significant difference ($p < 0.05$) in the alpha diversity index (Simpson), while no differences ($p > 0.05$) were observed in the ACE, Chao1, and Shannon indices between the SNE and BST groups. In addition, ACE, Chao1, and Shannon indices of broilers in the BST groups significantly increased ($p < 0.05$) compared with those in the Ctr group.

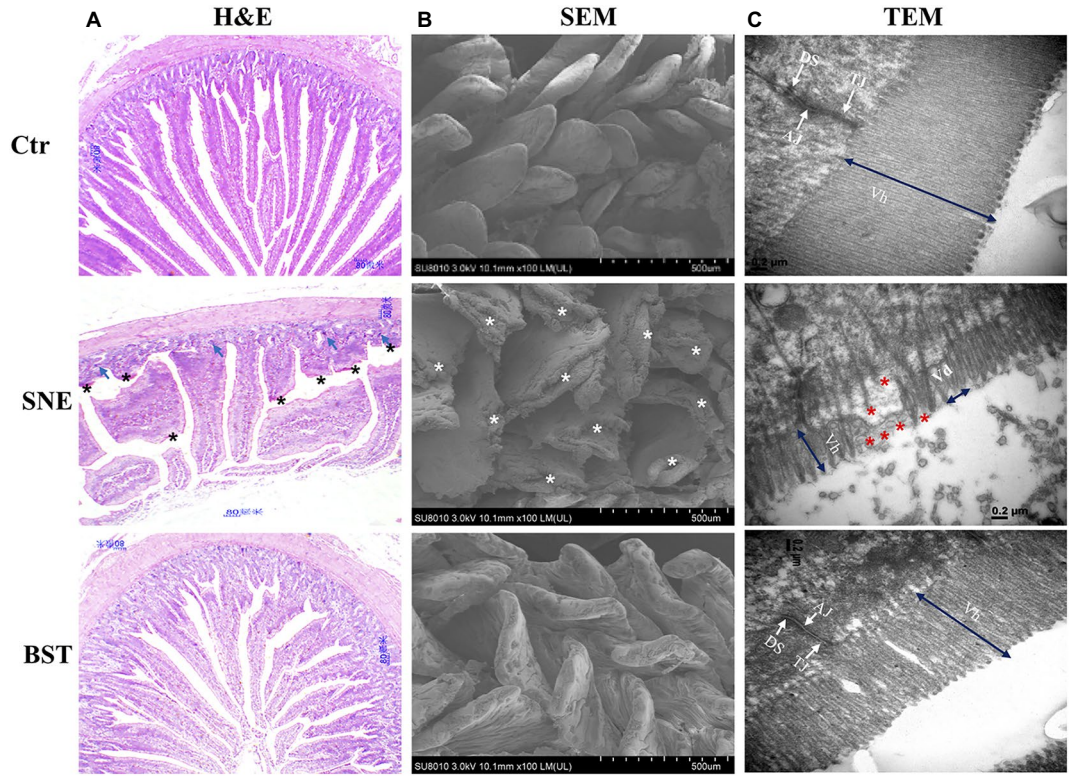

FIGURE 1 | (A) Representative haematoxylin and eosin (H&E)-stained images (top, scale bars = 80 μm); **(B)** Scanning electron micrograph (bottom, scale bars = 500 μm); and **(C)** Transmission electron microscopy (bottom, scale bars = 0.2 μm) of jejunal mucosal surface of broilers orally treated with or without coccidia and *Clostridium perfringens* infection. Vh, Villus height; Vd, Villus density; TJ, tight junction; AJ, adherens junction; DS, desmosomes. Shows the pathological (asterisk). Numerous enterocytes show all the features of necrotic cell death (blue arrows). Ctr group, basal diet in control group; SNE group, basal diet + SNE (20-fold dose coccidiosis vaccine) + 1 ml of *Clostridium perfringens* (2×10^8 cfu/ml coinfection); BST group, basal diet (days 1–21) + 1×10^9 colony-forming units (cfu)/kg BS diet (days 22–63) + SNE.

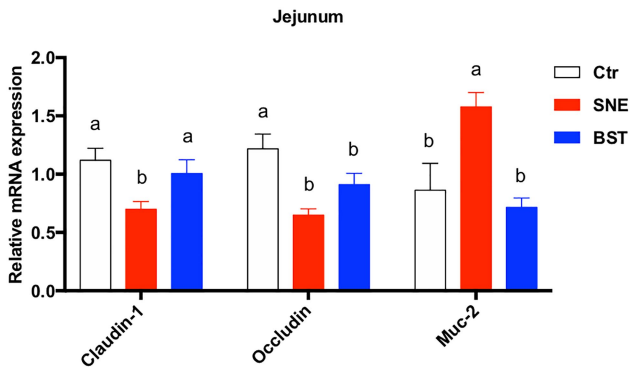

FIGURE 2 | Changes in relative expression of *claudin-1*, *occluding*, and *muc-2* in the jejunum. Data are means ± standard error ($n = 6$). [a,b]Mean values within a row with no common superscript differ significantly ($p < 0.05$). Ctr group, basal diet in control group; SNE group, basal diet + SNE (20-fold dose coccidiosis vaccine) + 1 ml of *Clostridium perfringens* (2×10^8 cfu/ml coinfection); BST group, basal diet (days 1–21) + 1×10^9 colony-forming units (cfu)/kg BS diet (days 22–63) + SNE. *Muc-2*, *mucin 2*.

TABLE 5 | Duodenal mucosa biochemistry parameters of SNE broilers treatment with *Bacillus subtilis* DSM29784 (mean ± SEM, $n = 8$ per treatment).

Items	Ctr	SNE	BST	SEM	*p*
Sucrase (U/mg prot)	62.97[a]	41.86[b]	46.51[ab]	9.019	0.070
Amylase (U/mg prot)	32.67	25.83	33.66	4.392	0.176
Maltase (U/mg prot)	104.79[a]	54.22[c]	90.52[b]	6.206	<0.001

[a,b,c]*Mean values with unlike letters between different groups were significantly different ($p < 0.05$).*

Ctr group, basal diet in control group; SNE group, basal diet + SNE (20-fold dose coccidiosis vaccine) + 1 ml of Clostridium perfringens (2×10^8 cfu/ml coinfection); BST group, basal diet (days 1–21) + 1×10^9 colony-forming units (cfu)/kg BS diet (days 22–63) + SNE.

Next, we applied PLS-DA to divide the samples into clusters, to identify differences between the harvested samples by establishing a model of the relationship between species abundance and sample category. As shown in **Figure 5C**, the Ctr, SNE, and BST groups were well separated, with 10.36 and 7.19% variation, explained by principal components 1 and 3, respectively.

A cladogram representative of the cecal microbiota and the predominant bacteria is shown in **Figures 5D,E**. The differences in taxa between the three groups are displayed. BST treatment significantly promoted the relative abundance of Ruminococcaceae (family), *Angelakisella* (genus), Bifidobacteriales (order),

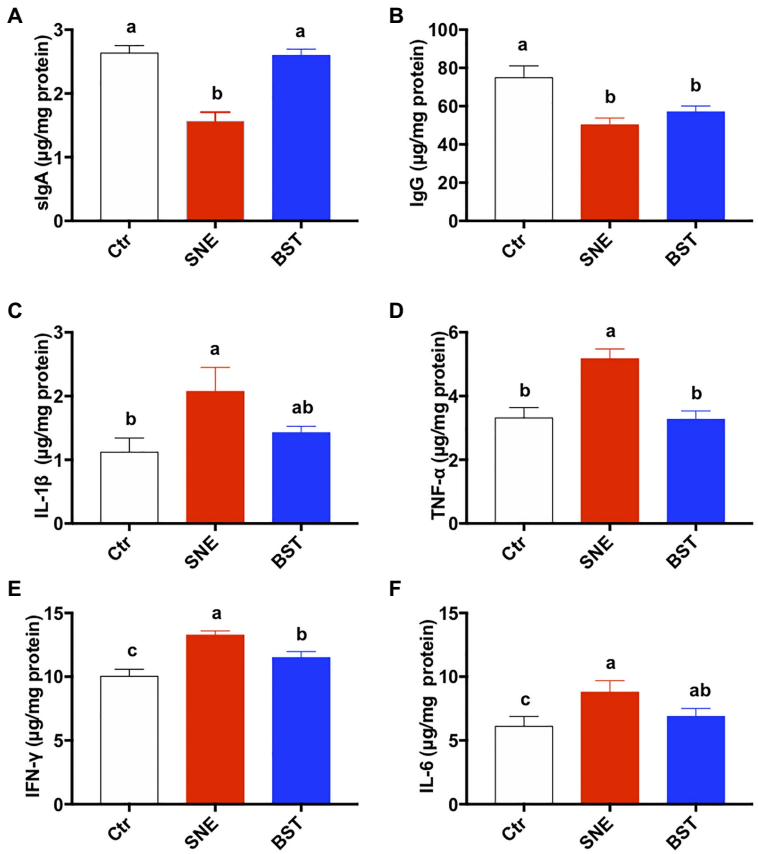

FIGURE 3 | Cytokine levels in the jejunum. Bars with different letters significantly differ on the basis of Turkey's multiple range tests ($p < 0.05$). Data are presented as mean ± SEM ($n = 8$). sIgA, secretory IgA; TNF-α, tumor necrosis factor-alpha; IFN-γ, interferon-gamma. Ctr group, basal diet in control group; SNE group, basal diet + SNE (20-fold dose coccidiosis vaccine) + 1 ml of *Clostridium perfringens* (2×10^8 cfu/ml coinfection); BST group, basal diet (days 1–21) + 1×10^9 colony-forming units (cfu)/kg BS diet (days 22–63) + SNE.

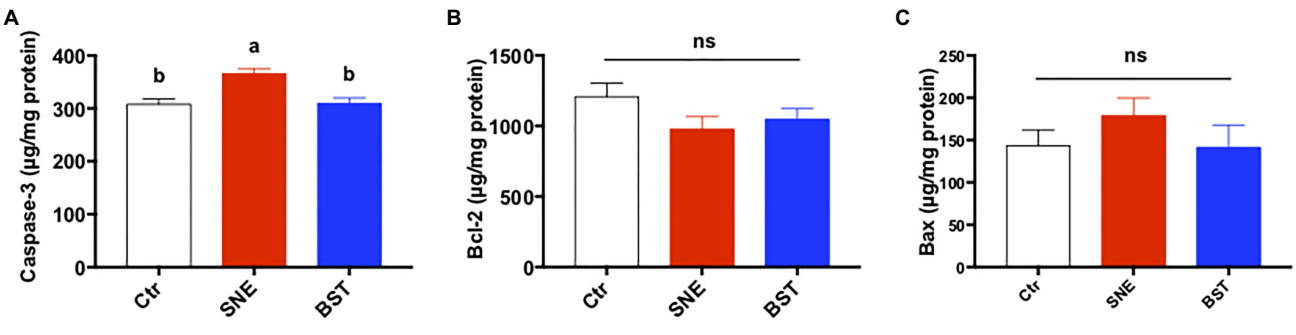

FIGURE 4 | Levels of apoptosis-related proteins [caspase-3 **(A)**, bcl2 **(B)**, and bax **(C)**] in the jejunum. Bars with different letters significantly differ on the basis of Turkey's multiple range tests ($p < 0.05$). Data are presented as mean ± SEM ($n = 8$). Ctr group, basal diet in control group; SNE group, basal diet + SNE (20-fold dose coccidiosis vaccine) + 1 ml of *Clostridium perfringens* (2×10^8 cfu/ml coinfection); BST group, basal diet (days 1–21) + 1×10^9 colony-forming units (cfu)/kg BS diet (days 22–63) + SNE.

Bifidobacteriaceae (family), *Bifidobacterium* (genus), and Actinobacteria (phylum). SNE treatment markedly increased the relative abundance of Bacillaceae (family), *Bacillus* (genus), Bacillales (order), *Negativibacillus* (genus), *Eisenbergiella* (genus), and *Oscillibacter* (genus).

Profiling of Cecal Metabolites

To identify differentially expressed metabolites in the cecum, we screened and compared the SNE and BST treatment groups by metabolomic profiling. **Figure 6A** shows the PCA score plot of the cecal samples from the two groups. There was a

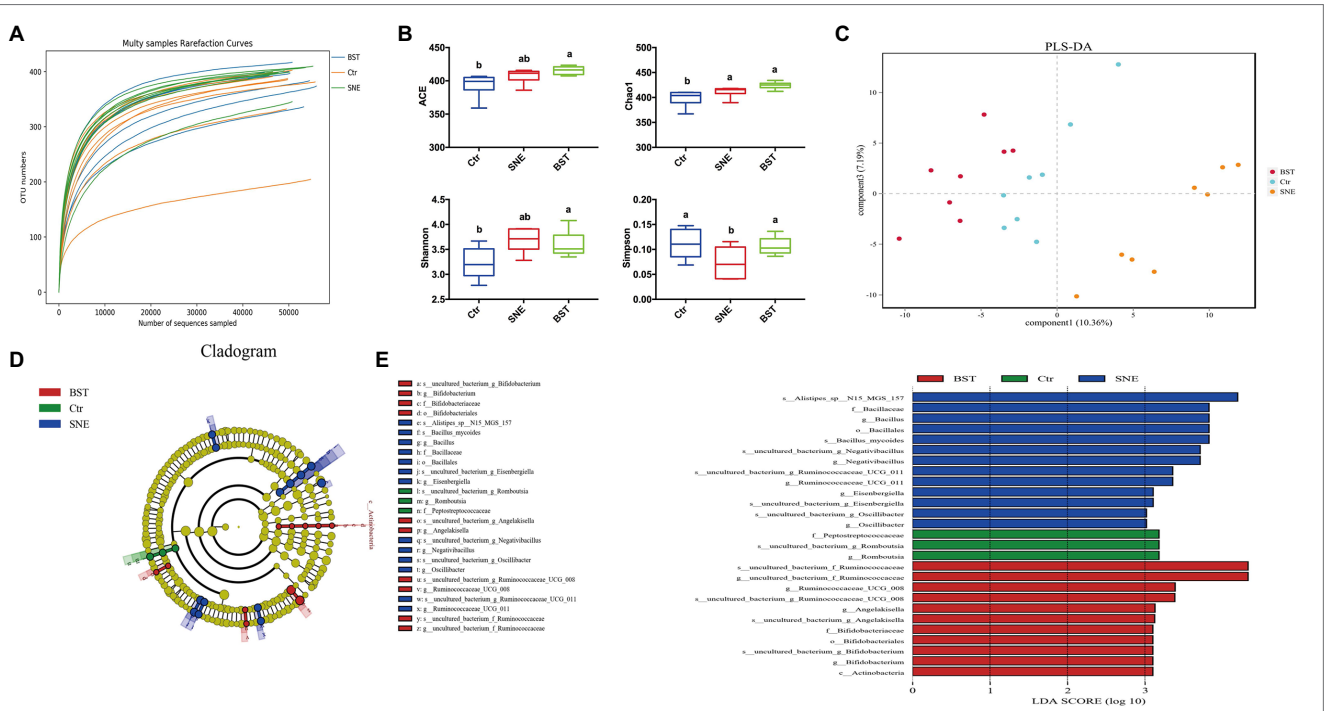

FIGURE 5 | The caecal bacterial community of broilers fed with dietary *Bacillus subtilis* DSM 29784 supplementation among Ctr, SNE and BST treatments. **(A)** Rarefaction curve for total OTUs; **(B)** α-Diversity of gut microbial was analyzed among Ctr, SNE, and BST treatments by determination of principal dimension ACE, chao1, Shannon, and Simpson indices; **(C)** Partial Least Squares Discriminant Analysis of gut microbiota at the operational taxonomic unit (OTU) level; **(D)** Cladogram; and **(E)** LDA value distribution histogram. Bacterial taxa significantly differentiated among Ctr, SNE, and BST treatments identified by linear discriminant analysis coupled with effect size (LEfSe) using the default parameters. Bacterial taxa with LDA score > 3 are selected as biomarker taxa (p: phylum level; c: class level; o: order level; f: family level; g: genus level). Ctr group, basal diet in control group; SNE group, basal diet + SNE (20-fold dose coccidiosis vaccine) + 1 ml of *Clostridium perfringens* (2×10^8 cfu/ml coinfection); BST group, basal diet (days 1–21) + 1×10^9 colony-forming units (cfu)/kg BS diet (days 22–63) + SNE.

clear separation along the t [1] axis, indicating that the cecal contents were different in each group. To obtain an improved separation, and for better understanding of the variables responsible for the classification, a latent structure-discriminant analysis (PLS-DA) model was applied to screen markers for the metabolites responsible for maximum separation, by removing the systematic variation unrelated to grouping. As shown in **Figure 6B**, all the samples in the PLS-DA score plots were within the 95% Hotelling's T^2 ellipse. The R2Y value of this model, which represents the explained variance, was 0.962. Cross-validation indicated good predictive ability of this model with a relatively high Q2 value of 0.551. Similar to the PCA model, PLS-DA also exhibited a distinct separation between the two groups. Furthermore, a permutation test (**Figure 6C**) was applied to assess the robustness and predictive ability of the PLS-DA model, and the corresponding R2Y and Q2 intercept values were 0.52, and 0.651, respectively. This indicated that this model was satisfactorily effective. Similar results were obtained using OPLS-DA (**Figure 6D**).

Differential Metabolite Analysis

We combined the multivariate OPLS-DA and VIP statistical analyses, and the *t*-test univariate statistical analysis value of *p* to screen for statistically differential metabolites between SNE and BST groups. A total of 86 metabolite biomarkers with similarity >700, VIP > 1, and $p < 0.05$ were filtered as shown in **Supplementary Figure S1**. These metabolites mainly comprise lipids, amino acids, carbohydrates, organic acids, and amines, such as lactic acid, fumaric acid, oleic acid, D-fructose, L-glutamic acid, and indole, which are involved in multiple biochemical processes. BST treatment group showed an upregulation of 35 metabolites, and a downregulation of 52 metabolites compared with SNE. Seventeen metabolites were selected and shown in a heat map (**Figure 6E**); the concentrations of succinic acid, uracil, malic acid, pyruvic acid, lactic acid, and adipic acid showed upregulation in BST group than the SNE group. On the contrary, the concentrations of azelaic acid, indole, oleic acid, L-glutamic acid, hydrocinnamic acid, valeric acid, hypoxanthine, D-glucose, 3-hydroxybenzoic acid, pantothenic acid, and nicotinic acid were higher in SNE. In short, there was a significantly differential expression pattern of metabolic profiles between chicks in the SNE and BST groups. The altered metabolome of the cecum during BS supplementation was associated with secondary metabolites involved in various amino acid and carbohydrate metabolic pathways. These metabolites included, d-glucose (galactose metabolism), l-glutamic acid (biosynthesis of amino acids), indole (protein digestion and absorption), succinic acid (tricarboxylic acid cycle), malic acid (carbon metabolism), and pyruvic acid (biosynthesis of amino acids).

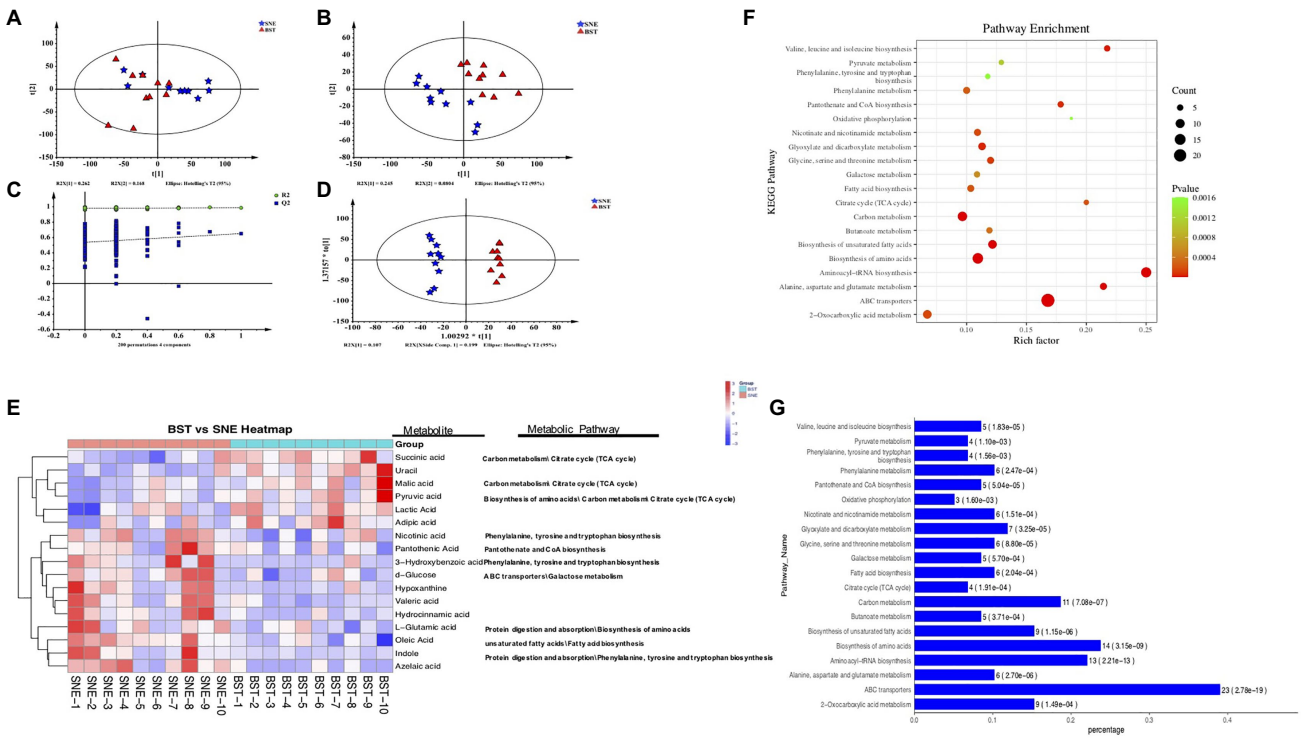

FIGURE 6 | (A) Principal component analysis (PCA) score plots (R2X = 0.534, Q2 = 0.252), **(B)** projections to latent structure-discriminant analysis (PLS-DA) score plots (R2X = 0.52, R2Y = 0.987, Q2 = 0.651), **(C)** permutation test of PLS-DA, and **(D)** orthogonal projections to latent structure-discriminant analysis (OPLS-DA) score plots (R2X = 0.52, R2Y = 0.987, Q2 = 0.507). Blue pentagon: SNE; red triangle: BST, green circle: R2; blue square: Q2. The dashed line represents the regression line for R2 and Q2; **(E)** Heatmap of metabolites in cecal contents between BST vs. SNE groups. The relative values for each of these metabolites are indicated by color intensity with the legend indicated at the right of the figure. Red and blue represent higher and reduced concentrations of metabolites in the BST and SNE groups; **(F)** Bubble (up) and **(G)** bar (down) charts of top 20 most KEGG enrichment analysis of the differential metabolites between BST vs. SNE groups. "Rich factor" means that the ratio of the DEMs number and the number of metabolites have been annotated in this pathway. The greater of the Rich factor, the greater the degree of enrichment (bubble chart); along *x*-axis values represents enrichment ratio. The horizontal axis represents the number of count, the corresponding value of *p* in brackets, and the vertical axis is pathway name (bar charts). Ctr group, basal diet in control group; SNE group, basal diet + SNE (20-fold dose coccidiosis vaccine) +1 ml of *Clostridium perfringens* (2×10^8 cfu/ml coinfection); BST group, basal diet (days 1–21) + 1×10^9 colony-forming units (cfu)/kg BS diet (days 22–63) + SNE.

Analysis of Metabolic Pathways

We compared various cecal metabolites between the SNE and BST groups and identified the pathways in which they participate. Seventy-seven enriched pathways displayed comprehensive impact values. The top 20 KEGG enrichment analyses of the differential metabolites between the SNE and BST groups are shown in **Figures 6F,G**. These pathways included ABC transporters, aminoacyl-tRNA biosynthesis, amino acid biosynthesis, carbon metabolism, biosynthesis of unsaturated fatty acids, alanine, aspartate, and glutamate metabolism, valine, leucine, and isoleucine biosynthesis, glyoxylate and dicarboxylate metabolism, pantothenate and CoA biosynthesis, and glycine, serine, and threonine metabolism.

Cecal Metabolome and Gut Microbiome Correlations

To further investigate the relationships between cecal metabolites and gut microbiota, Spearman correlation analysis was performed for cecal metabolites and microbiota in the BST an SNE groups (**Figure 7**). The relative abundance of Lactobacillales (order), Lactobacillaceae (family), and *Lactobacillus* (genus) were positively correlated with uracil and fumaric acid, and negatively correlated with pyroglutamic acid and D-arabinose. The relative abundance of *Negativibacillus* (genus), *Anaerofustis* (genus), *Holdemania* (genus), and *Alistipes* (genus) were positively correlated with palmitic acid, stearic acid, eicosanoic acid, heptadecanoic acid, and negatively correlated with lactic acid. In addition, the relative abundance of Ruminiclostridium was positively correlated with that of L-hydroxyproline and 2-hydroxyisocaproic acid.

DISCUSSION

SNE impairs growth performance, resulting in greater economic losses than the clinical form, as it can easily go unnoticed. Previous studies in have shown that probiotics have beneficial effects on the health of the host (Wang et al., 2017a). For example, the dietary probiotic *Bacillus* can effectively improve the growth

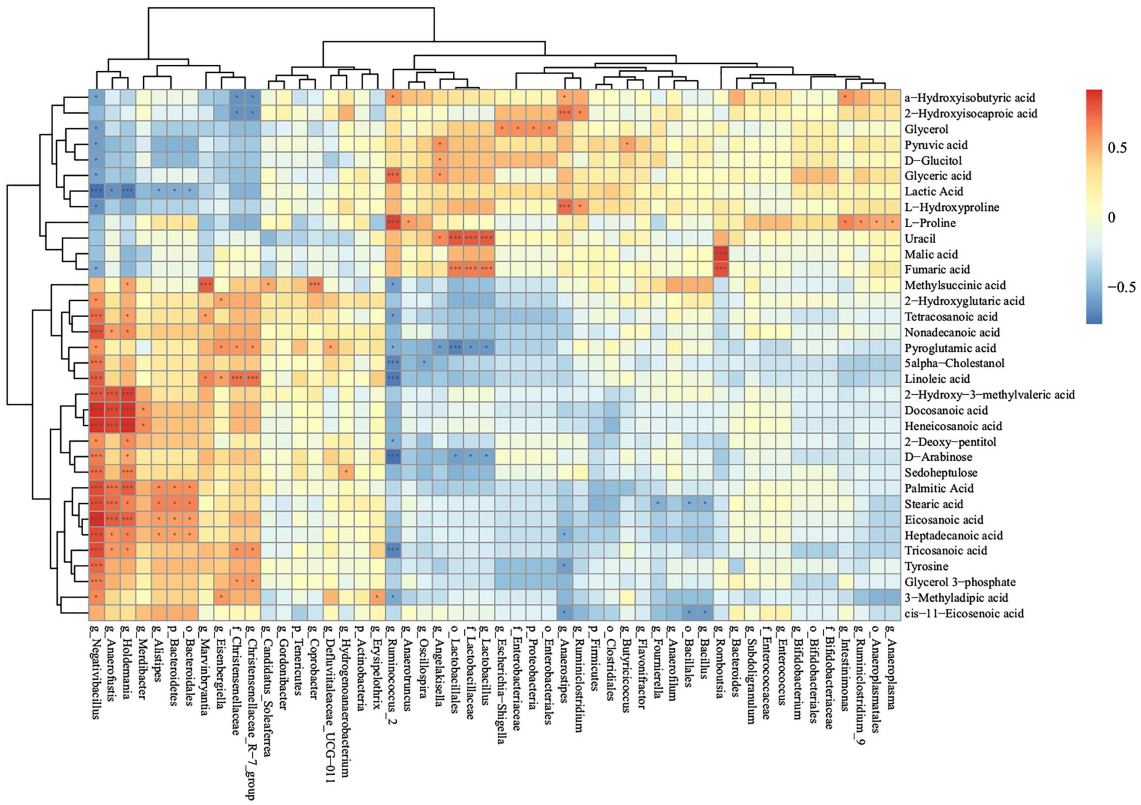

FIGURE 7 | Correlations of metabolome and microbiota in cecal contents according to the Spearman correlation coefficient distribution (SNE vs. BS). *$p > 0.01$ and $p < 0.05$; ***$p < 0.01$. Ctr group, basal diet in control group; SNE group, basal diet + SNE (20-fold dose coccidiosis vaccine) +1 ml of *Clostridium perfringens* (2×10^8 cfu/ml coinfection); BST group, basal diet (days 1–21) + 1×10^9 colony-forming units (cfu)/kg BS diet (days 22–63) + SNE.

performance and antioxidant capacity of animals and reduce the extent of intestinal lesions (Gobi et al., 2018; Jia et al., 2018; Musa et al., 2019). Our results show that the BST group, compared with the SNE group, showed beneficial effects in BW during the final phases of the experiment, and a higher ADG over the duration of the experiment. Moreover, previous findings are consistent with our current study. For instance, Jayaraman et al. (2017) reported that dietary supplementation with *B. subtilis* could be used as an alternative to antibiotic growth promoters in poultry farming, as it has exhibited good growth performance in birds.

Intestinal health and recovery are evaluated based on villi length and crypt depth. A higher ratio of villus length: crypt depth illustrates that the villus is longer and has a mature and active functional epithelium, accompanied by a shallow crypt and constant cell renewal (Jayaraman et al., 2013). Increasing villi length provides a greater intestinal surface area and improves nutrient absorption as well as the growth and production of broilers (Salim et al., 2013). In contrast, shorter villi and deeper crypts may lead to decreased disease resistance, poorer growth performance, and reduced nutrient absorption (Song et al., 2014; Mohammadagheri et al., 2016). Thus, changes in intestinal conditions can affect the nutrient absorption of birds. In this study, BS treatment effectively improved jejunum morphology, including villi length and the villi length: crypt depth ratio in the broilers. The same results were reported when broilers were administered *B. subtilis*, which improved the health of the intestine by enhancing the villus length, width and area, and the crypt depth in the small intestine (Bai et al., 2018). The above-mentioned findings illustrate that improved intestinal morphology development may contribute to the preventive of SNE.

Barrier function can be influenced by several luminal and systemic factors, leading to plasma protein leakage and watery diarrhea (Camilleri, 2019). Tight junctions provide paracellular permeability, which is integral to the intestinal mucosal barrier (Tugizov, 2021) and contain unique proteins, such as Claudin-1, occludin, and Muc-2 (Wang et al., 2018). Intestinal epithelial cells secrete mucus onto their surface, which is a major protective barrier against bacterial infection. However, intestinal mucus is an important nutritional source for CP, as it allows these bacteria to form part of the local microflora on the mucosal surface (Ficko-Blean et al., 2012). Here, we found that BST treatment significantly decreased the relative expressions of Muc-2 compared to the SNE group. Reduced mucus secretion may reduce CP localization, thus providing a preventive effect against SNE.

Previous studies have considered as an immune-metabolic perspective to identify the role of the inflammatory response mediating some diseases, such as obesity, diabetes, and other metabolic disorders. For instance, excessive fat deposition can

lead to an innate immune inflammatory response (Pothakam et al., 2021). Host–pathogen interactions in NE are complex and involve different components of the host immune system (Oh and Lillehoj, 2016). Cytokines are effective molecules for the transmission of information between immune cells. The composition of cytokines in the infection microenvironment determines the properties of the immune response (Fasina and Lillehoj, 2019). We observed a greater expression of pro-inflammatory cytokines in the SNE than other two groups, while excessive inflammation can lead to tissue damage (David and Lopez-Vales, 2021). Fasina and Lillehoj (2019) showed that CP infection could induce intestinal inflammation in broilers, which may be mediated by Threshold (Th) 2 and Th17 cells. sIgA antibody, as the first line of antigen-specific immune defense, protects the mucosal surface from environmental pathogens and antigens by combining with bacterial antigens (Tiboni et al., 2021). We also found that BST treatment upregulated the expression levels of sIgA in the jejunum. This is consistent with our previous results showing that probiotics increase the expression of sIgA and triggers the production of cytokines (Wang et al., 2015; Wu et al., 2019). The above-mentioned findings illustrate that BST treatment may help to relieve the inflammatory response and protect the intestine against pathogenic bacterial infection.

NE can alter the composition and quantity of gastrointestinal microbiota, which plays a pivotal role in the digestive tract of animals (Stanley et al., 2014; Azad et al., 2018). SNE is a type of dysbacteriosis, an imbalance of the normal flora in the proximal small intestine, caused by a variety of opportunistic pathogens (Palliyeguru and Rose, 2014). Previous studies have shown that probiotics can actively regulate the composition of the intestinal microbiota (Kristensen et al., 2016; Hu et al., 2017). *Ruminococcus* forms part of the natural flora in the intestinal tract of chickens. In human studies, some *Ruminococcus* flora help cells to absorb sugars and may contribute to weight gain (Correa et al., 2021), which explains why the BST chickens gained weight over the duration of the experiment, compared to the other treatment groups. The present study showed that the relative abundance of *Ruminococcaceae* in the BST group was higher than that in the other groups. Ahiwe et al. (2019) showed a decrease in the diversity of *Lactobacillus* and *Bifidobacterium* in the cecum of the CP challenged broilers. Notably, an increase in the population of *Bifidobacterium* spp. in the cecum was observed in the BST group, suggesting that BS treatment reduced the effect of NE on the composition and quantity of gastrointestinal microbiota. Khan et al. (2016) demonstrated that when *B. subtilis* was used as a probiotic, microbial balance in the chicken gut could be improved by immune stimulation and competitive exclusion. Similarly, *B. subtilis* can reduce the relative abundance of CPs in the intestine by changing the microflora (Bortoluzzi et al., 2019).

The greatest bacterial density in broilers is found in the cecum (Rehman et al., 2007). A complex microbial community in the intestine plays a key role in nutrition and health (Yang and Zhao, 2021). For example, probiotics and their metabolites can promote a symbiotic balance of microorganisms in the gut of the broilers (Perez-Chabela et al., 2020). Metabolomics provide novel insights into the dynamics of metabolites in the gut of broilers. For instance, different feed additives can directly affect the types of metabolites in the intestinal tract (Dittoe et al., 2018). Here, the higher concentrations of metabolites identified in BST group primarily include organic acids, amino acids, and alcohols. Various organic acids (such as lactic, succinic, nicotinic, acetic, propionic, and malic) are produced during intestinal fermentation and form barriers in the digestive tract, thereby preventing the colonization and reproduction of pathogenic bacteria. This enhances peristalsis and digestive enzyme secretion in the intestinal tract, thus promoting feed digestion, and improved nutrient absorption (Sun et al., 2020).

In chickens, most energy comes from glucose through the digestion of starch and long-chain fatty acids (Jozefiak et al., 2004). The decreased levels of D-glucose and sedoheptulose in the ceca of broilers in the BST treatment group might have been attributed to the increased adsorption of this carbohydrate. In addition, certain carbohydrates are metabolized by bacteria in the gut to produce different types of organic acids, together with volatile fatty acids produced from carbohydrate fermentation, such as branched chain fatty acids and lactic acid, which play an important role in the gastrointestinal tract of birds, for instance, by inhibiting the growth of certain pathogenic bacteria. This is achieved by fatty acids penetrating the bacterial cell membrane, leading to the dissociation of charged anions and protons, a decrease in intracellular bacterial pH, and inhibition of essential metabolic reactions, ultimately reducing bacterial replication (Cherrington et al., 1991; Youssef et al., 2020). Our results showed higher levels of lactic, succinic, α-hydroxyisobutyric, and malic acid in the BST group than in SNE broilers, which may explain the better health status of broilers in the BST group. Similar to our results, previous studies have reported a reduction in NE signs using butyric acid and sodium lauroyl lactylate in the diets of NE challenged birds (Biggs and Parsons, 2008; Huyghebaert et al., 2011).

Amino acids play a vital role in regulating the nutritional metabolism in broilers. Proteins consumed by broiler chickens are degraded into free amino acids by proteases and peptidases in the gastrointestinal tract and absorbed through the intestinal wall. Different types of amino acids were identified in BST broilers as compared to SNE broilers, with the composition observed in BST broilers more conducive to growth. Ammonia is generated by proteolytic bacteria, such as *Clostridium* spp., *Enterococcus* spp., and *Bacteroides* spp., and is released with potentially toxic metabolites such as biogenic amines, phenols, and indole (Macfarlane et al., 1992). Ammonia is easily absorbed by the intestine into the blood of birds and causes enterocytes toxicity (Marleen et al., 2003). Our data demonstrated that both the levels of indole and monoethanolamine were markedly increased in the cecal contents of SNE broilers compared to the BST group, suggesting that BS supplementation can alleviate the toxic side effects of CP infection. In addition, KEGG pathway annotation showed that several metabolic pathways were altered in the BS-treated broilers compared to the SNE group. This enrichment mainly involved lipid and amino acid metabolic pathways, such as protein digestion and absorption, biosynthesis of unsaturated fatty acids, and biosynthesis of amino acids.

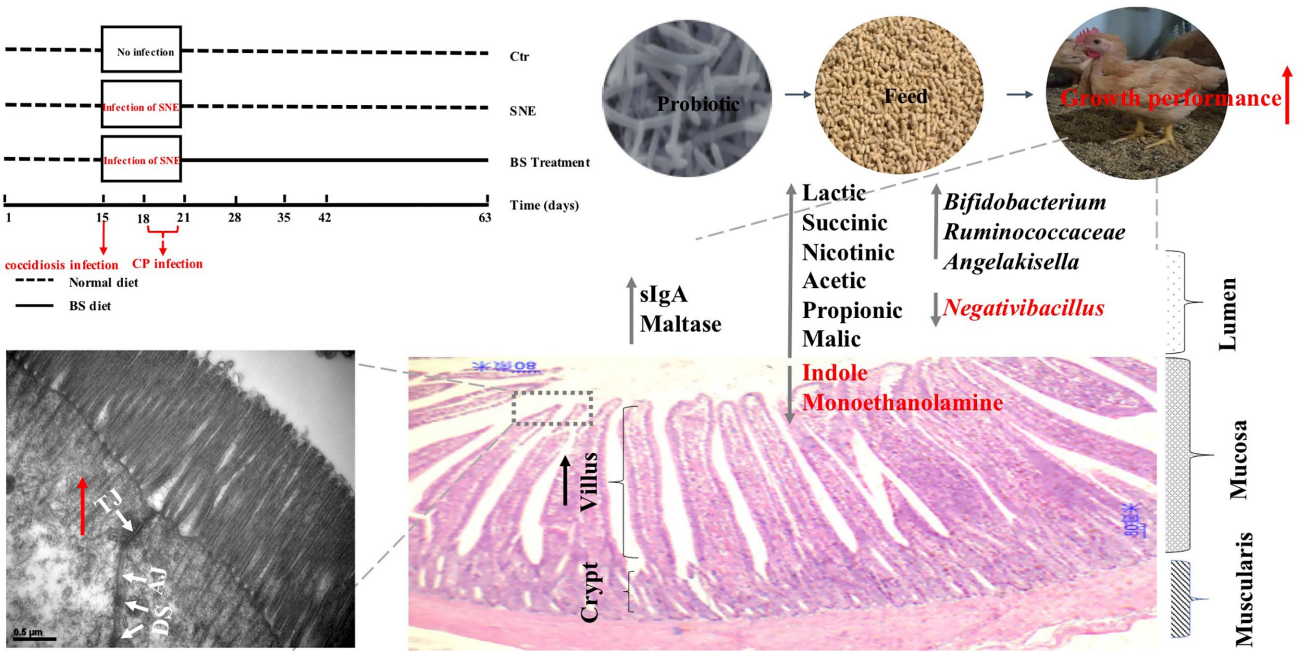

FIGURE 8 | Graphical summary of the effect of probiotic *Bacillus subtilis* DSM29784 (BS) exerts a protective effect against subclinical necrotic enteritis in broilers. BS reduces the risk of declined growth performance in chickens with SNE by enhancing exoenzyme secretion, intestinal barrier functions, and promoting the presence of beneficial commensal microorganisms and their metabolites in the intestine. SNE, subclinical enteritis; sIgA, secretory immunoglobulin A; CP, *Clostridium perfringens*; TJ, tight junction; AJ, adherens junction; DS, desmosomes. Ctr group, basal diet in control group; SNE group, basal diet + SNE (20-fold dose coccidiosis vaccine) +1 ml of *Clostridium perfringens* (2×10^8 cfu/ml coinfection); BST group, basal diet (days 1–21) + 1×10^9 colony-forming units (cfu)/kg BS diet (days 22–63) + SNE.

Microorganisms and their associated metabolites are a natural component of the developmental process and have a significant, yet underexplored, impact on the immune system (Wandro et al., 2018). In addition to the direct interaction with the immune system, the microbiota also interacts indirectly through the production of metabolites, which can be absorbed by the immune and epithelial cells (Wikoff et al., 2009; Dodd et al., 2017). In our study, the relative abundance of beneficial bacteria was positively correlated with a marked increase in metabolites in the BST group, and negatively correlated with the increase in metabolites in the SNE group. This suggests that the changes in cecal metabolites might have originated from the intestinal microbiota following co-infection of the coccidiosis vaccine and *C. perfringens*. The strong correlation between intestinal microflora and metabolites observed in the SNE broilers suggests that significant changes may cause an imbalance in the host immune response, which ultimately decline the growth performance of broilers.

In conclusion, results from the current study indicated that treatment with BS reduces the risk of declined BW in chickens with SNE by enhancing exoenzyme secretion, intestinal barrier functions, immunity, decreasing cell apoptosis, and promoting the presence of beneficial commensal microorganisms and their metabolites in the intestine (**Figure 8**). We intend to further investigate whether BS supplementation throughout the experimental period is a successful alternative for controlling clostridial infection in broilers.

DATA AVAILABILITY STATEMENT

The datasets presented in this study can be found in online repositories. The names of the repository/repositories and accession number(s) can be found in the article/**Supplementary Material**.

ETHICS STATEMENT

The animal study was reviewed and approved by the Zhejiang University Institutional Animal Care and Use Committee (permission number: ZJU2019-480-12).

AUTHOR CONTRIBUTIONS

XZ, YW, KW, and JY designed the experiments. SX, YW, and YX performed animal husbandry. YW and KW analyzed 16S rRNA data. YW and YX did the animal experiments. YW authored the final article. All authors contributed to the article and approved the submitted version.

FUNDING

This work was supported by a Zhejiang Province Key R&D Program of China (project: 2018C02035, Hangzhou, China), China Agriculture Research System of MOF and MARA (project:

CARS-41, Beijing, China), Agricultural Science and Technology Cooperation Program of Zhejiang Province (project: 2021SNLF024, Hangzhou, China), and Collaborative Extension Plan of Major Agricultural Technologies in Zhejiang Province (project: 2021XTTGXM04).

SUPPLEMENTARY MATERIAL

The Supplementary Material for this article can be found online at: https://www.frontiersin.org/articles/10.3389/fmicb.2021.723187/full#supplementary-material

REFERENCES

Ahiwe, E. U., Chang'a, E. P., Abdallh, M. E., Al-Qahtani, M., Kheravii, S. K., Wu, S., et al. (2019). Dietary hydrolysed yeast cell wall extract is comparable to antibiotics in the control of subclinical necrotic enteritis in broiler chickens. *Brit. Poultry. Sci.* 60, 757–765. doi: 10.1080/00071668.2019.1664727

Alagawany, M., Abd El-Hack, M. E., Farag, M. R., Sachan, S., Karthik, K., and Dhama, K. (2018). The use of probiotics as eco-friendly alternatives for antibiotics in poultry nutrition. *Environ. Sci. Pollut. R.* 25, 10611–10618. doi: 10.1007/s11356-018-1687-x

Awad, W. A., Ghareeb, K., Abdel-Raheem, S., and Bohm, J. (2009). Effects of dietary inclusion of probiotic and synbiotic on growth performance, organ weights, and intestinal histomorphology of broiler chickens. *Poult. Sci.* 88, 49–56. doi: 10.3382/ps.2008-00244

Azad, M. A., Sarker, M., Li, T. J., and Yin, J. (2018). Probiotic species in the modulation of gut microbiota: an overview. *Biomed. Res. Int.* 2018:9478630. doi: 10.1155/2018/9478630

Bai, K., Feng, C. C., Jiang, L. Y., Zhang, L. G., Zhang, J. F., Zhang, L. L., et al. (2018). Dietary effects of *Bacillus subtilis* fmbj on growth performance, small intestinal morphology, and its antioxidant capacity of broilers. *Poult. Sci.* 97, 2312–2321. doi: 10.3382/ps/pey116

Bani-Asadi, F. Z., Ahmadi, M., Rokni, N., Golestan, L., and Shahidi, S. A. (2021). Assessment of the distribution and concentration of residual antibiotics in chicken meat and liver samples collected in tehran by liquid chromatography and tandem mass spectrometry. *Egypt. J. Vet. Sci.* 52, 11–22. doi: 10.21608/ejvs.2020.26297.1162

Biggs, P., and Parsons, C. M. (2008). The effects of several organic acids on growth performance, nutrient digestibilities, and cecal microbial populations in young chicks. *Poult. Sci.* 87, 2581–2589. doi: 10.3382/ps.2008-00080

Bolger, A. M., Lohse, M., and Usadel, B. (2014). Trimmomatic: a flexible trimmer for Illumina sequence data. *Bioinformatics* 30, 2114–2120. doi: 10.1093/bioinformatics/btu170

Bortoluzzi, C., Vieira, B. S., Dorigam, J. C. D., Menconi, A., Sokale, A., Doranalli, K., et al. (2019). *Bacillus subtilis* DSM 32315 supplementation attenuates the effects of *Clostridium perfringens* challenge on the growth performance and intestinal microbiota of broiler chickens. *Microorganisms* 7:71. doi: 10.3390/microorganisms7030071

Caly, D. L., D'Inca, R., Auclair, E., and Drider, D. (2015). Alternatives to antibiotics to prevent necrotic enteritis in broiler chickens: a microbiologist's perspective. *Front. Microbiol.* 6:1336. doi: 10.3389/fmicb.2015.01336

Camilleri, M. (2019). Leaky gut: mechanisms, measurement and clinical implications in humans. *Gut* 68, 1516–1526. doi: 10.1136/gutjnl-2019-318427

Chen, Y. P., Wen, C., and Zhou, Y. M. (2018). Dietary synbiotic incorporation as an alternative to antibiotic improves growth performance, intestinal morphology, immunity and antioxidant capacity of broilers. *J. Sci. Food Agr.* 98, 3343–3350. doi: 10.1002/jsfa.8838

Cherrington, C. A., Hinton, M., Mead, G. C., and Chopra, I. (1991). Organic-acids - chemistry, antibacterial activity and practical applications. *Adv. Microb. Physiol.* 32, 87–108. doi: 10.1016/S0065-2911(08)60006-5

Correa, F., Luise, D., Castillo, M., Peris, S., Palomo-Yague, A., Bosi, P., et al. (2021). Effect of dietary supplementation with a blend of protected aromatic compounds, including benzoic acid, on growth performance and faecal microbial profile of weaned piglets as an alternative to Zinc Oxide. *Livest. Sci.* 246:1044455. doi: 10.1016/j.livsci.2021.104455

Dahiya, J. P., Wilkie, D. C., Van Kessel, A. G., and Drew, M. D. (2006). Potential strategies for controlling necrotic enteritis in broiler chickens in post-antibiotic era. *Anim. Feed Sci. Technol.* 129, 60–88. doi: 10.1016/j.anifeedsci.2005.12.003

David, S., and Lopez-Vales, R. (2021). Bioactive lipid mediators in the initiation and resolution of inflammation after spinal cord injury. *Neuroscience* 466, 273–297. doi: 10.1016/j.neuroscience.2021.04.026

Dittoe, D. K., Ricke, S. C., and Kiess, A. S. (2018). Organic acids and potential for modifying the avian gastrointestinal tract and reducing pathogens and disease. *Front. Vet. Sci.* 5:216. doi: 10.3389/fvets.2018.00216

Dodd, D., Spitzer, M. H., Van Treuren, W., Merrill, B. D., Hryckowian, A. J., Higginbottom, S. K., et al. (2017). A gut bacterial pathway metabolizes aromatic amino acids into nine circulating metabolites. *Nature* 551, 648–652. doi: 10.1038/nature24661

Duca, F., Gerard, P., Covasa, M., and Lepage, P. (2014). Metabolic interplay between gut bacteria and their host. *Front. Horm. Res.* 42, 73–82. doi: 10.1159/000358315

Edgar, R. C. (2013). UPARSE: highly accurate OTU sequences from microbial amplicon reads. *Nat. Methods* 10, 996–998. doi: 10.1038/nmeth.2604

Fasina, Y. O., and Lillehoj, H. S. (2019). Characterization of intestinal immune response to *Clostridium perfringens* infection in broiler chickens. *Poult. Sci.* 98, 188–198. doi: 10.3382/ps/pey390

Ficko-Blean, E., Stuart, C. P., Suits, M. D., Cid, M., Tessier, M., Woods, R. J., et al. (2012). Carbohydrate recognition by an architecturally complex alpha-N-acetylglucosaminidase from *Clostridium perfringens*. *PLoS One* 7:e33524. doi: 10.1371/journal.pone.0033524

Gobi, N., Vaseeharan, B., Chen, J. C., Rekha, R., Vijayakumar, S., Anjugam, M., et al. (2018). Dietary supplementation of probiotic bacillus licheniformis Dahb1 improves growth performance, mucus and serum immune parameters, antioxidant enzyme activity as well as resistance against Aeromonas hydrophila in tilapia Oreochromis mossambicus. *Fish Shellfish Immunol.* 74, 501–508. doi: 10.1016/j.fsi.2017.12.066

Gohari, I. M., Navarro, M. A., Li, J. H., Shrestha, A., Uzal, F., and McClane, B. A. (2021). Pathogenicity and virulence of *Clostridium perfringens*. *Virulence* 12, 723–753. doi: 10.1080/21505594.2021.1886777

Gu, C. Q., Lillehoj, H. S., Sun, Z. F., Lee, Y., Zhao, H. Y., Xianyu, Z. Z., et al. (2019). Characterization of virulent $netB^+$/$tpeL^+$ *Clostridium perfringens* strains from necrotic enteritis-affected broiler chicken farms. *Avian Dis.* 63, 461–467. doi: 10.1637/11973-092018-Reg.1

Hayashi, R. M., Lourenco, M. C., Kraieski, A. L., Araujo, R. B., Gonzalez-Esquerra, R., Leonardecz, E., et al. (2018). Effect of feeding *Bacillus subtilis* spores to broilers challenged with *Salmonella enterica* serovar Heidelberg Brazilian UFPR1 on performance, immune response, and gut health. *Front. Vet. Sci.* 5:13. doi: 10.3389/fvets.2018.00013

Hofacre, C. L., Smith, J. A., and Mathis, G. F. (2018). An optimist's view on limiting necrotic enteritis and maintaining broiler gut health and performance in today's marketing, food safety, and regulatory climate. *Poult. Sci.* 97, 1929–1933. doi: 10.3382/ps/pey082

Hu, L. S., Geng, S. J., Li, Y., Cheng, S. S., Fu, X. F., Yue, X. J., et al. (2018). Exogenous fecal microbiota transplantation from local adult pigs to crossbred newborn piglets. *Front. Microbiol.* 8:2663. doi: 10.3389/fmicb.2017.02663

Hu, S. L., Wang, L., and Jiang, Z. Y. (2017). Dietary additive probiotics modulation of the intestinal microbiota. *Protein Peptide Lett.* 24, 382–387. doi: 10.2174/0929866524666170223143615

Huyghebaert, G., Ducatelle, R., and Van Immerseel, F. (2011). An update on alternatives to antimicrobial growth promoters for broilers. *Vet. J.* 187, 182–188. doi: 10.1016/j.tvjl.2010.03.003

Jayaraman, S., Das, P. P., Saini, P. C., Roy, B., and Chatterjee, P. N. (2017). Use of bacillus Subtilis PB6 as a potential antibiotic growth promoter replacement in improving performance of broiler birds. *Poult. Sci.* 96, 2614–2622. doi: 10.3382/ps/pex079

Jayaraman, S., Thangavel, G., Kurian, H., Mani, R., Mukkalil, R., and Chirakkal, H. (2013). Bacillus subtilis PB6 improves intestinal health of broiler chickens

challenged with *Clostridium perfringens*-induced necrotic enteritis. *Poult. Sci.* 92, 370–374. doi: 10.3382/ps.2012-02528

Jia, P., Cui, K., Ma, T., Wan, F., Wang, W. Y., Yang, D., et al. (2018). Influence of dietary supplementation with bacillus licheniformis and Saccharomyces cerevisiae as alternatives to monensin on growth performance, antioxidant, immunity, ruminal fermentation and microbial diversity of fattening lambs. *Sci. Rep.* 8:16712. doi: 10.1038/s41598-018-35081-4

Johnson, J., and Reid, W. M. (1970). Anticoccidial drugs: lesion scoring techniques in battery and floor-pen experiments with chickens. *Exp. Parasitol.* 28, 30–36. doi: 10.1016/0014-4894(70)90063-9

Jozefiak, D., Rutkowski, A., and Martin, S. A. (2004). Carbohydrate fermentation in the avian ceca: a review. *Anim. Feed Sci. Technol.* 113, 1–15. doi: 10.1016/j.anifeedsci.2003.09.007

Khalique, A., Zeng, D., Shoaib, M., Wang, H. S., Qing, X. D., Rajput, D. S., et al. (2020). Probiotics mitigating subclinical necrotic enteritis (SNE) as potential alternatives to antibiotics in poultry. *AMB Express* 10:50. doi: 10.1186/s13568-020-00989-6

Khan, M. U. Z., Liu, B. H., Yang, S. L., Xu, X., Wang, Y. H., and Cai, J. P. (2021). Genetic diversity of clostridium perfringens strains isolated from broiler chickens revealed by PFGE analysis in China and Pakistan. *Pak. Vet. J.* 41, 85–91. doi: 10.29261/pakvetj/2020.087

Khan, R. U., Naz, S., Dhama, K., Karthik, K., Tiwari, R., Abdelrahman, M. M., et al. (2016). Direct-fed microbial: beneficial applications, modes of action and prospects as a safe tool for enhancing ruminant production and safeguarding health. *Int. J. Pharmacol.* 12, 220–231. doi: 10.3923/ijp.2016.220.231

Kristensen, N. B., Bryrup, T., Allin, K. H., Nielsen, T., Hansen, T. H., and Pedersen, O. (2016). Alterations in fecal microbiota composition by probiotic supplementation in healthy adults: a systematic review of randomized controlled trials. *Genome Med.* 8:10. doi: 10.1186/s13073-016-0300-5

Lee, K. W., Kim, D. K., Lillehoj, H. S., Jang, S. I., and Lee, S. H. (2015). Immune modulation by *Bacillus subtilis*-based direct-fed microbials in commercial broiler chickens. *Anim. Feed Sci. Technol.* 200, 76–85. doi: 10.1016/j.anifeedsci.2014.12.006

Li, J. V., Ashrafian, H., Bueter, M., Kinross, J., Sands, C., le Roux, C. W., et al. (2011). Metabolic surgery profoundly influences gut microbial-host metabolic cross-talk. *Gut* 60, 1214–1223. doi: 10.1136/gut.2010.234708

Li, Z., Wang, W., Lv, Z., Liu, D., and Guo, Y. (2017b). *Bacillus subtilis* and yeast cell wall improve the intestinal health of broilers challenged by *Clostridium perfringens*. *Br. Poult. Sci.* 58, 635–643. doi: 10.1080/00071668.2017.1370697

Li, Y. L., Wang, Y. Y., Wu, Y. P., Wang, B. K., Chen, X., Xu, X., et al. (2017a). Echinacea pupurea extracts promote murine dendritic cell maturation by activation of JNK, p38 MAPK and NF-kappa B pathways. *Dev. Comp. Immunol.* 73, 21–26. doi: 10.1016/j.dci.2017.03.002

Liu, C., Hu, B., Cheng, Y. L., Guo, Y. H., Yao, W. R., and Qian, H. (2021). In-depth analysis of the mechanisms of aloe polysaccharides on mitigating subacute colitis in mice via microbiota informatics. *Carbohyd. Polym.* 265:118041. doi: 10.1016/j.carbpol.2021.118041

Macfarlane, G. T., Gibson, G. R., Beatty, E., and Cummings, J. H. (1992). Estimation of short-chain fatty-acid production from protein by human intestinal bacteria based on branched-chain fatty-acid measurements. *FEMS Microbiol. Ecol.* 101, 81–88. doi: 10.1016/0378-1097(92)90829-D

Magoc, T., and Salzberg, S. L. (2011). FLASH: fast length adjustment of short reads to improve genome assemblies. *Bioinformatics* 27, 2957–2963. doi: 10.1093/bioinformatics/btr507

Marleen, H. M. C., van Nuenen, P., , Meyer, D., and Venema, K. (2003). The effect of various inulins and *Clostridium difficile* on the metabolic activity and composition of the human colonic microbiota *in vitro*. *Microb. Ecol. Health Dis.* 15, 137–144. doi: 10.1080/08910600310018959

Mohammadagheri, N., Najafi, R., and Najafi, G. (2016). Effects of dietary supplementation of organic acids and phytase on performance and intestinal histomorphology of broilers. *Vet. Res. Forum.* 7, 189–195.

Mohammadigheisar, M., Shirley, R. B., Barton, J., Welsher, A., Thiery, P., and Kiarie, E. (2019). Growth performance and gastrointestinal responses in heavy tom turkeys fed antibiotic free corn-soybean meal diets supplemented with multiple doses of a single strain Bacillus subtilis probiotic (DSM29784). *Poult. Sci.* 98, 5541–5550. doi: 10.3382/ps/pez305

Musa, B. B., Duan, Y. L., Khawar, H., Sun, Q. Z., Ren, Z. Z., Mohamed, M. A. E., et al. (2019). *Bacillus subtilis* B21 and Bacillus licheniformis B26 improve intestinal health and performance of broiler chickens with *Clostridium perfringens*-induced necrotic enteritis. *J. Anim. Physiol. Anim. Nutr.* 103, 1039–1049. doi: 10.1111/jpn.13082

Oh, S. T., and Lillehoj, H. S. (2016). The role of host genetic factors and host immunity in necrotic enteritis. *Avian Pathol.* 45, 313–316. doi: 10.1080/03079457.2016.1154503

Palliyeguru, M. W. C. D., and Rose, S. P. (2014). Sub-clinical necrotic enteritis: its aetiology and predisposing factors in commercial broiler production. *World. Poultry Sci. J.* 70, 803–815. doi: 10.1017/S0043933914000865

Perez-Chabela, M. D., Alvarez-Cisneros, Y. M., Soriano-Santos, J., and Perez-Hernandez, M. A. (2020). The probiotics and their metabolites in aquaculture. A review. *Hidrobiologica* 30, 93–105. doi: 10.24275/uam/izt/dcbs/hidro/2020v30n1/Perez

Pothakam, N., Supakankul, P., Norseeda, W., Liu, G. S., Teltathum, T., Naraballobh, W., et al. (2021). Association of adipocytokine IL-1A and IL-6 genes with intramuscular fat content and fatty acid composition in pigs. *Meat Sci.* 179:108554. doi: 10.1016/j.meatsci.2021.108554

Prescott, J. F., Smyth, J. A., Shojadoost, B., and Vince, A. (2016). Experimental reproduction of necrotic enteritis in chickens: a review. *Avian Pathol.* 45, 317–322. doi: 10.1080/03079457.2016.1141345

Rajput, D. S., Zeng, D., Khalique, A., Rajput, S. S., Wang, H. S., Zhao, Y., et al. (2020). Pretreatment with probiotics ameliorate gut health and necrotic enteritis in broiler chickens, a substitute to antibiotics. *Amb. Express.* 10:220. doi: 10.1186/s13568-020-01153-w

Rehman, H. U., Vahjen, W., Awad, W. A., and Zentek, J. (2007). Indigenous bacteria and bacterial metabolic products in the gastrointestinal tract of broiler chickens. *Arch. Anim. Nutr.* 61, 319–335. doi: 10.1080/17450390701556817

Rodjan, P., Soisuwan, K., Thongprajukaew, K., Theapparat, Y., Khongthong, S., Jeenkeawpieam, J., et al. (2018). Effect of organic acids or probiotics alone or in combination on growth performance, nutrient digestibility, enzyme activities, intestinal morphology and gut microflora in broiler chickens. *J. Anim. Physiol. Anim. Nutr.* 102, E931–E940. doi: 10.1111/jpn.12858

Rodrigues, I., Svihus, B., Bedford, M. R., Gous, R., and Choct, M. (2018). Intermittent lighting improves resilience of broilers during the peak phase of sub-clinical necrotic enteritis infection. *Poult. Sci.* 97, 438–446. doi: 10.3382/ps/pex315

Salim, H. M., Kang, H. K., Akter, N., Kim, D. W., Kim, J. H., Kim, M. J., et al. (2013). Supplementation of direct-fed microbials as an alternative to antibiotic on growth performance, immune response, cecal microbial population, and ileal morphology of broiler chickens. *Poult. Sci.* 92, 2084–2090. doi: 10.3382/ps.2012-02947

Sallam, E. A., Mohammed, L. S., Elbasuni, S. S., Azam, A. E., and Soliman, M. M. (2021). Impacts of microbial based therapy on growth performance, intestinal health, carcass traits and economic efficiency of clostridium perfringens-infected cobb and arbor acres broilers. *Vet. Med. Sci.* 7, 773–791. doi: 10.1002/vms3.412

Shini, S., and Bryden, W. L. (2021). Probiotics and gut health: linking gut homeostasis and poultry productivity. *Anim. Prod. Sci.* doi: 10.1071/AN20701

Shivaramaiah, S., Pumford, N. R., Morgan, M. J., Wolfenden, R. E., Wolfenden, A. D., Torres-Rodriguez, A., et al. (2011). Evaluation of bacillus species as potential candidates for direct-fed microbials in commercial poultry. *Poult. Sci.* 90, 1574–1580. doi: 10.3382/ps.2010-00745

Song, J., Xiao, K., Ke, Y. L., Jiao, L. F., Hu, C. H., Diao, Q. Y., et al. (2014). Effect of a probiotic mixture on intestinal microflora, morphology, and barrier integrity of broilers subjected to heat stress. *Poult. Sci.* 93, 581–588. doi: 10.3382/ps.2013-03455

Stanley, D., Wu, S. B., Rodgers, N., Swick, R. A., and Moore, R. J. (2014). Differential responses of cecal microbiota to fishmeal, Eimeria and *Clostridium perfringens* in a necrotic enteritis challenge model in chickens. *PLoS One* 9:e104739. doi: 10.1371/journal.pone.0104739

Sun, Z., Wang, T., Aschalew, N. D., Zhao, W., Chen, X., Zhang, X. F., et al. (2020). Effects of yeast cultures with different fermentation times on the growth performance, caecal microbial community and metabolite profile of broilers. *J. Anim. Physiol. Anim. Nutr.* 104, 212–223. doi: 10.1111/jpn.13241

Tiboni, M., Casettari, L., and Illum, L. (2021). Nasal vaccination against SARS-CoV-2: synergistic or alternative to intramuscular vaccines? *Int. J. Pharmaceut.* 603:120686. doi: 10.1016/j.ijpharm.2021.120686

Tugizov, S. (2021). Virus-associated disruption of mucosal epithelial tight junctions and its role in viral transmission and spread. *Tissue Barriers* 1943274. doi: 10.1080/21688370.2021.1943274 [Epub ahead of print].

Villagran-de la Mora, Z., Macias-Rodriguez, M. E., Arratia-Quijada, J., Gonzalez-Torres, Y. S., Nuno, K., and Villarruel-Lopez, A. (2020). *Clostridium perfringens* as foodborne pathogen in broiler production: pathophysiology and potential strategies for controlling necrotic enteritis. *Animals* 10:1718. doi: 10.3390/ani10091718

Wandro, S., Osborne, S., Enriquez, C., Bixby, C., Arrieta, A., and Whiteson, K. (2018). The microbiome and metabolome of preterm infant stool are personalized and not driven by health outcomes, including necrotizing enterocolitis and late-onset sepsis. *mSphere* 3, e00104–e00118. doi: 10.1128/mSphere.00104-18

Wang, Y. Y., Heng, C. A. N., Zhou, X. H., Cao, G. T., Jiang, L., Wang, J. S., et al. (2021). Supplemental Bacillus subtilis DSM 29784 and enzymes, alone or in combination, as alternatives for antibiotics to improve growth performance, digestive enzyme activity, anti-oxidative status, immune response and the intestinal barrier of broiler chickens. *Br. J. Nutr.* 125, 494–507. doi: 10.1017/S0007114520002755

Wang, L. F., Liu, C. H., Chen, M., Ya, T., Huang, W. C., Gao, P. F., et al. (2015). A novel *Lactobacillus plantarum* strain P-8 activates beneficial immune response of broiler chickens. *Int. Immunopharmacol.* 29, 901–907. doi: 10.1016/j.intimp.2015.07.024

Wang, H. S., Ni, X. Q., Qing, X. D., Liu, L., Lai, J., Khalique, A., et al. (2017a). Probiotic enhanced intestinal immunity in broilers against subclinical necrotic enteritis. *Front. Immunol.* 8:1592. doi: 10.3389/fimmu.2017.01592

Wang, H. S., Ni, X. Q., Qing, X. D., Zeng, D., Luo, M., Liu, L., et al. (2017b). Live probiotic *lactobacillus johnsonii* BS15 promotes growth performance and lowers fat deposition by improving lipid metabolism, intestinal development, and gut microflora in broilers. *Front. Microbiol.* 8:1073. doi: 10.3389/fmicb.2017.01073

Wang, Y. B., Wang, Y. Y., Wang, B. K., Mei, X. Q., Jiang, S. Q., and Li, W. F. (2019). Protocatechuic acid improved growth performance, meat quality, and intestinal health of Chinese yellow-feathered broilers. *Poult. Sci.* 98, 3138–3149. doi: 10.3382/ps/pez124

Wang, Y. Y., Wang, Y. B., Xu, H., Mei, X. Q., Gong, L., Wang, B. K., et al. (2018). Direct-fed glucose oxidase and its combination with *B. amyloliquefaciens* SC06 on growth performance, meat quality, intestinal barrier, antioxidative status, and immunity of yellow-feathered broilers. *Poult. Sci.* 97, 3540–3549. doi: 10.3382/ps/pey216

Wikoff, W. R., Anfora, A. T., Liu, J., Schultz, P. G., Lesley, S. A., Peters, E. C., et al. (2009). Metabolomics analysis reveals large effects of gut microflora on mammalian blood metabolites. *Proc. Natl. Acad. Sci. U. S. A.* 106, 3698–3703. doi: 10.1073/pnas.0812874106

Williams, R. B. (2005). Intercurrent coccidiosis and necrotic enteritis of chickens: rational, integrated disease management by maintenance of gut integrity. *Avian Pathol.* 34, 159–180. doi: 10.1080/03079450500112195

Wu, C. Y., Liao, S. Q., Qi, N. S., Peng, X. Y., Lv, M., and Sun, M. F. (2012). Molecullar typing, prevalence of netB and antimicrobial susceptibility among clinical isolates of clostridium perfringens from chickens in Southern China. *J. Anim. Vet. Adv.* 11, 1183–1187.

Wu, Y. Y., Shao, Y. J., Song, B. C., Zhen, W. R., Wang, Z., Guo, Y. M., et al. (2018). Effects of Bacillus coagulans supplementation on the growth performance and gut health of broiler chickens with *Clostridium perfringens*-induced necrotic enteritis. *J. Anim. Sci. Biotechnol.* 9:9. doi: 10.1186/s40104-017-0220-2

Wu, Y. P., Wang, B. K., Zeng, Z. H., Liu, R. R., Tang, L., Gong, L., et al. (2019). Effects of probiotics lactobacillus plantarum 16 and Paenibacillus polymyxa 10 on intestinal barrier function, antioxidative capacity, apoptosis, immune response, and biochemical parameters in broilers. *Poult. Sci.* 98, 5028–5039. doi: 10.3382/ps/pez226

Xu, X., Gong, L., Wu, Y., Wang, Y., Wang, B., Mei, X., et al. (2018). Glycyrrhizin attenuates salmonella enterica serovar Typhimurium infection: new insights into its protective mechanism. *Front. Immunol.* 9:2321. doi: 10.3389/fimmu.2018.02321

Yang, P., and Zhao, J. B. (2021). Variations on gut health and energy metabolism in pigs and humans by intake of different dietary fibers. *Food Sci. Nutr.* 9, 4639–4654. doi: 10.1002/fsn3.2421

Youssef, F. S., Eid, S. Y., Alshammari, E., Ashour, M. L., Wink, M., and El-Readi, M. Z. (2020). *Chrysanthemum indicum* and *Chrysanthemum morifolium*: chemical composition of their essential oils and their potential use as natural preservatives with antimicrobial and antioxidant activities. *Foods* 9:1460. doi: 10.3390/foods9101460

Zhang, J., Shi, H. T., Wang, Y. J., Li, S. L., Cao, Z. J., Ji, S. K., et al. (2017). Effect of dietary forage to concentrate ratios on dynamic profile changes and interactions of ruminal microbiota and metabolites in Holstein heifers. *Front. Microbiol.* 8:2206. doi: 10.3389/fmicb.2017.02206

Zhao, Y., Zeng, D., Wang, H. S., Qing, X. D., Sun, N., Xin, J. G., et al. (2020). Dietary probiotic *Bacillus licheniformis* H2 enhanced growth performance, morphology of small intestine and liver, and antioxidant capacity of broiler chickens against *Clostridium perfringens*-induced subclinical necrotic enteritis. *Probiotics Antimicrob. Proteins* 12, 883–895. doi: 10.1007/s12602-019-09597-8

Conflict of Interest: The authors declare that the research was conducted in the absence of any commercial or financial relationships that could be construed as a potential conflict of interest.

Publisher's Note: All claims expressed in this article are solely those of the authors and do not necessarily represent those of their affiliated organizations, or those of the publisher, the editors and the reviewers. Any product that may be evaluated in this article, or claim that may be made by its manufacturer, is not guaranteed or endorsed by the publisher.

frontiers in Microbiology

ORIGINAL RESEARCH
published: 06 October 2021
doi: 10.3389/fmicb.2021.746601

Oral Administration of *Latilactobacillus sakei* ADM14 Improves Lipid Metabolism and Fecal Microbiota Profile Associated With Metabolic Dysfunction in a High-Fat Diet Mouse Model

*Sung-Min Won†, Min Ju Seo†, Min Ju Kwon, Kye Won Park and Jung-Hoon Yoon**

Department of Food Science and Biotechnology, Sungkyunkwan University, Suwon, South Korea

OPEN ACCESS

Edited by:
Sabina Górska, Hirszfeld Institute of Immunology and Experimental Therapy, Polish Academy of Sciences (PAN), Poland

Reviewed by:
Filippo Rossi, Catholic University of the Sacred Heart, Italy
Aleksandr G. Bulaev, Federal Center Research Fundamentals of Biotechnology, Russian Academy of Sciences (RAS), Russia

***Correspondence:**
Jung-Hoon Yoon
jhyoon69@skku.edu

†These authors have contributed equally to this work

Specialty section:
This article was submitted to Food Microbiology, a section of the journal Frontiers in Microbiology

Received: *24 July 2021*
Accepted: *13 September 2021*
Published: *06 October 2021*

Citation:
Won S-M, Seo MJ, Kwon MJ, Park KW and Yoon J-H (2021) Oral Administration of Latilactobacillus sakei ADM14 Improves Lipid Metabolism and Fecal Microbiota Profile Associated With Metabolic Dysfunction in a High-Fat Diet Mouse Model. Front. Microbiol. 12:746601. doi: 10.3389/fmicb.2021.746601

Effects of *Latilactobacillus sakei* ADM14 on changes in lipid metabolism and fecal microbiota composition were studied in high-fat diet (HFD) mouse model. The mice were divided into three groups: normal diet (ND), high-fat diet (HD), and HFD plus *L. sakei* ADM14 (HDA). Oral administration of *L. sakei* ADM14 daily for 10 weeks decreased body weight gain, fat tissue mass, and liver weight in mice and reduced the size of histologically stained liver adipocytes. In addition, serum total cholesterol, triglycerides, and blood glucose decreased significantly. *Latilactobacillus sakei* ADM14 regulated the expression of genes related to lipid metabolism in epididymal adipose tissue and liver and induced changes in the composition of fecal microbiota, thereby improving energy harvests and changing metabolic disorder-related taxa. A significant decrease ($p < 0.05$) in the *Firmicutes* to *Bacteroidetes* ratio was found in the HDA group compared to the HD group, particularly due to the difference in the relative abundance of the *Bacteroidetes* between the two groups over 10 weeks. Differences in proportions of some taxa reported to have correlation with obesity were also found between HD and HDA groups. These results suggest that *L. sakei* ADM14 can have a positive effect on metabolic disorders such as obesity and fatty liver through effective regulation of host lipid metabolism and gut microbiota.

Keywords: ***Latilactobacillus sakei*, probiotics, obesity, lipid metabolism, microbiome**

INTRODUCTION

Obesity has emerged as an important health problem through a rapid increase in incidence worldwide. Excessive body weight gain and body fat accumulation pose a serious threat, leading to the onset of obesity and metabolic disorders such as diabetes and cardiovascular disease (Bastien et al., 2014). A high-fat diet (HFD) affects elevated serum cholesterol and triglycerides (TG) and increases the risk of chronic low-grade inflammation from obesity, along with adipose tissue enlargement (Dewulf et al., 2011). The influence of metabolic disorders in combination with the HFD can also damage the liver. Recently, the association and risk of obesity with

nonalcoholic fatty liver disease (NAFLD) has received a lot of attention. NAFLD includes a variety of symptoms ranging from simple steatosis to nonalcoholic fatty hepatitis, cirrhosis, or hepatocellular carcinoma (Wong et al., 2015), and more than 80% of obese individuals in western countries are affected by NAFLD (Younossi, 2019). Recently, several studies have focused on gut microbiota as a new environmental factor contributing to the relationship between obesity and NAFLD (Le Roy et al., 2013; Tilg et al., 2016; Da Silva et al., 2018). The gut microbial community consists of thousands of bacterial species, coexisting with the host, and has a significant influence on the physiology and metabolism of the host (Turnbaugh et al., 2006; Ridaura et al., 2013). Recently, a link between the effects of choline deficiency on fatty liver development and changes in the human gut microbiota was confirmed (Spencer et al., 2012), and it was revealed that changes in the gut microbiota regulate the progression of NAFLD (Buzzetti et al., 2016). Thus, the regulation of gut microbial communities may suggest new therapeutic strategies in the management of metabolic diseases such as obesity and NAFLD. Probiotics regulate the gut microbiome and have proven beneficial effects on metabolic symptoms. They are also known to be effective in improving lipid profiles and hyperlipidemia, while affecting lipid metabolism (Roller et al., 2004; Sun and Buys, 2015).

In our previous study, a lactic acid bacterium, designated ADM14, was found to have anti-adipogenic effect by reducing significantly intracellular triglyceride content on 3T3-L1 adipocytes and by decreasing the expression of five adipogenic marker genes (Won et al., 2020a). The strain ADM14 was identified as a member of *Lactobacillus sakei* in the study of Won et al. (2020a), but *L. sakei* has been recently reclassified as *L. sakei* (Zheng et al., 2020). The aim of this study was to investigate the effect of *L. sakei* ADM14 on host lipid metabolism, fatty liver, and metabolic problems in HFD mouse model. In addition, changes in gut microbiota structure on the host were analyzed through fecal microbiome analysis the relationship between the gut-liver axis was evaluated.

MATERIALS AND METHODS

Bacterial Strain Preparation and Growth Conditions

Latilactobacillus sakei (*L. sakei*) ADM14 was cultured using De Man-Rogosa-Sharpe (MRS, BD Difco, Sparks, MD, United States) agar at 30°C for 24 h and was stored at −80°C in 20% glycerol (v/v; Georgiachem, GA, United States) for cryopreservation until it was used in experiments.

Animals, Diets, and Experimental Design

The animal care and studies were conducted in accordance with the Animal Care and Use Committee of the College of Biotechnology at Sungkyunkwan University (approval date: 07-09-2019, approval number: SKKUIACUC-18-04-14-3). Male C57BL/6 J mice aged 5 weeks were purchased from RaonBio Inc. (Yongin, Republic of Korea) and maintained under controlled temperature and humidity (24 ± 2°C, 50 ± 10%) with a 12 h light/dark cycle. After a 1-week acclimation period, 6-week-old mice were randomly divided into three groups ($n = 8$): normal diet (ND), high-fat diet (HD), and high-fat diet plus *L. sakei* ADM14 (HDA, 10^8–10^9 CFU per 200 µl 0.85% saline). The ND group received a normal chow diet (10% of energy from fat, 16.1 kJ, RaonBio Inc.) for 10 weeks and the HD group received a HFD (60% of energy from fat, 21.9 kJ, RaonBio Inc.) for 10 weeks (**Supplementary Table S1**). The HDA group received a HFD for 10 weeks and *L. sakei* ADM14 by daily oral administration. Food and water were fed *ad libitum*. Live *L. sakei* ADM14 was administered by oral gavage at a concentration of 10^8–10^9 CFU per 200 µl 0.85% saline daily as recommended by the WHO and the Korea Food and Drug Administration. During the experiment, food intake and body weight were measured weekly. Fecal samples were collected weekly and stored at −80°C. The food efficiency ratio (FER) was expressed as total body weight gained from the diet divided by total diet consumed during the animal experiments, and total calorie intake was calculated as the total amount of diet consumed during the animal experiment multiplied by the caloric value of the diet. The mice that died during the experiment of 10 weeks were excluded, and the mice with the maximum and minimum values in weight were also excluded. Finally, 4–6 mice per group were used in further analyses. At the end of the experiment, mice were fasted for 16 h and sacrificed under anesthesia. After sacrifice, visceral organs (liver, spleen, and kidney) and epididymal and subcutaneous fat pad were collected and weighed. Epididymal fat pads and liver were preserved by freezing in liquid nitrogen for genetic analysis. A portion of the liver was frozen and stained with Oil Red O (Sigma-Aldrich, St. Louis, MO, United States) for histological study. Blood was collected *via* cardiac puncture and was centrifuged for 10 min at 3,000 rpm for serum separation.

Serum Analysis

Alanine transaminase (ALT), aspartate transaminase (AST), total cholesterol, glucose, triglyceride (TG), high-density lipoprotein (HDL), and low-density lipoprotein (LDL) levels were measured using a biochemical automatic analyzer (AU480, Beckman Coulter Inc., Brea, CA, United States) according to the manufacturer's instructions.

RNA Extraction and Quantitative Real-Time PCR

Total RNA was extracted from epididymal fat tissue and liver using an RNeasy Mini Kit (Qiagen, Hilden, Germany) and TRIzol (Invitrogen, Carlsbad, CA, United States) according to the manufacturer's protocol. First-strand complementary DNA was synthesized using a Veriti™ 96-Well Thermal Cycler machine (Thermo Scientific, Waltham, MA, United States) by mixing the extracted total RNA and ReverTra Ace Master Mix (Toyobo, Osaka, Japan). A mixture of Power SYBR Premix ExTaq (RP041A; Takara, Shiga, Japan), primers and cDNA was used for amplification using a thermal cycler machine (Takara). Gene expression was normalized by a housekeeping gene, *36B4*. The primer sequences for the genes are shown in **Supplementary Table S2**.

16S rRNA Gene Sequence Analysis of Gut Microbiota and Bioinformatics

For microbiome analysis, total genomic DNA was extracted from fecal samples using a QIAamp DNA Stool Mini Kit (Qiagen) according to the manufacturer's protocol. The first amplification from the total genomic DNA was performed in the V3 to V4 regions with primer sequences of 16S rRNA gene as shown in **Supplementary Table S3** (Fadrosh et al., 2014). A second amplification was performed by attaching an Illumina NexTera barcode to the first amplification product. Sequencing was performed according to the method of Chunlab Inc. (Seoul, Republic of Korea) using an Illumina MiSeq sequencing system (Illumina, San Diego, CA, United States). Taxonomic profiling and sequencing data analysis were performed using the Illumina platform (Chunlab Inc.). Alpha diversity was calculated using OTU information and expressed as the Chao 1 and Shannon index. The microbiota structure between groups was measured to principal coordinate analysis (PCoA) at the genus level using the beta diversity index. The linear discriminant analysis effect size (LEfSe) method was performed using latent Dirichlet allocation (LDA) score 3.0 cutoff and value of $p < 0.05$.

Statistical Analysis

Statistical analyses were conducted using SPSS ver. 19.0 (SPSS Inc., Chicago, IL, United States). Data are presented as mean ± SEM. Significant differences in the gene expression of tissue between animal experimental groups were determined by unpaired Student's *t*-test. For relative abundance analysis of the gut microbiome, significant differences between groups were determined using the Wilcoxon rank-sum test. Values were considered statistically significant when $p < 0.05$.

RESULTS

Effects of *L. sakei* ADM14 on Body, Liver, and Fat Tissue Weight

Changes in weight between the groups of mice were observed for 10 weeks. The weight of group fed the HFD increased more rapidly (**Figure 1A**). After 10 weeks, the average weight gains in the ND, HD, and HDA groups were 6.31 ± 0.56, 15.03 ± 1.25, and 11.30 ± 1.01 g, respectively. Compared with the HD group, the weight gain of the HDA group decreased significantly by 24.7% ($p < 0.05$). While the total caloric intake was significantly different (ND vs. HD, $p < 0.01$; ND vs. HDA, $p < 0.05$) between the ND and HFD intake groups, there was no significant difference between the HD and HDA groups (**Figure 1B**). The FER increased significantly ($p < 0.01$) in HD compared to ND, but there was no significant difference despite a 12.9% decrease in HDA compared to HD (**Figure 1C**). No significant weight changes were observed in the kidneys and spleen, of each group (**Figure 1D**). There was a significant increase ($p < 0.01$) in the mass of epididymal fat and subcutaneous fat in HD compared to ND (**Figure 1D**). In contrast, there was a significant decrease of 44.5% in epididymal fat ($p < 0.01$) and 33.8% in subcutaneous fat ($p < 0.05$) in HDA compared to HD (**Figure 1D**). The liver weight was not significantly different between ND and HD, but a significant decrease ($p < 0.05$) was observed in HDA compared to HD (**Figure 1D**). In the histological analysis of the liver using Oil Red O staining, it was observed that the size of stained adipocytes decreased in HDA compared to HD (**Figure 1E**).

Effects of *L. sakei* ADM14 on Serum Biochemical Parameters

The concentrations of total cholesterol, glucose, TG, and HDL of the serum in the HD group were significantly ($p < 0.01$) higher than those of the ND group (**Table 1**). Compared with the HD group, total cholesterol, glucose, and TG of the serum decreased in the HDA group administered with *L. sakei* ADM14 (**Table 1**). Total cholesterol decreased by 17.0% ($p < 0.05$), glucose decreased by 29.9% ($p < 0.05$), and TG decreased by 34.2% ($p < 0.01$). Compared to the HD group, the HDA group showed a significant increase ($p < 0.05$) in HDL, and the LDL decreased by 9.0% but there was no significant difference between them. ALT and AST were analyzed and there was no significant difference among the groups (**Supplementary Figure S1**).

Effects of *L. sakei* ADM14 on Genes of Lipid Metabolism in Epididymal Fat Tissue and Liver

The results for the mRNA expression of genes for lipid metabolism in epididymal fat tissue are shown in **Figure 2**. The expressions of genes related to lipid metabolism in epididymal fat tissue of HD group increased when compared to the ND group (**Figure 2**). Compared to the HD group, the HDA group administered with *L. sakei* ADM14 significantly downregulated ($p < 0.01$) peroxisome proliferator-activated receptor gamma (*Pparγ*), sterol regulatory element-binding protein-1C (*Srebp1C*), and fatty acid synthetase (*Fas*), of four genes related to fatty acid synthesis (**Figure 2B**). In addition, the expression of adipocyte protein 2 (*aP2*) was also significantly decreased ($p < 0.01$) in the HDA compared to the HD (**Figure 2A**). Likewise, the expressions of *Pparγ*-activated genes, lipoprotein-lipase (*Lpl*), and cluster of differentiation 36 (*CD36*) were significantly decreased ($p < 0.05$) in the HDA compared to the HD (**Figure 2A**). The expressions of tumor necrosis factor-alpha (*TNFα*; $p < 0.01$), interleukin 6 (*IL-6*; $p < 0.01$), and monocyte chemoattractant protein-1 (*MCP-1*; $p < 0.05$) related to pro-inflammatory cytokines in the HDA were significantly decreased compared to the HD group (**Figure 2C**).

To investigate the effect of *L. sakei* ADM14 on lipid metabolism in the liver, expression of overall related genes was investigated (**Figure 3**). There were also differences in the expressions of genes related to lipid metabolism in the liver between ND and HDA groups (**Figure 3**). Compared with HD, the lipid production-related genes, *Pparγ* ($p < 0.05$), *Srebp1C* ($p < 0.01$), *Fas* ($p < 0.05$), and acetyl-CoA carboxylase 1 (*Acc1*; $p < 0.05$), were significantly decreased in HDA (**Figure 3D**). In addition, the significantly increased

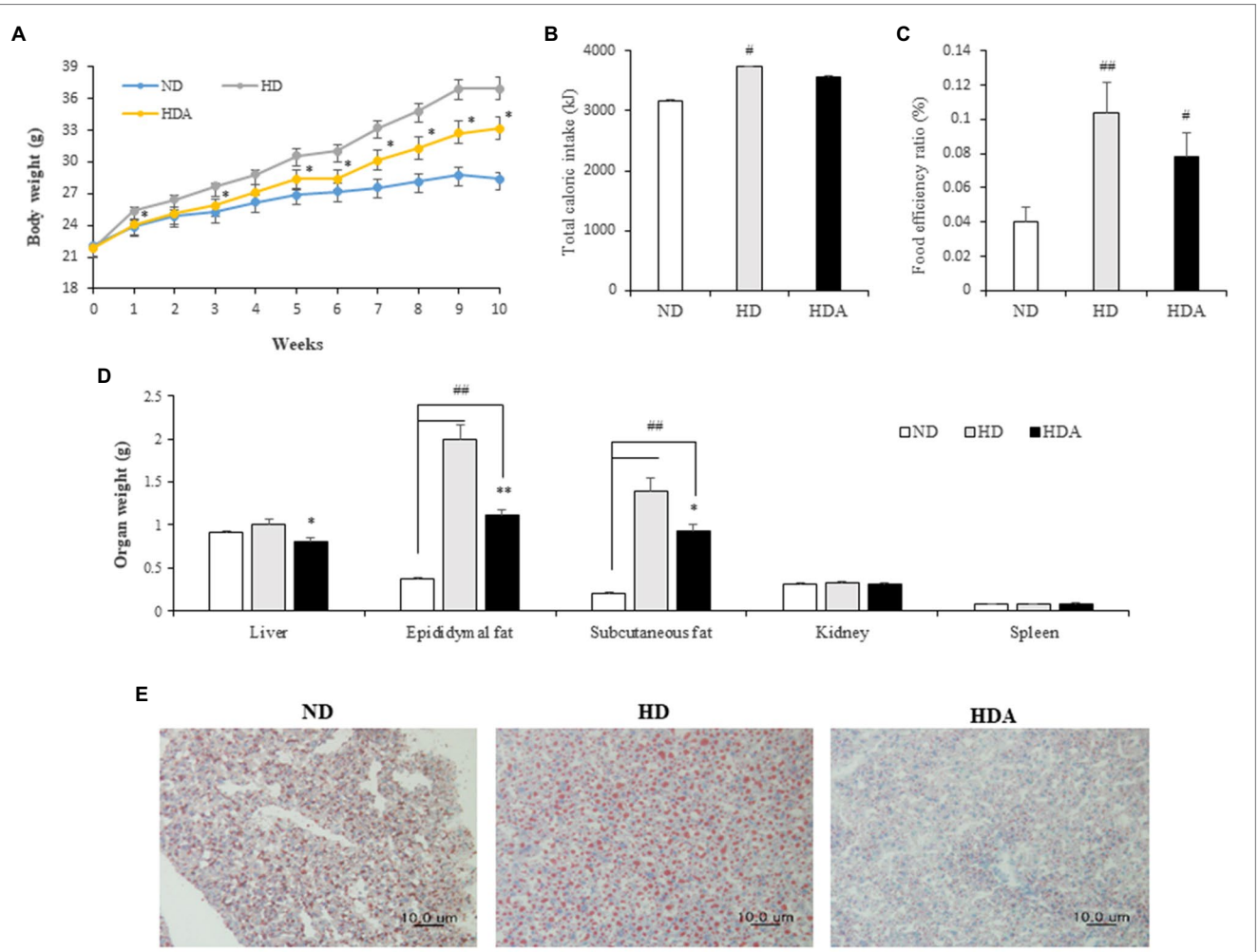

FIGURE 1 | Effect of administering *Lactobacillus sakei* ADM14 on body indicators in high-fat diet (HFD) mouse model. **(A)** Weight change of mice groups. **(B)** Total caloric intake for 10 weeks. **(C)** Food efficiency ratio (FER) for 10 weeks. **(D)** Organs weights of mice after sacrifice. **(E)** Histological analysis of liver stained with Oil Red O. ND, normal diet group; HD, high-fat diet group; and HDA, high-fat diet plus *L. sakei* ADM14 group. The results are shown as mean ± SEM ($n = 5–7$). Significant differences between HD and ND are indicated as $^{\#}p < 0.05$ and $^{\#\#}p < 0.01$. Significant differences between HDA and ND are indicated as $^{\#}p < 0.05$ and $^{\#\#}p < 0.01$. Significant differences between HD and HDA are indicated as $^{*}p < 0.05$ and $^{**}p < 0.01$.

TABLE 1 | Biochemical parameter of serum.

	ND	HD	HDA
Total cholesterol	105.00 ± 3.67	185.25 ± 11.12$^{\#\#}$	153.75 ± 6.41*
Glucose	70.75 ± 3.33	162.75 ± 7.39$^{\#\#}$	114.00 ± 15.64*
TG	61.00 ± 1.87	86.25 ± 4.96$^{\#\#}$	56.75 ± 2.53**
HDL	83.25 ± 1.89	101.25 ± 1.89$^{\#\#}$	110.25 ± 3.09*
LDL	21.75 ± 1.44	24.75 ± 0.75	22.50 ± 0.87

Values are shown as the means ± SEM ($n = 4–5$). Significant differences between HD and ND are indicated as follow: $^{\#\#}p < 0.01$. Significant differences between HD and HDA are indicated as follow: $^{*}p < 0.05$; $^{**}p < 0.01$.

expressions ($p < 0.05$) of β-oxidation-related genes, carnitine palmitoyltransferase1 alpha (*Cpt1α*) and peroxisome proliferator-activated receptor alpha (*Pparα*), were found in HDA (**Figure 3B**). Carbohydrate-response element-binding proteins, *ChREBPα* ($p < 0.01$) and *ChREBPβ* ($p < 0.05$), which are major transcriptional regulatory factors that are activated by glucose catabolism in the liver and regulates lipogenesis, were observed to be significantly downregulated in HDA (**Figure 3A**). There was no significant change in the level of *Lpl* expression, but *CD36* expression showed a significant decrease ($p < 0.05$) in HDA (**Figure 3C**). As a result of observing the expression of diglyceride acyltransferase (*Dgat*) that catalyzes TG formation, it was found that both *Dgat1* ($p < 0.05$) and *Dgat2* ($p < 0.01$) were significantly decreased (**Figure 3E**).

Effects of *L. sakei* ADM14 on Changes in Ratio and Composition of Fecal Microbiota

On analyzing alpha diversity, there was no significant difference in the Chao1 index of each group, but there was a significant increase ($p < 0.05$) in the HDA group in the Shannon index compared to the ND group (**Supplementary Figure S2**). On the other hand, there was no significant change between the HD group and the HDA group.

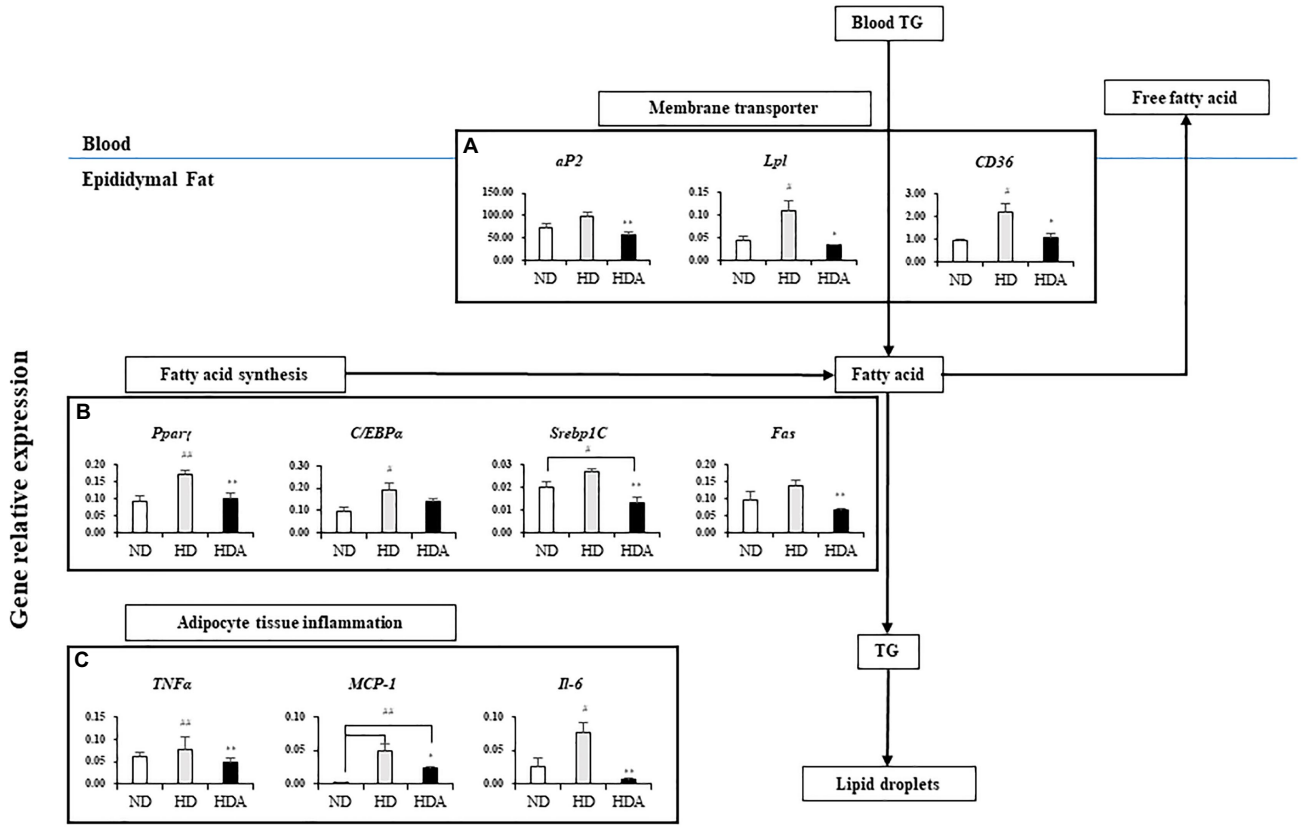

FIGURE 2 | Effects of administering *L. sakei* ADM14 on the transcription of genes related to lipid metabolism in epididymal fat tissue. The results are shown as mean ± SEM ($n = 5$). Significant differences between HD and ND are indicated as $^{\#}p < 0.05$ and $^{\#\#}p < 0.01$. Significant differences between HDA and ND are indicated as $^{\#}p < 0.05$ and $^{\#\#}p < 0.01$. Significant differences between HD and HDA are indicated as $^{*}p < 0.05$ and $^{**}p < 0.01$.

Changes of fecal microbiota in the phylum level were assessed at 1, 6, and 10 weeks using each group (**Figure 4A**). An increase in *Firmicutes* and a decrease in *Bacteroidetes* from 1 to 10 weeks were observed in both HD and HDA groups, but each showed a difference in the range of variation. The *Firmicutes* ratios at 1, 6, and 10 weeks were 49.02, 70.55, and 74.98%, respectively, in the HD group and 43.58, 70.02, and 74.04%, respectively, in the HDA group. There was no significant difference in the *Firmicutes* ratio between the two groups at 6 and 10 weeks. The *Bacteroidetes* ratios at 1, 6, and 10 weeks were 37.14, 22.37, and 3.56%, respectively, in the HD group and 38.49, 19.20, and 16.72%, respectively, in the HDA group. At 10 weeks, the *Bacteroidetes* ratios of the two groups showed a significant difference ($p < 0.05$). In addition, the *Proteobacteria* ratios at 1, 6, and 10 weeks were 2.95, 5.28, and 14.16%, respectively, in the HD group and 2.01, 9.50, and 7.21% at 1, 6, and 10 weeks, respectively, in the HDA group. The HD group showed a steady increase in the *Proteobacteria* ratios, but the HDA group decreased again from 6 to 10 weeks in the *Proteobacteria* ratios. The proportions of the three major phyla, *Firmicutes*, *Bacteroidetes*, and *Proteobacteria*, at 10 weeks of HD and HDA groups were similar with those of the two groups shown in cecal microbiota from our previous study (Won et al., 2020b), even though the proportion of the *Proteobacteria* in HDA group is higher than that of *Bacteroidetes* in the study of Won et al. (2020b). However, the *Verrucomicrobia*, which was the second major phylum in the cecal microbiota of HD group, was found only as minor phylum at 6 and 10 weeks in fecal microbiota of this study (Won et al., 2020b; **Figure 4A**).

Two dominant phyla, *Firmicutes* and *Bacteroidetes*, were compared between the three groups at 10 weeks (**Figure 4B**). The *Firmicutes* to *Bacteroidetes* ratio was significantly decreased ($p < 0.05$) in the HDA group compared to the HD group as well as ND group. At the genus level, UniFrac PCoA showed a tendency to separate among the three groups (**Figure 4C**). The percentage of major genus composition in the ND, HD, and HDA groups were investigated (**Figure 4D**). The proportions of genera *Bacteroides*, *Oscillibacter*, *Helicobacter*, *Pseudoflavonifractor*, *Alistipes*, KE159600_g, PAC002482_g, and PAC001118_g were higher in the HDA group than in other two groups. On the other hand, the proportions of genera *Faecalibaculum*, *Lactobacillus*, *Desulfovibrio*, *Staphylococcus*, *Olsenella*, and *Romboutsia* were lower in the HDA group compared to the HD group. Significant increases ($p < 0.05$) in levels of family *Muribaculaceae* and *Bacteroides acidifaciens* were found between the HDA and HD groups (**Figure 4E**). Significant increase ($p < 0.05$) in genus *Alistipes* was found in the HDA group compared to the ND and HD groups (**Figure 4E**).

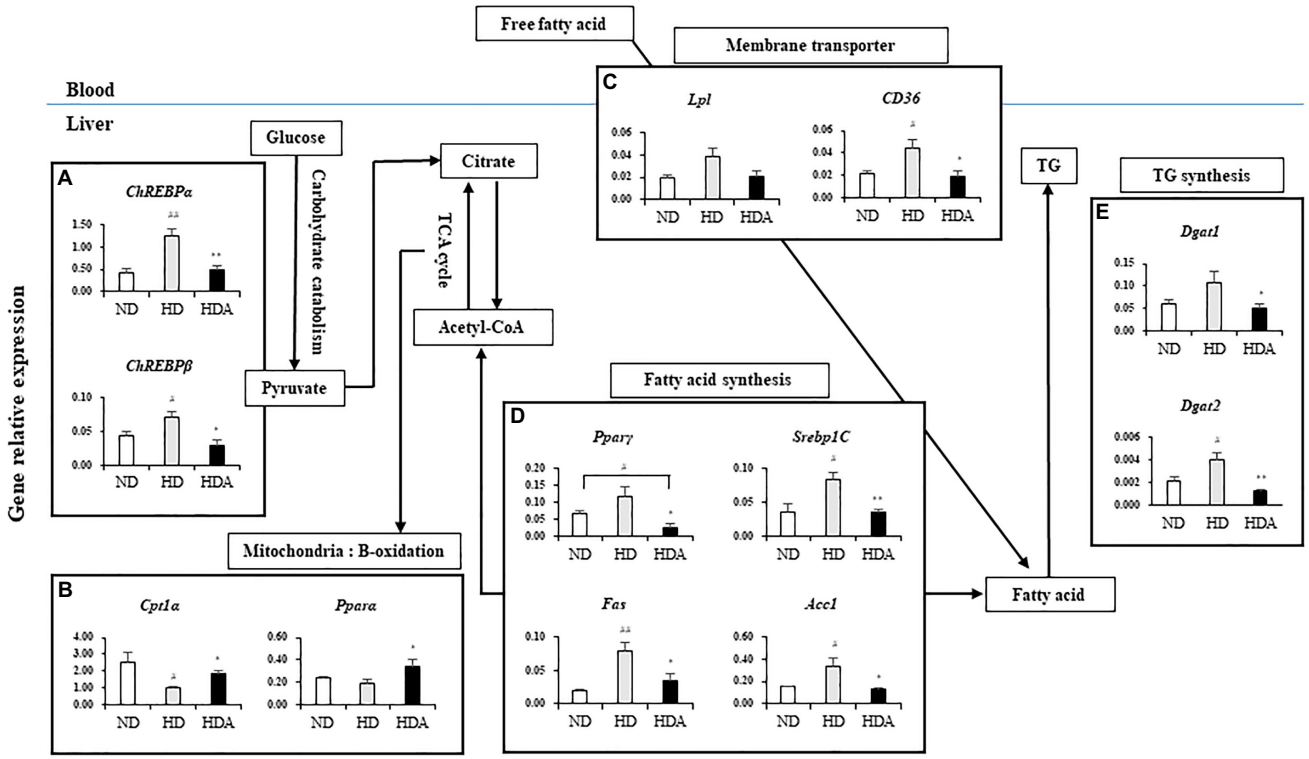

FIGURE 3 | Effects of administered *L. sakei* ADM14 on the transcription of genes related to glucose and lipid metabolism in the liver. The results are shown as mean ± SEM ($n = 5$). Significant differences between HD and ND are indicated as $^{\#}p < 0.05$ and $^{\#\#}p < 0.01$. Significant differences between HDA and ND are indicated as $^{\#}p < 0.05$ and $^{\#\#}p < 0.01$. Significant differences between HD and HDA are indicated as $^{*}p < 0.05$ and $^{**}p < 0.01$.

LEfSe analysis was calculated to identify specific bacterial taxa dominant in the HD and HDA groups (**Figure 5**). *Pseudomonas* and PAC000677_g were the core genus microbiota of the HD group, and *Bacteroides*, PAC002482_g, *Alistipes*, PAC001063_g, PAC000198_g, and PAC001066_g were identified as the dominant genus microbiota of the HDA group.

DISCUSSION

The incidence and severity of obesity and metabolic complications are constantly rising, and drug therapy has the potential to cause adverse effects (Sonnenburg and Bäckhed, 2016; Dahiya et al., 2017). The necessity for alternative therapy is increasing, and attention has been drawn by the effectiveness and utilization of probiotic lactobacilli (Aryana and Olson, 2017). Animal studies and clinical studies have reported the anti-obesity effects of probiotic lactic acid bacteria and improvements in metabolic disorders (Dahiya et al., 2017). In this study, the administration of *L. sakei* AMD14 suppressed weight gain and reduced body fat mass in a high-fat mouse model as shown in our previous study (Won et al., 2020b). Although, there is no significant difference in total caloric consumption, the difference in physical indicators is confirmed to be an inhibitory effect by *L. sakei* ADM14 (**Figure 1**). The reduction in the weight of subcutaneous fat tissue, as well as reduction in the weight of the epididymal fat tissue also observed previous study (Won et al., 2020b), appears to induce the overall decrease in lipid accumulation in mice administered with *L. sakei* AMD14. In this study, it was found that the weight of the liver was decreased, and as a result of microscopic observation through Oil Red O staining of the liver tissue, a decrease in the size of the adipocytes was observed (**Figures 1D,E**). This is seen as evidence that the expansion of adipocytes and accumulation of lipids in the liver were inhibited. Cardiovascular disease and lipidemia are major metabolic complications that occur and intensify because of obesity (Cani and Delzenne, 2009). These metabolic disorders are mainly caused by an increase in blood cholesterol and TGs (Yoo and Kim, 2016). The significant increases in total cholesterol, TG, and glucose in serum of the HD group were consistent with the predicted characteristics of obesity. Administration of *L. sakei* ADM14 suppressed and improved these indicators and confirmed the possibility of preventing symptoms related to lipidemia. The improvement in blood lipids after administration of *L. sakei* ADM14 could be evaluated on the basis of another case that the probiotic lactic acid bacteria effectively improved the serum markers of high-fat diet mice (Wang et al., 2012).

To confirm the potential mechanism by which *L. sakei* ADM14 inhibits obesity in a high-fat diet mouse model, genetic expression analysis of epididymal adipose tissue was

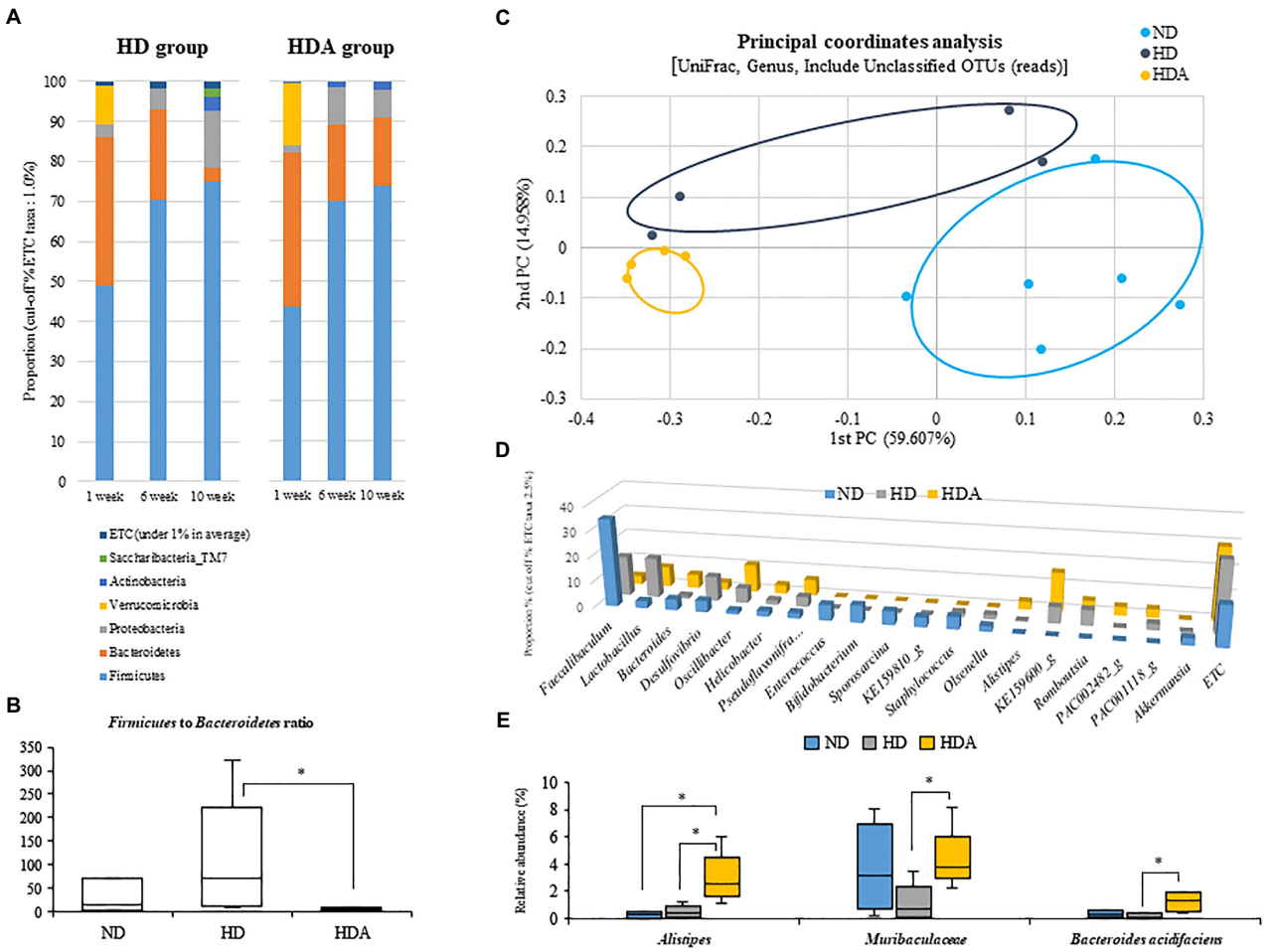

FIGURE 4 | Effect of administered *L sakei* ADM14 on fecal microbiome composition. **(A)** Changes in fecal microbiota in HD and HDA groups at the phylum level in 1, 6, and 10 weeks. **(B)** *Firmicutes* to *Bacteroidetes* ratios between groups at 10 weeks. **(C)** Fecal microbiota composition of groups at 10 weeks is shown by the genus level UniFrac principal coordinates analysis (PCoA). **(D)** Main fecal microbiota composition of genus level (cut off taxa 2.5%) at 10 weeks. **(E)** The relative abundance of specific taxa in fecal microbiota at 10 weeks. The results are shown as mean ± SEM ($n = 4$–6). Significant differences between groups are indicated as $^{*}p < 0.05$.

performed (**Figure 2**). Adipose tissue is one of the important organs that regulate lipid metabolism (Schneeberger et al., 2015). Adipocyte transcription factors *Pparγ* and *C/EBPα* play an important role in the development of adipocytes (Rosen et al., 1999; Jeong et al., 2008), and our results showed a tendency to decrease in the expression of both genes. It has been reported that these transcription factors have a positive correlation with lipid accumulation rates (Park et al., 2009). Additionally, the decreased expression of *Srebp1C*, which is involved in fatty acid synthesis, and *Fas*, which is involved in regulating lipid production, suggests that the accumulation of lipids in adipocytes was inhibited. Likewise, *aP2*, which is related to adipose production, and *CD36* and *Lpl*, which are related to lipid storage showed decreased expression and through this, it could be confirmed that a change occurred in adipose tissue metabolism. The expression of *Pparγ*, *C/EBPα*, *Fas*, *aP2*, and *CD36* in epididymal fat was confirmed to decrease also in this study as shown previously (Won et al., 2020b). From these results, it could be confirmed that administration of *L. sakei* ADM14 may cause changes in adipose tissue metabolism by affecting transcription factors, lipid production, or lipid storage. Low-grade chronic inflammation of adipose tissue is one of the major factors in obesity-induced insulin resistance and metabolic disorders (Gregor and Hotamisligil, 2011). As the expression of inflammation-related genes in adipose tissue was decreased, it was also confirmed that low-grade inflammation was alleviated (**Figure 2**; Won et al., 2020b).

Nonalcoholic fatty liver disease is representative of the symptoms induced by obesity (Canfora et al., 2019). The balance of lipid metabolism in the liver is disrupted, causing excessive lipogenesis and hepatic lipid accumulation (Rotman and Sanyal, 2017; Friedman et al., 2018). NAFLD can lead to liver damage and develop into fatty hepatitis, cirrhosis, or hepatocellular carcinoma (Le Roy et al., 2013). Fundamentally, the increase in the expression of major genes

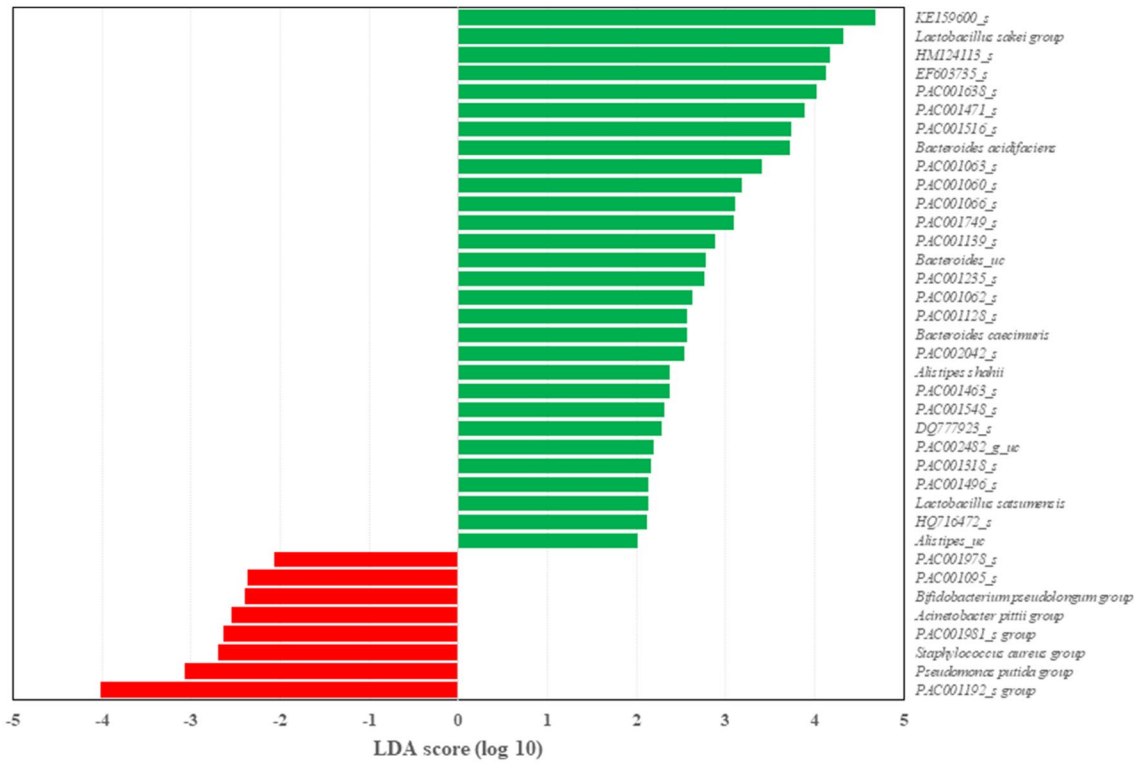

FIGURE 5 | Differentially represented genus between HD and HDA group through linear discriminant analysis effect size (LEfSe) analysis. Latent Dirichlet allocation (LDA) score indicates the effect size. $n = 4$–6 per group.

related to lipogenesis in liver tissue seems to be one of the biggest causes. Glucose absorbed in the intestine regulates the transcription of lipogenic genes through *ChREBP* (Kawaguchi et al., 2001). In our results, it appears that the decreased expression of *ChREBPα/β* resulted in the decreased expression of adipogenic genes, thus affecting the reduction of hepatic lipid accumulation in the liver. The expression of fatty acid synthesis-related genes such as *Pparγ*, *Fas*, and *Acc1* decreased with the inhibition of glucose catabolism. The expression of *Srebp1C* targeting *Fas* and *Acc1* also decreased. The main characteristic of NAFLD is the accumulation of TG in the liver (Eslamparast et al., 2013). In a state of excess energy such as obesity, the activity of *Dgat*, which catalyzes TG synthesis, increases (Choi and Diehl, 2008). The increase in free fatty acid delivered to the liver also upregulates the synthesis of TG and ultimately increases the likelihood of developing NAFLD (Choi and Diehl, 2008). The results of our study showed that the expression of *Dgat1* and *Dgat2* was reduced in the final stage of TG synthesis. Likewise, a reduction in the uptake of free fatty acid through the reduction of *Lpl* and *CD36* expression seems to affect the process of TG synthesis. In our results, it was confirmed that the expression of *Dgat1* and *Dgat2*, which catalyzes TG synthesis, was decreased. Likewise, it appears that a reduction in the uptake of free fatty acid to the liver through a decrease in *Lpl* and *CD36* expression influenced the TG synthesis. β-oxidation is one of the key pathways for fatty acid metabolism in the liver (Lu et al., 2014). *Pparα* and *Cpt1α* were upregulated in the HDA group compared to the HD group. This has been shown to upregulate lipolysis and fatty acid oxidation. In this study, although NAFLD is shown not to be caused by high-fat diet, genetic analysis in the mechanisms of lipid metabolism in the liver suggests that *L. sakei* ADM14 downregulates lipid production and upregulates fatty acid oxidation-related genes, while regulating hepatocytes lipid accumulation and a reduction in TG synthesis (**Figure 3**).

A high-fat diet can contribute to changes in the gut microbiome and can lead to metabolic imbalances caused by gut microbiota dysbiosis (Wang et al., 2011; Wu et al., 2017). In addition, gut microbiota dysbiosis has recently been reported to be associated with liver diseases as well as metabolic diseases such as obesity (Da Silva et al., 2018; Kong et al., 2018). Therefore, for the prevention and treatment of metabolic diseases, an analysis targeting the gut microbiota must be conducted (Li et al., 2020). As a result of analyzing the fecal microbiota, we observed a significant decrease ($p < 0.05$) in the *Firmicutes* to *Bacteroidetes* ratio in the HDA group compared to the HD group at the phylum level as also shown in cecal microbiota from our previous study (Won et al., 2020b; **Figure 2**). The main cause was the difference in the relative abundance of the *Bacteroidetes* between HDA and HD groups over 10 weeks. In particular, relative abundance of the *Bacteroidetes* after 10 weeks from

the HDA group was also similar with that of cecum shown in the study of Won et al. (2020b). In the analyses of the fecal microbiota at three different times (1, 6, and 10 weeks), the increase in *Firmicutes* ratios from 1 to 6 weeks was much greater than that from 6 to 10 weeks in both the HD and HDA groups, whereas the decrease in *Bacteroidetes* ratios was greater from 6 to 10 weeks in the HD group but was greater from 1 to 6 weeks in the HDA group (**Figure 4A**). The *Proteobacteria* ratios from 6 to 10 weeks were decreased in the HDA group unlike in the HD group (**Figure 4A**). The administration of *L. sakei* ADM14 from 1 to 10 weeks does not affect *Firmicutes* ratios between the HD and HDA groups but affect the ratios of *Bacteroidetes* and *Proteobacteria* in the HDA group. In the study of Won et al. (2020b), administration of *L. sakei* ADM14 was shown to increase *Firmicutes* ratios in the cecal microbiota. These results suggest that the failure to increase the *Firmicutes* ratio in fecal microbiota despite the administration of *L. sakei* might be due to colonization of *L. sakei* ADM14 in the intestine. The *Firmicutes* can produce more harvestable energy than *Bacteroidetes*, and when the relative abundance of *Firmicutes* increases and *Bacteroidetes* decreases, the absorption of calories in the digestive tract increases (Turnbaugh et al., 2006; Komaroff, 2017). This difference in terms of energy harvesting promotes metabolic diseases such as obesity. In our results, the administration of *L. sakei* ADM14 induces a change in the proportion of the dominant taxa at the phylum level and suggests that differences in energy resources may occur. At the genus level, *Bacteroides*, *Oscillibacter*, and *Alistipes*, which have higher proportions in the HDA group compared to the HD group, were reported to have a negative correlation with obesity (Dahiya et al., 2017; Thingholm et al., 2019). *Bacteroides* and *Alistipes* were also observed to have higher proportions in cecal sample of the HDA group in previous study by Won et al. (2020b). *Bacteroides* and *Alistipes* are known to be the major producers of short chain fatty acids such as acetic acid and butyric acid (Borton et al., 2017; Yin et al., 2018). In fecal microbiota, members of genus *Alistipes*, family *Muribaculaceae* and species *Bacteroides acidifaciens* were notable bacteria whose relative abundance was significantly changed by the administration of *L. sakei* ADM14 (**Figure 4E**). The genus *Alistipes* is found at low levels in the intestines of patients with hepatocellular carcinoma, colitis, and NAFLD and has been reported to have protective effects against some diseases including liver fibrosis, colitis, and cardiovascular disease (Parker et al., 2020). *Muribaculaceae*, previously known as family S24-7, was reported as representative bacteria with low abundance in mice fed a high-fat diet (Lagkouvardos et al., 2016). *Bacteroides acidifaciens* has been reported to be effective in preventing metabolic disorders such as obesity by controlling the host lipid metabolism (Yang et al., 2017). Overall, *L. sakei* ADM14 changed the composition of gut microbiota, suggesting the possibility of preventing metabolic disorders caused by dysbiosis. In particular, an increase in the abundance of *Alistipes* through gut microbiota modification helps to prevent diseases such as fatty liver through gut-liver axis modulation.

CONCLUSION

In this study, *Latilactobacillus sakei* ADM14 was found to inhibit adipogenesis by regulating the expression level of lipid metabolism in adipose tissue and liver tissue in a high-fat diet mouse model. In addition, fecal microbial community analysis suggested that the composition and ratio of gut microbiota were modified to induce changes in energy harvest, and the possibility of preventing metabolic disorders through modulation of the gut-liver axis. To our knowledge, there are few studies to evaluate the relationships among obesity, lipid metabolism in both epididymal fat and liver, and fecal microbiomes at different times by probiotic strain, particularly lactic acid bacteria isolated from kimchi. Further research and clinical studies are needed to evaluate their applicability and effectiveness in human.

DATA AVAILABILITY STATEMENT

The datasets presented in this study can be found in online repositories. The names of the repository/repositories and accession number(s) can be found at: https://www.ncbi.nlm.nih.gov/ (PRJNA751416, PRJNA751419, PRJNA751420, PRJNA751421, PRJNA751431, and PRJNA751433).

ETHICS STATEMENT

The animal study was reviewed and approved by Animal Care and Use Committee of the College of Biotechnology at Sungkyunkwan University (approval number: SKKUIACUC-18-04-14-3).

AUTHOR CONTRIBUTIONS

S-MW and MS performed the experiments of this study and reviewed the manuscript. MK supported some experiments of this study. KP discussed the results of this study. J-HY designed this study and wrote manuscript. All authors contributed to the article and approved the submitted version.

FUNDING

This work was supported by the "Cooperative Research Program for Agriculture Science and Technology Development (project no. PJ015247)" of the Rural Development Administration, Republic of Korea and a Research Initiative Program of Sungkyunkwan University, Republic of Korea.

SUPPLEMENTARY MATERIAL

The Supplementary Material for this article can be found online at: https://www.frontiersin.org/articles/10.3389/fmicb.2021.746601/full#supplementary-material

REFERENCES

Aryana, K. J., and Olson, D. W. (2017). A 100-year review: yogurt and other cultured dairy products. *J. Dairy Sci.* 100, 9987–10013. doi: 10.3168/jds.2017-12981

Bastien, M., Poirier, P., Lemieux, I., and Després, J. P. (2014). Overview of epidemiology and contribution of obesity to cardiovascular disease. *Prog. Cardiovasc. Dis.* 56, 369–381. doi: 10.1016/j.pcad.2013.10.016

Borton, M. A., Sabag-Daigle, A., Wu, J., Solden, L. M., and Wrighton, K. C. (2017). Chemical and pathogen-induced inflammation disrupt the murine intestinal microbiome. *Microbiome* 5, 1–15. doi: 10.1186/s40168-017-0264-8

Buzzetti, E., Pinzani, M., and Tsochatzis, E. A. (2016). The multiple-hit pathogenesis of non-alcoholic fatty liver disease (NAFLD). *Metabolism* 65, 1038–1048. doi: 10.1016/j.metabol.2015.12.012

Canfora, E. E., Meex, R. C. R., Venema, K., and Blaak, E. E. (2019). Gut microbial metabolites in obesity, NAFLD and T2DM. *Nat. Rev. Endocrinol.* 15, 261–273. doi: 10.1038/s41574-019-0156-z

Cani, P., and Delzenne, N. (2009). The role of the gut microbiota in energy metabolism and metabolic disease. *Curr. Pharm. Des.* 15, 1546–1558. doi: 10.2174/138161209788168164

Choi, S. S., and Diehl, A. M. (2008). Hepatic triglyceride synthesis and nonalcoholic fatty liver disease. *Curr. Opin. Lipidol.* 19, 295–300. doi: 10.1097/MOL.0b013e3282ff5e55

Da Silva, H. E., Teterina, A., Comelli, E. M., Taibi, A., Arendt, B. M., and Allard, J. P. (2018). Nonalcoholic fatty liver disease is associated with dysbiosis independent of body mass index and insulin resistance. *Sci. Rep.* 8:1466. doi: 10.1038/s41598-018-19753-9

Dahiya, D. K., Renuka, Puniya, M., Shandilya, U. K., Dhewa, T., and Shukla, P. (2017). Gut microbiota modulation and its relationship with obesity using prebiotic fibers and probiotics: a review. *Front. Microbiol.* 8:563. doi: 10.3389/fmicb.2017.00563

Dewulf, E. M., Cani, P. D., Neyrinck, A. M., Possemiers, S., and Delzenne, N. M. (2011). Inulin-type fructans with prebiotic properties counteract GPR43 overexpression and PPARγ-related adipogenesis in the white adipose tissue of high-fat diet-fed mice. *J. Nutr. Biochem.* 22, 712–722. doi: 10.1016/j.jnutbio.2010.05.009

Eslamparast, T., Eghtesad, S., Hekmatdoost, A., and Poustchi, H. (2013). Probiotics and nonalcoholic fatty liver disease. *Middle East J. Dig. Dis.* 5, 129–136.

Fadrosh, D. W., Ma, B., Gajer, P., Sengamalay, N., Ott, S., Brotman, R. M., et al. (2014). An improved dual-indexing approach for multiplexed 16S rRNA gene sequencing on the Illumina MiSeq platform. *Microbiome* 2:6. doi: 10.1186/2049-2618-2-6

Friedman, S. L., Neuschwander-Tetri, B. A., Rinella, M., and Sanyal, A. J. (2018). Mechanisms of NAFLD development and therapeutic strategies. *Nat. Med.* 24, 908–922. doi: 10.1038/s41591-018-0104-9

Gregor, M. F., and Hotamisligil, G. S. (2011). Inflammatory mechanisms in obesity. *Annu. Rev. Immunol.* 29, 415–445. doi: 10.1146/annurev-immunol-031210-101322

Jeong, H. J., Yoon, S. J., and Pyun, Y. R. (2008). Polysaccharides from edible mushroom Hinmogi (*Tremella fuciformis*) inhibit differentiation of 3T3-L1 adipocytes by reducing mRNA expression of PPARγ, C/EBPα, and leptin. *Food Sci. Biotechnol.* 17, 267–273. doi: 10.1016/j.bbrc.2011.05.086

Kawaguchi, T., Takenoshita, M., Kabashima, T., and Uyeda, K. (2001). Glucose and cAMP regulate the L-type pyruvate kinase gene by phosphorylation/dephosphorylation of the carbohydrate response element binding protein. *Proc. Natl. Acad. Sci. U. S. A.* 98, 13710–13715. doi: 10.1073/pnas.231370798

Komaroff, A. L. (2017). The microbiome and risk for obesity and diabetes. *JAMA* 317, 355–356. doi: 10.1001/jama.2016.20099

Kong, C., Gao, R., Yan, X., Huang, L., and Qin, H. (2018). Probiotics improve gut microbiota dysbiosis in obese mice fed a high-fat or high-sucrose diet. *Nutrition* 60, 175–184. doi: 10.1016/j.nut.2018.10.002

Lagkouvardos, I., Pukall, R., Abt, B., Foesel, B. U., and Clavel, T. (2016). The mouse intestinal bacterial collection (miBC) provides host-specific insight into cultured diversity and functional potential of the gut microbiota. *Nat. Microbiol.* 1, 1–16. doi: 10.1038/nmicrobiol.2016.131

Le Roy, T., Llopis, M., Lepage, P., Bruneau, A., Rabot, S., and Gérard, P. (2013). Intestinal microbiota determines development of non-alcoholic fatty liver disease in mice. *Gut* 62, 1787–1794. doi: 10.1136/gutjnl-2012-303816

Li, H., Liu, F., Lu, J., Shi, J., Guan, J., Yan, F., et al. (2020). Probiotic mixture of *lactobacillus plantarum* strains improves lipid metabolism and gut microbiota structure in high fat diet-fed mice. *Front. Microbiol.* 11:512. doi: 10.3389/fmicb.2020.00512

Lu, H.-J., Tzeng, T.-F., Liou, S.-S., Chang, C. J., Yang, C., Wu, M.-C., et al. (2014). Ruscogenin ameliorates experimental nonalcoholic steatohepatitis via suppressing lipogenesis and inflammatory pathway. *Biomed Res. Int.* 2014:652680. doi: 10.1155/2014/652680

Park, H. J., Della-Fera, M. A., Hausman, D. B., Rayalam, S., and Baile, C. A. (2009). Genistein inhibits differentiation of primary human adipocytes. *J. Nutr. Biochem.* 20, 140–148. doi: 10.1016/j.jnutbio.2008.01.006

Parker, B. J., Wearsch, P. A., Veloo, A. C. M., and Rodriguez-Palacios, A. (2020). The genus *Alistipes*: gut bacteria with emerging implications to inflammation, cancer, and mental health. *Front. Immunol.* 11:906. doi: 10.3389/fimmu.2020.00906

Ridaura, V. K., Faith, J. J., Rey, F. E., Cheng, J., Duncan, A. E., and Gordon, J. I. (2013). Gut microbiota from twins discordant for obesity modulate metabolism in mice. *Science* 341:1241214. doi: 10.1126/science.1241214

Roller, M., Rechkemmer, G., and Watzl, B. (2004). Prebiotic inulin enriched with oligofructose in combination with the probiotics *Lactobacillus rhamnosus* and *Bifidobacterium lactis* modulates intestinal immune functions in rats. *J. Nutr.* 134, 153–156. doi: 10.1093/jn/134.1.153

Rosen, E. D., Sarraf, P., Troy, A. E., Bradwin, G., Moore, K., and Mortensen, R. M. (1999). PPARγ is required for the differentiation of adipose tissue in vivo and in vitro. *Mol. Cell* 4, 611–617. doi: 10.1016/S1097-2765(00)80211-7

Rotman, Y., and Sanyal, A. J. (2017). Current and upcoming pharmacotherapy for non-alcoholic fatty liver disease. *Gut* 66, 180–190. doi: 10.1136/gutjnl-2016-312431

Schneeberger, M., Everard, A., Gómez-Valadés, A. G., and Cani, P. D. (2015). *Akkermansia muciniphila* inversely correlates with the onset of inflammation, altered adipose tissue metabolism and metabolic disorders during obesity in mice. *Sci. Rep.* 5:16643. doi: 10.1038/srep16643

Sonnenburg, J. L., and Bäckhed, F. (2016). Diet-microbiota interactions as moderators of human metabolism. *Nature* 535, 56–64. doi: 10.1038/nature18846

Spencer, M. D., Hamp, T. J., Reid, R. W., Fischer, L. M., Steven, H., and Fodor, A. A. (2012). Association between composition of the human gastrointestinal microbiome and development of fatty liver with choline deficiency. *Gastroenterology* 140, 976–986. doi: 10.1053/j.gastro.2010.11.049

Sun, J., and Buys, N. (2015). Effects of probiotics consumption on lowering lipids and CVD risk factors: a systematic review and meta-analysis of randomized controlled trials. *Ann. Med.* 47, 430–440. doi: 10.3109/07853890.2015.1071872

Thingholm, L. B., Rühlemann, M. C., Koch, M., Fuqua, B., and Huttenhower, C. (2019). Obese individuals with and without type 2 diabetes show different gut microbial functional capacity and composition. *Cell Host Microbe* 26, 252.e10–264.e10. doi: 10.1016/j.chom.2019.07.004

Tilg, H., Cani, P. D., and Mayer, E. A. (2016). Gut microbiome and liver diseases. *Gut* 65, 2035–2044. doi: 10.1136/gutjnl-2016-312729

Turnbaugh, P. J., Ley, R. E., Mahowald, M. A., Magrini, V., Mardis, E. R., and Gordon, J. I. (2006). An obesity-associated gut microbiome with increased capacity for energy harvest. *Nature* 444, 1027–1031. doi: 10.1038/nature05414

Wang, Z., Klipfell, E., Bennett, B. J., Koeth, R., Levison, B. S., and Hazen, S. L. (2011). Gut flora metabolism of phosphatidylcholine promotes cardiovascular disease. *Nature* 472, 57–65. doi: 10.1038/nature09922

Wang, J., Zhang, H., Chen, X., Chen, Y., Menghebilige, and Bao, Q. (2012). Selection of potential probiotic lactobacilli for cholesterol-lowering properties and their effect on cholesterol metabolism in rats fed a high-lipid diet. *J. Dairy Sci.* 95, 1645–1654. doi: 10.3168/jds.2011-4768

Won, S. M., Chen, S., Park, K. W., and Yoon, J.-H. (2020a). Isolation of lactic acid bacteria from kimchi and screening of *Lactobacillus sakei* ADM14 with anti-adipogenic effect and potential probiotic properties. *LWT* 126:109296. doi: 10.1016/j.lwt.2020.109296

Won, S. M., Chen, S., Lee, S. Y., Lee, K. E., Park, K. W., and Yoon, J.-H. (2020b). *Lactobacillus sakei* ADM14 induces anti-obesity effects and changes in gut microbiome in high-fat diet-induced obese mice. *Nutrients* 12:3703. doi: 10.3390/nu12123703

Wong, R. J., Aguilar, M., Cheung, R., Perumpail, R. B., Harrison, S. A., and Ahmed, A. (2015). Nonalcoholic steatohepatitis is the second leading etiology

of liver disease among adults awaiting liver transplantation in the United States. *Gastroenterology* 148, 547–555. doi: 10.1053/j.gastro.2014.11.039

Wu, H., Esteve, E., Tremaroli, V., Khan, M. T., Caesar, R., and Bäckhed, F. (2017). Metformin alters the gut microbiome of individuals with treatment-naive type 2 diabetes, contributing to the therapeutic effects of the drug. *Nat. Med.* 23, 850–858. doi: 10.1038/nm.4345

Yang, J.-Y., Lee, Y.-S., Kim, Y., Lee, S.-H., Ryu, S., Fukuda, S., et al. (2017). Gut commensal *Bacteroides acidifaciens* prevents obesity and improves insulin sensitivity in mice. *Mucosal Immunol.* 10, 104–116. doi: 10.1038/mi.2016.42

Yin, J., Li, Y., Han, H., Chen, S., Gao, J., Liu, G., et al. (2018). Melatonin reprogramming of gut microbiota improves lipid dysmetabolism in high-fat diet-fed mice. *J. Pineal Res.* 65, 1–18. doi: 10.1111/jpi.12524

Yoo, J., and Kim, S. (2016). Probiotics and prebiotics: present status and future perspectives on metabolic disorders. *Nutrients* 8:173. doi: 10.3390/nu8030173

Younossi, Z. M. (2019). Non-alcoholic fatty liver disease: a global public health perspective. *J. Hepatol.* 70, 531–544. doi: 10.1016/j.jhep.2018.10.033

Zheng, J., Wittouck, S., Salvetti, E., Franz, C. M. A. P., Harris, H. M. B., Mattarelli, P., et al. (2020). A taxonomic note on the genus *Lactobacillus*: description of 23 novel genera, emended description of the genus *Lactobacillus* Beijerinck 1901, and union of *Lactobacillaceae* and *Leuconostocaceae*. *Int. J. Syst. Evol. Microbiol.* 70, 2782–2858. doi: 10.1099/ijsem.0.004107

Conflict of Interest: The authors declare that the research was conducted in the absence of any commercial or financial relationships that could be construed as a potential conflict of interest.

Publisher's Note: All claims expressed in this article are solely those of the authors and do not necessarily represent those of their affiliated organizations, or those of the publisher, the editors and the reviewers. Any product that may be evaluated in this article, or claim that may be made by its manufacturer, is not guaranteed or endorsed by the publisher.

frontiers in Nutrition

ORIGINAL RESEARCH
published: 13 October 2021
doi: 10.3389/fnut.2021.708096

Lactobacillus plantarum TWK10 Attenuates Aging-Associated Muscle Weakness, Bone Loss, and Cognitive Impairment by Modulating the Gut Microbiome in Mice

Chia-Chia Lee[1], Yi-Chu Liao[1,2], Mon-Chien Lee[3], Kun-Ju Lin[4,5], Han-Yin Hsu[1], Shiou-Yun Chiou[1], San-Land Young[1], Jin-Seng Lin[1], Chi-Chang Huang[3] and Koichi Watanabe[1,6,7]**

[1] Culture Collection & Research Institute, SYNBIO TECH INC., Kaohsiung, Taiwan, [2] Institute of Population Health Sciences, National Health Research Institutes, Miaoli, Taiwan, [3] Graduate Institute of Sports Science, National Taiwan Sport University, Taoyuan, Taiwan, [4] Department of Nuclear Medicine, Linkou Chang Gung Memorial Hospital, Taoyuan, Taiwan, [5] Department of Medical Imaging and Radiological Sciences, Chang Gung University, Taoyuan, Taiwan, [6] Bioresource Collection and Research Center, Food Industry Research and Development Institute, Hsinchu, Taiwan, [7] Department of Animal Science and Technology, National Taiwan University, Taipei, Taiwan

OPEN ACCESS

Edited by:
De-Xing Hou,
Kagoshima University, Japan

Reviewed by:
Shusong Wu,
Hunan Agricultural University, China
Sylvie Françoise Rebuffat,
Muséum National d'Histoire Naturelle, France

***Correspondence:**
Chi-Chang Huang
john5523@ntsu.edu.tw
Koichi Watanabe
koichi_wtnb@yahoo.co.jp

Specialty section:
This article was submitted to Nutrition and Microbes, a section of the journal Frontiers in Nutrition

Received: *13 May 2021*
Accepted: *13 September 2021*
Published: *13 October 2021*

Citation:
Lee C-C, Liao Y-C, Lee M-C, Lin K-J, Hsu H-Y, Chiou S-Y, Young S-L, Lin J-S, Huang C-C and Watanabe K (2021) Lactobacillus plantarum TWK10 Attenuates Aging-Associated Muscle Weakness, Bone Loss, and Cognitive Impairment by Modulating the Gut Microbiome in Mice. Front. Nutr. 8:708096. doi: 10.3389/fnut.2021.708096

In humans, aging is characterized by the progressive decline in biological, physiological, and psychological functions, and is a major risk factor in the development of chronic diseases. Therefore, the development of strategies aimed at attenuating aging-related disorders and promoting healthy aging is critical. In a previous study, we have demonstrated that *Lactobacillus plantarum* TWK10 (TWK10), a probiotic strain isolated from Taiwanese pickled cabbage, improved muscle strength, exercise endurance, and overall body composition in healthy humans. In this study, the effect of TWK10 on the progression of age-related impairments was investigated in mice. We found that TWK10 not only enhanced muscle strength in young mice, but also prevented the aging-related loss of muscle strength in aged mice, which was accompanied by elevated muscle glycogen levels. Furthermore, TWK10 attenuated the aging-associated decline in learning and memory abilities, as well as bone mass. Further analyses of gut microbiota using next-generation sequencing (NGS) of the 16S rRNA gene showed that the pattern of gut microbial composition was clearly altered following 8 weeks of TWK10 administration. TWK10-treated mice also experienced an increase in short-chain fatty acid (SCFA)-producing bacteria and higher overall levels of gut SCFA. Furthermore, TWK10 administration to some extent reversed the aging-associated accumulation of pathogenic bacterial taxa. In conclusion, TWK10 could be viewed as a potential therapeutic agent that attenuates aging-related disorders and provides health benefits by modulating the imbalance of gut microbiota.

Keywords: ***Lactobacillus plantarum*** **TWK10, aging, sarcopenia, gut microbiota, muscle, memory, osteoporosis**

INTRODUCTION

Aging is a progressive process associated with negative changes in the physical performance, body composition, learning and memory, social and psychological responses, joints, and metabolic regulation. Aging-associated decline in the functions of tissues and organs represents a major risk factor in the development of chronic disease (1). Aging is accompanied by a reduction in body lean mass and bone mineral density, and an increase in fat mass. Sarcopenia is generally defined as the progressive loss of skeletal muscle mass and strength that occurs with aging (2, 3). Muscle mass drops by ∼3–8% per decade after age 30 and its declining rate is accelerated after age 60 (4). Muscle loss is closely correlated with an increased risk of falls and fractures, physical disability, poor quality of life, and death. Furthermore, fat mass usually increases progressively with age, and is particularly localized to the abdominal region. Accumulation of abdominal fat mass is closely related to the onset of metabolic disorders, including cardiovascular disease and diabetes (5).

Low bone mass, a condition known as osteoporosis, usually happens as a result of aging. Osteoporosis is associated with an increased risk of bone fracture and fracture-associated mortality. In humans, bone mass gradually increases and peaks in the 30s and starts to decline again in the 40s (6). Meanwhile, learning and memory start to gradually decline as early as in the 20s and 30s, with the decline becoming more prominent after reaching 60 years of age. Learning and memory impairment interferes with the daily lives of elderly individuals. Approximately 40% of people aged 60 years or older have memory impairments, and each year ∼1% of them will go on to develop dementia (7, 8).

The gut microbiome plays an important role in health maintenance, and the imbalances of gut microbiota are closely related to aging (9, 10). It has been shown that elderly people have a different gut microbiome compared to younger adults. With aging, the diversity of gut microbiota appears to decline while levels of opportunistic microbes, such as members of enterobacteria and *Clostridium* spp. become more abundant (10, 11). Short-chain fatty acids (SCFAs) are produced by anaerobic intestinal bacteria as end products of dietary fiber fermentation. Butyrate, propionate, and acetate account for 90% of total SCFAs present in the colon. These metabolites have been shown to play important roles in host physiology, by modulating metabolism, gut permeability, inflammatory responses, and immune function (12–15). SCFAs also protect the host from several diseases, including colorectal cancer, inflammatory bowel disease, and diabetes (16–18). *Bacteroidetes* and *Firmicutes* are the most abundant phyla in the human gut, accounting for over 85% of microbial composition (19). In the human gut, *Bacteroidetes* members mainly produce acetate and propionate, while *Firmicutes* populations mostly produce butyrate (20). Administration of *Lactobacillus acidophilus* DDS-1 in an aging mouse model has been shown to trigger gut microbial composition shifts, leading to an improvement in the metabolic phenotype, and enhancing the production of cecal and mucosal SCFAs (21, 22). Therefore, stimulation of SCFA production and enrichment of SCFA-producing bacteria in the gut are essential for improving overall health.

Population aging is becoming a serious problem facing all humans. By 2050, the number of people aged 65 or older is expected to reach 1.5 billion globally (World Population Aging 2019 Highlights, https://digitallibrary.un.org/record/3846855). With a fast-growing elderly population, the development of strategies for attenuating aging-related disorders and promoting healthy aging, has become a crucial issue. Recent reports have highlighted the use of probiotic supplements as potential therapeutic agents to combat aging. For example, *Lactobacillus salivarius* FDB89 has been shown to promote the growth and prolong the lifespan of *Caenorhabditis elegans* (23). Lee et al. (24) also demonstrated the skin anti-aging property of *Lactobacillus plantarum* HY7714 in humans. Supplementation of *Lactococcus lactis* subsp. *lactis* strain Plasma reduced the expression of genes associated with muscle degeneration and decelerated senescence (25). Moreover, consumption of *Lactobacillus paracasei* PS23 attenuated aging-related cognitive decline and muscle loss (26, 27). Other research groups demonstrated that supplementation of *Lactobacillus* spp. prevented bone loss in an ovariectomized (OVX) induced osteoporotic mouse model (28, 29). However, the underlying mechanisms implicated as well as the impact of these probiotics on the gut microbiome remain unclear.

In our previous studies, we have demonstrated that *Lactobacillus plantarum* TWK10 (TWK10) exerted beneficial effects on body composition, particularly on muscle mass, muscle quality, and fat mass, in mice and humans (30, 31). In this study, we aimed to (i) analyze the potential role of TWK10 in attenuating the progression of aging, namely muscle loss, reduced muscle strength, cognitive deficits, body fat accumulation, and bone density loss; and (ii) investigate the impact of TWK10 on the gut microbiome.

MATERIALS AND METHODS

Animals, Probiotics, and Study Design

Male ICR mice were purchased from BioLASCO (Charles River Licensee Corp., Yi-Lan, Taiwan). All mice were housed under humidity-controlled (65 ± 5%), temperature-controlled (24 ± 2°C) conditions, kept on a 12:12 light-dark cycle, provided with a standard laboratory diet (No. 5001; PMI Nutrition International, Brentwood, MO, USA) and distilled water *ad libitum*. All experimental procedures were approved by the Institutional Animal Care and Use Committee (IACUC) of National Taiwan Sport University, Taoyuan City, Taiwan (IACUC-10712). TWK10, a plant-derived *L. plantarum* strain [recently reclassified as *Lactiplantibacillus plantarum* (32)], isolated from Taiwanese pickled cabbage (33), was obtained from the SYNBIO TECH INC. Culture Collection (Kaohsiung, Taiwan). The concentration of TWK10 was adjusted to 1×10^9 CFU in 200 μl PBS for administration to mice. All mice were first grouped by age into the young (age 4 months; $n = 17$) and the aged groups (age 19–22 months; $n = 16$). Next, these two groups of mice were each randomly assigned to two experimental groups: Y-Control (young mice receiving PBS, 200

μl/mouse/day) and Y-TWK10 (young mice receiving TWK10, 1×10^9 CFU/mouse/day), and A-Control (aged mice receiving PBS, 200 μl/mouse/day) and A-TWK10 (aged mice receiving TWK10, 1×10^9 CFU/mouse/day). During the experimental trial, body weight, food intake, and water intake were recorded on a weekly basis. Freshly voided fecal samples were also collected at baseline and at 8 weeks after treatment initiation, for microbiome analysis. Forelimb grip strength was monitored at baseline (before TWK10 administration), 4, and 8 weeks (after TWK10 administration). After 8 weeks of TWK10 administration, all mice were assessed in terms of body composition and cognitive function. The mice were then sacrificed to obtain measurements relating to tissue weight, bone quality, and muscle glycogen, and perform histological analysis.

Forelimb Grip Strength

A low-force testing system (Model-RX-5, Aikoh Engineering, Nagoya, Japan) was used to measure the absolute forelimb grip strength of treated mice as previously described (34). Briefly, the mouse was grasped at the base of the tail and lowered vertically toward the bar. The mouse was pulled slightly backwards by the tail while its two paws (forelimbs) grasped the bar, which triggered a "counter pull." The maximal grip force in 10 trials was recorded as absolute forelimb grip strength. Forelimb grip strength was monitored at baseline, 4, and 8 weeks after TWK10/PBS administration.

The Morris Water Maze

The Morris water maze (MWM) was used to assess the spatial learning and memory of mice as described previously (35). Briefly, the MWM test was performed in a round pool (100 cm in diameter and 30 cm in depth) containing water ($26 \pm 1°C$) that is colored opaque with non-toxic tempera paint. The platform and extra-mazal cues remained in the same position throughout the learning trials (day 1 and day 2) and the mice were trained to find a platform below the water surface three times per day. The water maze has three starting positions, and the mice were made to start the exercise from a different starting position each day. Maximum swim time was set at 90 s. Escape latencies of the mice on day 3 were used to examine their spatial learning and memory.

Body Composition

A micro-CT scan (Bioscan, Washington, DC, USA) was used for the measurement of adipose and lean tissues in living mice. A micro-CT air/water phantom scan (CT QC Phantom, Mediso, Hungary) was performed regulatory for Hounsfield unit (HU) calibration. All mice were anesthetized by 1% isoflurane inhalation in the prone position with legs extended. CT imaging was performed using 180 projections per rotation with 65 kVp, 1,000 ms, 0.123 mAs exposure, and a 1:1 binning factor. Sequential transaxial images through the lower body (between the femurs and abdominal region at L1 level) were obtained. The CT projections were reconstructed with a voxel size of $0.1475 \times 0.1475 \times 0.1477$ mm^3. Image analysis was performed using the PMOD (version 3.7 PMOD Technologies LTD, Zurich, Switzerland) analysis software. Images were first smoothed using a Gaussian 3D filter, then segmented according to tissue density, first for total volume and then for fat volume (36). A histogram of the abdominal volume of interest from L1 to L5 was generated and the distribution was bi-modal in nature, with one mode representing adipose tissue voxels, and the other lean tissue voxels (37). We used a fixed threshold of −300 to +3,500 HU for total volume, and −200 to −50 HU for fat volume, according to the best separation method for known fat and lean tissue regions, for all mice in this study.

Bone Quality and Serum Vitamin D Measurements

Femur bones were harvested from mice and stored in methanol until analysis. Micro-CT images of each specimen were obtained using the SkyScan 1076 micro-CT (Bruker, Kontich, Belgium). The scanning parameters were set to 50 kV, 200 μA, a rotation step of 0.5°, exposure time 2.1 s, 0.5 mm Al filter, and 9 μm/pixel scan resolution. Bone quality parameters were calculated using CT-Analyser software (Bruker). The following three-dimensional (3-D) parameters were assessed: tissue volume (TV), bone volume (BV), bone volume fraction (BV/TV), bone surface (BS), bone surface density (BS/BV), trabecular thickness (Tb.Th), trabecular spacing (Tb.Sp), trabecular number (Tb.N), trabecular pattern factor (Tb.Pf), structure model index (SMI), and bone mineral density (BMD). Serum vitamin D ($1,25\text{-}(OH)_2$ vitamin D) was measured using an automated analyzer (Hitachi 7060, Hitachi, Tokyo, Japan).

Muscle Glycogen Levels

Gastrocnemius muscles of mice were isolated and stored at −80°C until subsequent analysis. Glycogen content was measured as described previously (38). Briefly, 100 mg of muscle tissue was homogenized in 0.5 ml cold perchloric acid. The homogenate was centrifuged at 15,000 × g for 15 min at 4°C and the supernatant was collected prior to determining glycogen concentration. Levels of glycogen (mg/g muscle) were determined by commercial assay kit (Sigma-Aldrich, St. Louis, MO, USA) according to the manufacturer's instructions.

Histological Analysis

After 8 weeks of treatment, the epididymal fat pad (EFP), interscapular brown adipose tissue (BAT), and gastrocnemius muscle were carefully removed, fixed with 10% formalin overnight, and then embedded within paraffin. Paraffin-embedded tissues were sectioned at 4 μm and stained with hematoxylin and eosin (H&E) for histological examination of the EFP and BAT using a light microscope (BX-51; Olympus, Tokyo, Japan). The cross-sectional area (CSA, μm^2) of an adipocyte, the mean number of BAT adipocytes observed per high-power-field (HPF), and the mean relative brown area in BAT (%) after H&E staining, were measured and analyzed using ImageJ software (NIH, MD, USA).

DNA Extraction and 16S rRNA Gene Sequence Analysis

Freshly voided fecal samples were collected from mice after 8 weeks of treatment. For extraction of bacterial genomic DNA, fecal samples were washed three times with 1.0 ml of

PBS and centrifugated at 14,000 × g for 5 min. The fecal pellets were resuspended in 180 μl TE buffer containing lysozyme (final conc 10 mg/ml), and the suspension with glass beads (300 mg, 0.1 mm in diameter; Biospec, Bartesville, OK, USA) was homogenized for 30 s using a FastPrep 24 homogenizer (MP Biomedicals, USA) to ensures complete disruption of cell walls and release of the DNA molecules into solution. Bacterial genomic DNA was then extracted using the Genomic DNA Mini Kit (Geneaid, Taipei, Taiwan) according to the manufacturer's instructions. DNA concentrations were determined by spectrophotometry using a BioDrop instrument (Biochrom, Biochrom Ltd., Cambridge, UK). DNA samples were stored at −20°C until further processing. The V3–V4 region of the 16S rRNA gene was amplified using specific primers (319F: 5′-CCTACGGGNGGCWGCAG-3′ and 806R: 5′-GACTACHVGGGTATCTAATCC-3′) (39) according to the 16S Metagenomic Sequencing Library Preparation procedure (Illumina).

The amplicon pool was sequenced on the Illumina MiSeq™ sequencing platform (Illumina, San Diego, CA, USA). Raw sequence data were demultiplexed using the q2-demux plugin and minimally quality-filtered with DADA2 (40) (via q2-dada2) using the QIIME 2 2019.7 (41), with resulting amplicon sequence variants (ASVs). Taxonomy was assigned to ASVs using the q2-feature-classifier (42), the classify-sklearn naive Bayes taxonomy classifier against the SILVA database (release 132), and representative sequences with a 99% of similarity (43). Both alpha diversity (Shannon and Richness indices) and beta diversity were estimated with QIIME2, using a rarefaction of 30,000 sequences. Beta diversity analysis was performed using a non-metric multidimensional scaling (NMDS) ordination plot based on the weighted UniFrac or unweighted UniFrac distances by metaMDS function in the "vegan" package of R software (Vegan: Community Ecology Package. R package version 2.5-6). Permutational multivariate analysis of variance (PERMANOVA)/Adonis test was applied to explore the significant differences on the basis of 999 permutations with vegan package in R software. Raw sequence files supporting the findings of this article are deposited at NCBI Sequence Read Archive (SRA) database with project accession number PRJNA726848.

Measurement of Short-Chain Fatty Acid (SCFA) Levels

Ceca of mice were harvested, frozen immediately in liquid nitrogen, and stored at −80°C until further processing. One milligram of cecal content was mixed with 10 μl 70% ethanol solution, and then homogenized with appropriate amounts of glass beads (1.0 mm in diameter; Biospec Products) by vortexing at 3,000 rpm for 10 min. Homogenized samples were centrifuged at 14,000 × g for 10 min, and the supernatants were collected and processed for fatty acid derivatization according to the method described previously (44). The derivatized supernatants were filtered using a 0.22-μm polycarbonate syringe filter (Millipore, St. Charles, MO, USA). Analysis of SCFAs was performed using high-performance liquid chromatography (HPLC) (HITACHI, Tokyo, Japan). SCFAs were separated using a C18 HTec column (NUCLEODUR, Macherey-Nagel, Düren, Germany) with a 40°C column temperature, flow rate at 1 ml/min, and detection wavelength set to 400 nm.

Statistical Analysis

Data are expressed as mean ± SD. Statistical analyses were performed using GraphPad Prism 7.04 (GraphPad Software, San Diego, CA). For comparisons of multiple groups, data were analyzed by two-way ANOVA with a *post-hoc* Tukey-Kramer test. The Kruskal-Wallis test with a *post-hoc* Dunn's test was used for multiple non-parametric comparisons. For comparisons of two groups, the Student unpaired *t*-test and the Mann-Whitney *U*-test were used for parametric or non-parametric data analyses, respectively. The Pearson's correlation coefficient and the Spearman's correlation coefficient were used for correlation analyses between forelimb grip strength and muscle glycogen levels, and between gut microbiota abundance and aging-related phenotypic features, respectively. Differences were considered statistically significant if $P < 0.05$.

RESULTS

The Effect of TWK10 on the Aging-Related Decline in Skeletal Muscle Strength

All mice in the four experimental groups (Y-Control, Y-TWK10, A-Control, and A-TWK10) were fed for 8 weeks with identical diets, and their average body weight, food, and water intake are summarized in **Table 1**. No significant differences were observed in the body weight, food, or water intake among the four groups.

To evaluate baseline levels of muscle strength in the young and aged mouse groups, all mice were subjected to measurements of forelimb grip strength before TWK10 administration. The forelimb grip strength in the aged mouse groups (A-Control and A-TWK10; 106.1 ± 3.7 g, $n = 16$) was significantly ($P < 0.001$) lower than in the young mouse groups (Y-Control and Y-TWK10; 144.7 ± 20.7 g, $n = 17$) (**Figure 1A**). At week 0, no significant differences in the grip strength between the Y-Control and Y-TWK10 groups, and A-Control and A-TWK10 groups, respectively, while the levels of the grip strength in the young mouse groups were significantly higher ($P < 0.001$) than those in the aged mouse groups. Two-way ANOVA indicated that the factors "aging (young vs. aged)" and "treatment (control vs. TWK10 administration)" significantly ($P < 0.05$) affected the grip strength at week 8. After 4 and 8 weeks of TWK10 administration, the grip strength in the aged mouse groups were significantly lower [Y-TWK10 at week 4 and 8 ($P < 0.001$), and A-TWK10 at week 4 ($P < 0.001$) and week 8 ($P < 0.01$)] than those in the young mouse groups, respectively. Meanwhile, the grip strength in the TWK10 administered groups were significantly higher [Y-TWK10 at week 4 and 8 ($P < 0.05$), and A-TWK10 at week 4 ($P < 0.05$) and week 8 ($P < 0.01$)] compared with those in the Y-Control and A-Control groups, respectively. A significant reduction ($P < 0.001$) in the grip strength was observed in the control aged mice (A-Control) at both weeks 4 and 8, compared with that at week 0 (**Figure 1B**). Furthermore, the gastrocnemius muscle weights in the aged mouse group were significantly lower

TABLE 1 | General characteristics of the animals.

	Group			
	Y-Control	**Y-TWK10**	**A-Control**	**A-TWK10**
	$n = 8$	$n = 9$	$n = 9$	$n = 7$
Age (month)	4	4	19–22	19–22
Basal body weight (g)	41.1 ± 3.0^a	43.4 ± 1.6^a	44.0 ± 3.8^a	44.2 ± 3.4^a
Final body weight (g)	44.1 ± 3.2^a	48.0 ± 2.4^a	48.4 ± 4.2^a	48.5 ± 6.0^a
Food intake [(g/mouse)/day]	7.6 ± 0.7^a	7.8 ± 0.7^a	7.6 ± 1.1^a	7.9 ± 2.2^a
Water intake [(ml/mouse)/day]	14.3 ± 3.0^a	14.0 ± 3.2^a	13.4 ± 1.3^a	13.5 ± 2.8^a

Data are represented as mean ± SD. Statistical differences among groups were analyzed by Tukey-Kramer test. Within a row, same superscript letter (a) indicates no significant difference, P > 0.05.

($P < 0.05$), relative to those in the young mouse group. However, no significant differences in the gastrocnemius muscle weights were observed following TWK10 administration in both young and aged mice (**Figure 1C**). The gastrocnemius muscle glycogen levels were significantly lower in the aged mice (A-Control) compared with young mice (Y-Control). However, on TWK10 administration, the glycogen levels were significantly increased ($P < 0.05$) in the young mouse group, and slightly increased in the aged mice (**Figure 1D**). Positive correlations between the grip strength and muscle glycogen levels were observed in both young mice (Pearson's correlation coefficient, $r = 0.630$, $P = 0.007$) and aged mice (Pearson's correlation coefficient, $r = 0.578$, $P = 0.019$) (**Figure 1E**).

The Effect of TWK10 on Aging-Associated Bone Loss

To evaluate the efficacy of TWK10 in restoring bone quality, murine femur bones were harvested after 8 weeks of treatment, and the cortical and trabecular microstructures were analyzed using micro-CT. The impact of TWK10 on femur BMD and trabecular parameters is summarized in **Table 2**. Age-related bone loss was demonstrated as a significant reduction ($P < 0.05$) in Tb.N and an increase in Tb.Sp ($P = 0.1547$), when comparing the Y-Control and A-Control groups. The BV/TV values were significantly higher ($P < 0.05$) in the Y-TWK10 group compared to the Y-Control mice, whereas the values of Tb.Sp in the Y-TWK10 group were significantly lower ($P < 0.05$). Administration of TWK10 resulted in a significant increase ($P < 0.05$) in the Tb.N of Y-TWK10 and A-TWK10 mice, compared to the control mice (the Y-Control and A-Control groups). The serum levels of vitamin D in the A-TWK10 were also increased ($P = 0.0584$), compared with those in the A-Control group. No significant differences in Tb.Th, Tb.Pf, SMI, or BMD values were observed among the four groups (Y-Control, Y-TWK10, A-Control, and A-TWK10).

The Effect of TWK10 on Aging-Related Spatial Learning and Memory Deficits

To evaluate the effect of TWK10 on the aging-related decline in spatial learning and memory, the Morris water maze (MWM) test was carried out. Two-way ANOVA indicated that the factor "aging (control vs. aged)" significantly affected ($P < 0.05$) the spatial learning and memory on days 1, 2, and 3, respectively. The mean escape latency of the aged mice (A-Control at day 3) was significantly higher ($P < 0.01$) than that of the young mice (Y-Control at day 3).The mean escape latency of the Y-TWK10 group on day 2 and day 3 was significantly lower ($P < 0.05$, and $P < 0.01$, respectively) compared to that of the Y-TWK10 group on day 1, whereas no significant differences were observed at any of the time points (days 1, 2, and 3) in the Y-Control mice (**Figure 2A**). The differences in the mean escape latency between day 1 and day 3 in the Y-TWK10 group showed a decreasing trend ($P = 0.1388$) compared to the Y-Control mice (**Figure 2B**) whereas those in the A-TWK10 group were significantly lower ($P < 0.05$) than those in the A-Control group (**Figure 2C**).

The Effect of TWK10 on Body Fat Regulation

The mean abdominal fat mass (%) of the A-Control group showed a decreasing trend ($P = 0.1330$) when compared to the Y-Control mice. Following the administration of TWK10 for 8 weeks, the mean abdominal fat mass of Y-TWK10 mice became significantly lower ($P < 0.05$) than that of the Y-Control group, whereas no significant differences were observed between the aged mouse groups (**Figures 3A,B**). Significant interactions ($P < 0.05$) [aging (young vs. aged) × treatment (control vs. TWK10 administration)] were observed in the mean of EFP weights and CSA of adipocytes in EFP, respectively. The mean EFP weight and the mean CSA of adipocytes in EFP of Y-TWK10 mice were significantly lower ($P < 0.05$) than in the Y-Control group (**Figures 3C–E**). The mean number of BAT adipocytes in the A-Control group was no different compared to the Y-Control mice. However, TWK10 administration resulted in significantly higher BAT adipocyte numbers in A-TWK10 group compared to the control group (**Figures 3F,G**). To better understand the effect of TWK10 treatment on BAT composition, the relative BAT brown area (%) (visualized following H&E staining), as the proportion of the mitochondria-containing area, was quantified. The mean relative brown area (%) in the BATs of mice in the Y-TWK10 and A-TWK10 groups showed strong increasing trends ($P = 0.0858$) as compared to those in the control groups (**Figure 3H**).

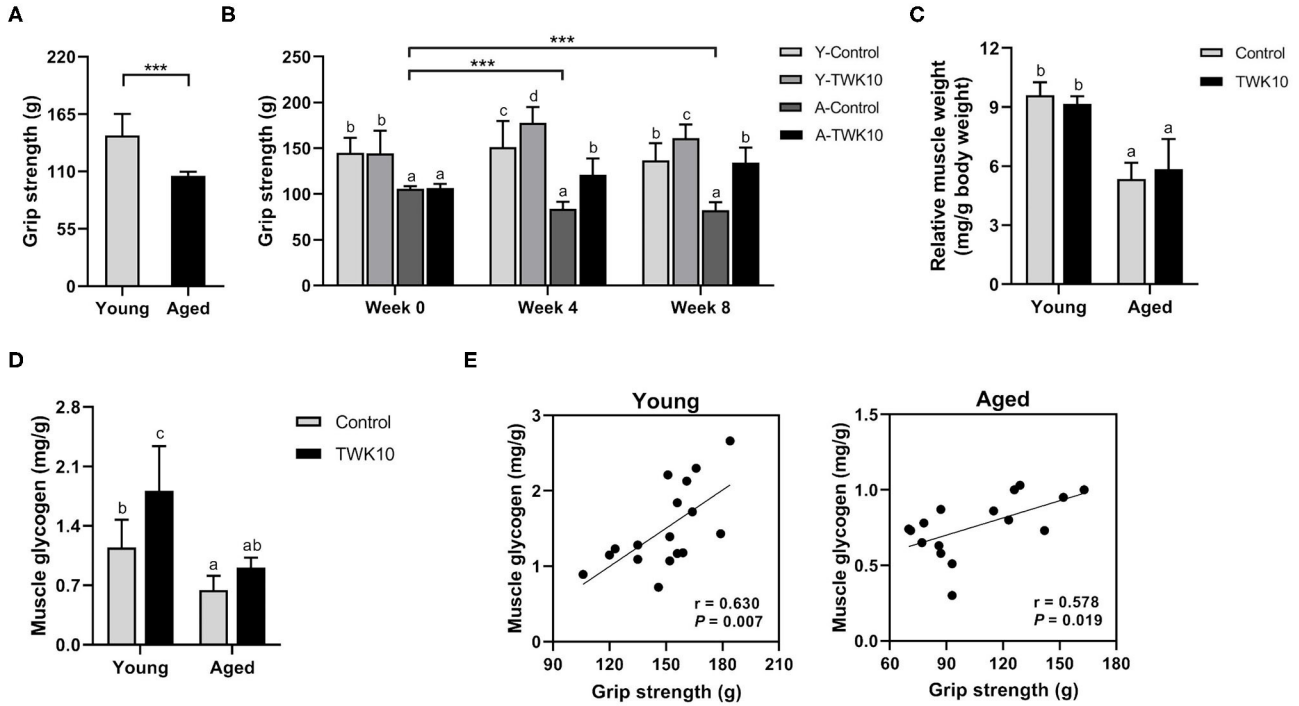

FIGURE 1 | *Lactobacillus plantarum* TWK10 attenuated the age-related decline in skeletal muscle strength by improving muscle quality. **(A)** Forelimb grip strength of young ($n = 17$) and aged mice ($n = 16$) was measured before administration. **(B)** Mice were treated with *Lactobacillus plantarum* TWK10 or PBS for 8 weeks, and forelimb grip strength was measured at week 0, week 4, and week 8. **(C,D)** Gastrocnemius muscles were harvested and subjected to measurements of muscle wet weight and glycogen levels. Data are represented as mean ± SD. Statistical differences among groups were analyzed by two-way ANOVA with the *post-hoc* Tukey-Kramer test. Different letters (a, b, c) indicate significant differences among groups, $P < 0.05$. Two group comparison was analyzed using the unpaired Student *t*-test. ***$P < 0.001$. **(E)** Pearson's correlation, after 8 weeks of TWK10/PBS administration, between grip strength and muscle glycogen levels in the young and aged mice.

The Effect of TWK10 on the Gut Microbiota

To address the impact of TWK10 on the gut microbiota, freshly voided fecal samples were collected following 8 weeks of TWK10/PBS administration and subjected to 16S rRNA gene sequencing analysis. Sequencing of fecal microbiota resulted in a total 5,314,481 quality filtered reads, corresponding to an average of 69,927 reads per sample. After chimera removal, the reads per sample were rarefied to 52,190. Based on the analysis of sequencing data, a total of 580 operational taxonomic units (OTUs) were obtained, with 267 genera of microorganisms identified. Taxonomic and phylogenetic information relating to the OTUs is provided in **Supplementary Table 1**.

To determine how the overall profile of microbial composition was altered by TWK10 administration, alpha-diversity and beta-diversity were analyzed. No significant differences in Shannon indices for α-diversity were observed between the TWK10-treated and control young and aged mice, whereas the richness indices in the A-TWK10 group were significantly lower ($P < 0.05$) than those in the Y-TWK10 group (**Figure 4A**). To evaluate the differences in the microbial community structures among the four groups, beta-diversities were measured by non-metric multidimensional scaling (NMDS) ordinations of unweighted and weighted UniFrac distance matrices followed by PERMANOVA. As showed in **Figure 4B**, the fecal microbial composition of the Y-Control group was significantly (PERMANOVA, $P < 0.05$) different from the A-Control group by NMDS analysis with consideration of the presence/absence of taxa (unweighted UniFrac distance). The Y-TWK10 mice showed a distinctly different (PERMANOVA, $P < 0.05$) β-diversity profile compared to the Y-Control mice while considering the presence/absence as well as relative abundance of taxa (weighted UniFrac distance), suggesting that TWK10 induced a rearrangement in the gut microbial composition of young mice. However, the A-TWK10 mice had a similar microbial composition profile to the A-Control group, as determined by NMDS, with weighted UniFrac distance ($P = 0.309$).

To further investigate these alterations in microbial composition, relative abundances of the major taxa at phylum and family levels were analyzed. At the phylum level, the A-TWK10 group showed no significant but slightly higher abundances of *Bacteroidetes* and *Fusobacteria*, with slightly lower abundances of *Firmicutes* and *Proteobacteria* than the A-Control mice. In addition, TWK10 administration tended to decrease the *Firmicutes*/*Bacteroidetes* (F/B) ratio in aged mice (**Supplementary Figure 1A**). The abundance of *Actinobacteria* in the Y-TWK10 group was significantly higher ($P < 0.05$) than in the Y-Control mice (**Figure 4C**, **Supplementary Figure 1A**).

TABLE 2 | Bone quality was improved by *Lactobacillus plantarum* TWK10.

Item	Group			
	Y-Control	Y-TWK10	A-Control	A-TWK10
BV/TV (%)	$7.61 \pm 2.68^{a,b}$	$13.57 \pm 5.67^{b\#1}$	4.56 ± 2.56^{a}	$7.89 \pm 10.15^{a,b}$
Tb.Th (mm)	0.09 ± 0.01^{a}	0.09 ± 0.01^{a}	0.10 ± 0.01^{a}	0.10 ± 0.02^{a}
Tb.Sp (mm)	$0.53 \pm 0.16^{a,b}$	$0.35 \pm 0.10^{a\#2}$	0.76 ± 0.25^{b}	0.70 ± 0.32^{b}
Tb.N (1/mm)	0.92 ± 0.24^{b}	1.94 ± 0.43^{c}	0.45 ± 0.26^{a}	0.91 ± 0.20^{b}
Tb.Pf (1/mm)	20.53 ± 3.21^{a}	17.40 ± 3.89^{a}	19.23 ± 5.40^{a}	17.03 ± 4.90^{a}
SMI	2.54 ± 0.18^{a}	2.32 ± 0.30^{a}	2.61 ± 0.34^{a}	2.51 ± 0.64^{a}
BMD (g/cm^3)	0.53 ± 0.05^{a}	0.53 ± 0.02^{a}	0.55 ± 0.04^{a}	0.57 ± 0.08^{a}
Serum vitamin D (ng/ml)	35.85 ± 6.25^{a}	33.99 ± 5.63^{a}	30.45 ± 7.89^{a}	$36.95 \pm 2.94^{a\#3}$

Data are represented as mean ± SD. Statistical differences among groups were analyzed by two-way ANOVA with post-hoc Tukey-Kramer test. Non-parametric data were statistically analyzed by Kruskal-Wallis test with Dunn's test. Within a row, different letters (a,b,c) indicate significant differences between the groups, $P < 0.05$. Statistical differences between Control and TWK10-adminitstered young groups on BV/TV ($P = 0.0274$)#1 were analyzed by Mann-Whiney U-test. Statistical differences between Control and TWK10-administered young mice groups on Tb.Sp ($P = 0.0173$)#2, and those between Control and TWK10-administered aged mice groups on serum vitamin D ($P = 0.0584$)#3 were analyzed by Student unpaired t-test, respectively. BV/TV, bone volume fraction; Tb.N, trabecular number; Tb.Sp, trabecular spacing; Tb.Pf, trabecular bone pattern factor; BMD, bone mineral density; SMI, structure model index.

At family level, the relative abundances of *Lachnospiraceae* and *Eggerthellaceae* in the Y-TWK10 group were significantly higher ($P < 0.05$) compared to the Y-Control mice, whereas the abundance of *Lactobacillaceae* in the Y-TWK10 group was significantly lower ($P < 0.01$) than in the Y-Control group. The abundances of *Eubacteriaceae* ($P = 0.0823$) and *Ruminococcaceae* ($P = 0.0927$) in the Y-TWK10 group, as well as *Muribaculaceae* ($P = 0.1119$) and *Eggerthellaceae* ($P = 0.1308$) in the A-TWK10 group followed a weak increasing trend toward significance when compared to the abundance of these populations in the Y-Control and A-Control mice, respectively (**Supplementary Figure 1B**).

To analyze the specific characteristic taxa within each mouse group, LEfSe [Linear discriminant analysis (LDA) Effect Size] was performed based on the discrepancies between groups. Enriched phylotypes in the Y-TWK10 group included the phylum *Actinobacteria* and genera mainly belonging to the class *Clostridia*, namely, *Lachnospiraceae* UCG-006*, Lachnoclostridium, Phascolarctobacterium, Ruminiclostridium* 6*, Tyzzerella,* the *Eubacterium* brachy group, and *Ruminococcaceae* UCG-004, whereas those in Y-Control group belonged to the class *Bacilli* (**Supplementary Figure 2A**). In A-TWK10 mice, the phylum *Bacteroidetes* was the most differentially abundant bacterial taxon, whereas the microbiota of the A-Control group was dominated by the phylum *Firmicutes* (LDA score [log10] > 3) (**Supplementary Figure 2B**).

The Effect of TWK10 on Gut Bacterial Networks

To investigate the variation in bacterial interactions in the gut microbial community after TWK10 administration in both young and aged mice, microbial correlation network analysis was performed using SparCC. In the Y-Control mice, *Prevotellaceae*, *Lactobacillaceae*, and *Ruminococcaceae* correlated positively with *Bacteroidaceae* and *Burkholderiaceae*, *Anaeroplasmataceae*, and *Staphylococcaceae*, respectively (**Figure 5A**). In the Y-TWK10 group, the predominant *Ruminococcaceae* correlated negatively with *Anaeroplasmataceae*, *Enterobacteriaceae,* and *Enterococcaceae*, and positively with the *Clostridiales* vadinBB60 group. *Eggerthellaceae* correlated positively with *Fusobacteriaceae* (**Figure 5B**). In the A-Control group, the most predominant *Lachnospiraceae* correlated negatively with *Enterobacteriaceae* and *Enterococcaceae*, and positively with *Peptococcaceae*. The three families, *Chitinibacteraceae*, *Fusobacteriaceae,* and *Rhodocyclaceae* showed positive correlations with each other (**Figure 5C**). In A-TWK10 mice, *Lachnospiraceae* correlated negatively with *Desulfovibrionaceae*, *Lactobacillaceae*, *Muribaculaceae*, *Prevotellaceae*, *Ruminococcaceae,* and *Streptococcaceae*. *Ruminococcaceae* correlated negatively with *Chitinibacteraceae*, *Prevotellaceae*, *Staphylococcaceae*, *Streptococcaceae,* and *Lachnospiraceae*, and positively with the *Clostridiales* vadinBB60 group and *Desulfovibrionaceae*. *Muribaculaceae* correlated positively with *Streptococcaceae*, and negatively with *Christensenellaceae*. The four families, *Chitinibacteraceae*, *Chromatiaceae*, *Fusobacteriaceae,* and *Rhodocyclaceae* showed positive correlations with each other. Three of them (*Chitinibacteraceae*, *Fusobacteriaceae,* and *Rhodocyclaceae*) also correlated negatively with *Christensenellaceae* (**Figure 5D**).

The Effect of TWK10 on the Abundance of SCFA-Producing Gut Bacteria and Gut SCFA Levels

Short-chain fatty acids (SCFAs), such as acetate, propionate, and butyrate are important metabolites in the maintenance of intestinal homeostasis. We therefore next investigated whether TWK10 could facilitate the production of SCFAs through the modulation of gut microbiota in young and aged mice. The concentrations of acetate, propionate, as well as butyrate in the cecal contents of Y-TWK10 mice were significantly ($P < 0.05$)

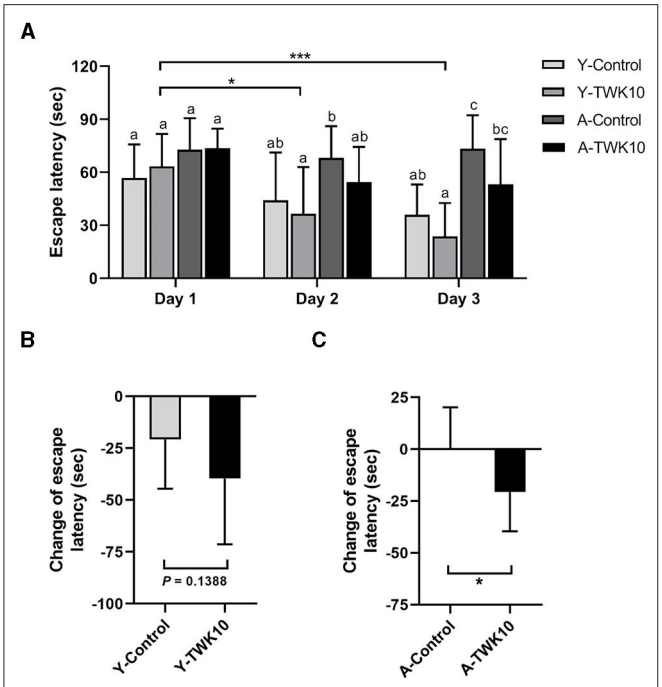

FIGURE 2 | The decline in spatial learning and memory was attenuated by *Lactobacillus plantarum* TWK10. Spatial learning and memory ability were evaluated using the Morris Water Maze after 8 weeks of TWK10 or PBS administration. **(A)** Mean escape latency to the platform were recorded during trial days 1, 2, and 3. **(B,C)** The differences in escape latency between day 1 and day 3 were examined in young and aged mice. Data are represented as mean ± SD. Statistical differences among groups in mean escape latency during the trial days were statistically analyzed by two-way ANOVA with the *post-hoc* Tukey-Kramer test. Different letters (a, b, c) indicate significant differences among the groups, $P < 0.05$. Two group comparison was analyzed using the unpaired Student *t*-test. ***$P < 0.001$. The differences in delta time of escape latency between the Control and TWK10-administered groups were analyzed using the Mann-Whitney *U*-test. *$P < 0.05$.

higher, compared to those in the Y-Control group, whereas no significant differences were observed between the A-Control and A-TWK10 groups.

In young mice, we found that the administration of TWK10 resulted in higher abundances of SCFA-producing bacteria. In the case of acetate-producing bacteria, members of the family *Peptococcaceae* ($P < 0.01$) and genus *Ruminococcaceae* UCG-004 ($P < 0.01$) were significantly higher in abundance, with strong increasing trends being observed for the genera *Prevotella* 9 ($P = 0.1111$), *Ruminiclostridium* 6 ($P = 0.0755$), and *Ruminiclostridium* 9 ($P = 0.0745$), in Y-TWK10 mice compared to those in the Y-Control group. The abundances of butyrate-producing bacteria, namely members of the family *Lachnospiraceae* ($P < 0.05$) and the genus *Lachnospiraceae* UCG-006 ($P < 0.001$) were significantly increased as a result of TWK10 administration, and significant increasing trends were observed for members of the family *Ruminococcaceae* ($P = 0.0927$) and the genera *Eubacterium* spp. ($P = 0.1388$) and *Roseburia* ($P = 0.1388$) in Y-TWK10 mice, compared to those in the Y-Control group. Administration of TWK10 to aged mice increased the abundance of acetate-producing bacteria, particularly belonging to the genus *Prevotellaceae* UCG-001 albeit not significantly ($P = 0.1519$). There were no significant differences in the abundances of butyrate-producing bacteria in the A-TWK10 group compared to the control mice. In addition, the propionate-producing genus *Phascolarctobacterium* was observed in both Y-TWK10 and A-TWK10 groups (**Table 3**).

The Correlation Between Gut Microbiome Composition and TWK10-Mediated Health Benefits

The correlation between the relative abundance of gut bacterial taxa and seven age-related host phenotypic features: including spatial learning and memory, muscle and bone qualities, in young and aged mice, were assessed using Spearman's correlation analysis. The escape latency was significantly lower following the treatment of aged mice with TWK10 (A-TWK10 group, **Figure 2C**). The change in escape latency was significantly and positively correlated with the abundance of the family *Enterobacteriaceae* (**Figure 6**), whereas the abundance of *Enterococcaceae* and *Prevotellaceae* populations in A-Control mice were negatively correlated with the change in escape latency. In young mice, the abundance of *Chitinibacteriaceae, Fusobacteriaceae,* and *Rhodocyclaceae* (in the Y-Control group) correlated positively with the change in escape latency. The reduction in abdominal fat mass (%) mediated by TWK10 administration to Y-TWK10 mice was significantly positively and negatively correlated with the presence of *Prevotellaceae*, and *Desulfovibrionaceae* and *Staphylococcaceae* populations, respectively. Meanwhile, *Enterococcaceae* abundance correlated positively with the fat mass of A-TWK10 mice. The abundance of *Clostridiaceae* and *Erysipelotrichaceae*, and *Enterococcaceae* were positively and negatively correlated with the fat mass in the Y-Control group, respectively, while *Lachnospiraceae* abundances correlated positively with the fat mass of A-Control mice. For muscle aging-associated parameters, *Burkholderiaceae* abundances correlated positively with grip strength, whereas *Helicobacteraceae*, *Lachnospiraceae,* and *Marinifilaceae* populations correlated negatively with grip strength, in the Y-Control group. In aged mice, the presence of *Erysipelotrichaceae* correlated positively with grip strength in the A-Control group, whereas no significant correlations were observed in the A-TWK10 or Y-TWK10 mice. Additionally, muscle glycogen levels were increased by TWK10 administration in both young and aged mice (**Figure 1D**), and correlated positively with the abundance of *Lactobacillaceae*. In the Y-Control group, the abundance of *Bacteroidaceae* and *Prevotellaceae* correlated positively with muscle glycogen levels, whereas no significant correlations were observed in the A-Control group (**Figure 6**). Strong negative correlations between phylum *Proteobacteria* abundance and levels of muscle glycogen in the A-TWK10 mice were also observed (**Supplementary Figure 3**). In relation

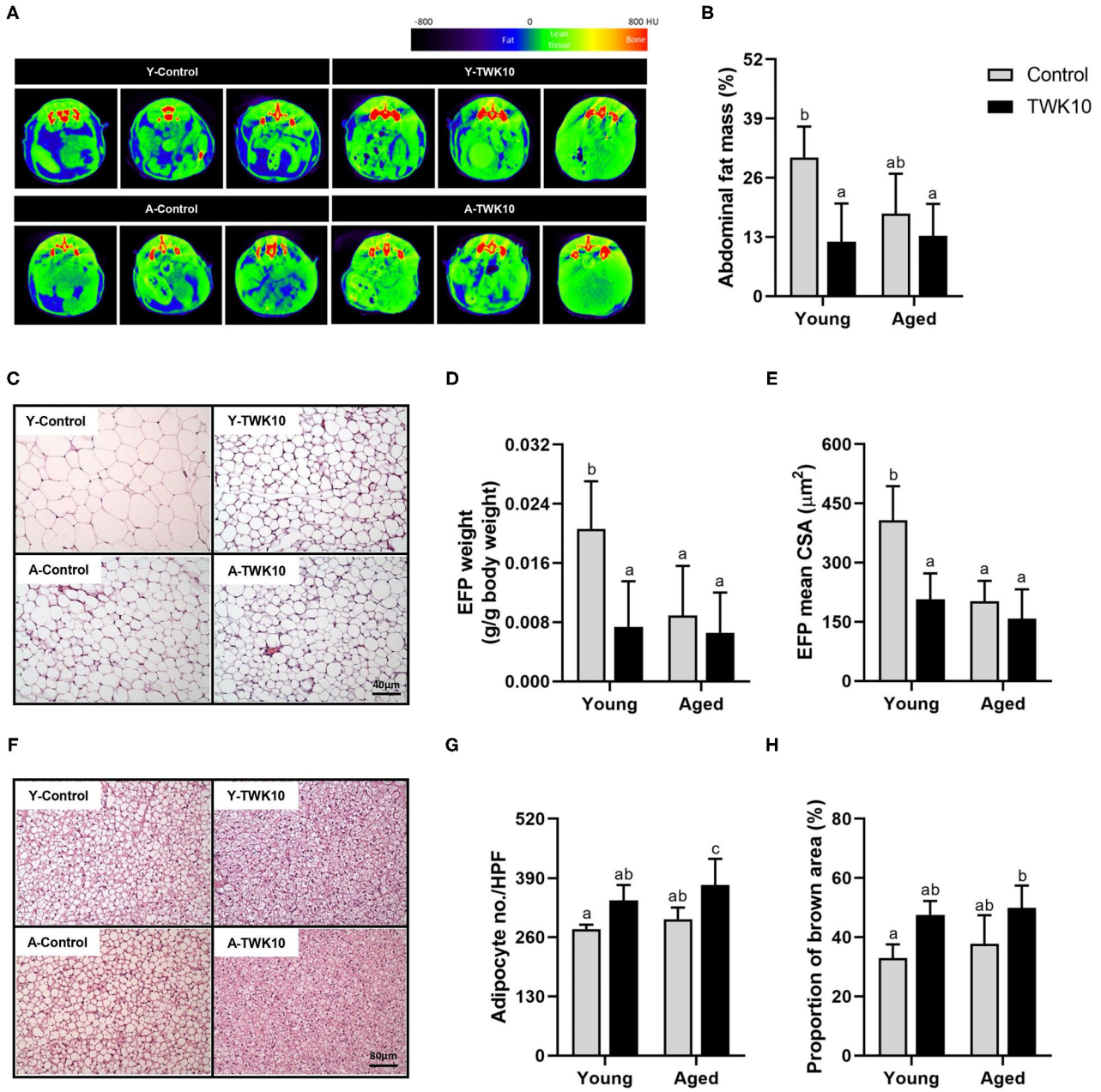

FIGURE 3 | The impact of *Lactobacillus plantarum* TWK10 on body fat regulation. **(A)** Representative micro-CT images showing abdominal region composition. **(B)** Quantification of fat mass at abdominal regions L1 to L5 after 8 weeks of PBS or TWK10 treatment. Epididymal fat pad (EFP) and interscapular brown adipose tissue (BAT) were harvested after 8 weeks of TWK10/PBS administration, and subjected to histological analysis. **(C)** Representative images of EFP obtained by hematoxylin and eosin (H&E) staining. **(D,E)** Measurements of EFP wet weight, and the mean cross-section area of EFP adipocytes. **(F)** Representative images of BAT obtained by H&E staining. **(G)** Quantification of BAT adipocyte number per high-power-field (HPF). **(H)** Quantification of BAT brown area after H&E staining. Data are represented as mean ± SD. Statistical differences among groups were analyzed by two-way ANOVA with the *post-hoc* Tukey-Kramer test and different letters (a, b, c) indicate significant differences, $P < 0.05$. Non-parametric data were statistically analyzed by Kruskal-Wallis test with Dunn's test.

to bone health parameters, Tb.N and BV/TV values were higher in young and aged groups after TWK10 administration (**Table 2**). *Enterobacteriaceae* correlated positively with Tb.N in the femur of Y-TWK10 mice. There were no bacterial families showing strong correlations with Tb.N in the aged mouse groups. In the Y-TWK10 mice, however, *Enterobacteriaceae* and *Peptostreptococcaceae* presence correlated positively with BV/TV, whereas *Fusobacteriaceae* and *Streptococcaceae* populations

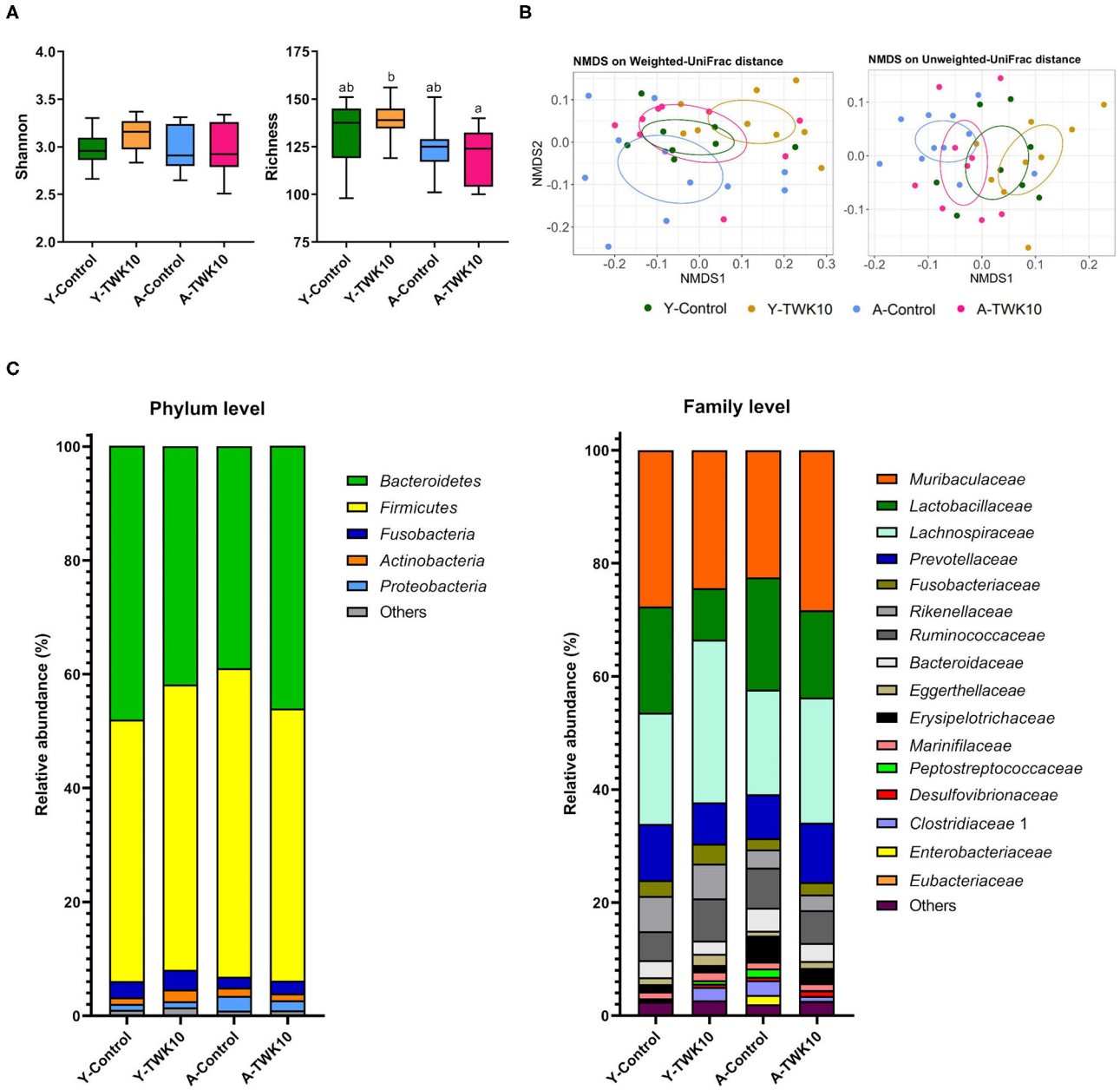

FIGURE 4 | Modulation of gut microbial composition by *Lactobacillus plantarum* TWK10. Gut microbiota signatures were expressed in terms of **(A)** Alpha-diversity (Shannon and Richness indices). The box plots show the smallest and largest values, 25 and 75% quartiles and the median, **(B)** Beta-diversity represented by non-metric multidimensional scaling (NMDS) plots based on weighted and unweighted UniFrac distances, and **(C)** Cumulative bar chart of average relative abundance of bacterial taxa at phylum and family levels. Statistical differences among groups were analyzed by two-way ANOVA with *post-hoc* Tukey-Kramer test, and different letters (a, b, c) indicate significant differences between the groups, $P < 0.05$. Non-parametric data were statistically analyzed by Kruskal-Wallis test with Dunn's test.

correlated negatively with BV/TV in the Y-Control group. Serum vitamin D levels in A-TWK10 were also higher when compared to the A-Control mice ($P = 0.0584$) (**Table 2**). However, no significant correlations between bacterial taxa and serum vitamin D levels were observed in the A-TWK10 group. The abundance of the *Clostridiales* vadinBB60 group members as well as *Eggerthellaceae*, *Helicobacteraceae,* and *Marinifilaceae* correlated positively with serum vitamin D levels in A-Control mice, whereas *Erysipelotrichaceae* and *Peptostreptococcaceae* exhibited a negative correlation. In the Y-Control mice, *Lactobacillaceae* abundance correlated negatively with serum vitamin D levels.

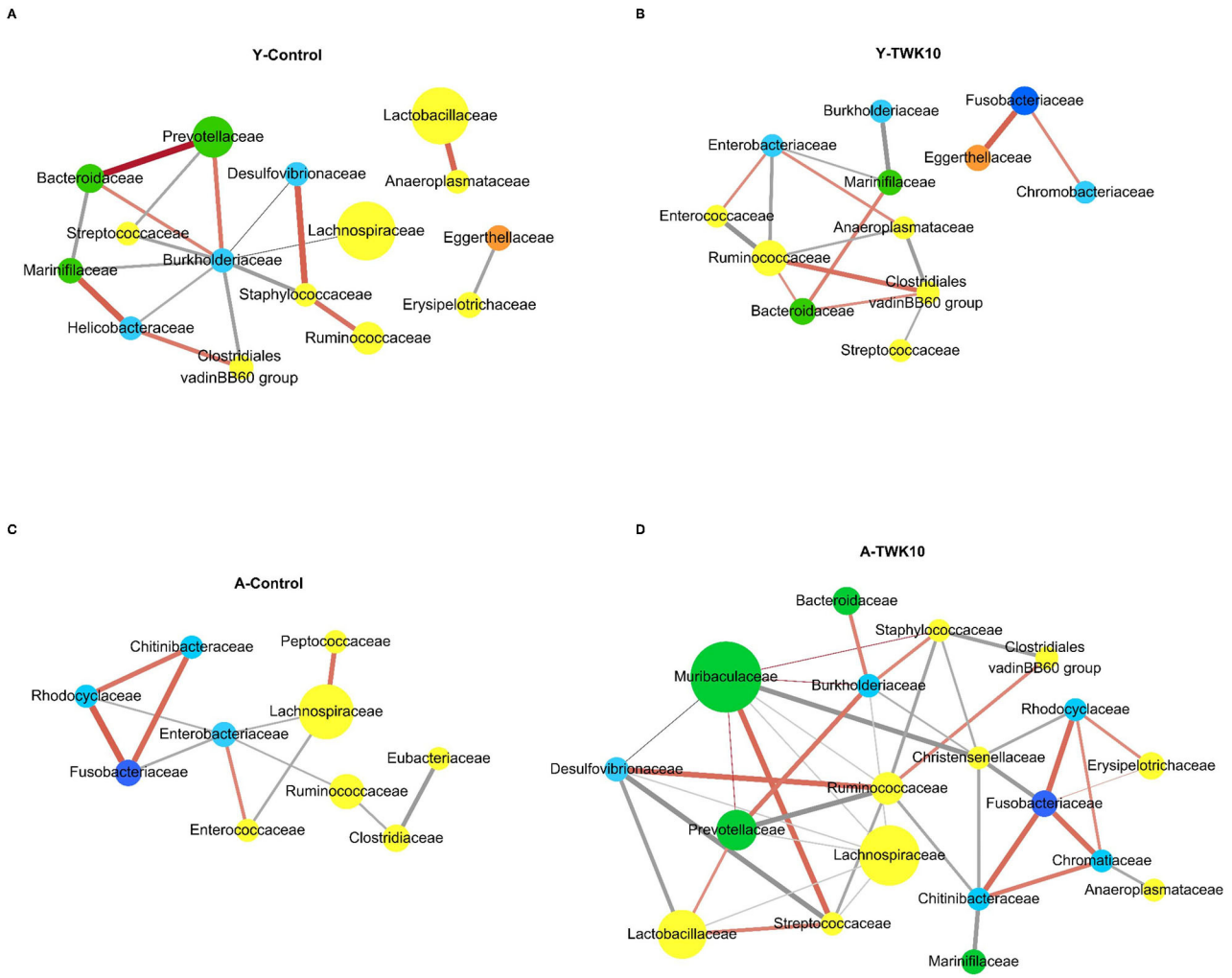

FIGURE 5 | Co-occurrence network analysis of the gut microbiota. Co-occurrence networks were performed at the family level on the basis of relative abundances in the **(A)** young control mice (Y-Control), **(B)** young TWK10-treated mice (Y-TWK10), **(C)** aged control mice (A-Control), and **(D)** aged TWK10-treated mice (A-TWK10). A connection indicated a strong (SParCC's rho cut-off = 0.6) and significant ($P < 0.01$) correlation. Each node represents a family and is colored according to its phylum; yellow: *Firmicutes*, green: *Bacteroidetes*, light blue: *Proteobacteria*, dark blue: *Fusobacteria*, orange: *Actinobacteria*. The node size represents the relative abundance of each family (if >1%) in each group. Each edge represents a positive correlation (orange red line) or a negative correlation (gray line) between the two families with a SparCC's correlation coefficient of ±0.6, and edge shading indicating correlation magnitude.

DISCUSSION

The Effect of TWK10 on Muscle Strength

Aging usually brings about anabolic impairment of skeletal muscle, which in turn leads to reductions in muscle mass and strength (45). Mounting evidence has indicated that declining muscle mass and strength is closely associated with mortality rates in the elderly. Of the two, it appears that muscle strength is more important than muscle mass as a determinant of functional limitation and poor health in the elderly (2, 3, 46–49). Glycogen is an essential energy substrate supporting skeletal muscle activity in humans and animals, and the rate of glycogenesis in muscle decreases with age (50). As demonstrated in our previous studies, TWK10 administration enhanced muscle strength and increased muscle mass, and improved muscle quality and endurance performance in mice and humans (30, 31). However, the impact of TWK10 on slowing down the progression of muscle aging was not clear.

In the present study, we aimed to demonstrate the effect of oral TWK10 administration on the progression of aging-related disorders, such as muscle weakness in naturally aging mice. Therefore, the forelimb grip strength (a marker used widely for the evaluation of *in vivo* neuromuscular performance),

TABLE 3 | *Lactobacillus plantarum* TWK10 enriched SCFA-producing gut bacteria and promoted the production of SCFAs.

	Group					
	Y-Control	**Y-TWK10**	***P*-value**	**A-Control**	**A-TWK10**	***P*-value**
SCFA (μmol/g cecal content)						
Acetate	28.01 ± 26.91	119.90 ± 101.20	0.0130	44.00 ± 26.70	49.08 ± 45.08	0.7823
Butyrate	10.55 ± 7.86	46.04 ± 43.53	0.0211	15.47 ± 12.15	23.13 ± 28.11	0.4724
Propionate	3.50 ± 3.06	12.18 ± 10.34	0.0212	6.57 ± 3.85	6.64 ± 6.56	0.9802
Acetate-producing bacteria (%)						
Bacteroides	3.0305 ± 2.3119	2.2954 ± 1.5848	0.8148	4.0741 ± 2.7387	3.2048 ± 1.7169	0.5027
Blautia	0.0957 ± 0.0392	0.1562 ± 0.0951	0.2766	0.4425 ± 0.4702	0.5243 ± 0.8987	0.8868
Eggerthellaceae	1.1709 ± 0.5187	2.0119 ± 1.1364	0.0360	0.9072 ± 0.3313	1.2209 ± 0.4666	0.1308
Fusobacteriaceae	2.8120 ± 0.7184	3.4779 ± 1.3763	0.4234	1.9417 ± 0.8716	2.1964 ± 1.0041	0.6556
Prevotellaceae UCG-001	6.6855 ± 4.3685	5.6362 ± 2.8759	0.7430	6.0641 ± 3.4124	9.1604 ± 4.1470	0.1519
Prevotella 9	0.0081 ± 0.0044	0.0107 ± 0.0042	0.1111	0.0083 ± 0.0020	0.0059 ± 0.0018	0.4000
Peptococcaceae	0.0977 ± 0.0594	0.2516 ± 0.1093	0.0016	0.1171 ± 0.0777	0.1707 ± 0.0933	0.2060
Ruminococcaceae UCG-004	0.0390 ± 0.0255	0.1144 ± 0.0631	0.0016	0.0677 ± 0.0623	0.0759 ± 0.0673	0.8238
Ruminiclostridium 9	0.2943 ± 0.1438	0.5067 ± 0.2774	0.0745	0.2439 ± 0.2088	0.4522 ± 0.4725	0.4119
Ruminiclostridium 6	0.0269 ± 0.0385	0.1137 ± 0.1328	0.0755	0.0989 ± 0.0983	0.2440 ± 0.2440	0.4396
Streptococcus	0.1604 ± 0.1029	0.2083 ± 0.1344	0.5414	0.0831 ± 0.0626	0.1167 ± 0.0836	0.3562
Propionate-producing bacteria (%)						
Megamonas	0.0060 ± 0.0017	0.0068 ± 0.0012	0.8000	0.0055 ± 0.0029	0.0047 ± 0.0010	0.8000
Phascolarctobacterium	n.d.	0.0061 ± 0.0021	–	n.d.	0.0040 ± 0.0000	–
Butyrate-producing bacteria (%)						
Eubacterium spp.	0.2803 ± 0.3138	0.5180 ± 0.2924	0.1388	0.4041 ± 0.4617	0.5456 ± 0.8300	0.7103
Faecalibacterium prausnitzii	0.0086 ± 0.0022	0.0141 ± 0.0019	0.2000	0.0107 ± 0.0051	0.0075 ± 0.0000	–
Lachnospiraceae	19.6801 ± 7.6001	28.7954 ± 9.6799	0.0464	18.4889 ± 12.9901	22.1170 ± 13.0379	0.4561
Lachnospiraceae UCG-006	0.1681 ± 0.1416	1.9809 ± 2.0960	< 0.001	1.3084 ± 2.3146	0.4179 ± 0.2934	0.9048
Odoribacter	1.1620 ± 0.6283	1.5569 ± 0.9212	0.3704	1.2450 ± 0.6954	1.2187 ± 0.8926	0.8820
Oscillibacter	0.4131 ± 0.3367	0.5855 ± 0.5635	0.6058	0.3599 ± 0.3216	0.4936 ± 0.4787	0.8238
Roseburia	0.1446 ± 0.1095	0.3088 ± 0.2865	0.1388	0.3245 ± 0.2431	0.4554 ± 0.6009	> 0.9999
Ruminococcaceae	5.1385 ± 2.0922	7.4884 ± 2.7297	0.0927	7.0488 ± 4.4442	5.7306 ± 2.9812	0.6027

Relative abundances of SCFA-associated gut bacteria and the contents of cecal SCFAs in young and aged mice. Data are represented as mean ± SD. Statistical differences between Control and TWK10-administered groups on the basis of the relative abundances of SCFA-producing gut bacteria were analyzed by Mann-Whiney U-test. Statistical significances between the cecal SCFA content of Control and TWK10-administered groups were analyzed by Student unpaired t-test. $P < 0.05$ represents statistically significant differences. n.d, not detected.

gastrocnemius muscle weight, and muscle glycogen levels were determined in young and aged mice.

As our results showed, a significant reduction in the forelimb grip strength ($P < 0.001$), muscle weight ($P < 0.05$), and glycogen levels ($P < 0.05$) was observed in aged mice when compared to young mice (**Figures 1A–D**). Although TWK10 administration did not seem to significantly increase the muscle weight of either young or aged mice when compared to those in the control groups, it did significantly increase their grip strength and muscle glycogen levels. In addition, significant positive correlations between the grip strength and muscle glycogen levels were observed in both the young ($P < 0.01$) and aged ($P < 0.05$) mice (**Figure 1E**). These findings indicate that the muscle strength-improving benefits exerted by TWK10 could be attributed to the improvement in muscle quality, specifically by increasing glycogen concentration in the muscle tissue. The effect of TWK10 on improving muscle strength and preventing muscle loss in aged mice is consistent with a previous study investigating the use of *L. paracasei* PS23 in senescence-accelerated mouse prone-8 (SAMP8) mice (27). In our previous study, we found that TWK10 administration could boost muscle mass in 6-week-old mice (30). However, in the present study, muscle mass was not increased by TWK10 administration (**Figure 1C**), although the myofiber cross-sectional area was enlarged in TWK10-treated young mice (data not shown; Y-Control vs. Y-TWK10 groups, 531 ± 73 vs. 641 ± 92 μm^2). These inconsistent results relating to muscle mass may be due to the difference in the ages of study animals. Generally, 3–6 month-old mice are considered as mature adults, and are usually used as the reference group in aging-associated studies. Since mice undergo a period of rapid growth until they reach 2–3 months of age, administration of TWK10 during the developmental stage may promote growth more easily than at the mature adult stage.

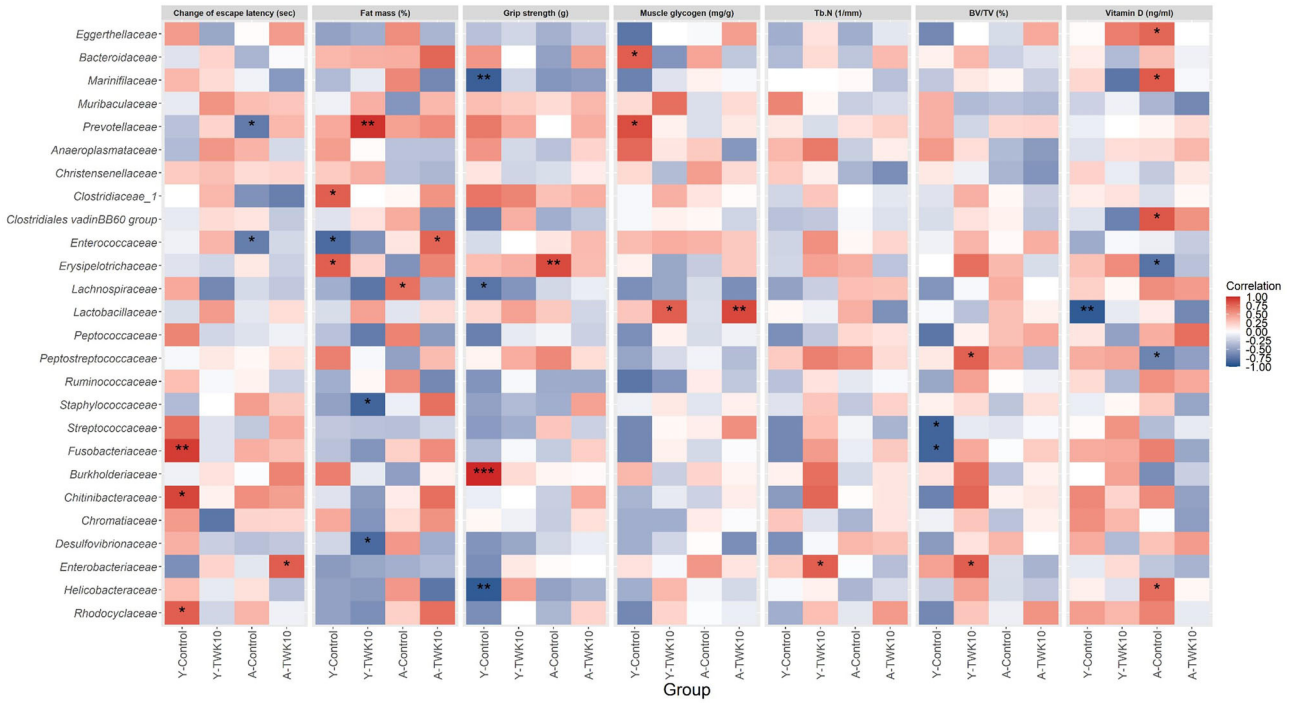

FIGURE 6 | Heatmap of Spearman's correlation analysis between the gut microbiota and the altered age-related host phenotypic features. Spearman's correlation analysis was performed to investigate the correlations between the relative abundances of 26 major families and the values of seven altered aged-related host phenotypic features selected from the differential analysis between Y-Control and Y-TWK10 or A-Control and A-TWK10 groups. Red squares indicate positive correlations and blue squares indicate negative correlations. $^{*}P < 0.05$, $^{**}P < 0.01$, $^{***}P < 0.001$.

Muscular glycogen content affects muscle quantity and muscle quality, together with mitochondrial quality, dietary nutrition, and the levels of inflammation-related cytokines and anabolic hormones. Although the above results confirmed that TWK10 administration significantly improved muscle strength in aged mice, further investigations are needed to elucidate the underlying mechanisms involved. In addition, Khandelwal et al. (51) reported that the reduced activities of liver glycogen synthase and phosphorylase in aged rats are indicative of a likely diminution in the turnover of glycogen in liver during aging. The synthesis of glycogen in muscle decreases with age (50). Skeletal muscle is the major tissue where insulin stimulates glucose uptake from the blood via translocation of GLUT4 (52). Therefore, TWK10 may play a role in regulation of age-associated deficit in glycogen metabolism contributing to the generally observed glucose intolerance upon aging.

The Effect of TWK10 on Bone Quality

Osteoporosis is a common age-related disorder, which is characterized by reduced bone mass and density in the aged population (6). With aging or the onset of osteoporosis, BV/TV, Tb.Th, Tb.N, and BMD decrease, whereas Tb.Sp, Tb.Pf, and SMI usually increase (53). Vitamin D is an essential factor involved in calcium metabolism and is therefore necessary for bone formation. With aging, the risk of vitamin D deficiency is also significantly increased (54). In the A-Control mice, aging-related bone loss was observed by detecting a significant reduction in Tb.N ($P < 0.05$), accompanied by a slight increase in Tb.Sp ($P = 0.1547$), when compared to the Y-Control group. TWK10 administration significant increased ($P < 0.05$) the BV/TV and Tb.N values in both young and aged mice, while significantly decreasing ($P < 0.05$) Tb.Sp in young mice. A near-significant increase ($P = 0.0584$) in serum vitamin D levels was also observed in A-TWK10 mice (**Table 2**). These results demonstrate that TWK10 administration not only showed a protective potential against age-related bone loss but also improved bone quality in mice, which is consistent with a previous study investigating the effect of *L. paracasei* GKS6 and *L. plantarum* KM3 supplementation in ovariectomized SAMP8 mice (29).

The Effect of TWK10 on Body Fat

In general, aging not only brings about the loss of lean mass but increases the amount of body fat (55). With aging, fat is redistributed from the subcutaneous to the visceral region. Accumulation of adipose tissue in the abdominal compartment is associated with an increased risk of chronic disease, such as cardiovascular disease, insulin resistance, and type 2 diabetes mellitus (56, 57). Here, we evaluated the age-associated alterations in body composition and the impact of TWK10 on body fat by micro-CT. We found that TWK10

administration significantly lowered ($P < 0.05$) the mean abdominal fat mass, mean EFP weight, and mean CSA of EFP adipocytes in young mice compared to the Y-Control group (**Figures 3A–E**), which was consistent with our previous findings (30). Although we expected to see the age-associated increase in body fat in the A-Control group (compared to the Y-control mice), no significant change in fat mass was observed. As Hamrick et al. (58) have previously reported, this unfavorable result may be due to the significant decline in fat mass that occurs naturally in aging mice. Since the aged mice used in this study were 27–30 months old at the time of fat mass evaluation, they may have been too old to investigate the impact of TWK10 on the age-associated accumulation in body fat. In addition, aging is associated with the reduction in BAT mass and activity (59). The reduction in BAT that occurs with aging is linked to the loss of mitochondrial function, increased inflammation, impairment of the sympathetic nervous system, and changes in endocrine signaling (60–63). According to our data, no significant changes affecting BAT were detected when comparing the Y-Control and A-Control mice. However, TWK10 administration increased the mean adipocyte number and the size of the area containing mitochondria in both the Y-TWK10 and A-TWK10 mice (**Figures 3F–H**), suggested that TWK10 may facilitate the browning of adipose tissue. To the best of our knowledge, BAT is crucial for heat generation and energy consumption. It is thus worthwhile to further evaluate BAT activity and the brown-to-white fat ratio in order to elucidate the impact of TWK10 on body fat. These results demonstrate that TWK10 has the potential to alter body composition, promoting a healthier configuration and improving metabolism.

The Effect of TWK10 on Learning and Memory

Impairment of learning and memory is another common health issue affecting the elderly. The Morris water maze (MWM), which assesses rodent spatial learning and memory, is one of the most widely used behavioral tests (35). We conducted the MWM test to evaluate the effect of TWK10 on aging-related spatial learning and memory decline in mice.

We observed a significant increase ($P < 0.001$) in escape latency with aging, whereas TWK10 administration significantly lowered escape latency on days 2 and 3 in young mice (**Figure 2A**). The change in escape latency between days 1 and 3 for the A-TWK10 and Y-TWK10 mice showed a significant decrease ($P < 0.05$) and a decreasing trend ($P = 0.1388$), respectively (**Figures 2B,C**). These results demonstrate that TWK10 improved the learning and memory capacities of young mice, and attenuated memory loss in aged mice. These observations are consistent with previous studies: *L. paracasei* PS23 in SAMP8 mice (26), probiotic mixture of *L. paracasei* BCRC 12188, *L. plantarum* BCRC 12251 and *Streptococcus thermophilus* BCRC 13869 in D-galactose-induced aging C57BL/6 mice (64), and a multi-strain probiotic preparation composed of *Bifidobacterium bifidum*, *Bifidobacterium lactis*, *L. acidophilus,* and *Lactobacillus casei* in SAMP8 mice (65).

The Effect of TWK10 on the Gut Microbiota

Age-related degeneration is usually associated with gut microbiota imbalance (9, 11, 66–68). Our results are in agreement with previous findings showing that aging alters the gut microbiota in mice (69). The fecal microbial structures of A-Control mice was enriched in *Firmicutes*, with a lower abundance of *Bacteroidetes,* compared to the Y-Control group (**Supplementary Figure 1A**). Larger *Firmicutes* and smaller *Bacteroidetes* populations are commonly associated with a dysbiotic microbial signature and poor health (70, 71). Probiotics modulate gut microbial composition imbalances and confer beneficial functions to gut microbial communities (72). Our results indicate that TWK10 administration reduced the *Firmicutes*/*Bacteroidetes* (F/B) ratio in aging mice compared to the A-Control group (**Supplementary Figure 1A**), although this decrease was not statistically significant, which could be due to the small sample size used in our study. This finding suggests that TWK10 administration could modify the F/B ratio to restore gut microbial balance and confer health benefits.

Higher abundances of phylum *Proteobacteria* and family *Enterobacteriaceae* members were present in aged mice compared to young mice (**Supplementary Figures 1A,B**). The phylum *Proteobacteria* comprises a wide variety of Gram-negative pathogens, including the families *Enterobacteriaceae*, *Pseudomonadaceae*, *Vibrionaceae,* and *Yersiniaceae*. Among them, *Enterobacteriaceae* represents a core bacterial group, comprising over 30 genera and 130 species. These enterobacteria include potentially pathogenic bacteria (termed pathobionts), which exert specific effects on the host mucosal immune system and are the primary cause of infections when host resistance mechanisms fail as a result of aging (73, 74). In addition, the aging-related increase in the intestinal abundance of *Enterobacteriaceae* and other Gram-negative bacteria may result in an increased endotoxin challenge against the weakened intestinal barrier, leading to chronic inflammation (74). Our results show that TWK10 was able to reduce the abundance of *Enterobacteriaceae* in aged mice (**Supplementary Figure 1B**). Significant reductions in the abundances of major families in the phylum *Proteobacteria*, such as *Chitinibacteraceae*, *Enterobacteriaceae*, *Helicobacteraceae*, *Rhodobacteraceae,* and *Rhodocyclaceae* (except *Burkholderiaceae*) in young and aged mice after TWK10 administration were observed (**Supplementary Figure 4**). These findings are consistent with previous reports (75, 76), which suggested that TWK10 has the potential to promote gut health in the elderly.

Furthermore, we found differences in the microbial community co-occurrence patterns between young and aged mice. The co-occurrence networks indicated that microorganisms belonging to the phylum *Bacteroidetes* had strong positive correlations in the Y-Control group (**Figure 5A**). Meanwhile in the A-Control mice, Gram-negative opportunistic pathogens belonging to the phylum *Proteobacteria* (*Chitinibacteraceae*, *Enterobacteriaceae,* and *Rhodocyclaceae*), and the family *Enterococcaceae* were positively correlated with each other (**Figure 5C**). In the Y-TWK10 group, the topology of the co-occurrence network was altered after TWK10 administration. As the most abundant bacterial families in the

main network of the Y-TWK10 group, *Ruminococcaceae* showed mutual restriction with *Anaeroplasmataceae*, *Enterobacteriaceae,* and *Enterococcaceae* (**Figure 5B**). The family *Christensenellaceae,* which is linked to metabolic health and longevity (77–80), showed negative correlations with *Chitinibacteraceae*, *Fusobacteriaceae,* and *Rhodocyclaceae*. Additionally, we also found that the connections between pathogenic microorganisms were disrupted by TWK10 administration in aged mice (**Figure 5D**), which suggested that the disruption of the correlated interactions among pathogenic microorganisms may have potential applications in slowing the aging process.

Gut microbiota-derived SCFAs, including acetate, propionate, and butyrate, are key mediators in the maintenance of gut and metabolic health (20, 81, 82). An increase in microbial SCFA production is regarded as beneficial for health. Lactate, which is produced by lactic acid bacteria (LAB) as the major end-product of sugar fermentation, is also one of the important growth factors for SCFA-producing gut bacteria (83). Therefore, LAB are extensively used as probiotics. (84, 85). Chen et al. (86) reported that the administration of *L. paracasei* PS23 significantly decreased the abundance of butyrate-producing *Lachnospiraceae* UCG 001 in aged SAMP8 mice. In contrast, we observed that on TWK10 administration, the abundance of *Lachnospiraceae* was significantly increased ($P = 0.0464$) in Y-TWK10 mice and maintained at a high level (comprising >20% of total fecal microbiota) in the A-TWK10 group. Wang et al. (87) reported that probiotic *L. plantarum* P-8 could improve human gastrointestinal health by increasing the fecal concentrations of acetate and propionate in all age groups, including the elderly. In addition, probiotic *L. acidophilus* DDS-1 modulated intestinal microbiota by increasing *Akkermansia muciniphila* and *Lactobacillus* spp. and reducing *Proteobacteria* spp. abundances, which was accompanied by an increase in cecal propionate and butyrate levels in aged C57BL/6J mice (21, 22). Given that TWK10 administration appears to modulate the gut microbiota of young and aged mice, we hypothesized that TWK10 could be used to boost gut SCFA production. Consequently, we found no significant difference in the levels of cecal SCFAs between the Y-Control and A-Control groups, whereas a significant increase in SCFA levels was observed in the Y-TWK10 group compared to Y-Control mice (**Table 3**). An overall increase in acetate- and butyrate-producing bacteria was observed in the Y-TWK10 group compared to Y-Control mice. We also observed that TWK10 administration caused a slight increase in the gut acetate and butyrate levels of aged mice. These results imply that TWK10 may exert its health benefits via microbiota modulation and consequently SCFA production, especially in young mice.

In our previous study, we have demonstrated that TWK10 administration significantly increased skeletal muscle mass and strength in mice (30). Growing evidence has led to the notion of the 'gut-muscle axis', which implies that gut microbiota may act as the mediator for muscle health (88, 89), and hold therapeutic promise for muscle-related diseases, such as sarcopenia (90). Numerous studies have highlighted the close relationship between muscle glycogen levels and fatigue resistance (91). However, the mechanism linking muscle glycogen concentration to muscle function remains elusive. SCFAs have been shown to increase skeletal muscle glycogen levels (92–95), and have the potential to increase skeletal muscle mass and physical function (96). In the present study, we found that the muscle glycogen levels were significantly and positively correlated with muscle strength in young ($P = 0.007$) and aged ($P = 0.019$) mice (**Figure 1E**), and the abundances of *Lactobacillaceae* members displayed significant positive correlations with muscle glycogen levels in Y-TWK10 and A-TWK10 mice (**Figure 6**). We also evaluated whether altered age-related host phenotypic features in each treatment group correlated with the SCFA levels. However, only a few of these correlations were statistically significant ($P < 0.05$). In the young mouse group, muscle glycogen concentration was positively correlated with SCFA levels after TWK10 administration. In addition, a negative correlation between butyric acid and muscle glycogen levels was observed in the Y-Control group (**Supplementary Figure 5**). It remains important to determine whether these correlations arose as a consequence of TWK10 administration. Further studies are needed to understand the mechanisms by which SCFAs produced by gut microbiota affect skeletal muscle following TWK10 administration.

CONCLUSIONS

In the present study, we have for the first time presented evidence of TWK10 attenuating aging-related disorders in naturally aging mice. We found that TWK10 administration attenuated aging-related muscle weakness by improving muscle quality and increasing muscle glycogen levels. TWK10 slowed down the progression of age-related bone loss and increased trabecular numbers in the murine femur. TWK10 treatment also significantly attenuated the cognitive impairment of aged mice by shortening their MWM test mean escape latencies. Moreover, gut microbiota analysis by next-generation sequencing (NGS) of the 16S rRNA gene demonstrated that the gut microbial composition was significantly altered following TWK10 administration, reducing the natural accumulation of pathogenic organisms (such as *Enterobacteriaceae* and *Enterococcaceae*) that occurs with age, while boosting the abundances of beneficial SCFA-producing bacteria.

Conclusively, we have confirmed that *Lactobacillus plantarum* TWK10 could be considered as a potential therapeutic agent to promote healthy aging by attenuating aging-related disorders and modulating the imbalance of gut microbiota. Future studies are needed to validate the results obtained using animal models in a clinical setting, prior to confirming the health-promoting benefits of TWK10 in humans.

DATA AVAILABILITY STATEMENT

The datasets presented in this study can be found in online repositories. The names of the repository/repositories and accession number(s) can be found at: https://www.ncbi.nlm.nih.gov/bioproject/PRJNA726848.

ETHICS STATEMENT

The animal study was reviewed and approved by Institutional Animal Care and Use Committee (IACUC) of National Taiwan Sport University, Taoyuan City, Taiwan.

AUTHOR CONTRIBUTIONS

C-CL and Y-CL analyzed and interpreted the data and wrote the manuscript. M-CL, H-YH, and S-YC conducted the experiments and collected data. S-LY, J-SL, and C-CH designed and oversaw the study. KW interpreted the data and edited the manuscript. All authors read and approved the final manuscript.

ACKNOWLEDGMENTS

We would like to thank the National Laboratory Animal Center (NLAC), NARLabs, Taiwan, for technical support relating to Micro-CT image analysis.

SUPPLEMENTARY MATERIAL

The Supplementary Material for this article can be found online at: https://www.frontiersin.org/articles/10.3389/fnut.2021.708096/full#supplementary-material

REFERENCES

1. Kennedy BK, Berger SL, Brunet A, Campisi J, Cuervo AM, Epel ES, et al. Aging: a common driver of chronic diseases and a target for novel interventions. *Cell.* (2014) 159:709–13. doi: 10.1016/j.cell.2014.10.039
2. Marzetti E, Leeuwenburgh C. Skeletal muscle apoptosis, sarcopenia and frailty at old age. *Exp Gerontol.* (2006) 41:1234–8. doi: 10.1016/j.exger.2006.08.011
3. Siparsky PN, Kirkendall DT, Garrett WE. Muscle changes in aging: understanding sarcopenia. *Sports Health.* (2014) 6:36–40. doi: 10.1177/1941738113502296
4. Melton LJ, Khosla S, Crowson CS, O'Connor MK, O'Fallon WM, Riggs BL. Epidemiology of sarcopenia. *J Am Geriatr Soc.* (2000) 48:625–30. doi: 10.1111/j.1532-5415.2000.tb04719.x
5. Després JP. Body fat distribution and risk of cardiovascular disease: an update. *Circulation.* (2012) 126:1301–13. doi: 10.1161/CIRCULATIONAHA.111.067264
6. Mc Donnell P, Mc Hugh PE, O'Mahoney D. Vertebral osteoporosis and trabecular bone quality. *Ann Biomed Eng.* (2007) 35:170–89. doi: 10.1007/s10439-006-9239-9
7. Hänninen T, Koivisto K, Reinikainen KJ, Helkala EL, Soininen H, Mykkänen L, et al. Prevalence of ageing-associated cognitive decline in an elderly population. *Age Ageing.* (1996) 25:201–5. doi: 10.1093/ageing/25.3.201
8. Small SA. Age-related memory decline: current concepts and future directions. *Arch Neurol.* (2001) 58:360–4. doi: 10.1001/archneur.58.3.360
9. O'Toole PW, Jeffery IB. Gut microbiota and aging. *Science.* (2015) 350:1214–5. doi: 10.1126/science.aac8469
10. Nagpal R, Mainali R, Ahmadi S, Wang S, Singh R, Kavanagh K, et al. Gut microbiome and aging: physiological and mechanistic insights. *Nutr Heal Aging.* (2018) 4:267–85. doi: 10.3233/NHA-170030
11. Odamaki T, Kato K, Sugahara H, Hashikura N, Takahashi S, Xiao JZ, et al. Age-related changes in gut microbiota composition from newborn to centenarian: a cross-sectional study. *BMC Microbiol.* (2016) 16:90. doi: 10.1186/s12866-016-0708-5
12. Kim MH, Kang SG, Park JH, Yanagisawa M, Kim CH. Short-chain fatty acids activate GPR41 and GPR43 on intestinal epithelial cells to promote inflammatory responses in mice. *Gastroenterology.* (2013) 145:396–406. doi: 10.1053/j.gastro.2013.04.056
13. Corrêa-Oliveira R, Fachi JL, Vieira A, Sato FT, Vinolo MAR. Regulation of immune cell function by short-chain fatty acids. *Clin Transl Immunol.* (2016) 5:e73. doi: 10.1038/cti.2016.17
14. Feng W, Wu Y, Chen G, Fu S, Li B, Huang B, et al. Sodium butyrate attenuates diarrhea in weaned piglets and promotes tight junction protein expression in colon in a GPR109A-dependent manner. *Cell Physiol Biochem.* (2018) 47:1617–29. doi: 10.1159/000490981
15. Hu J, Lin S, Zheng B, Cheung PCK. Short-chain fatty acids in control of energy metabolism. *Crit Rev Food Sci Nutr.* (2018) 58:1243–9. doi: 10.1080/10408398.2016.1245650
16. Puddu A, Sanguineti R, Montecucco F, Viviani GL. Evidence for the gut microbiota short-chain fatty acids as key pathophysiological molecules improving diabetes. *Mediators Inflamm.* (2014) 2014:162021. doi: 10.1155/2014/162021
17. Gomes SD, Oliveira CS, Azevedo-Silva J, Casanova MR, Barreto J, Pereira H, et al. The role of diet related short-chain fatty acids in colorectal cancer metabolism and survival: prevention and therapeutic implications. *Curr Med Chem.* (2018) 27:4087–108. doi: 10.2174/0929867325666180530102050
18. Russo E, Giudici F, Fiorindi C, Ficari F, Scaringi S, Amedei A. Immunomodulating activity and therapeutic effects of short chain fatty acids and tryptophan post-biotics in inflammatory bowel disease. *Front Immunol.* (2019) 10:2754. doi: 10.3389/fimmu.2019.02754
19. Eckburg PB, Bik EM, Bernstein CN, Purdom E, Dethlefsen L, Sargent M, et al. Microbiology: diversity of the human intestinal microbial flora. *Science.* (2005) 308:1635–8. doi: 10.1126/science.1110591
20. Koh A, DeVadder F, Kovatcheva-Datchary P, Bäckhed F. From dietary fiber to host physiology: short-chain fatty acids as key bacterial metabolites. *Cell.* (2016) 165:1332–45. doi: 10.1016/j.cell.2016.05.041
21. Vemuri R, Shinde T, Gundamaraju R, Gondalia SV, Karpe AV, Beale DJ, et al. *Lactobacillus acidophilus* DDS-1 modulates the gut microbiota and improves metabolic profiles in aging mice. *Nutrients.* (2018) 10:1255. doi: 10.3390/nu10091255
22. Vemuri R, Gundamaraju R, Shinde T, Perera AP, Basheer W, Southam B, et al. *Lactobacillus acidophilus* DDS-1 modulates intestinal-specific microbiota, short-chain fatty acid and immunological profiles in aging mice. *Nutrients.* (2019) 11:1297. doi: 10.3390/nu11061297
23. Zhao Y, Zhao L, Zheng X, Fu T, Guo H, Ren F. *Lactobacillus salivarius* strain FDB89 induced longevity in *Caenorhabditis elegans* by dietary restriction. *J Microbiol.* (2013) 51:183–8. doi: 10.1007/s12275-013-2076-2
24. Lee DE, Huh CS, Ra J, Choi ID, Jeong JW, Kim SH, et al. Clinical evidence of effects of *Lactobacillus plantarum* HY7714 on skin aging: a randomized, double blind, placebo-controlled study. *J Microbiol Biotechnol.* (2015) 25:2160–8. doi: 10.4014/jmb.1509.09021
25. Tsuji R, Komano Y, Ohshio K, Ishii N, Kanauchi O. Long-term administration of pDC stimulative lactic acid bacteria, *Lactococcus lactis* strain Plasma, prevents immune-senescence and decelerates individual senescence. *Exp Gerontol.* (2018) 111:10–16. doi: 10.1016/j.exger.2018.06.028
26. Huang SY, Chen LH, Wang MF, Hsu CC, Chan CH, Li JX, et al. *Lactobacillus paracasei* PS23 delays progression of age-related cognitive decline in senescence accelerated mouse prone 8 (SAMP8) mice. *Nutrients.* (2018) 10:894. doi: 10.3390/nu10070894
27. Chen LH, Huang SY, Huang KC, Hsu CC, Yang KC, Li LA, et al. *Lactobacillus paracasei* PS23 decelerated age-related muscle loss by

ensuring mitochondrial function in SAMP8 mice. *Aging.* (2019) 11:756–70. doi: 10.18632/aging.101782
28. Dar HY, Shukla P, Mishra PK, Anupam R, Mondal RK, Tomar GB, et al. *Lactobacillus acidophilus* inhibits bone loss and increases bone heterogeneity in osteoporotic mice via modulating Treg-Th17 cell balance. *Bone Rep.* (2018) 8:46–56. doi: 10.1016/j.bonr.2018.02.001
29. Yang LC, Lin SW, Li IC, Chen YP, Tzu SY, Chou W, et al. *Lactobacillus plantarum* gkm3 and *Lactobacillus paracasei.* gks6 supplementation ameliorates bone loss in ovariectomized mice by promoting osteoblast differentiation and inhibiting osteoclast formation. *Nutrients.* (2020) 12:1914. doi: 10.3390/nu12071914
30. Chen YM, Wei L, Chiu YS, Hsu YJ, Tsai TY, Wang MF, et al. *Lactobacillus plantarum* TWK10 supplementation improves exercise performance and increases muscle mass in mice. *Nutrients.* (2016) 8:205. doi: 10.3390/nu8040205
31. Huang WC, Lee MC, Lee CC, Ng KS, Hsu YJ, Tsai TY, et al. Effect of *Lactobacillus plantarum* TWK10 on exercise physiological adaptation, performance, and body composition in healthy humans. *Nutrients.* (2019) 11:2836. doi: 10.3390/nu11112836
32. Zheng J, Wittouck S, Salvetti E, Franz, C. M. A. P., Harris HMB, et al. A taxonomic note on the genus *Lactobacillus:* description of 23 novel genera, emended description of the genus *Lactobacillus* Beijerinck 1901, and union of *Lactobacillaceae* and *Leuconostocaceae. Int J Syst Evol Microbiol.* (2020) 70:2782–858. doi: 10.1099/ijsem.0.004107
33. Chen YM, Shih TW, Chiu CP, Pan TM, Tsai TY. Effects of lactic acid bacteria-fermented soy milk on melanogenesis in B16F0 melanocytes. *J Funct Foods.* (2013) 5:395–405. doi: 10.1016/j.jff.2012.11.012
34. Li X, Mohan S, Gu W, Wergedal J, Baylink DJ. Quantitative assessment of forearm muscle size, forelimb grip strength, forearm bone mineral density, and forearm bone size in determining humerus breaking strength in 10 inbred strains of mice. *Calcif Tissue Int.* (2001) 68:365–9. doi: 10.1007/s00223-001-0004-7
35. Vorhees CV, Williams MT. Morris water maze: procedures for assessing spatial and related forms of learning and memory. *Nat Protoc.* (2006) 1:848–58. doi: 10.1038/nprot.2006.116
36. Sasser TA, Chapman SE, Li S, Hudson C, Orton SP, Diener JM, et al. Segmentation and measurement of fat volumes in murine obesity models using X-ray computed tomography. *J Vis Exp.* (2012) 62:e3680. doi: 10.3791/3680
37. Luu YK, Lublinsky S, Ozcivici E, Capilla E, Pessin JE, Rubin CT, et al. In vivo quantification of subcutaneous and visceral adiposity by micro-computed tomography in a small animal model. *Med Eng Phys.* (2009) 31:34–41. doi: 10.1016/j.medengphy.2008.03.006
38. Huang CC, Hsu MC, Huang WC, Yang HR, Hou CC. Triterpenoid-rich extract from antrodia camphorata improves physical fatigue and exercise performance in mice. *Evid Based Complement Alternat Med.* (2012) 2012:364741. doi: 10.1155/2012/364741
39. Klindworth A, Pruesse E, Schweer T, Peplies J, Quast C, Horn M, et al. Evaluation of general 16S ribosomal RNA gene PCR primers for classical and next-generation sequencing-based diversity studies. *Nucleic Acids Res.* (2013) 41:e1. doi: 10.1093/nar/gks808
40. Callahan BJ, McMurdie PJ, Rosen MJ, Han AW, Johnson AJA, Holmes SP. DADA2: high-resolution sample inference from Illumina amplicon data. *Nat Methods.* (2016) 13:581–3. doi: 10.1038/nmeth.3869
41. Bolyen E, Rideout JR, Dillon MR, Bokulich NA, Abnet CC, Al-Ghalith GA, et al. Reproducible, interactive, scalable and extensible microbiome data science using QIIME 2. *Nat Biotechnol.* (2019) 37:852–7. doi: 10.1038/s41587-019-0209-9
42. Bokulich NA, Kaehler BD, Rideout JR, Dillon M, Bolyen E, Knight R, et al. Optimizing taxonomic classification of marker-gene amplicon sequences with QIIME 2's q2-feature-classifier plugin. *Microbiome.* (2018) 6:90. doi: 10.1186/s40168-018-0470-z
43. Quast C, Pruesse E, Yilmaz P, Gerken J, Schweer T, Yarza P, et al. The SILVA ribosomal RNA gene database project: improved data processing and web-based tools. *Nucleic Acids Res.* (2013) 41:D590–6. doi: 10.1093/nar/gks1219
44. Torii T, Kanemitsu K, Wada T, Itoh S, Kinugawa K, Hagiwara A. Measurement of short-chain fatty acids in human faeces using high-performance liquid chromatography: specimen stability. *Ann Clin Biochem.* (2010) 41:447–52. doi: 10.1258/acb.2010.010047
45. Wilkinson DJ, Piasecki M, Atherton PJ. The age-related loss of skeletal muscle mass and function: measurement and physiology of muscle fibre atrophy and muscle fibre loss in humans. *Ageing Res Rev.* (2018) 47:123–32. doi: 10.1016/j.arr.2018.07.005
46. Landers KA, Hunter GR, Wetzstein CJ, Bamman MM, Weinsier RL. The interrelationship among muscle mass, strength, and the ability to perform physical tasks of daily living in younger and older women. *J Gerontol A Biol Sci Med Sci.* (2001) 56:B443–8. doi: 10.1093/gerona/56.10.B443
47. Visser M, Goodpaster BH, Kritchevsky SB, Newman AB, Nevitt M, Rubin SM, et al. Muscle mass, muscle strength, and muscle fat infiltration as predictors of incident mobility limitations in well-functioning older persons. *J Gerontol A Biol Sci Med Sci.* (2005) 60:324–33. doi: 10.1093/gerona/60.3.324
48. Newman AB, Kupelian V, Visser M, Simonsick EM, Goodpaster BH, Kritchevsky SB, et al. Strength, but not muscle mass, is associated with mortality in the health, aging and body composition study cohort. *J Gerontol A Biol Sci Med Sci.* (2006) 2014:162021. doi: 10.1093/gerona/61.1.72
49. Ruiz JR, Sui X, Lobelo F, Morrow JR, Jackson AW, Sjöström M, et al. Association between muscular strength and mortality in men: prospective cohort study. *BMJ.* (2008) 337:a439. doi: 10.1136/bmj.a439
50. Dall'Aglio E, Chang H, Reaven GM, Azhar S. Age-related changes in rat muscle glycogen synthase activity. *J Gerontol.* (1987) 42:168–72. doi: 10.1093/geronj/42.2.168
51. Khandelwal RL, Enno TL, Narayanan N. Effects of age on glycogen synthase and phosphorylase activities in rat liver. *Mech Ageing Dev.* (1984) 28:13–22. doi: 10.1016/0047-6374(84)90149-0
52. Larance M, Ramm G, James DE. The GLUT4 code. *Mol Endocrinol.* (2008) 22:226–33. doi: 10.1210/me.2007-0282
53. Willinghamm MD, Brodt MD, Lee KL, Stephens AL, Ye J, Silva MJ. Age-related changes in bone structure and strength in female and male BALB/c Mice. *Calcif Tissue Int.* (2010) 86:470–83. doi: 10.1007/s00223-010-9359-y
54. Holick MF, Binkley NC, Bischoff-Ferrari HA, Gordon CM, Hanley DA, Heaney RP, et al. Evaluation, treatment, and prevention of vitamin D deficiency: an endocrine society clinical practice guideline. *J Clin Endocrinol Metab.* (2011) 96:1911–30. doi: 10.1210/jc.2011-0385
55. St-Onge MP. Relationship between body composition changes and changes in physical function and metabolic risk factors in aging. *Curr Opin Clin Nutr Metab Care.* (2005) 8:523–8. doi: 10.1097/01.mco.0000171150.49248.14
56. Hughes VA, Roubenoff R, Wood M, Frontera WR, Evans WJ, Fiatarone Singh MA. Anthropometric assessment of 10-y changes in body composition in the elderly. *Am J Clin Nutr.* (2004) 80:475–82. doi: 10.1093/ajcn/80.2.475
57. Karpe F, Pinnick KE. Biology of upper-body and lower-body adipose tissue - link to whole-body phenotypes. *Nat Rev Endocrinol.* (2015) 11:90–100. doi: 10.1038/nrendo.2014.185
58. Hamrick MW, Ding KH, Pennington C, Chao YJ, Wu YD, Howard B, et al. Age-related loss of muscle mass and bone strength in mice is associated with a decline in physical activity and serum leptin. *Bone.* (2006) 39:845–53. doi: 10.1016/j.bone.2006.04.011
59. Cypess AM, Lehman S, Williams G, Tal I, Rodman D, Goldfine AB, et al. Identification and importance of brown adipose tissue in adult humans. *N Engl J Med.* (2009) 360:1509–17. doi: 10.1056/NEJMoa0810780
60. Valle A, Santandreu FM, García-Palmer FJ, Roca P, Oliver J. The serum levels of 17β-estradiol, progesterone and triiodothyronine correlate with brown adipose tissue thermogenic parameters during aging. *Cell Physiol Biochem.* (2008) 22:337–46. doi: 10.1159/000149812
61. Bahler L, Verberne HJ, Admiraal WM, Stok WJ, Soeters MR, Hoekstra JB, et al. Differences in sympathetic nervous stimulation of brown adipose tissue between the young and old, and the lean and obese. *J Nucl Med.* (2016) 57:372–7. doi: 10.2967/jnumed.115.165829
62. Cedikova M, Kripnerov,á M, Dvorakova J, Pitule P, Grundmanova M, Babuska V, et al. Mitochondria in white, brown, beige adipocytes. *Stem Cells Int.* (2016) 2016:6067349. doi: 10.1155/2016/6067349
63. Villarroya F, Cereijo R, Gavaldà-Navarro A, Villarroya J, Giralt M. Inflammation of brown/beige adipose tissues in obesity and metabolic disease. *J Intern Med.* (2018) 284:492–504. doi: 10.1111/joim.12803

64. Ho ST, Hsieh YT, Wang SY, Chen MJ. Improving effect of a probiotic mixture on memory and learning abilities in D-galactose–treated aging mice. *J Dairy Sci.* (2019) 102:1901–9. doi: 10.3168/jds.2018-15811
65. Yang X, Yu D, Xue L, Li H, Du J. Probiotics modulate the microbiota–gut–brain axis and improve memory deficits in aged SAMP8 mice. *Acta Pharm Sin B.* (2020) 10:475–87. doi: 10.1016/j.apsb.2019.07.001
66. Biagi E, Nylund L, Candela M, Ostan R, Bucci L, Pini E, et al. Through ageing, and beyond: gut microbiota and inflammatory status in seniors and centenarians. *PLOS One.* (2010) 5:e10667. doi: 10.1371/journal.pone.0010667
67. Claesson MJ, Cusack S, O'Sullivan O, Greene-Diniz R, de Weerd H, Flannery E, et al. Composition, variability, and temporal stability of the intestinal microbiota of the elderly. *Proc Natl Acad Sci USA.* (2011) 108:4586–91. doi: 10.1073/pnas.1000097107
68. Xu C, Zhu H, Qiu P. Aging progression of human gut microbiota. *BMC Microbiol.* (2019) 19:236. doi: 10.1186/s12866-019-1616-2
69. Langille MG, Meehan CJ, Koenig JE, Dhanani AS, Rose RA, Howlett SE, et al. Microbial shifts in the aging mouse gut. *Microbiome.* (2014) 2:50. doi: 10.1186/s40168-014-0050-9
70. Mariat D, Firmesse O, Levenez F, Guimarães VD, Sokol H, Dor,é J, et al. The *Firmicutes/Bacteroidetes* ratio of the human microbiota changes with age. *BMC Microbiol.* (2009) 9:123. doi: 10.1186/1471-2180-9-123
71. Razavi AC, Potts KS, Kelly TN, Bazzano LA. Sex, gut microbiome, and cardiovascular disease risk. *Biol Sex Differ.* (2019) 10:29. doi: 10.1186/s13293-019-0240-z
72. Liu G, Huang Y, Zhai L. Impact of nutritional and environmental factors on inflammation, oxidative stress, the microbiome. *Biomed Res Int.* (2018) 2018:5606845. doi: 10.1155/2018/5606845
73. Cerf-Bensussan N, Gaboriau-Routhiau V. The immune system and the gut microbiota: friends or foes? *Nat Rev Immunol.* (2010) 10:735–44. doi: 10.1038/nri2850
74. Schiffrin EJ, Morley JE, Donnet-Hughes A, Guigoz Y. The inflammatory status of the elderly: the intestinal contribution. *Mutat Res.* (2010) 690:50–6. doi: 10.1016/j.mrfmmm.2009.07.011
75. Ahmed M, Prasad J, Gill H, Stevenson L, Gopal P. Impact of consumption of different levels of *Bifidobacterium lactis* HN019 on the intestinal microflora of elderly human subjects. *J Nutr Health Aging.* (2007) 11:26–31.
76. Pérez Martínez G, Bäuerl C, Collado MC. Understanding gut microbiota in elderly's health will enable intervention through probiotics. *Benef Microbes.* (2014) 5:235–46. doi: 10.3920/BM2013.0079
77. Goodrich JK, Waters JL, Poole AC, Sutter JL, Koren O, Blekhman R, et al. Human genetics shape the gut microbiome. *Cell.* (2014) 159:789–99. doi: 10.1016/j.cell.2014.09.053
78. Kong F, Hua Y, Zeng B, Ning R, Li Y, Zhao J. Gut microbiota signatures of longevity. *Curr Biol.* (2016) 26:R832–3. doi: 10.1016/j.cub.2016.08.015
79. Oki K, Toyama M, TBanno T, Chonan O, Benno Y, Watanabe K. Comprehensive analysis of the fecal microbiota of healthy Japanese adults reveals a new bacterial lineage associated with a phenotype characterized by a high frequency of bowel movements and a lean body type. *BMC Microbiol.* (2016) 16:284. doi: 10.1186/s12866-016-0898-x
80. Waters JL, Ley RE. The human gut bacteria Christensenellaceae are widespread, heritable, and associated with health. *BMC Biol.* (2019) 17:83. doi: 10.1186/s12915-019-0699-4
81. Duncan SH, Barcenilla A, Stewart,C. S., Pryde SE. Flint HJ. Acetate utilization and butyryl coenzyme A (CoA): Acetate-CoA transferase in butyrate-producing bacteria from the human large intestine. ppl. *Environ Microbiol.* (2002) 68:5186–90. doi: 10.1128/AEM.68.10.5186-5190.2002
82. Gibson GR, Hutkins R, Sanders ME, Prescott SL, Reimer RA, Salminen SJ, et al. Expert consensus document: the International Scientific Association for Probiotics and Prebiotics (ISAPP) consensus statement on the definition and scope of prebiotics. *Nat Rev Gastroenterol Hepatol.* (2017) 14:491–502. doi: 10.1038/nrgastro.2017.75
83. Duncan SH, Louis P, Flint HJ. Lactate-utilizing bacteria, isolated from human feces, that produce butyrate as a major fermentation product. *Appl Environ Microbiol.* (2004) 70:5810–7. doi: 10.1128/AEM.70.10.5810-5817.2004
84. Yadav H, Jain S, Sinha PR. Production of free fatty acids and conjugated linoleic acid in probiotic dahi containing *Lactobacillus acidophilus* and *Lactobacillus casei* during fermentation and storage. *Int Dairy J.* (2007) 17:1006–10. doi: 10.1016/j.idairyj.2006.12.003
85. Pessione E. Lactic acid bacteria contribution to gut microbiota complexity: lights and shadows. *Front Cell Infect Microbiol.* (2012) 2:86. doi: 10.3389/fcimb.2012.00086
86. Chen LH, Wang MF, Chang CC, Huang SY, Pan CH, Yeh YT, et al. Lacticaseibacillus paracasei PS23 effectively modulates gut microbiota composition and improves gastrointestinal function in aged SAMP8 mice. *Nutrients.* (2021) 13:1116. doi: 10.3390/nu13041116
87. Wang L, Zhang J, Guo Z, Kwok L, Ma C, Zhang W, et al. Effect of oral consumption of probiotic *Lactobacillus plantarum* P-8 on fecal microbiota, SIgA, SCFAs, and TBAs of adults of different ages. *Nutrition.* (2014) 30:776–83. doi: 10.1016/j.nut.2013.11.018
88. Ticinesi A, Lauretani F, Milani C, Nouvenne A, Tana C, DelRio D, et al. Aging gut microbiota at the cross-road between nutrition, physical frailty, and sarcopenia: is there a gut–muscle axis? *Nutrients.* (2017) 9:1303. doi: 10.3390/nu9121303
89. Grosicki GJ, Fielding RA, Lustgarten MS. Gut microbiota contribute to age-related changes in skeletal muscle size, composition, and function: biological basis for a gut-muscle axis. *Calcif Tissue Int.* (2018) 102:433–442. doi: 10.1007/s00223-017-0345-5
90. Liao X, Wu M, Hao Y, Deng H. Exploring the preventive effect and mechanism of senile sarcopenia based on "gut–muscle axis." *Front Bioeng Biotechnol.* (2020) 8:590869. doi: 10.3389/fbioe.2020.590869
91. Ørtenblad N, Westerblad H. Nielsen J. Muscle glycogen stores and fatigue. *J Physiol.* (2013) 591.18:4405–13. doi: 10.1113/jphysiol.2013.251629
92. Fushimi T, Tayama K, Fukaya M, Kitakoshi K, Nakai N, Tsukamoto Y, et al. Acetic acid feeding enhances glycogen repletion in liver and skeletal muscle of rats. *J Nutr.* (2001) 131:1973–9. doi: 10.1093/jn/131.7.1973
93. Nakao C, Yamada E, Fukaya M, Tayama K, Tsukamoto Y, Sato Y. Effect of acetate on glycogen replenishment in liver and skeletal muscles after exhaustive swimming in rats. *Scand J Med Sci Sport.* (2001) 11:33–7. doi: 10.1034/j.1600-0838.2001.011001033.x
94. Fushimi T, Sato Y. Effect of acetic acid feeding on the circadian changes in glycogen and metabolites of glucose and lipid in liver and skeletal muscle of rats. *Br J Nutr.* (2005) 94:714–9. doi: 10.1079/BJN200 51545
95. Sakakibara S, Yamauchi T, Oshima Y, Tsukamoto Y, Kadowaki T. Acetic acid activates hepatic AMPK and reduces hyperglycemia in diabetic KK-A(y) mice. *Biochem Biophys Res Commun.* (2006) 344:597–604. doi: 10.1016/j.bbrc.2006.03.176
96. Lahiri S, Kim H, Garcia-Perez I, Reza MM, Martin KA, Kundu P, et al. The gut microbiota influences skeletal muscle mass and function in mice. *Sci Transl Med.* (2019) 11:eaan5662. doi: 10.1126/scitranslmed.aan5662

Conflict of Interest: C-CL, Y-CL, H-YH, S-YC, S-LY, J-SL, and KW are employed by SYNBIO TECH INC.

The remaining authors declare that the research was conducted in the absence of any commercial or financial relationships that could be construed as a potential conflict of interest.

Publisher's Note: All claims expressed in this article are solely those of the authors and do not necessarily represent those of their affiliated organizations, or those of the publisher, the editors and the reviewers. Any product that may be evaluated in this article, or claim that may be made by its manufacturer, is not guaranteed or endorsed by the publisher.

frontiers in Microbiology

ORIGINAL RESEARCH
published: 01 November 2021
doi: 10.3389/fmicb.2021.759378

Protective Effect of an Exopolysaccharide Produced by *Lactiplantibacillus plantarum* BGAN8 Against Cadmium-Induced Toxicity in Caco-2 Cells

*Emilija Brdarić[1], Svetlana Soković Bajić[1], Jelena Đokić[1], Slađana Đurđić[2], Patricia Ruas-Madiedo[3], Magdalena Stevanović[4], Maja Tolinački[1], Miroslav Dinić[1], Jelena Mutić[2], Nataša Golić[1] and Milica Živković[1]**

[1] Group for Probiotics and Microbiota-Host Interaction, Laboratory for Molecular Microbiology, Institute of Molecular Genetics and Genetic Engineering, University of Belgrade, Belgrade, Serbia, [2] Faculty of Chemistry, University of Belgrade, Belgrade, Serbia, [3] Department of Microbiology and Biochemistry of Dairy Products, Instituto de Productos Lácteos de Asturias – Consejo Superior de Investigaciones Científicas (IPLA-CSIC), Asturias, Spain, [4] Institute of Technical Sciences, Serbian Academy of Sciences and Arts, Belgrade, Serbia

OPEN ACCESS

Edited by:
Martin Schwarzer, Academy of Sciences of the Czech Republic (ASCR), Czechia

Reviewed by:
Daniele Maria-Ferreira, Pelé Pequeno Príncipe Research Institute, Brazil
Corina-Diana Ceapa, Universidad Nacional Autónoma de México, Mexico

***Correspondence:**
Milica Živković
milicanikolic@imgge.bg.ac.rs

Specialty section:
This article was submitted to Food Microbiology, a section of the journal Frontiers in Microbiology

Received: *16 August 2021*
Accepted: *01 October 2021*
Published: *01 November 2021*

Citation:
Brdarić E, Soković Bajić S, Đokić J, Đurđić S, Ruas-Madiedo P, Stevanović M, Tolinački M, Dinić M, Mutić J, Golić N and Živković M (2021) Protective Effect of an Exopolysaccharide Produced by Lactiplantibacillus plantarum BGAN8 Against Cadmium-Induced Toxicity in Caco-2 Cells. Front. Microbiol. 12:759378. doi: 10.3389/fmicb.2021.759378

Cadmium (Cd) ranks seventh on the list of most significant potential threats to human health based on its suspected toxicity and the possibility of exposure to it. It has been reported that some bacterial exopolysaccharides (EPSs) have the ability to bind heavy metal ions. We therefore investigated the capacity of eight EPS-producing lactobacilli to adsorb Cd in the present study, and *Lactiplantibacillus plantarum* BGAN8 was chosen as the best candidate. In addition, we demonstrate that an EPS derived from BGAN8 (EPS-AN8) exhibits a high Cd-binding capacity and prevents Cd-mediated toxicity in intestinal epithelial Caco-2 cells. Simultaneous use of EPS-AN8 with Cd treatment prevents inflammation, disruption of tight-junction proteins, and oxidative stress. Our results indicate that the EPS in question has a strong potential to be used as a postbiotic in combatting the adverse effects of Cd. Moreover, we show that higher concentrations of EPS-AN8 can alleviate Cd-induced cell damage.

Keywords: cadmium, exopolysaccharides, *Lactiplantibacillus plantarum*, intestinal epithelial cells, inflammation, oxidative stress, cellular junctions

INTRODUCTION

Cadmium (Cd) is a toxic metal and widespread environmental pollutant with serious adverse effects on human and animal health. In 1993, Cd was classified as a human carcinogen and teratogen (IARC Monographs on the Evaluation of Carcinogenic Risks to Humans, 1993). Cd intoxication has been linked with various diseases, including cancer, diabetes mellitus, cardiovascular diseases, neurodegeneration, and osteomalacia (Genchi et al., 2020). Development of industry, fume inhalation, and use of Cd in paint pigments, Cd–nickel batteries, electroplating, and fertilizers have resulted in high exposure to this metal, with a mortality rate of 17% (International Programme On Chemical Safety, 1992; Nawrot et al., 2010). In addition, its long half-life and low level of excretion make Cd an even more dangerous toxicant. Cd is readily transported from soil to plants with a high bioconcentration factor. In rice, for example, as one of the major staple cereal crops

for most of the world's population, the bioconcentration factor of Cd is from 0.300 to 1.112, and it affects the major physiological properties of the plant (Liu et al., 2015). In that context, it is important to mention the so-called "itai-itai" disease that hit Japan during the last century and was a consequence of prolonged intake of Cd-contaminated rice (Huang et al., 2009). An increase of Cd concentration leads to high contamination of the food chain, making food and drinking water the main sources of Cd exposure for the nonsmoking population (Satarug et al., 2010). The first target of orally taken Cd is preferentially the gastrointestinal tract (GIT) (Goon and Klaassen, 1989). Cadmium causes intestinal inflammation, death of epithelial cells, and morphological alterations of cell junctions, which leads to a leaky intestinal barrier (Blais et al., 1999; Prozialeck, 2000; Zhao et al., 2006; Ninkov et al., 2015). After absorption by intestinal epithelium, Cd is transported via blood circulation to different organs and tissues. Thus, keeping the intestinal barrier's integrity intact is of crucial importance.

In view of all these facts, it is urgent to find novel strategies to prevent and neutralize the toxic effect of Cd. It has been reported that some lactic acid bacteria such as lactobacilli, which are commonly present in the GIT and have GRAS status, can bind toxic metal ions and detoxify them (Halttunen et al., 2008; Mrvcic et al., 2009). These abilities often correlate with the presence of different surface biomolecules [e.g., exopolysaccharides (EPSs)] responsible for the probiotic activity of lactobacilli (Yi et al., 2017). EPSs are carbohydrate polymers, which are covalently or loosely bound to the cell surface or secreted in the cell environment and can have antioxidative and immunomodulatory properties (Kanmani et al., 2011; Jones et al., 2014; Caggianiello et al., 2016). Besides, EPS might be used as a postbiotics (Wegh et al., 2019), which are defined as a preparation of inanimate microorganisms and/or their components that confers a health benefit on the host (Salminen et al., 2021). Adsorption of heavy metals by EPSs is mainly a metabolism-independent process based on physicochemical interactions between metal cations and negatively charged acidic functional groups of EPSs (Morillo Pérez et al., 2008). Sequestration of metals is attributable to the presence of various functional groups such as carboxyl, acetate, hydroxyl, amine, phosphate, and sulfate in extracellular bacterial polymers, and the result of metal sequestration may be physical sorption, ion exchange, complexation, and/or precipitation (Gadd and White, 1989; Liu and Fang, 2002). It is now well known that EPS molecules from different bacteria are very potent Cd binders in aqueous solution (Polak-Berecka et al., 2014), but to the best of our knowledge, evidence on how they act in other conditions is insufficient.

The aims of the present study were to select EPS-producing lactobacilli with the highest ability to adsorb Cd from our laboratory collection and show whether the action of EPSs can lead to *in vitro* prevention of Cd-induced inflammation, oxidative stress, and disruption of the cell junctions of differentiated Caco-2 cells, which are well-known test objects frequently used as *in vitro* models to estimate the ability of chemicals to cross the gut barrier and define their mechanisms in humans (Yee, 1997; Angelis and Turco, 2011). Providing information about EPS efficiency is particularly significant in view of the current trend of replacement of live bacteria with nonviable bacterial extracts and metabolic by-products in order to reduce health risks (Konstantinov et al., 2013; Patel and Denning, 2013) and/or exclude biological effects that rely on bacterial metabolism, which might be variable under different conditions (Tsilingiri et al., 2012; Tsilingiri and Rescigno, 2013).

MATERIALS AND METHODS

Bacterial Strains, Media, and Growth Conditions

The eight EPS-producing lactobacilli used in this study are listed in **Table 1**. All strains were grown in De Man–Rogosa–Sharpe medium [MRS (Merck, GmbH, Darmstadt, Germany)]. We prepared MRS agar plates by adding 1.7% agar (Torlak, Belgrade, Serbia). Bacterial strains were grown under anaerobic or aerobic conditions at 30°C or 37°C, depending on the strain.

Exopolysaccharide Extraction and Purification

Exopolysaccharide (EPS) molecules were isolated from *Lactiplantibacillus plantarum* BGAN8 (EPS-AN8), the selected strain with the best Cd-binding ability. For EPS isolation, 100 μL of overnight BGAN8 culture was spread on 200 MRS agar plates and incubated for 48 h at 30°C. Isolation of EPSs was done according to the protocol provided by Ruas-Madiedo et al. (2006) with additional steps described by Dinić et al. (2018). Dialysis was performed twice, after the isolation and purification steps, and lasted for 5 days, each time with daily changes of Milli-Q water. The dialysis bag (Sigma–Aldrich, St. Louis, MO, United States) had a 12- to 14-kDa molecular mass cutoff. At the end of dialysis, extracted and purified EPS molecules were lyophilized (Alpha 1-4 LSC plus freeze dryer, Martin Christ, Germany).

Analysis of EPS-AN8 Structure by Size Exclusion Chromatography–Multiangle Laser Light Scattering and Testing of Sugar Composition of the Purified Exopolysaccharide

First, the purified EPS was assessed by means of size exclusion chromatography (SEC) coupled with a multiangle laser light

TABLE 1 | List of strains used in this study.

Species	Strain	Origin
Lactiplantibacillus plantarum	BGAN8	Cow white cheese
	BGPKM22	Cow sour milk
	BGVL2a-18	Goat cheese
	BGMI1	Cow white cheese
	BGSJ2-3	Cow white cheese
Lacticaseibacillus rhamnosus	BGHI22	Human intestinal tract
	BGHV954	Human vaginal tract
	BGHV20	Human vaginal tract

scattering (MALLS) detector as described by Nikolic et al. (2012). The chromatographic system (Waters, Milford, MA, United States) was composed of an Alliance 2690 module injector, a Photodiode Array PDA 996 detector (set at 280 nm), a 410 refractive index detector, and the Empower software (Waters). The MALLS detector (Dawn Heleos II, Wyatt Europe GmbH, Dambach, Germany) was coupled in series, and the Astra 3.5 software was used for analysis of molar mass distribution. Separation was carried out in two SEC columns placed in series, TSK-Gel G3000 PW_{XL} + TSK-Gel G5000 PW_{XL}, protected with a TSK-Gel guard column (Supelco-Sigma), at a temperature of 40°C and flow rate of 0.45 mL/min using 0.1 M $NaNO_3$ as the mobile phase. Experiments were repeated three times.

For analysis of neutral sugars in testing EPS monosaccharide composition, polysaccharides (approximately 1.6 mg) were first hydrolyzed with 3M TFA (121°C, 90 min). Monosaccharides were converted into their corresponding alditol acetate by reduction with $NaBH_4$ and subsequent acetylation (Laine et al., 1972). Identification and quantification were performed by gas–liquid chromatography (GLC) on a gas chromatograph equipped with a DB-5HT column (Agilent, Santa Clara, CA, United States; 30 m × 0.25-mm internal diameter; 0.10-mm film thickness) coupled to a quadrupole mass detector. The oven program started at 175°C for 1 min and was increased by 2.5°C min/min until 204°C was reached. Helium was used as the carrier gas at a flow rate of 1 mL/min. Identification was performed on the basis of coincidence of the retention time of sample components with those previously measured for standards analyzed in identical conditions, using inositol as an internal standard. GLC was performed in the Centro de Investigaciones Biológicas (CIB) by Margarita Salas, CSIC, 28040 Madrid, Spain.

Fourier Transform Infrared Spectroscopy

As a powerful analytical technique to investigate the structural characteristics of biomacromolecules (Verhoef et al., 2005), Fourier transform infrared spectroscopy (FTIR) spectroscopy was used to confirm the qualitative composition of EPS-AN8 molecules. The FTIR spectrum of samples was acquired in the transmittance mode on a Nicolet iS10 spectrometer (Thermo Fisher Scientific, Waltham, MA, United States) to confirm the qualitative composition of samples, that is, to confirm that extracted and purified material from BGAN8 is an EPS. Measurements were performed in the spectral range of 400 to 4,000 cm^{-1} with a resolution of 4 cm^{-1}, the number of scans being 32. Spectra were collected using the attenuated total reflectance mode, whereas the OMNIC software was used to acquire, process, analyze, and manage FTIR data in a graphical environment.

Preparation of Cadmium Solutions

Cadmium (Cd) was added in the form of $CdCl_2$ (Sigma–Aldrich). It was dissolved in Milli-Q water at a concentration of 1 mM and kept at 4°C. Working solutions were freshly made by dissolving $CdCl_2$ in Milli-Q water or cell culture medium.

TABLE 2 | List of primers used for real-time PCR analysis in this study.

Primer name	Primer sequence	References
IL-8	5′-ACACAGAGCTGCAGAAATCAGG-3′	Angrisano et al., 2010
	5′-GGCACAAACTTTCAGAGACAG-3′	
CDH1	5′-AGCCTGTCGAAGCAGGATTG-3′	Popović et al., 2020
	5′-AGAAACAGCAAGAGCAGCAGA-3′	
OCLN	5′-TCAGGGAATATCCACCTATCACTTCAG-3′	Elamin et al., 2012
	5′-CATCAGCAGCAGCCATGTACTCTTCAC-3′	
ZO-1	5′-AGGGGCAGTGGTGGTTTTCTGTTCTTTC-3′	Elamin et al., 2012
	5′-GCAGAGGTCAAAGTTCAAGGCTCAAGAGG-3′	
NQO1	5′-GGATTGGACCGAGCTGGAAA-3′	This work
	5′-CAAACTGAAACACCCAGCCG-3′	
GAPDH	5′-GTGAAGGTCGGAGTCAACG-3′	Freudenberger et al., 2014
	5′-TGAGGTCAATGAAGGGGTC-3′	

Cadmium-Binding Experiments

The ability of live EPS-producing lactobacilli to bind Cd was investigated using the protocol provided by Zhai et al. (2013) with slight modifications. Overnight cultures were washed twice in phosphate-buffered saline (PBS). A volume of 1 mL (10^9 CFU/mL) was taken and centrifuged at 13 000 revolutions/min (rpm) for 10 min at room temperature (RT). Cell pellets were resuspended in 1 mL of dissolved $CdCl_2$ (50 μM) and incubated at 30°C for 1 h. After 1 h, the mixtures were centrifuged (13 000 rpm, 20 min, RT), and supernatants were collected and kept at −20°C for residual Cd content analysis. The concentration of 50 μM $CdCl_2$ used in this protocol corresponded to the doses of Cd present in the environment (Blanusa et al., 2002; Damek-Poprawa and Sawicka-Kapusta, 2004).

The EPS of a strain with the highest ability to adsorb Cd ions was isolated, and its adsorption of Cd was measured, following the protocol of Polak-Berecka et al. (2014) with a few modifications. Briefly, 1 mg/mL of EPS was resuspended in Milli-Q water and placed in a dialysis bag. The EPS-containing dialysis bag was placed in a glass cup filled with an aqueous solution of $CdCl_2$ and stirred for 24 h at 30°C.

Determination of Cadmium Concentration

Concentrations of Cd ions were determined by inductively coupled plasma mass spectrometry with ICP-QMS (iCAP Q, Thermo Scientific X series 2, United Kingdom). A standard stock solution of Cd containing of 1,000.0 ± 0.2 mg/L (Alfa Aesar, Germany) was used to prepare intermediate standard solutions for ICP-MS measurements. Operating conditions for ICP-QMS were as follows: RF power—1548 W; lens voltage—7 V; pulse stage voltage—950 V; sample uptake rate—24 rpm;

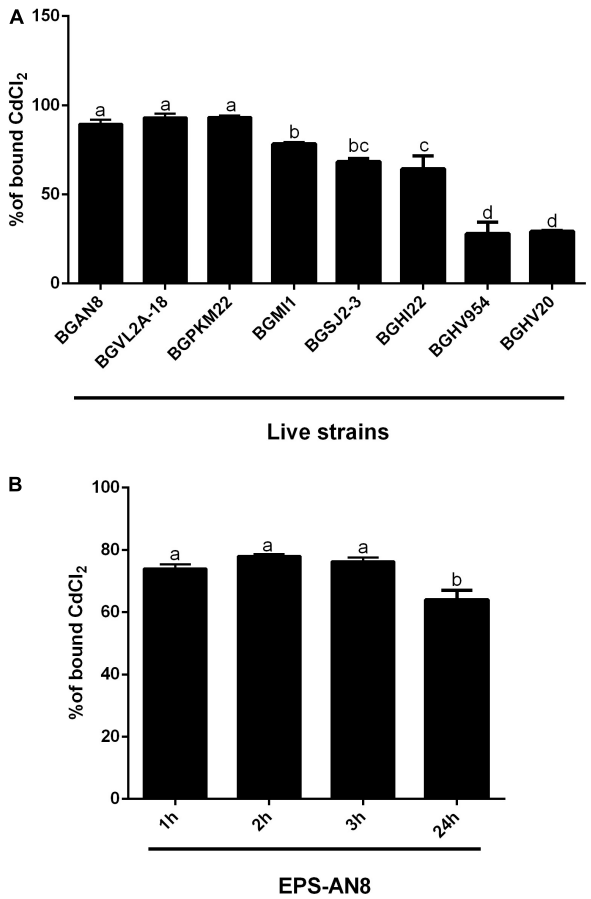

FIGURE 1 | Ability of live exopolysaccharide (EPS)–producing lactobacillus strains to bind Cd **(A)** and ability of EPS isolated from the selected *Lactiplantibacillus plantarum* AN8 strain (EPS-AN8) to adsorb Cd ions after 1, 2, 3, and 24 h of exposure **(B)**. Values that do not share a common letter are significantly ($p < 0.05$) different.

gas flow rates—13.9, 1.09, and 0.8 L/min; acquisition time—3 × 50 s; points per peak - 3; dwell time—10 ns; detector mode—analog/pulse; replicates—3; measured isotope—^{113}Cd.

Cell Culture

Differentiated human enterocyte-like Caco-2 cells were used as a model system to analyze the adverse effects of Cd and putative protection by the EPS. The Caco-2 cells were grown and maintained in the same manner as described by Popović et al. (2019). The medium was replaced every second day for 21 days.

Treatment of Caco-2 Cells

For all assays, cells were differentiated in 24-well plates, except in the case of the Lucifer yellow test, where cells were differentiated in 24-well plates covered with Transwell inserts (pore diameter 0.4 μm, Sarstedt, Nümbrecht, Germany). Here 21-day cells were washed three times with PBS and then treated. First, in order to find subtoxic concentrations of $CdCl_2$, cells were treated with $CdCl_2$ in a range of different concentrations (50, 100, and 200 μM) for 24 h. EPS-AN8 was added in two concentrations: in a lower concentration (50 μg/mL), which corresponds to approximately 1 × 10^9 CFU/mL *L. plantarum* BGAN8 and in a two times higher concentration (100 μg/mL). Both were in a range of concentrations usually used in different studies (Liu et al., 2019). Besides, none of used EPS-AN8 concentrations caused cytotoxic effect on Caco-2 (**Supplementary Data**). Further on, Caco-2 cells were simultaneously treated with EPS-AN8 and with a subtoxic concentration of $CdCl_2$ for 3 h, which was enough time to observe Cd-induced changes in gene expression (Rusanov et al., 2015) and 24 h to measure protein expression (Zhai et al., 2016). At the end of the treatment, cell culture supernatants were collected and stored at -20°C for cytotoxicity assay and superoxide dismutase (SOD) activity measurements. Cells were detached with trypsin-EDTA solution (Torlak) and stored at -80°C for quantitative real-time polymerase chain reaction (PCR) and Western blot analysis. Also, to see if the EPS could be used to alleviate the effect of $CdCl_2$ on the cell, Caco-2 was first treated with a subtoxic concentration of $CdCl_2$ for 24 h. The next day the medium was changed, the EPS was added in lower and higher concentrations, and the incubation lasted another 24 h.

Cytotoxicity Assay

The level of lactate dehydrogenase (LDH) released in supernatants, which correlates with the number of dead cells (Bajić et al., 2020b), was measured by using an LDH cytotoxicity assay kit (Thermo Fisher Scientific, Waltham, MA, United States). Activity of LDH was measured in cell culture supernatants, following the manufacturer's instructions. Absorbance was read at 450 nm using a microplate reader (Tecan Austria GmbH, Grödig, Austria).

Quantitative Real-Time Polymerase Chain Reaction

Total RNA was isolated following the protocol described by Sokovic Bajic et al. (2019). For reverse transcription, the RevertAid RT kit was used according to the manufacturer's protocol (Thermo Fisher Scientific). Amplification of synthesized cDNA was done in a 7500 real-time PCR system (Applied Biosystems, Foster City, CA, United States). The SYBR™ Green PCR Master Mix (Applied Biosystems) was used following the instructions for reaction conditions, viz.: activation at 95°C for 10 min, 40 cycles of 15 s at 95°C, and 60 s at 60°C. The primers used are listed in **Table 2**. Expression of mRNA was normalized against the *GAPDH* gene utilizing the $2^{-\Delta\Delta Ct}$ method. All primers were purchased from Thermo Fisher Scientific.

Western Blot

Protein isolation and Western blotting were performed following the protocol provided by Popović et al. (2019). Isolated proteins were separated on 12% sodium dodecyl sulfate–polyacrylamide gel electrophoresis and transferred to a 0.2-mm nitrocellulose membrane (GE Healthcare). Anti-GAPDH (as loading control; 1:1,000; Invitrogen), anticlaudin (CLDN-4, 1:1,000; Thermo Fisher Scientific), and anti-p65 [nuclear factor κB (NF-κB), 1:500; Cell Signaling Technology] were used during the night at +4°C. Proteins were detected by a ChemiDoc apparatus and quantified in ImageJ software (National Institutes of Health).

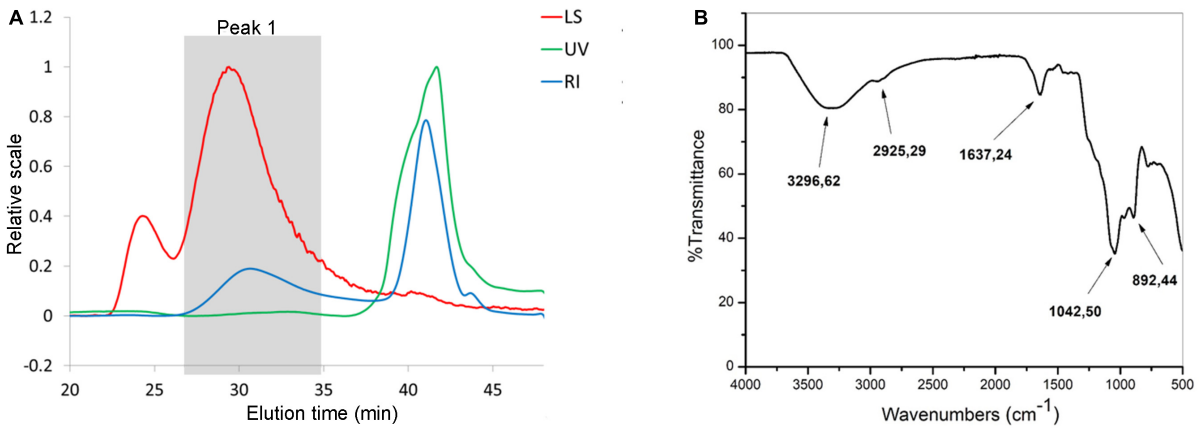

FIGURE 2 | SEC analysis **(A)** of EPS-AN8. Ultraviolet (UV, 280 nm) detector, multiangle light scattering (LS, angle 90°), refraction index (RI). **(B)** FTIR spectra of EPS-AN8.

Permeability Assay

Integrity of the monolayer barrier was determined by measuring the passive passage of Lucifer yellow dye (Invitrogen, Thermo Fisher Scientific). The protocol described by Yamaura et al. (2016), with a few modifications, was followed. Initially, Lucifer yellow was dissolved in dimethyl sulfoxide and then diluted 1,000-fold in PBS solution. The mixture was added to the apical membrane of Caco-2 cells and incubated for 1 h at 37°C. A microplate reader (Tecan) with excitation and emission of 428 and 536 nm, respectively, was used for fluorescence detection.

Superoxide Dismutase Activity

Superoxide dismutase (SOD) activity was measured in supernatants of Caco-2 cells using the SOD Assay Kit (Sigma–Aldrich) after 24 h of treatments. The manufacturer's instructions were followed, and absorbance was measured at 440 nm, using a microplate reader (Tecan).

Statistical Analysis

GraphPad Prism 8 software was used in performing statistical analysis and preparing graphs. All experiments were repeated at least three times. After checking normal distribution of values with the Kolmogorov–Smirnov test, one-way analysis of variance and Dunnett and Tukey tests were used for multiple comparison. Values that do not share a common letter are significantly different at $p < 0.05$. Data are presented as mean values ± standard deviation from different experiments.

RESULTS AND DISCUSSION

Ability of Exopolysaccharide-Producing Lactobacilli to Adsorb Cd Ions and Characterization of EPS-AN8

It is known that microorganisms can interact with heavy metals via biosorption of metal ions on the cell surface, intracellular uptake, and chemical transformation (Hassan et al., 2009). Also, it was previously reported that the greatest amount of metals is bound to the surface and adsorbed, in contrast to an exceedingly small part of ions that was actively taken up (Mrvcic et al., 2009). Lactobacilli turned out to be a promising solution for the growing problem of Cd pollution (Mrvčić et al., 2012). They can adsorb a great number of different metals ions, in a strain-specific manner (Zhai et al., 2013). For example, lactobacilli showed a protective effect against acute Cd poisoning in mice. More precisely, both live and dead lactobacilli decreased intestinal absorption of Cd ions, leading to a lower level of Cd in tissues and increased concentration in feces, which indicates the involvement of surface biomolecules of lactobacilli in the Cd-binding process (Zhai et al., 2013). Lactobacilli have the ability to produce homopolysaccharides and heteropolysaccharides with enormous structural diversity and different biological properties (Caggianiello et al., 2016). Among other activities, the potential of different EPS-producing bacterial species to adsorb metal ions was described by Yi et al. (2017). Therefore, in the present study, we tested the potential of eight EPS-producing lactobacilli strains from our laboratory collection to adsorb Cd. *L. plantarum* BGAN8, *L. plantarum* BGVL2A-18, and *L. plantarum* BGPKM22 showed the highest ability to bind Cd ions in aqueous solution and did not significantly differ from each other (**Figure 1A**). *L. plantarum* BGAN8 has been well characterized as an EPS producer and microvesicle releaser (Bajic et al., 2020a), and it was therefore chosen for further work. Further, isolated EPS-AN8 was tested for binding Cd. As shown in **Figure 1B**, EPS-AN8 has a great capacity for binding Cd ions. After the first, second, and third hour of EPS and $CdCl_2$ coincubation, the percentage of Cd binding did not differ significantly, ranging between 72 and 78% of the total amount of $CdCl_2$ in solution. Interestingly, a slight decrease in adsorbed Cd ions was observed after 24 h of coincubation, suggesting that a smaller amount of Cd is reversibly bound to EPS molecules. This observation is in agreement with earlier studies that showed the same phenomenon of a short-term reduction of Cd ion binding between 24 and 48 h (Polak-Berecka et al., 2014). Examination of the SEC profile reveals the presence of one major peak with average retention time of

about 32 min (**Figure 2A**). Furthermore, SEC- MALLS analyses showed that EPS-AN8 has a high molecular weight (**Table 3**), the value of which is within the expected range of weight among characterized HePSs of other lactobacilli from the *L. plantarum* group, ranging from 10^4 to 10^6 Da (Tallon et al., 2003; Sánchez et al., 2006; Nikolic et al., 2012). Also, radius of gyration was similar to values for EPS of other lactobacilli (Bachtarzi et al., 2020). Analysis of neutral sugar content of EPS-AN8 revealed that glucose, galactose, rhamnose, and mannose are present in a ratio of 1:0.33:0.19:0.05, respectively, and in percentages of 12.91%, 4.23%, 2.45%, and 0.60% (**Table 3**). It is well known that heteropolysaccharides consist of different monosaccharides, such as D-glucose, D-galactose, and L-rhamnose (De Vuyst and Degeest, 1999). The presence of mannose was also reported in other HePSs as well, such as in *Lactococcus lactis* subspecies *cremoris* Ropy352, *Lactobacillus pentosus* LPS26, or *Lactobacillus paraplantarum* BGCG11 (Cerning et al., 1994; Knoshaug et al., 2000; Sánchez et al., 2006). The FTIR spectrum of EPS-AN8 is presented on **Figure 2B**. The spectrum contains typical groups for polysaccharides, that is, carboxyl, hydroxyl, and amide groups (Dinić et al., 2018). A broad-stretching absorption band at 3,296.62 cm^{-1} corresponds to –OH or –NH vibrations (Coates, 2006). From the literature, it is well known that hydroxyl groups are ubiquitous in polysaccharide structure, which exhibits an intense broad stretching vibration in the region characteristic of the carbohydrate ring (Dinić et al., 2018). The affinity of polysaccharides for water molecules depends on the presence of these multi-OH groups (Hu et al., 2017). The small absorption band at 2,925.29 cm^{-1} corresponds to the C-H stretching vibrations of methyl or methylene groups, regularly present in hexoses such as glucose or galactose and in deoxyhexoses such as rhamnose or fucose (Ismail and Nampoothiri, 2010). The band at 1,637.24 cm^{-1} represents vibration of the C = O stretch of the amide I band or carboxyl group (Shen et al., 2013). This may indicate the presence in the examined EPS of acidic sugars (monosaccharides with a carboxyl group at one end or both ends of their chain), which are important in view of the heavy metal–binding properties of this polymer (Angyal, 1989). Also, carboxyl and hydroxyl groups are important for the coordination responsible for stability of the EPS-metal bond (Moppert et al., 2009). The band at 1,041.50 cm^{-1} corresponds to a C-O stretch vibration or a phosphorus out-of-phase P-O-C stretch (Corbrjdge, 2007). EPSs are known to be composed of carbohydrates (sugar residues) substituted with proteins, DNA, phospholipids, and noncarbohydrate substituents such as acetate, glycerol, pyruvate, sulfate, carboxylate, succinate, and phosphate (Angelin and Kavitha, 2020). The strongest absorption band at 1,041.50 cm^{-1} indicates that the substance is an EPS. A possible explanation for the effective binding of metal cations is that the phosphate group undergoes deprotonation under physiological conditions, which results in negative charges along the phosphate backbone (Pal and Paul, 2008; Ruan et al., 2008). The resulting negative charges tend to be stabilized and neutralized by the binding of metal cations, such as, in our case, Cd, and result in immobilization of the metal. The absorption band at 892.44 cm^{-1} corresponds to vibrations of the glycoside link C-O-C (Nikonenko et al., 2000). Apart from the aforementioned peaks, there are no other peaks that can be observed in the spectrum of our sample.

TABLE 3 | Physicochemical characteristics of EPS-AN8.

Parameters		
Molecular weight (g/mol = Da)	$2.27 \pm 0.07 \times 10^5$	
Radius of gyration (nm)	86.65 ± 3.46	
Monosaccharides	**%**	**Ratio**
Glucose	12.91	21.5
Galactose	4.23	7.1
Rhamnose	2.45	4.1
Manose	0.60	1

Protective Effect of EPS-AN8 on Cd-Induced Inflammation of Caco-2 Cells

In order to investigate the ability of EPS-AN8 to protect differentiated Caco-2 cells from Cd-induced inflammation, we determined the subtoxic concentration of $CdCl_2$ on Caco-2 cells (**Figure 3A**), which were used as an *in vitro* model of the intestinal epithelium. Concentrations of $CdCl_2$ higher than 50 μM were toxic, which is in accordance with published data (Hyun et al., 2007), so 50 μM of $CdCl_2$ was used as a subtoxic concentration in our further experiments. Intestinal epithelial cells are very important, not only as a physical barrier, but also as a part of innate mucosal immunity–producing antimicrobial molecules, as well as the cytokines and chemokines required for immune response activation (Stadnyk, 1994; Turner, 2009). It has been shown that Cd induces inflammation via overproduction of interleukin 8 (IL-8) (Hyun et al., 2007). IL-8 is a chemotactic cytokine that attracts and activates leukocytes, leading to acute inflammation, which is very important for the resolution of infection (Baggiolini and Clark-Lewis, 1992). On the other hand, in the case of stimuli that cannot be removed and persist as a stimulator of the epithelial barrier and immune response, overexpression of IL-8 has a destructive effect on the local tissue (Baggiolini and Clark-Lewis, 1992). In the present study, we demonstrate that treatment of Caco-2 cells with Cd for 3 h leads to a statistically significant increase in *IL-8* gene expression (**Figure 3B**), but cotreatment, at the same time, with the higher concentration of EPS-AN8 provided protection from this overexpression, and the level of mRNA for IL-8 did not differ statistically from the level in the control cells (**Figure 3B**). On the contrary, cotreatment with the lower EPS-AN8 concentration did not affect the up-regulation of IL-8 induced by Cd. NF-κB is defined as one of the most significant regulators of inflammation in different types of cells, including intestinal epithelial cells (Mitchell et al., 2016). In addition, there are binding regions in the promoter of the IL-8 coding gene, confirming the regulatory role of NF-κB in IL-8 production (Wu et al., 1997). Importantly, it has been shown that activation of NF-κB is essential for up-regulation of IL-8 in Caco-2 cells treated with Cd (Hyun et al., 2007). Accordingly,

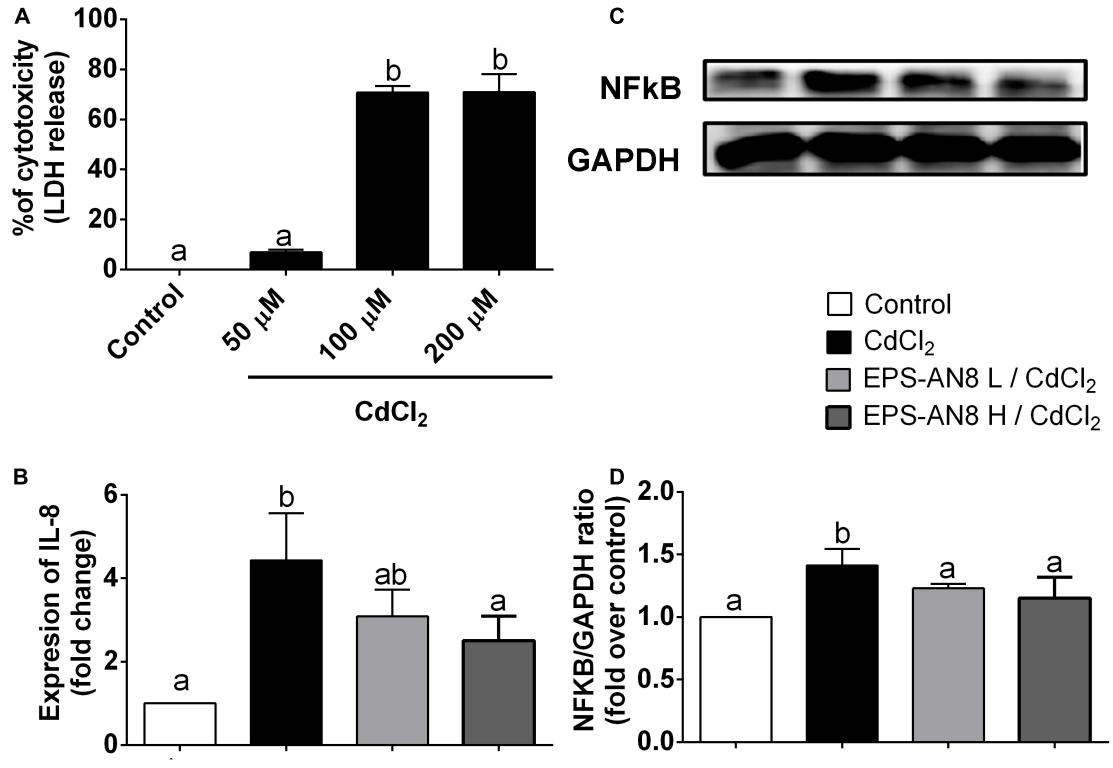

FIGURE 3 | Protection from Cd-induced inflammation. **(A)** Percentage (%) of cytotoxicity measured in differentiated Caco-2 cells treated with different concentrations (50, 100, and 200 μM) of $CdCl_2$. **(B)** Effect of Cd and cotreatment with Cd and EPS-AN8 in lower and higher concentrations (L and H) on *IL-8* mRNA expression after 3 h. **(C,D)** P65 protein levels after 24 h of incubation and Western blot and densitometric analysis, respectively. Values that do not share a common letter are significantly ($p < 0.05$) different.

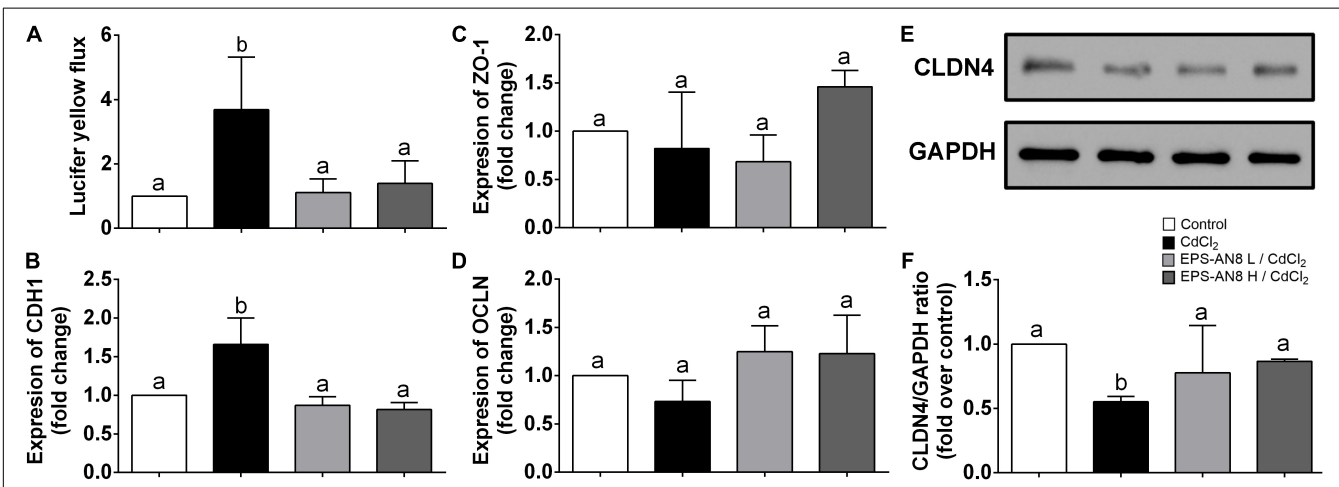

FIGURE 4 | Protection from Cd-induced disruption of cell junctions by EPS-AN8. **(A)** Rate of passive transport of Lucifer yellow through Caco-2 cell monolayer after Cd exposure and coexposure with Cd and EPS-AN8 (L and H). **(B)** Effect on mRNA of adherence junction protein *CDH1* after 3 h. Effect on mRNA of tight junction proteins *ZO-1* **(C)** and *OCLN* **(D)** after 3 h. **(E,F)** Effect on expression of CLDN4 protein and representative Western blot and densitometric analysis after 24 h of incubation, respectively. Values that do not share a common letter are significantly ($p < 0.05$) different.

we investigated the effect of Caco-2 cotreatment with Cd and EPS-AN8 on activation of NF-κB by estimating protein levels of phosphorylated p65, which represents a transcriptionally active form of NF-κB. As shown on **Figures 3C,D**, both concentrations of EPS-AN8 neutralized the stimulatory effect of Cd on NF-κB activation, but only the higher concentration of EPS-AN8

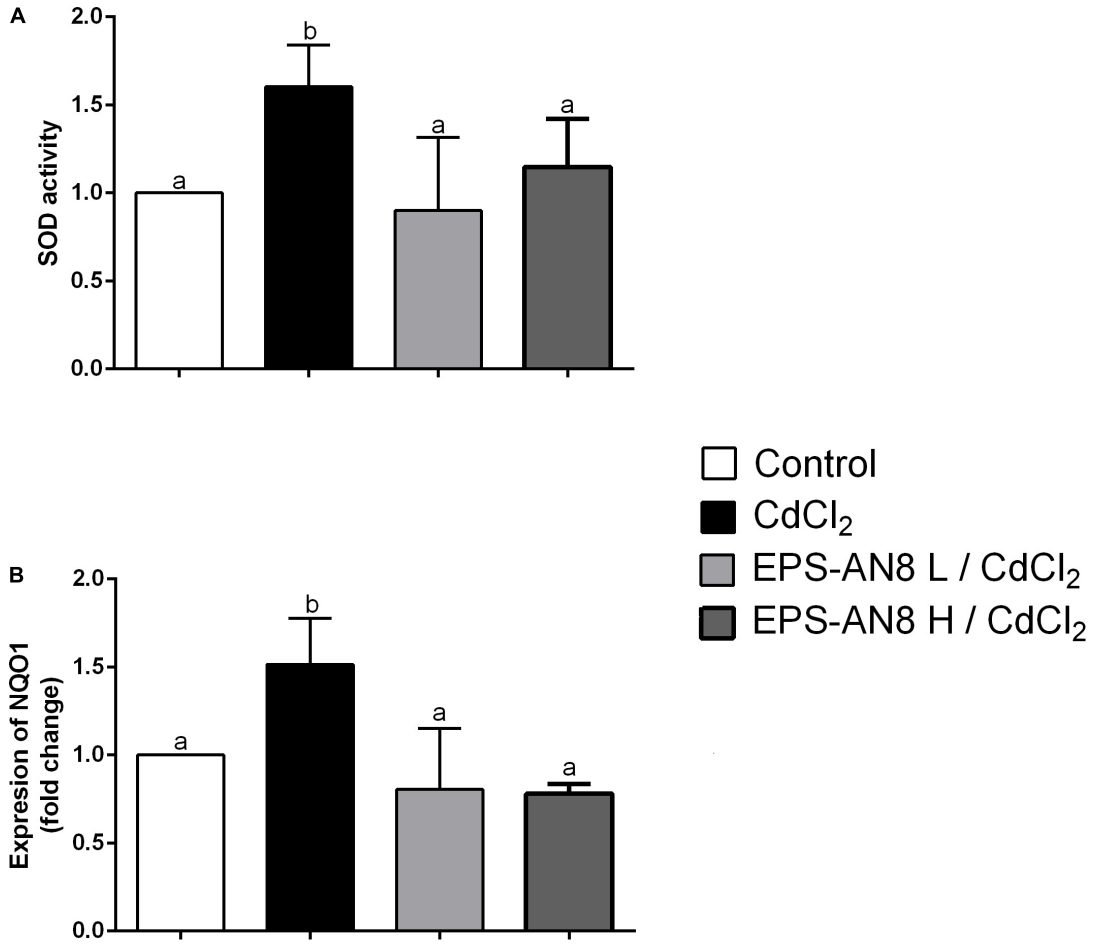

FIGURE 5 | Role of EPS (L and H) in protection of Cd-induced oxidative stress. **(A)** Effect on SOD activity and **(B)** mRNA expression of *NQO1*. Values that do not share a common letter are significantly ($p < 0.05$) different.

reduced IL-8m RNA levels. These results suggest that EPS-AN8, when applied simultaneously with Cd, most likely decreases Cd-induced inflammation through the sequestration of Cd ions by EPS-AN8, which inhibits entry of Cd into the cells, and imply that with the lower EPS-AN8 concentration, it is not sufficient to bind all available Cd ions responsible for mild stimulation of IL-8.

Protective Effect of EPS-AN8 on Cd-Induced Disruption of Intercellular Junctions

Maintenance of the intestinal barrier is very important in the restriction of Cd spreading in the organism (Tinkov et al., 2018). For that reason, the permeability of a differentiated layer of Caco-2 cells was analyzed after exposure of cells to Cd and to Cd and EPS simultaneously. According to the results presented in **Figure 4A**, Cd strongly increased permeability of the monolayer, but integrity of the monolayer was preserved in the culture cotreated with EPS-AN8. Oral administration of Cd disrupts adherence and tight junctions (TJs) in epithelial surfaces, resulting in amplified Cd absorption (Rusanov et al., 2015). Hence, the primary therapeutic targets are proteins involved in intercellular junctions. E-cadherin is defined as the most sensitive to Cd exposure, as Ca ions are substituted with ions of Cd at the sites of its binding to the cells (Prozialeck, 2000). In connection with this, we investigated the potential of two concentrations of EPS-AN8, simultaneously added to Cd, as a treatment of differentiated Caco-2 cells to neutralize the harmful effects of Cd. After 3 h of treatment, only Cd exposure significantly increased the expression of E-cadherin (*CDH1*) mRNA (**Figure 4B**), whereas coexposure to both concentrations of EPS-AN8 molecules retained the control value of expression. These results can be explained by the aforementioned Ca–Cd substitution and sensitivity of this protein to an increased concentration of divalent ions. Further, claudin (*CLDN-4*), zonulin-1 (*ZO-1*), and occludin (*OCLN*) are crucial proteins in forming TJs (Günzel and Fromm, 2012). In our study, the level of mRNAs for *ZO-1* and *OCLN* did not change in response to either treatment compared to the control (**Figures 4C,D**). In contrast, after 24-h treatment, Cd down-regulated the level of CLDN-4 (**Figure 4C**), whereas cotreatment with EPS-AN8

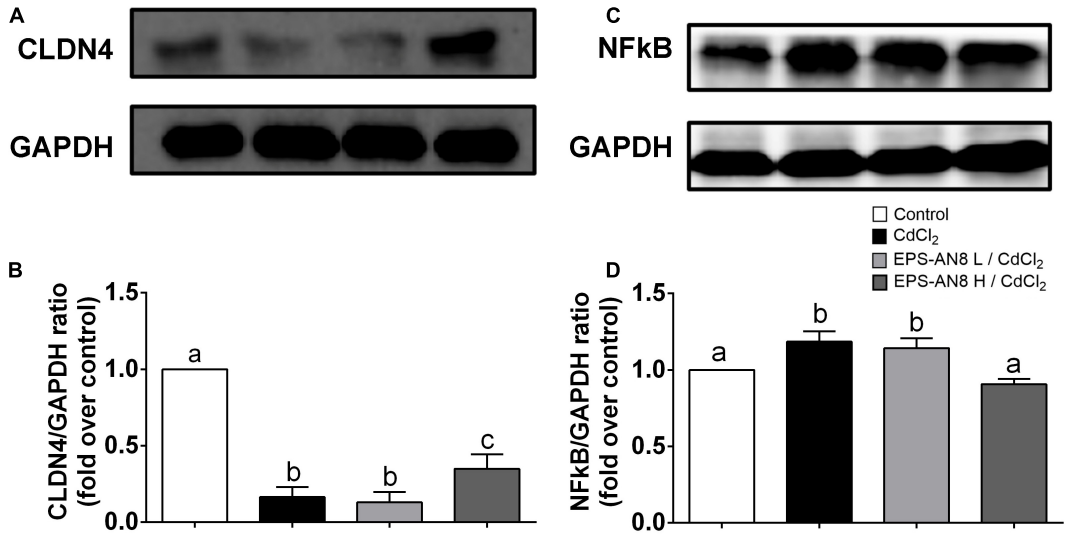

FIGURE 6 | EPS-AN8 as a potential agent for alleviation of Cd-induced damage. **(A,B)** Effect of EPS (L and H) on Cd-induced down-regulation of tight junction protein CLDN-4 and representative Western blot and densitometric analysis, respectively. **(C,D)** Effect of EPS (L and H) on Cd-induced overexpression of NF-κB and representative Western blot and densitometric analysis, respectively. Values that do not share a common letter are significantly ($p < 0.05$) different.

in both concentrations inhibited the downregulation of this protein's expression (**Figures 4E,F**). In light of these results, it can be concluded that EPS-AN8 prevents Cd-induced destruction of the intestinal barrier by protecting against CLDN-4 degradation.

Protective Effect of EPS-AN8 on Cd-Induced Oxidative Stress

It has been repeatedly shown that the main mechanism of Cd-induced toxicity is based on induction of oxidative stress in exposed cells (Genchi et al., 2020). We therefore investigated the activity of two enzymes important for oxidative/antioxidative responses of cells: SOD and NAD(P)H quinone reductase (NQO1). Superoxide dismutase is one of the enzymes essential for the antioxidative balance of cells, catalyzing dismutation of the superoxide anion into hydrogen peroxide and molecular oxygen (Canada and Calabrese, 1989). We were able to demonstrate that after 24 h of treatment of Caco-2 with Cd, SOD activity was significantly higher than in the control and in the case where EPS-AN8 was applied to the cells at the same time with Cd. Both concentrations of EPS were shown to be similarly efficient in inhibiting the induction of oxidative stress by Cd through activation of SOD in Caco-2 cells (**Figure 5A**). As SOD protects cells from the activity of reactive oxygen species (ROS), higher activity implies higher production of ROS (He et al., 2017; Wang et al., 2018). Based on this, it can be concluded that cells are in a better oxidative state in the presence of EPS-AN8 simultaneously with Cd. In addition, NQO1 is also a key enzyme of antioxidant cell defense, one that catalyzes reduction of quinones and a variety of other substrates (Pey et al., 2019). As in the case of SOD, Cd stimulated the level of mRNA for NQO1, which is consistent with data from the literature (Rusanov et al., 2015). The addition of EPS-AN8 in both lower and higher concentrations at the same time with it protected from this effect of Cd as well (**Figure 5B**).

EPS-AN8 as a Potential Agent for Alleviation of Cd-Induced Damage

From the results obtained when Caco-2 cells were exposed to Cd and EPS-AN8 at the same time, we conclude that EPS-AN8, in both the lower and higher tested concentrations, provides strong protection against the damage caused by Cd toxicity. We presume that such a protective effect is a consequence of the ability of EPS-AN8 to sequester Cd ions and disable the entry of ions into the cells. It was reported elsewhere that *L. plantarum* CCFM8610, besides initially sequestrating Cd ions, can also reverse damage induced by Cd in HT29 cells and mice (Zhai et al., 2016). To see if EPS-AN8 has a therapeutic effect as well, we analyzed changes in the expression of CLDN-4 and NF-κB when Caco-2 cells were previously exposed to Cd. To be specific, after 24 h of treatment of Caco-2 cells with Cd, EPS-AN8 was added to the culture as a putative agent for alleviation of Cd-induced damage and incubated for the next 24 h. Although we noticed some positive changes after treatment with the lower concentration of EPS-AN8, the higher concentration of EPS-AN8 was far more effective in this study (**Figure 6**). The higher concentration of EPS-AN8 significantly increased expression of CLDN-4 compared to Cd treatment (**Figures 6A,B**) and significantly decreased the level of p65 protein expression in comparison with Cd treatment and treatment with a lower concentration of EPS (**Figures 6C,D**). These results imply that EPS-AN8, besides sequestration of Cd ions, also triggered intestinal cell responses that lead to alleviation of Cd-induced damage. This assumption is in accordance with results of a previous study that demonstrated that EPS molecules might have a strong anti-inflammatory potential in conditions of high inflammation via modulation of Toll-like receptor

expression and inhibition of mitogen-activated protein kinase and NF-κB in intestinal epithelial cells (Gao et al., 2017). Also, some EPSs act as a stabilizer of intestinal barrier integrity by activating signal transducers, activating transcription of signaling (STAT-3) pathways, and up-regulating TJ proteins, respectively, in cases of intestinal barrier dysfunction (e.g., inflammatory bowel disease, colitis) (Zhou et al., 2018).

CONCLUSION

Our findings indicate an important role of probiotic-derived EPSs in protection against the hazardous effects of Cd on intestinal epithelial cells. To our knowledge, the present study is the first one providing information about EPSs as a potent postbiotic agent against this environmental pollutant and its possible use as a functional food supplement or dairy food additive in areas highly exposed to Cd. This pioneering work calls for further studies analyzing the use of EPSs as a putative therapeutic strategy.

DATA AVAILABILITY STATEMENT

The original contributions presented in the study are included in the article/**Supplementary Material**, further inquiries can be directed to the corresponding author.

AUTHOR CONTRIBUTIONS

EB performed all the work, analyzed and interpreted the data, and drafted this manuscript. MŽ, JĐ, and MT planned, designed, and performed some of the experiments and critically revised the manuscript. SSB performed Western blot analysis, participated in EPS extraction, analyzed the data, and interpreted the results. PR-M performed SEC-MALLS analysis, analyzed data and interpreted the results. MS analyzed FTIR spectrum of EPS-AN8 and interpreted the results. MD participated in Caco-2 cell culture experiments and qPCR. JM and SĐ performed Cd-binding research. MŽ and NG supervised all the work. All authors contributed to the article and approved the submitted version.

FUNDING

This work was funded by the Ministry of Education, Science, and Technological Development of the Republic of Serbia (Registration No. 451-03-9/2021-14/200042) in an agreement on the implementation and financing of research work in 2021.

ACKNOWLEDGMENTS

EB is grateful to Nemanja Mirković from the University of Belgrade-Faculty of Agriculture for necessary lyophilization of EPS-AN8. EB is also grateful to Leonor Rodrigues-Sanchez and Alicia Prieto from CIB-CSIC, Madrid, Spain, for the GLC analysis of EPS-AN8.

SUPPLEMENTARY MATERIAL

The Supplementary Material for this article can be found online at: https://www.frontiersin.org/articles/10.3389/fmicb.2021.759378/full#supplementary-material

REFERENCES

Angelin, J., and Kavitha, M. (2020). Exopolysaccharides from probiotic bacteria and their health potential. *Int. J. Biol. Macromol.* 162, 853–865. doi: 10.1016/j.ijbiomac.2020.06.190

Angelis, I. D., and Turco, L. (2011). Caco-2 cells as a model for intestinal absorption. *Curr. Protoc. Toxicol.* Chapter 20:Unit20.6. doi: 10.1002/0471140856.tx2006s47

Angrisano, T., Pero, R., Peluso, S., Keller, S., Sacchetti, S., Bruni, C. B., et al. (2010). LPS-induced IL-8 activation in human intestinal epithelial cells is accompanied by specific histone H3 acetylation and methylation changes. *BMC Microbiol.* 10:172. doi: 10.1186/1471-2180-10-172

Angyal, S. J. (1989). "Complexes of metal cations with carbohydrates in solution," in *Advances in Carbohydrate Chemistry and Biochemistry*, eds R. S. Tipson and D. Horton (Cambridge, MA: Academic Press), 1–43. doi: 10.1016/S0065-2318(08)60411-4

Bachtarzi, N., Speciale, I., Kharroub, K., De Castro, C., Ruiz, L., and Ruas-Madiedo, P. (2020). Selection of exopolysaccharide-producing *Lactobacillus Plantarum* (*Lactiplantibacillus Plantarum*) isolated from algerian fermented foods for the manufacture of skim-milk fermented products. *Microorganisms* 8:E1101. doi: 10.3390/microorganisms8081101

Baggiolini, M., and Clark-Lewis, I. (1992). Interleukin-8, a chemotactic and inflammatory cytokine. *FEBS Lett.* 307, 97–101. doi: 10.1016/0014-5793(92)80909-z

Bajić, S. S., Đokić, J., Dinić, M., Tomić, S., Popović, N., Brdarić, E., et al. (2020b). GABA potentiate the immunoregulatory effects of *Lactobacillus brevis* BGZLS10-17 via ATG5-dependent autophagy in vitro. *Sci. Rep.* 10:1347. doi: 10.1038/s41598-020-58177-2

Bajic, S. S., Cañas, M.-A., Tolinacki, M., Badia, J., Sánchez, B., Golic, N., et al. (2020a). Proteomic profile of extracellular vesicles released by *Lactiplantibacillus plantarum* BGAN8 and their internalization by non-polarized HT29 cell line. *Sci. Rep.* 10:21829. doi: 10.1038/s41598-020-78920-z

Blais, A., Lecoeur, S., Milhaud, G., Tomé, D., and Kolf-Clauw, M. (1999). Cadmium uptake and transepithelial transport in control and long-term exposed Caco-2 cells: the role of metallothionein. *Toxicol. Appl. Pharmacol.* 160, 76–85. doi: 10.1006/taap.1999.8735

Blanusa, M., Mrković-Milić, R., and Durbesić, P. (2002). Lead and cadmium in soil and Isopoda woodlice in Croatia. *Ecotoxicol. Environ. Saf.* 52, 198–202. doi: 10.1006/eesa.2002.2173

International Programme On Chemical Safety, (1992). *Cadmium – Environmental Aspects (EHC 135, 1992)*. Available online at: http://www.inchem.org/documents/ehc/ehc/ehc135.htm [Accessed May 24, 2021].

Caggianiello, G., Kleerebezem, M., and Spano, G. (2016). Exopolysaccharides produced by lactic acid bacteria: from health-promoting benefits to stress tolerance mechanisms. *Appl. Microbiol. Biotechnol.* 100, 3877–3886. doi: 10.1007/s00253-016-7471-2

Canada, A. T., and Calabrese, E. J. (1989). Superoxide dismutase: its role in xenobiotic detoxification. *Pharmacol. Ther.* 44, 285–295. doi: 10.1016/0163-7258(89)90068-5

Cerning, J., Renard, C. M., Thibault, J. F., Bouillanne, C., Landon, M., Desmazeaud, M., et al. (1994). Carbon source requirements for exopolysaccharide production

by lactobacillus casei cg11 and partial structure analysis of the polymer. *Appl. Environ. Microbiol.* 60, 3914–3919. doi: 10.1128/aem.60.11.3914-3919.1994

Coates, J. (2006). "Interpretation of infrared spectra, a practical approach," in *Encyclopedia of Analytical Chemistry*, eds R. A. Meyers and M. L. McKelvy (Atlanta, GA: American Cancer Society), doi: 10.1002/9780470027318.a5606

Corbrjdge, D. (2007). Infrared analysis of phosphorous compounds. *J. Appl. Chem.* 6, 456–465. doi: 10.1002/jctb.5010061007

Damek-Poprawa, M., and Sawicka-Kapusta, K. (2004). Histopathological changes in the liver, kidneys, and testes of bank voles environmentally exposed to heavy metal emissions from the steelworks and zinc smelter in Poland. *Environ. Res.* 96, 72–78. doi: 10.1016/j.envres.2004.02.003

De Vuyst, L., and Degeest, B. (1999). Heteropolysaccharides from lactic acid bacteria. *FEMS Microbiol. Rev.* 23, 153–177. doi: 10.1111/j.1574-6976.1999.tb00395.x

Dinić, M., Pecikoza, U., Djokić, J., Stepanović-Petrović, R., Milenković, M., Stevanović, M., et al. (2018). Exopolysaccharide produced by probiotic strain *Lactobacillus paraplantarum* BGCG11 reduces inflammatory hyperalgesia in rats. *Front. Pharmacol.* 9:1. doi: 10.3389/fphar.2018.00001

Elamin, E., Jonkers, D., Juuti-Uusitalo, K., van Ijzendoorn, S., Troost, F., Duimel, H., et al. (2012). Effects of ethanol and acetaldehyde on tight junction integrity: in vitro study in a three dimensional intestinal epithelial cell culture model. *PLoS One* 7:e35008. doi: 10.1371/journal.pone.0035008

Freudenberger, T., Deenen, R., Kretschmer, I., Zimmermann, A., Seiler, L. F., Mayer, P., et al. (2014). Synthetic gestagens exert differential effects on arterial thrombosis and aortic gene expression in ovariectomized apolipoprotein E-deficient mice. *Br. J. Pharmacol.* 171, 5032–5048. doi: 10.1111/bph.12814

Gadd, G. M., and White, C. (1989). Uptake and intracellular compartmentation of thorium in *Saccharomyces cerevisiae*. *Environ Pollut* 61, 187–197. doi: 10.1016/0269-7491(89)90240-6

Gao, K., Wang, C., Liu, L., Dou, X., Liu, J., Yuan, L., et al. (2017). Immunomodulation and signaling mechanism of *Lactobacillus rhamnosus* GG and its components on porcine intestinal epithelial cells stimulated by lipopolysaccharide. *J. Microbiol. Immunol. Infect.* 50, 700–713. doi: 10.1016/j.jmii.2015.05.002

Genchi, G., Sinicropi, M. S., Lauria, G., Carocci, A., and Catalano, A. (2020). The effects of cadmium toxicity. *Int. J. Environ. Res. Public Health* 17:3782. doi: 10.3390/ijerph17113782

Goon, D., and Klaassen, C. D. (1989). Dosage-dependent absorption of cadmium in the rat intestine measured in situ. *Toxicol. Appl. Pharmacol.* 100, 41–50. doi: 10.1016/0041-008x(89)90090-2

Günzel, D., and Fromm, M. (2012). Claudins and other tight junction proteins. *Compr. Physiol.* 2, 1819–1852. doi: 10.1002/cphy.c110045

Halttunen, T., Collado, M. C., El-Nezami, H., Meriluoto, J., and Salminen, S. (2008). Combining strains of lactic acid bacteria may reduce their toxin and heavy metal removal efficiency from aqueous solution. *Lett. Appl. Microbiol.* 46, 160–165. doi: 10.1111/j.1472-765X.2007.02276.x

Hassan, S. H. A., Kim, S.-J., Jung, A.-Y., Joo, J. H., Eun Oh, S., and Yang, J. E. (2009). Biosorptive capacity of Cd(II) and Cu(II) by lyophilized cells of *Pseudomonas* stutzeri. *J. Gen. Appl. Microbiol.* 55, 27–34. doi: 10.2323/jgam.55.27

He, L., He, T., Farrar, S., Ji, L., Liu, T., and Ma, X. (2017). Antioxidants maintain cellular redox homeostasis by elimination of reactive oxygen species. *Cell Physiol. Biochem.* 44, 532–553. doi: 10.1159/000485089

Hu, X., Wang, C., and Ai, L. (2017). Polysaccharides: structure and Solubility. *Solubility Polysacch* 2017, 7–21. doi: 10.5772/intechopen.71570

Huang, Y., Hu, Y., and Liu, Y. (2009). Heavy metal accumulation in iron plaque and growth of rice plants upon exposure to single and combined contamination by copper, cadmium and lead. *Acta Ecol. Sin.* 29, 320–326. doi: 10.1016/j.chnaes.2009.09.011

Hyun, J. S., Satsu, H., and Shimizu, M. (2007). Cadmium induces interleukin-8 production via NF-kappaB activation in the human intestinal epithelial cell, Caco-2. *Cytokine* 37, 26–34. doi: 10.1016/j.cyto.2007.02.011

IARC Monographs on the Evaluation of Carcinogenic Risks to Humans (1993). *Beryllium, Cadmium, Mercury, and Exposures in the Glass Manufacturing Industry*. Lyon, FR: International Agency for Research on Cancer.

Ismail, B., and Nampoothiri, K. M. (2010). Production, purification and structural characterization of an exopolysaccharide produced by a probiotic *Lactobacillus plantarum* MTCC 9510. *Arch. Microbiol.* 192, 1049–1057. doi: 10.1007/s00203-010-0636-y

Jones, S., Paynich, M. L., and Knight, K. (2014). *Exopolysaccharides: Sweet Success With Probiotic Therapeutics*. Available online at: /paper/Exopolysaccharides%3A-Sweet-success-with-probiotic-Jones-Paynich/40da44f5a9698e28fcc3ec20a9b6984501eaf6f4 [Accessed May 24, 2021].

Kanmani, P., Satish kumar, R., Yuvaraj, N., Paari, K. A., Pattukumar, V., and Arul, V. (2011). Production and purification of a novel exopolysaccharide from lactic acid bacterium *Streptococcus phocae* PI80 and its functional characteristics activity in vitro. *Bioresour. Technol.* 102, 4827–4833. doi: 10.1016/j.biortech.2010.12.118

Knoshaug, E. P., Ahlgren, J. A., and Trempy, J. E. (2000). Growth associated exopolysaccharide expression in *Lactococcus lactis* subspecies cremoris Ropy352. *J. Dairy Sci.* 83, 633–640. doi: 10.3168/jds.S0022-0302(00)74923-X

Konstantinov, S. R., Kuipers, E. J., and Peppelenbosch, M. P. (2013). Functional genomic analyses of the gut microbiota for CRC screening. *Nat. Rev. Gastroenterol. Hepatol.* 10, 741–745. doi: 10.1038/nrgastro.2013.178

Laine, R. A., Esselman, W. J., and Sweeley, C. C. (1972). Gas-liquid chromatography of carbohydrates. *Methods Enzymol.* 28, 159–167. doi: 10.1016/0076-6879(72)28012-0

Liu, F., Liu, X., Ding, C., and Wu, L. (2015). The dynamic simulation of rice growth parameters under cadmium stress with the assimilation of multi-period spectral indices and crop model. *Field Crops Res.* 183, 225–234. doi: 10.1016/j.fcr.2015.08.004

Liu, H., and Fang, H. H. P. (2002). Characterization of electrostatic binding sites of extracellular polymers by linear programming analysis of titration data. *Biotechnol. Bioeng.* 80, 806–811. doi: 10.1002/bit.10432

Liu, Z., Dong, L., Jia, K., Zhan, H., Zhang, Z., Shah, N. P., et al. (2019). Sulfonation of *Lactobacillus plantarum* WLPL04 exopolysaccharide amplifies its antioxidant activities in vitro and in a Caco-2 cell model. *J. Dairy Sci.* 102, 5922–5932. doi: 10.3168/jds.2018-15831

Mitchell, S., Vargas, J., and Hoffmann, A. (2016). Signaling via the NFκB system. *Wiley Interdiscip. Rev. Syst. Biol. Med.* 8, 227–241. doi: 10.1002/wsbm.1331

Moppert, X., Le Costaouec, T., Raguenes, G., Courtois, A., Simon-Colin, C., Crassous, P., et al. (2009). Investigations into the uptake of copper, iron and selenium by a highly sulphated bacterial exopolysaccharide isolated from microbial mats. *J. Ind. Microbiol. Biotechnol.* 36, 599–604. doi: 10.1007/s10295-009-0529-8

Morillo Pérez, J. A., García-Ribera, R., Quesada, T., Aguilera, M., Ramos-Cormenzana, A., and Monteoliva-Sánchez, M. (2008). Biosorption of heavy metals by the exopolysaccharide produced by *Paenibacillus jamilae*. *World J. Microbiol. Biotechnol.* 24, 2699–2704. doi: 10.1007/s11274-008-9800-9

Mrvcic, J., Stanzer, D., Bacun-Druzina, V., and Stehlik-Tomas, V. (2009). Copper binding by lactic acid bacteria (LAB). *Biosci. Microflora* 28, 1–6. doi: 10.12938/bifidus.28.1

Mrvčić, J., Stanzer, D., Solić, E., and Stehlik-Tomas, V. (2012). Interaction of lactic acid bacteria with metal ions: opportunities for improving food safety and quality. *World J. Microbiol. Biotechnol.* 28, 2771–2782. doi: 10.1007/s11274-012-1094-2

Nawrot, T. S., Staessen, J. A., Roels, H. A., Munters, E., Cuypers, A., Richart, T., et al. (2010). Cadmium exposure in the population: from health risks to strategies of prevention. *Biometals* 23, 769–782. doi: 10.1007/s10534-010-9343-z

Nikolic, M., López, P., Strahinic, I., Suárez, A., Kojic, M., Fernández-García, M., et al. (2012). Characterisation of the exopolysaccharide (EPS)-producing *Lactobacillus paraplantarum* BGCG11 and its non-EPS producing derivative strains as potential probiotics. *Int. J. Food Microbiol.* 158, 155–162. doi: 10.1016/j.ijfoodmicro.2012.07.015

Nikonenko, N. A., Buslov, D. K., Sushko, N. I., and Zhbankov, R. G. (2000). Investigation of stretching vibrations of glycosidic linkages in disaccharides and polysaccharides with use of IR spectra deconvolution. *Biopolymers* 57, 257–262.

Ninkov, M., Popov Aleksandrov, A., Demenesku, J., Mirkov, I., Mileusnic, D., Petrovic, A., et al. (2015). Toxicity of oral cadmium intake: impact on gut immunity. *Toxicol. Lett.* 237, 89–99. doi: 10.1016/j.toxlet.2015.06.002

Pal, A., and Paul, A. K. (2008). Microbial extracellular polymeric substances: central elements in heavy metal bioremediation. *Indian J. Microbiol.* 48, 49–64. doi: 10.1007/s12088-008-0006-5

Patel, R. M., and Denning, P. W. (2013). Therapeutic use of prebiotics, probiotics, and postbiotics to prevent necrotizing enterocolitis: what is the current evidence? *Clin. Perinatol.* 40, 11–25. doi: 10.1016/j.clp.2012.12.002

Pey, A. L., Megarity, C. F., and Timson, D. J. (2019). NAD(P)H quinone oxidoreductase (NQO1): an enzyme which needs just enough mobility, in just the right places. *Biosci. Rep.* 39:BSR20180459. doi: 10.1042/BSR20180459

Polak-Berecka, M., Szwajgier, D., and Waśko, A. (2014). Biosorption of Al(+3) and Cd(+2) by an exopolysaccharide from *Lactobacillus rhamnosus*. *J. Food Sci.* 79, T2404–T2408. doi: 10.1111/1750-3841.12674

Popović, N., Brdarić, E., Đokić, J., Dinić, M., Veljović, K., Golić, N., et al. (2020). Yogurt produced by novel natural starter cultures improves gut epithelial barrier in vitro. *Microorganisms* 8:1586. doi: 10.3390/microorganisms8101586

Popović, N., Djokić, J., Brdarić, E., Dinić, M., Terzić-Vidojević, A., Golić, N., et al. (2019). The Influence of heat-killed *Enterococcus faecium* BGPAS1-3 on the tight junction protein expression and immune function in differentiated Caco-2 cells infected with *Listeria monocytogenes* ATCC 19111. *Front. Microbiol.* 10:412. doi: 10.3389/fmicb.2019.00412

Prozialeck, W. C. (2000). Evidence that E-cadherin may be a target for cadmium toxicity in epithelial cells. *Toxicol. Appl. Pharmacol.* 164, 231–249. doi: 10.1006/taap.2000.8905

Ruan, C., Huang, H., and Rodgers, M. T. (2008). A simple model for metal cation-phosphate interactions in nucleic acids in the gas phase: alkali metal cations and trimethyl phosphate. *J. Am. Soc. Mass Spectrom.* 19, 305–314. doi: 10.1016/j.jasms.2007.10.006

Ruas-Madiedo, P., Gueimonde, M., Margolles, A., de los Reyes-Gavilán, C. G., and Salminen, S. (2006). Exopolysaccharides produced by probiotic strains modify the adhesion of probiotics and enteropathogens to human intestinal mucus. *J. Food Prot.* 69, 2011–2015. doi: 10.4315/0362-028x-69.8.2011

Rusanov, A. L., Smirnova, A. V., Poromov, A. A., Fomicheva, K. A., Luzgina, N. G., and Majouga, A. G. (2015). Effects of cadmium chloride on the functional state of human intestinal cells. *Toxicol. Vitro* 29, 1006–1011. doi: 10.1016/j.tiv.2015.03.018

Salminen, S., Collado, M. C., Endo, A., Hill, C., Lebeer, S., Quigley, E. M. M., et al. (2021). The international scientific association of probiotics and prebiotics (ISAPP) consensus statement on the definition and scope of postbiotics. *Nat. Rev. Gastroenterol. Hepatol.* 18, 649–667. doi: 10.1038/s41575-021-00440-6

Sánchez, J.-I., Martínez, B., Guillén, R., Jiménez-Díaz, R., and Rodríguez, A. (2006). Culture conditions determine the balance between two different exopolysaccharides produced by *Lactobacillus pentosus* LPS26. *Appl. Environ. Microbiol.* 72, 7495–7502. doi: 10.1128/AEM.01078-06

Satarug, S., Garrett, S. H., Sens, M. A., and Sens, D. A. (2010). Cadmium, environmental exposure, and health outcomes. *Environ. Health Perspect.* 118, 182–190. doi: 10.1289/ehp.0901234

Shen, J.-W., Shi, C.-W., and Xu, C. (2013). Exopolysaccharides from *Pleurotus pulmonarius*: fermentation optimization, characterization and antioxidant activity. *Food Technol. Biotechnol.* 51, 520–527.

Sokovic Bajic, S., Djokic, J., Dinic, M., Veljovic, K., Golic, N., Mihajlovic, S., et al. (2019). GABA-producing natural dairy isolate from artisanal zlatar cheese attenuates gut inflammation and strengthens gut epithelial barrier in vitro. '. *Microbiol.* 10:527. doi: 10.3389/fmicb.2019.00527

Stadnyk, A. W. (1994). Cytokine production by epithelial cells. *FASEB J.* 8, 1041–1047. doi: 10.1096/fasebj.8.13.7926369

Tallon, R., Bressollier, P., and Urdaci, M. C. (2003). Isolation and characterization of two exopolysaccharides produced by *Lactobacillus plantarum* EP56. *Res. Microbiol.* 154, 705–712. doi: 10.1016/j.resmic.2003.09.006

Tinkov, A. A., Gritsenko, V. A., Skalnaya, M. G., Cherkasov, S. V., Aaseth, J., and Skalny, A. V. (2018). Gut as a target for cadmium toxicity. *Environ. Pollut.* 235, 429–434. doi: 10.1016/j.envpol.2017.12.114

Tsilingiri, K., and Rescigno, M. (2013). Postbiotics: what else? *Benef. Microbes* 4, 101–107. doi: 10.3920/BM2012.0046

Tsilingiri, K., Barbosa, T., Penna, G., Caprioli, F., Sonzogni, A., Viale, G., et al. (2012). Probiotic and postbiotic activity in health and disease: comparison on a novel polarised ex-vivo organ culture model. *Gut* 61, 1007–1015. doi: 10.1136/gutjnl-2011-300971

Turner, J. R. (2009). Intestinal mucosal barrier function in health and disease. *Nat. Rev. Immunol.* 9, 799–809. doi: 10.1038/nri2653

Verhoef, R., Schols, H. A., Blanco, A., Siika-aho, M., Rättö, M., Buchert, J., et al. (2005). Sugar composition and FT-IR analysis of exopolysaccharides produced by microbial isolates from paper mill slime deposits. *Biotechnol. Bioeng.* 91, 91–105. doi: 10.1002/bit.20494

Wang, Y., Branicky, R., Noë, A., and Hekimi, S. (2018). Superoxide dismutases: dual roles in controlling ROS damage and regulating ROS signaling. *J. Cell Biol.* 217, 1915–1928. doi: 10.1083/jcb.201708007

Wegh, C. A. M., Geerlings, S. Y., Knol, J., Roeselers, G., and Belzer, C. (2019). Postbiotics and their potential applications in early life nutrition and beyond. *Int. J. Mol. Sci.* 20:E4673. doi: 10.3390/ijms20194673

Wu, G. D., Lai, E. J., Huang, N., and Wen, X. (1997). Oct-1 and CCAAT/enhancer-binding protein (C/EBP) bind to overlapping elements within the interleukin-8 promoter. The role of Oct-1 as a transcriptional repressor. *J. Biol. Chem.* 272, 2396–2403.

Yamaura, Y., Chapron, B. D., Wang, Z., Himmelfarb, J., and Thummel, K. E. (2016). Functional comparison of human colonic carcinoma cell lines and primary small intestinal epithelial cells for investigations of intestinal drug permeability and first-pass metabolism. *Drug Metab. Dispos.* 44, 329–335. doi: 10.1124/dmd.115.068429

Yee, S. (1997). In vitro permeability across Caco-2 cells (colonic) can predict in vivo (small intestinal) absorption in man–fact or myth. *Pharm. Res.* 14, 763–766. doi: 10.1023/a:1012102522787

Yi, Y.-J., Lim, J.-M., Gu, S., Lee, W.-K., Oh, E., Lee, S.-M., et al. (2017). Potential use of lactic acid bacteria *Leuconostoc mesenteroides* as a probiotic for the removal of Pb(II) toxicity. *J. Microbiol.* 55, 296–303. doi: 10.1007/s12275-017-6642-x

Zhai, Q., Tian, F., Zhao, J., Zhang, H., Narbad, A., and Chen, W. (2016). Oral administration of probiotics inhibits absorption of the heavy metal cadmium by protecting the intestinal barrier. *Appl. Environ. Microbiol.* 82, 4429–4440. doi: 10.1128/AEM.00695-16

Zhai, Q., Wang, G., Zhao, J., Liu, X., Tian, F., Zhang, H., et al. (2013). Protective effects of Lactobacillus plantarum CCFM8610 against acute cadmium toxicity in mice. *Appl. Environ. Microbiol.* 79, 1508–1515. doi: 10.1128/AEM.03417-12

Zhao, Z., Hyun, J. S., Satsu, H., Kakuta, S., and Shimizu, M. (2006). Oral exposure to cadmium chloride triggers an acute inflammatory response in the intestines of mice, initiated by the over-expression of tissue macrophage inflammatory protein-2 mRNA. *Toxicol. Lett.* 164, 144–154. doi: 10.1016/j.toxlet.2005.12.004

Zhou, X., Qi, W., Hong, T., Xiong, T., Gong, D., Xie, M., et al. (2018). Exopolysaccharides from *Lactobacillus plantarum* NCU116 regulate intestinal barrier function via STAT3 signaling pathway. *J. Agric. Food Chem.* 66, 9719–9727. doi: 10.1021/acs.jafc.8b03340

Conflict of Interest: The authors declare that the research was conducted in the absence of any commercial or financial relationships that could be construed as a potential conflict of interest.

Publisher's Note: All claims expressed in this article are solely those of the authors and do not necessarily represent those of their affiliated organizations, or those of the publisher, the editors and the reviewers. Any product that may be evaluated in this article, or claim that may be made by its manufacturer, is not guaranteed or endorsed by the publisher.

frontiers in Microbiology

ORIGINAL RESEARCH
published: 14 December 2021
doi: 10.3389/fmicb.2021.799173

Probiotic Potential Analysis and Safety Evaluation of *Enterococcus durans* A8-1 Isolated From a Healthy Chinese Infant

Yi Zhou[1†], Lu Shi[1†], Juan Wang[1], Jia Yuan[1], Jin Liu[1], Lijuan Liu[1], Rong Da[2], Yue Cheng[1] and Bei Han[1,3*]*

[1] School of Public Health, Health Science Center, Xi'an Jiaotong University, Xi'an, China, [2] Department of Clinical Laboratory, The First Affiliated Hospital of Xi'an Jiaotong University, Xi'an, China, [3] Key Laboratory for Disease Prevention and Control and Health Promotion of Shaanxi Province, Xi'an, China

OPEN ACCESS

Edited by:
Irma Schabussova, Medical University Vienna, Austria

Reviewed by:
Abdelazeem Algammal, Suez Canal University, Egypt
Yousef Nami, Agricultural Biotechnology Research Institute of Iran, Iran

***Correspondence:**
Yue Cheng
chengy@mail.xjtu.edu.cn
Bei Han
hanbei@mail.xjtu.edu.cn

[†] These authors have contributed equally to this work

Specialty section:
This article was submitted to Food Microbiology, a section of the journal Frontiers in Microbiology

Received: *21 October 2021*
Accepted: *11 November 2021*
Published: *14 December 2021*

Citation:
Zhou Y, Shi L, Wang J, Yuan J, Liu J, Liu L, Da R, Cheng Y and Han B (2021) Probiotic Potential Analysis and Safety Evaluation of Enterococcus durans A8-1 Isolated From a Healthy Chinese Infant. Front. Microbiol. 12:799173. doi: 10.3389/fmicb.2021.799173

To evaluate the probiotic characteristics and safety of *Enterococcus durans* isolate A8-1 from a fecal sample of a healthy Chinese infant, we determined the tolerance to low pH, survival in bile salts and NaCl, adhesion ability, biofilm formation, antimicrobial activity, toxin gene distribution, hemolysis, gelatinase activity, antibiotic resistance, and virulence to *Galleria mellonella* and interpreted the characters by genome resequencing. Phenotypically, *E. durans* A8-1 survived at pH 5.0 in 7.0% NaCl and 3% bile salt under aerobic and anaerobic condition. The bacterium had higher adhesion ability toward mucin, collagen, and Bovine Serum Albumin (BSA) *in vitro* and showed high hydrophobicity (79.2% in chloroform, 49.2% in xylene), auto-aggregation activity (51.7%), and could co-aggregate (66.2%) with *Salmonella typhimurium*. It had adhesion capability to intestinal epithelial Caco-2 cells (38.74%) with moderate biofilm production and antimicrobial activity against several Gram-positive pathogenic bacteria. A8-1 can antagonize the adhesion of *S. typhimurium* ATCC14028 on Caco-2 cells to protect the integrity of the cell membrane by detection of lactate dehydrogenase (LDH) and AKP activities. A8-1 also helps the cell relieve the inflammation induced by lipopolysaccharide by reducing the expression of cytokine IL-8 ($P = 0.002$) and TNF-α ($P > 0.05$), and increasing the IL-10 ($P < 0.001$). For the safety evaluation, A8-1 showed no hemolytic activity, no gelatinase activity, and had only *asa1* positive in the seven detected virulence genes in polymerase chain reaction (PCR), whereas it was not predicted in the genome sequence. It was susceptible to benzylpenicillin, ampicillin, ciprofloxacin, levofloxacin, moxifloxacin, tigecycline, nitrofurantoin, linezolid, vancomycin, erythromycin, and quinupristin/dalofopine except clindamycin, which was verified by the predicted *lasA*, *lmrB*, *lmrC*, and *lmrD* genes contributing to the clindamycin resistance. The virulence test of *G. mellonella* showed that it had toxicity lower than 10% at 1×10^7 CFU. According to the results of these evaluated attributes, *E. durans* strain A8-1 could be a promising probiotic candidate for applications.

Keywords: *Enterococcus durans*, stress tolerance, probiotic characters, safety evaluation, whole-genome sequencing

INTRODUCTION

Gut microbiota contributes a lot to human health and the occurrence of diseases. It is called the "invisible endocrine organ," which is the place where the body digests food and absorbs nutrients (Scarpellini et al., 2010). *Enterococcus*, as one of the indigenous bacteria in the intestine, belongs to the class of facultative anaerobic lactic acid bacteria (LAB). *Enterococcus* spp. is distributed widely and can be separated from the environment, food, and human and animal gastrointestinal tract and has strong resistance to harsh stress and can survive at different conditions (Starke et al., 2015; Cirrincione et al., 2019).

Probiotics are defined as "live microorganisms which consumes in sufficient amounts, affect beneficially the health of the host [*sic*]." Enterococci have biological properties of probiotics; some strains usually show high resistance to acids and bile salts (Gu et al., 2008), antioxidant and free radical scavenging activity, improve host immunity by intestinal adhesion and localization (Starke et al., 2015; Li et al., 2018), and enhance apoptosis of human cancer cells (Nami et al., 2014); at the same time, some strains have antibacterial activity and anti-inflammatory effects (Popović et al., 2019). With the continuous discovery and exploration of the probiotic characteristics of *Enterococcus*, many strains have proven to be effective and safe and developed into applications, such as the commercial microecological probiotics in human (Medilac-Vita®, live *Bacillus subtilis* and *Enterococcus faecium*) and veterinary medicine (Bonvital®, *E. faecium* DSM 7134) (Li et al., 2020), and the food industry (Cernivet®, *E. faecium* SF68®; Symbioflor®, *E. faecalis*) (Strompfová et al., 2004).

At the same time, *Enterococcus* has both probiotic character and potential pathogenicity, and some strains can cause important infections and diseases, such as endocarditis; bacteremia; and urinary, intra-abdominal, pelvic infections, and central nervous system infections (O'Driscoll and Crank, 2015). It is generally known that antibiotic resistance and virulence are the main factors for *enterococci* pathogenicity. The main concern for the safety evaluation of *enterococci* is focused on the potential infectivity and transferable drug-resistant genes (Yang et al., 2015). Pathogenic enterococci may cause concerns about the safety using of probiotics, so to screen the potential probiotic enterococci, assessing and evaluating the safety is necessary and a priority.

Enterococcus is one of the most controversial LAB (Martino et al., 2018). The development of new enterococcal probiotics needs a strict assessment with regard to safety aspects for selecting the truly harmless strains for safe applications. The potential probiotic enterococci isolates can be applied to biotechnology development, and a broader application can be obtained by strain improvement. The aim of this study was to evaluate the probiotic characteristics and safety of *E. durans* A8-1 isolated from a fecal sample of a healthy Chinese infant and its potential in future probiotic development and application.

MATERIALS AND METHODS

Bacterial Strains and Cell Culture

Enterococcus durans A8-1 were isolated from a fecal sample by the microbiology lab of the Nutrition and Food Safety Engineering Research Center of Shaanxi province, Xi'an, China. Fecal samples were taken from a healthy infant born 1–7 days earlier at the Maternal and Child Health Hospital of Bin County of Shaanxi province, China. There was no history of being treated with antibiotics after birth. The fecal sample was collected after the informed consent form was signed by the guardian. This study was reviewed and approved by the ethics committee of the Health Science Center, Xi'an Jiaotong University, Xi'an, China (No. 2016114).

Enterococcus durans A8-1, *Enterococcus faecalis* ATCC29212, *Lactobacillus rhamnosus* GG BL379, and *Bifidobacterium infantis* CICC6069 were inoculated into de Man, Rogosa and Sharpe (MRS) medium (CM187, Beijing Land Bridge Technology Co., Ltd., Beijing, China) and incubated aerobically with constant temperature shaker at 37°C for 18–24 h. About the streak-plating growth, A8-1 and BL379 were cultured on MRS agar using MRS broth with 15 g/L agar for 18 h. For the anaerobic culture, the bacterial cells were inoculated on the same medium and incubated in an anaerobic chamber (Coy Laboratory Products Inc., Ann Arbor, MI, United States) with a modified atmosphere of 82% N_2, 15% CO_2, and 3% H_2 without shaking. For the growth of *Staphylococcus aureus* ATCC25923, *Pseudomonas aeruginosa* PA01, *P. aeruginosa* ATCC27853, *Enterococcus hormaechei* ATCC700323, *Salmonella typhimurium* ATCC14028, and *Escherichia coli* ATCC35218, nutrient broth was used (CP142, Beijing Land Bridge Technology Co., Ltd., Beijing, China).

Caco-2 cells were cultured in Dulbecco's modified Eagle's minimal essential medium (DMEM, Hyclone) supplemented with 10% fetal bovine serum (FBS, Hyclone) without antibody. The cells were kept at 37°C in an atmosphere containing 5% CO_2.

Isolation and Identification of A8-1

One gram of stool sample was mixed with 0.9% sterile saline solution to a final volume of 10 mL, and 0.1 mL of this dilution was spread on the MRS agar plate (MRS broth with 15 g/L agar) and cultured anaerobically at 37°C for 48 h. After incubation, colonies were randomly selected from each sample and subcultured on MRS plates for further analysis. Single colonies were picked out for Gram staining and microscopic observation and catalase, oxidase production, and nitrate reduction tests (Mansour et al., 2014).

For further confirmation, the 16S rRNA gene sequence (1.4 kb) was amplified, and sequenced by Sangon Biotech (Shanghai, China) Co., Ltd. Primers used were 16S-27F: 5′ AGA GTT TGA TCC TGG CTC AG 3′, 16S-1492R: 5′ GGT ACC TTG TTA CGA CTT 3′. The polymerase chain reaction (PCR) amplification conditions were as follows: initial denaturation for 5 min at 94°C, 35 cycles of denaturation for 30 s at 94°C, annealing at 60°C for 30 s, extension at 72°C for 60 s, and a final elongation step of 5 min at 72°C. Multiple alignments with

sequences of closest similarity were analyzed using CLUSTAL W, and a phylogenetic tree was constructed by using the neighbor-joining method.

Acid, NaCl, and Bile Salt Tolerance

A8-1 was inoculated into MRS broth at 37°C overnight in an aerobic incubator and anaerobic chamber separately. The overnight culture was centrifuged, and the collected cells were washed twice by sterile phosphate buffered solution (PBS) and resuspended in OD_{600} = 0.1 at fresh MRS with different pH 3.0, 4.0, and 5.0; bile salts (0.5, 1, 2, and 3%) and NaCl (1.75, 3.5, and 7%). The negative control was MRS blank medium at pH 6.5. Three replicates were set for each medium. Growth was monitored by optical density at 600 nm every 30 min at 37°C for 21 h in a microtiter plate reader (PolarStar, BMG Labtech, Germany) (Banwo et al., 2013; Li et al., 2020). Maximal growth, the lag phase duration, and the increment in OD values were considered by using the Gompertz growth analysis mode of non-linear regression in GraphPad Prism 7 (Wang et al., 2020).

Antibacterial Ability

The minimum inhibitory concentration (MIC) method was used to determine the antibacterial activity of A8-1. The indicator bacteria were as follows: *E. faecalis* ATCC29212, *S. aureus* ATCC25923, *P. aeruginosa* PA01, *P. aeruginosa* ATCC27853, *E. hormaechei* ATCC700323, *S. typhimurium* ATCC14028, and *E. coli* ATCC35218. A8-1 was inoculated into MRS broth and incubated at 37°C for 24 h. The cells were removed by centrifugation at 9,710 × *g* for 2 min at 4°C. The supernatants were filter sterilized and added to 96-well plates at 0, 25, 50, 100, 150, and 200 μL, made up to 200 μL with fresh medium. Finally, each test indicator bacteria was added to the well at the concentration of OD_{600} = 0.1. Growth of test indicator bacteria was monitored every 30 min by optical density at 600 nm with an automatic microplate reader for 12 h at 37°C (Wang et al., 2020).

In vitro Hydrophobicity, Auto-Aggregation, and Co-aggregation

The hydrophobicity, auto-aggregation, and co-aggregation assays were performed according to Fonseca et al. (2021). The cell surface hydrophobicity of each strain was assessed by measuring microbial affinity to xylene and chloroform. The A8-1 was incubated overnight and washed in PBS twice, and then resuspended in PBS with OD_{600} of 0.8 (A0). Then, 1 mL xylene and 1 mL chloroform were added separately to 3 mL of A8-1 cell suspension and mixed thoroughly. Then, the water and xylene phases were separated for 30 min at room temperature. The aqueous phase was removed, and the new OD_{600} was measured (A1). The cell surface hydrophobicity (%) was calculated using the following formula: Hydrophobicity (%) = [(A0−A1)/A0] × 100%. The strain was classified into low (0–29%), moderate (30–59%), and high hydrophobicity (60–100%).

For auto-aggregation, A8-1 was incubated overnight and washed in PBS twice and then resuspended in PBS with OD_{600} about 0.6 (A0). Bacterial cell suspensions were vortexed for 10 s and subsequently incubated at room temperature for 5 h, and the new OD_{600} was measured (At). The auto-aggregation percentage was determined using the following equation:

$$\text{Auto} - \text{aggregation}\ (\%) = (1 - \text{At}/\text{A0}) \times 100\%.$$

For co-aggregation, *E. durans* A8-1 and *S. typhimurium* ATCC14028 were incubated overnight separately and washed in PBS twice and then resuspended in PBS with OD_{600} about 0.8. Equal volumes (2 mL) of A8-1 and *S. typhimurium* ATCC14028 were mixed and incubated at room temperature without agitation for 5 h. Control tubes contained 2 mL of the suspension of each bacterial cells. The OD_{600} of the mixtures and controls were measured after incubation. The percentage of co-aggregation was calculated using the following formula: Co−aggregation (%) = [(Ax + Ay)/2−A(x + y)]/(Ax + Ay) × 100%, where Ax and Ay refer to the OD_{600} of the A8-1 and *S. typhimurium* ATCC14028 cell suspension, respectively, Ax + y represents the absorbance of the mixed bacterial suspension tested after 5 h.

In vitro Binding to Bovine Serum Albumi, Mucin, and Collagen

Strain binding to different substrates was evaluated as reported previously (Muñoz-Provencio et al., 2009; Wang et al., 2020). Mucin (500 μg/mL, porcine stomach, Sigma-Aldrich, St. Louis, MO, United States), Bovine Serum Albumi (BSA) (500 μg/mL, Sigma-Aldrich, St. Louis, MO, United States), and collagen (50 μg/mL, type I, Roche, Mannheim, Germany) were added separately to the 96-well microplates and incubated overnight at 4°C. Then, wells were washed three times with PBS and dried at room temperature. Two milliliters of A8-1 were labeled by 20 μL cFDA [5-(6-)-carboxyfluorescein diacetate, Sigma Aldrich, St. Louis, MO, United States] to the plate wells. After mixing, the cells were incubated at room temperature for 1 h and kept away from light. The strain labeled by cFDA was added to the plate wells and separately incubated with immobilization at 4°C overnight and kept away from light. After incubation, each well was washed three times by PBS and dried at room temperature. The 100 μL cFDA-labeled A8-1 cells were added into wells with no immobilization and set as control. Fluorescence intensity of the well plate was measured by a microplate reader, and the adhesion rate of A8-1 cells to mucin, collagen, and BSA was calculated according to the following formula. *L. rhamnosus* GG BL379 was used as a positive control; its adhesion rate was set as 100%, and the relative adhesion of A8-1 cell to BL379 was calculated.

Adhesion (%) = (fluorescence intensity of A8-1)/(the free cFDA-labeled BL379) × 100.

Adhesion Ability to Caco-2 Cells

The A8-1 was incubated overnight and washed in PBS twice and then resuspended in 1 mL DMEM medium (without antibiotic) with a final concentration of 10^7 CFU/mL. Caco-2 cells cultured by high-glucose DMEM were seeded in 96-well plates and incubated at 37°C. The 200 μL of A8-1 suspension was added to each well containing Caco-2 cells and then incubated for 2 h. Caco-2 cells with DMEM was set as control. The Caco-2 cells

were collected and washed three times by PBS to remove the unadhered A8-1. Then, trypsin was added to Caco-2 cells to lyse the adherent A8-1. Finally, the mixture of each well was cultured on an MRS solid plate to count the adhered bacteria (Nami et al., 2014; Popović et al., 2019).

The adhesion (%) = [(CFU/mL) adhered bacteria/(CFU/mL) added bacteria] × 100.

Antibiotic Susceptibility

VITEK 2 Compact with AST-GP67 (REF 22226, bioMererieux, France) was used to access the antimicrobial susceptibility of the A8-1 to 15 clinical antibiotics, which included penicillin (PEN, 0.125–64 μg/mL), ampicillin (AMP, 0.5–32 μg/mL), high-level gentamicin (synergistic) (HLG, 500 μg/mL; GEN, 8–64 μg/mL), high-level streptomycin (HLS, 1,000 μg/mL), ciprofloxacin (CIP, 1–4 μg/mL), levofloxacin (LVX, 0.25–8 μg/mL), moxifloxacin (MXF, 0.25–8 μg/mL), erythromycin (ERY, 0.25–2 μg/mL), clindamycin (CLI, 0.15–2 μg/mL), quinupristin/dalofopine (QDA, 0.25–2 μg/mL), linezolid (LZD, 0.15–2 μg/mL), vancomycin (VAN, 1–16 μg/mL), tetracycline (TET, 0.15–2 μg/mL), tigecycline (TGC, 0.25–1 μg/mL), and nitrofurantoin (NIT, 16–64 μg/mL). According to the MIC obtained, the results were judged according to Clinical Laboratory Standard Institute criteria (CLSI M100 S28) (Clinical and Laboratory Standards Institute, 2018) and the European Food Safety Authority (EFSA) for assessment of bacterial resistance to antimicrobials (EFSA Panel on Additives and Products or Substances used in Animal Feed [FEEDAP], 2012).

Hemolysis and Gelatinase Activity

Hemolytic activity of A8-1 was evaluated as described previously (Maturana et al., 2017). A8-1 was inoculated on Columbia agar supplemented with 5% (v/v) sheep blood and cultured at 37°C for 48 h. The hemolysis of single colonies on the plate was observed. Hemolytic activity can be divided into α-hemolysis, β-hemolysis, and γ -hemolysis.

Overnight cultured A8-1 was inoculated into gelatin medium (120 g/L gelatin, 5 g/L peptone, and 3 g/L beef extract, pH 6.8 ± 0.2) and incubated at 37°C for 48 h. Then, the tube was placed at 4°C for 1 h and it was observed whether there is liquefaction immediately. If the bacteria could produce gelatinase, there was liquid in the tube.

Quantitative Assessment of Biofilm Formation

Quantitative assessment of biofilm formation was evaluated as shown previously (Zhang et al., 2016). Overnight bacterial cultures were washed with PBS twice and adjusted to OD_{600} = 1.0. The 50 μL of bacterial suspension was added to 150 μL of fresh MRS broth and incubated in 96-well plates at 37°C for 24 h. Also, 200 μL of MRS broth without bacteria was set as negative control. After 24 h, the culture medium was poured out. The wells were washed with sterile PBS three times to remove free-floating planktonic bacteria and then dried at room temperature. The biofilm was then fixed with methanol and stained with crystal violet. The control hole was rinsed with sterile water three times until it turned colorless. Then, 200 μL ethanol was added into each well, and optical density of stained adherent cells was measured at 595 nm by microplate reader. According to the cutoff OD (ODC), the biofilm-producing ability was determined as follows: OD ≤ ODC set as non-biofilm-producer (0), ODC < OD ≤ 2ODC set as weak biofilm producer (+), 2ODC < OD ≤ 4ODC set as moderate biofilm producer (++), and OD > 4ODC set as strong biofilm producer (+++).

Virulence Gene and Virulence Activity Assay

The presence of virulence genes of A8-1 were detected by PCR, which included *gelE* (gelatinase), *cylA* (cytolysin), *hyl* (hyaluronidase), *asa1*/*agg* (aggregation substance), *esp* (enterococcal surface protein), *efaA* (endocarditis antigen), and *ace*/*acm* (collagen adhesion) (Wang et al., 2020). The primers and PCR conditions are listed in **Supplementary Table 1**.

For the virulence activity assay, tests in wax moth (*Galleria mellonella*) larvae were arranged (Martino et al., 2018). The *G. mellonella* larvae weighing about 300 mg (purchased from Tianjin Huiyude Biotech Company, Tianjin, China) were maintained on woodchips in the dark at 15°C until being used. The overnight cultures of *E. durans* A8-1, *E. faecalis* ATCC29212, and *B. infantis* CICC6069 suspension were adjusted with concentrations of 1×10^6, 1×10^7, and 1×10^8 CFU/mL. Ten randomly selected larvae were used in each group. Each larva was inoculated the bacterial suspension *via* the rear left proleg using a 10 μL Hamilton animal syringe. The MRS medium was injected into the larvae and set as negative control. The treated *G. mellonella* larvae incubated at 37°C for 3 days, and the survival rate of the *G. mellonella* were recorded every 12 h.

Impact of A8-1 on the Caco-2 Cell Membrane Integrity

Caco-2 cells were seeded into 24-well plates (1×10^5 cells per well) and cultivated to a single layer. For the treatment, there were three treatment groups, S-A8-1 (competition group), A8-1 + S (exclusion group), and S + A8-1 (replacement group). S-A8-1, 1×10^7 CFU/mL *S. typhimurium* ATCC14028 and 1×10^7 CFU/mL A8-1 culture were added into the cell wells at the same time and incubated for 2 h; A8-1 + S, 1×10^7 CFU/mL A8-1 culture were added into the cell wells and incubated for 2 h and then 1×10^7 CFU/mL *S. typhimurium* ATCC14028 was added and incubated for another 2 h; S + A8-1, 1×10^7 CFU/mL *S. typhimurium* ATCC14028 culture was added into the cell wells and incubated for 2 h and then 1×10^7 CFU/mL A8-1 added and incubated for another 2 h. Finally, 1×10^7 CFU/mL *S. typhimurium* ATCC14028 incubating solely with Caco-2 cells for 2 h was set as control. After incubation, the cell wells were washed three times by PBS to remove the unadhered *S. typhimurium* ATCC14028 cells. The amount of adhered *S. typhimurium* ATCC14028 to the Caco-2 cells were counted by bismuth sulfite agar plate (Popović et al., 2018; Kouhi et al., 2021). The inhibition rate of *S. typhimurium* adhesion to Caco-2 was calculated as:

Inhibition rate (%) = the counted adhered *S. typhimurium* ATCC14028 in treatment group (CFU/mL)/the counted adhered *S. typhimurium* ATCC14028 in control (CFU/mL).

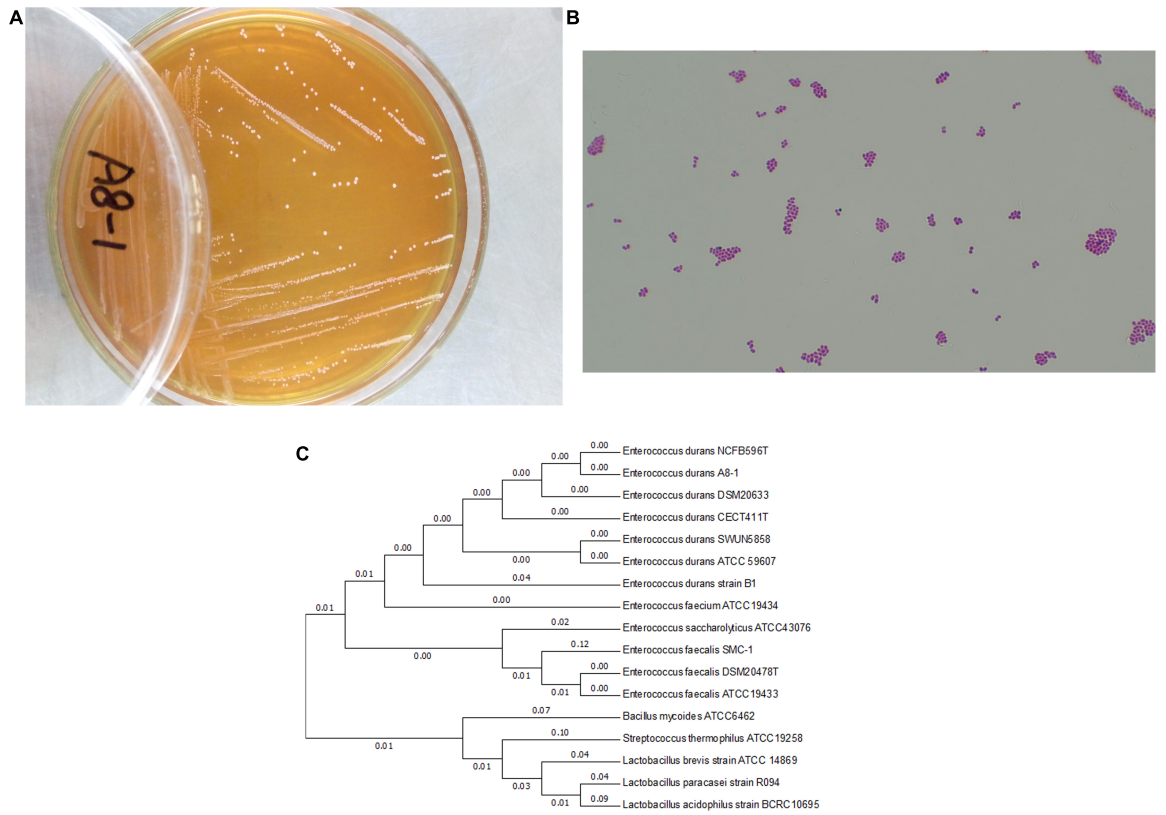

FIGURE 1 | The growth of *Enterococcus durans* A8-1 on MRS plate **(A)**; the Gram staining observation at microscope **(B)** (Olympus CX23, 40×); and phylogenetic tree based on the 16S rRNA gene sequences **(C)**, which was inferred by using the maximum likelihood method and conducted in MEGA7.

Caco-2 cells were cultured and treated as mentioned into four treatment groups (*S. typhimurium* ATCC14028, A8-1, A8-1 + S, S + A8-1) and one control. After incubation, the supernatant of cell culture was collected after centrifuging at 1,500 rpm for 10 min at 4°C. The activity of extracellular alkaline phosphatase (AKPase) was assayed in the collected supernatant using a kit (Nanjing Jiancheng Technology Co., Ltd., Nanjing, China) as described (Lv et al., 2020). The AKPase unit was defined as 1 mg of phenol produced by 100 mL of cell culture supernatant reacted with the substrate at 37°C for 15 min. Cells treated with the same amount of sterile water were used as negative control. The release of lactate dehydrogenase (LDH) into the culture medium through damaged membranes was measured spectrophotometrically using a LDH Cytotoxicity Assay Kit Nanjing Jiancheng Technology Co., Ltd., Nanjing, China) according to the manufacturer's protocol (García-Cayuela et al., 2014).

Anti-inflammation Study Using Caco-2 Cells

Measurement of Cell Viability by 3-(4,5-Dimethylthiazol-2-yl)-2,5-Diphenyltetrazolium Bromide

It was carried out as described previously by Carasi et al. (2017). An 3-(4,5-Dimethylthiazol-2-yl)-2,5-diphenyltetrazolium bromide (MTT) colorimetric assay was used to monitor cell viability. Briefly, Caco-2 cells were seeded into 96-well plates (1×10^5 cells per well). After treatment, cells were washed twice with PBS and incubated with 5 mg/mL MTT working solution for 4 h at 37°C. Then, the supernatant was removed, and the culture was resuspended in 150 μL of DMSO to dissolve MTT formazan crystals, followed by mixing on a shaker for 15 min. The absorbance was measured at 570 nm using a microplate reader. The effect of A8-1 culture and Lipopolysaccharides (LPS) on cell viability was assessed as the percentage of viable cells in each treatment group relative to untreated control cells, which were arbitrarily assigned a viability of 100%.

Measurement of Cell Cytokines by Enzyme-Linked Immunosorbent Assay and q-PCR

Quantification of cytokine levels in cell culture supernatants was determined by enzyme-linked immunosorbent assay (ELISA) and quantitative PCR (qPCR) (Mansour et al., 2014). Caco-2 cells were added into a 24-well cell culture plate according to 1×10^5 cell/well and incubated until the cells grew to monolayer. There were two treatment groups, A8-1 + LPS and LPS + A8-1. For the A8-1 + LPS group, 2.5×10^6 CFU A8-1 cells were added into Caco-2 cells and incubated for 6 h; the wells were washed three times by PBS, and 1 mL fresh DMEM was supplied and then 10 μg LPS was added and incubated for another 6 h. For the LPS + A8-1 group, 10 μg LPS was added into Caco-2 cells and

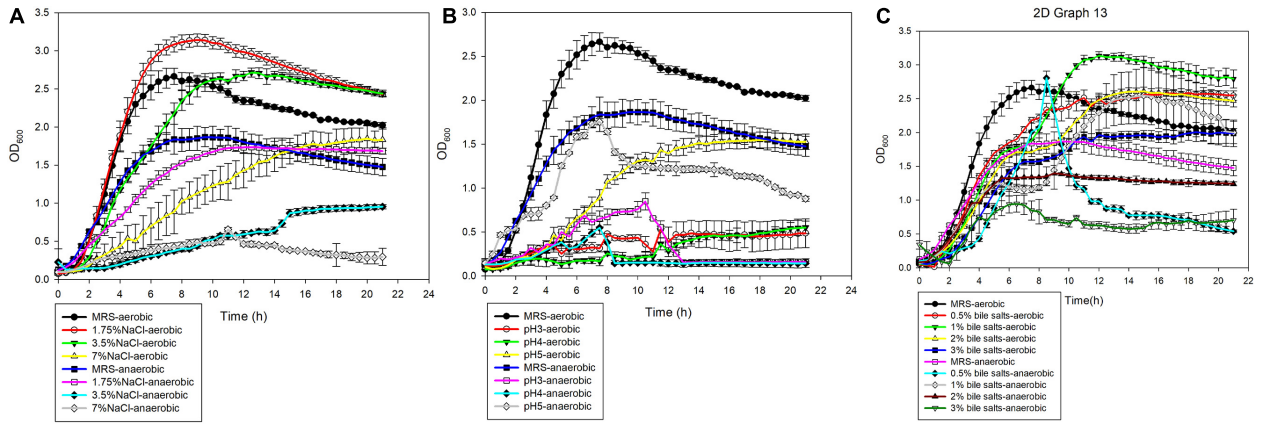

FIGURE 2 | *In vitro* tolerance of *Enterococcus durans* A8-1 under aerobic and anaerobic conditions with **(A)** 1.75, 3.5, and 7% NaCl; **(B)** pH 3, 4, and 5; **(C)** 0.5, 1, 2, and 3% bile salts.

incubated for 6 h; the wells were washed three times by PBS, and 1 mL fresh DMEM was supplied and then 2.5 × 10^6 CFU A8-1 cells were added and incubated for another 6 h. The different treated Caco-2 cells and cell culture supernatant were collected at 6 and 12 h, separately. The contents of IL-8, IL-10, and TNF-α in the supernatant were detected by an ELISA kit (Sigma-Aldrich). Cell RNA extraction and relative mRNA expression of IL-8, IL-10, and TNF-α were determined according to the instructions of corresponding kits (Sigma-Aldrich). GAPDH was selected as the internal reference gene, and the relative mRNA expression levels of IL-8, IL-10, and TNF-α were calculated according to the $2^{-\Delta\Delta CT}$ method. The untreated Caco-2 cells were used as control, and all tests were performed in triplicate.

Whole-Genome Sequence of A8-1

Whole-genome DNA of A8-1 was extracted by a kit (Applied Biosystems® 4413021). The DNA concentration and purity was quantified with the NanoDrop2000. It was sequenced on the Illumina HiSeq™2000 platform at Gene *de novo* Biotechnology Co., Ltd. (Guangzhou, China). The reads were *de novo* assembled by SOAPdenovo version 2.04, Li et al. (2009) and the genome sequence was improved by GapCloser. For the analysis of specific gene sequences, such as virulence genes, heavy metal resistance genes, antibiotic resistance genes, and efflux gene sequences in the bacterial genome, the genomes were analyzed and retrieved in the BIGSdb.[1] The predicted genes of *E. durans* A8-1 were compared with the comprehensive antibiotic resistance database (CARD)[2] (McArthur et al., 2013) and virulence factors database (VFDB)[3] (Chen et al., 2016) for identifying antibiotic resistance and virulence factors. Furthermore, the ResFinder 3.0[4] (Zankari et al., 2012) and PathogenFinder 1.1[5] (Cosentino et al., 2013) were used for identifying the acquired antibiotic resistance genes and pathogenicity factors, respectively. Clustered regularly interspersed short palindromic repeats (CRISPR) and prophage sequences were identified by CRISPR Finder[6] (Grissa et al., 2007). The genome sequences have been submitted to antiSMASH bacterial version[7] to search for the secondary metabolite biosynthetic gene clusters.

Statistical Analysis

The test and analysis of variance (ANOVA), STAMP10, GraphPad Prism 7, and SPSS V20.0 (IBM Inc., IL, United States) were used to perform statistical analyses. Data were presented as means ± SEM. $P < 0.05$ was considered significant differences.

RESULTS

Isolation and Identification of A8-1

The Gram-positive and cocci-shaped bacteria were selected from a fecal sample of healthy infants. The colony morphology had a sticky, translucent white and mucoid appearance on MRS agar. Except cell morphology, Gram staining (G^+), catalase (negative) and oxidase production (negative), nitrate reduction test (negative), a final strain of A8-1 was confirmed by 16S rRNA sequence analysis (**Figures 1A–C**). The 16S rRNA was submitted to NCBI with the accession number of MH385353.

Analysis of Probiotic Characteristics of *Enterococcus durans* A8-1

Acid and Bile Salt Tolerance Under Aerobic and Anaerobic Conditions

A8-1 had different tolerance in different environments in our experiment. Under aerobic conditions, A8-1 could survive at pH 5.0 in MRS medium, and the maximum cell density reached about 50% of the density in normal MRS under aerobic conditions

[1]https://bigsdb.pasteur.fr/

[2]http://arpcard.mcmaster.ca/

[3]http://www.mgc.ac.cn/VFs/main.htm

[4]https://cge.cbs.dtu.dk//services/ResFinder/

[5]https://cge.cbs.dtu.dk/services/PathogenFinder/

[6]http://crispr.i2bc.paris-saclay.fr/Server/

[7]https://antismash.secondarymetabolites.org/

TABLE 1 | Comparison of acid, NaCl, and bile salt tolerance of *Enterococcus durans* A8-1 cultured at aerobic and anaerobic conditions.

Medium	Aerobic			Anaerobic		
	ODmax	LSD (h)	R^2	ODmax	LSD (h)	R^2
MRS	2.322	1.5944	0.9266	1.713	0.6206	0.9375
1.75% NaCl	2.841	1.6536	0.948	1.739	0.3693	0.9947
3.5% NaCl	2.619	1.5034	0.9889	0.396	0.5392	0.7078
7% NaCl	1.974	1.1152	0.9982	1.418	0.2969	0.9764
pH 3	0.476	NA*	NA	0.5662	NA	NA
pH 4	1.513	1.1036	0.9363	0.209	NA	NA
pH 5	1.585	2.1805	0.9927	1.234	0.933	0.5311
0.5% Bile salts	2.539	1.0611	0.9956	1.104	NA	NA
1% Bile salts	3.018	1.496	0.9735	2.497	0.1764	0.9209
2% Bile salts	2.595	0.7329	0.9825	1.288	0.8741	0.9382
3% Bile salts	1.97	1.5058	0.9946	0.704	NA	NA

**NA, not fit for the Gompertz growth curve analysis.*

(**Figure 2**). A8-1 showed great tolerance to bile salt and NaCl. It was found that the growth of A8-1 in 1.75 and 3.5% NaCl was better than that in MRS (ODmax: 2.841 vs. 2.322, $P < 0.05$; 2.619 vs. 2.322, $P < 0.05$). The maximum biomass of A8-1 in a 0.5, 1, and 2% bile salt environment were higher than that of the control group (**Figure 2A**). Under anaerobic conditions, the maximum OD_{600} of A8-1 was close to the control at pH 5.0 (**Figure 2B**), and the strain could grow well under 1% bile salt (ODmax: 2.497 vs. 1.713, $P < 0.01$) and 1.75% NaCl (ODmax: 1.739 vs. 1.713, $P > 0.05$) (**Figure 2C**). Under aerobic conditions, compared with the MRS control group, the lag phase of A8-1 was the shortest at 2% bile salts and 7% NaCl, was delayed under pH 5. Under anaerobic conditions, compared with MRS control, the lag phase of A8-1 was the shortest at 1% bile salt, and the lag phase of A8-1 was shortened with NaCl added (**Table 1**).

In vitro Adherence Assay

Compared with *L. rhamnosus* GG BL379 (positive control), A8-1 showed higher adhesion to mucin ($P < 0.01$), BSA ($P < 0.01$), and collagen. The adhesion ability of A8-1 to mucin, collagen, and BSA was 5.2, 1.6, and 5.6 times higher than *L. rhamnosus* GG BL379. For the adhesion to Caco-2 cells, the adhesion of A8-1 was 38.47%, which is higher than *L. rhamnosus* GG BL379 (38.47 vs. 11.7%, $P < 0.05$) determined in our study.

For the surface adhesion ability, A8-1 showed a high hydrophobicity of 79.2 ± 3.1% in chloroform and moderate hydrophobicity of 49.2 ± 4.4% in xylene; it had 51.7 ± 4.5% for the auto-aggregation after 5 h of incubation and was able to co-aggregate with *S. typhimurium* with a co-aggregation percentage of 66.2 ± 2.9%.

Antibacterial Activity Analysis

The fermentation supernatant of A8-1 showed different antibacterial activity against the indicator strains for *P. aeruginosa* PA01 and *E. coli* ATCC35218, the MIC was 25 μL supernatant, and for the *S. aureus* ATCC25923, *P. aeruginosa* ATCC27853, *E. hormaechei* ATCC700323, *S. typhimurium* ATCC14028, the MIC was 50 μ L supernatant.

Protect Effect to the Caco-2 Cell

Protection Effect of A8-1 to the Caco-2 Cell Membrane Integrity

The enzyme activities of LDH and AKP in the supernatant of cell culture were selected as indicators for the integrity of the Caco-2 cell membrane (**Figures 3A,B**). Compared with the control group, it was found that the LDH activity in the A8-1 group was significantly reduced compared with the control group (467.20 vs. 535.58, $P = 0.005$) and was increased in the *S. typhimurium* ATCC14028 group (577.92 vs. 535.58, $P = 0.042$), whereas AKP activity was changed with a similar trend to LDH but no statistical difference. In the A8-1 + S group, activities of LDH and AKP in the Caco-2 cell supernatant were all significantly decreased compared with that of the Salmonella group (470.46 vs. 577.92, $P < 0.001$; 2.21 vs. 2.51, $P = 0.007$). Even in the S + A8-1 group, LDH activity was still significantly lower than that of the Salmonella group (445.61 vs. 577.92, $P < 0.001$). Those results show that strain A8-1 could protect the integrity of the Caco-2 cell membrane in pretreatment and inhibit the damage of *Salmonella* to Caco-2 cells.

A8-1 Competitively Inhibited the Adhesion of *Salmonella typhimurium* to Caco-2 Cell

The plate counting method was used to explore the antagonism of A8-1 against the adhesion of *S. typhimurium* ATCC14028 to Caco-2 cells. It is found that, in S-A8-1 (competition group), A8-1 can reduce the adhesion of *S. typhimurium* to cells without statistical difference (19.8 vs. 16.5%, $P > 0.05$). In A8-1 + S (exclusion group), the adhesion of *S. typhimurium* to Caco-2 cells was significantly reduced (19.8 vs. 10.5%, $P = 0.002$) possibly because A8-1 could inhibit the growth of *S. typhimurium* and occupied the binding sites on the surface of the Caco-2 cells. However, there was no statistical difference for the adhesion to Caco-2 cells between S + A8-1 (replacement group) and the *S. typhimurium* group (19.8 vs. 22.1%, $P = 0.592$) (**Figure 3C**). Those results showed that A8-1 competitively inhibited the adhesion of *S. typhimurium* to Caco-2 cell.

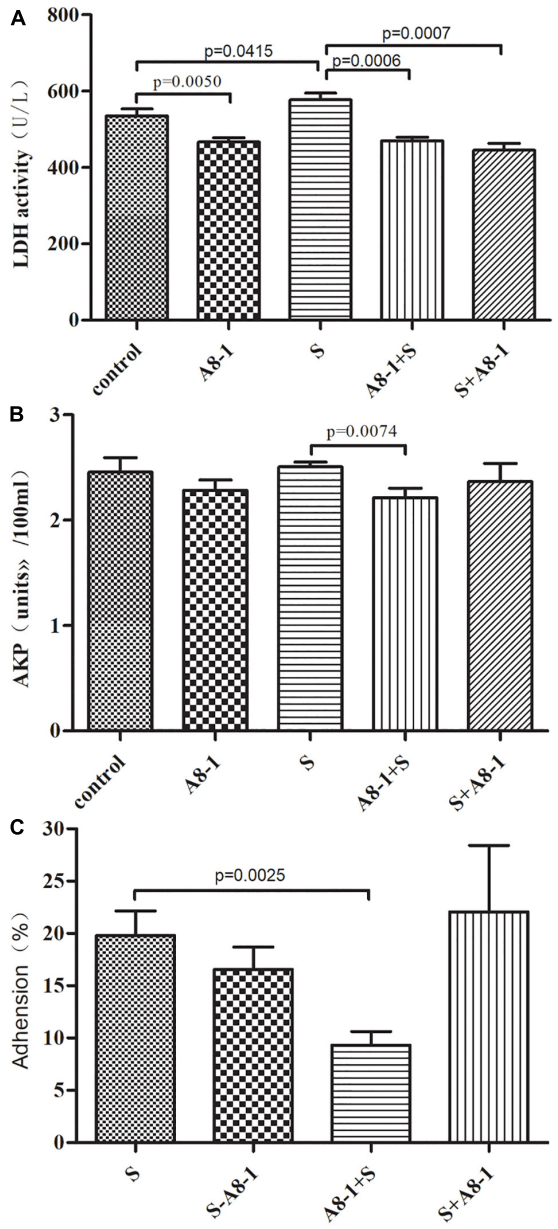

FIGURE 3 | Protective effect of *Enterococcus durans* A8-1 to the Caco-2 cell membrane integrity by lactate dehydrogenase (LDH) **(A)** and AKP **(B)** activity assay and the adhesion rate of A8-1 to the Caco-2 cell **(C)**.

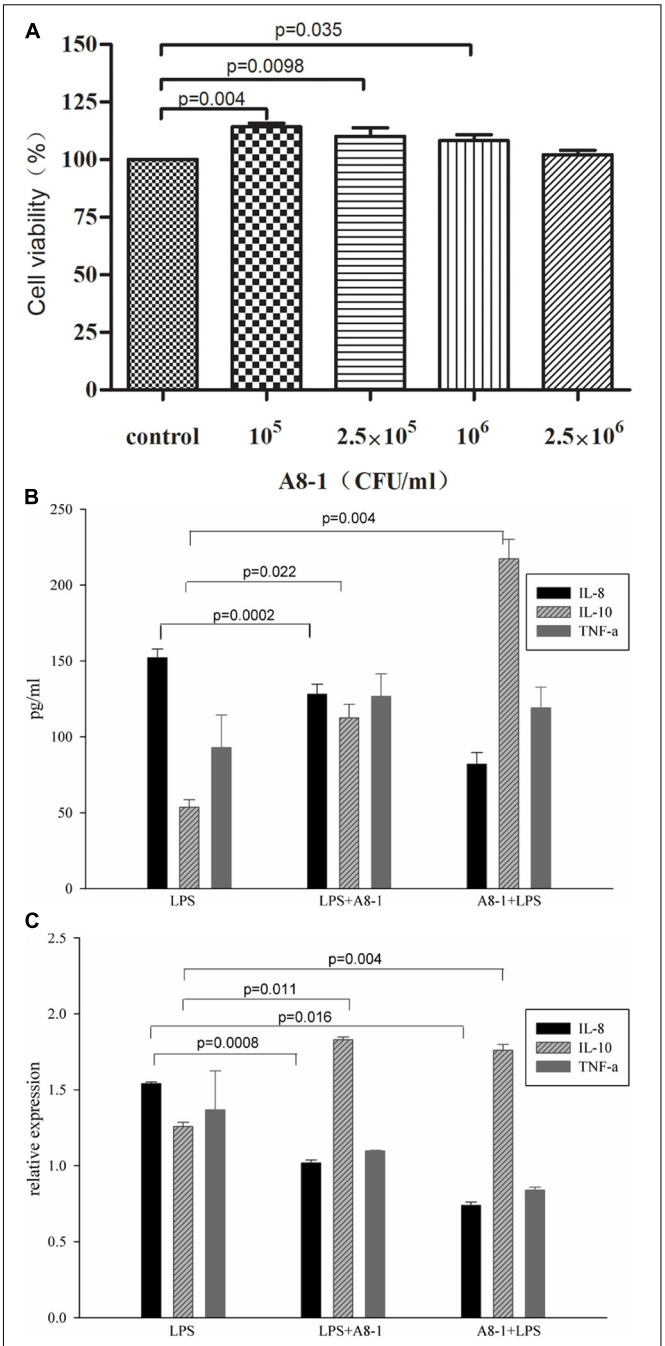

FIGURE 4 | The Caco-2 cell viability with incubation of 10^5, 2.5×10^5, 10^6, and 2.5×10^6 CFU/mL of A8-1 **(A)**. Then, 10 μg/mL LPS was added to the medium to induce the inflammation of Caco-2 cells, the anti-inflammation ability of 2.5×10^6 CFU/mL A8-1 was detected by IL-8, IL-10, and TNF-α through ELISA **(B)** and qPCR **(C)**.

A8-1 Reduced IL-8 and Increased IL-10, TNF-α Secretion in Response to LPS Stimulation in Caco-2 Cells

Results of cell viability treated by A8-1 are shown in **Figure 4A**. Different concentrations of A8-1 cells with 1×10^5, 2.5×10^5, and 1×10^6 CFU/mL could all significantly increase the Caco-2 cell viability (114.18 vs. 100%, $P = 0.004$; 110.04 vs. 100%, $P = 0.0098$; 108.14 vs. 100%, $P = 0.035$) except the 2.5×10^6 CFU/mL group (102.10 vs. 100%, $P = 0.140$). So 2.5×10^6 CFU/mL of A8-1 cells was selected for the following assays.

The 10 μg/mL LPS was added to the medium and induced the inflammation of Caco-2 cells, and the anti-inflammation ability of A8-1 was detected by IL-8, IL-10, and TNF-α through ELISA

TABLE 2 | Minimum inhibitory concentrations (MICs) of *Enterococcus durans* A8-1 against 15 antimicrobials, and the antimicrobial susceptibility was evaluated by CLSI-2018 and FEEDAP-EFSA-2012.

Antimicrobials	MIC	Cutoff values		Antimicrobial susceptibility
		CLSI	FEEDAP-EFSA	
Penicillin	2	8	4	S
Ampicillin	≤2	8	4	S
Ciprofloxacin	≤0.5	1	4	S
Levofloxacin	0.25	2	NA	S
Moxifloxacin	≤0.25	0.5	NA	S
Erythromycin	≤0.25	0.5	4	S
Clindamycin	≥8	8	8	R*
Quinupristin/dalofopine	1	4	NA	S
Linezolid	2	4	NA	S
Vancomycin	≤0.5	4	4	S
Tetracycline	≤1	4	2	S
Tigecycline	≤0.12	0.2	NA	S
Nitrofurantoin	32	64	NA	S
high-level gentamicin (synergistic)				SYN-S
high-level streptomycin				SYN-S

**For Enterococcus spp., clindamycin may appear active in vitro but is not effective clinically and should not be reported as susceptible as described in CLSI.*
NA, Not available.

and qPCR (**Figures 4B,C**). Compared with the LPS treatment cells, IL-8 were decreased in both A8-1 + LPS and LPS + A8-1 groups and showed significant difference between LPS + A8-1 and LPS groups (82.11 vs. 152.23 pg/mL, $P = 0.002$); the IL-10 were significantly increased in both A8-1 + LPS and LPS + A8-1 groups (217.3 vs. 53.7 pg/mL, $P = 0.004$; 112.5 vs. 53.7 pg/mL, $P = 0.022$). TNF-α increased in both intervention groups, but there was no significant difference compared with LPS group (126.7 vs. 93.0 pg/mL, $P = 0.265$; 119.1 vs. 93.0 pg/mL, $P = 0.362$). For the relative expression of mRNA, the IL-8 in A8-1 + LPS and LPS + A8-1 groups were significantly decreased (1.54 vs. 1.02, $P = 0.0016$; 1.54 vs. 0.74, $P = 0.0008$); IL-10 were significantly increased in both A8-1 + LPS and LPS + A8-1 groups (1.83 vs. 1.26, $P = 0.004$; 1.76 vs. 1.26, $P = 0.011$). TNF-α expression was decreased in both groups without statistical difference (1.36 vs. 1.09, $P = 0.4059$; 1.36 vs. 0.84, $P = 0.1784$). Those results showed that A8-1 could reduce the secretion of IL-8 and increase the secretion of IL-10 and TNF-α in response to LPS stimulation in Caco-2 cells.

Safety Evaluation of A8-1

Susceptibility of *E. durans* A8-1 to antibiotics was determined by measuring MICs, and the results were compared to the cutoff values for *Enterococcus* species as defined by EFSA and CLSI. *E. durans* A8-1 was found to be resistant only to clindamycin but was susceptible to penicillin, ampicillin, high-level gentamicin (synergistic), high-level streptomycin, ciprofloxacin, levofloxacin, moxifloxacin, erythromycin, quinupristin/dalofopine, linezolid, vancomycin, tetracycline, tigecycline, and nitrofurantoin (**Table 2**). A8-1 showed no hemolytic activity (**Supplementary Figure 1A**) and no gelatin hydrolysis activity (**Supplementary Figure 1B**). It was identified as a weak biofilm producer (++). In the nine tested virulence related genes, there showed only *asa1* gene positive in A8-1.

For the virulence assay with *G. mellonella* larvae, after 72 h injection, except the 10^8 CFU/mL group of *E. faecalis* ATCC29212, all larvae had a 90% survival rate in both the 10^7 and 10^8 CFU/mL groups. All larvae survived in the control and the 10^6 CFU/mL groups. The survival curves were analyzed statistically using Log-rank (Mantel-Cox) Test, and there were no statistical differences in *E. durans* A8-1 and *B. infantis* CICC6096 within 10^7 and 10^8 CFU/mL groups ($P > 0.05$). Apparently, A8-1 could be considered safe (**Figure 5**).

Whole-Genome Sequence of A8-1

The circular chromosome of *E. durans* A8-1 contains 2,877,218 bp, 37.92% GC-content, and 56 tRNA genes (**Table 3**). Genome annotation at the RAST server showed that the C-1 genome encodes 2,752 proteins, and the corresponding functional categorization by COG annotation is in **Supplementary Table 2**. The sequence data of the *E. durans* A8-1 genome were deposited into NCBI and can be accessed *via* accession number PRJNA769572. The GO function annotation map of genome is shown in **Supplementary Table 3**. There were 1,123 genes related to biological process (BP), 590 genes related to cell composition (CC), and 757 genes related to molecular function (MF). Among the genes involved in BP, there were two bio-adhesion–related genes (A8-1_0276, Zinc-binding lipoprotein *adcA*; A8-1_2290, Metal ABC transporter substrate-binding lipoprotein), 85 cell colonization–related genes, 268 binding ability genes, and four antioxidant genes (A8-1_0078, Glutathione peroxidase; A8-1_2302, Manganese catalase; A8-1_2334, carboxymuconolactone decarboxylase; A8-1_2613, peroxiredoxin).

The probiotic-related genes in the genome were also analyzed. The cholylglycine hydrolase (EC 3.5.1.24) gene responsible for bile salt hydrolysis action was identified in one copy within the A8-1 genome (A8-1_2053). Fibronectin/fibrinogen-binding protein (A8-1_2247) and collagen-binding protein (A8-1_0314) were found in the genome allowing them to bind the GI tract, suggesting an important role in adhesion and colonization in intestinal mucosal surfaces. Also, the resistance to hydrogen peroxide is imparted by genes alkyl hydroperoxide reductase (*ahp*, A8-1_2612, A8-1_2613) and NADH peroxidase (npr, A8-1_1888, A8-1_2186, and A8-1_2466) that were found in the genome. For the polysaccharide biosynthesis–related genes, there were eight genes located in the genome, including A8-1_ 0155 (polysaccharide biosynthesis glycosyltransferase), A8-1_0235 (polysaccharide core biosynthesis protein RfaS), A8-1_0854 (polysaccharide transport system ATP-binding protein), A8-1_1612 (sugar transferase), A8-1_1617 (polysaccharide cholinephosphotransferase), A8-1_1621 (polysaccharide core biosynthesis protein RfaS), A8-1_1639 (polysaccharide chain length determining protein CapA), and A8-1_1764 (polysaccharide biosynthesis protein). In addition, based on the

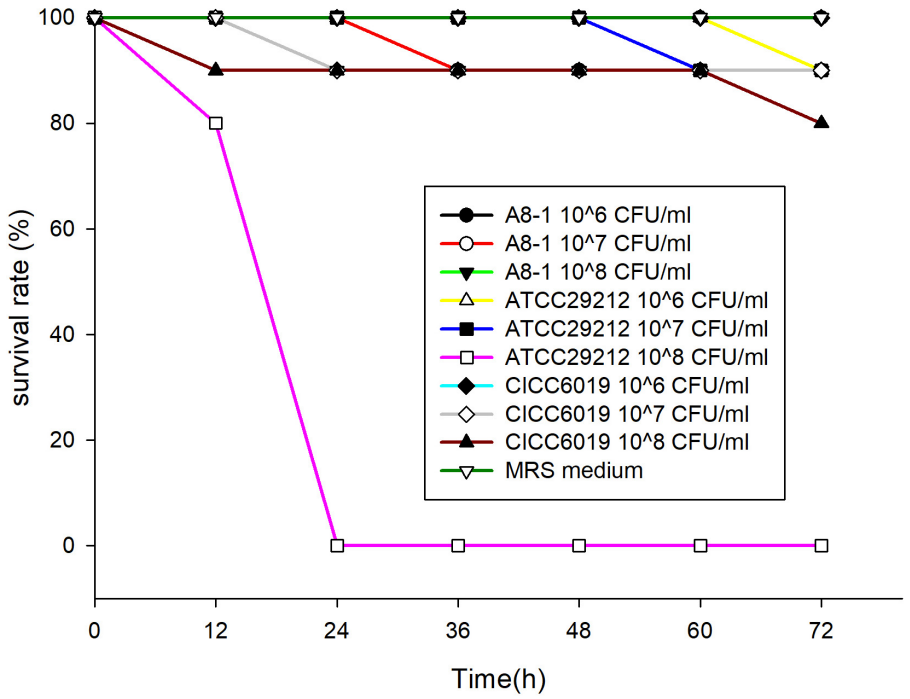

FIGURE 5 | Survival curves of *Galleria mellonella* larvae were recorded for 72 h after injection with 10 μL of *Enterococcus durans* A8-1, *Enterococcus faecalis* ATCC29212, and *Bifidobacterium infantis* CICC6096 at concentrations of 1×10^6, 1×10^7, and 1×10^8 CFU/mL, respectively, and the 10 μL of MRS medium was used as negative controls.

TABLE 3 | Genomic analysis of A8-1.

Characteristic	Number	Characteristic	Number
Genome size (bp)	2,877,218	CRISPR	2
Scaffolds	102	tRNA	56
GC content (%)	37.92	Transposon PSI	17
Code genes	2,752	GIs	15

previous studies, we also screened for a set of genes involved in imparting important probiotic functions as described in **Table 3**.

The drug-resistance and virulence genes were annotated by database of CARD and VFDB. Two aminoglycoside resistance–related genes *AAC (6′)-IIH* and *AAC (6′)-IID*; three β-lactam resistance genes *mecC*, *mecB*, and *mecA*; and one fluoroquinolone resistance gene *mfd* were predicted in CARD. Regarding the possibility of acquired resistance by horizontal gene transfer (HGT), there was no detection of any acquired antibiotic resistance genes. In addition, *efaA/scbA* was found in virulence gene prediction (A8-1_2290, endocarditis specific antigen); however, the similarity score was only 50.1%. Meanwhile, the *asa1* gene detected by PCR was not found in the genome sequencing results, which may explain the non-toxic activity to the *G. mellonella* larvae. In addition to the above genes, there predicated some genes responsible for the secondary metabolites, such as *bsh* (A8-1_2053, bile salt hydrolase), which may be related to the bile salt tolerance and survival in the intestinal tract for A8-1; *cap8E* (A8-1_1630, capsular polysaccharide synthesis enzyme), *cap8E* (A8-1_1631, capsular polysaccharide synthesis enzyme), *cas4J* (A8-1_1631, capsular polysaccharide biosynthesis protein) genes related to capsular polysaccharide synthesis were also found in the genome, which may contribute to protect bacteria itself and resist the phagocytosis of host cells; *fliN* (A8-1_1957, flagella motor switch protein), which is involved in synthesis of flagellin, which could be recognized by Toll like receptor *TLR5*, and activate innate immunity, upregulate the expression of tight junction protein Occludin and mucin and protect the intestinal barrier.

DISCUSSION

Probiotics, the microorganisms referred to are non-pathogenic bacteria and are considered "friendly germs" due to the benefits they offer to the gastrointestinal tract and immune system. Probiotic *Enterococcus* spp. are mainly from the gut of human and animal and can be detected in fecal samples, which are more competitive than isolates from other environments and deserve more attention for probiotic screening (Rodríguez et al., 2015; Zheng et al., 2015). Except the origin host, in the screening for new probiotic strains, probiotic characteristics of the isolates should be analyzed, including stress tolerance, adhesion, antibacterial ability, anti-inflammatory ability, antibiotic resistance, and toxicity (AlKalbani et al., 2019). Our study aimed to assess the potential probiotic properties

and safety of an *E. durans* strain A8-1 isolated from feces of a healthy Chinese infant.

In our results, A8-1 grew faster and showed higher antistress ability. By simulating the gastrointestinal environment,it was found that, under the aerobic conditions of pH 5.0, 3% bile salt, and 7% NaCl, the growth of *E. durans* A8-1 could reach more than 50% of the control group, and this indicated that A8-1 has the potential to pass through the intestinal contents and reach the intestinal colonization site. Bile salt tolerance has generally been considered more important during probiotic selection than that of other properties, such as gastric and pancreatic tolerance (Masco et al., 2007). The growth of the strain was stimulated under bile salt and NaCl, which suggested that we can optimize the fermentation conditions to promote better growth and faster enrichment of bacteria cells. In the genome of A8-1, the bile salt hydrolase–related gene *bsh* was found, and the presence of bile salt hydrolase in probiotics renders them more tolerant to bile salts (Hussein et al., 2020), which may interpret the better tolerance of A8-1 to higher concentration of bile salt.

The first step for good probiotics to exert probiotics in the host is to adhere to the cell surface, which is also the basis for probiotics to show the barrier protection function. Also, for probiotic enterococci, it is an important factor in colonization and competitive exclusion of enteropathogens (Nueno-Palop and Narbad, 2011). The stronger the adhesion ability of the bacteria, the higher the probability of colonization and survival in the intestinal tract. Compared with *L. rhamnosus* BL379, A8-1 had higher adhesion ability to the tested proteins of mucin, BSA, and collagen. The human intestinal epithelial-like Caco-2 cell line is often used as an intestinal epithelial cell model (Jose et al., 2017). The adhesion rate of A8-1 to Caco-2 cells was 30%, and this result showed that the adhesion performance of the A8-1 to various proteins and cells was different. Also, the considerably high level of hydrophobicity, auto-aggregation, and co-aggregation of A8-1 could enable the bacterial cell to adhere to host epithelial cells and allow the formation of a barrier to prevent the colonization of pathogens on surfaces of the mucosa (Nami et al., 2020; Fonseca et al., 2021). Similarly, whether the strain has the same adhesion ability *in vivo* and *in vitro* also needs to be considered (Banwo et al., 2013). Metabolites produced by probiotics have antibacterial activities, such as organic acids, hydrogen peroxide, and bacteriocin (İspirli et al., 2015). A8-1 has a better antibacterial effect on G^- than G^+, which may be related to the similar bacterial structure of A8-1 (G^+) and two G + indicator bacteria (*E. faecalis* ATCC 29212 and *S. aureus* ATCC 5923). Moreover, bacteriocin showed a narrow antibacterial spectrum against the same related strains. In this study, the growth of the indicator bacteria was used to determine the antibacterial ability of *Enterococcus* isolates, but the specific types and production of antibacterial active substances were not discussed. To further analyze the bacteriostatic mechanism of A8-1, the eight specific polysaccharide biosynthesis–related genes, which were annotated in the genome sequence of A8-1, deserve more attention.

Lipopolysaccharide is often used as a substance to induce an inflammatory reaction, which can make cells produce inflammation and stimulate the expression of inflammatory cytokines (Drakes et al., 2004). Our results show that the inflammatory response induced by LPS could be alleviated and IL-8 mRNA could be reduced after being pretreated with A8-1. The expression of TNF-α mRNA was decreased, but there was no significant change in the supernatant of each treatment group ($P > 0.05$). A8-1 may have the potential to inhibit inflammatory response. When inflammation occurs, A8-1 can reduce the expression of cytoinflammatory factors to reduce the inflammatory response of cells to LPS. It is worth noting that probiotics have highly diverse effects on the level of immune regulatory cytokines, mainly related to the specificity of strains and cell lines (Kook et al., 2019).

Enterococcus, as the original symbiotic bacteria in the intestine, has dual characteristics of probiotic function and potential pathogenicity. Therefore, it is necessary to compare and analyze the functional characteristics and safety at the strain level (Klimko et al., 2020). To evaluate the safety of A8-1, susceptibility to antibiotics, hemolytic activity, gelatin hydrolysis activity, virulence-related genes, and the virulence assay were all carried out. In the antibiotic susceptibility test, A8-1 was only resistant to clindamycin, which may be related to the inherent resistance of enterococci, which was verified in *E. durans* KLDS 6.0930 (Li et al., 2018). Antibiotics linezolid and vancomycin are often used as the last resort for G^+ pathogen infection. β-lactams (penicillin, ampicillin), and aminoglycoside antibiotics are generally the preferred drugs for the treatment of *enterococci* infection, which may make the strains more resistant to such antibiotics (Tsai et al., 2012). A8-1 was sensitive to the above antibiotics. Bacterial toxicity should be evaluated by phenotype and genotype. The *esp* gene may be involved in the formation of biofilm, but it is not the only factor determining the producing of biofilm (Fallah et al., 2017; Kook et al., 2019). No *esp* gene was detected in A8-1. The ability of producing biofilm was considerate lower, which may be related to the lack of *esp* gene. A8-1 was *gleE* gene negative with no gelatin hydrolase (Popović et al., 2018). Furthermore, there were no obvious pathogenicity or virulence genes found in A8-1. This correlates with the observed phenotype in the *G. mellonella* model due to the low mortality rates that were obtained, which is similar behavior to the larvae inoculated with *L. lactis* strains reported by Martino (Martino et al., 2018).

The whole-genome sequencing of bacteria is a convenient way to determine antibiotic-resistant genotypes and predict the corresponding resistance phenotypes, and the phenotype does not always completely reflect the genotype. Through comparative analysis of ARDB, it predicted aminoglycosides, β-lactam antibiotics, and fluoroquinolone-related genes in A8-1, but A8-1 had no corresponding resistance phenotype. It may be because the expression of the drug-resistant gene was silenced or the transcription process was not completed, resulting in the absence of resistance phenotype. A8-1 is resistant to clindamycin, which is usually an inherent antibiotic resistant to *Enterococcus*, and the predicted *lasA*, *lmrB*, *lmrC*, and *lmrD* genes contributed to the clindamycin-resistance through the efflux pump function (Hollenbeck and Rice, 2012). However, antibiotic resistance may have a positive effect on probiotics. For some antibiotic-resistant

enterococci, it can effectively maintain the natural balance of intestinal flora in the process treatment (Strompfová et al., 2004).

In the current research, we only explored the impact of potential probiotic A8-1 on intestinal epithelial cell membranes and the regulation of cell inflammation. In the follow-up experiments, the transepithelial electrical resistance (TER) should be measured, and the cell tight junction protein can be further detected to explain the effect of A8-1 on the maintenance of gut permeability and intestinal barrier function and interpret the mechanism of inflammation suppression through the inflammatory response-related signal pathways. Furthermore, animal models will be established to evaluate the safety and functionality of *E. durans* A8-1 before potential use in applications.

CONCLUSION

In summary, we have identified a strain of *E. durans* that is able to tolerate and survive the simulated gastric and intestinal juices and has the potential to colonize the intestinal epithelial cells. Furthermore, we also showed that it contains no obvious pathogenicity or virulence genes. Taken together, our findings suggest the efficacy of probiotic *E. durans* A8-1 in exerting an adherence to the cell surface to show the barrier protection function and competitive exclusion of enteropathogens with reductions in the levels of inflammatory cytokines. According to the results of these evaluated attributes, *E. durans* strain A8-1 could be a promising probiotic candidate for applications.

DATA AVAILABILITY STATEMENT

The datasets presented in this study can be found in online repositories. The names of the repository/repositories and accession number(s) can be found in the article/ **Supplementary Material**.

AUTHOR CONTRIBUTIONS

BH and YC: conceptualization and writing—review and editing. YZ, JW, and LS: main experiments. LL and JY: genome analysis. RD: data and bacterial curation. BH and YZ: writing—original draft preparation. BH: supervision. BH and RD: funding acquisition. All authors agreed to be accountable for the content of the work.

FUNDING

This research was funded by the National Natural Science Foundation of China (Nos. 81673199 and 82173526) and the Natural Science Basic Research Program of Shaanxi Province, China (No. 2019JM-445).

SUPPLEMENTARY MATERIAL

The Supplementary Material for this article can be found online at: https://www.frontiersin.org/articles/10.3389/fmicb.2021.799173/full#supplementary-material

REFERENCES

AlKalbani, N. S., Turner, M. S., and Ayyash, M. M. (2019). Isolation, identification, and potential probiotic characterization of isolated lactic acid bacteria and in vitro investigation of the cytotoxicity, antioxidant, and antidiabetic activities in fermented sausage. *Microb. Cell Fact.* 18:188. doi: 10.1186/s12934-019-1239-1

Banwo, K., Sanni, A., and Tan, H. (2013). Technological properties and probiotic potential of *Enterococcus faecium* strains isolated from cow milk. *J. Appl. Microbiol.* 114, 229–241. doi: 10.1111/jam.12031

Carasi, P., Racedo, S. M., Jacquot, C., Elie, A. M., Serradell, M. L., and Urdaci, M. C. (2017). *Enterococcus durans* EP1 a promising anti-inflammatory probiotic able to stimulate sIgA and to increase *Faecalibacterium prausnitzii* abundance. *Front. Immunol.* 8:88. doi: 10.3389/fimmu.2017.00088

Chen, L., Zheng, D., Liu, B., Yang, J., and Jin, Q. (2016). VFDB 2016: hierarchical and refined dataset for big data analysis–10 years on. *Nucleic Acids Res.* 44, D694–D697. doi: 10.1093/nar/gkv1239

Cirrincione, S., Neumann, B., Zühlke, D., Riedel, K., and Pessione, E. (2019). Detailed soluble proteome analyses of a sairy-isolated *Enterococcus faecalis*: a possible approach to assess food safety and potential probiotic value. *Front. Nutr.* 6:71. doi: 10.3389/fnut.2019.00071

Clinical and Laboratory Standards Institute (2018). *Performance Standards for Antimicrobial Susceptibility Testing; 27th Informational Supplement.* M100-S28. Wayne, PA: Clinical and Laboratory Standards Institute.

Cosentino, S., Voldby Larsen, M., Møller Aarestrup, F., and Lund, O. (2013). PathogenFinder–distinguishing friend from foe using bacterial whole genome sequence data. *PLoS One* 8:e77302. doi: 10.1371/journal.pone.0077302

Drakes, M., Blanchard, T., and Czinn, S. (2004). Bacterial probiotic modulation of dendritic cells. *Infect. Immun.* 72, 3299–3309. doi: 10.1128/iai.72.6.3299-3309.2004

EFSA Panel on Additives and Products or Substances used in Animal Feed [FEEDAP] (2012). Guidance on the assessment of bacterial susceptibility to antimicrobials of human and veterinary importance. *EFSA J.* 10:2740. doi: 10.2903/j.efsa.2012.2740

Fallah, F., Yousefi, M., Pourmand, M. R., Hashemi, A., Nazari Alam, A., and Afshar, D. (2017). Phenotypic and genotypic study of biofilm formation in *Enterococci* isolated from urinary tract infections. *Microb. Pathog.* 108, 85–90. doi: 10.1016/j.micpath.2017.05.014

Fonseca, H. C., de Sousa, M. D., Ramos, C. L., Dias, D. R., and Schwan, R. F. (2021). Probiotic properties of *Lactobacilli* and their ability to inhibit theadhesion of enteropathogenic bacteria to Caco-2 and HT-29 cells. *Probiot. Antimicrob. Proteins* 13, 102–112. doi: 10.1007/s12602-020-09659-2

García-Cayuela, T., Korany, A. M., Bustos, I., Cadiñanos, L. P. G. D., Requena, T., Peláez, C., et al. (2014). Adhesion abilities of dairy *Lactobacillus plantarum* strains showing an aggregation phenotype. *Food Res. Intern.* 57, 44–50. doi: 10.1016/j.foodres.2014.01.010

Grissa, I., Vergnaud, G., and Pourcel, C. (2007). CRISPRFinder: a web tool to identify clustered regularly interspaced short palindromic repeats. *Nucleic Acids Res.* 35, W52–W57. doi: 10.1093/nar/gkm360

Gu, R. X., Yang, Z. Q., Li, Z. H., Chen, S. L., and Luo, Z. L. (2008). Probiotic properties of lactic acid bacteria isolated from stool samples of longevous people in regions of Hotan, Xinjiang and Bama, Guangxi, China. *Anaerobe* 14, 313–317. doi: 10.1016/j.anaerobe.2008.06.001

Hollenbeck, B. L., and Rice, L. B. (2012). Intrinsic and acquired resistance mechanisms in enterococcus. *Virulence* 3, 421–433. doi: 10.4161/viru.21282

Hussein, W. E., Abdelhamid, A. G., Rocha-Mendoza, D., García-Cano, I., and Yousef, A. E. (2020). Assessment of safety and probiotic traits of *Enterococcus durans* OSY-EGY, isolated from Egyptian artisanal cheese, using comparative genomics and phenotypic analyses. *Front. Microbiol.* 11:608314. doi: 10.3389/fmicb.2020.608314

İspirli, H., Demirbaş, F., and Dertli, E. (2015). Characterization of functional properties of *Enterococcus faecium* strains isolated from human gut. *Can. J. Microbiol.* 61, 861–870. doi: 10.1139/cjm-2015-0446

Jose, N. M., Bunt, C. R., McDowell, A., Chiu, J. Z. S., and Hussain, M. A. (2017). Short communication: a study of *Lactobacillus* isolates' adherence to and influence on membrane integrity of human Caco-2 cells. *J. Dairy Sci.* 100, 7891–7896. doi: 10.3168/jds.2017-12912

Klimko, A. I., Cherdyntseva, T. A., Brioukhanov, A. L., and Netrusov, A. I. (2020). In vitro evaluation of probiotic potential of selected lactic acid bacteria strains. *Probiot. Antimicrob. Proteins* 12, 1139–1148. doi: 10.1007/s12602-019-09599-6

Kook, S. Y., Chung, E. C., Lee, Y., Lee, D. W., and Kim, S. (2019). Isolation and characterization of five novel probiotic strains from Korean infant and children faeces. *PLoS One* 14:e0223913. doi: 10.1371/journal.pone.0223913

Kouhi, F., Mirzaei, H., Nami, Y., Khandaghi, J., and Javadi, A. (2021). Potential probiotic and safety characterisation of *Enterococcus* bacteria isolated from indigenous fermented Motal cheese. *Int. Dairy J.* 126:105247. doi: 10.1016/j.idairyj.2021.105247

Li, B., Zhan, M., Evivie, S. E., Jin, D., Zhao, L., Chowdhury, S., et al. (2018). Evaluating the safety of potential probiotic *Enterococcus durans* KLDS6.0930 using whole genome sequencing and oral toxicity study. *Front. Microbiol.* 9:1943. doi: 10.3389/fmicb.2018.01943

Li, M., Wang, Y., Cui, H., Li, Y., Sun, Y., and Qiu, H. J. (2020). Characterization of lactic acid bacteria isolated from the gastrointestinal tract of a wild boar as potential probiotics. *Front. Vet. Sci.* 7:49. doi: 10.3389/fvets.2020.00049

Li, R., Yu, C., Li, Y., Lam, T. W., Yiu, S. M., Kristiansen, K., et al. (2009). SOAP2: an improved ultrafast tool for short read alignment. *Bioinformatics* 25, 1966–1967. doi: 10.1093/bioinformatics/btp336

Lv, J., Da, R., Cheng, Y., Tuo, X., Wei, J., Jiang, K., et al. (2020). Mechanism of antibacterial activity of *Bacillus amyloliquefaciens* C-1 lipopeptide toward anaerobic *Clostridium difficile*. *Biomed. Res. Int.* 2020:3104613. doi: 10.1155/2020/3104613

Mansour, N. M., Heine, H., Abdou, S. M., Shenana, M. E., Zakaria, M. K., and El-Diwany, A. (2014). Isolation of *Enterococcus faecium* NM113, *Enterococcus faecium* NM213 and *Lactobacillus casei* NM512 as novel probiotics with immunomodulatory properties. *Microbiol. Immunol.* 58, 559–569. doi: 10.1111/1348-0421.12187

Martino, G. P., Espariz, M., Gallina Nizo, G., Esteban, L., Blancato, V. S., and Magni, C. (2018). Safety assessment and functional properties of four *Enterococci* strains isolated from regional Argentinean cheese. *Int. J. Food Microbiol.* 277, 1–9. doi: 10.1016/j.ijfoodmicro.2018.04.012

Masco, L., Crockaert, C., Van Hoorde, K., Swings, J., and Huys, G. (2007). In vitro assessment of the gastrointestinal transit tolerance of taxonomic reference strains from human origin and probiotic product isolates of Bifidobacterium. *J. Dairy Sci.* 90, 3572–3578. doi: 10.3168/jds.2006-548

Maturana, P., Martinez, M., Noguera, M. E., Santos, N. C., Disalvo, E. A., Semorile, L., et al. (2017). Lipid selectivity in novel antimicrobial peptides: implication on antimicrobial and hemolytic activity. *Colloids Surf. B Biointerf.* 153, 152–159. doi: 10.1016/j.colsurfb.2017.02.003

McArthur, A. G., Waglechner, N., Nizam, F., Yan, A., Azad, M. A., Baylay, A. J., et al. (2013). The comprehensive antibiotic resistance database. *Antimicrob. Agents Chemother.* 57, 3348–3357. doi: 10.1128/aac.00419-13

Muñoz-Provencio, D., Llopis, M., Antolín, M., de Torres, I., Guarner, F., Pérez-Martínez, G., et al. (2009). Adhesion properties of *Lactobacillus casei* strains to resected intestinal fragments and components of the extracellular matrix. *Arch. Microbiol.* 191, 153–161. doi: 10.1007/s00203-008-0436-9

Nami, Y., Abdullah, N., Haghshenas, B., Radiah, D., Rosli, R., and Yari Khosroushahi, A. (2014). A newly isolated probiotic *Enterococcus faecalis* strain from vagina microbiota enhances apoptosis of human cancer cells. *J. Appl. Microbiol.* 117, 498–508. doi: 10.1111/jam.12531

Nami, Y., Panahi, B., Jalaly, H. M., Bakhshayesh, R. V., and Hejazi, M. A. (2020). Application of unsupervised clustering algorithm and heat-map analysis for selection of lactic acid bacteria isolated from dairy samples based on desired probiotic properties. *LWT Food Sci. Technol.* 118:108839. doi: 10.1016/j.lwt.2019.108839

Nueno-Palop, C., and Narbad, A. (2011). Probiotic assessment of *Enterococcus faecalis* CP58 isolated from human gut. *Int. J. Food Microbiol.* 145, 390–394. doi: 10.1016/j.ijfoodmicro.2010.12.029

O'Driscoll, T., and Crank, C. W. (2015). Vancomycin-resistant enterococcal infections: epidemiology, clinical manifestations, and optimal management. *Infect. Drug Resist.* 8, 217–230. doi: 10.2147/idr.S54125

Popović, N., Dinič, M., Tolinaèki, M., Mihajlović, S., Terzić-Vidojević, A., Bojić, S., et al. (2018). New insight into biofilm formation ability, the presence of virulence genes and probiotic potential of *Enterococcus sp*. dairy isolates. *Front. Microbiol.* 9:78. doi: 10.3389/fmicb.2018.00078

Popović, N., Djokić, J., Brdarić, E., Dinić, M., Terzić-Vidojević, A., Golić, N., et al. (2019). The influence of heat-killed *Enterococcus faecium* BGPAS1-3 on the tight junction protein expression and immune function in differentiated Caco-2 cells infected with *Listeria monocytogenes* ATCC 19111. *Front. Microbiol.* 10:412. doi: 10.3389/fmicb.2019.00412

Rodríguez, J. M., Murphy, K., Stanton, C., Ross, R. P., Kober, O. I., Juge, N., et al. (2015). The composition of the gut microbiota throughout life, with an emphasis on early life. *Microb. Ecol. Health Dis.* 26:26050. doi: 10.3402/mehd.v26.26050

Scarpellini, E., Campanale, M., Leone, D., Purchiaroni, F., Vitale, G., Lauritano, E. C., et al. (2010). Gut microbiota and obesity. *Intern. Emerg. Med.* 5(Suppl. 1), S53–S56. doi: 10.1007/s11739-010-0450-1

Starke, I. C., Zentek, J., and Vahjen, W. (2015). Effects of the probiotic *Enterococcus faecium* NCIMB 10415 on selected lactic acid bacteria and enterobacteria in co-culture. *Benef. Microb.* 6, 345–352. doi: 10.3920/bm2014.0052

Strompfová, V., Lauková, A., and Ouwehand, A. C. (2004). Selection of *Enterococci* for potential canine probiotic additives. *Vet. Microbiol.* 100, 107–114. doi: 10.1016/j.vetmic.2004.02.002

Tsai, H. Y., Liao, C. H., Chen, Y. H., Lu, P. L., Huang, C. H., Lu, C. T., et al. (2012). Trends in susceptibility of vancomycin-resistant *Enterococcus faecium* to tigecycline, daptomycin, and linezolid and molecular epidemiology of the isolates: results from the Tigecycline In vitro surveillance in Taiwan (TIST) study, 2006 to 2010. *Antimicrob. Agents Chemother.* 56, 3402–3405. doi: 10.1128/aac.00533-12

Wang, J., Da, R., Tuo, X., Cheng, Y., Wei, J., Jiang, K., et al. (2020). Probiotic and safety properties screening of *Enterococcus faecalis* from healthy Chinese infants. *Probiot. Antimicrob. Proteins* 12, 1115–1125. doi: 10.1007/s12602-019-09625-7

Yang, J. X., Li, T., Ning, Y. Z., Shao, D. H., Liu, J., Wang, S. Q., et al. (2015). Molecular characterization of resistance, virulence and clonality in vancomycin-resistant *Enterococcus faecium* and *Enterococcus faecalis*: a hospital-based study in Beijing, China. *Infect. Genet. Evol.* 33, 253–260. doi: 10.1016/j.meegid.2015.05.012

Zankari, E., Hasman, H., Cosentino, S., Vestergaard, M., Rasmussen, S., Lund, O., et al. (2012). Identification of acquired antimicrobial resistance genes. *J. Antimicrob. Chemother.* 67, 2640–2644. doi: 10.1093/jac/dks261

Zhang, F., Jiang, M., Wan, C., Chen, X., Chen, X., Tao, X., et al. (2016). Screening probiotic strains for safety: evaluation of virulence and antimicrobial susceptibility of *Enterococci* from healthy Chinese infants. *J. Dairy Sci.* 99, 4282–4290. doi: 10.3168/jds.2015-10690

Zheng, W., Zhang, Y., Lu, H. M., Li, D. T., Zhang, Z. L., Tang, Z. X., et al. (2015). Antimicrobial activity and safety evaluation of *Enterococcus faecium* KQ 2.6 isolated from peacock feces. *BMC Biotechnol.* 15:30. doi: 10.1186/s12896-015-0151-y

Conflict of Interest: The authors declare that the research was conducted in the absence of any commercial or financial relationships that could be construed as a potential conflict of interest.

Publisher's Note: All claims expressed in this article are solely those of the authors and do not necessarily represent those of their affiliated organizations, or those of the publisher, the editors and the reviewers. Any product that may be evaluated in this article, or claim that may be made by its manufacturer, is not guaranteed or endorsed by the publisher.

frontiers in Microbiology

ORIGINAL RESEARCH
published: 17 December 2021
doi: 10.3389/fmicb.2021.760385

A Rapid Screening Method of Candidate Probiotics for Inflammatory Bowel Diseases and the Anti-inflammatory Effect of the Selected Strain *Bacillus smithii* XY1

Xuedi Huang, Fang Ai, Chen Ji, Pengcheng Tu, Yufang Gao, Yalan Wu, Fujie Yan and Ting Yu**

National Engineering Laboratory of Intelligent Food Technology and Equipment, College of Biosystems Engineering and Food Science, Zhejiang University, Hangzhou, China

OPEN ACCESS

Edited by:
Martin Schwarzer, Academy of Sciences of the Czech Republic (ASCR), Czechia

Reviewed by:
Jose Luiz De Brito Alves, Federal University of Paraíba, Brazil
Daniela Pinto, Giuliani S.p.A., Italy

***Correspondence:**
Ting Yu
yuting@zju.edu.cn
Fujie Yan
fjyan@zju.edu.cn

Specialty section:
This article was submitted to Food Microbiology, a section of the journal Frontiers in Microbiology

Received: *18 August 2021*
Accepted: *18 November 2021*
Published: *17 December 2021*

Citation:
Huang X, Ai F, Ji C, Tu P, Gao Y, Wu Y, Yan F and Yu T (2021) A Rapid Screening Method of Candidate Probiotics for Inflammatory Bowel Diseases and the Anti-inflammatory Effect of the Selected Strain Bacillus smithii XY1. Front. Microbiol. 12:760385. doi: 10.3389/fmicb.2021.760385

Inflammatory bowel disease (IBD) is a chronic intestinal disease associated with the inflammatory gastrointestinal tract and microbiome dysbiosis. Probiotics are a promising intervention, and several probiotics have been reported to positively affect IBD remission and prevention, particularly on ulcerative colitis (UC). However, there is still a limitation in the knowledge of effectiveness and safety of probiotics therapies for IBD. Exploring more potential probiotics helps to find extensive evidence for probiotic intervention. This study established a rapid method for probiotics candidate screening and finally screened out one strain with the best protective effect. Forty strains isolated from four different sources were used for this screening. Hemolysis tests and acute toxic test evaluated strain safety. Zebrafish were first treated with dextran sodium sulfate (DSS) for colitis induction, and every bacteria were individually added to the fish water subsequently. Results showed eight strains could lower the larvae mortality within 3 days under a 0.6% DSS concentration, including *Lacticaseibacillus rhamnosus* GG, *L. rhamnosus* NBRC3425, *Bacillus smithii* DSM4216, *B. smithii* XY1, *Bacillus coagulans* NBRC12583, *Bacillus coagulans* XY2, *Lactobacillus parafarraginis* XYRR2, and *Bacillus licheniformis* XYT3. Among eight, *B. smithii* XY1 was the only strain having the equal ability to alleviate neutrophil infiltration in the larvae intestine with that ability of prednisolone under a 0.5% DSS concentration. *Bacillus smithii* XY1 restored intestinal epithelial cell integrity after DSS damage, as well as regulated the gene expression inflammation-related factors, indicating its bio-function of inflammatory response alleviation.

Keywords: inflammatory bowel disease, ulcerative colitis, probiotics, *Bacillus smithii*, lactic acid bacteria, zebrafish

INTRODUCTION

Inflammatory bowel diseases (IBD), types of chronic intestinal diseases characterized by immune-mediated intestinal inflammation of the gastrointestinal tract, affect millions of people every year (Ng et al., 2017). In recent decades, an increasing incidence rate has been characterized in newly industrialized countries, especially those transforming a western lifestyle, indicating

that IBD has become a global disease in the 21st century (Ananthakrishnan et al., 2020). Due to the burden of the continuous rising IBD cases and growing health care costs, future therapeutics are suggested to achieve sustained durability of benefit and prevention and global sustainability, which is cost-effective, safe, and simple (Ananthakrishnan et al., 2020).

Probiotics are considered experimental interventions for functional symptoms of IBD (Colombel et al., 2019). Until now, the cause of the disease has still been hard to clarify. However, dysbiosis in the microbiota, mucosal immune system, and genetic factors play essential parts in the IBD's pathogenesis (Fritsch and Abreu, 2019). Normal intestinal microbial flora is vital for the host to maintain the gut's well-being and integrity of gut immunity (Zareef et al., 2020). In human subjects, the gut microbiome is different in patients with IBD compared with that in healthy control subjects (Glassner et al., 2020). The alteration of normal gut microbiota in the patients contributes to IBD incidence (Zareef et al., 2020). The host-microbial relationships lead to a sight of viable therapeutic approaches (Ni et al., 2017). Fecal microbiota transplantation (FMT) has been proved available not only in *Clostridium difficile* infection but also in some IBD clinical trials (Friedman et al., 2014; Browne and Kelly, 2017). Further evidence is needed before FMT or probiotics could be used in practice treatment, and probiotic or prebiotic therapies could be the next step (Friedman et al., 2014).

Contrary to most other therapeutics, multiple agent interventions in probiotics therapy show a low risk of harm (Colombel et al., 2019). Probiotics have succeeded widely in several IBD cases, especially in ulcerative colitis (UC), one of the two main entities of IBD (Basso et al., 2018). According to two double blind trials and mice model experiments, *Escherichia coli* Nissle 1917 has the equal ability of remission and prevention with mesalamine (Kruis et al., 1997; Rembacken et al., 1999; Kruis et al., 2004; Souza et al., 2020). Multiple lactic acid bacteria (LAB) and probiotic mixture also show positive effects, like *Lactobacillus acidophilus*, *Lacticaseibacillus rhamnosus* GG, *Bifidobacterium longum* 536, and VSL#3 (Zocco et al., 2006; Sood et al., 2009; Tursi et al., 2010; Wildt et al., 2011; Tamaki et al., 2016). Some strains have succeeded in some cases, while some strains are reported failed in clinical UC trials. The conclusion that extensive probiotics have beneficial effects on IBD patients is still controversial (Ng et al., 2010; Petersen et al., 2014). These failures suggest that the functional properties may be strain determined, encouraging establishment of new probiotics screening work and efficient methods for evaluating functions of different strains (Geier et al., 2007). Most research focuses on verifying the function of familiar strains like VSL#3 or *E. coli* Nissle (Kruis et al., 2004; Sood et al., 2009; Matthes et al., 2010). However, beneficial bacteria could come from various resources like food, air, soil, and animals (Zielińska and Kołożyn-Krajewska, 2018), though probiotics are initially believed to originate from the gastrointestinal tract of a healthy individual (Guarner et al., 2005). This study tried to isolate a wider range of anti-inflammatory bacteria from diverse resources, especially fermented foods. Fermented foods are promising bio-resources, especially those rich in multiple LAB. LAB are one of the most popular probiotics pools of probiotic therapies for diseases. For example, *Lactobacillus* and *Bifidobacterium* have been proved to be effective in clinical trials. So we used one commercialized probiotic, *L. rhamnosus* GG, to compare with the effect of other isolated strains on IBD improvement.

Multiple processing is required to finally define a microbe as a probiotic (Pereira et al., 2018). *In vitro* and *in vivo* safety test is the first step (Sanders et al., 2010). Using high-throughput experimental animal models with low cost is encouraged in screening lots of bacteria. Zebrafish has become one of the most common vertebrate models in cellular microbiology because of its benefits such as high throughput and ease of operation with simple immersion (Flores et al., 2020). The zebrafish gastrointestinal (GI) systems are highly homologous in functions and genes with the mammalian GI system. Over 100 IBD susceptibility genes found in IBD and zebrafish share homologous genes like NOD1, NOD2, e-cadherin, hnf4a, and ttc7a, suggesting it is a suitable animal model (Oehlers et al., 2011; Jostins et al., 2012; Zhao et al., 2018). Intestinal epithelial damage induced by chemical dextran sodium sulfate (DSS) mimics one of the critical features of IBD pathology. A DSS-induced IBD zebrafish model successfully represents the neutrophils infiltration at a medium 0.5% DSS concentration and high mortality at a high 0.6% DSS concentration (Oehlers et al., 2013, 2017). Acute mortality and the level of colitis inflammation set a scale for evaluating strains' effectiveness.

In this study, we constructed a rapid isolating and screening method to efficiently isolate novel strains and expand the probiotics library for IBD remission or prevention. One novel strain with the best protective effect was discovered and underlying mechanisms were further investigated.

MATERIALS AND METHODS

Bacterial Strains and Culture

Bacteria Strains and Culture

Forty *Bacillus* strains and LAB strains newly isolated and preserved in the laboratory were used. Twenty-one strains were isolated from fermented coffee grounds in Hangzhou, China. Seven strains were introduced by China Center of Industrial Culture Collection (CICC). Four strains were introduced by China General Microbiological Culture Collection Center (CGMCC). Three strains were isolated from dairy products and four from an "Effective Microorganisms" EM bacteria product (**Supplementary Table S1**). The isolation method is described in **Supplementary Table S1**. *Lactobacillus rhamnosus GG*, a strain widely used as a commercialized probiotic, was used as the reference strain.

Culture of Strains

Strains were grown for 18 h in suitable media and conditions in which they were isolated (**Supplementary Table S1**). All of the bacteria were subcultured three times before their use in the experiments. The bacterial broth was centrifuged at 12,000 rpm for 1 min at 4°C. Then, the precipitation was washed

twice and resuspended with sterile PBS buffer. The suspension concentration was calculated with the Helber bacteria counting chamber (Auvon Helber Thoma; Rea et al., 2015, pp. 127–128).

Identification of the Strains by 16S-rRNA

Genomic DNA of the novel bacteria was extracted with TaKaRa No.9164, Japan, and 16S rRNA gene was amplified with Vazyme 2 x Phanta Max Master Mix, China. Sanger sequencing was conducted through the commercial service of Qingke, China. Gene sequences were analyzed in the BLAST Gene database. Phylogenetic analysis was constructed based on the 16S rRNA gene sequence through the neighbor-joining method by MEGA X software. The phylogenetic tree was plotted using EvolView.[1] The 16S rRNA sequences have been deposited under GenBank NCBI (accession numbers and all strains used are shown in **Supplementary Table S2**). The number on a branch is the bootstrap value that indicates the extent of relatedness between two subjects.

Zebrafish Manipulations

Adult zebrafish lines wild-type (WT: TU) and Tg (mpx:eGFP^{il14}) were from core facilities, Zhejiang University school of medicine (CFZSM), and were kept there at a 14:10 light: dark cycle at 28°C. Fertilized embryos collected following natural spawning were cultured at 28.5°C in E3 water (5 mM NaCl, 0.17 mM KCl, 0.33 mM $CaCl_2$, and 0.33 mM $MgSO_4$) containing methylene blue (0.002 g/L). To observe fluorescent better at Tg (mpx:eGFP^{il14}) fish line, an additional 75 μM 1-phenyl 2-thiourea was added into E3 water 24 h post-fertilization to prevent the pigment-cell formation. Methylene blue was removed 1 day before live imaging. Batches of 200 larvae were kept in sterile fish boxes in 80 ml E3 water, which was changed every day to 3 days post-fertilization (dpf). The Zhejiang University Laboratory Animal Center approved the protocols.

The protocol of DSS-induced intestine injury models was adapted and modified from Oehlers et al. (2013) and Chuang et al. (2019, p. 7). Fresh 0.6 and 0.5% (w/v) colitis grade DSS (36,000–50,000 MW) was prepared to induce high and medium levels of enterocolitis of 3 dpf larvae. All analyses were performed at 6 dpf unless otherwise noted.

Safety Assessment of Strains

Hemolysis tests were used to do *in vitro* safety evaluation of the strains. Colonies were streaked on blood agar (10 g/L of tryptone, 10 g/L of NaCl, and 5 g/L of yeast extract; 100 ml/L of sterile defibrinated sheep blood was added after sterilization of the other medium components) plates with aseptic processing. Results were observed after 24 h of cultivation. γ hemolysis (lack of hemolysis; Savardi et al., 2018) means safe. For the *in vivo* safety test, the bacteria virulence assessment adapted from Ran et al. (2018, p. 3452) was done. Zebrafish larvae (4 dpf) were placed into 12-well plate (10 larvae per well) with 2 ml bacteria suspension (concentration of 1×10^6 CFU/ml) of each bacteria strain for 3 days. *Escherichia coli* DH5α was used as a negative control. The larvae mortality was recorded after 3 days. Dead fish were removed from the wells during the experiments. Each experiment had three biological replications.

Bacteria Screening

Each strain's liquid culture was diluted into the same OD_{600} aseptically. Then, 100 μl of the culture dilution was inoculated into a 5 ml medium. After incubation, one strain with the highest final OD_{600} was selected from strains belonging to the same species isolated from the same sample. The strain culture was prepared at a concentration of 1×10^6 CFU/ml. Prednisolone, an anti-inflammatory drug commonly prescribed for IBD treatment, was used as a positive control. Batches of 10 TU 3 dpf larvae were placed into each well (24-well plate) at a total volume of 2 ml 0.6% DSS E3 water with a final bacteria concentration of 1×10^6 CFU/ml or 25 μg/ml positive drug prednisolone. A hit was defined as the higher mean value of survival compared to water control group. All first-round hits were rescreened with an inflammation assessment. Batches of 6 Tg (mpx:EGFP)^{i114} 3 dpf larvae were placed into 0.5% DSS E3 water. After 2 days of incubation, the 5 dpf larvae were washed with E3 water once and placed into bacteria or prednisolone dilution (same final concentration as above) for 24 h. The significant reduction of neutrophils infiltration was defined as a hit.

Gene Expression Analysis

Total RNA used for real-time PCR from dissected intestines was isolated using RNAiso Plus (TaKaRa, Japan). Six larvae were used for one RNA extract. cDNA synthesis was performed using Prime Script™ RT reagent Kit with gDNA Eraser (TaKaRa, Japan). Real-time PCR was performed with the SYBR green method using TB Green Premix Ex Taq™ (TaKaRa, Japan). Triplicate PCRs were carried out for each sample analyzed. The data obtained were analyzed using StepOne Software v2.3. Modification of gene expression is reported concerning the control sample. The relative abundance of mRNA was determined by normalization to rpl13 levels, and the results were expressed as relative expression levels. The data were quantified by the comparative threshold cycle (ΔΔCt) method.

The primer sequences are rpl13 forward TCTGGAGGAC TGTAAGAGGTATGC, rpl13 reverse TCAGACGCACAATCTT GAGAGCAG, IL-1β forward GAGACAGACGGTGCTGTTTA, IL-1β reverse GTAAGACGGCACTGAATCCA, TNF-α forward CAGAGTTGTATCCACCTGTTA, TNF-α reverse TTCACGCT CCATAAGACCCA, IL-6 forward TCAACTTCTCCAGCGT GATG, IL-6 reverse TCTTTCCCTCTTTTCCTCCTG, NOD2 forward AGTTTCTGGGATTATGGGGT, an NOD2 reverse ACTGCCCACACCATTATCCA (Qin et al., 2018; Yi et al., 2019).

Analysis of Neutrophilic Infiltration by Live Imaging

Six dpf larvae were anesthetized with 120 μg/ml tricaine for 30 s, mount larvae in 3% (w/v) methylcellulose for live imaging by epifluorescent microscopy (Oehlers et al., 2013). Inflammation

[1]https://www.evolgenius.info/evolview/

level was indicated by the number of neutrophils congested in the intestine. Fluorescent neutrophils around the larval intestine were enumerated by manual counting. Larvae images were taken using a Nikon SMZ18 stereoscope.

Hematoxylin and Eosin Staining

Zebrafish larvae were fixed in 4% paraformaldehyde overnight at 4°C and then dehydrated and embedded according to standard protocols. Transverse sections were prepared with LEICA RM2235 paraffin slicing machine and stained by auto Hematoxylin and Eosin (H&E) staining with Thermo GEMINI AS.

Statistical Analysis

All analyses were performed using IBM SPSS Statistics 22. Differences were considered statistically significant when at $p < 0.05$. The mean ± SEM are used to display data. Neutrophil quantification data were analyzed using one-way ANOVA. RT-PCR data were analyzed using two-tailed Student's *t*-tests for comparisons between the control group with other groups.

RESULTS

Construction of a Strain Library

The strains isolation strategy and the potential probiotics strain library were constructed as the implementation:

a. Bacteria isolation (**Figure 1**). More strains and more sources need to be considered. In this study, 29 novel strains were isolated from food samples (e.g., dairy products and fermented coffee grounds) and EM products (product contains multiple bacteria for agricultural usage; **Table 1**). Eleven other commercialized strains (from culture centers) were also included in the preliminary strain library.

b. Hemolysis test. Safety assessment of potential probiotics is vital. Hemolysis-positive strains are considered to have safety risks. In very rare immunosuppression, chronic diseases, or surgical interventions cases, several LAB strains of *L. rhamnosus* and some other *Lactobacillus* species, which caused human infection were detected to be hemolysis positive (Baumgartner et al., 1998; **Figure 1**). Among the preliminary strain library, 34 strains were hemolysis-negative (γ-lysis). The other six strains were hemolysis-positive (α-lysis or β-lysis; **Table 1**). All food samples and EM product isolates were hemolysis-negative, while nearly half of the strains from the culture centers were hemolysis-positive.

c. Acute toxic test. Being proved *in vivo* safety is another requirement of probiotics for medicine and food use. The high throughput zebrafish larvae model, a time-efficient and low-cost *in vivo* vertebrate model, was used to evaluate each strain's virulence (**Figure 1**). Three-day exposure to 1×106 CFU/ml bacteria suspension of eight strains from coffee grounds resulted in larvae death. Other strains resulted in no mortality at the concentration of 1×10^6 CFU/ml. The number of candidate strains in the lists was reduced to 26.

d. Growth ability test. All strains found *in vitro* and *in vivo* safety in this study were sequenced based on 16S rRNA. Most novel strains belonged to the genus *Lactobacillus* and *Bacillus*. Several new isolates from the same sample were also identified as the same species (**Figure 2**). These were defined as one group. One strain with the highest final concentration (represented by OD_{600}) after incubation among the group was particularly picked out as a representative strain (**Figures 1, 2**). Strains with higher growth ability are prone to be easier to be commercialized. After the test, the probiotic strains in the library were reduced from 26 to 18. They are four from EM products, six from coffee grounds, five from culture center, and three from dairy products.

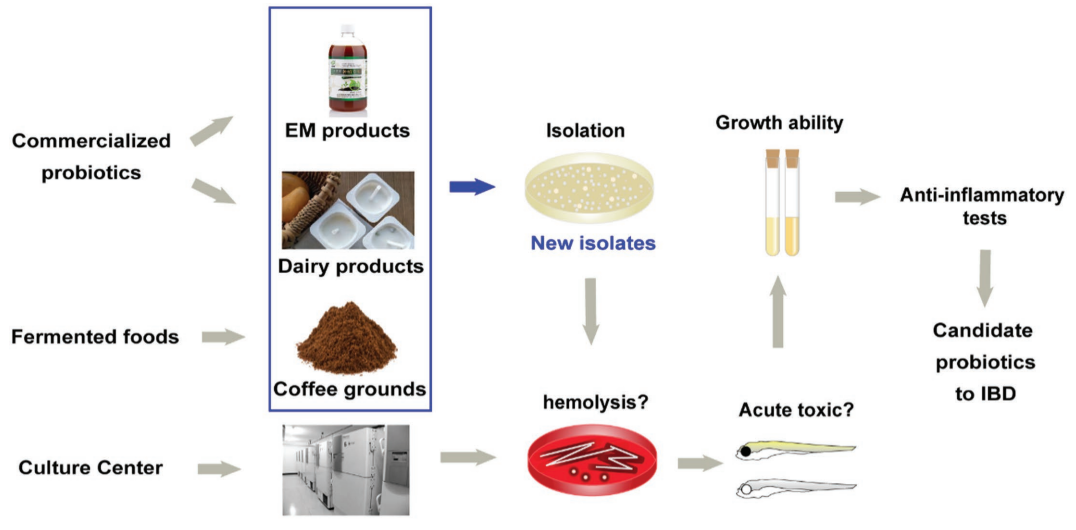

FIGURE 1 | Source of strains and the screening method of candidate probiotics for inflammatory bowel diseases.

TABLE 1 | Result of *in vivo* and *in vitro* safety assessment of strains.

Source	Strain ID	Hemolysis tests	Acute toxicity (survival %)
Coffee grounds	XY1	–	100 ± 0
	XY2	–	100 ± 0
	XY3	–	100 ± 0
	XY4	–	100 ± 0
	XY5	–	100 ± 0
	XY6	–	100 ± 0
	XY7	–	100 ± 0
	XY8	–	100 ± 0
	XY9	–	100 ± 0
	XY10	–	100 ± 0
	XY11	–	100 ± 0
	XY12	–	3 ± 1
	XY13	–	3 ± 1
	XY14	–	3 ± 1
	XY15	–	3 ± 1
	XY16	–	100 ± 0
	XY17	–	90 ± 0
	XY18	–	90 ± 0
	XY19	–	90 ± 2
	XY20	–	73 ± 3
	XY21	–	100 ± 0
	XY22	–	100 ± 0
Culture Collection	LGG	–	100 ± 0
	CICC 20022	–	100 ± 0
	NBRC 3425	–	100 ± 0
	CICC 10309	+	–
	CICC 23632	+	–
	CGMCC 1.4261	+	–
	CICC 10580	+	–
	CICC 23057	+	–
	CICC 10061	+	–
	NBRC 12583	–	100 ± 0
	DSM 4216	–	100 ± 0
EM product	XYB	–	100 ± 0
	XYR	–	100 ± 0
	XYT3	–	100 ± 0
	XYT2	–	100 ± 0
Fermented dairy product	XYRR3	–	100 ± 0
	XYRR2	–	100 ± 0
	XYHYN	–	100 ± 0

Strains Screening for Mortality Reduction of Acute Colitis

The DSS-induced zebrafish acute colitis model has a dose-effect relationship for different mortality levels and intestinal inflammation (Oehlers et al., 2013). A high concentration of 0.6% DSS was first added to record the survival of larvae because acute mortality is more straightforward to observe than live imaging (**Figure 3A**). The 0.6% DSS dose results in 62.5% mortality in larvae after 3 days of exposure (**Figure 3B**). Prednisolone, the commercial drug for the treatment of IBD, reduces the mortality of larvae. The first anti-inflammatory test identified eight hits with higher survival and causing no malformation of larvae compared to the negative control, namely, *L. rhamnosus GG*, *B. smithii* DSM4216, *B. smithii* XY1, *L. parafarraginis* XYRR2, *L. rhamnosus* NBRC3425, *B.s coagulans* NBRC 12583, *B. coagulans* XY2, and *B. licheniforms* XYT3. Other strains may have side effects like edema (or different deformation results) or severe toxicity, causing greater mortality. Among them, two strains (*L.s plantarum* CICC20022 and *B. subtilis* XYT2) independently caused malformations. One strain (*B. subtilis subsp.* CICC20643) increased mortality. Furthermore, six strains (*L. paracasei* XYRR3, *B. licheniformis* XY16, *L. lactis subsp. hordniae* XYR, *L. buchneri* XYB, *B. coagulans* XYHYN, and *B. subtilis* XY12) caused both side effects (**Figure 3B**).

Effects of Different Strains on Medium Intestinal Inflammation Alleviation

The eight hits from the first anti-inflammatory test were subsequently further screened. Larvae were kept under a condition at a lower concentration of 0.5% DSS, which caused lower mortality (less than 2%) and a medium level of intestinal inflammation (**Figure 4A**). The localization of neutrophils in the intestine was assessed by live imaging of Tg (mpx:EGFP)^{i114} larvae (**Figure 4B**). Among the strains that increased the survival rate of zebrafish damaged by a relatively high dose DSS, *Bacillus smithii* XY1 was the only one to significantly reduce neutrophil mobilization. Its improvement effect is equivalent to prednisolone (**Figure 4C**). Other strains have no significant impact on inflammation alleviation.

Bacillus smithii XY1 Rescues Abnormal Intestinal Features in the IBD Zebrafish Model

Exposure to DSS for 2 days has been documented to cause gross changes to intestinal morphology. Zebrafish sections were taken longitudinally along the zebrafish mid and posterior segments of the 6 dpf larval intestines. Sections were assessed for villus structure, a clear and discernable epithelial monolayer, intestinal epithelial cell integrity, and the presence of mature goblet cells with large secretory vesicles (Jardine et al., 2019). Abnormal intestinal phenotypes, such as shorter and thinner villi, were observed in the DSS-induced model, resulting in apparent gaps. Other abnormal intestinal phenotypes include smaller goblet cells and signs of apoptosis (**Figure 5A**). Rescue of these changes with *B. smithii* XY1 and prednisolone was observed.

Bacillus smithii XY1 Effects on Disturbed Innate Immune Genes Expression

Expression levels of the inflammatory cytokine gene IL-1β and TNF-α in the DSS group were significantly higher than in the negative control. The expression of the two genes was not significantly different in *B. smithiii* XY1, LGG, and prednisolone intervention compared with the control (**Figure 5B**). IL-6 gene expression was not significantly different in the treatment groups and the control group. NOD2 is a vital gene that is closely related to IBD pathogenesis. The NOD2 gene was highly expressed in the DSS group but similarly expressed in *B. smithiii* XY1, LGG, and prednisolone intervention groups. Though the TNF-α and NOD2 gene expression of the *B. smithiii* XY1 group was not significantly different from and LGG group,

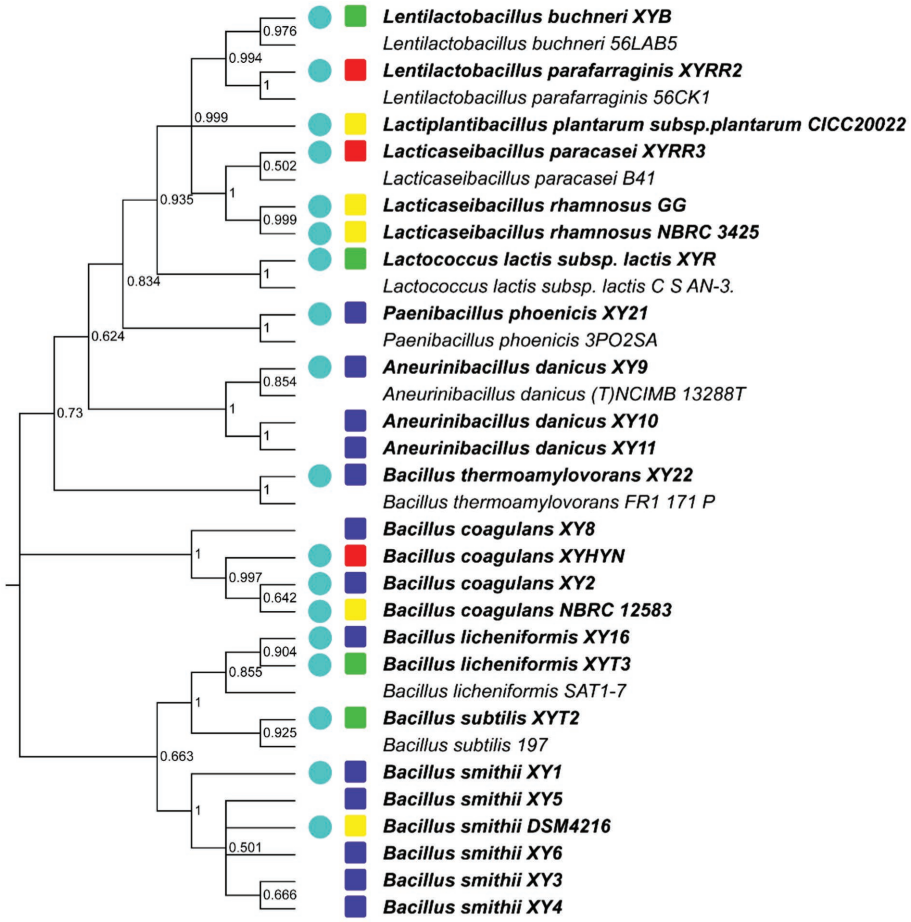

FIGURE 2 | Phylogenetic relatedness of 16S rRNA between *in vivo* and *in vitro* safe strains isolated from different sources. Bold fonts mean strains used in this test. The circle indicates that the strain has the best growth ability from the same species and is isolated from the same sample. The colors of squares represent the sources of strains. Green, EM products; Red, dairy products; Yellow, culture centers; and Blue, coffee grounds.

the mean of the LGG group is higher than the mean of the *B. smithii* XY1 group, which may relate to the result of the difference in **Figure 4C**.

DISCUSSION

A rapid and preliminary bacteria screening approach for IBD remission was designed for this work. The methodology involves six main steps: isolation, hemolysis test, acute toxic test, growth ability test, lethality reduction test for acute colitis, and reducing inflammation test. It takes care of both safety and function, and more safety assessments should be included in the screening process when considering uncommon bacteria species (Pereira et al., 2018). The approach is exceptionally suitable for labs possessing zebrafish infrastructure. Screening work, especially the acute toxic and anti-inflammatory tests, consumes many model animals. The high-throughput characteristic of the zebrafish larvae model meets the need. When we were conducting the methodology, coffee grounds were presented to be a promising bio-resource. Among the 22 novel strains isolated from coffee grounds, 14 were proven preliminary *in vitro* and *in vivo* safe, and 50% of best-grown strains passed the first screening to reduce acute colitis mortality. Although only *Bacillus smithii* XY1 isolated from coffee grounds passed the final screening, others are still worth further exploitation, especially those Generally Recognized as Safe (GRAS) or the qualified presumption of safety (QPS) recommended strains. *Baciillus smithii* XY1 also shows good tolerance to acid, especially bile (**Supplementary Figure S1**), suggesting that *Bacillus smithii* XY1 is prone to survive well in the intestine environment. It is better to include the acid and bile tolerance assessment after the growth ability test, but it is unnecessary. Live or dead bacteria may both have functions.

As a food-originated bacteria pool, dairy products present one strain of *L. parafarraginis* XYRR2, reducing mortality of acute colitis. EM products and their bacteria may not be suitable for anti-inflammation use because no strain from EM products presents effectiveness in the final two screening steps. This study also suggests fermented foods are treasuries for finding new IBD remission probiotics, though the number of tested sample strains was limited. Searching for candidates in a culture

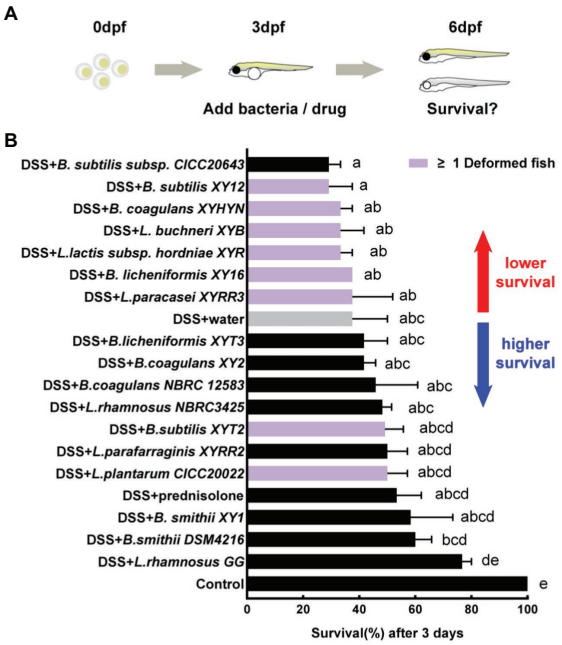

FIGURE 3 | First hits on reducing mortality of acute colitis. **(A)** Schematic depicts the screening methodology to reduce the mortality of 0.6% dextran sodium sulfate (DSS) induced acute colitis. **(B)** Survival of larvae after 1-day immersion of bacteria suspension, data are presented as mean ± SEM, $n \geq 8$ biologically independent animals from three independent experiments. Strain is considered an effective candidate when the mean survival rate exceeds water control (gray). Values indicated by the bars with different letters are significantly different ($p < 0.05$, one-way ANOVA).

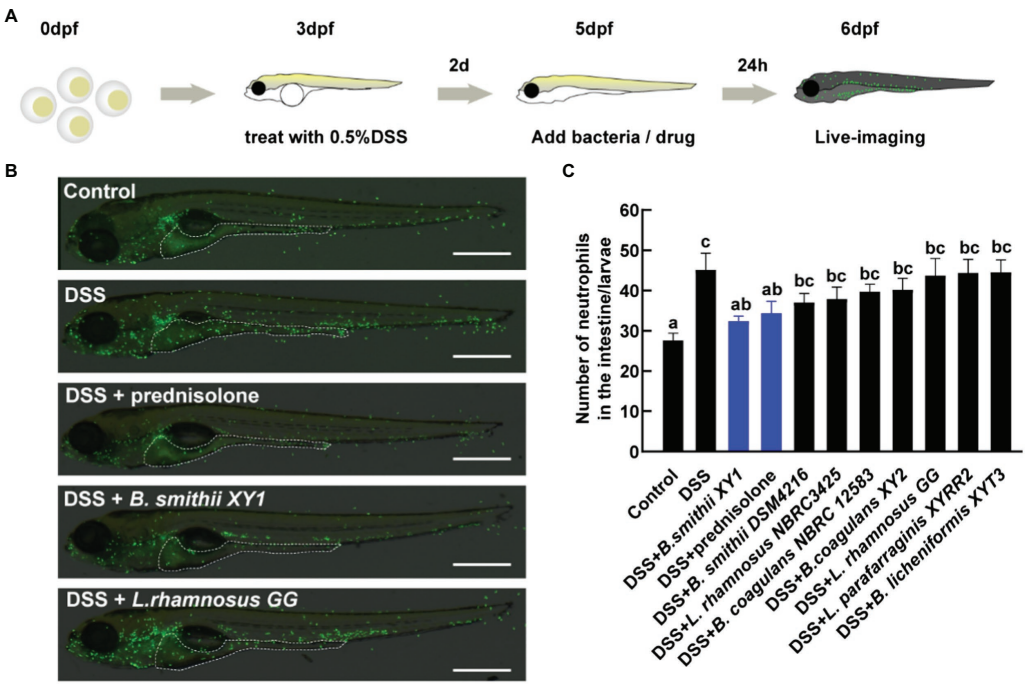

FIGURE 4 | Second hits on reducing intestinal inflammation. **(A)** Schematic depicts the screening methodology to suppress neutrophilic inflammation. **(B)** Representative images of live imaging in 6 days post-fertilization (dpf) Tg (mpx:EGFP)^{i114} larvae exposed to 0.5% DSS at 3 dpf and treated with a drug and bacteria at 5 dpf. The area of the intestine is illustrated by a white dotted line, scale bars, 500 μm. **(C)** The number of neutrophils in the intestine per larvae, data are presented as mean ± SEM. Values indicated by the bars with different letters are significantly different ($p < 0.05$, one-way ANOVA). $n \geq 8$ biologically independent animals from three independent experiments.

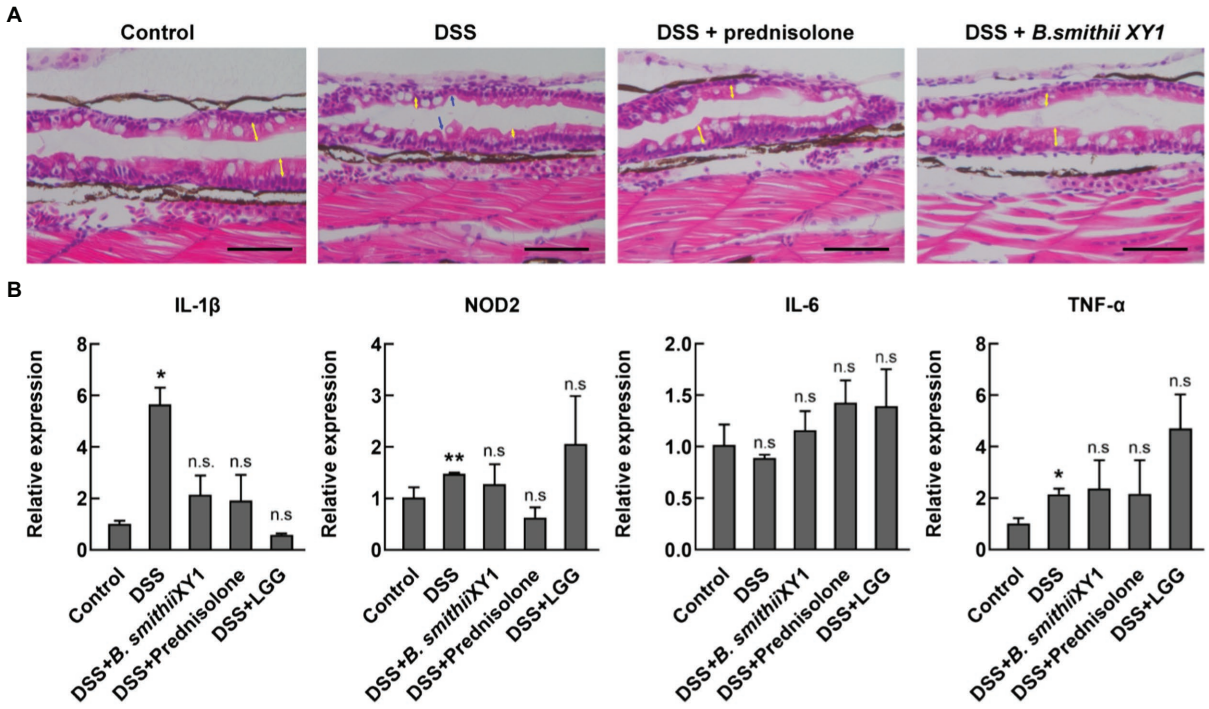

FIGURE 5 | *Bacillus smithii* XY1 protects the intestine epithelium. **(A)** Hematoxylin and eosin (H&E) staining of a longitudinal section of zebrafish larvae intestine, scale bars, 50 μm, and yellow arrows indicate the length of the villi. Blue arrows indicate obvious gaps because of the thinner mucosal layer. **(B)** The mRNA level of immune-related genes including IL-1β, NOD2, IL-6, and TNF-α in the 6 dpf larvae. Data are presented as mean ± SEM. $^{*}p < 0.05$ and $^{**}p < 0.01$, analyzed by two-tail test. Every character represents the significance of a treatment group compared to the control group. $n = 6$ from three independent experiments.

center is also a good option. Bacteria from the culture centers may be another probable candidate probiotic resource for IBD remission, particularly LAB species like *L. rhamnosus*, *B. smithii*, and *B. coagulans*, except some *L. licheniformis* strains. Nevertheless, an effort is needed to draft lists, which could be more costly in expense and time.

Protective effects of bacteria in the IBD zebrafish model are found to be strain-determined. Over 50% of bacteria used in the first anti-inflammatory test were beneficial. However, the other seven strains do not have anti-inflammatory effects and even result in harmful effects like lower survival and deformation. The inner differences within the strains also exist. For species like *B. coagulans* and *L. licheniformis*, *B. coagulans* XY2 and *L. licheniformis* XYT3 have positive effects on reducing acute colitis mortality in zebrafish models, but *B. coagulans* XYHYN and *L. licheniformis* XY16 could result in lower survival and deformation. There is a risk to using probiotics casually in the host with a damaged gut without testing first. This suggests that probiotics treatment should be more careful and we should regulate the specific strains used in IBD therapies.

Lactic acid bacteria were presented to be beneficial in anti-inflammation function again. Active strains like *L. rhamnosus* and *B. coagulans* were found to be anti-inflammatory in mice models already (Yan et al., 2017; Shinde et al., 2020). In this experiment, we confirmed their anti-inflammatory function in the DSS-induced acute colitis zebrafish model. On the other hand, *L. parafarraginis* and *B. smithii* are rarely reported as anti-inflammatory bacteria. This study provides evidence for these two species in exploring their bio-functions.

Bacillus smithii XY1 is found to be especially effective in anti-inflammation compared with any other strain. In this study, *B. smithii* XY1 is the only strain that could both reduce the mortality in acute colitis zebrafish models and significantly relieve inflammation in the intestine. *Bacillus smithii* XY1 used to be classified as *B. coagulans* until the late nineteenth century, suggesting that characteristics like oral safe and some immunomodulatory function of *B. coagulans* could also come from *B. smithii* (Nakamura et al., 1988). Species *B. smithii* has been added to the list of QPS-recommended biological agents intentionally added to food or feed as notified to EFSA since 2017 (Ricci et al., 2017). Another *B. smithii* strain has also been reported to present some anti-inflammatory function on animal models recent years. *Bacillus smtihii TBMI 12* is proved to protect against *C. difficile* infection in mice, and its spores protect against the Salmonella serotype enteritidis in mice, though its protective mechanisms have not been described (Jõogi et al., 2007; Suitso et al., 2007). Combining the former research on *B. smtihii TBMI 12* and our study, we found that *B. smithii* show its probiotics potential on anti-inflammation.

Bacillus smithii XY1 might be involved in immune regulation. RT-qPCR analysis shows gene expression of pro-inflammatory

cytokines IL-1β and TNF-α could be restored to normal level after *B. smithii* XY1 intervention. The two cytokines are involved in NF-κB and IRF pathways. Unmoral high expression of these two genes reflects the inflammation in the host. However, whether *B. smithii* XY1 reduces inflammation levels by downregulating these genes expression directly is still unverified, and this needs further study. NOD2 also participates in the NF-κB signaling pathway. NOD2 is an innate immune sensor. It encodes a protein that helps NF-κB be responsive to bacterial lipopolysaccharides (Ogura et al., 2001; Strober and Watanabe, 2011). The changes of NOD2 gene expression levels may suggest that lipopolysaccharides change in the inner gut microbiome, which may lead a way to explore the mechanism of anti-inflammatory function of *B. smithii* XY1. Moreover, *B. smithii* XY1 helps the host to restore the intestinal epithelial cell integrity after DSS damage. Integral intestinal epithelial construction helps the host to insulate harmful microbes from the body.

As a promising and sustainable potential therapy of IBD, probiotics therapies still need efforts to find more effective strains and study the relationship between the probiotics, the host, and the gut microbiomes. Conventionally, human gastrointestinal is recommended as the source of probiotics by FAO and WHO. However, probiotics may also be isolated from unconventional sources. The physiological structure of zebrafish still differs from rodents and humans, so it is better to confirm strains' beneficial effects in other models. Broader species screening would help set up a larger potential IBD remission probiotics library. Not only LAB but also some uncommonly used *Bacillus* like *B. smithii* and *B. licheniformis* presented to be anti-inflammatory. For specific strains, the mechanisms that their better anti-inflammatory effects differ from other strains of the same species are worth studying.

In conclusion, we firstly established a rapid method for choosing suitable bacteria and screened out one novel strain *Bacillus smithii* XY1 that successfully worked against DSS-induced intestinal damage in zebrafish larvae. *Bacillus smithii* XY1 intervention alleviated inflammatory response including neutrophil mobilization reduction, abnormal intestinal phenotypes rescue, and downregulation of inflammatory cytokine genes' expressions. The present work has demonstrated the excellently protective effects of *Bacillus smithii* XY1 on intestinal inflammation recovery in the zebrafish model, which is meaningful for application in IBD therapy.

DATA AVAILABILITY STATEMENT

The datasets presented in this study can be found in online repositories. The names of the repository/repositories and accession number(s) can be found in the article/**Supplementary Material**.

ETHICS STATEMENT

The animal study was reviewed and approved by Zhejiang University Laboratory Animal Center.

AUTHOR CONTRIBUTIONS

XH: conceptualization, methodology, writing – original draft preparation, and writing – reviewing and editing. FA and CJ: investigation. PT, YG, and YW: supervision. FY: supervision and writing – reviewing and editing. TY: project administration and funding acquisition. All authors contributed to the article and approved the submitted version.

ACKNOWLEDGMENTS

We thank Li Yingniang and Chen Jingyao from the core facility platform of Zhejiang University School of Medicine for their technical support.

SUPPLEMENTARY MATERIAL

The Supplementary Material for this article can be found online at: https://www.frontiersin.org/articles/10.3389/fmicb.2021.760385/full#supplementary-material

REFERENCES

Ananthakrishnan, A. N., Kaplan, G. G., and Ng, S. C. (2020). Changing global epidemiology of inflammatory bowel diseases: sustaining health care delivery into the 21st century. *Clin. Gastroenterol. Hepatol.* 18, 1252–1260. doi: 10.1016/j.cgh.2020.01.028

Basso, P. J., Câmara, N. O. S., and Sales-Campos, H. (2018). Microbial-Based Therapies in the Treatment of Inflammatory Bowel Disease—An Overview of Human Studies. *Front. Pharmacol.* 9:1571. doi: 10.3389/fphar.2018.01571

Baumgartner, A., Kueffer, M., Simmen, A., and Grand, M. (1998). Relatedness of Lactobacillus rhamnosus Strains Isolated from Clinical Specimens and Such from Food-stuffs, Humans and Technology. *LWT* 31, 489–494. doi: 10.1006/fstl.1998.0395

Browne, A. S., and Kelly, C. R. (2017). Fecal transplant in inflammatory bowel disease. *Gastroenterol. Clin. N. Am.* 46, 825–837. doi: 10.1016/j.gtc.2017.08.005

Chuang, L.-S., Morrison, J., Hsu, N.-Y., Labrias, P. R., Nayar, S., Chen, E., et al. (2019). Zebrafish modeling of intestinal injury, bacterial exposures and medications defines epithelial in vivo responses relevant to human inflammatory bowel disease. *Dis. Model. Mech.* 12:dmm037432. doi: 10.1242/dmm.037432

Colombel, J.-F., Shin, A., and Gibson, P.R. (2019). AGA clinical practice update on functional gastrointestinal symptoms in patients With inflammatory bowel disease: expert review. *Clin. Gastroenterol. Hepatol.* 17, 380-390.e1. doi: 10.1016/j.cgh.2018.08.001

Flores, E. M., Nguyen, A. T., Odem, M. A., Eisenhoffer, G. T., and Krachler, A. M. (2020). The zebrafish as a model for gastrointestinal tract-microbe interactions. *Cell. Microbiol.* 22:e13152. doi: 10.1111/cmi.13152

Friedman, S. L., Quigley, E. M. M., Sharkey, K. A., Sung, J. J. Y., and Whitcomb, D. C. (2014). The past 10 years of gastroenterology and hepatology-reflections and predictions. *Nat. Rev. Gastroenterol. Hepatol.* 11, 692–700. doi: 10.1038/nrgastro.2014.167

Fritsch, J., and Abreu, M. T. (2019). The microbiota and the immune response: what is the chicken and what is the egg? *Gastrointest. Endosc. Clin. N. Am.* 29, 381–393. doi: 10.1016/j.giec.2019.02.005

Geier, M. S., Butler, R. N., Giffard, P. M., and Howarth, G. S. (2007). Lactobacillus fermentum BR11, a potential new probiotic, alleviates symptoms of colitis induced by dextran sulfate sodium (DSS) in rats. *Int. J. Food Microbiol.* 114, 267–274. doi: 10.1016/j.ijfoodmicro.2006.09.018

Glassner, K. L., Abraham, B. P., and Quigley, E. M. M. (2020). The microbiome and inflammatory bowel disease. *J. Allergy Clin. Immunol.* 145, 16–27. doi: 10.1016/j.jaci.2019.11.003

Guarner, F., Perdigon, G., Corthier, G., Salminen, S., Koletzko, B., and Morelli, L. (2005). Should yoghurt cultures be considered probiotic? *Br. J. Nutr.* 93, 783–786. doi: 10.1079/bjn20051428

Jardine, S., Dhingani, N., and Muise, A. M. (2019). TTC7A: steward of intestinal health. *Cell. Mol. Gastroenterol. Hepatol.* 7, 555–570. doi: 10.1016/j.jcmgh.2018.12.001

Jõogi, E., Suitso, I., Talpsep, E., Naaber, P., Lõoivukene, K., and Nurk, A. (2007). P1767 probiotic infiuence of Bacillus smithii TBMI 12 against *Clostridium difficile* infection in mice and hamster model. *Int. J. Antimicrob. Agents* 29:S502. doi: 10.1016/S0924-8579(07)71606-0

Jostins, L., Ripke, S., Weersma, R. K., Duerr, R. H., McGovern, D. P., Hui, K. Y., et al. (2012). Host-microbe interactions have shaped the genetic architecture of inflammatory bowel disease. *Nature* 491, 119–124. doi: 10.1038/nature11582

Kruis, W., Fric, P., Pokrotnieks, J., Lukás, M., Fixa, B., Kascák, M., et al. (2004). Maintaining remission of ulcerative colitis with the probiotic *Escherichia coli* Nissle 1917 is as effective as with standard mesalazine. *Gut* 53, 1617–1623. doi: 10.1136/gut.2003.037747

Kruis, W., Schütz, E., Fric, P., Fixa, B., Judmaier, G., and Stolte, M. (1997). Double-blind comparison of an oral *Escherichia coli* preparation and mesalazine in maintaining remission of ulcerative colitis. *Aliment. Pharmacol. Ther.* 11, 853–858. doi: 10.1046/j.1365-2036.1997.00225.x

Matthes, H., Krummenerl, T., Giensch, M., Wolff, C., and Schulze, J. (2010). Clinical trial: probiotic treatment of acute distal ulcerative colitis with rectally administered *Escherichia coli* Nissle 1917 (EcN). *BMC Complement. Altern. Med.* 10:13. doi: 10.1186/1472-6882-10-13

Nakamura, L. K., Blumenstock, I., and Claus, D. (1988). Taxonomic study of *Bacillus coagulans* hammer 1915 with a proposal for *Bacillus smithii* sp. nov. *Int. J. Syst. Bacteriol.* 38, 63–73. doi: 10.1099/00207713-38-1-63

Ng, S. C., Plamondon, S., Kamm, M. A., Hart, A. L., Al-Hassi, H. O., Guenther, T., et al. (2010). Immunosuppressive effects via human intestinal dendritic cells of probiotic bacteria and steroids in the treatment of acute ulcerative colitis. *Inflamm. Bowel Dis.* 16, 1286–1298. doi: 10.1002/ibd.21222

Ng, S. C., Shi, H. Y., Hamidi, N., Underwood, F. E., Tang, W., Benchimol, E. I., et al. (2017). Worldwide incidence and prevalence of inflammatory bowel disease in the 21st century: a systematic review of population-based studies. *Lancet* 390, 2769–2778. doi: 10.1016/S0140-6736(17)32448-0

Ni, J., Wu, G. D., Albenberg, L., and Tomov, V. T. (2017). Gut microbiota and IBD: causation or correlation? *Nat. Rev. Gastroenterol. Hepatol.* 14, 573–584. doi: 10.1038/nrgastro.2017.88

Oehlers, S. H., Flores, M. V., Hall, C. J., Okuda, K. S., Sison, J. O., Crosier, K. E., et al. (2013). Chemically induced intestinal damage models in Zebrafish larvae. *Zebrafish* 10, 184–193. doi: 10.1089/zeb.2012.0824

Oehlers, S. H., Flores, M. V., Hall, C. J., Swift, S., Crosier, K. E., and Crosier, P. S. (2011). The inflammatory bowel disease (IBD) susceptibility genes NOD1 and NOD2 have conserved anti-bacterial roles in zebrafish. *Dis. Model. Mech.* 4, 832–841. doi: 10.1242/dmm.006122

Oehlers, S. H., Flores, M. V., Hall, C. J., Wang, L., Ko, D. C., Crosier, K. E., et al. (2017). A whole animal chemical screen approach to identify modifiers of intestinal neutrophilic inflammation. *FEBS J.* 284, 402–413. doi: 10.1111/febs.13976

Ogura, Y., Bonen, D. K., Inohara, N., Nicolae, D. L., Chen, F. F., Ramos, R., et al. (2001). A frameshift mutation in NOD2 associated with susceptibility to Crohn's disease. *Nature* 411, 603–606. doi: 10.1038/35079114

Pereira, G. V. D. M., Oliveira Coelho, B. D., Júnior, M. A. I., Thomaz-Soccol, V., and Soccol, C. R. (2018). How to select a probiotic? A review and update of methods and criteria. *Biotechnol. Adv.* 36, 2060–2076. doi: 10.1016/j.biotechadv.2018.09.003

Petersen, A. M., Mirsepasi, H., Halkjær, S. I., Mortensen, E. M., Nordgaard-Lassen, I., and Krogfelt, K. A. (2014). Ciprofloxacin and probiotic *Escherichia coli* Nissle add-on treatment in active ulcerative colitis: a double-blind randomized placebo controlled clinical trial. *J. Crohns Colitis* 8, 1498–1505. doi: 10.1016/j.crohns.2014.06.001

Qin, C., Xie, Y., Wang, Y., Li, S., Ran, C., He, S., et al. (2018). Impact of *Lactobacillus casei* BL23 on the host transcriptome, growth and disease resistance in larval Zebrafish. *Front. Physiol.* 9:1245. doi: 10.3389/fphys.2018.01245

Ran, C., Qin, C., Xie, M., Zhang, J., Li, J., Xie, Y., et al. (2018). Aeromonas veronii and aerolysin are important for the pathogenesis of motile aeromonad septicemia in cyprinid fish. *Environ. Microbiol.* 20, 3442–3456. doi: 10.1111/1462-2920.14390

Rea, S. M., McSweeney, N. J., Degens, B. P., Morris, C., Siebert, H. M., and Kaksonen, A. H. (2015). Salt-tolerant microorganisms potentially useful for bioleaching operations where fresh water is scarce. *Miner. Eng.* 75, 126–132. doi: 10.1016/j.mineng.2014.09.011

Rembacken, B. J., Snelling, A. M., Hawkey, P. M., Chalmers, D. M., and Axon, A. T. R. (1999). Non-pathogenic *Escherichia coli* versus mesalazine for the treatment of ulcerative colitis: a randomised trial. *Lancet* 354, 635–639. doi: 10.1016/S0140-6736(98)06343-0

Ricci, A., Allende, A., Bolton, D., Chemaly, M., Davies, R., Girones, R., et al. (2017). Update of the list of QPS-recommended biological agents intentionally added to food or feed as notified to EFSA 5: suitability of taxonomic units notified to EFSA until September 2016. *EFSA J.* 15:e04663. doi: 10.2903/j.efsa.2017.4663

Sanders, M. E., Akkermans, L. M. A., Haller, D., Hammerman, C., Heimbach, J., Hörmannsperger, G., et al. (2010). Safety assessment of probiotics for human use. *Gut Microbes* 1, 164–185. doi: 10.4161/gmic.1.3.12127

Savardi, M., Ferrari, A., and Signoroni, A. (2018). Automatic hemolysis identification on aligned dual-lighting images of cultured blood agar plates. *Comput. Methods Prog. Biomed.* 156, 13–24. doi: 10.1016/j.cmpb.2017.12.017

Shinde, T., Perera, A. P., Ravichandra, V., Gondalia, S. V., Beale, D. J., Karpe, A. V., et al. (2020). Synbiotic supplementation with prebiotic green banana resistant starch and probiotic Bacillus coagulans spores ameliorates gut inflammation in mouse model of inflammatory bowel diseases. *Eur. J. Nutr.* 59, 3669–3689. doi: 10.1007/s00394-020-02200-9

Sood, A., Midha, V., Makharia, G. K., Ahuja, V., Singal, D., Goswami, P., et al. (2009). The probiotic preparation, VSL#3 induces remission in patients with mild-to-moderately active ulcerative colitis. *Clin. Gastroenterol. Hepatol.* 7, 1202–9,1209.e1. doi: 10.1016/j.cgh.2009.07.016

Souza, E. L. S., Campos, C. L. V., Reis, D. C., Cassali, G. D., Generoso, S. V., Cardoso, V. N., et al. (2020). Beneficial effects resulting from oral administration of *Escherichia coli* Nissle 1917 on a chronic colitis model. *Benefic. Microbes* 11, 779–790. doi: 10.3920/BM2020.0045

Strober, W., and Watanabe, T. (2011). NOD2, an intracellular innate immune sensor involved in host defense and Crohn's disease. *Mucosal Immunol.* 4, 484–495. doi: 10.1038/mi.2011.29

Suitso, I., Jögi, E., Talpsep, E., Naaber, P., and Nurk, A. (2007). P1763 *Bacillus smithii* TBMI12 spores as a potential competitive exclusion agent against *Salmonella enteritidis*. *Int. J. Antimicrob. Agents* 29:S501. doi: 10.1016/S0924-8579(07)71602-3

Tamaki, H., Nakase, H., Inoue, S., Kawanami, C., Itani, T., Ohana, M., et al. (2016). Efficacy of probiotic treatment with Bifidobacterium longum 536 for induction of remission in active ulcerative colitis: A randomized, double-blinded, placebo-controlled multicenter trial. *Dig. Endosc.* 28, 67–74. doi: 10.1111/den.12553

Tursi, A., Brandimarte, G., Papa, A., Giglio, A., Elisei, W., Giorgetti, G. M., et al. (2010). Treatment of relapsing mild-to-moderate ulcerative colitis with the probiotic VSL#3 as adjunctive to a standard pharmaceutical treatment: a double-blind, randomized, placebo-controlled study. *Am. J. Gastroenterol.* 105, 2218–2227. doi: 10.1038/ajg.2010.218

Wildt, S., Nordgaard, I., Hansen, U., Brockmann, E., and Rumessen, J. J. (2011). A randomised double-blind placebo-controlled trial with *Lactobacillus* acidophilus La-5 and Bifidobacterium animalis subsp. lactis BB-12 for maintenance of remission in ulcerative colitis. *J. Crohns Colitis* 5, 115–121. doi: 10.1016/j.crohns.2010.11.004

Yan, F., Liu, L., Cao, H., Moore, D. J., Washington, M. K., Wang, B., et al. (2017). Neonatal colonization of mice with LGG promotes intestinal development and decreases susceptibility to colitis in adulthood. *Mucosal Immunol.* 10, 117–127. doi: 10.1038/mi.2016.43

Yi, C.-C., Liu, C.-H., Chuang, K.-P., Chang, Y.-T., and Hu, S.-Y. (2019). A potential probiotic Chromobacterium aquaticum with bacteriocin-like activity enhances the expression of indicator genes associated with nutrient metabolism, growth performance and innate immunity against pathogen infections in zebrafish (Danio rerio). *Fish Shellfish Immunol.* 93, 124–134. doi: 10.1016/j.fsi.2019.07.042

Zareef, R., Younis, N., and Mahfouz, R. (2020). Inflammatory bowel disease: A key role for microbiota? *Meta Gene* 25:100713. doi: 10.1016/j.mgene.2020.100713

Zhao, S., Xia, J., Wu, X., Zhang, L., Wang, P., Wang, H., et al. (2018). Deficiency in class III PI3-kinase confers postnatal lethality with IBD-like features in zebrafish. *Nat. Commun.* 9:2639. doi: 10.1038/s41467-018-05105-8

Zielińska, D., and Kołożyn-Krajewska, D. (2018). Food-origin lactic acid bacteria may exhibit probiotic properties: review. *Biomed. Res. Int.* 2018:5063185. doi: 10.1155/2018/5063185

Zocco, M. A., dal Verme, L. Z., Cremonini, F., Piscaglia, A. C., Nista, E. C., Candelli, M., et al. (2006). Efficacy of *Lactobacillus* GG in maintaining remission of ulcerative colitis. *Aliment. Pharmacol. Ther.* 23, 1567–1574. doi: 10.1111/j.1365-2036.2006.02927.x

Conflict of Interest: The authors declare that the research was conducted in the absence of any commercial or financial relationships that could be construed as a potential conflict of interest.

Publisher's Note: All claims expressed in this article are solely those of the authors and do not necessarily represent those of their affiliated organizations, or those of the publisher, the editors and the reviewers. Any product that may be evaluated in this article, or claim that may be made by its manufacturer, is not guaranteed or endorsed by the publisher.

frontiers in Microbiology

REVIEW
published: 24 December 2021
doi: 10.3389/fmicb.2021.812536

The Possible Link Between Manufacturing and Probiotic Efficacy; a Molecular Point of View on *Bifidobacterium*

Stéphane Duboux[1,2], Myrthe Van Wijchen[1,2] and Michiel Kleerebezem[2]*

[1] Nestlé Research, Lausanne, Switzerland, [2] Host-Microbe Interactomics Group, Wageningen University and Research, Wageningen, Netherlands

OPEN ACCESS

Edited by:
Corine Sandström, Swedish University of Agricultural Sciences, Sweden

Reviewed by:
Maria de los Angeles Serradell, Consejo Nacional de Investigaciones Científicas y Técnicas (CONICET), Argentina
Cristian Botta, University of Turin, Italy

***Correspondence:**
Stéphane Duboux
stephane.duboux@rdls.nestle.com

Specialty section:
This article was submitted to Food Microbiology, a section of the journal Frontiers in Microbiology

Received: *10 November 2021*
Accepted: *06 December 2021*
Published: *24 December 2021*

Citation:
Duboux S, Van Wijchen M and Kleerebezem M (2021) The Possible Link Between Manufacturing and Probiotic Efficacy; a Molecular Point of View on Bifidobacterium. Front. Microbiol. 12:812536. doi: 10.3389/fmicb.2021.812536

Probiotics for food or supplement use have been studied in numerous clinical trials, addressing a broad variety of diseases, and conditions. However, discrepancies were observed in the clinical outcomes stemming from the use of lactobacillaceae and bifidobacteria strains. These differences are often attributed to variations in the clinical trial protocol like trial design, included target population, probiotic dosage, or outcome parameters measured. However, a contribution of the methods used to produce the live bioactive ingredients should not be neglected as a possible additional factor in the observed clinical outcome variations. It is well established that manufacturing conditions play a role in determining the survival and viability of probiotics, but much less is known about their influence on the probiotic molecular composition and functionality. In this review, we briefly summarize the evidence obtained for *Lacticaseibacillus rhamnosus* GG and *Lactiplantibacillus plantarum* WCFS1, highlighting that expression and presence of probiotic niche factor (NF) and/or effector molecules (EM) may be altered during production of those two well-characterized lactobacillaceae probiotic strains. Subsequently, we summarize in more depth what is the present state of knowledge about bifidobacterial probiotic NF and EM; how their expression may be modified by manufacturing related environmental factors and how that may affect their biological activity in the host. This review highlights the importance of gathering knowledge on probiotic NF and EM, to validate them as surrogate markers of probiotic functionality. We further propose that monitoring of validated NF and/or EM during production and/or in the final preparation could complement viable count assessments that are currently applied in industry. Overall, we suggest that implementation of molecular level quality controls (i.e., based on validated NF and EM), could provide mode of action based *in vitro* tests contributing to better control the health-promoting reliability of probiotic products.

Keywords: probiotic, niche factors, effector molecules, lactobacillaceae, bifidobacteria, manufacturing

INTRODUCTION

Initially formulated by the World Health Organization in 2002 (Joint Fao/Who Working Group Report on Drafting, 2002) and slightly corrected by experts in the field in 2014 (Hill et al., 2014), probiotics are today defined as "live microorganisms that, when administered in adequate amounts, confer a health benefit to the host." Overall, probiotic bacteria for food or supplement use (mainly lactobacillaceae and bifidobacteria) have been studied in a large number of clinical trials, targeting a wide array of diseases and conditions (Dronkers et al., 2020).

Two distinguishable classes of health benefits are attributed to probiotics: a "general" class of effects that groups beneficial effects exerted by various well-studied microbial species; and a "strain-specific" class of effects that are expected to be driven by specific probiotics strains. An expert panel convened in 2013 has acknowledged those two classes, concluding that "general" benefits such as "creating a more favorable gut environment" and "supporting a healthy digestive tract" (regrouping a diversity of clinical end points such as diarrhea, antibiotic-associated diarrhea (AAD), gut transit, abdominal pain, bloating, and necrotizing enterocolitis) are displayed by a large number of probiotic strains representing various commonly studied species. The mechanisms of action supporting those "general" probiotic beneficial effects (e.g., probiotic and/or microbiome mediated SCFA production, regulation of intestinal transit, competitive exclusion of pathogens) are similarly believed to be shared by a large number, if not all, of the probiotic strains (Hill et al., 2014). Furthermore, "general" benefits (e.g., AAD prevention) provided by the commonly used *Lacticaseibacillus rhamnosus* GG strain have be shown to be relatively consistent throughout different clinical trials in children (Szajewska and Hojsak, 2020).

In contrast, "strain-specific" benefits are defined as effects that are likely exerted by a limited number of strains, such as "prevention of allergic disease," "downregulation of inflammation," "enhancement of anti-infection activities," or "support of specific organs health" (e.g., reproductive tract, lungs) (Hill et al., 2014). Those beneficial effects are believed to be driven by specific molecules present within or at the surface of the probiotic bacterial cells (Lebeer et al., 2008; Remus et al., 2012; Lee et al., 2013). In the last decade, it was shown that a range of molecules produced by probiotic contribute to their robustness and stress tolerance, supporting their survival and establishment when they transit through the gastro-intestinal tract (i.e., so-called niche factors; NF). In addition, various probiotic effector molecules (EM) have been identified to drive *in situ* host-microbe interactions, thus determining the specific health benefit of different probiotic strains (Lebeer et al., 2018). Disentangling the NF or EM role of specific probiotic molecules is not trivial, especially when adhesive-like phenotypes are affected. Adhesion to the host cells or to the intestinal mucus can be regarded as a factor promoting the bacterial colonization but could as well contribute to the exposure of different structures present on the bacterial cell envelope.

Variability in health effects is not uncommonly observed in clinical trials with probiotic for food or supplement use (Osborn and Sinn, 2007; Johnston et al., 2011; Guo et al., 2019). The inconsistency in results is usually attributed to variations in the design of the clinical studies, including differences in dosage of the probiotic, selection of different target population (i.e., inclusion and exclusion factors at enrollment), powering of the studies according to the primary and secondary objectives, duration of the studies, probiotic delivery format and schedule, data collection, and further analysis performed. Indeed, these factors have been suggested to explain part of the discrepancies observed in the reported clinical health-outcomes (Forssten et al., 2020). Furthermore, probiotics need to exert their effects in the complex microbiome. Inter-individual microbiota variability represent hence a challenge in ensuring probiotic effect consistency in different populations, and new stratification as well as personalized nutrition approaches have been recently proposed to improve the situation (Veiga et al., 2020). Moreover, the way the probiotic strains themselves are produced and formulated is often not well-described in clinical trial studies, while it could play an important role in the health-promoting efficacy that a product elicits. This is well illustrated by the discrepancies observed in randomized clinical trials using *L. rhamnosus* GG targeting the prevention of allergic disease, which are summarized by Segers and Lebeer (2014). Initially, Kalliomaki et al. (2001, 2007) showed in a landmark study that *L. rhamnosus* GG treatment significantly lowered the risk of eczema in young children belonging to families with a history of atopic disease. However, in a subsequent attempt to reproduce this Finnish study protocol, Kopp et al. (2008) failed to detect similar beneficial effects in a German cohort. Population (Finnish vs. Germans) and dosage differences (2^{E10} vs. 1^{E10} CFU daily) are potential confounding factor in those two studies, but it is important to note that the source (and possibly the manufacturing process) of *L. rhamnosus* GG in the studies by Kalliomaki et al. (2001, 2007) and Kopp et al. (2008) was different, which deserves attention because it may have as well contributed to the differences in clinical outcomes (Tripathi et al., 2012). At present, probiotic manufacturing procedures remain largely unexplored as a potential source of variation in probiotic clinical trials outcomes and hence deserves to be studied in more details (Sanders et al., 2014; Brussow, 2019), especially in the light of the increasing knowledge about specific NF and EM that play a role in the efficacy of intestinal delivery and health promotion following consumption of the product.

Production of dried probiotic supplements consists generally of (a) a series of fermentations of different scale where bacterial biomass is produced using specific media and growth conditions, (b) a centrifugation step to remove the culture supernatant and concentrate the biomass, (c) a mixing step where protectants are added, followed by (d) a drying step (Fenster et al., 2019). Throughout these manufacturing stages, probiotics encounter a range of different stress conditions, including variations in temperature, acid exposure, osmotic and oxidative stress, all of which can modulate their physiology and molecular composition. These modulations may impact their survival during manufacturing as well as their fitness during gastrointestinal tract transit (Corcoran et al., 2008; Gaucher et al., 2019). We suggest that not only the expression of NF (e.g., proteins that contribute to robustness and stress

tolerance) can be affected by the production conditions, but also effector molecule expression levels may differ, leading to variable presence of molecules that have been shown to mediate the health-benefit elicited by the strain. The required presence of NF and/or EM is further supported by the fact that probiotic cells rendered metabolically inactive by the mean of heat-treatment can still elicit beneficial health effects (Pique et al., 2019), highlighting the potential limitation of using live cells enumeration alone to ascertain efficacy of probiotic preparations. Therefore, monitoring the expression of validated NF as well as EM during probiotic manufacturing may enable better control of product properties at a molecular level, which goes beyond the traditionally used colony forming units (CFU), and could contribute to an increased robustness of clinical outcomes (**Figure 1**).

In this review, we first briefly highlight that expression and presence of probiotic EM may be altered during production using two well-characterized examples among the lactobacillaceae probiotic, i.e., *Lacticaseibacillus rhamnosus* GG and *Lactiplantibacillus plantarum* WCFS1 (**Figure 2**). Subsequently, we focus with more depth on bifidobacteria and their probiotic NF and EM, summarizing what is the present state of knowledge about bifidobacterial NF and EM; how their expression may be modified by manufacturing related environmental factors and how that may affect their biological activity in the host (**Table 1**). Overall, this review highlights the importance of gathering knowledge on probiotic NF and EM, to validate them as surrogate markers of probiotic functionality. We further hypothesize that understanding the dynamics of these molecules during production could contribute to better control the health-promoting reliability of dried probiotic products. Hence, NF/EM based *in vitro* assays represent molecular-level quality controls that adds to the limited information coming from viable count assessments that are currently applied in industry and research.

MODIFICATION OF *LACTICASEIBACILLUS RHAMNOSUS* GG EFFECTOR MOLECULES BY PROCESSING

L. rhamnosus GG is among the probiotic strains with the best described set of EM, several of which play diverse roles in the probiotic activity of this strain as assessed mainly in preclinical models. Those include the major secreted proteins p40 and p75 that prevent cytokine-induced inflammatory damage, lipoteichoic acid (LTA) that negatively modulate colitis, CpG-rich DNA motifs that dampen allergen-specific IgE, and exopolysaccharides (EPS) that reduce adipogenesis in high-fat-diet fed mice (Lebeer et al., 2018). *L. rhamnosus* GG *spaCBA* encoded sortase-dependent pilin anchored at the surface of the bacteria are important NF as they are involved in the mucus and intestinal epithelium adhesion capacity of the strain. However, they were also shown *in vitro* to act as EM as they contribute to the immunomodulatory capacities of the strain when incubated with monocytes and dentritic cells

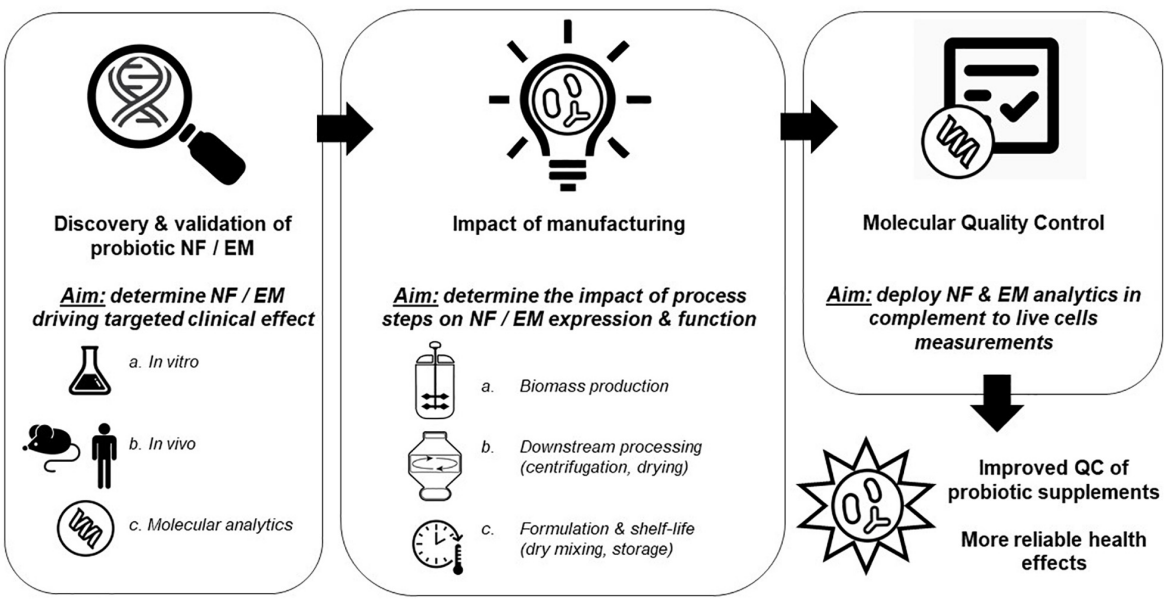

FIGURE 1 | Stepwise approach leveraging probiotic niche factors (NF) and effector molecules (EM) knowledge to improve probiotic supplements consistency. As a first step, a robust link between the presence of probiotic NF or EM and the desired clinical outcome needs to be established. This step will also allow the development of sets of molecular analytics that can be used in the subsequent steps. Then, the different manufacturing steps need to be evaluated to understand their contribution to NF or EM expression and function. Finally, the NF/EM molecular analytics developed earlier can be used as quality control (QC), complementing traditional CFU/live cells measurements, which overall should enable production of probiotic supplements with increased consistency in their attributed health benefits.

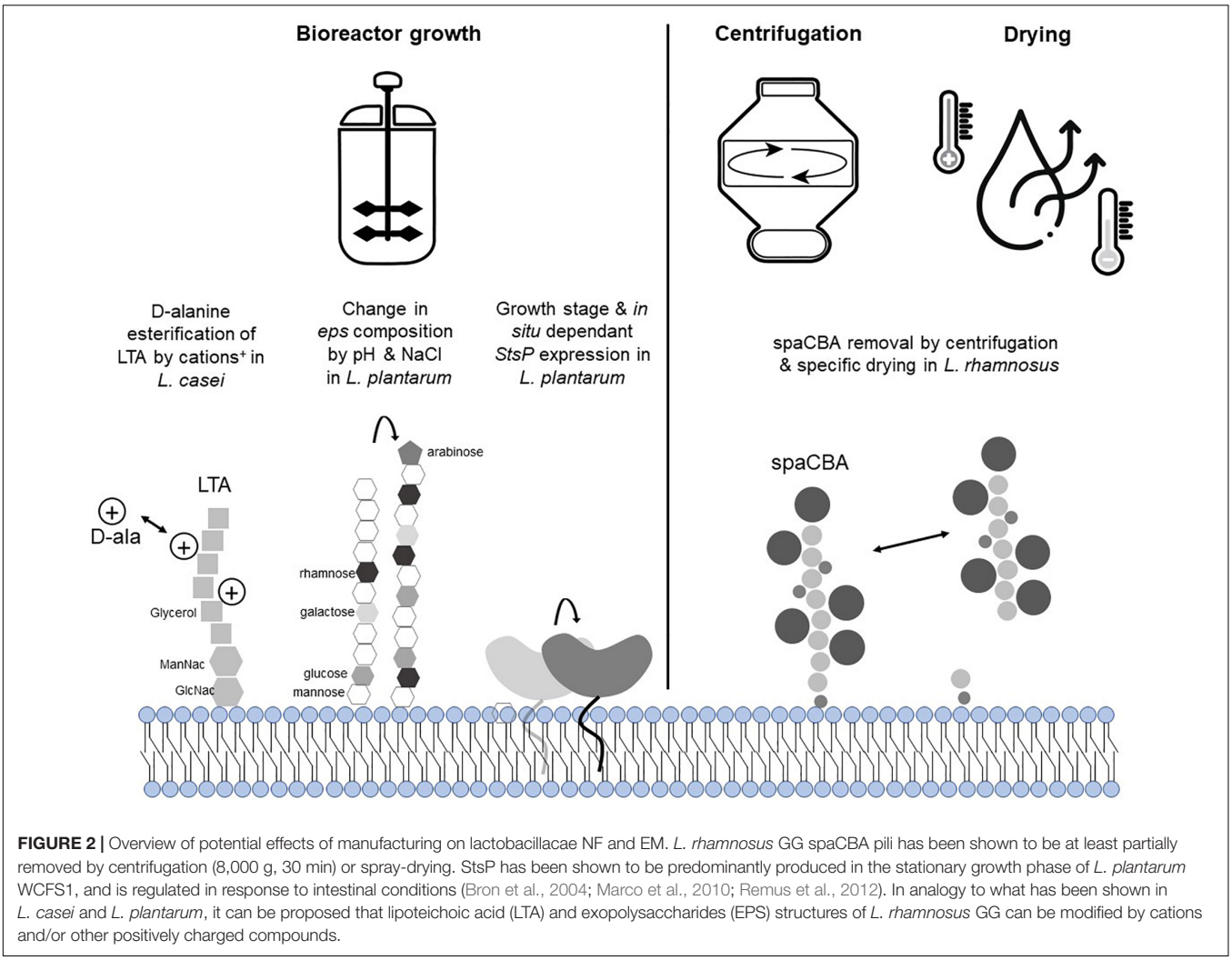

FIGURE 2 | Overview of potential effects of manufacturing on lactobacillacae NF and EM. *L. rhamnosus* GG spaCBA pili has been shown to be at least partially removed by centrifugation (8,000 g, 30 min) or spray-drying. StsP has been shown to be predominantly produced in the stationary growth phase of *L. plantarum* WCFS1, and is regulated in response to intestinal conditions (Bron et al., 2004; Marco et al., 2010; Remus et al., 2012). In analogy to what has been shown in *L. casei* and *L. plantarum*, it can be proposed that lipoteichoic acid (LTA) and exopolysaccharides (EPS) structures of *L. rhamnosus* GG can be modified by cations and/or other positively charged compounds.

(Lebeer et al., 2012; Vargas Garcia et al., 2015), and stimulate cell proliferation that protects against radiologically induced intestinal epithelial damage (Ardita et al., 2014). Nevertheless, the regulation of expression and functional properties of the pili as well as the other EM during manufacturing of *L. rhamnosus* GG remains largely unexplored.

For example, the regulation of the genes encoding p40 and p75 remains unknown. Additionally, these bioactive molecules are derived from cell wall associated muramidases and are at least partially secreted in the culture supernatant (Yan et al., 2013), which is usually removed during dried probiotic manufacturing (Fenster et al., 2019), raising doubts about their functional availability in supplement products. Similarly, although the role of specific genes involved in LTA biosynthesis in lactobacilli (including *L. rhamnosus* GG) has been studied (Debabov et al., 1996, 2000), their regulation by environmental conditions remains largely unknown. For example, Dlt mediated LTA D-alanylation has been long recognized as an important modulator of the host-effects elicited by LTA (Claes et al., 2012), but we do not know whether *dlt* expression is regulated by environmental conditions in *L. rhamnosus* GG. Notably, it has been demonstrated that the *dlt* gene of *Staphylococcus aureus*, is regulated by cations levels in the medium [Na^{+}, $Mg^{(2+)}$, $Ca^{(2+)}$] (Koprivnjak et al., 2006), and in *L. casei* (a close relative of *L. rhamnosus*) is regulated by the presence of charged molecules like antimicrobial peptides (Revilla-Guarinos et al., 2013). These findings suggest that *dlt* regulation in lactobacilli may be coordinated similarly to what was observed in *S. aureus*, and that the concentrations of positively charged components in the growth medium may affect D-alanylation of LTA. A specific galactose-rich exopolysaccharide in *L. rhamnosus* GG has been previously identified to play a role in the adhesion capacity of the strain (Lebeer et al., 2009). Although regulation of the production of this EPS in *L. rhamnosus* GG has not been studied in detail, recent studies in *L. plantarum* VAL6 indicated that expression of *eps* genes eliciting structural changes of the polysaccharides produced in this species is regulated by pH and sodium chloride induced stress (Nguyen et al., 2021), conditions that may occur during industrial growth. Importantly, manufacturing was demonstrated to influence the presence of the SpaCBA pili at *L. rhamnosus* GG's surface and could thus affect the presence and function of this important niche factor

and effector molecule in preparations of this strain. It has been shown that centrifugation at 8,000 g for 30 min was sufficient to break and separate the pili from the surface of the bacteria (Tripathi et al., 2012), while a specific type of drying (spray-drying without addition of any protectants, which is not a common manufacturing practice) diminished the adherence capacity of *L. rhamnosus* GG correlated with the disappearance of the SpaCBA pili (Kiekens et al., 2019; **Figure 2**). It is not known today if the presence of this importance protein structure can be influenced by other types of drying. However, freeze-drying was shown to decrease the adherence capacity of *L. rhamnosus* GG, while it did not exert the same effect on *L. casei* Shirota (du Toit et al., 2013). Moreover, besides the physical presence or absence of the pili structure in preparations of this strain, the genetic region encoding the SpaCBA pili was shown to be relatively unstable (Sybesma et al., 2013), which may also contribute to variations in *in vivo* behavior of *L. rhamnosus* GG isolates originating from different products (Grzeskowiak et al., 2011). Altogether, these lines of evidence indicate that upstream (e.g., fermentation conditions) or downstream processing conditions (e.g., centrifugation, type of drying) can play a role in the presence and bioavailability of NF as well as EM of *L. rhamnosus* GG. *In vivo* demonstration of the impact of those processing induced modifications has not yet been pursued, but we hypothesize that they may have contributed to the different outcomes obtained in clinical trials like those reported by Kalliomaki et al. (2001, 2007) and Kopp et al. (2008).

LACTIPLANTIBACILLUS PLANTARUM WCSF1 GROWTH PHASE INFLUENCES ITS HOST IMMUNODULATORY CAPACITY

To the best of our knowledge, the only substantiated example demonstrating that production parameters (i.e., growth phase harvesting) can influence the way a probiotic can interact with the human body has been obtained with the well-characterized *L. plantarum* WCFS1 strain. Freeze-dried preparations of heat-killed or live *L. plantarum* WCFS1 were administered to healthy adults. In addition, the live preparations consisted of cells harvested during mid-logarithmic or during the stationary phase of growth. Following consumption of these distinct preparations of the same strain, duodenal tissue biopsies were analyzed by array-based transcriptomics, revealing that both live and dead (heat treated) stationary phase harvested bacterial preparations were able to modulate Nfκ-B responses in human duodenum mucosal tissues, which were interpreted to play an important role in the establishment of immune tolerance. Conversely, the bacteria harvested mid-exponentially failed to induce such responses, but modified the expression of human genes involved in immune-suppressing activities such as BCL3, Iκ-B, and ADM, as well as several functions involved in cell-cycle and metabolic regulation (van Baarlen et al., 2009). As a follow-up, it was found that the *lp_0800* gene, coding for a serine- and threonine-rich surface protein (StsP) that is anchored to the peptidoglycan by sortase was shown to be expressed predominantly during the stationary growth phase, albeit at low levels during growth under laboratory conditions. Notably, previous studies of *L. plantarum* had established that the expression of *lp_0800* was *in situ* induced during the transit through the murine and human intestinal tract, supporting that specific environmental conditions can modulate its expression (Bron et al., 2004; Marco et al., 2007, 2010). Importantly, using isogenic *L. plantarum* WCFS1 lacking or overexpressing StsP, it was shown that StsP surface derived peptides obtained by whole-cell trypsin-shaving could strongly inhibit flagellin induced Nfκ-B activation in a CaCo-2-derived reporter cell line. Finally, gel-purified StsP protein derived tryptic peptides potently suppressed NFkB activation, unambiguously pinpointing this activity to peptides derived from this surface protein (Remus et al., 2012). These findings demonstrate that the growth phase as well as specific growth conditions (i.e., gut-like conditions) of *L. plantarum* WCFS1 can influence the expression level or bioavailability of the important immunomodulatory StsP, which was proposed to play a prominent role in the clinically observed duodenal transcriptional responses (**Figure 2**).

Of note, the host responses were determined in the duodenum of the participating volunteers. In fact, upon ingestion, the relatively short transit time to reach the duodenal mucosa likely allows a limited molecular adaptation of the probiotic bacteria. At this moment it is unclear whether similar transcriptome response differences would be observed in the colonic mucosa when applying these distinct *L. plantarum* WCFS1 preparations. One the one hand, the different molecular make-up of the preparations may change during gastrointestinal transit, and on the other hand it is known that *stsP* expression is induced in the intestinal tract. We hence hypothesize that ensuring NF and EM presence and function in probiotic products may be especially relevant when the probiotic is expected to elicit its health benefit in the proximal regions of the intestine.

Overall, the *L. plantarum* WCFS1 example strongly indicates that upstream processing (e.g., harvesting time) can impact probiotic bioactivities *in vivo,* and underlines the importance of harvesting probiotic cells at stationary phase, which is today a common practice in industry. Moreover, it supports that quantification of StsP in preparations of *L. plantarum* WCFS1 could serve as a molecular quality control parameter to complement the traditionally used CFU enumeration.

AND WHAT ABOUT *BIFIDOBACTERIUM*?

Similar to probiotics belonging to the *Lactobacillaceae* family, we propose that manufacturing procedures used for bifidobacteria should be investigated for their possible contribution to the discrepancies observed in clinical trial outcomes (Szajewska and Hojsak, 2020). To date, there are only few studies focusing on the effect of manufacturing on bifidobacteria bioactivities and most focused on the potential impact of downstream processing (i.e., drying). Moreover, the available studies did not include an assessment of specific effector molecule presence and bioavailability but were mostly driven by functional assays. For example, Laconelli et al. (2015) showed that different drying

TABLE 1 | Summary of known bifidobacterial NF and EM, their validation level and related evidence supporting an effect of manufacturing.

Protein	Bioactivity class and validation level	Evidence of potential manufacturing Impact
Sortase dependent pili	Niche factor; *in vitro* (Turroni et al., 2013)	Growth phase dependent transcription in *B. bifidum* (Westermann et al., 2012)
	Effector molecule; *in vitro* and *in vivo* (Turroni et al., 2013)	Carbohydrate regulated transcription in *B. bifidum* (Foroni et al., 2011; Serafini et al., 2014) and *B. adolescentis* (Duranti et al., 2014)
		Lysine presence is necessary for protein production in *B. bifidum* (Turroni et al., 2014)
Type IVb TAD pili	Niche factor; *in vivo* (O'Connell Motherway et al., 2011)	Growth phase dependent transcription in *B. bifidum* (Westermann et al., 2012)
	Effector molecule; *in vitro* and *in vivo* (O'Connell Motherway et al., 2019)	
Serpin	Niche factor; *in vitro* (Ivanov et al., 2006)	Carbohydrate substrate controls protein presence in *B. longum* (Duboux et al., 2021)
	Effector molecule; *in vivo* (McCarville et al., 2017)	Protease presence controls expression in *B. breve* (Turroni et al., 2010; Alvarez-Martin et al., 2012)
Moonlighting proteins (transaldolase, enolase, DnaK)	Niche factor; *in vitro* (Candela et al., 2007; Gleinser et al., 2012; González-Rodríguez et al., 2012)	Unknown metabolite presence during growth enhance extracellular vehicle production in *B. longum* (Nishiyama et al., 2020)
EPS	Niche factor; *in vitro* (Wu et al., 2010; Xu et al., 2011; Amiri et al., 2019)	Carbohydrate substrate modified transcription (Audy et al., 2010) and yield in *B. longum* (Roberts et al., 1995)
	Effector molecule; *in vitro* (López et al., 2012; Hidalgo-Cantabrana et al., 2013, 2016) and *in vivo* (Xu et al., 2017), but lack structure/function relationship	Growth conditions modulate EPS yield in *B. animalis* (Amiri et al., 2019) and *B. longum* (Ninomiya et al., 2009)

procedures (air-, freeze-, spray-drying) impacted on the anti-inflammatory properties of *B. bifidum*, as determined by cytokine production profiling in Peripheral Blood Mononuclear Cells (PBMC) following co-incubation with the differently processed bacterial preparations of the same strain. In addition, this study demonstrated that different down-stream process may affect the hydrophobicity of the strain, which is indicative of changes in cell-surface properties (Laconelli et al., 2015). Conversely, similar analyses showed that spray-drying did not alter the immunomodulatory potential of two *B. animalis* subsp. *lactis* strains (INL1 and BB12), nor did it modify their preventive effect on colitis *in vivo* (Burns et al., 2017). Similarly, although freeze-drying was proposed to enhance the adherence capacity of *B. animalis* subsp. *lactis* BB12, increasing its capacity to outcompete *C. difficile in vitro* (du Toit et al., 2013), these effects were not observed for other strains of *B. animalis* subsp. *lactis* (Charnchai et al., 2016). These studies illustrate the rather limited information concerning the potential impact of manufacturing on bifidobacteria bioactivity, and highlight the contradictory findings described to date on the potential role of downstream processing (e.g., drying) in influencing *Bifidobacterium* probiotic functionality. However, these studies mostly addressed the consequences of different downstream-processing conditions (i.e., drying procedures) on *in vitro* outcomes (O'Connell Motherway et al., 2011; Westermann et al., 2016), whereas the upstream processing (e.g., fermentation parameters) effects on the expression of NF and/or EM in these bacteria remain to be deciphered.

Metabolic Regulation of Pili Production

Two types of pili have been described in bifidobacteria to act as NF and EM, the sortase dependant pili and the Type IV TAD pili. Sortase dependent pili gene clusters consisting of major (fimA or fimP) and minor (fimB or fimQ) subunit structural proteins are widely distributed amongst *Bifidobacterium* species (Foroni et al., 2011). However, their genetic distribution among strains and species within this genus appears quite disperse. For example, *B. adolescentis* contains five distinct pili encoding gene clusters, while other bifidobacteria, like *B. bifidum*, contains "only" three of these clusters. Out of the three pili gene clusters found in *B. bifidum* PRL2010, only *pil2* and *pil3* were found to be functional, and *pil1* being disrupted by a frameshift (Foroni et al., 2011; Turroni et al., 2013; Duranti et al., 2014). Importantly, and analogous to what was shown for *L. rhamnosus GG*, the sortase dependent pili of *B. bifidum* PRL2010 were demonstrated to play a role in both adhesive and anti-inflammatory properties of the strain using recombinant *L. lactis* harboring the *pil2* or *pil3* gene clusters. While Pil2 was shown to act as a NF and mediated binding to extracellular matrix, Pil3 was also able to modify both *in vitro* and *in vivo* inflammatory responses (Turroni et al., 2013).

Similarly to the sortase dependent pili, type IVb TAD pili are also conserved and widely distributed in both gram positive and gram negative bacteria (Pu et al., 2018), and has been identified in multiple *B. breve* and *B. bifidum* strains (O'Connell Motherway et al., 2011; Westermann et al., 2012). It was demonstrated that the Type IVb TAD pili of *B. breve* UCC2003 act as NF, as disruption of the ATPase encoding gene $tadA_{2003}$, which is essential for its assembly, resulted in a decreased capacity of the strain to colonize the mouse intestine (O'Connell Motherway et al., 2011). Additionally, using a set of recombinant *B. breve*

UCC 2003 strains it was shown that the same pilin structure (and particularly its TadE pilin subunit) could contribute to the maturation of the naïve gut, since it promoted epithelial proliferation both *in vitro* and *in vivo* (O'Connell Motherway et al., 2019), demonstrating its additional EM role.

Limited information is available about the regulation of production of the various pili that are encoded by bifidobacteria. In *B. bifidum* S17 it was demonstrated that sortase-dependent pili encoded by the *pil2* and *pil3* clusters were higher expressed during exponential growth as compared to the stationary phase of growth (Westermann et al., 2012). In another strain of the same species, *B. bifidum* PRL2010, the *pil2* and *pil3* clusters were transcribed both during growth in laboratory medium (MRS) as well as in the mouse cecum, whereas transcription of the *pil1* cluster could not be detected under either of these conditions (Turroni et al., 2013). Culturing of this strain in bovine milk led to activation transcription of the *pil1* cluster genes, indicating that growth (i.e., production) conditions can influence the repertoire of pilin produced by *B. bifidum* PRL2010. This observation was expanded by demonstrating that the other *pil* clusters in this strain were subject to substrate regulation, which is exemplified by the induction of transcription of the *pil2* cluster during growth on fructo-oligosaccharides (FOS) and the induction of the *pil3* cluster during both growth on bovine milk or polysaccharides derived from kefir (Foroni et al., 2011; Serafini et al., 2014). Analogously, the expression of *pil* gene clusters was also regulated by the carbon source used for growth in *B. adolescentis* 22L, where maltodextrin or cellobiose as substrates for growth resulted in an increase of gene expression (compared to growth on glucose) for *pil3*, *pil4*, and *pil5*, which coincided with increased adhesion of the strain to laminin, fibrinogen, and fibronectin, albeit that direct relatedness of these observations remains to be established (Duranti et al., 2014). Besides the carbon source for growth, also the available nitrogen source in the medium has been reported to control pilin expression. For example, the presence of lysine in the growth medium appeared to be essential for Pil2 and Pil3 production by *B. bifidum* PRL2010 (Turroni et al., 2014).

In both *B. breve* and *B. bifidum*, part of the genes encoding the Type IVb TAD pili were found to be expressed during standard growth conditions in the laboratory (O'Connell Motherway et al., 2011; Westermann et al., 2012). However, the transcriptional levels of the Type IVb TAD pilus encoding genes in *B. breve* were strongly induced (25–62-fold) when the bacteria were inhabiting the murine intestinal tract. This was further supported by immunogold staining demonstrating that the pili structures could only be observed when the strain was harvested from the murine gut (O'Connell Motherway et al., 2011). Even though the Type IVb TAD pili protein presence was not assessed in laboratory-grown (MRS) *B. bifidum* S17, the encoding genes (*tadZ, tadA,* and *tadB*) were expressed in a growth phase dependent manner, with higher transcriptional levels in the exponential phase compared to the stationary phase (Westermann et al., 2012).

Although, the specific environmental factors that regulate pili production of specific bifidobacterial pili are quite diverse (e.g., carbon source, nitrogen source, "intestinal conditions," etc.) and/or remain unknown, it is clear from the observations presented above that pilin expression by *Bifidobacterium* probiotics may be modulated by the growth conditions (e.g., substrate) employed during production. In addition, more work deserves to be pursued to decipher the role of downstream processing, as analogous to what has been described for the pili of *L. rhamnosus* GG, we can hypothesis that the presence of the pili on the cell-surface of the bifidobacteria may be impacted by drying procedures.

Environmental Factors Regulating Serine Protease Inhibitor Production

The serine protease inhibitor (serpin) of pancreatic and neutrophilic elastases was has initially described in *B. longum* NCC 2705 (Ivanov et al., 2006). This protein was shown to be conserved in a broad range of bifidobacteria and has been proposed to protect them against host produced proteases, thus providing them with a survival and colonization advantage (Ivanov et al., 2006; Turroni et al., 2010). The serpin's capacity to inhibit the Human Neutrophil Elastase (Ivanov et al., 2006) may also be involved in the immunomodulatory capacities of the strain (Riedel et al., 2006) as elastase is released by activated neutrophils at the sites of intestinal inflammation in the gastro-intestinal tract (Burg and Pillinger, 2001). In line with this role in dampening innate immunity, serpin was demonstrated to play a key role in the anti-inflammatory effect of *B. longum* NCC 2705 in a mouse model of gluten sensitivity (McCarville et al., 2017). In addition, it was recently reported that the serpin of the NCC 2705 strain prevented enteric nerve activation *in vitro*, which was proposed to potentially play a role in pain reduction in Irritable Bowel Syndrome (IBS) patients (Buhner et al., 2018). These findings indicate that analogous to the bifidobacterial pili, the role of the serpin is dualistic in the sense that it acts as both NF and EM.

Transcriptional regulation studies of the *B. breve* UCC2003 serpin-encoding gene showed that it involves a protease inducible two-component system encoded directly adjacent to the serpin encoding operon, which was shown to activate serpin production upon exposure of the strain to proteases (e.g., papain) (Alvarez-Martin et al., 2012). However, a similar two-component system appears to be absent in *B. longum* subsp. *longum* strains (including NCC 2705), and variable gene-syntenies encountered in the serpin encoded region in different bifidobacterial (sub-)species suggests that serpin regulation may involve (sub-)species specific mechanisms (Turroni et al., 2010). This notion is further confirmed by our recent study that demonstrated that in *B. longum* subsp. *longum*, serpin production is regulated by the carbohydrate-substrates used for growth, revealing galactose and fructose (or galacto- or fructo- di/oligo-saccharides) as inducing substrates, while the presence of glucose repressed serpin production almost completely (Duboux et al., 2021). These studies illustrate the diverse environmental factors and regulatory mechanisms involved in controlling serpin production in *Bifidobacterium* (sub-) species, indicating that growth conditions (e.g., substrate) could be tailored to ensure, or even enhance the production and function of this NF and/or EM in the final probiotic preparation.

Bifidobacterial Exopolysaccharides Biosynthesis and Potential Link to Bioactivities

Exopolysaccharides (EPS) are extracellular carbohydrates polymers synthesized by a vast variety of micro-organisms, including gram positive bacteria. In bifidobacteria, EPS can be covalently or non-covalently bound to the cell surface (sometimes referred to as capsular polysaccharides; CPS), or can be predominantly secreted. The EPS produced by bifidobacteria are heteropolysaccharides (HePS) that have been reported to vary in molecular weight (between 4.9×10^3 and 3×10^6 Da) (Leivers et al., 2011) and monosaccharide composition and linkage (Hidalgo-Cantabrana et al., 2012). The synthesis of HePS by *Bifidobacterium* strains involves gene clusters (*eps* clusters) and biosynthesis mechanisms that are similar to those described for other microbes, involving a membrane associated synthesis machinery that utilizes cytoplasmic sugar nucleotides as building blocks for the assembly of repeating units that are exported and polymerized to form the HePS (Altmann et al., 2016; Schiavi et al., 2016; Castro-Bravo et al., 2017). Most of the bifidobacterial HePS are predominantly composed of D-galactose and D-glucose, but can also contain other monosaccharides like L-rhamnose, D-mannose, L-arabinose, or D-fructose in ratios that can vary between species and likely also between strains of the same species (Xu et al., 2011; Amiri et al., 2019). This notion is supported by the fact that *eps* gene clusters are highly variable between different species and strains of bifidobacteria (Hidalgo-Cantabrana et al., 2014; Altmann et al., 2016; Schiavi et al., 2016; Castro-Bravo et al., 2017).

Purified EPS produced by *B. longum* BCRC14634 showed an anti-microbial effect on four pathogenic and three food spoiling bacteria (Wu et al., 2010), which could provide a competitive advantage to the strain in the complex gut ecosystem, supporting its role as NF. In addition, bifidobacterial EPS has also been proposed to affect host responses, suggesting that these molecules may also act as EM in bifidobacteria. Firstly, EPS produced by two *B. animalis* strains (*B. animalis* RH and *B. animalis* subsp. *lactis* BB12) was shown to possess anti-oxidant capacities *in vitro* (Xu et al., 2011; Amiri et al., 2019), which could be relevant in order to alleviate intestinal oxidative damages. Then, the EPS produced by different *B. longum* and *B. animalis* strains has been proposed to modulate the immune response of the host based on the role of these molecules in inducing immune cell proliferation and modulating cytokine production in peripheral blood mononuclear cells (PBMCs) (López et al., 2012; Xu et al., 2017). Notably, the immunomodulatory effect of EPS observed in this study was shown to be strain specific, which was exemplified by the finding that out of eight strains of *B. longum* and *B. animalis* tested, only the EPS produced by *B. animalis* A1 and *B. longum* NB667 elicited a significant increase of PBMC proliferation (López et al., 2012). The immunomodulatory capacities of specific bifidobacterial EPS molecules has been reported to be quite diverse, including reports on the induction of pro-inflammatory profiles *in vitro* (López et al., 2012; Hidalgo-Cantabrana et al., 2016) or *in vivo* (Xu et al., 2017) but also cases where anti-inflammatory responses were detected (Wu et al., 2010; Schiavi et al., 2016). However, these studies provided very limited information on the physical and chemical characteristics or the monosaccharide composition of the EPS molecules produced by these different bifidobacterial strains, leaving the relationships of EPS structure and its immunomodulatory function unaddressed. A study by Hidalgo-Cantabrana et al. (2013) partly elucidated how EPS characteristics might affect its biological activity. In this study they used *B. animalis* subsp. *lactis* A1 and two mutant derivatives (A1dO and A1dOxR) that produce EPS with distinct monosaccharide composition and molecular size characteristics compared to the wild-type strain. Strain A1dOxR harbored a mutation in the *Balat_1410* tyrosine kinase encoding gene (Hidalgo-Cantabrana et al., 2015) and expressed the enzyme dTDP-glucose 4,6-dehydratase that catalyzes the production of dTDP-rhamnose at an elevated level, leading to the production of a high molecular weight, rhamnose-rich EPS. The changes in polymer length and monosaccharide composition in this mutant strain were associated with increased production of the anti-inflammatory cytokine IL-10 by PBMCs exposed to the A1dOxR strain relative to its parental strain (Hidalgo-Cantabrana et al., 2013). To the best of our knowledge this is one of the few studies where the EPS structure-function relationship is investigated in the context of immunomodulatory capacities, illustrating that there is a large gap in our mechanistic understanding of the postulated role of EPS as EM in bifidobacteria.

Several studies have demonstrated that growth conditions modulate both the level of production as well as the structural properties of EPS produced by bifidobacteria. As an example, the carbon substrate applied during growth influences the expression of *eps* related genes in *B. longum* CRC002 (Audy et al., 2010), which is potentially influencing the EPS produced by the strain. Indeed, the carbon source used for growth of *B. longum* BB79 affected the level of EPS produced, with lactose leading to the highest level of production when compared to glucose, fructose, or sucrose (Roberts et al., 1995). Besides the influence of the carbon source, differences in concentration of yeast extract, growth temperature and incubation time modulated the EPS production by *B. animalis* BB12 (Amiri et al., 2019), and the level of dissolved oxygen and CO2 concentrations affected EPS production in *B. longum* JBL05 (Ninomiya et al., 2009). Although these studies did not investigate the potential compositional changes in the EPS that was produced, they do highlight that various growth conditions can influence EPS production. In this context, it should be noted that in *L. rhamnosus* E/N, the carbon source used for growth did not only affect the quantity of EPS produced but also its monosaccharide composition (Berecka et al., 2013). Taken together, the existing information illustrates the limited and scattered knowledge of the regulatory mechanisms underlying the production of (different) EPS molecules in bifidobacteria. Especially when the role of EPS as a NF or EM is to be further substantiated, better understanding of the regulation of EPS production and composition will be required to reliably investigate the role played by these molecules in *Bifidobacterium* probiotics. Such knowledge would also be required to design manufacturing procedures that aim to improve the presence and abundance of bioactive EPS molecules in *Bifidobacterium* probiotic products, in order to enhance their health benefit reliability as we propose in this review.

Environmental Regulation of Surface Enzymes Involved in Adhesion

Different cytoplasmic enzymes are also found on the surface of bacterial cells, such as transaldolase, enolase, and DnaK. These surface attached proteins were suggested to act as bifidobacterial NF, based on their *in vitro* demonstrated role in the adhesive properties of *Bifidobacterium* strains. The example proteins mentioned serve typical cytoplasmic functions in glycolysis (transaldolase and enolase) or stress response (DnaK is a chaperonin), but were suggested to be secreted via a yet unknown non-classical secretion mechanism (González-Rodríguez et al., 2012). This class of surface exposed cytoplasmic proteins is often referred to as moonlighting proteins (Candela et al., 2007; Gleinser et al., 2012) defined by the fact that they can perform two or more physiologically relevant biochemical or biophysical functions (Jeffery, 1999). It could be that these proteins become deposited on the cell surface upon lysis of surrounding bacteria that release their cytoplasmic content in the environment. Alternatively, it was recently proposed that in *B. longum* NCC 2705 those type of surface exposed cytoplasmic (moonlighting) proteins could be excreted through the formation of extracellular vesicles (Nishiyama et al., 2020), of which the formation was shown to occur through membrane bubbling upon peptidoglycan damage in *Bacillus subtilis* (Toyofuku et al., 2017).

Modulation of the expression of these cytoplasmic proteins could also affect their surface exposure levels. Although such relation has to the best of our knowledge not been investigated in detail, it has been reported that different environmental factor (pH, bile salts) or mild stress conditions (Sánchez et al., 2007; Candela et al., 2010) can increase expression levels of moonlighting proteins. Finally, extracellular vesicles are one of the purported export-mechanism for adhesive proteins and may be modulated during growth as the presence of yet unidentified gut microbiota derived metabolites (in *in vitro* fecal fermentations) increased their formation (Nishiyama et al., 2020). More work is required to understand how these proteins are ending up on the cell surface, and if different manufacturing steps (e.g., steps inducing lysis of cells or growth condition inducing extracellular vesicles formation) might influence this process.

CONCLUSION AND DISCUSSION

Discrepancies in clinical trial outcomes stemming from the use of probiotics belonging to the *Lactobacillaceae* family or the *Bifidobacterium* genus has been previously reported. Variations in trial design (population, dose, outcome measurement, etc.) have been advocated to at least in part explain the differences in the outcomes. However, the information summarized in the present review indicates that manufacturing conditions can influence on the presence and/or function of probiotic molecules that play critical roles in the survival of the bacteria in the intestinal tract (NF) and/or their interaction with host cells (EM), which may in turn be an additional cause for the observed variations in clinical outcomes. This review argues that knowledge of probiotic NF and/or EM molecules can provide means to assess the impact of manufacturing conditions on the functionality of the studied strain. Ensuring the presence of validated NF and EM in the final probiotic product could ultimately contribute to improve the consistency of the probiotic's clinical effect.

As mentioned above, ensuring the presence and function of NF and EM during manufacturing could be particularly relevant for upper-gastrointestinal tract mediated health-benefits. An interesting example supporting this hypothesis is the serpin produced by *B. longum* NCC 2705 that was shown to reduce gliadin-induced immune responses in a mouse model, which was proposed to compensate the duodenal serine protease inhibitor decrease observed in active celiac disease. Recently, it was shown that the level of serpin production by this strain can be strongly modulated by the carbon source applied for growth, which allows the production of serpin-rich and serpin-poor probiotic preparations that can subsequently be evaluated *in vivo*. Such approach could establish the relevance of EM presence and function in the probiotic product for health benefits elicited in the proximal region of the intestine. Conversely, the Type IVb TAD pili of *B. breve* UCC 2003 was demonstrated to act as EM in the promotion of colonic epithelial cell proliferation. In this case, it would be interesting to study if the presence or absence of those EM in the initial preparation influences their mediated effect in the distal regions of the intestine, as pili expression was shown to be induced during intestinal transit.

Overall, this review highlights that beyond an improvement of the current clinical trial designs, there is a need to better understand the impact of manufacturing on clinical efficacy of probiotic products. First, NF and EM molecules have to be established as surrogate markers for probiotic functionality, linking their presence or absence to functional readouts. Work around this topic is relatively advanced for *Lactobacillaceae* (e.g., with the cases of *L. plantarum* WCFS1 and *L. rhamnosus* GG). However, for *Bifidobacterium* probiotics, only a few molecules were identified to act as EM in preclinical animal studies, like the sortase dependant pili of *B. bifidum* PRL2010, the Type IVb TAD pili of *B. breve* UCC 2003 and the serpin of *B. longum* NCC 2705. Overall, additional work, including *in vivo* demonstrations, is needed to identify and validate the molecules driving the host-bifidobacteria interactions. Once NF or EM established as surrogate markers of functionality, implementation of molecular level quality controls (i.e., based on NF and EM), could nicely complement the traditional live cells (e.g., CFU) enumeration in the final probiotic preparation, hence providing more insight on the functional consistency of dried probiotics.

AUTHOR CONTRIBUTIONS

SD took the lead in writing the manuscript, under direct supervision of MK. MV provided initial literature survey for several sections, under supervision of SD. All authors provided critical feedback and helped shape the manuscript.

ACKNOWLEDGMENTS

We thank B. Bogicevic, A. Mercenier, J. A. Muller, E. Ananta, and E. van der Beek for their critical review of the manuscript.

REFERENCES

Altmann, F., Kosma, P., O'Callaghan, A., Leahy, S., Bottacini, F., Molloy, E., et al. (2016). Genome analysis and characterisation of the exopolysaccharide produced by *Bifidobacterium longum* subsp. longum 35624^{TM}. *PLoS One* 11:e0162983. doi: 10.1371/journal.pone.0162983

Alvarez-Martin, P., O'Connell Motherway, M., Turroni, F., Foroni, E., Ventura, M., and van Sinderen, D. (2012). A two-component regulatory system controls autoregulated serpin expression in *Bifidobacterium breve* UCC2003. *Appl. Environ. Microbiol.* 78, 7032–7041. doi: 10.1128/AEM.01776-12

Amiri, S., Rezaei Mokarram, R., Sowti Khiabani, M., Rezazadeh Bari, M., and Alizadeh Khaledabad, M. (2019). Exopolysaccharides production by *Lactobacillus acidophilus* LA5 and *Bifidobacterium animalis* subsp. lactis BB12: optimization of fermentation variables and characterization of structure and bioactivities. *Int. J. Biol. Macromol.* 123, 752–765. doi: 10.1016/j.ijbiomac.2018.11.084

Ardita, C. S., Mercante, J. W., Kwon, Y. M., Luo, L., Crawford, M. E., Powell, D. N., et al. (2014). Epithelial adhesion mediated by pilin SpaC is required for Lactobacillus rhamnosus GG-induced cellular responses. *Appl. Environ. Microbiol.* 80, 5068–5077. doi: 10.1128/AEM.01039-14

Audy, J., Labrie, S., Roy, D., and LaPointe, G. (2010). Sugar source modulates exopolysaccharide biosynthesis in *Bifidobacterium longum* subsp. longum CRC 002. *Microbiology* 156, 653–664. doi: 10.1099/mic.0.033720-0

Berecka, M. P., Waśko, A., Szwajgier, D., and Choma, A. (2013). Bifidogenic and antioxidant activity of exopolysaccharides produced by *Lactobacillus rhamnosus* E/N cultivated on different carbon sources. *Pol. J. Microbiol.* 62, 181–189.

Bron, P. A., Grangette, C., Mercenier, A., de Vos, W. M., and Kleerebezem, M. (2004). Identification of *Lactobacillus plantarum* genes that are induced in the gastrointestinal tract of mice. *J. Bacteriol.* 186, 5721–5729. doi: 10.1128/JB.186.17.5721-5729.2004

Brussow, H. (2019). Probiotics and prebiotics in clinical tests: an update. *F1000Res.* 8, F1000FacultyRev–1157. doi: 10.12688/f1000research.19043.1

Buhner, S., Hahne, H., Hartwig, K., Li, Q., Vignali, S., Ostertag, D., et al. (2018). Protease signaling through protease activated receptor 1 mediate nerve activation by mucosal supernatants from irritable bowel syndrome but not from ulcerative colitis patients. *PLoS One* 13:e0193943. doi: 10.1371/journal.pone.0193943

Burg, N. D., and Pillinger, M. H. (2001). The neutrophil: function and regulation in innate and humoral immunity. *Clin. Immunol.* 99, 7–17. doi: 10.1006/clim.2001.5007

Burns, P., Alard, J., Hrdy, J., Boutillier, D., Paez, R., Reinheimer, J., et al. (2017). Spray-drying process preserves the protective capacity of a breast milk-derived Bifidobacterium lactis strain on acute and chronic colitis in mice. *Sci. Rep.* 7:43211. doi: 10.1038/srep43211

Candela, M., Bergmann, S., Vici, M., Vitali, B., Turroni, S., Eikmanns, B. J., et al. (2007). Binding of human plasminogen to Bifidobacterium. *J. Bacteriol.* 189, 5929–5936.

Candela, M., Centanni, M., Fiori, J., Biagi, E., Turroni, S., Orrico, C., et al. (2010). DnaK from Bifidobacterium animalis subsp. lactis is a surface-exposed human plasminogen receptor upregulated in response to bile salts. *Microbiology* 156, 1609–1618. doi: 10.1099/mic.0.038307-0

Castro-Bravo, N., Hidalgo-Cantabrana, C., Rodriguez-Carvajal, M. A., Ruas-Madiedo, P., and Margolles, A. (2017). Gene replacement and fluorescent labeling to study the functional role of exopolysaccharides in bifidobacterium animalis subsp. lactis. *Front. Microbiol.* 8:1405. doi: 10.3389/fmicb.2017.01405

Charnchai, P., Jantama, S. S., Prasitpuriprecha, C., Kanchanatawee, S., and Jantama, K. (2016). Effects of the food manufacturing chain on the viability and functionality of bifidobacterium animalis through simulated gastrointestinal conditions. *PLoS One* 11:e0157958. doi: 10.1371/journal.pone.0157958

Claes, I. J., Segers, M. E., Verhoeven, T. L., Dusselier, M., Sels, B. F., De Keersmaecker, S. C., et al. (2012). Lipoteichoic acid is an important microbe-associated molecular pattern of *Lactobacillus rhamnosus* GG. *Microb. Cell Fact.* 11:161. doi: 10.1186/1475-2859-11-161

Corcoran, B. M., Stanton, C., Fitzgerald, G., and Ross, R. P. (2008). Life under stress: the probiotic stress response and how it may be manipulated. *Curr. Pharm. Des.* 14, 1382–1399. doi: 10.2174/138161208784480225

Debabov, D. V., Heaton, M. P., Zhang, Q., Stewart, K. D., Lambalot, R. H., and Neuhaus, F. C. (1996). The D-Alanyl carrier protein in *Lactobacillus casei*: cloning, sequencing, and expression of dltC. *J. Bacteriol.* 178, 3869–3876. doi: 10.1128/jb.178.13.3869-3876.1996

Debabov, D. V., Kiriukhin, M. Y., and Neuhaus, F. C. (2000). Biosynthesis of lipoteichoic acid in *Lactobacillus rhamnosus*: role of DltD in D-alanylation. *J. Bacteriol.* 182, 2855–2864. doi: 10.1128/JB.182.10.2855-2864.2000

Dronkers, T. M. G., Ouwehand, A. C., and Rijkers, G. T. (2020). Global analysis of clinical trials with probiotics. *Heliyon* 6:e04467.

du Toit, E., Vesterlund, S., Gueimonde, M., and Salminen, S. (2013). Assessment of the effect of stress-tolerance acquisition on some basic characteristics of specific probiotics. *Int. J. Food Microbiol.* 165, 51–56. doi: 10.1016/j.ijfoodmicro.2013.04.022

Duboux, S., Golliard, M., Muller, J. A., Bergonzelli, G., Bolten, C. J., Mercenier, A., et al. (2021). Carbohydrate-controlled serine protease inhibitor (serpin) production in *Bifidobacterium longum* subsp. longum. *Sci. Rep.* 11:7236. doi: 10.1038/s41598-021-86740-y

Duranti, S., Turroni, F., Lugli, G. A., Milani, C., Viappiani, A., Mangifesta, M., et al. (2014). Genomic characterization and transcriptional studies of the starch-utilizing strain bifidobacterium adolescentis 22L. *Appl. Environ. Microbiol.* 80, 6080–6090. doi: 10.1128/AEM.01993-14

Fenster, K., Freeburg, B., Hollard, C., Wong, C., Ronhave Laursen, R., and Ouwehand, A. C. (2019). The production and delivery of probiotics: a review of a practical approach. *Microorganisms* 7:83. doi: 10.3390/microorganisms7030083

Foroni, E., Serafini, F., Amidani, D., Turroni, F., He, F., Bottacini, F., et al. (eds) (2011). Genetic analysis and morphological identification of pilus-like structures in members of the genus Bifidobacterium. *Microb. Cell Fact.* 10:S16. doi: 10.1186/1475-2859-10-S1-S16

Forssten, S. D., Laitila, A., Maukonen, J., and Ouwehand, A. C. (2020). Probiotic triangle of success; strain production, clinical studies and product development. *FEMS Microbiol. Lett.* 367:fnaa167. doi: 10.1093/femsle/fnaa167

Gaucher, F., Bonnassie, S., Rabah, H., Marchand, P., Blanc, P., Jeantet, R., et al. (2019). Review: adaptation of beneficial propionibacteria, *Lactobacilli*, and bifidobacteria improves tolerance toward technological and digestive stresses. *Front. Microbiol.* 10:841. doi: 10.3389/fmicb.2019.00841

Gleinser, M., Grimm, V., Zhurina, D., Yuan, J., and Riedel, C. U. (2012). Improved adhesive properties of recombinant bifidobacteria expressing the Bifidobacterium bifidum-specific lipoprotein BopA. *Microbial. Cell Fact.* 11:80. doi: 10.1186/1475-2859-11-80

González-Rodríguez, I., Sánchez, B., Ruiz, L., Turroni, F., Ventura, M., Ruas-Madiedo, P., et al. (2012). Role of extracellular transaldolase from *Bifidobacterium bifidum* in mucin adhesion and aggregation. *Appl. Environ. Microbiol.* 78, 3992–3998. doi: 10.1128/AEM.08024-11

Grzeskowiak, L., Isolauri, E., Salminen, S., and Gueimonde, M. (2011). Manufacturing process influences properties of probiotic bacteria. *Br. J. Nutr.* 105, 887–894. doi: 10.1017/S0007114510004496

Guo, Q., Goldenberg, J. Z., Humphrey, C., El Dib, R., and Johnston, B. C. (2019). Probiotics for the prevention of pediatric antibiotic-associated diarrhea. *Cochrane Database Syst. Rev.* 4:CD004827.

Hidalgo-Cantabrana, C., Algieri, F., Rodriguez-Nogales, A., Vezza, T., Martínez-Camblor, P., Margolles, A., et al. (2016). Effect of a ropy exopolysaccharide-producing Bifidobacterium animalis subsp. lactis strain orally administered on DSS-induced colitis mice model. *Front. Microbiol.* 7:868. doi: 10.3389/fmicb.2016.00868

Hidalgo-Cantabrana, C., López, P., Gueimonde, M., Clara, G., Suárez, A., Margolles, A., et al. (2012). Immune modulation capability of exopolysaccharides synthesised by lactic acid bacteria and bifidobacteria. *Probiotics Antimicrob. Proteins* 4, 227–237. doi: 10.1007/s12602-012-9110-2

Hidalgo-Cantabrana, C., Sanchez, B., Alvarez-Martin, P., Lopez, P., Martinez-Alvarez, N., Delley, M., et al. (2015). A single mutation in the gene responsible for the mucoid phenotype of Bifidobacterium animalis subsp. lactis confers surface and functional characteristics. *Appl. Environ. Microbiol.* 81, 7960–7968. doi: 10.1128/AEM.02095-15

Hidalgo-Cantabrana, C., Sánchez, B., Milani, C., Ventura, M., Margolles, A., and Ruas-Madiedo, P. (2014). Genomic overview and biological functions of exopolysaccharide biosynthesis in *Bifidobacterium spp*. *Appl. Environ. Microbiol.* 80, 9–18. doi: 10.1128/AEM.02977-13

Hidalgo-Cantabrana, C., Sanchez, B., Moine, D., Berger, B., de Los Reyes-Gavilan, C. G., Gueimonde, M., et al. (2013). Insights into the ropy phenotype of the exopolysaccharide-producing strain Bifidobacterium animalis subsp. lactis A1dOxR. *Appl. Environ. Microbiol.* 79, 3870–3874. doi: 10.1128/AEM.00633-13

Hill, C., Guarner, F., Reid, G., Gibson, G. R., Merenstein, D. J., Pot, B., et al. (2014). Expert consensus document. the international scientific association for probiotics and prebiotics consensus statement on the scope and appropriate use of the term probiotic. *Nat. Rev. Gastroenterol. Hepatol.* 11, 506–514. doi: 10.1038/nrgastro.2014.66

Ivanov, D., Emonet, C., Foata, F., Affolter, M., Delley, M., Fisseha, M., et al. (2006). A serpin from the gut bacterium *Bifidobacterium longum* inhibits eukaryotic elastase-like serine proteases. *J. Biol. Chem.* 281, 17246–17252. doi: 10.1074/jbc.M601678200

Jeffery, C. J. (1999). Moonlighting proteins. *Trends Biochem. Sci.* 24, 8–11.

Johnston, B. C., Goldenberg, J. Z., Vandvik, P. O., Sun, X., and Guyatt, G. H. (2011). Probiotics for the prevention of pediatric antibiotic-associated diarrhea. *Cochrane Database Syst. Rev.* 4:CD004827.

Joint Fao/Who Working Group Report on Drafting (2002). *Guidelines for the Evaluation of Probiotics in Food*. London: Food and Agriculture Organization.

Kalliomaki, M., Salminen, S., Arvilommi, H., Kero, P., Koskinen, P., and Isolauri, E. (2001). Probiotics in primary prevention of atopic disease: a randomised placebo-controlled trial. *Lancet* 357, 1076–1079. doi: 10.1016/S0140-6736(00)04259-8

Kalliomaki, M., Salminen, S., Poussa, T., and Isolauri, E. (2007). Probiotics during the first 7 years of life: a cumulative risk reduction of eczema in a randomized, placebo-controlled trial. *J. Allergy Clin. Immunol.* 119, 1019–1021. doi: 10.1016/j.jaci.2006.12.608

Kiekens, S., Vandenheuvel, D., Broeckx, G., Claes, I., Allonsius, C., De Boeck, I., et al. (2019). Impact of spray-drying on the pili of *Lactobacillus rhamnosus* GG. *Microb. Biotechnol.* 12, 849–855. doi: 10.1111/1751-7915.13426

Kopp, M. V., Hennemuth, I., Heinzmann, A., and Urbanek, R. (2008). Randomized, double-blind, placebo-controlled trial of probiotics for primary prevention: no clinical effects of Lactobacillus GG supplementation. *Pediatrics* 121, e850–e856. doi: 10.1542/peds.2007-1492

Koprivnjak, T., Mlakar, V., Swanson, L., Fournier, B., Peschel, A., and Weiss, J. P. (2006). Cation-induced transcriptional regulation of the dlt operon of *Staphylococcus aureus*. *J. Bacteriol.* 188, 3622–3630. doi: 10.1128/JB.188.10.3622-3630.2006

Laconelli, C., Lemetais, G., Kechaou, N., Chain, F., Bermudez-Humaran, L. G., Langella, P., et al. (2015). Drying process strongly affects probiotics viability and functionalities. *J. Biotechnol.* 214, 17–26. doi: 10.1016/j.jbiotec.2015.08.022

Lebeer, S., Bron, P. A., Marco, M. L., Van Pijkeren, J. P., O'Connell Motherway, M., Hill, C., et al. (2018). Identification of probiotic effector molecules: present state and future perspectives. *Curr. Opin. Biotechnol.* 49, 217–223. doi: 10.1016/j.copbio.2017.10.007

Lebeer, S., Claes, I., Tytgat, H. L., Verhoeven, T. L., Marien, E., von Ossowski, I., et al. (2012). Functional analysis of *Lactobacillus rhamnosus* GG pili in relation to adhesion and immunomodulatory interactions with intestinal epithelial cells. *Appl. Environ. Microbiol.* 78, 185–193. doi: 10.1128/AEM.06192-11

Lebeer, S., Vanderleyden, J., and De Keersmaecker, S. C. (2008). Genes and molecules of lactobacilli supporting probiotic action. *Microbiol. Mol. Biol. Rev.* 72, 728–764. doi: 10.1128/MMBR.00017-08

Lebeer, S., Verhoeven, T. L., Francius, G., Schoofs, G., Lambrichts, I., Dufrene, Y., et al. (2009). Identification of a gene cluster for the biosynthesis of a long, galactose-rich exopolysaccharide in *Lactobacillus rhamnosus* GG and functional analysis of the priming glycosyltransferase. *Appl. Environ. Microbiol.* 75, 3554–3563. doi: 10.1128/AEM.02919-08

Lee, I. C., Tomita, S., Kleerebezem, M., and Bron, P. A. (2013). The quest for probiotic effector molecules–unraveling strain specificity at the molecular level. *Pharmacol. Res.* 69, 61–74. doi: 10.1016/j.phrs.2012.09.010

Leivers, S., Hidalgo-Cantabrana, C., Robinson, G., Margolles, A., Ruas-Madiedo, P., and Laws, A. P. (2011). Structure of the high molecular weight exopolysaccharide produced by *Bifidobacterium animalis* subsp. lactis IPLA-R1 and sequence analysis of its putative eps cluster. *Carbohydr. Res.* 346, 2710–2717. doi: 10.1016/j.carres.2011.09.010

López, P., Monteserín, D. C., Gueimonde, M., de los Reyes-Gavilán, C. G., Margolles, A., Suárez, A., et al. (2012). Exopolysaccharide-producing *Bifidobacterium strains* elicit different in vitro responses upon interaction with human cells. *Food Res. Int.* 46, 99–107.

Marco, M. L., Bongers, R. S., de Vos, W. M., and Kleerebezem, M. (2007). Spatial and temporal expression of *Lactobacillus plantarum* genes in the gastrointestinal tracts of mice. *Appl. Environ. Microbiol.* 73, 124–132. doi: 10.1128/AEM.01475-06

Marco, M. L., de Vries, M. C., Wels, M., Molenaar, D., Mangell, P., Ahrne, S., et al. (2010). Convergence in probiotic Lactobacillus gut-adaptive responses in humans and mice. *ISME J.* 4, 1481–1484. doi: 10.1038/ismej.2010.61

McCarville, J. L., Dong, J., Caminero, A., Bermudez-Brito, M., Jury, J., Murray, J. A., et al. (2017). A commensal *Bifidobacterium longum* strain improves gluten-related immunopathology in mice through expression of a serine protease inhibitor. *Appl. Environ. Microbiol.* 83, e1323–e1317. doi: 10.1128/AEM.01323-17

Nguyen, P. T., Nguyen, T. T., Vo, T. N., Nguyen, T. T., Hoang, Q. K., and Nguyen, H. T. (2021). Response of *Lactobacillus plantarum* VAL6 to challenges of pH and sodium chloride stresses. *Sci. Rep.* 11:1301. doi: 10.1038/s41598-020-80634-1

Ninomiya, K., Matsuda, K., Kawahata, T., Kanaya, T., Kohno, M., Katakura, Y., et al. (2009). Effect of CO2 concentration on the growth and exopolysaccharide production of Bifidobacterium longum cultivated under anaerobic conditions. *J. Biosci. Bioeng.* 107, 535–537. doi: 10.1016/j.jbiosc.2008.12.015

Nishiyama, K., Takaki, T., Sugiyama, M., Fukuda, I., Aiso, M., Mukai, T., et al. (2020). Extracellular vesicles produced by *Bifidobacterium longum* export mucin-binding proteins. *Appl. Environ. Microbiol.* 86, e1464–e1420. doi: 10.1128/AEM.01464-20

O'Connell Motherway, M., Houston, A., O'Callaghan, G., Reunanen, J., O'Brien, F., O'Driscoll, T., et al. (2019). A Bifidobacterial pilus-associated protein promotes colonic epithelial proliferation. *Mol. Microbiol.* 111, 287–301. doi: 10.1111/mmi.14155

O'Connell Motherway, M., Zomer, A., Leahy, S. C., Reunanen, J., Bottacini, F., Claesson, M. J., et al. (2011). Functional genome analysis of *Bifidobacterium breve* UCC2003 reveals type IVb tight adherence (Tad) pili as an essential and conserved host-colonization factor. *Proc. Natl. Acad. Sci. U.S.A.* 108, 11217–11222. doi: 10.1073/pnas.1105380108

Osborn, D. A., and Sinn, J. K. (2007). Probiotics in infants for prevention of allergic disease and food hypersensitivity. *Cochrane Database Syst. Rev.* 4:CD006475. doi: 10.1002/14651858.CD006475.pub2

Pique, N., Berlanga, M., and Minana-Galbis, D. (2019). Health benefits of heat-killed (Tyndallized) probiotics: an overview. *Int. J. Mol. Sci.* 20:2534. doi: 10.3390/ijms20102534

Pu, M., Duriez, P., Arazi, M., and Rowe-Magnus, D. A. (2018). A conserved tad pilus promotes *Vibrio vulnificus* oyster colonization. *Environ. Microbiol.* 20, 828–841. doi: 10.1111/1462-2920.14025

Remus, D., Kleerebezem, M., and Bron, P. A. (2012). *Molecular Analysis of Candidate Probiotic Effector Molecules of Lactobacillus plantarum*. Netherlands: Wageningen University.

Revilla-Guarinos, A., Gebhard, S., Alcantara, C., Staron, A., Mascher, T., and Zuniga, M. (2013). Characterization of a regulatory network of peptide antibiotic detoxification modules in *Lactobacillus casei* BL23. *Appl. Environ. Microbiol.* 79, 3160–3170. doi: 10.1128/AEM.00178-13

Riedel, C. U., Foata, F., Philippe, D., Adolfsson, O., Eikmanns, B. J., and Blum, S. (2006). Anti-inflammatory effects of bifidobacteria by inhibition of LPS-induced NF-kappaB activation. *World J. Gastroenterol.* 12, 3729–3735. doi: 10.3748/wjg.v12.i23.3729

Roberts, C. M., Fett, W. F., Osman, S. F., Wijey, C., O'Connor, J. V., and Hoover, D. G. (1995). Exopolysaccharide production by *Bifidobacterium longum* BB-79. *J. Appl. Bacteriol.* 78, 463–468.

Sánchez, B., Champomier-Vergès, M.-C., Collado, M. D. C., Anglade, P., Baraige, F., Sanz, Y., et al. (2007). Low-pH adaptation and the acid tolerance response of *Bifidobacterium longum* Biotype longum. *Appl. Environ. Microbiol.* 73, 6450–6459. doi: 10.1128/AEM.00886-07

Sanders, M. E., Klaenhammer, T. R., Ouwehand, A. C., Pot, B., Johansen, E., Heimbach, J. T., et al. (2014). Effects of genetic, processing, or product formulation changes on efficacy and safety of probiotics. *Ann. N. Y. Acad. Sci.* 1309, 1–18. doi: 10.1111/nyas.12363

Schiavi, E., Gleinser, M., Molloy, E., Groeger, D., Frei, R., Ferstl, R., et al. (2016). The surface-associated exopolysaccharide of *Bifidobacterium longum* 35624 plays an essential role in dampening host proinflammatory responses and repressing local TH17 responses. *Appl. Environ. Microbiol.* 82, 7185–7196. doi: 10.1128/AEM.02238-16

Segers, M. E., and Lebeer, S. (2014). Towards a better understanding of *Lactobacillus rhamnosus* GG–host interactions. *Microb. Cell Fact.* 13(Suppl. 1):S7. doi: 10.1186/1475-2859-13-S1-S7

Serafini, F., Turroni, F., Ruas-Madiedo, P., Lugli, G. A., Milani, C., Duranti, S., et al. (2014). Kefir fermented milk and kefiran promote growth of *Bifidobacterium bifidum* PRL2010 and modulate its gene expression. *Int. J. Food Microbiol.* 178, 50–59. doi: 10.1016/j.ijfoodmicro.2014.02.024

Sybesma, W., Molenaar, D., van, I. W., Venema, K., and Kort, R. (2013). Genome instability in *Lactobacillus rhamnosus* GG. *Appl Environ Microbiol.* 79, 2233–2239.

Szajewska, H., and Hojsak, I. (2020). Health benefits of *Lactobacillus rhamnosus* GG and *Bifidobacterium animalis* subspecies lactis BB-12 in children. *Postgrad. Med.* 132, 441–451. doi: 10.1080/00325481.2020.1731214

Toyofuku, M., Carcamo-Oyarce, G., Yamamoto, T., Eisenstein, F., Hsiao, C. C., Kurosawa, M., et al. (2017). Prophage-triggered membrane vesicle formation through peptidoglycan damage in *Bacillus subtilis*. *Nat. Commun.* 8:481. doi: 10.1038/s41467-017-00492-w

Tripathi, P., Dupres, V., Beaussart, A., Lebeer, S., Claes, I. J., Vanderleyden, J., et al. (2012). Deciphering the nanometer-scale organization and assembly of *Lactobacillus rhamnosus* GG pili using atomic force microscopy. *Langmuir* 28, 2211–2216. doi: 10.1021/la203834d

Turroni, F., Foroni, E., O'Connell Motherway, M., Bottacini, F., Giubellini, V., Zomer, A., et al. (2010). Characterization of the serpin-encoding gene of *Bifidobacterium breve* 210B. *Appl. Environ. Microbiol.* 76, 3206–3219. doi: 10.1128/AEM.02938-09

Turroni, F., Serafini, F., Foroni, E., Duranti, S., O'Connell Motherway, M., Taverniti, V., et al. (2013). Role of sortase-dependent pili of *Bifidobacterium bifidum* PRL2010 in modulating bacterium–host interactions. *Proc. Natl. Acad. Sci. U.S.A.* 110, 11151–11156. doi: 10.1073/pnas.1303897110

Turroni, F., Serafini, F., Mangifesta, M., Arioli, S., Mora, D., van Sinderen, D., et al. (2014). Expression of sortase-dependent pili of *Bifidobacterium bifidum* PRL2010 in response to environmental gut conditions. *FEMS Microbiol. Lett.* 357, 23–33. doi: 10.1111/1574-6968.12509

van Baarlen, P., Troost, F. J., van Hemert, S., van der Meer, C., de Vos, W. M., de Groot, P. J., et al. (2009). Differential NF-kappaB pathways induction by Lactobacillus plantarum in the duodenum of healthy humans correlating with immune tolerance. *Proc. Natl. Acad. Sci. U.S.A.* 106, 2371–2376. doi: 10.1073/pnas.0809919106

Vargas Garcia, C. E., Petrova, M., Claes, I. J., De Boeck, I., Verhoeven, T. L., Dilissen, E., et al. (2015). Piliation of *Lactobacillus rhamnosus* GG promotes adhesion, phagocytosis, and cytokine modulation in macrophages. *Appl. Environ. Microbiol.* 81, 2050–2062. doi: 10.1128/AEM.03949-14

Veiga, P., Suez, J., Derrien, M., and Elinav, E. (2020). Moving from probiotics to precision probiotics. *Nat. Microbiol.* 5, 878–880. doi: 10.1038/s41564-020-0721-1

Westermann, C., Gleinser, M., Corr, S. C., and Riedel, C. U. (2016). A critical evaluation of bifidobacterial adhesion to the host tissue. *Front. Microbiol.* 7:1220. doi: 10.3389/fmicb.2016.01220

Westermann, C., Zhurina, D. S., Baur, A., Shang, W., Yuan, J., and Riedel, C. U. (2012). Exploring the genome sequence of *Bifidobacterium bifidum* S17 for potential players in host-microbe interactions. *Symbiosis* 58, 191–200.

Wu, M.-H., Pan, T.-M., Wu, Y.-J., Chang, S.-J., Chang, M.-S., and Hu, C.-Y. (2010). Exopolysaccharide activities from probiotic bifidobacterium: immunomodulatory effects (on J774A.1 macrophages) and antimicrobial properties. *Int. J. Food Microbiol.* 144, 104–110. doi: 10.1016/j.ijfoodmicro.2010.09.003

Xu, R., Shen, Q., Ding, X., Gao, W., and Li, P. (2011). Chemical characterization and antioxidant activity of an exopolysaccharide fraction isolated from *Bifidobacterium animalis* RH. *Eur. Food Res. Technol.* 232, 231–240.

Xu, R., Shen, Q., Wu, R., and Li, P. (2017). Structural analysis and mucosal immune regulation of exopolysaccharide fraction from *Bifidobacterium animalis* RH. *Food Agric. Immunol.* 28, 1226–1241.

Yan, F., Liu, L., Dempsey, P. J., Tsai, Y. H., Raines, E. W., Wilson, C. L., et al. (2013). A *Lactobacillus rhamnosus* GG-derived soluble protein, p40, stimulates ligand release from intestinal epithelial cells to transactivate epidermal growth factor receptor. *J. Biol. Chem.* 288, 30742–30751. doi: 10.1074/jbc.M113.492397

Conflict of Interest: SD and MV performed the work as employees of Nestlé (Société des Produits Nestlé SA).

The remaining author declares that the research was conducted in the absence of any commercial or financial relationships that could be construed as a potential conflict of interest.

Publisher's Note: All claims expressed in this article are solely those of the authors and do not necessarily represent those of their affiliated organizations, or those of the publisher, the editors and the reviewers. Any product that may be evaluated in this article, or claim that may be made by its manufacturer, is not guaranteed or endorsed by the publisher.

frontiers in Nutrition

ORIGINAL RESEARCH
published: 04 February 2022
doi: 10.3389/fnut.2022.804210

Heat-Killed *Lacticaseibacillus paracasei* GMNL-653 Exerts Antiosteoporotic Effects by Restoring the Gut Microbiota Dysbiosis in Ovariectomized Mice

*Jhih-Hua Jhong[1], Wan-Hua Tsai[2], Li-Chan Yang[3], Chia-Hsuan Chou[2], Tzong-Yi Lee[4,5], Yao-Tsung Yeh[6,7], Cheng-Hsieh Huang[6,8] and Yueh-Hsia Luo[9]**

[1] Department of Computer Science and Engineering, Yuan Ze University, Taoyuan, Taiwan, [2] Research and Development Department, GenMont Biotech Incorporation, Tainan, Taiwan, [3] Department of Pharmacy, China Medical University, Taichung, Taiwan, [4] School of Life and Health Sciences, The Chinese University of Hong Kong, Shenzhen, China, [5] Warshel Institute for Computational Biology, The Chinese University of Hong Kong, Shenzhen, China, [6] Aging and Diseases Prevention Research Center, Fooyin University, Kaohsiung, Taiwan, [7] Biomed Analysis Center, Fooyin University Hospital, Pingtung, Taiwan, [8] Ph.D. Program in Environmental and Occupational Medicine, Kaohsiung Medical University, Kaohsiung, Taiwan, [9] Department of Life Sciences, National Central University, Taoyuan, Taiwan

OPEN ACCESS

Edited by:
Sabina Górska,
Polish Academy of Sciences, Poland

Reviewed by:
Guoju Hong,
University of Alberta, Canada
Giovanni Iolascon,
University of Campania Luigi Vanvitelli, Italy
Hailing Xin,
Second Military Medical University, China

***Correspondence:**
Yueh-Hsia Luo
yhluo@ncu.edu.tw

Specialty section:
This article was submitted to Nutritional Immunology, a section of the journal Frontiers in Nutrition

Received: 29 October 2021
Accepted: 13 January 2022
Published: 04 February 2022

Citation:
Jhong JH, Tsai WH, Yang LC, Chou CH, Lee TY, Yeh YT, Huang CH and Luo YH (2022) Heat-Killed Lacticaseibacillus paracasei GMNL-653 Exerts Antiosteoporotic Effects by Restoring the Gut Microbiota Dysbiosis in Ovariectomized Mice. Front. Nutr. 9:804210. doi: 10.3389/fnut.2022.804210

Osteoporosis is a metabolic inflammatory disease, an imbalance occurs between bone resorption and formation, leading to bone loss. Anti-inflammatory diet is considered having the potential to ameliorate osteoporosis. Heat-killed probiotics exhibit health benefits in relation to their immunomodulatory effects, but the detail mechanism involved in gut microbiota balance, host metabolism, immunity, and bone homeostasis remains unclear. In this study, we evaluated the antiosteoporotic effects of heat-killed *Lacticaseibacillus paracasei* GMNL-653 *in vitro* and in ovariectomized (OVX) mice. Furthermore, whole-genome sequencing and comparative genomics analysis demonstrated potentially genes involved in antiosteoporotic activity. The GMNL-653 exerts anti-inflammatory activity which restored gut microbiota dysbiosis and maintained intestinal barrier integrity in the OVX mice. The levels of IL-17 and LPS in the sera decreased following GMNL-653 treatment compared with those of the vehicle control; mRNA levels of *RANKL* were reduced and *TGF-β* and *IL-10* enhanced in OVX-tibia tissue after treatment. The levels of IL-17 were significantly associated with gut microbiota dysbiosis. Gut microbial metagenomes were further analyzed by PICRUSt functional prediction, which reveal that GMNL-653 intervention influence in several host metabolic pathways. The analysis of whole-genome sequencing accompanied by comparative genomics on three *L. paracasei* strains revealed a set of GMNL-653 genes that are potentially involved in antiosteoporotic activity. Our findings validated antiosteoporotic activity of heat-killed GMNL-653 using *in vitro* and *in vivo* models, to whole-genome sequencing and identifying genes potentially involved in this gut microbiota–bone axis.

Keywords: *Lacticaseibacillus paracasei*, gut microbiota, dysbiosis, whole-genome sequencing, gut-bone axis, IL-17A, RANKL (receptor activator for nuclear factor k B ligand), antiosteoporotic effects

INTRODUCTION

Environmental factors influence host health through gut microbiota (1). Gut microbial communities can tune host immunity, modulate gut endocrine function and neurological signaling, and produce vital metabolites that influence the host (2). Gut dysbiosis is associated with many diseases, including metabolic liver diseases, cardiometabolic diseases, obesity, and type 2 diabetes (1). Moreover, studies and emerging evidence have indicated that dysregulated gut microbiota correlate with decreased bone density, and inflammatory bowel disease (IBD) (3–5). A close relationship between bone health and gut microbiota exist that may involve in calcium absorption, bone mineralization, and immune signaling (6, 7). Osteoporosis, a common metabolic inflammatory disease, is characterized by low bone density and the destruction of bone tissue; an imbalance occurs between bone resorption and formation, leading to bone loss. Osteoporosis-induced fractures of the femur and vertebrae profoundly affect the life quality and mortality of aging populations, representing a serious public health problem, and incurring high medical care costs. Postmenopausal osteoporosis increases the expression of proinflammatory and osteogenic cytokines, including interleukin 1 (IL-1), interleukin 6 (IL-6), tumor necrosis factor-alpha (TNF-α), macrophage colony stimulating factor (MCSF), and the receptor activator of nuclear factor kappa-light-chain-enhancer of activated B cells ligand (RANKL) from osteoblasts, T cells, and B cells (8–11). Gut dysbiosis not only induces local or systemic inflammation but also dysregulates nutrients and calcium across the intestine and into systemic circulation. Several drugs (e.g., bisphosphonates, denosumab, teriparatide, and abaloparatide) are used to treat osteoporosis through the blocking of bone reabsorption, stimulating of bone formation, or both (12). Combined use of drugs and probiotic supplementation may represent a safe and potentially effective therapy strategy for osteoporosis.

Although probiotics are considered non-pathogenic live microorganisms, the safety profile of live probiotic supplement remains unclear in certain circumstances, particularly in regard to the translocation of bacteria from intestinal tissue to systemic circulation (13). Hence, the utilization of nonviable heat-killed probiotics has drawn increased attention. Several studies have reported that heat-killed probiotics exhibit health benefits in terms of their immunomodulatory effect (14, 15) in *in vitro* and *in vivo* models. Furthermore, inactivated *Lactobacillus* decreases the production of IgE in an ovalbumin (OVA) mice model (16), mediates the Th1/Th2 switch, and exhibits potential protective effects in food allergies (17). The structural components of probiotics, particularly the cell envelope, capsule, and cell wall components, may play a role in these immunological effects (18, 19). However, the possible mechanisms underlying the influence of heat-killed probiotics on gut microbiota balance, host metabolism, immunity, and bone homeostasis remain undetermined.

In the present study, we investigated the antiosteoporotic effects of three heat-killed *Lacticaseibacillus paracasei* (previously classified as *Lactobacillus paracasei*) strain GMNL-653 *in vitro* and in ovariectomized (OVX) mice. First, we observed that one *L. paracasei* GMNL-653 strain reduced lipopolysaccharide (LPS)-stimulated IL-6 and NO production in the mouse macrophage RAW264.7. Heat-killed GMNL-653 also increased calcium mineralization in human osteosarcoma MG63 cells mineralizing in culture and protected the OVX mice from bone loss, including increasing bone volume over tissue volume (BV/TV) and bone mineral density (BMD). Our results revealed that GMNL-653 restored ovariectomy-induced gut microbiota dysbiosis and maintained intestinal barrier integrity. Additionally, in the OVX mice, GMNL-653 treatment reduced the IL-17 and LPS levels compared with those of the vehicle control group, reduced the mRNA levels of *RANKL*, and increased the anti-inflammatory cytokines *TGF-β* and *IL-10* in tibia tissue. We applied the whole-genome sequencing technique and comparative genomics analysis to further examine these three *L. paracasei*. Our results indicated that the genes related to carbohydrate transport/metabolism and the cell wall/membrane/envelope biogenesis of GMNL-653 are worthy of future investigation. In summary, our results revealed that heat-killed GMNL-653 exhibited antiosteoporotic activity through the gut microbiota–bone axis.

EXPERIMENTAL PROCEDURES

Bacterial Culture and Heat-Inactive Preparations

Lactobacilli were cultured in 1 mL of MRS broth at 37°C for 20 h, and subcultured at a 1:100 ratio in fresh MRS medium. After 20 h of subculture, the bacteria were centrifuged at 13,000 rpm for 1 min, and the bacterial pellet was then washed twice with PBS. The bacteria were suspended in PBS, with the bacterial concentration adjusted to 1×10^{10} cells/mL. The heat-killing method was performed at 90°C for 30 min or through autoclaving at 121°C for 15 min. *Lactobacilli* used in this study were *Limosilactobacillus reuteri* (previously classified as *Lactobacillus reuteri*; CCTCC M 209263), *Lacticaseibacillus rhamnosus* (CCTCC M 203098), *Lacticaseibacillus salivarius* (GMNL-678), and five *Lacticaseibacillus. paracasei* strains (#1:CCTCC M 204012; #2: CCTCC M 2011331; #3: GMNL-653/BCRC-910721; #4: GMNL-855; and #5: BCRC-16100/ATCC 11582) were provided by GenMont Biotech (Tainan, Taiwan).

Cell Culture

The RAW 264.7 cells were cultured in Dulbecco's modified Eagle's complete medium (DMEM) and supplemented with 10% fetal bovine serum (FBS; Invitrogen, MA, Unites States) and 20 μg/mL gentamicin. The cells were seeded with 4×10^5 cells/well in a 24-well plate and then incubated in a humidified atmosphere at 37°C with 5% CO_2. The supernatant was removed, and the adhered cells were washed twice with sterile PBS. Next, fresh DMEM without FBS was added for 2 h of starvation. The cells were treated with or without heat-killed bacteria for 2 h, and then LPS (*Escherichia coli* O111:B4; SI-L4391, Sigma-Aldrich, St. Louis, MO, United States) was added to yield a final concentration of 100 ng/mL for a further 20 h of incubation. The supernatant was collected for cytokine and NO measurement.

In vitro Model for Calcium Mineralization

Mineralization was induced on confluent monolayers through the addition of osteogenic culture medium (OIM) containing 10% (v/v) FBS, 10 mM glycerol-phosphate, 100 mM dexamethasone, and 0.05 mM vitamin C. Human osteosarcoma osteoblastic MG63 cells were cultured in a 24-well plate (3×10^4 cells/well) with DMEM containing 10% FBS. Heat-killed GMNL-653 were adjusted to an appropriate density using OIM medium, and MG63 cells were added. Alizarin red S (ARS) staining was employed to evaluate calcium deposits. The cultures were incubated at 37°C with 5% CO_2 with changes of OIM medium every 7 days. After 28 days, the cells were washed twice with PBS and then fixed with 70% acetic acid for 1 h. The cells were stained with 2% ARS (pH 4.1–4.5) at room temperature for 30 min with gentle shaking. Following the removal of the ARS dye, the cells were washed with H_2O five times. Excess water was removed from the plates, which were then stored at −20°C prior to dye extraction. For quantification of the ARS staining, 200 μL of 10% (v/v) acetic acid was added to each well in the 24-well plate, and the plate was incubated at room temperature for 30 min with gentle shaking. The cells were then scraped from the plate and transferred into a 1.5-mL microcentrifuge tube. After being vortexed for 30 s, the tubes were heated to 85°C for 10 min and then placed into ice for 5 min. The tubes were centrifuged at 20,000 g for 15 min, and 200 μL of the supernatant was transferred into a new 1.5-mL microcentrifuge tube. Next, 75 μL of 10% (v/v) ammonium hydroxide was added to neutralize the acid. Aliquots (50 μL) of the supernatant and standard were measured at 405 nm in a 96-well format.

Enzyme-Linked Immunosorbent Assay

Levels of IL-6 and interleukin 17 (IL-17A) were measured through enzyme-linked immunosorbent assay (BioLegend) according the instructions of the manufacturer. Sera LPS was detected using a Pierce LAL Chromogenic Endotoxin Quantitation Kit (Thermo Scientific, MA, United State).

Animals

Twenty-four female ICR mice aged 8 to 10 weeks were housed in standard cages, maintained under specific pathogen-free conditions, and fed sterilized food and autoclaved water. The mice were either OVX or sham-operated with an intraperitoneal injection of anesthetic following standard protocol and were divided into three categories with eight mice in each group (sham, OVX + H_2O, and OVX + GMNL-653). Mice in OVX + GMNL653 received GMNL-653 treatment once per day after the OVX or sham surgery for 28 days. At the end of experiment (4 weeks), the animals were sacrificed for further analysis.

Micro-Computed Tomography Measures

The alterations in trabecular site of tibia were determined using a high resolution tomography image system micro-CT (SkyScan 1076, kontizh, Belgiumm resolution 18 μm per slice). After positioning right tibia, parameters such as total volume (TV, mm^3), bone volume/total volume (BV/TV, %), apparent density refer to bone mineral density (BMD) (mgHA·ccm-1) were scanned. The locations of analysis were selected under proximal to the growth plate 100 slices and excluded cortical bone.

RNA Isolation and Quantitative Real-Time Reverse Transcription-Polymerase Chain Reaction

The tibia from the OVX and sham mice were dissected, and the soft tissue was removed. The sample was pulverized using liquid nitrogen, and TRIzol reagent was added for RNA isolation. The purified RNA concentration was measured and stored at −80°C, and cDNA was synthesized with the total RNA (5 μg). Quantitative real-time reverse transcription-polymerase chain reaction (PCR) was used to measure *TGF-β*, *RANKL*, *IL-10*, *bone morphogenetic proteins 2 (BMP2), tartrate-resistant acid phosphatase 5b (Trap-5)*, and *glyceraldehyde-3-phosphate dehydrogenase (GAPDH)* expression, with the assays performed using 2× Rotor-Gene SYBR Green PCR Master Mix (204076; QIAGEN). The reaction mixtures were prepared by mixing aliquots of cDNA, 3 μL of forward and reverse primer, and 5 μL of 2× Rotor-Gene SYBR Green PCR Master Mix to obtain a final volume of 10 μL. The reaction mixtures were analyzed on a Rotor-Gene Q 2plex system. Quantitative values were obtained from the threshold cycle (Ct) number. The relative mRNA levels of the target genes were derived using the equation $2 - \Delta Ct$, where ΔCt is $Ct_{targetgene} - Ct_{GAPDH}$. Data were presented as the fold relative to the control value.

16S Ribosomal RNA Gene Amplicon Sequencing

Fecal samples were collected after 28 days of GMNL-653 treatment, and all specimens were extracted using a QIAGEN DNA kit according to the manufacturer's instructions. DNA samples were analyzed with a 260/280 OD in the range of 1.8 to 2.0. 16S ribosomal RNA (rRNA) PCR was performed using metagenomic DNA as a template, which was amplified with the bacterial-specific primers S17 (5′-TCG TCG GCA GCG TCA GAT GTG TAT AAG AGA CAG CCT ACG GGN GGC WGC AG-3′) and A21 (5′-GTC TCG TGG GCT CGG AGA TGT GTA TAA GAG ACA GGA CTA CHV GGG TAT CTA ATC C-3′). The amplified DNA sizing was verified using a fragment analyzer (5300; Agilent Technologies), and sequencing was conducted using a Illumina MiSeq platform. DNA samples were assigned indices and Illumina sequencing adapters with the Nextera XT Index Kit v2. After library construction, the samples were mixed using a 600-cycle MiSeq Reagent Kit v3 at a final concentration of 4 pM, loaded onto a MiSeq cartridge, and then transferred onto the instrument. Automated cluster generation and a 2 × 300 bp paired-end sequencing run was performed. The sequences generated passed through a filtering process to obtain the qualified reads. The total reads were merged, low-quality and chimera sequences were removed, and OTUs at a 97% similarity with the Greengenes database (v13.8) were clustered. We employed the QIAGEN CLC Microbial Genomics Module (v10.1.1) for further analysis.

Processing and Statistical Analysis of Metataxonomic Data

The alpha diversity of taxonomic composition was measured using the Shannon diversity index, which evaluates the overall diversity of each group including the number of observed species (richness) and the evenness of the observed taxonomic composition. Beta diversity was measured using PCoA-Weighted UniFrac to determine the difference in microbial composition among groups. The OTU table was generated using the QIAGEN CLC Microbial Genomics Module combined with linear discriminant analysis effect size (LEfSe). LEfSe was performed using the Galaxy/Hutlab webtool to identify specific microbial markers among groups, with an 0.05 alpha value for the factorial Kruskal–Wallis test and pairwise Wilcoxon test and a linear discriminant analysis (LDA) score cutoff of 2.0. The results revealed that the functional pathways had a significantly different abundance at level 3 among the groups. Additionally, Spearman's correlation (calculated using the corrplot package v0.84) and principal component analysis (PCA; performed using the ade4 package v1.7-16) were applied through the use of R language (v4.0.2). A comparison of the groups was undertaken through two-tailed *t*-test analysis, and a $p < 0.05$ was considered statistically significant. We used GraphPad Prism 8 (GraphPad Software, San Diego, CA, USA) to identify taxonomic differences and generate relative abundance plots.

Library Preparation and Sequencing on the Illumina Platform

For the *L. paracasei* strain GMNL-653, library preparation was conducted in accordance with the Illumina TruSeq Nano DNA Sample Preparation Kit protocol. First, 200 ng of genomic DNA was sonicated to approximately 550 bp. Fragmented DNA was processed to convert the overhangs into blunt ends, and the library size was selected using beads. After ends repair, a single "A" nucleotide was added to the 3′ ends of the blunt fragments, and the corresponding single "T" nucleotide on the adapter with index was ligated to the fragments. The library size was verified through electrophoresis, and the quantification was validated with the NanoPhotometer. All validated libraries were mixed, denatured, and diluted to the appropriate concentration for pair-end 250-cycle sequencing on MiSeq.

For the GMNL-855 and BCRC-16100 strains, 1 μg DNA per sample was used as the input material for the DNA sample preparations. Sequencing libraries were generated using NEBNext Ultra DNA Library Prep Kit for Illumina (New England Biolabs, Ipswich, MA, USA) following the manufacturer's recommendations, and index codes were added to attribute sequences to each sample. In brief, the DNA sample was fragmented through sonication to the size of 350 bp, and DNA fragments were then end-polished, A-tailed, and ligated using the full-length adaptor for Illumina sequencing with further PCR amplification. The PCR products were purified (AMPure XP); the libraries were then analyzed for size distribution by using an Agilent 2100 Bioanalyzer and quantified using real-time PCR. The clustering of the index-coded samples was performed on a cBot Cluster Generation System according to the manufacturer's instructions. After cluster generation, the library preparations were sequenced on an Illumina NovaSeq 6000 platform, and paired-end reads were generated.

Sample Preparation and Sequencing on Oxford Nanopore Technologies GridION

DNA extraction was conducted in accordance with the EasyPure Genomic DNA Kit protocol (TransGen Biotech). Library preparation was performed following Oxford Nanopore Technologies (ONT) protocols in the form of native barcoding genomic DNA (with EXP-NBD103 and SQK-LSK108). Next, 400 ng of genomic DNA was fragmented with transposome randomly, with a barcode added at the same time. DNA was subsequently purified using AMPureXP beads and ligated using motor protein-complexed adapter to DNA ends. The library was quantified using the Qubit Fluorometer, and the prepared library was loaded onto a running buffer-primed flow cell for sequencing. Sequencing of the native genomic DNA was performed on a single R9.4/FLO-MIN106 flow cell on the GridION.

Hybrid Assembly and Genome Annotation

Genomes were constructed through a hybrid assembly method of low-coverage ONT long-read (approximate mean of 6.2, 7.8, and 7.8 kbp for GMNL-653, GMNL-855, and BCRC-16100, respectively), sequencing for generating scaffolds and high-coverage Illumina short-read (550 bp) sequencing for determining the consensus sequence. The *de novo* hybrid genome assembly approach was applied using the MaSuRCA v3.3.1 assembler (20). Specifically, the MaSuRCA assembler first reduces high-coverage Illumina reads to long super reads and then aligns them with long ONT reads to generate even longer super reads (21). Illumina short reads and ONT long reads were input into the MaSuRCA assembler without any preprocessing, as recommended in the MaSuRCA documentation. In addition, the MaSuRCA uses a high coverage of error-prone long reads generated by ONT to construct consensus sequences for regions not captured by the short Illumina reads. Consequently, this approach combines the advantages of the accuracy of Illumina short reads and the coverage of ONT long reads. Furthermore, Benchmarking Universal Single-Copy Orthologs (BUSCO; v.4.0.0) (22) was used for genome completeness assessment through comparison with the lactobacillales_odb10 gene database, which contains 402 orthologs of 304 species (23). The comparison of each chromosome with the reference sequences was conducted using BLASTN and visualized with Easyfig (24).

The genome was annotated through a multipronged approach consisting of the use of Prokka software (25) and a combination of *ab initio* and evidence-driven gene prediction, including protein-coding regions and RNA genes (i.e., tRNA, rRNA). Then, functional classification of these annotated genes was carried out using eggNOG-mapper (26, 27) for annotation and classification in conjunction with the database of Clusters of Orthologous Groups (COGs) of proteins. The CRISPRFinder program was employed to search for CRISPR direct repeats and spacers (28). Mobile genetic elements such as conjugative plasmids,

bacteriophages, and transposons are regarded as a determinant force of horizontal gene transfer. Plasmid identification and typing were conducted using PlasFlow (29), and the genomes were screened for prophages using the PHASTER tool (30); transposon sequences were predicted using RepeatMasker software. Additionally, genes related to the production of bacteriocins were predicted using BAGEL4 (31). Following annotation, the circular genome atlas was generated using the Circos visualization tool (32).

16S rRNA Phylogenetic Analysis

To evaluate the quality of genome assembly, we compared the genome sequence of our strains with that of 12 reported *Lacticaseibacillus* strains from four *L. paracasei* species. The publicly available 16S rRNA sequences of *Lacticaseibacillus* spp. (*L. acidophilus*, *L. amylovorus*, *L. casei*, *L. crispatus*, *L. delbrueckii*, *L. fermentum*, *L. gasseri*, *L. johnsonii*, *L. plantarum*, *L. reuteri*, *L. rhamnosus*, and *L. salivarius*) were retrieved from the National Center for Biotechnology Information nucleotide database (https://www.ncbi.nlm.nih.gov/nuccore/?term=Lactobacillus). Then, the phylogenetic tree was constructed using Molecular Evolutionary Genetics Analysis (MEGA X) software (33). In addition, the multiple sequence alignment program ClustalW was employed to reconstruct the molecular evolution tree using the maximum-likelihood estimation method, with genetic distances computed using the Kimura two-parameter model. Confidence values for the phylogenetic trees were estimated through bootstrap analyses with 1,000 replicates.

Whole-Genome Average Nucleotide Identity Analysis

Although the 16S rRNA sequence-based division into higher taxa is the most widely used classification system for prokaryotes, the sequence of 16S rRNA genes is too conservative to distinguish between closely related species. Hence, to measure the nucleotide-level genomic similarity between our strain and other related *Lactobacillus* genomes, the OrthoANI (34), regarded as the gold standard for prokaryotes at the genomic level, was calculated using the BLASTN program based on the modified algorithm of average nucleotide identity (ANI) (35).

Determination of Virulence Factors and Antimicrobial Resistance Properties

After genome annotation, each homolog of the *L. paracasei* genes was searched in the BLAST database against the Integrated Microbial Genomes and Microbiomes database v.5.0 (36), Virulence Factor Database (VFDB) (37), and Comprehensive Antibiotic Resistance Database (CARD) (38) to identify candidate virulence genes and antibiotic-resistant genes using genotypic methods. The protein-coding gene was submitted into the Resistance Gene Identifier in the CARD for identification of antimicrobial resistance genes under the default settings (perfect/strict option). The BLAST hit cutoff values, and an $E < 1E\text{-}30$ were used to identify the possible virulence genes and antibiotic-resistant genes for further investigation of mobile genetic elements such as bacteriophages, plasmids, naked DNA, or horizontal transposons. In addition, the BlastKOALA (39) search tool v.2.2 in the Kyoto Encyclopedia of Genes and Genomes (KEGG) database (https://www.kegg.jp/) was used for the investigation of undesirable genes.

RESULTS

Heat-Killed *L. paracasei* (GMNL-653) Reduced Levels of IL-6 and NO in LPS-Stimulated Mouse RAW 264.7 Macrophages

The inflammation and bone cells are highly related. We used the macrophage *in vitro* model to screen a variety of strains of heat-killed probiotics with anti-inflammatory activity, namely *L. reuteri*, *L. rhamnosus*, *L. salivarius*, and *L. paracasei.* These bacteria were inactivated at 90 °C for 30 min and then added to mouse RAW264.7 macrophages with or without LPS stimulation. Our results revealed that only *L. salivarius* GMNL-678 *and L. paracasei* GMNL-653 (**Figure 1A**, column 5 and 8) reduced LPS-induced IL-6 production in the macrophages. The other *Lactobacilli* had no inhibitory effect on the production of IL-6 and NO in LPS-stimulated macrophages (**Figure 1A**). GMNL-653 inhibited IL-6 and NO production under LPS stimulation in a dose-dependent manner (**Figures 1B,C**).

Heat-Killed GMNL-653 Increased Calcium Mineralization in Human Osteosarcoma MG63 Cells in Osteoinduction Medium

Bone is a mineralized tissue that continuously undergoes remodeling, with homeostasis achieved through the balance of osteoblasts and osteoclasts (40). First, we employed ARS staining to evaluate calcium deposits using *in vitro* culture (41), demonstrating that a high dose (1×10^8/mL) of GMNL-653 markedly increased calcium deposits in the MG63 cells (**Figure 2**). Furthermore, we investigated whether heat-killed GMNL-653 triggered the differentiation of macrophages into osteoclasts. Acid phosphatase-positive multinucleated (>3 nuclei) cells were counted as osteoclasts, revealing that GMNL-653 did not influence osteoclast differentiation under RANKL stimulation *in vitro* (**Supplementary Figure 1**).

GMNL-653 Protects Mice From Ovariectomy-Induced Bone Loss

To determine the effect of heat-killed probiotic GMNL-653 treatment on OVX-induced bone loss, 8-week-old ICR mice were treated with a vehicle (H_2O), GMNL-653, and GMNL-678 once a day following OVX or sham surgery for 28 days. Alendronate treatment acted as a positive control to treat and prevent osteoporosis in OVX mice (**Table l**). We performed high resolution micro-computed tomography for evaluation right tibia bone morphology and architecture with treatment GMNL-653 in OVX mice. The result showed that GMNL-653 enhances bone microarchitecture in OVX mice (**Supplementary Figure 2**). In the vehicle-treated mice, OVX decreased BV/TV and BMD, whereas the GMNL-653-treated mice exhibited increased BV/TV and BMN. The effects of GMNL-678 were not as obvious as those of GMNL-653. Decreased mRNA levels of

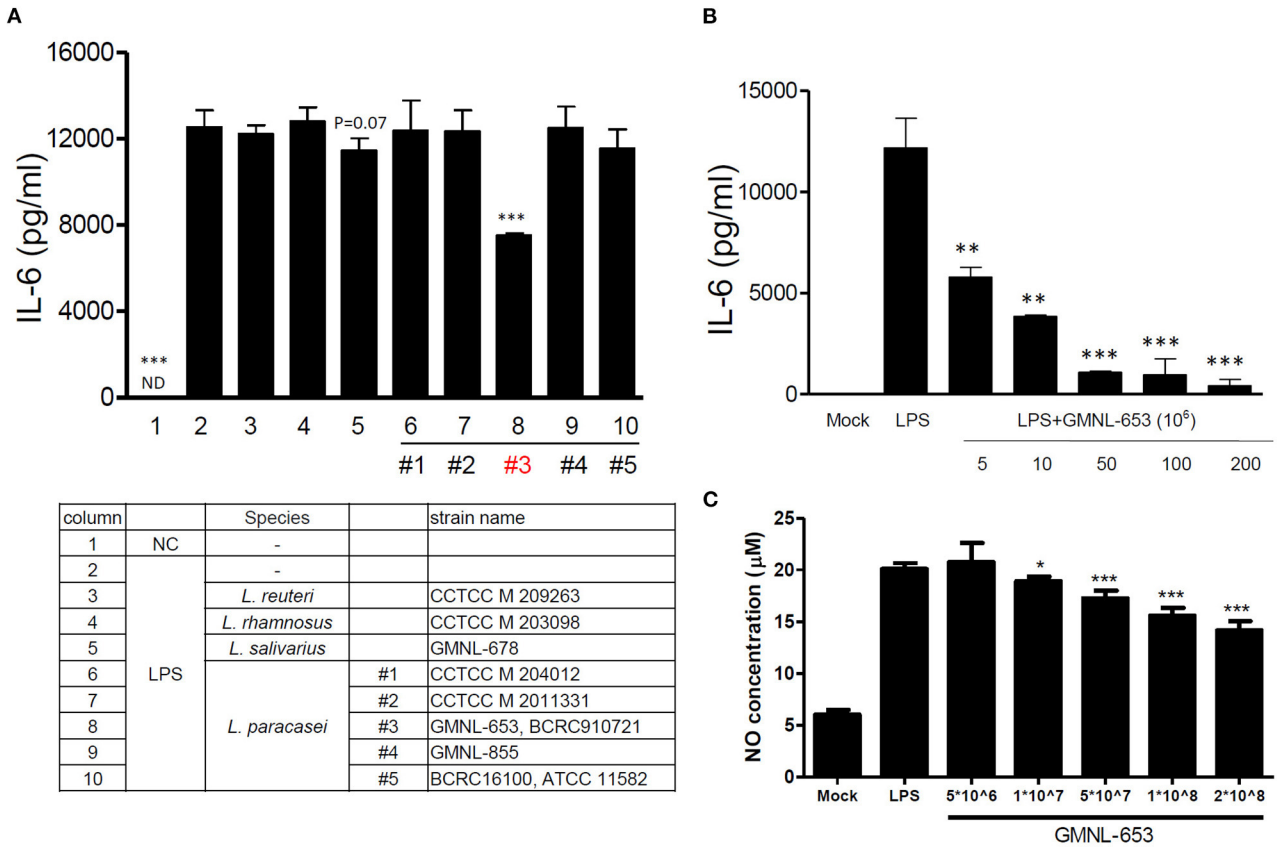

column		Species		strain name
1	NC	-		
2	LPS	-		
3		*L. reuteri*		CCTCC M 209263
4		*L. rhamnosus*		CCTCC M 203098
5		*L. salivarius*		GMNL-678
6		*L. paracasei*	#1	CCTCC M 204012
7			#2	CCTCC M 2011331
8			#3	GMNL-653, BCRC910721
9			#4	GMNL-855
10			#5	BCRC16100, ATCC 11582

FIGURE 1 | Heat-killed probiotics reduced IL-6 and NO levels through LPS stimulation in mouse RAW 264.7 macrophages. An appropriate number of cells were seeded in a 24-well plate. Probiotics (*L. reuteri*, *L. rhamnosus*, *L. salivarius*, and five strains of *L. paracasei*) were cultured in MRS broth for 20 h, with the bacterial concentration adjusted through centrifugation. These bacteria were heat killed (90°C for 30 min) and then added to cells with or without LPS stimulation. After 20 h, the culture supernatant was collected for measurement of the IL-6 production **(A,B)** and NO **(C)**. $^{*}P < 0.05$, $^{**}P < 0.01$, and $^{***}P < 0.001$ compared with the group treated with LPS alone.

TGF-β and *IL-10* and increased *RANKL* in the tibia were observed in the OVX mice treated with H_2O (**Figures 3A–C**). However, GMNL-653 restored the *TGF-β* and *IL-10* levels and decreased the *RANKL* mRNA levels in the OVX mice. We also detect mRNA levels of *bone morphogenetic proteins 2 (BMP2)* and *tartrate-resistant acid phosphatase 5b (TRAP-5)* in OVX mice (**Supplementary Figure 3**). BMP-2 plays a critical role in osteoblast differentiation (42). TRAP-5 has been used as a reliable biomarker of bone resorption and osteoclast number (43). There has been an increasing trend in mRNA levels of *BMP-2* in GMNL-653 treated OVX mice. The GMNL-653 decreased *TRAP-5* levels in OVX mice. In the OVX mice, IL-17A, and LPS levels in the sera also increased, though GMNL-653 decreased these levels (**Figures 3D,E**). These data indicated that GMNL-653 protects mice from ovariectomy-induced bone loss and enhances gut barrier integrity.

GMNL-653 Modulated Gut Microbiota Composition in OVX Mice

Because gut barrier integrity may have been affected in the OVX mice, we further analyzed the gut microbiota compositions. Relative abundance (**Figure 4A**) and diversity (**Figure 4B**) of the fecal microbiota in the sham and OVX mice treated with either the vehicle (H_2O) or GMNL-653 are depicted; at the genus level, the dominant gut microbiota were *rc4-4*, *Ruminococcus*, *Lachnospiracear*, *Mucispirillum*, *Oscillospira*, *Parabacteroides*, *Ruminococcaceae*, *Bacteroides*, *S24-7*, and *Clostridiales* (**Figure 4A**). The results of the PCoA plot of beta diversity (**Figure 4B**) indicated that the microbial community, compared with the sham, OVX, and GMNL-653-treated OVX mice groups, exhibited a significantly distinct cluster that was separate from the other groups.

The differential microbiota from the three groups were identified through LEfSe analysis (**Figure 5A**), which demonstrated that *Tenericutes* (phylum) and *Mollicutes* (class) were enriched in the OVX group and *Lachnospiraceae* (family), *Rhizobiales* (order), *Aeromonadaceae* (family), *Bifidobacteriales* (order), *Bifidobacterium* (genus), *Bifidobacteriaceae* (family), and *Rikenellaceae* (family) were enriched in the OVX+GMNL-653 group. A PCA biplot was generated to investigate the microbial composition differences between the sham, OXV, and OVX + GMNL-653 groups (**Figure 5B**). This biplot revealed that

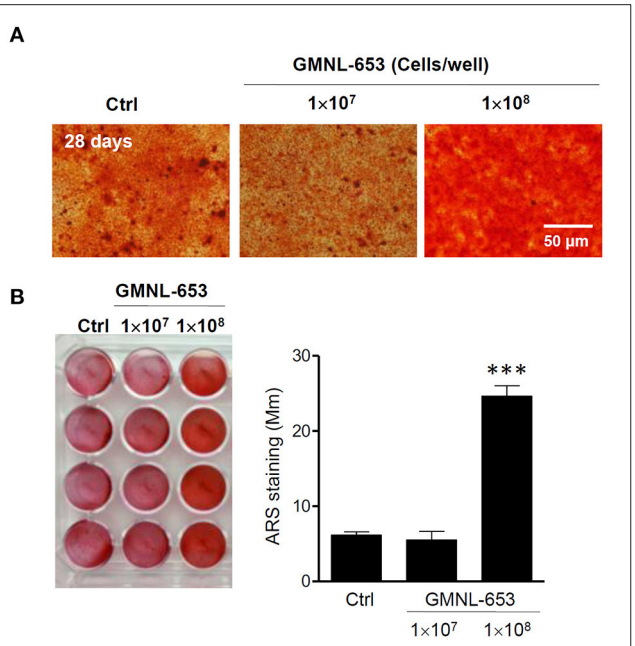

FIGURE 2 | Heat-killed *L. paracasei* (GMNL-653) increased calcium mineralization in human osteosarcoma MG63 cells mineralizing in culture. **(A)** Human osteosarcoma MG63 cells are incubated with heat-killed GMNL-653 in osteoinduction medium for 28 days. Following fixation, the cells are stained with Alizarin Red S to measure calcium deposits. **(B)** Quantification of Alizarin Red S stain by the absorbance (405 nm) of the red extracts according to the manufacturer's instructions. ***$P < 0.001$ compared with the control group.

TABLE 1 | Heat-killed *L. paracasei* (GMNL-653) protect mice from ovariectomy-induced bone loss.

Control	OVX + H_2O	OVX + GMNL-653	OVX + GMNL-678	OVX + alendronate
BV/TV (%)				
42.12 ± 2.4**	30.9 ± 1.1	36.80 ± 1.6**	32.38 ± 0.8*	34.88 ± 0.9**
BMD (g/cm^3)				
0.502 ± 0.04**	0.344 ± 0.04	0.444 ± 0.043**	0.38 ± 0.027*	0.426 ± 0.02*

*$P < 0.05$ and **$P < 0.01$ compared with the OVX+H_2O group.

dimension 1 and dimension 2 explained 51.6 and 20.7% of the variation in gut microbiota composition, respectively. Obvious intergroup distances tended to form distinct clusters between the OVX group and the other two groups, indicating dissimilar gut microbiota. These results suggested that dysbiosis occurred in the OVX mice, which was then modulated through GMNL-653 intervention, leading to a similar configuration to the sham control group. The relative abundance of gut bacteria indicated that the enrichment of *Tenericutes* (phylum) and *Mollicutes* (class) in the OVX mice could be reduced through GMNL-653 supplementation. Likewise, the decreased *Bifidobacteriales* (order), *Bifidobacteriaceae* (family), and *Rikenellaceae* (family) abundance in the OVX mice was enriched by GMNL-653 (**Figure 5C**).

GMNL-653 Intervention Influenced the Relative Abundance of the PICRUSt Functional Prediction of Colonic Microbiota in OVX Mice

To investigate the effect of GMNL-653 on the functional profiles of microbiome communities in the OVX mice, we used PICRUSt to predict metagenomes based on 16S rRNA marker gene sequences and the KEGG database. The results revealed that the relative abundance of several metabolic pathways associated with pathways of cancer, pyruvate metabolism, carbohydrate digestion and absorption, nitrogen metabolism, and geraniol degradation in the colon of OVX mice were altered through GMNL-653 treatment (**Figure 6A**). The relative abundance of the functional pathways in carbohydrate digestion and absorption, fatty acid biosynthesis, ion channels, nitrogen metabolism, and other ion-coupled transporters as well as the pathways of cancer, phenylalanine, tyrosine, and tryptophan biosynthesis, and pyruvate metabolism were downregulated in the OXV group compared with those in the sham group; they were, however, upregulated through GMNL-653 treatment (**Figure 6B**).

Correlation Between Gut Microbiota Composition and Sera Concentrations of IL-17 and LPS in OVX Mice

Our results indicated that sera IL-17 and LPS increased in the OVA mice, implying that gut microbiota composition may be associated with immune responses to osteoporosis. Because GMNL-653 intervention could reverse the dysbiosis of gut microbiota, we further investigated the associations between gut microbiota composition and IL-17 and LPS levels in the OVX mice. We then assessed which specific species were enriched or depleted in the OVA mice and whether this correlated with the cytokine and LPS concentrations. Using Spearman's correlation coefficient, we also investigated the correlation strength of the phylum counted in the OVX mice (**Figure 7A**), with the results demonstrating that the enriched *Bifidobacteriales* (order), *Rikenellaceae* (family), *Bifidobacteriaceae* (family), and *Bifidobacterium* spp. in the OVX + GMNL653 group had significantly negative correlations with sera IL-17. Moreover, the enriched *Tenericutes* (phylum) and *Mollicutes* (class) in the OVX group exhibited positive correlations with sera LPS, whereas the enriched *Aeromonadacae* (family) in the OVX + GMNL-653 group was negatively correlated with sera LPS (**Figure 7B**).

General Genome Features and Comparative Genome Analysis

Whole-genomic DNA–DNA hybridization (DDH) is the gold standard for bacterial species delineation (44). NGS-based genome sequencing has also been widely applied to the taxonomy of microorganisms and was successfully used to distinguish between *L. casei* and *L. paracasei* strains (45). However, these technologies are time intensive, costly, and difficult to use routinely in laboratories. Comparison of the DNA sequences of protein-encoding genes is an alternative approach to the analysis of whole-genome relatedness and has become increasingly critical in the use of these sequences

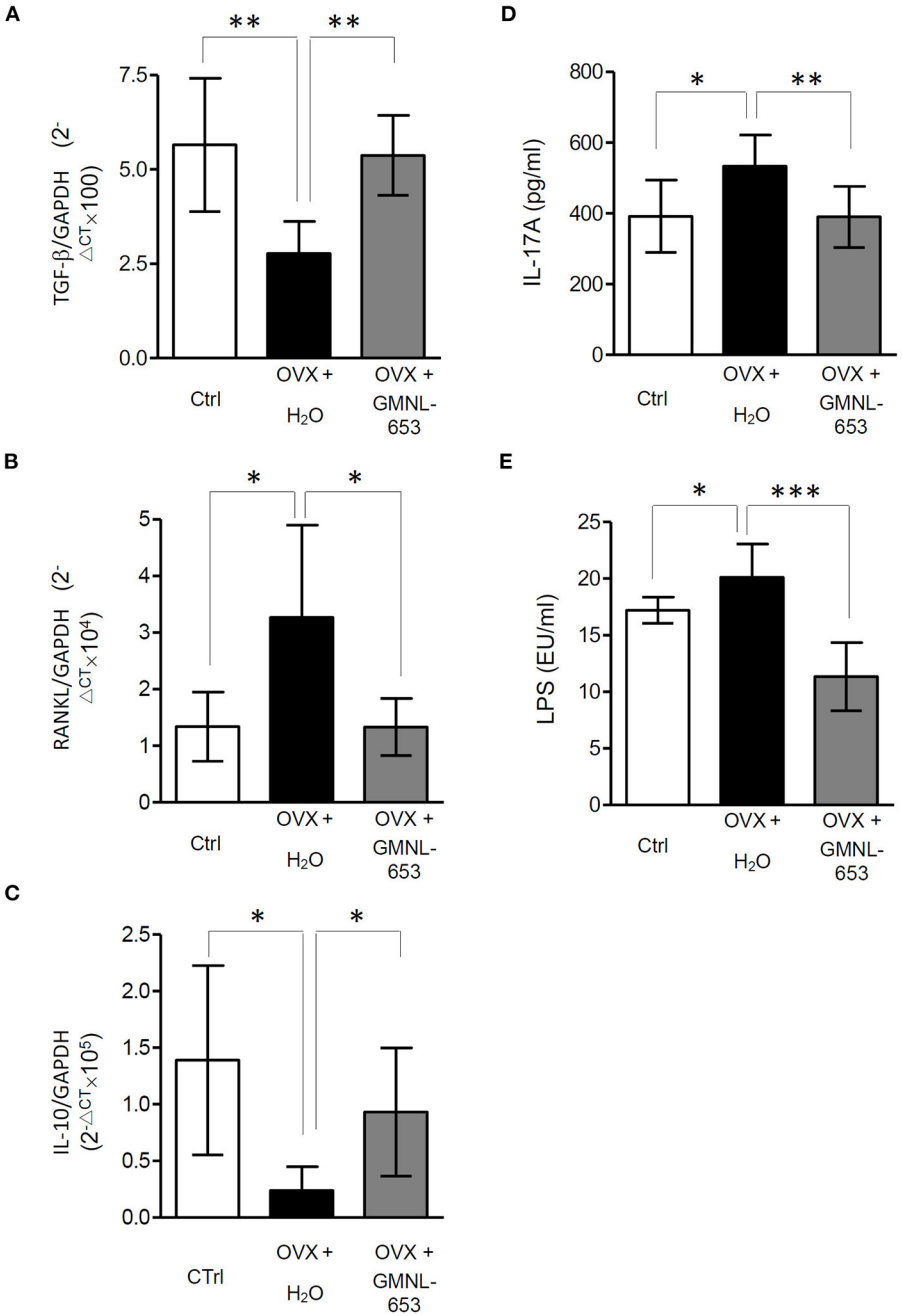

FIGURE 3 | (A–C) The mRNA levels of *TGF-α*, *RANKL*, and *IL-10* in the tibia. **(D,E)** The IL-17A and LPS levels in the sera of ovariectomized (OVX) mice treated with either the vehicle (H_2O) or heat-killed *L. paracasei* (GMNL-653). qRT-PCR analysis of the expression of genes known to promote bone formation, *TGF-β* and *IL-10* **(A,C)**, and bone resorption, *RANKL*, in the tibia of OVX mice. The levels of IL-17A and LPS in the sera are measured through ELISA. $^*P < 0.05$, $^{**}P < 0.01$, and $^{***}P < 0.001$ compared with the OVX+H_2O group.

as molecular targets for microbial species identification. We identified and verified the distinct nature of the three strains of *L. paracasei* (GMNL-653, GMNL-855, and BCRC-16100) by using SEM, RAPD analysis, and carbohydrate fermentation features (**Supplementary Figure 4**). Furthermore, we performed genome sequencing and characterization of the strains to identify genes potentially involved in probiotic activity.

Three *L. paracasei* strains (GMNL-653, GMNL-855, and BCRC-16100) were characterized at the genotypic and phenotypic level (**Figure 8**). High-molecular-weight DNA from three isolates of the *L. paracasei* strain was sequenced using ONT long reads and Illumina short reads for the hybrid assembly of their genomes using the MaSuRCA assembler v3.3.1 (20). As detailed in **Table 2**, the assembly of the GMNL-653 draft genome

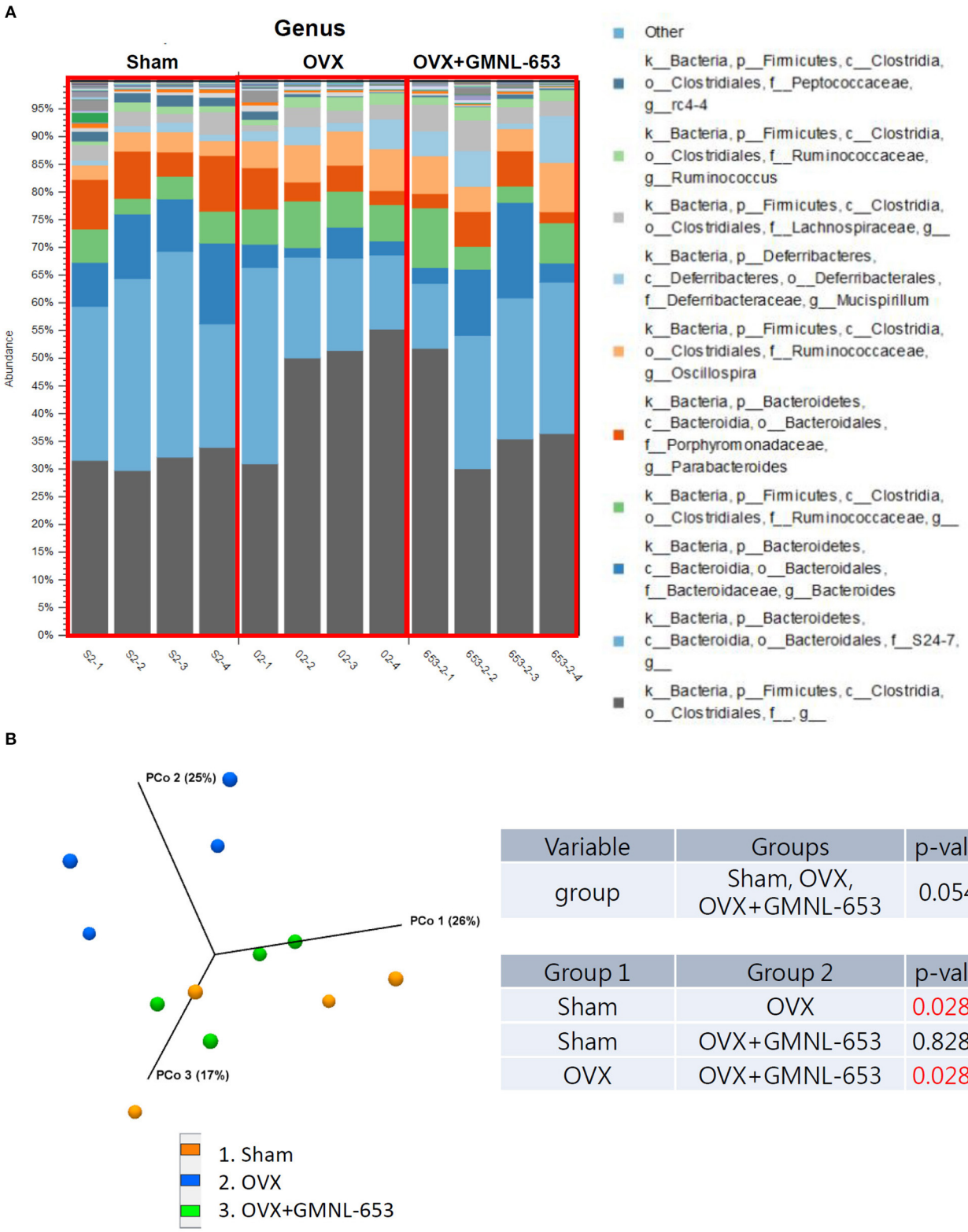

Variable	Groups	p-value
group	Sham, OVX, OVX+GMNL-653	0.0542

Group 1	Group 2	p-value
Sham	OVX	0.02857
Sham	OVX+GMNL-653	0.82857
OVX	OVX+GMNL-653	0.02857

FIGURE 4 | Relative abundance and diversity of stool microbiota in the sham and OVX mice treated with either the vehicle (H_2O) or heat-killed GMNL-653. **(A)** Each column in the stacked histogram represents one sample; the differently colored bars are proportional to the percentage of relative bacterial abundance of each taxon within the sample (summing up to 100%). **(B)** Principal coordinate analysis of the beta diversity among the three groups.

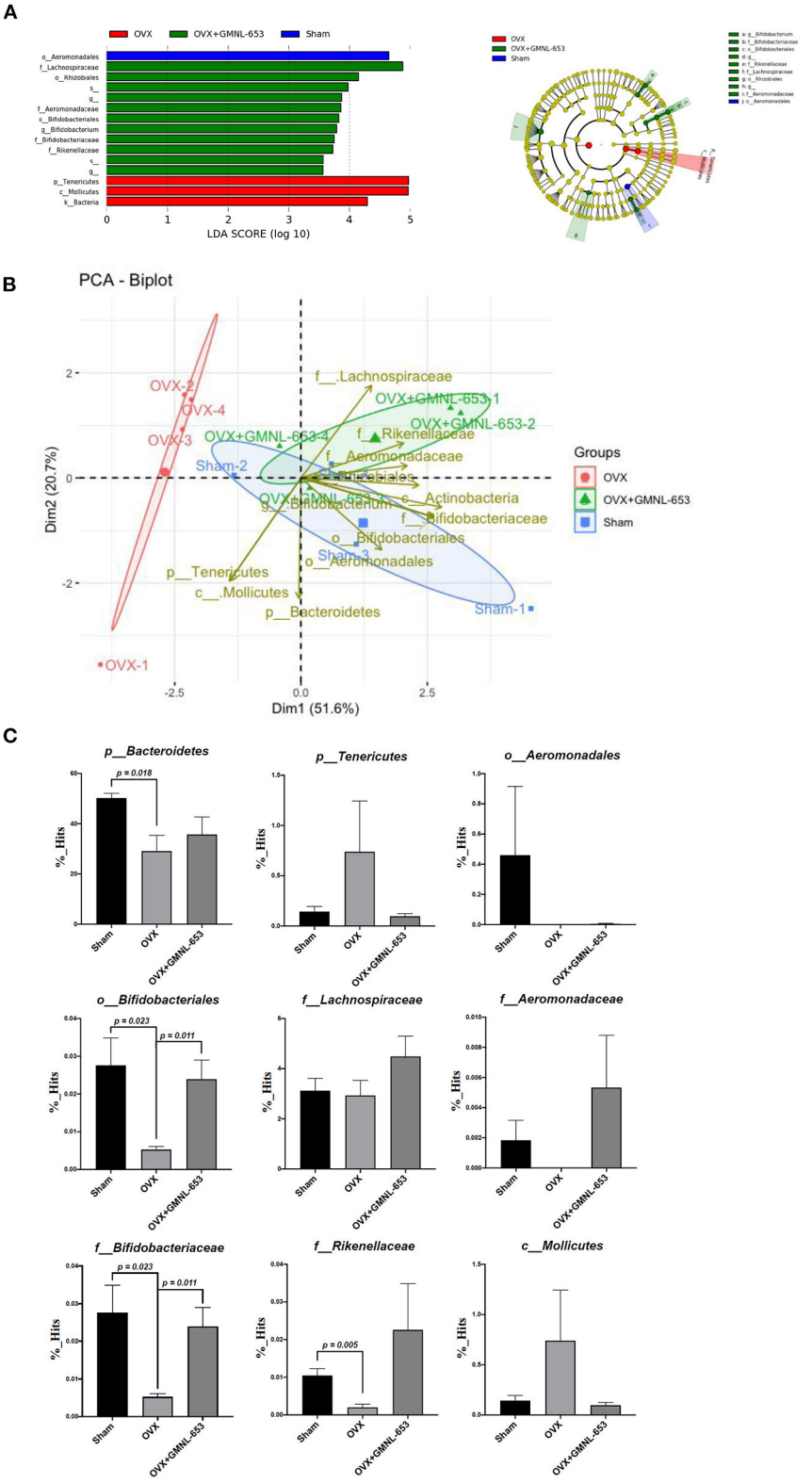

FIGURE 5 | Taxonomic differences and relative abundance of fecal microbiota in the sham and OVX mice treated with either the vehicle (H_2O) or heat-killed GMNL-653. **(A)** Linear discriminant analysis and cladogram revealed the phylogenetic distribution of fecal microbiota associated with the sham, OVX, and OVX + GMNL-653 groups. The biplot of the principal component analysis **(B)** and relative abundances **(C)** of bacterial communities in the sham, OVX, and OVX+GMNL-653 groups.

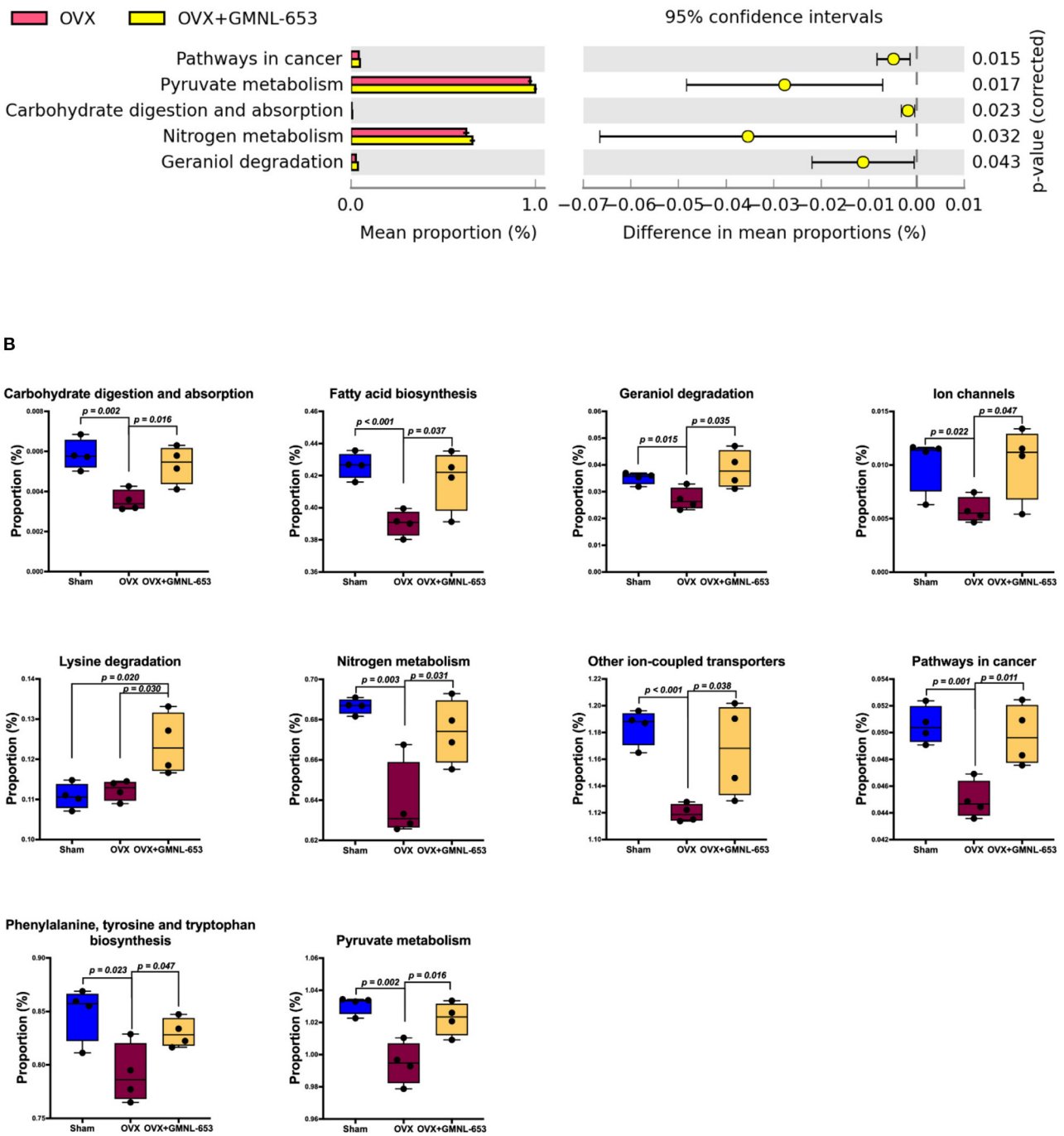

FIGURE 6 | Predicted function of the involved gut microbial using the phylogenetic investigation of communities by the reconstruction of unobserved states 2 (PICRUSt2) in the sham and OVX mice treated with either the vehicle (H_2O) or heat-killed GMNL-653. **(A)** Pairwise comparison showed that five function pathways were significantly increased in mice treated with GMNL-653 vs. OVX mice. Among them, 4 of 5 function pathways were included in the metabolism of pyruvate, carbohydrate, nitrogen, and geraniol. **(B)** There were nine function pathways overlapped between OVX vs. GMNL-653 and Sham vs. OVX and were significantly decreased in the OVX mice as compared to the Sham group, but further increased upon GMNL-653 treatment. It is noted that only Lysine degradation pathway was overlapping between OVX vs. GMNL-653 and Sham vs. GMNL-653 and was significantly increased in the OVX mice as compared to the Sham group, but was further increased when treated with GMNL-653. $p < 0.05$ is considered as statistically significant.

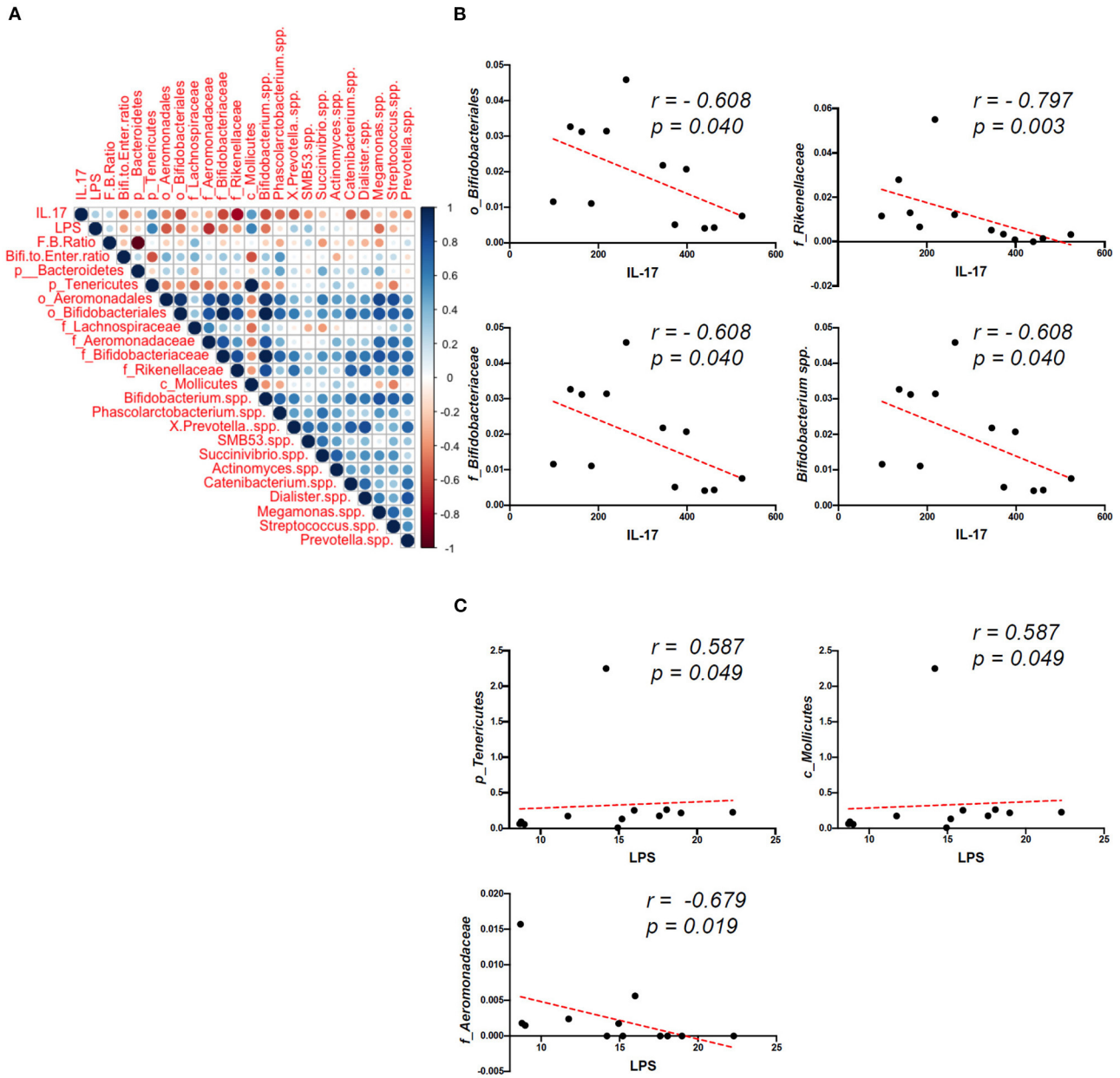

FIGURE 7 | Correlations between the gut microbiota composition and plasma concentrations of IL-17 and LPS in the sham and OVX mice treated with either the vehicle (H_2O) or heat-killed GMNL-653. **(A)** Spearman's correlation coefficient strength of the phylum counts from the OVX mice. Correlations with $P < 0.05$ are indicated, and the strength of the coefficient is represented by the change in color intensity. **(B)** The enriched *Bifidobacteriales* (order), *Rikenellaceae* (family), *Bifidobacteriaceae* (family), and *Bifidobacterium* spp. in the OVX + GMNL653 group exhibited a significant negative correlation with sera IL-17. **(C)** The enriched *Tenericutes* (phylum) and *Mollicutes* (class) in the OVX group were positively correlated with sera LPS. The enriched *Aeromonadacae* (family) in the OVX + GMNL-653 group exhibited a negative correlation with sera LPS.

sequence consists of three contigs amounting to 3,329,730 bp. The first contigs (3,121,847 bp) were regarded as a circular chromosome predicted using PlasFlow (29), with a GC content of 46.19%. Prokka (25) software was used to annotate 3,375 protein-coding genes and identify 60 tRNA genes and five rRNA operons. The genetic organization of GMNL-653 was illustrated as a genome atlas constructed with Circos software (**Figure 8A**) (32). For completeness assessment for genomics data quality control, BUSCO analysis was employed, revealing that 400 of the 402 reference genes were complete (99.5%, 391 single-copy and 9 duplicated), 2 (0.5%) were fragmented, and none were missing in the draft assembly; thus, the assembly represents most of the genomic content (**Supplementary Figure 5**). One separate CRISPR loci (**Table 2**, **Supplementary Table 1**) was discovered

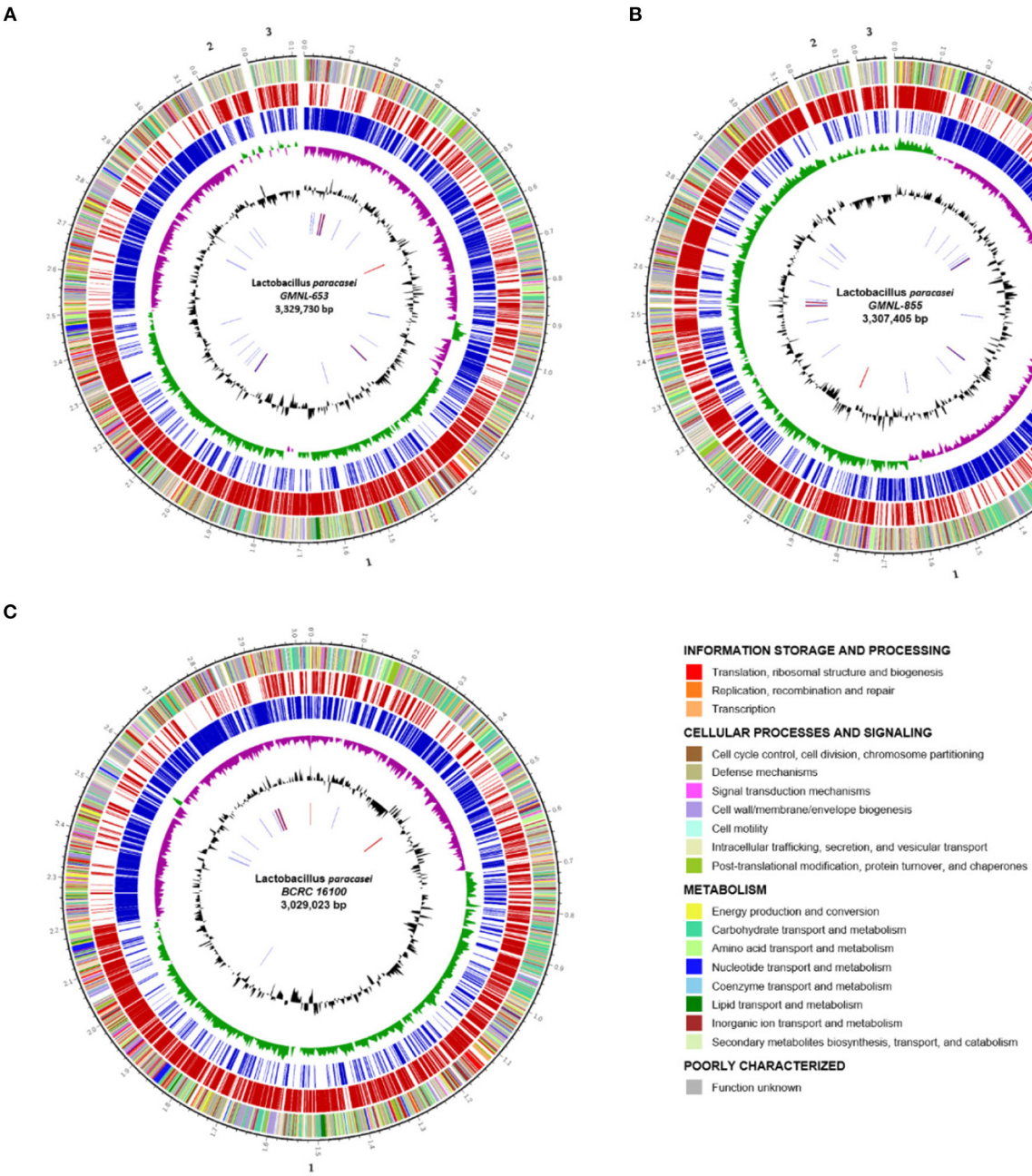

FIGURE 8 | Circular genome graph **(A–C)** of the *L. paracasei* strain. **(A)** The GMNL-653, **(B)** GMNL-855, and **(C)** BCRC-16100 genome. The outer to inner circles depict the (1) DNA coordinates; (2) function-based color-coded mapping of the genes, colored according to the COG category whose code and meaning is provided in the table below the plot; (3, 4) coding sequences predicted on the forward (red) and reverse (blue) strands, respectively; (5) GC skew (G – C/G + C), calculated for a window of 4,000 bp and shifted by 1,000 bp over the genome sequence, with the above- and below-average regions indicated in green and purple; (6) GC content (black); and the (7) RNA genes (tRNA, blue; rRNA, red; other RNAs, black).

in the genome of GMNL-653 by using the CRISPRFinder (28). Additionally, eight prophage regions were identified, of which four regions were intact, two were incomplete, and two were questionable (**Supplementary Table 2**); a type IIa bacteriocin operon (**Supplementary Table 3**) was also identified in GMNL-653.

The complete genome sequence of GMNL-855 and BCRC-16100 comprised a circular chromosome (3,118,787 and 3,029,023 in contigs 1, respectively), with average GC values of 46.4 and 46.19%, respectively. **Figures 8B,C** illustrates the orthologous genes shared among strains, presenting the position and color-coded function of each specific gene. Through BUSCO

TABLE 2 | General features of *L. paracasei* genomes.

	GMNL-653	GMNL-855	BCRC 16100
Size (bp)	3,329,730	3,307,405	3,029,023
G + C content (%)	46.19	46.19	46.4
Total genes	3,375	3,328	2,902
Coding content (%)	88.82	86.27	85.88
Gene average length (bp)	852	857	896
Genes assigned to COGs	2,627 (77.8%)	2,669 (80.2%)	2,387 (82.2%)
Chromosome	1	1	1
rRNA operons	5	5	5
tRNA	60	60	62
Plasmids	0	0	0
Transposases	16	104	13
CRISPR loci	1	1	2
Prophage-Like clusters	4	5	0
Bacteriocin	3	3	2

analysis, we determined that 99.5% of reference genes were complete in both strains, 2 (0.5%) were fragmented, and none were missing (**Supplementary Figure 5**). In total, over 99% of complete BUSCOs were present in the three *L. paracasei* strains, indicating high-quality assemblies. Of the 3,328 and 2,902 genes that were predicted in GMNL-855 and BCRC-16100, respectively, 86.27 and 85.88% were protein-coding genes, respectively. Gene prediction demonstrated the presence of the following putative genes: three CRISPR/CRISPR-associated (cas) gene loci (type I and IIA; **Supplementary Table 1**), five intact prophage-like regions (**Supplementary Table 2**), and several type IIb bacteriocin operons (**Supplementary Table 3**).

Genotypic Identification of the *L. paracasei* Strain

The beneficial health attributes and safety concerns of probiotic cultures are closely related; thus, categorical identification of the probiotic strain is paramount (46). A maximum-likelihood tree of four *L. paracasei* genomes and 12 reported *Lactobacillus* strains (*L. acidophilus*, *L. amylovorus*, *L. casei*, *L. crispatus*, *L. delbrueckii*, *L. fermentum*, *L. gasseri*, *L. johnsonii*, *L. plantarum*, *L. reuteri*, *L. rhamnosus*, and *L. salivarius*) was created based on 16S rRNA gene sequences. Genome-wide phylogenetic analysis in combination with alignment fraction analysis indicated that GMNL-653, GMNL-855, BCRC-16100, and *L. casei* spp. were grouped together (**Supplementary Figure 6**). Another work documented an approximately 90% sequence identity among *L. casei*, *L. paracasei*, and *L. rhamnosus* (47). Furthermore, to measure genomic similarity at the nucleotide level between GMNL-653 and other *Lactobacillus* genomes, the average nucleotide identity (ANI) was calculated using an improved algorithm (34). The ANI values were calculated and revealed that three *L. paracasei* strains were most closely related to *L. paracasei LC2W* in terms of their nucleotide sequences (ANI > 98%; **Supplementary Figure 7**). The values between the two strains were extracted from the junction point of the diagonals departing from each strain. The critical ANI value aligned to other species was between 64.94 and 79.55%. A BLAST comparison of GMNL-653 against the GMNL-855 and BCRC-16100 strains was performed using Easyfig (**Supplementary Figure 8**). Genome-wide comparison indicated a high degree of synteny among the characterized *L. paracasei* GMNL-653, GMNL-855, and BCRC-16100 strains, with only a few regions disrupted throughout the chromosome. Therefore, the whole-genome data verified that the GMNL-653 strain belongs to the species *L. paracasei*. The functional classification of Clusters of Orthologous Groups (COGs) predicted using eggNOG-mapper (26, 27) revealed that 2,627 (77.8%) putative coding sequences were homologous to known gene families. The distribution of genes into COG functional categories is summarized in **Table 3**. Functional analysis of GMNL-653 genes revealed that, in addition to hypothetical proteins, a relative abundance of the gene was involved in the basic mechanisms of DNA replication and recombination, carbohydrate metabolism, and cell wall/membrane/envelope biogenesis. Additionally, in the putative regions of genomic coding, 2,669 (80.2%) and 2,387 (82.2%) genes were attributed to a COG family (**Table 3**). A core- and pan-genome analysis indicated that 72, 40, and 34 genes were specific to GMNL-653, GMNL-855, and BCRC-16100, respectively (**Supplementary Table 4**).

Cell wall components are key mediators influence on the interactions between host and associated microbiota. *Lacticaseibacillus* not only utilize and metabolize a variety of carbohydrates but also synthesized extensive exopolysaccharides which may affect other commensal bacteria resulting in health benefits in host. Therefore, genome sequencing of many *Lactobacillus* strains have revealed many genes involved in the metabolism of carbohydrate. Based on our results, we proposed that the bacterial cell wall components or carbohydrate metabolism exclusively expressing in GMNL-653 may be involved in the antiosteoporotic activity. We compared genes related to carbohydrate transport and metabolism (**Figure 9A**) and cell wall/membrane/envelope biogenesis (**Figure 9B**) among the three *L. paracasei* strains. Thirteen genes were annotated to carbohydrate transport and metabolism, which are sucrose-6-phosphate hydrolase, phosphotransferase (PTS) system, glycerate kinase, sucrose phosphorylase, phosphotransfer between the C1 and C5 carbon atoms of pentose, glycoside hydrolase family 4, repressor, ORF, kinase (ROK) family, glycosyl hydrolase family 1, and sugar kinase (**Table 4**). Six genes were related to cell wall/membrane/envelope biogenesis, which are phage tail tape measure protein, udp-galactopyranose mutase, glycosyl transferase, licD family, and catalyzes the conversion of a range of fructosamine 6-phosphates to glucose 6phosphate, and a free amino acid (**Table 4**). According to the KEGG BRITE database, these thirteen genes annotated to carbohydrate transport and metabolism have functional hierarchy classification of starch and sucrose metabolism, fructose-specific II-like component, biosynthesis of secondary metabolism, pentose phosphate pathway/purine metabolism, mitochondrial DNA transcription and translation factors, fructose like PTS system EIIA component, and fructoselysine 6-kinase. Six genes related to cell wall/membrane/envelope biogenesis have functional

TABLE 3 | COG functional categories of *L. paracasei* strain.

COG class	Description	GMNL-653	GMNL-855	BCRC 16100
J	Translation, ribosomal structure, and biogenesis	107 (4.1%)	157 (5.9%)	149 (6.2%)
L	Replication, recombination, and repair	304 (11.6%)	258 (9.7%)	135 (5.7%)
K	Transcription	209 (8.0%)	212 (8.0%)	201 (8.4%)
D	Cell cycle control, cell division, chromosome partitioning	29 (1.1%)	28 (1.1%)	25 (1.0%)
V	Defense mechanisms	104 (4.0%)	103 (3.9%)	81 (3.4%)
T	Signal transduction mechanisms	60 (2.3%)	62 (2.3%)	64 (2.7%)
M	Cell wall/membrane/envelope biogenesis	129 (4.9%)	136 (5.1%)	138 (5.8%)
N	Cell motility	2 (0.1%)	1 (0.1%)	1 (0.1%)
U	Intracellular trafficking, secretion, and vesicular transport	20 (0.8%)	24 (0.9%)	16 (0.7%)
O	Post-translational modification, protein turnover, and chaperones	71 (2.7%)	65 (2.4%)	61 (2.6%)
C	Energy production and conversion	107 (4.1%)	113 (4.2%)	110 (4.6%)
G	Carbohydrate transport and metabolism	270 (10.3%)	314 (11.8%)	307 (12.9%)
E	Amino acid transport and metabolism	207 (7.9%)	203 (7.6%)	196 (8.2%)
F	Nucleotide transport and metabolism	88 (3.3%)	88 (3.3%)	87 (3.6%)
H	Coenzyme transport and metabolism	47 (1.8%)	46 (1.7%)	47 (2.0%)
I	Lipid transport and metabolism	55 (2.1%)	54 (2.0%)	52 (2.2%)
P	Inorganic ion transport and metabolism	113 (4.3%)	113 (4.2%)	114 (4.8%)
Q	Secondary metabolites biosynthesis, transport, and catabolism	18 (0.7%)	13 (0.5%)	16 (0.7%)
S	Function unknown	687 (26.2%)	676 (25.4%)	587 (24.6%)

hierarchy classification of glycan biosynthesis and metabolism, lipopolysaccharide cholinephosphotransferase and fructoselysine 6-phosphate deglycase.

DISCUSSION

In present study, we observed that one *L. paracasei* GMNL-653 strain reduced LPS-stimulated IL-6 and NO production in the mouse macrophage RAW264.7. GMNL-653 increased calcium mineralization in human osteosarcoma MG63 cells mineralizing in culture and protected the OVX mice from bone loss, including increasing bone volume over tissue volume (BV/TV) and bone mineral density (BMD). Our results revealed that GMNL-653 restored ovariectomy-induced gut microbiota dysbiosis and maintained intestinal barrier integrity. Additionally, in the OVX mice, GMNL-653 treatment reduced the IL-17 and LPS levels compared with those of the vehicle control group, reduced the mRNA levels of RANKL, and increased the anti-inflammatory cytokines TGF-β and IL-10 in tibia tissue. Furthermore, we applied the whole-genome sequencing technique and comparative genomics analysis to further examine these three *L. paracasei*. Our results indicated that the genes related to carbohydrate transport/metabolism and the cell wall/membrane/envelope biogenesis of GMNL-653 are worthy of future investigation. In summary, our results showed that heat-killed GMNL-653 exhibited antiosteoporotic activity through the gut microbiota–bone axis (**Supplementary Figure 9**).

Many studies have explored the potential role of the intestinal microbiome and its associated metabolomics in metabolic health and disease. Several metabolic diseases have been linked to altered gut microbiota, such as type 2 diabetes, cardiometabolic diseases, and non-alcoholic fatty liver disease. Disruption of gut microbiota, also called dysbiosis, is also related to multiple host disorders and is closely associated with an increased risk of bone loss (48), inflammatory bowel disease (49), diabetes, and obesity (50). Although the potential causality between various microbial components and diseases must be clarified, the intervention of probiotics or prebiotics can still provide beneficial metabolic health effects. In this study, we applied *in vitro* and *in vivo* models to validate the antiosteoporotic effect of heat-killed *L. paracasei* (GMNL-653) and employed comparative genomics analysis to explore the potentially vital genes involved.

Osteoporosis is mediated by a variety of inflammatory mediators, including TNF-α, RANKL, interleukin 1 beta, IL-6, and interferon gamma. Furthermore, chronic inflammatory disease such as inflammatory bowel disease can affect bone metabolism and is frequently associated with occurrence of osteoporosis (5, 7, 51). Although our understanding of the underlying mechanism of the relationship between inflammation and osteoporosis is incomplete, increasing evidence continues demonstrated that inflammation may intrinsically contribute to osteoporosis. Based on these findings indicating the contribution of inflammation to bone loss, we screened the anti-inflammatory activity in various strains of heat-killed probiotics in RAW 264.7 macrophages under LPS stimulation. We observed that one heat-killed *L. paracasei* GMNL-653 reduced macrophage IL-6 secretion and NO production following LPS treatment. RANKL is a key regulator of osteoclast activity and acts as a therapeutic target in osteoporosis (52). Our results indicated that the levels of *RANKL* mRNA increased in OVX mice, though subsequent treatment with heat-killed GMNL-653 once per day resulted in decreased *RANKL* mRNA expression in the tibia.

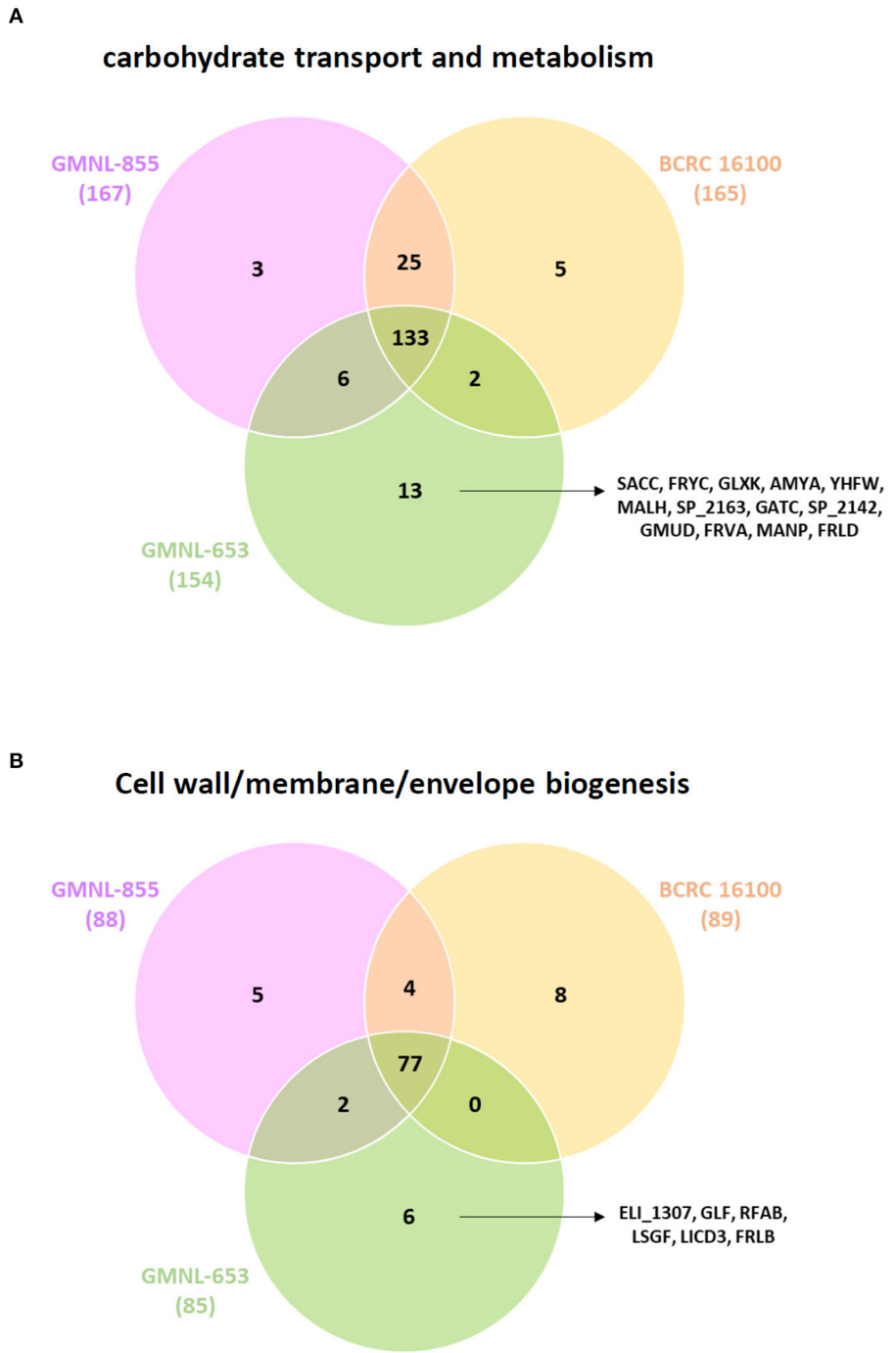

FIGURE 9 | Comparison of the genes related to **(A)** carbohydrate transport and metabolism and **(B)** cell wall/membrane/envelope biogenesis among the three *L. paracasei* strains.

Furthermore, GMNL-653 increased *TGF-β* and *IL-10* mRNA levels in the OVX mice. These results demonstrated that GMNL-653 exhibits anti-inflammatory effects, with anti-inflammatory cytokines potentially enhancing gut epithelial barrier function (53, 54) and proinflammatory cytokines attenuating intestinal barrier dysfunction (55).

IL-17A is also a vital mediator of bone absorption in inflammatory diseases associated with osteoporosis, and elevated serum concentrations of IL-17A have been observed in patients with postmenopausal osteoporosis (56). We determined that elevated IL-17A was downregulated through GMNL-653 treatment in OVX mice and that IL-17 can also promote

TABLE 4 | EggNOG functional annotations of *L. paracasei* (GMNL-653).

Functional categories	Predicted gene name	eggNOG annot	KEGG brite
Carbohydrate transport and metabolism (G)	SACC	Sucrose-6-phosphate hydrolase	Starch and sucrose metabolism
	FRYC	PTS System	Fructose-specific II-like component
	GLXK	Glycerate kinase	Biosynthesis of secondary metabolites
	AMYA	Sucrose phosphorylase	Starch and sucrose metabolism
	YHFW	Phosphotransfer between the C1 and C5 carbon atoms of pentose (By similarity)	Pentose phosphate pathway/Purine metabolism
	MALH	Glycoside hydrolase family 4	Starch and sucrose metabolism
	SP_2163	PTS system	
	GATC	PTS system, galactitol-specific IIc component	Mitochondrial DNA transcription and translation factors
	SP_2142	ROK family	
	GMUD	Glycosyl hydrolase family 1	Starch and sucrose metabolism
	FRVA	PTS system	Fructose-like PTS system EIIA component
	MANP	PTS system	
	FRLD	Sugar kinase	Fructoselysine 6-kinase
Cell wall/ membrane/ envelope biogenesis (M)	ELI_1307	Phage tail tape measure protein	
	GLF	udp-galactopyranose mutase	Glycan biosynthesis and metabolism
	RFAB	Glycosyl transferase (Group 1 family protein)	Glycan biosynthesis and metabolism
	LSGF	Glycosy ltransferase	
	LICD3	licD family	lipopolysaccharide cholinephosphotransferase
	FRLB	Catalyzes the conversion of a range of fructosamine 6-phosphates to glucose 6-phosphate and a free amino acid (By similarity)	fructoselysine 6-phosphate deglycase

osteoclast differentiation and RANKL secretion. Our results indicated that elevated IL-17 may enhance RANKL expression in OVX mice. Blocking the IL-17A pathway may have a positive effect on bone and cartilage damage in inflammatory disease (57). Furthermore, GMNL-653 may reduce IL-17A production, preventing bone loss in OVX mice. In terms of the influence of GMNL-653 osteoblast and osteoclast differentiation, we discovered that GMNL-653 does not influence osteoclast differentiation under RANKL stimulation. These results demonstrated that GMNL-653 can promote osteoblast differentiation leading to mineralization. The use of the OVX mice model verified that the GMNL-653 protects mice from ovariectomy-induced bone loss.

In the OVX mice, gut integrity was also altered, leading to elevated LPS in the sera. Notably, the gut microbiota composition changed in the OVX group. The PCoA plot of our beta diversity analysis indicated that the microbial communities in the OVX mice exhibited a significantly distinct cluster separate from the sham and OVX + GMNL-653 groups. Accumulated evidence revealed that the gut microbiome was associated with specific dysbiosis in osteoporosis, though the causal mechanism remains unclear. Epidemiological study also reported that the gut microbiome was altered in postmenopausal women with osteoporosis and osteopenia (58). A potential mechanism is that dysbiosis of gut microbiota may increase the permeability of the intestinal cell, increasing LPS levels in the circulation system. LPS can upregulate the inflammatory mediators in bone tissue (59). LPS has identified as the vital factor in inflammatory-induced osteoclast differentiation leading to bone loss (60, 61). Levels of sera IL-17A and LPS correlated with certain gut microorganisms in the OVX mice, indicating a link between immune responses and changes in gut microbiome composition. In addition, gut microbiota may be involved in the regulation of IL-17A production and functions (62). Therefore, we speculated that GMNL influences gut microbiota, leading to decreased IL-17A and LPS production in OVX mice.

The enriched *Bifidobacteriales* (order), *Rikenellaceae* (family), *Bifidobacteriaceae* (family), and *Bifidobacterium* spp. in the OVX + GMNL653 group exhibited significantly negative correlations with sera IL-17A. GMNL-653 intervention can enhance the abundance of these microorganisms, resulting in decreased IL-17A production. Our results demonstrated that GMNL-653 modulated gut microbiota composition in OVX mice. This result implied that the interactions of *Rikenellaceae* (family), *Bifidobacteriales* (order), *Bifidobacteriaceae* (family), *Bifidobacterium spp*. may be highly associated with IL-17. These subset of gut microbiota may have selective effects on IL-17. Previous study reported that *Bifidobacterium* suppress IL-17 production in murine splenocytes and dextran sodium sulfate-induced intestinal inflammation (63). However, whether the alterations in the abundances of *Bifidobacterium* and *Rikenellaceae* contribute to the functional consequence on the homeostasis of osteoblast and osteoclast development are issues that need further clarified. Our finding is consistent with a study reporting that gut *Rikenellaceae* involved in Th17 development (64). The enriched *Tenericutes* (phylum) and *Mollicutes* (class) in OVX group have positive correlations with sera LPS. *Tenericutes* has been reported as one of biomarkers in rat model of senile osteoporosis (65). Our result indicated that enriched *Tenericutes* was highly associated with gut barrier integrity which may result from intestinal inflammations. We further investigated the effect of GMNL-653 on the functional profiles of microbiome communities in the OVX mice and used PICRUSt to predict metagenomes mapped to the KEGG database. Carbohydrate digestion and absorption, fatty acid biosynthesis, ion channels,

nitrogen metabolism, other ion-coupled transporters, pathways in cancer, phenylalanine, tyrosine, and tryptophan biosynthesis, and pyruvate metabolism were all downregulated in the OXV group compared with those in the sham group but were upregulated following GMNL-653 treatment. Several pathways have been associated with bone homeostasis; for example, essential fatty acids have been demonstrated to increase calcium absorption from the gut, reducing the urinary excretion of calcium, enhancing calcium deposition in bones, and improving bone strength (66). The dysfunction of various of ion channels is connected to perturbations in osteoblast bone formation and osteoclast bone resorption (67). Hence, ion channels play critical roles in sustaining bone homeostasis. A cohort study reported that amino acid metabolism, such as tyrosine and tryptophan metabolism, was significantly related to gut dysbiosis and osteoporosis (68). Pyruvate also plays a pivotal role in various physiological processes as a counterion and could affect the absorption and availability of calcium through the epithelial cells (69).

Our comparative genomics analysis classified genes of GMNL-653 dependent on functional categories to explore potential vital genes involved in anti-osteoporotic effects. Scanning electron microscope analysis showed that GMNL-653 has a unique longer rod-shape which may result from multicell aggregates. The carbohydrate structure and components influence bacterial adhesion and colonization. Bacterial glycans are typically display at the cell surface and interact with environment, so they have significant biomedical importance. Moreover, cell wall components are key mediators influence on the interactions between host and other microbiota. *Lacticaseibacillus* not only utilize and metabolize a variety of carbohydrates but also synthesized extensive exopolysaccharides which may affect other commensal bacteria resulting in health benefits in host. Therefore, we focus on genes exclusive express in GMNL-653 categorized as carbohydrate transport and metabolism and cell wall/membrane/envelope biogenesis. Nineteen unique genes were responsible for carbohydrate transport and metabolism and cell wall/membrane/envelope biogenesis in GMNL-653. Four genes (SACC, AMYA, MALH, and GMUD) involved in starch and sucrose metabolism. SACC, annotated as sucrose-6-phosphate hydrolase, participate in glucose 6-phosphate and fructose production. Fructooligosaccharides (FOS) are polymers of fructose with a prebiotic activity (70) which may facilitate maintaining gut barrier integrity. It was reported that FOS from *Stevia rebaudiana* roots enhanced the growth of specific strains of both *Bifidobacteria* and *Lactobacilli* (70, 71). AMYA gene encode a sucrose phosphorylase, which is a glucosyltransferase transferring glucose from sucrose to acceptor molecules further production of glucose-1-phosphate and fructose (72). The MALH gene was annotated as glycoside hydrolase, which allows the utilization of different oligosaccharides with prebiotic properties (73). Meanwhile, FRYC and FRVA gene were annotated as fructose-specific II-like component and Fructose-like PTS system EIIA component. FRLD gene classified as fructoselysine 6-kinase, which catalyzed the ATP-dependent phosphorylation of fructoselysine to fructoselysine 6-phosphate. The function of FRLB catalyze the conversion of fructoselysine to fructoselysine 6-phosphate and lysine. Lysine has been reported to enhance osteoblast proliferation, Ca^{2+} absorption and healing of bone fracture (74, 75). Therefore, GMNL-653 has sophisticated and complex genes participated in metabolisms of sucrose and fructose which may play important roles in maintaining gut barrier, symbiosis and bone metabolism.

The genes of GLF and RFAB were classified in glycan biosynthesis and metabolism. The predicted gene GLF of GMNL-653 was annotated as udp-galactopyranose mutase, which is involved in the biosynthesis of the cell wall residue of d-galactofuranose (76). The RFAB and LSGF genes were predicated as glycosyl transferase, which is responsible for exopolysaccharide production, cell aggregation, and bile resistance in *Lactobacillus* probiotic strains (77). We proposed that several bacterial cell wall components, such as lipoteichoic acids, peptidoglycans, and exopolysaccharides, may be involved in the antiosteoporotic activity of heat-killed GMNL-653. Peptidoglycan accounts for ∼90% of the cell wall component of Gram-positive bacteria and is largely composed of glycan strands and pentapeptides, which present as strain-specific for *Lactobacilli* (78). Purified peptidoglycans from *L. salivarius* Ls-33 exhibited anti-inflammatory properties through the induction of IL-10 production (79).

CONCLUSION

In summary, we demonstrated that heat-killed *L. paracasei* (GMNL-653) exerts antiosteoporotic effects by restoring the gut microbiota dysbiosis in ovariectomized mice. The possible mechanism of this antiosteoporotic activity involves the reduced production of inflammatory mediators (RANKL and IL-17A) and gut microbiota dysbiosis through GMNL-653 treatment. We also clarified that fluctuation in gut microbiota is closely associated with sera IL-17A and LPS levels in OVX mice. Metagenomes mapped to the KEGG database revealed that bone homeostasis is affected by gut microbial function pathways, including carbohydrate digestion and absorption, fatty acid biosynthesis, ion channels, phenylalanine, tyrosine, and tryptophan biosynthesis, and pyruvate metabolism. Whole-genome sequencing and comparative genomics analysis revealed that genes related to carbohydrate transport and metabolism and cell wall/membrane/envelope biogenesis may be associated with antiosteoporotic activity of GMNL-653. To the best of our knowledge, this is the first study linking antiosteoporotic activity, as validated using *in vitro* and *in vivo* models, to whole-genome sequencing and identifying genes potentially involved in antiosteoporotic activity.

DATA AVAILABILITY STATEMENT

The datasets presented in this study can be found in online repositories. The names of the repository/repositories and accession number(s) can be found in the article/ **Supplementary Material**.

ETHICS STATEMENT

The animal study was reviewed and approved by all animal experiments and housing were conducted in accordance with protocol by IACUC laboratory animal center of China Medical University and GenMont Biotech Incorporation (Taiwan IACUC Approval No. 148 IACUC 2016-165 and Approval No. 194 GenMont Biotech Incorporation Approval No. 107004).

AUTHOR CONTRIBUTIONS

J-HJ and T-YL analyzed the whole genome sequence, prepare figures, and wrote manuscript. W-HT analyzed and prepare figures. L-CY designed and performed the animal experiment, analyzed data, and prepared figures. C-HC designed and performed the *in vitro* experiment, analyzed data, and prepared figures. Y-TY and C-HH analyzed the gut microbiome, prepared figures, and wrote manuscript. Y-HL contributed to the study concept, wrote manuscript, and revised the final content of the manuscript. All authors contributed to the article and approved the submitted version.

FUNDING

This study was supported by grants MOST-110-2320-B-008-003 from the Ministry of Science and Technology in Taiwan.

SUPPLEMENTARY MATERIAL

The Supplementary Material for this article can be found online at: https://www.frontiersin.org/articles/10.3389/fnut.2022.804210/full#supplementary-material

Supplementary Figure 9 | Pictorial description of heat-killed Lacticaseibacillus paracasei GMNL-653 exerts antiosteoporotic effects by restoring the gut microbiota dysbiosis in ovariectomized mice.

REFERENCES

1. Fan Y, Pedersen O. Gut microbiota in human metabolic health and disease. *Nat Rev Microbiol.* (2021) 19:55–71. doi: 10.1038/s41579-020-0433-9
2. Lynch SV, Pedersen O. The human intestinal microbiome in health and disease. *N Engl J Med.* (2016) 375:2369–79. doi: 10.1056/NEJMra1600266
3. Yatsonsky Ii D, Pan K, Shendge VB, Liu J, Ebraheim NA. Linkage of microbiota and osteoporosis: A mini literature review. *World J Orthop.* (2019) 10:123–7. doi: 10.5312/wjo.v10.i3.123
4. Collins FL, Rios-Arce ND, Schepper JD, Parameswaran N, McCabe LR. The potential of probiotics as a therapy for osteoporosis. *Microbiol Spectr.* (2017) 5:1–16. doi: 10.1128/microbiolspec.BAD-0015-2016
5. Ke K, Arra M, Abu-Amer Y. Mechanisms underlying bone loss associated with gut inflammation. *Int J Mol Sci.* (2019) 20:6323. doi: 10.3390/ijms20246323
6. Chedid VG, Kane SV. Bone health in patients with inflammatory bowel diseases. *J Clin Densitom.* (2020) 23:182–9. doi: 10.1016/j.jocd.2019.07.009
7. Sgambato D, Gimigliano F, De Musis C, Moretti A, Toro G, Ferrante E, et al. Bone alterations in inflammatory bowel diseases. *World J Clin Cases.* (2019) 7:1908–25. doi: 10.12998/wjcc.v7.i15.1908
8. Pfeilschifter J, Koditz R, Pfohl M, Schatz H. Changes in proinflammatory cytokine activity after menopause. *Endocr Rev.* (2002) 23:90–119. doi: 10.1210/edrv.23.1.0456
9. Bismar H, Diel I, Ziegler R, Pfeilschifter J. Increased cytokine secretion by human bone marrow cells after menopause or discontinuation of estrogen replacement. *J Clin Endocrinol Metab.* (1995) 80:3351–5. doi: 10.1210/jcem.80.11.7593450
10. D'Amelio P, Grimaldi A, Di Bella S, Brianza S Z M, Cristofaro M A, Tamone C, et al. Estrogen deficiency increases osteoclastogenesis up-regulating T cells activity: a key mechanism in osteoporosis. *Bone.* (2008) 43:92–100. doi: 10.1016/j.bone.2008.02.017
11. Eghbali-Fatourechi G, Khosla S, Sanyal A, Boyle WJ, Lacey DL, Riggs BL. Role of RANK ligand in mediating increased bone resorption in early postmenopausal women. *J Clin Invest.* (2003) 111:1221–30. doi: 10.1172/JCI200317215
12. Locantore P, Del Gatto V, Gelli S, Paragliola RM, Pontecorvi A. The interplay between immune system and microbiota in osteoporosis. *Mediators Inflamm.* (2020) 2020:3686749. doi: 10.1155/2020/3686749
13. Pique N, Berlanga M, Minana-Galbis D. Health benefits of heat-killed (tyndallized) probiotics: an overview. *Int J Mol Sci.* (2019) 20:2534. doi: 10.3390/ijms20102534
14. Jorjao AL, de Oliveira FE, Leao MV, Carvalho CA, Jorge AO, de Oliveira LD. Live and heat-killed lactobacillus rhamnosus ATCC 7469 may induce modulatory cytokines profiles on macrophages RAW 264.7. *ScientificWorldJournal.* (2015) 2015:716749. doi: 10.1155/2015/716749
15. Li N, Russell WM, Douglas-escobar M, Hauser N, Lopez M, Neu J. Live and heat-killed *Lactobacillus rhamnosus* GG: effects on proinflammatory and anti-inflammatory cytokines/chemokines in gastrostomy-fed infant rats. *Pediatr Res.* (2009) 66:203–7. doi: 10.1203/PDR.0b013e3181aabd4f
16. Matsuzaki T, Chin J. Modulating immune responses with probiotic bacteria. *Immunol Cell Biol.* (2000) 78:67–73. doi: 10.1046/j.1440-1711.2000.00887.x
17. Murosaki S, Yamamoto Y, Ito K, Inokuchi T, Kusaka H, Ikeda H, et al. Heat-killed *Lactobacillus plantarum* L-137 suppresses naturally fed antigen-specific IgE production by stimulation of IL-12 production in mice. *J Allergy Clin Immunol.* (1998) 102:57–64. doi: 10.1016/S0091-6749(98)70055-7
18. Chapot-Chartier MP, Vinogradov E, Sadovskaya I, Andre G, Mistou MY, Trieu-Cuot P, et al. Cell surface of *Lactococcus lactis* is covered by a protective polysaccharide pellicle. *J Biol Chem.* (2010) 285:10464–71. doi: 10.1074/jbc.M109.082958
19. Jensen GS, Benson KF, Carter SG, Endres JR. GanedenBC30 cell wall and metabolites: anti-inflammatory and immune modulating effects in vitro. *BMC Immunol.* (2010) 11:15. doi: 10.1186/1471-2172-11-15
20. Zimin AV, Marcais G, Puiu D, Roberts M, Salzberg SL, Yorke JA. The MaSuRCA genome assembler. *Bioinformatics.* (2013) 29:2669–77. doi: 10.1093/bioinformatics/btt476
21. Zimin AV, Puiu D, Luo MC, Zhu T, Koren S, Marcais G, et al. Hybrid assembly of the large and highly repetitive genome of Aegilops tauschii, a progenitor of bread wheat, with the MaSuRCA mega-reads algorithm. *Genome Res.* (2017) 27:787–92. doi: 10.1101/gr.213405.116
22. Seppey M, Manni M, Zdobnov EM. BUSCO: assessing genome assembly and annotation completeness. *Methods Mol Biol.* (2019) 1962:227–45. doi: 10.1007/978-1-4939-9173-0_14
23. Kriventseva EV, Kuznetsov D, Tegenfeldt F, Manni M, Dias R, Simao FA, et al. OrthoDB v10: sampling the diversity of animal, plant, fungal, protist, bacterial and viral genomes for evolutionary and functional annotations of orthologs. *Nucleic Acids Res.* (2019) 47:D807–11. doi: 10.1093/nar/gky1053
24. Sullivan MJ, Petty NK, Beatson SA. Easyfig: a genome comparison visualizer. *Bioinformatics.* (2011) 27:1009–10. doi: 10.1093/bioinformatics/btr039
25. Seemann T. Prokka: rapid prokaryotic genome annotation. *Bioinformatics.* (2014) 30:2068–9. doi: 10.1093/bioinformatics/btu153
26. Huerta-Cepas J, Forslund K, Coelho LP, Szklarczyk D, Jensen LJ, von Mering C, et al. Fast genome-wide functional annotation through orthology assignment by eggNOG-mapper. *Mol Biol Evol.* (2017) 34:2115–22. doi: 10.1093/molbev/msx148

27. Huerta-Cepas J, Szklarczyk D, Heller D, Hernandez-Plaza A, Forslund SK, Cook H, et al. eggNOG 5.0: a hierarchical, functionally and phylogenetically annotated orthology resource based on 5090 organisms and 2502 viruses. *Nucleic Acids Res.* (2019) 47:D309–14. doi: 10.1093/nar/gky1085
28. Grissa I, Vergnaud G, Pourcel C. CRISPRFinder: a web tool to identify clustered regularly interspaced short palindromic repeats. *Nucleic Acids Res.* (2007) 35:W52–7. doi: 10.1093/nar/gkm360
29. Krawczyk PS, Lipinski L, Dziembowski A. PlasFlow: predicting plasmid sequences in metagenomic data using genome signatures. *Nucleic Acids Res.* (2018) 46:e35. doi: 10.1093/nar/gkx1321
30. Arndt D, Grant JR, Marcu A, Sajed T, Pon A, Liang Y, et al. PHASTER: a better, faster version of the PHAST phage search tool. *Nucleic Acids Res.* (2016) 44:W16–21. doi: 10.1093/nar/gkw387
31. van Heel AJ, de Jong A, Song C, Viel JH, Kok J, Kuipers OP. BAGEL4: a user-friendly web server to thoroughly mine RiPPs and bacteriocins. *Nucleic Acids Res.* (2018) 46:W278–81. doi: 10.1093/nar/gky383
32. Krzywinski M, Schein J, Birol I, Connors J, Gascoyne R, Horsman D, et al. Circos: an information aesthetic for comparative genomics. *Genome Res.* (2009) 19:1639–45. doi: 10.1101/gr.092759.109
33. Kumar S, Stecher G, Li M, Knyaz C, Tamura K. MEGA X: molecular evolutionary genetics analysis across computing platforms. *Mol Biol Evol.* (2018) 35:1547–9. doi: 10.1093/molbev/msy096
34. Lee I, Ouk Kim Y, Park SC, Chun J. OrthoANI: an improved algorithm and software for calculating average nucleotide identity. *Int J Syst Evol Microbiol.* (2016) 66:1100–3. doi: 10.1099/ijsem.0.000760
35. Richter M, Rossello-Mora R. Shifting the genomic gold standard for the prokaryotic species definition. *Proc Natl Acad Sci USA.* (2009) 106:19126–31. doi: 10.1073/pnas.0906412106
36. Chen IA, Chu K, Palaniappan K, Pillay M, Ratner A, Huang J, et al. IMG/M v.5.0: an integrated data management and comparative analysis system for microbial genomes and microbiomes. *Nucleic Acids Res.* (2019) 47:D666–77. doi: 10.1093/nar/gky901
37. Liu B, Zheng D, Jin Q, Chen L, Yang J. VFDB 2019: a comparative pathogenomic platform with an interactive web interface. *Nucleic Acids Res.* (2019) 47:D687–92. doi: 10.1093/nar/gky1080
38. Alcock BP, Raphenya AR, Lau TTY, Tsang KK, Bouchard M, Edalatmand A, et al. CARD 2020: antibiotic resistome surveillance with the comprehensive antibiotic resistance database. *Nucleic Acids Res.* (2020) 48:D517–25. doi: 10.1093/nar/gkz935
39. Kanehisa M, Sato Y, Morishima K. BlastKOALA and GhostKOALA: KEGG tools for functional characterization of genome and metagenome sequences. *J Mol Biol.* (2016) 428:726–31. doi: 10.1016/j.jmb.2015.11.006
40. Yamaguchi T, Movila A, Kataoka S, Wisitrasameewong W, Ruiz Torruella M, Murakoshi M, et al. Proinflammatory M1 macrophages inhibit RANKL-induced osteoclastogenesis. *Infect Immun.* (2016) 84:2802–12. doi: 10.1128/IAI.00461-16
41. Gregory CA, Gunn WG, Peister A, Prockop DJ. An alizarin red-based assay of mineralization by adherent cells in culture: comparison with cetylpyridinium chloride extraction. *Anal Biochem.* (2004) 329:77–84. doi: 10.1016/j.ab.2004.02.002
42. Medici M, van Meurs JB, Rivadeneira F, Zhao H, Arp PP, Hofman A, et al. BMP-2 gene polymorphisms and osteoporosis: the rotterdam study. *J Bone Miner Res.* (2006) 21:845–54. doi: 10.1359/jbmr.060306
43. Lv Y, Wang G, Xu W, Tao P, Lv X, Wang Y. Tartrate-resistant acid phosphatase 5b is a marker of osteoclast number and volume in RAW 264.7 cells treated with receptor-activated nuclear kappaB ligand. *Exp Ther Med.* (2015) 9:143–6. doi: 10.3892/etm.2014.2071
44. Stackebrandt E, Frederiksen W, Garrity GM, Grimont PAD, Kampfer P, Maiden MCJ, et al. Report of the ad hoc committee for the re-evaluation of the species definition in bacteriology. *Int J Syst Evol Microbiol.* (2002) 52:1043–7. doi: 10.1099/00207713-52-3-1043
45. Toh H, Oshima K, Nakano A, Takahata M, Murakami M, Takaki T, et al. Genomic adaptation of the *Lactobacillus casei* group. *PLoS ONE.* (2013) 8:e75073. doi: 10.1371/journal.pone.0075073
46. Sanders ME, Akkermans L M, Haller D, Hammerman C, Heimbach J, Hormannsperger G, et al. Safety assessment of probiotics for human use. *Gut Microbes.* (2010) 1:164–85. doi: 10.4161/gmic.1.3.12127
47. Smokvina T, Wels M, Polka J, Chervaux C, Brisse S, Boekhorst J, et al. Lactobacillus paracasei comparative genomics: towards species pan-genome definition and exploitation of diversity. *PLoS ONE.* (2013) 8:e68731. doi: 10.1371/journal.pone.0068731
48. Ohlsson C, Sjogren K. Effects of the gut microbiota on bone mass. *Trends Endocrinol Metab.* (2015) 26:69–74. doi: 10.1016/j.tem.2014.11.004
49. Manichanh C, Borruel N, Casellas F, Guarner F. The gut microbiota in IBD. *Nat Rev Gastroenterol Hepatol.* (2012) 9:599–608. doi: 10.1038/nrgastro.2012.152
50. Marik PE. Colonic flora, probiotics, obesity and diabetes. *Front Endocrinol.* (2012) 3:87. doi: 10.3389/fendo.2012.00087
51. Tilg H, Moschen AR, Kaser A, Pines A, Dotan I. Gut, inflammation and osteoporosis: basic and clinical concepts. *Gut.* (2008) 57:684–94. doi: 10.1136/gut.2006.117382
52. McClung M. Role of RANKL inhibition in osteoporosis. *Arthritis Res Ther.* (2007) 9 (Suppl. 1):S3. doi: 10.1186/ar2167
53. Kim KW, Kang SS, Woo SJ, Park OJ, Ahn KB, Song KD, et al. Lipoteichoic acid of probiotic lactobacillus plantarum attenuates poly I:C-induced IL-8 production in porcine intestinal epithelial cells. *Front Microbiol.* (2017) 8:1827. doi: 10.3389/fmicb.2017.01827
54. Wang J, Ji H, Wang S, Liu H, Zhang W, Zhang D, et al. Probiotic *Lactobacillus plantarum* promotes intestinal barrier function by strengthening the epithelium and modulating gut microbiota. *Front Microbiol.* (2018) 9:1953. doi: 10.3389/fmicb.2018.01953
55. Donato KA, Gareau MG, Wang YJJ, Sherman PM. Lactobacillus rhamnosus GG attenuates interferon-{gamma} and tumour necrosis factor-alpha-induced barrier dysfunction and pro-inflammatory signalling. *Microbiology.* (2010) 156:3288–97. doi: 10.1099/mic.0.040139-0
56. Zhang J, Fu Q, Ren Z, Wang Y, Wang C, Shen T, et al. Changes of serum cytokines-related Th1/Th2/Th17 concentration in patients with postmenopausal osteoporosis. *Gynecol Endocrinol.* (2015) 31:183–90. doi: 10.3109/09513590.2014.975683
57. Le Goff B, Bouvard B, Lequerre T, Lespessailles E, Marotte H, Pers YM, et al. Implication of IL-17 in bone loss and structural damage in inflammatory rheumatic diseases. *Mediators Inflamm.* (2019) 2019:8659302. doi: 10.1155/2019/8659302
58. Rettedal EA, Ilesanmi-Oyelere BL, Roy NC, Coad J, Kruger MC. The gut microbiome is altered in postmenopausal women with osteoporosis and osteopenia. *JBMR Plus.* (2021) 5:e10452. doi: 10.1002/jbm4.10452
59. Li L, Rao S, Cheng Y, Zhuo X, Deng C, Xu N, et al. Microbial osteoporosis: the interplay between the gut microbiota and bones via host metabolism and immunity. *Microbiologyopen.* (2019) 8:e00810. doi: 10.1002/mbo3.810
60. Wang J, Wu X, Duan Y. Magnesium lithospermate b protects against lipopolysaccharide-induced bone loss by inhibiting RANKL/RANK pathway. *Front Pharmacol.* (2018) 9:64. doi: 10.3389/fphar.2018.00064
61. Park HJ, Gholam Zadeh M, Suh JH, Choi HS. Dauricine protects from LPS-induced bone loss via the ROS/PP2A/NF-kappaB axis in osteoclasts. *Antioxidants.* (2020) 9:588. doi: 10.3390/antiox9070588
62. Douzandeh-Mobarrez B, Kariminik A. Gut microbiota and IL-17A: physiological and pathological responses. *Probiotics Antimicrob Proteins.* (2019) 11:1–10. doi: 10.1007/s12602-017-9329-z
63. Tanabe S, Kinuta Y, Saito Y. Bifidobacterium infantis suppresses proinflammatory interleukin-17 production in murine splenocytes and dextran sodium sulfate-induced intestinal inflammation. *Int J Mol Med.* (2008) 22:181–5. doi: 10.3892/ijmm_00000006
64. Shih VF, Cox J, Kljavin NM, Dengler HS, Reichelt M, Kumar P, et al. Homeostatic IL-23 receptor signaling limits Th17 response through IL-22-mediated containment of commensal microbiota. *Proc Natl Acad Sci USA.* (2014) 111:13942–7. doi: 10.1073/pnas.1323852111
65. Ma S, Qin J, Hao Y, Fu L. Association of gut microbiota composition and function with an aged rat model of senile osteoporosis using 16S rRNA and metagenomic sequencing analysis. *Aging.* (2020) 12:10795–808. doi: 10.18632/aging.103293
66. Kruger MC, Horrobin DF. Calcium metabolism, osteoporosis and essential fatty acids: a review. *Prog Lipid Res.* (1997) 36:131–51. doi: 10.1016/S0163-7827(97)00007-6
67. An H. Ion channels and bone homeostasis imbalance. *Biomed J Sci Techn Res.* (2019) 16:1–6. doi: 10.26717/BJSTR.2019.16.002862

68. Ling CW, Miao Z, Xiao ML, Zhou H, Jiang Z, Fu Y, et al. The association of gut microbiota with osteoporosis is mediated by amino acid metabolism: multiomics in a large cohort. *J Clin Endocrinol Metab.* (2021) 106:e3852–64. doi: 10.1210/clinem/dgab492
69. Rzymski P, Pischel I, Conrad F, Zwingers T, Rzymski P, Opala T. The bioavailability of calcium in the form of pyruvate, carbonate, citrate–malate in healthy postmenopausal women. *Euro Food Res Technol.* (2015) 242:45–50. doi: 10.1007/s00217-015-2516-9
70. de Lima MZT, de Almeida LR, Mera AM, Bernardes A, Garcia W, Muniz JRC. Crystal structure of a sucrose-6-phosphate hydrolase from *Lactobacillus gasseri* with potential applications in fructan production and the food industry. *J Agric Food Chem.* (2021) 69:10223–34. doi: 10.1021/acs.jafc.1c03901
71. Sanches Lopes SM, Francisco MG, Higashi B, de Almeida RTR, Krausova G, Pilau EJ, et al. Chemical characterization and prebiotic activity of fructo-oligosaccharides from *Stevia rebaudiana* (Bertoni) roots and in vitro adventitious root cultures. *Carbohydr Polym.* (2016) 152:718–25. doi: 10.1016/j.carbpol.2016.07.043
72. Vandamme EJ, Soetaert W. Biotechnical modification of carbohydrates. *Fems Microbiol Rev.* (1995) 16:163–86. doi: 10.1111/j.1574-6976.1995.tb00164.x
73. Pokusaeva K, Fitzgerald GF, van Sinderen D. Carbohydrate metabolism in bifidobacteria. *Genes Nutr.* (2011) 6:285–306. doi: 10.1007/s12263-010-0206-6
74. Torricelli P, Fini M, Giavaresi G, Giardino R, Gnudi S, Nicolini A, et al. L-arginine and L-lysine stimulation on cultured human osteoblasts. *Biomed Pharmacother.* (2002) 56:492–7. doi: 10.1016/S0753-3322(02)00287-1
75. Torricelli P, Fini M, Giavaresi G, Giardino R. Bone tissue cultures: an in vitro model for the evaluation of bone defect healing after L-arginine and L-lysine administration. *Artif Cells Blood Substit Immobil Biotechnol.* (2001) 29:325–34. doi: 10.1081/BIO-100104234
76. Sanders DA, Staines AG, McMahon SA, McNeil MR, Whitfield C, Naismith JH. UDP-galactopyranose mutase has a novel structure and mechanism. *Nat Struct Biol.* (2001) 8:858–63. doi: 10.1038/nsb1001-858
77. Fukao M, Zendo T, Inoue T, Nakayama J, Suzuki S, Fukaya T, et al. Plasmid-encoded glycosyltransferase operon is responsible for exopolysaccharide production, cell aggregation, and bile resistance in a probiotic strain, *Lactobacillus brevis* KB290. *J Biosci Bioeng.* (2019) 128:391–7. doi: 10.1016/j.jbiosc.2019.04.008
78. Asong J, Wolfert MA, Maiti KK, Miller D, Boons GJ. Binding and cellular activation studies reveal that toll-like receptor 2 can differentially recognize peptidoglycan from gram-positive and gram-negative bacteria. *J Biol Chem.* (2009) 284:8643–53. doi: 10.1074/jbc.M806633200
79. Teame T, Wang A, Xie M, Zhang Z, Yang Y, Ding Q, et al. Paraprobiotics and postbiotics of probiotic lactobacilli, their positive effects on the host and action mechanisms: a review. *Front Nutr.* (2020) 7:570344. doi: 10.3389/fnut.2020.570344

Conflict of Interest: Authors W-HT and C-HC are employed by GenMont Biotech Incorporation.

The remaining authors declare that the research was conducted in the absence of any commercial or financial relationships that could be construed as a potential conflict of interest.

Publisher's Note: All claims expressed in this article are solely those of the authors and do not necessarily represent those of their affiliated organizations, or those of the publisher, the editors and the reviewers. Any product that may be evaluated in this article, or claim that may be made by its manufacturer, is not guaranteed or endorsed by the publisher.

frontiers in Microbiology

REVIEW
published: 30 March 2022
doi: 10.3389/fmicb.2022.864720

Probiotics, Their Extracellular Vesicles and Infectious Diseases

*A. Paula Domínguez Rubio[1,2], Cecilia L. D'Antoni[1,2], Mariana Piuri[1,2] and Oscar E. Pérez[1,2]**

[1] Departamento de Química Biológica, Facultad de Ciencias Exactas y Naturales, Universidad de Buenos Aires, Buenos Aires, Argentina, [2] Instituto de Química Biológica de la Facultad de Ciencias Exactas y Naturales, Universidad de Buenos Aires, Consejo Nacional de Investigaciones Científicas y Técnicas, Buenos Aires, Argentina

Probiotics have been shown to be effective against infectious diseases in clinical trials, with either intestinal or extraintestinal health benefits. Even though probiotic effects are strain-specific, some "widespread effects" include: pathogen inhibition, enhancement of barrier integrity and regulation of immune responses. The mechanisms involved in the health benefits of probiotics are not completely understood, but these effects can be mediated, at least in part, by probiotic-derived extracellular vesicles (EVs). However, to date, there are no clinical trials examining probiotic-derived EVs health benefits against infectious diseases. There is still a long way to go to bridge the gap between basic research and clinical practice. This review attempts to summarize the current knowledge about EVs released by probiotic bacteria to understand their possible role in the prevention and/or treatment of infectious diseases. A better understanding of the mechanisms whereby EVs package their cargo and the process involved in communication with host cells (inter-kingdom communication), would allow further advances in this field. In addition, we comment on the potential use and missing knowledge of EVs as therapeutic agents (postbiotics) against infectious diseases. Future research on probiotic-derived EVs is needed to open new avenues for the encapsulation of bioactives inside EVs from GRAS (Generally Regarded as Safe) bacteria. This could be a scientific novelty with applications in functional foods and pharmaceutical industries.

Keywords: probiotics, GRAS, postbiotics, extracellular vesicles, membrane vesicles, infectious diseases

OPEN ACCESS

Edited by:
Martin Schwarzer, Institute of Microbiology, Academy of Sciences of the Czech Republic (ASCR), Czechia

Reviewed by:
Maria de los Angeles Serradell, Universidad Nacional de La Plata, Argentina
Arthur C. Ouwehand, International Flavors and Fragrances, Finland

***Correspondence:**
Oscar E. Pérez
oscarperez@qb.fcen.uba.ar

Specialty section:
This article was submitted to Food Microbiology, a section of the journal Frontiers in Microbiology

Received: *28 January 2022*
Accepted: *07 March 2022*
Published: *30 March 2022*

Citation:
Domínguez Rubio AP, D'Antoni CL, Piuri M and Pérez OE (2022) Probiotics, Their Extracellular Vesicles and Infectious Diseases. Front. Microbiol. 13:864720. doi: 10.3389/fmicb.2022.864720

INTRODUCTION

Infectious diseases are disorders caused by organisms such as viruses, bacteria, fungi, or parasites. Could probiotics deal with infectious diseases? A lot of clinical trials have brought this question to the forefront with positive effects on prevention and/or treatment of infectious diseases. In this review, we conducted a search for probiotic bacteria utilized for treatment of infectious diseases and then discussed the current knowledge about extracellular vesicles (EVs) released by these probiotic species. It is important to highlight that according to the generally accepted definition of probiotic, probiotic effects are strain-specific. However, various effects of probiotics can be ascribed to the species level (Hill et al., 2014). Moreover, the study of EVs released by the probiotic strains is still in its infancy and has not been widely analyzed so far. For these two reasons, to collect the current evidence of probiotic-derived EVs we decided to extrapolate our search to the species level. In this line, EV-producing strains were shown to mediate beneficial effects both *in vitro* and *in vivo* models,

but human trials (a requirement for probiotic claim) are still pending.

PROBIOTICS

Definition

Probiotics are defined as "live microorganisms that, when administered in adequate amounts, confer a health benefit on the host" (Hill et al., 2014). In a position statement an expert panel of the International Scientific Association for Probiotics and Prebiotics (ISAPP) set four minimum criteria for probiotic claims (Binda et al., 2020). Probiotics must: (1) be identified to the genus, species and strain level, (2) be safe for the intended use, (3) have demonstrated health benefits in at least one clinical trial, and (4) have a suitable viable count at end of shelf life.

Before clinical trials are conducted, potential probiotics must be selected by a comprehensive approach including multiple steps. According to the "Guidelines for the Evaluation of Probiotics in Food" (FAO/WHO, 2002), candidate strains are suggested to be assessed for their stress tolerance, antimicrobial properties, epithelium adhesion ability, and safety. At the same time, *in vitro* and *in vivo* experiments should be performed to evaluate probiotic effects (de Melo Pereira et al., 2018; Santos et al., 2020).

As stated above, for validation of treatment safety and efficacy, probiotics must be subjected to at least one clinical trial, which must be conducted based on generally accepted scientific standards (Binda et al., 2020). In general, the weight ascribed to a trial result is higher when sources of bias are avoided (Higgins et al., 2019), and therefore randomized controlled trials are usually considered the most appropriate methodology for validating a probiotic health claim (Tamayo, 2008). In the last decades, there has been a rapid growth in the number of clinical trials for the use of probiotics for prophylactic and/or therapeutic applications in various fields: infectious diseases, cancer, depression and obesity (Zommiti et al., 2020).

Even though probiotics must be identified to the strain level, various meta-analyses indicate that "shared benefits" are achieved by many different strains of the same species, due to similar biological pathways (Sanders et al., 2018). In that regard, the ISAPP panel considered that well-studied beneficial species may be considered as "probiotics" even in the absence of randomized controlled trials that support this claim (Hill et al., 2014). Although clinical trials rarely compare different strains of the same species, certain health effects such as immunomodulation have been ascribed to many strains of the same species (Zhao et al., 2020, 2021).

Many probiotic lactic acid bacteria have long been used in dairy products, being awarded the status of GRAS (Ghosh et al., 2019). The projection of the global probiotics market is expected to grow at a compound annual growth rate of 7.2% from 2021 to 2028 (Grand View Research, 2021). The popularity of probiotic use has increased dramatically in the last decades, not only for their clinical use, but also in healthy individuals wishing to maintain a healthy gut microbiota (Fleming et al., 2016; Su et al., 2020).

Probiotics and Microbiota: Inter-Kingdom Communication

Our bodies are composed of human cells and microbiota, which is composed of viruses, bacteria, fungi and parasites (Cao and Mortha, 2020). These complex and dynamic populations of microorganisms are crucial for maintaining health and playing a decisive defensive role against pathogens (Sokol, 2019). Inside the human body there exist different microbiotas according to their localization: skin, lung, urethra, vagina, etc. In the last decade, organs that had been previously considered sterile today are hypothesized to have a microbiota. For example, despite it was always thought that the fetus was developed under sterile conditions, recent data suggested the presence of microorganisms in the uterus and placenta (Agostinis et al., 2019; Tang et al., 2020). Moreover, contrary to a long-held dogma, today we know that human milk is not sterile (McGuire and McGuire, 2017). The hypothesis of how bacteria from the maternal gastrointestinal tract (GIT) are translocated to human milk is that dendrites from dendritic cells (DCs) could cross the gut epithelium and transport gut lumen bacteria to the mammary gland through the lymphoid system (Olivares et al., 2015; Demmelmair et al., 2020).

Nowadays, the gut microbiota is considered a new "vital organ" of the human body and is connected with other organs through different axis via neural, endocrine and immune interactions (Ding et al., 2019; Ahlawat et al., 2021). In this line, the consumption of probiotics has been reported to have beneficial effects on the gut–brain axis, the gut–skin axis, etc. (Banfi et al., 2021; Park et al., 2021). In addition, it has recently been demonstrated that the consumption of probiotics can modulate other microbiotas too, e.g., vaginal microbiota (Silvia Ventimiglia et al., 2021).

Fermented foods and probiotics (these terms should not be confused) increase gut microbiota diversity with benefits on human health (Aljutaily et al., 2020; Vinderola and Pérez-Marc, 2021). Frequently, a disruption in the microbiota composition results in a less diverse or less "rich" microbiota, which is often linked to a leaky gut syndrome, higher gut inflammation and more oxidative stress. This microbiota imbalance is linked to various diseases including obesity, diabetes, irritable bowel syndrome, inflammatory bowel disease, depression, and cardiovascular disease (Hills et al., 2019).

It is important to emphasize that many probiotic strains do not colonize the gut and are no longer recoverable in stool 1–4 weeks after stopping their consumption. For example, the probiotic-containing fermented milk Activia did not change the bacterial composition in the gut, but instead altered gene expression patterns that are relevant to carbohydrate metabolism in the gut microbiota. These changes in the gut function were confined only to the time of probiotic consumption (Maguire and Maguire, 2019).

Probiotics for Infectious Diseases

In the context of probiotics against infectious diseases, widespread effects or "shared benefits" of probiotics include mechanisms that act directly by inhibiting pathogens and

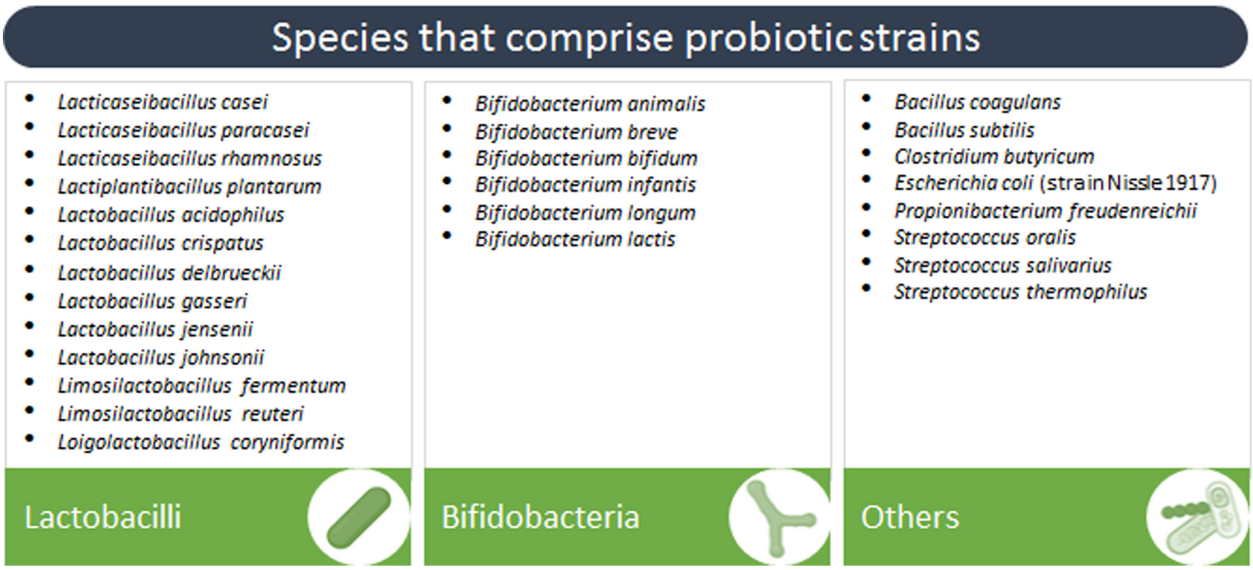

FIGURE 1 | Species that comprise probiotic strains assessed for the prevention or treatment of infectious diseases in clinical trials.

indirectly by reinforcing the host epithelial barrier function and immune responses (Lebeer et al., 2010; Sassone-Corsi and Raffatellu, 2016; Raheem et al., 2021). Even though probiotic effects are strain-specific, in this review we collected a series of clinical trials where probiotic species benefits were assessed against infectious diseases (**Figure 1**). According to our search, nearly 50% of these species were reported to release EVs (**Table 1**). Seven out of 24 strains released EVs that have had beneficial effects against pathogens in *in vitro*, *ex vivo* or *in vivo* models (**Table 1**, indicated by asterisks). In fact, some of these strains are well-known probiotics: i.e., *Escherichia coli* Nissle 1917 and *Lacticaseibacillus rhamnosus* GG. We limited our search to bacteria, although some fungi are also considered to be probiotics.

Probiotic bacteria with successful results against infectious diseases mainly include bifidobacteria and lactobacilli, which represent the most studied probiotics (Stavropoulou and Bezirtzoglou, 2020), and other Gram (+) bacteria belonging to the genera *Streptococcus*, *Bacillus*, *Propionibacterium* and *Clostridium*. On the other hand, to our knowledge the only Gram (−) bacterial strain that was found to be effective in clinical trials is *E. coli* Nissle 1917. *E. coli* Nissle 1917 has been considered a probiotic for over a century and used to treat intestinal diseases. However, the strain contains a pathogenicity island (*pks*) that codes for colibactin, a genotoxin that mediates anti-inflammatory effects (Olier et al., 2012) and is now linked to causative mutations found in human colorectal cancer (Nougayrède et al., 2021).

Probiotics are commonly consumed in food or supplements (Hill et al., 2014; **Figure 2**). Oral administration, which is the most usual route of administration of probiotics, has resulted in satisfactory outcomes in clinical trials, even when the beneficial effect occurred in extraintestinal sites (Maldonado-Lobón et al., 2015; Panigrahi et al., 2017; Vladareanu et al., 2018; Lazou Ahrén et al., 2021). Possible mechanisms by which oral administration of probiotics may have extraintestinal and systemic effects on the host will be discussed in the following sections. However, there are many possible routes of administration of probiotics, such as mouth rinses and lozenges for periodontal disease (Tsubura et al., 2009; Invernici et al., 2018), vaginal suppositories for trichomoniasis, bacterial vaginosis and recurrent urinary tract infections (Stapleton et al., 2011; Sgibnev and Kremleva, 2020), intranasal administration for upper respiratory tract infections (Passali et al., 2019), and topical application for skin wounds (Peral et al., 2009). In the case of respiratory and skin infections, although topical administration could be advantageous (Lopes et al., 2017; Spacova et al., 2021), their study in clinical trials is currently underrepresented.

It is important to note that many clinical trials examine the use of probiotics as a supplementation to conventional therapy against infectious diseases, such as antibiotic and antifungal agents (Shi et al., 2019; Joseph et al., 2021). In general terms, probiotics have shown effectiveness in preventing infectious diseases in different organ systems, from the respiratory and gastrointestinal tracts to the female urogenital system, among others. As regards gastrointestinal diseases, probiotics were effective in reducing frequency and duration of diarrhea (Francavilla et al., 2012; Park et al., 2017; Sharifi-Rad et al., 2020), reducing symptoms of gastroenteritis and *H. pylori* gastritis (Shafaghi et al., 2016; Shin et al., 2020), and preventing necrotizing enterocolitis (Chang et al., 2017). In respect of respiratory diseases, the benefit of probiotics has been mostly associated with prevention of infections, especially in the upper respiratory tract (Aryayev et al., 2018; Anaya-Loyola et al., 2019; Lazou Ahrén et al., 2021). Finally, certain probiotics were successful in reducing symptoms and frequency of recurrent vulvovaginal candidiasis, bacterial vaginosis and urinary tract infections (Laue et al., 2018; Russo et al., 2019; Sgibnev and Kremleva, 2020), possibly mainly by restoring the normal vaginal

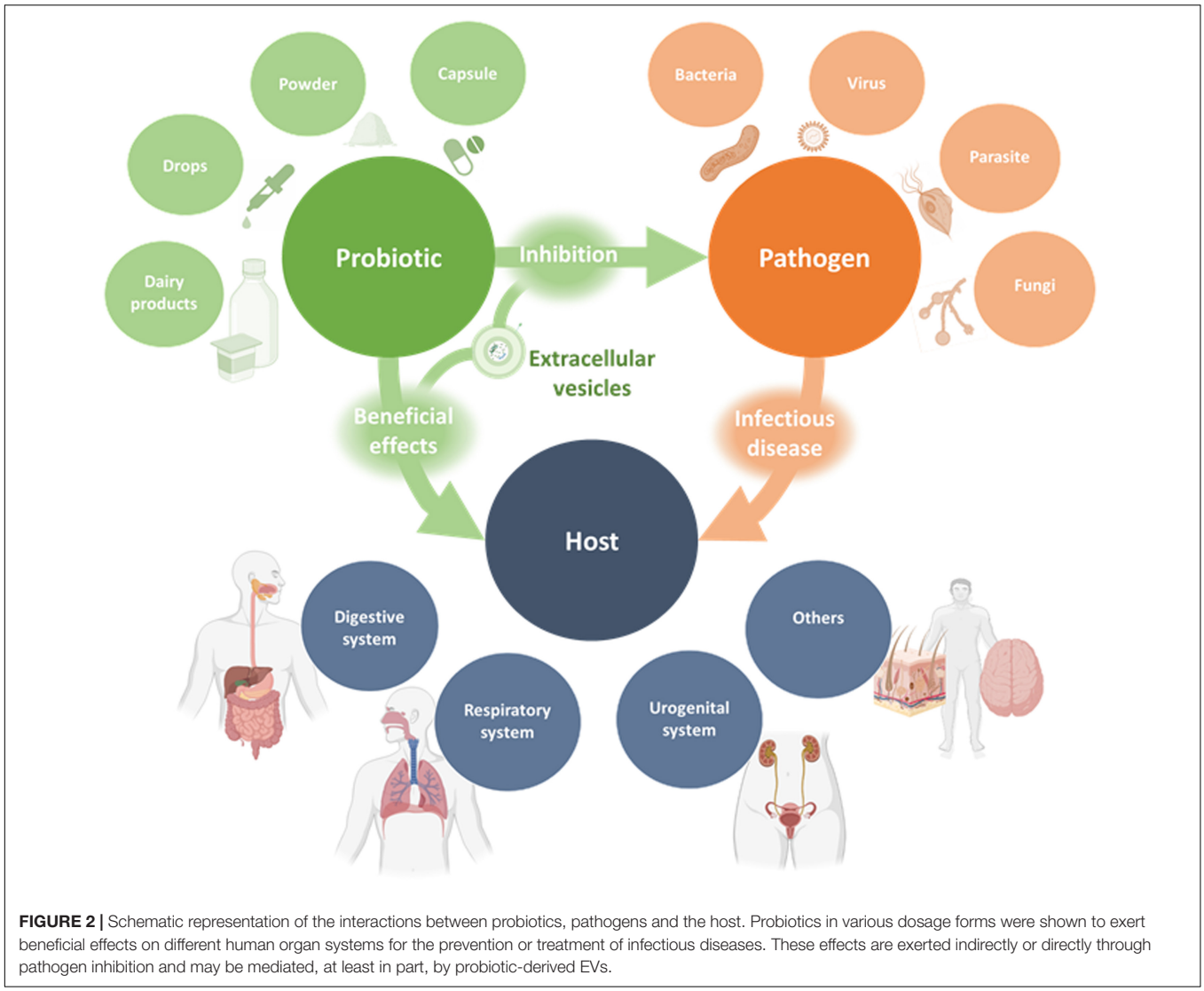

FIGURE 2 | Schematic representation of the interactions between probiotics, pathogens and the host. Probiotics in various dosage forms were shown to exert beneficial effects on different human organ systems for the prevention or treatment of infectious diseases. These effects are exerted indirectly or directly through pathogen inhibition and may be mediated, at least in part, by probiotic-derived EVs.

microbiota. Other benefits of probiotics demonstrated in clinical trials involve other organ systems, such as skin and the nervous system (Kotzampassi et al., 2015; Xia et al., 2018). Further high-quality clinical trials and meta-analyses should be undertaken to provide stronger evidence for the therapeutic use of probiotics (Stavropoulou and Bezirtzoglou, 2020).

EXTRACELLULAR VESICLES

Bacterial Extracellular Vesicles

Probiotics seem to act through a wide repertoire of mechanisms but the specific pathways and key regulatory molecules underlying their beneficial effects are largely unknown (Plaza-Diaz et al., 2019). In this line, EVs have been associated with diverse functions in cell-to-cell communication and appear to be a common language between kingdoms (i.e., bacteria and eukaryotic cells) (Ñahui Palomino et al., 2021).

Extracellular vesicles are produced by all domains of life: archaea, bacteria and eukarya. To this day it has been seen that EVs appear to be produced by all cell types of all studied organisms. All EVs are composed of a lipid bilayer with membrane proteins and contain DNA, RNA and proteins (Théry et al., 2018). The level of knowledge about bacterial EVs is lower than eukaryotic EVs, but the number of studies is continuously increasing (Ñahui Palomino et al., 2021). In particular, EVs from Gram (+) bacteria have been less studied, and our understanding of their biogenesis and interaction with host cells is just being started (Briaud and Carroll, 2020).

The size of bacterial EVs is in the nanoscale (below 500 nm), and has been related to bacterial physiology including probiotic and pathogenic effects. In the case of Gram (+) bacteria, EVs are called membrane vesicles (MVs) and the lipid bilayer encloses cytosolic material. In contrast, in the case of Gram (−) bacteria, EVs are called outer-membrane vesicles (OMVs) and the lipid bilayer encloses periplasmic material. Gram (+) and Gram (−) bacterial EVs are also different in their surface composition for

TABLE 1 | Biological effects of EVs released by species that comprise probiotic strains.

Genus and species	Strain	Current evidence	Pathogen inhibition	Barrier function	Immune system	Composition	Transport	Other biological effects	References
Escherichia coli	Nissle 1917	EVs improved epithelial barrier function in intestinal epithelial cells (T-84 and Caco-2)		•					Alvarez et al., 2016
Escherichia coli	Nissle 1917	EVs protected barrier function in human intestinal epithelial cells (T-84 and Caco-2) infected with *E. coli* (EPEC)		•					Alvarez et al., 2019 *
Escherichia coli	Nissle 1917	EVs were endocytosed in a clathrin-dependent manner by human intestinal epithelial cells (HT-29)					•		Cañas et al., 2016
Escherichia coli	Nissle 1917	EVs incubation with human intestinal epithelial cells (Caco-2) activated NOD1-signaling cascades and NF-κB, and increased IL-6 and IL-8 levels			•				Cañas et al., 2018
Escherichia coli	Nissle 1917	EVs increased TNF-α, IL-6, IL-8, IL-10 and MIP1α levels in PBMC, human intestinal epithelial cells (Caco-2)/PMBCs co-culture and *ex vivo* colonic mucosa explants		•	•		•		Fábrega et al., 2016
Escherichia coli	Nissle 1917	EVs improved clinical symptoms and histological scores, protected intestinal epithelial barrier function, and mediated anti-inflammatory effects in a dextran sulfate sodium-induced colitis mouse model		•	•				Fábrega et al., 2017
Escherichia coli	Nissle 1917	EVs incubation with mouse macrophage cells (RAW264.7) increased TNF-α, IL-4, IL-6, IL-10 and IL-12 levels, and stimulated bacteria-killing ability against *E. coli*, *S. typhimurium, and S. aureus*			•				Hu et al., 2020 *
Escherichia coli	Nissle 1917	Vaccination with engineered EVs (modified bacteria that express the enterotoxin ClyA) had a strong adjuvant capability on the immune response in mice			•				Rosenthal et al., 2014
Bacillus subtilis	168	EVs were transported across human intestinal epithelial cells (Caco-2)					•		Domínguez Rubio et al., 2020
Bifidobacterium bifidum	LMG13195	EVs incubation with human dendritic cells induced Treg differentiation and increased IL-10 levels			•				López et al., 2012
Bifidobacterium longum	NCC2705	EVs contained several mucin-adhesion proteins				•			Morishita et al., 2021
Bifidobacterium longum	–	EVs incubation with mouse macrophage cells (RAW264.7) and dendritic cells (DC2.4) increased TNF-α and IL-6 levels			•	•	•		Morishita et al., 2021
Clostridium butyricum	–	EVs incubation with mouse macrophage cells (RAW264.7) and dendritic cells (DC2.4) increased TNF-α and IL-6 levels			•	•	•		Morishita et al., 2021
Lacticaseibacillus casei	ATCC 393	EVs contain the protein p75 associated with probiotic effects				•			Dean et al., 2019
Lacticaseibacillus casei	ATCC 393	EVs incubation with human intestinal epithelial cells (Caco-2) decreased TLR9 gene expression and IFN-γ levels, and increased IL-4 and IL-10 levels			•				Vargoorani et al., 2020
Lacticaseibacillus casei	BL23	EVs contain proteins p40 and p75 associated with probiotic effects				•			Domínguez Rubio et al., 2017

(Continued)

TABLE 1 | (Continued)

Genus and species	Strain	Current evidence	Pathogen inhibition	Barrier function	Immune system	Composition	Transport	Other biological effects	References
Lacticaseibacillus casei	BL23	EVs increased NF-κB levels and induced phosphorylation of epidermal growth factor receptor (EGFR) in human intestinal epithelial cells (HT-29 and T-84, respectively)			•	•			Bäuerl et al., 2020
Lacticaseibacillus paracasei	–	EVs decreased NF-κB levels and mRNA levels of TNFα, IL-1α, IL-1β and IL-2, and increased mRNA levels of TGFβ and IL-10 in LPS-induced inflammation in human intestinal epithelial cells (HT-29) and reduce inflammation symptoms of dextran sulfate sodium-induced colitis in mice.			•				Choi et al., 2020
Lactiplantibacillus plantarum	APsulloc 331261	EVs increased IL-10, IL-1β and GM-CSF levels in *ex vivo* human skin cultures, and induced monocyte-to-macrophage transition and polarization to M2b in human monocytic cells (THP-1)			•				Kim et al., 2020
Lactiplantibacillus plantarum	BGAN8	EVs were endocytosed in a clathrin-dependent manner by human intestinal epithelial cells (HT29)				•	•		Bajic et al., 2020
Lactiplantibacillus plantarum	KCTC 11401BP	EVs decreased IL-6 levels and protected cell viability against treatment with *S. aureus* EVs in human epidermal keratinocytes (HaCaT), and reduced skin inflammation in *S. aureus* EV-induced atopic dermatitis in mice			•				Kim et al., 2018 *
Lactiplantibacillus plantarum	KCTC 11401BP	EVs increased Brain Derived Neurotrophic Factor (BDNF) levels in mouse hippocampal neurons (HT22) and produced antidepressant-like effects in mice with chronic restraint stress						•	Choi et al., 2019
Lactiplantibacillus plantarum	WCFS1	EVs prolonged the survival of *C. elegans* infected with vancomycin-resistant enterococci		•		•			Li et al., 2017 *
Lactiplantibacillus plantarum	WCFS1	EVs incubation with mouse macrophage cells (RAW264.7) and dendritic cells (DC2.4) increased TNF-α and IL-6 levels			•	•	•		Morishita et al., 2021
Lacticaseibacillus rhamnosus	GG	EVs decreased TNF-α, IL-1β, IL-6 and MCP-1 levels in LPS-induced inflammation in mouse macrophage cells (RAW264.7), increased IL-22 levels and decreased hepatic bacterial translocation by reinforcing the intestinal barrier function in alcohol-associated liver disease in mice		•	•	•			Gu et al., 2021
Lacticaseibacillus rhamnosus	GG	EVs increased apoptosis in human hepatic cells (hepG2)				•			Behzadi et al., 2017
Lacticaseibacillus rhamnosus	GG	EVs decreased IFN-γ and IL-17A levels in *S. aureus*-stimulated human PBMC			•				Mata Forsberg et al., 2019 *
Lacticaseibacillus rhamnosus	GG	EVs inhibited TLR4-NF-κB-NLRP3 axis activation in colonic tissues, and decreased TNF-α, IL-1β, IL-2 and IL-6 levels in dextran sulfate sodium-colitis in mice			•				Tong et al., 2021
Lacticaseibacillus rhamnosus	JB-1	EVs increased IL-10 and HO-1 levels via Dectin-1, SIGNR1, TLR-2 and TLR-9 activation in dendritic cells, and increased Treg cells in Peyer's patch from mice			•				Al-Nedawi et al., 2015
Lacticaseibacillus rhamnosus	JB-1	EVs appeared in blood 2.5 h after oral consumption and contained bacteriophage DNA			•	•	•		Champagne-Jorgensen et al., 2021a

(Continued)

TABLE 1 | (Continued)

Genus and species	Strain	Current evidence	Pathogen inhibition	Barrier function	Immune system	Composition	Transport	Other biological effects	References
Lacticaseibacillus rhamnosus	JB-1	EVs were endocytosed in a likely clathrin-dependent manner by mouse (MODE-K) and human intestinal epithelial cells (HT-29) and by mouse intestinal epithelial cells *in vivo*. They expose lipoteichoic acid that activated TLR2 and increased IL-10 levels			•	•	•		Champagne-Jorgensen et al., 2021b
Lactobacillus acidophilus	ATCC 53544	EVs contain bacteriocins	•			•			Dean et al., 2019
Lactobacillus acidophilus	ATCC 53544	Bacteriocin-enriched EVs fused with other bacteria	•			•			Dean et al., 2020
Lactobacillus crispatus	BC3	EVs protected human cervico-vaginal and tonsillar tissues, and human CD4+ T cell lines (MT-4 and Jurkat-tat) from HIV-1 infection by decreasing viral attachment	•			•			Ñahui Palomino et al., 2019 *
Lactobacillus gasseri	BC12	EVs protected human cervico-vaginal and tonsillar tissues, and human CD4+ T cell lines (MT-4 and Jurkat-tat) from HIV-1 infection by decreasing viral attachment	•			•			Ñahui Palomino et al., 2019 *
Lactobacillus gasseri	JCM 1131	EVs expose lipoteichoic acid on the surface during logarithmic phase				•			Shiraishi et al., 2018
Lactobacillus johnsonii	N6.2	EV expose proteins that are recognized by IgA and IgG from plasma of individuals who had consumed the probiotic			•				Harrison et al., 2021
Latilactobacillus sakei	NBRC15893	EVs promoted IgA production by murine Peyer's patch cells via TLR2			•				Yamasaki-Yashiki et al., 2019
Limosilactobacillus reuteri	ATCC 23272	EVs contain no bacteriocins, even though this strain produces high levels of these antibacterial molecules				•			Dean et al., 2019
Limosilactobacillus reuteri	BBC3	EVs decreased mRNA levels of TNF-α, IL-1β, IL-6, IL-17 and IL-8, and increased mRNA levels of IL-10 and TGF-β in LPS-induced inflammation in chicken			•	•			Hu et al., 2021
Limosilactobacillus reuteri	DSM 17938	EVs decreased IFN-γ and IL-17A levels in *S. aureus*-stimulated human PBMC			•				Mata Forsberg et al., 2019 *
Limosilactobacillus reuteri	DSM 17938	EVs mimicked the effect of the bacteria on gut motility in mice						•	West et al., 2020
Propionibacterium freudenreichii	CIRM-BIA 129	EVs decreased NF-κB and IL-8 levels in LPS-induced inflammation in human intestinal epithelial cells (HT-29)			•	•			Rodovalho et al., 2020

EVs that have had beneficial effect against pathogens in in vitro, ex vivo, or in vivo models are indicated by asterisks.

example the presence of lipopolysaccharide (LPS). The diversity in cargo molecules contained in EVs might explain the variety of described roles ranging from decoys for viral and antibiotic attack, quorum sensing as well as regulation of host immune defense (Kaparakis-Liaskos and Kufer, 2020).

Postbiotics, a New Concept

As mentioned before, probiotics comprise live microorganisms that confer a health benefit on the host when administered in adequate amounts. At the same time, there is increasing evidence of the health effects of non-viable microorganisms and their bioactive compounds (metabolites that they can produce by fermentation or by their action on food components) (Collado et al., 2019). An expert panel of ISAPP defined a postbiotic as a "preparation of inanimate microorganisms and/or their components that confers a health benefit on the host" (Salminen et al., 2021). In this line, EVs are secretory components associated with probiotic bacteria health benefits and consequently could be considered postbiotics (Wegh et al., 2019).

Extracellular vesicles play a central role in many physiological and pathological processes due to their capacity to transport biologically active macromolecules that can effectively alter the biological properties of target cells. Due to this property, they can be considered novel agents with different therapeutic applications. There are many clinical trials investigating the use of human EVs for various therapeutic approaches, including pathogen vaccination, anti-tumor therapy, regenerative therapies and drug delivery (Lener et al., 2015; Théry et al., 2018). In the case of EVs against infectious diseases there exist two different strategies: evaluation of EVs released naturally by the pathogen or infected cells, and EVs from *in vitro* antigen-pulsed DCs (Wahlund et al., 2017; Riley and Blanton, 2018; Santos and Almeida, 2021). However, to our knowledge there are no clinical trials related to the use of EVs from probiotic bacteria for the prevention and/or treatment of any infectious disease.

EXTRACELLULAR VESICLES FROM PROBIOTIC BACTERIA AND INFECTIOUS DISEASES

In order to organize the information, we divided the current evidence of the knowledge about the role of EVs as mediators of probiotic beneficial effects into six categories. The first category addresses the role of EVs against pathogens. The second and third categories are related to their function in the host immune system that can also be divided into three lines of defense: physical and chemical barriers, innate immunity and adaptive immunity. The last categories describe EVs composition, how EVs are uptaken and transported across human cells and other functions.

Pathogen Inhibition

Probiotics can inhibit pathogens through production of antimicrobial agents and through competitive exclusion of pathogens by competing for adhesion or nutrients in the GIT (Surendran Nair et al., 2017; van Zyl et al., 2020; Raheem et al., 2021).

Antimicrobial agents mainly include reactive oxygen species, lactic acid, and bacteriocins (Rajilić-Stojanović, 2013). Bacteriocins are peptides with antimicrobial activity that have shown to inhibit not only bacteria, but also viruses, fungi and parasites (Dicks and Grobbelaar, 2021; Huang et al., 2021). Furthermore, bacteriocins might be an interesting alternative to the use of antibiotics for infectious diseases caused by antibiotic-resistant bacteria due to their high potency and low toxicity (Cui et al., 2021; Gradisteanu Pircalabioru et al., 2021).

Recent studies show that EVs released by *L. acidophilus* ATCC 53544 could deliver bacteriocins and thus kill other bacteria (Dean et al., 2019, 2020). Proteomic analyses revealed bacteriocins are enriched in EVs. Even though bacteriocins investigated by these authors are directed against a *L. delbrueckii* strain (Dean et al., 2020), other bacteriocins synthesized by probiotics are able to inhibit or kill pathogens, such as *Listeria monocytogenes*, *Staphylococcus aureus, Acinetobacter baumannii*, *Gardnerella vaginalis*, *Streptococcus agalactiae*, and *Pseudomonas aeruginosa,* in both *in vitro* and *in vivo* models (Gaspar et al., 2018; van Zyl et al., 2019; Hassan et al., 2020). It is noteworthy that EVs may protect bacteriocins from proteases and inactivation molecules that are normally present in the intestine. Whether EVs from probiotics can deliver bacteriocins to pathogens is still unknown and holds great potential for future research.

Several clinical trials have shown that probiotics improved vaginal microbiota composition (Ho et al., 2016; Laue et al., 2018; Vladareanu et al., 2018) and it has been demonstrated that a vaginal microbiota dominated by lactobacilli prevents infections caused by various pathogens, including HIV-1 (Chee et al., 2020). A possible relevant mechanism of EVs related to pathogen inhibition is their ability to prevent pathogen interaction with host cells. It has been demonstrated that some *L. crispatus* and *L. gasseri* EVs reduced HIV-1 attachment to host cells and in this way prevented infection in human cell lines and tissues (Ñahui Palomino et al., 2019). This effect was associated with the reduced accessibility of gp120 (a viral envelope protein) to host target cells after incubating HIV-1 virions with EVs.

Regarding competitive exclusion, probiotics can compete with enteric pathogens for adhesion sites on the mucus layer or on intestinal epithelial cells, and hence prevent pathogen colonization and infection (van Zyl et al., 2020). Competitive exclusion of pathogens has been demonstrated in *in vitro* models (Singh et al., 2017; Tuo et al., 2018), and possibly takes place not only in the GIT but also in the oral cavity and urogenital tract. Numerous authors have investigated the role of pathogenic bacteria EVs in transporting virulence factors and toxins into host cells (Macion et al., 2021). On the other hand, to the best of our knowledge, the only existing report of EVs from probiotics mediating the competition between pathogenic and probiotic bacteria was published by Kim et al. (2018). In this study, it was shown that EVs from *L. plantarum* prevented skin inflammation in a murine model of *S. aureus* EV-induced atopic dermatitis. Concerning the GIT, EVs from probiotics expose adhesion proteins that may interact with the mucus layer and human cells. Although it is likely that this interaction may affect viral and bacterial

attachment, there remains a need for *in vitro* and *in vivo* studies addressing this question.

Barrier Function: Physical and Chemical Defense

The intestinal epithelial barrier acts as the first line of defense by avoiding the entrance of antigens and pathogens (Barbara et al., 2021). The alteration of the gut microbiota is the most important factor that disrupts the integrity of the intestinal epithelial barrier, leading to intestinal inflammation and diseases (Gareau et al., 2010). Probiotics, in this context, as transient constituents of the microbiota, are able to improve barrier function by surface components and secreted factors (postbiotics), among them, EVs (Liu et al., 2020). Since the exposure to infection can lead to the loss of epithelial integrity (König et al., 2016; Invernizzi et al., 2020), probiotic EVs participation in the improvement of barrier function could be an important point to regard them as potential prophylactic or therapeutic agents against infections.

As for the physical barrier, *in vitro* and *in vivo* experiments have demonstrated that EVs released by *E. coli* Nissle 1917 can mediate anti-inflammatory effects and protect the intestinal epithelial barrier function (Alvarez et al., 2016; Fábrega et al., 2016, 2017). A key role in the maintenance of intestinal epithelial barrier integrity is played by tight junctions, which are composed of a network of proteins that regulate paracellular permeability, such as claudins, zonula occludens (ZO) and occludin (Barbara et al., 2021). EVs released by *E. coli* Nissle 1917 have been shown to upregulate ZO-1 and claudin-14, downregulate claudin-2 (a gene that codes for a leaky protein), and in turn improve epithelial barrier function in an *in vitro* intestinal epithelium models (T-84 and Caco-2 cell lines) (Alvarez et al., 2016). This function of EVs has also been reported in these same cell lines infected with enteropathogenic *E. coli* (EPEC), an enteric pathogen that disrupts tight junctions as a way to increase invasion. In this work, EVs released by *E. coli* Nissle 1917 were able to counteract EPEC-altered mRNA levels of claudin-14 and occludin, preserve subcellular localization of ZO-1 and occludin, and maintain F-actin at the intercellular junctions. Barrier integrity restoration was further confirmed by measuring transepithelial electrical resistance (TEER) and the flux of FITC-dextran (Alvarez et al., 2019). In addition, restoration of epithelial integrity by EVs has been observed in an *in vivo* model of experimental colitis (Fábrega et al., 2017). In this regard, these authors demonstrated that oral administration of EVs from *E. coli* Nissle 1917 increased: trefoil factor 3 (TFF-3) mRNA levels, a marker of intestinal barrier function; and decreased MMP-9 mRNA levels, a protein involved in tissue injury.

Regarding the intestinal chemical defense, antimicrobial peptides and the mucus layer (mainly produced by the goblet cells) are further key factors that maintain intestinal barrier integrity by protecting epithelial cells from bacteria and other challenges (Hansson, 2020; Yong et al., 2020; Barbara et al., 2021; Fusco et al., 2021). In an *in vivo* model of experimental colitis, treatment with EVs from *E. coli* Nissle 1917 resulted in the restoration of the mucin content in goblet cells and in a smaller ulceration surface, as evidence of barrier integrity (Fábrega et al., 2017). On the other hand, a recent study conducted by Gu and colleagues showed that EVs from *L. rhamnosus* GG increased nuclear factor erythroid 2-related factor 2 (Nrf2) expression and, in turn, increased tight junction proteins and antimicrobial peptide Reg3 levels, which is involved in the prevention of *Listeria monocytogenes* and *Salmonella enteritidis* infections (Loonen et al., 2014; Gu et al., 2021). Furthermore, mRNA Reg3 levels increased after incubation of Caco-2 cells with EVs from *L. plantarum* WCFS1 (Li et al., 2017). In an *in vivo* model, the administration of these EVs prolonged the survival of *Caenorhabditis elegans* infected with vancomycin-resistant enterococci. In this line, EV-mediated protection against antimicrobial resistant pathogens could be useful to limit the development of antibiotic resistance that results from the widespread use of antibiotics.

Innate and Adaptive Immunity

As mentioned before, intestinal epithelial cells provide a physical barrier that separates the host from the external environment and form not merely static physical barriers: on the contrary, intestinal epithelial cells engage in a complex dynamic crosstalk between the microbiota and the intestinal immune system (Takiishi et al., 2017). Both bacteria and host-derived EVs are key players of such inter-kingdom crosstalk. There is now an accumulating body of evidence that bacterial EVs regulate the innate and adaptive immune system of the host. Consequently, EVs released by the gut microbiota may have great influence on human health and disease. EVs also carry a set of molecules known as microbe-associated molecular patterns (MAMPs) that are recognized by specific receptors expressed by host epithelial and immune cells. These pattern recognition receptors (PRRs), such as TLR2 and NOD1, are key components of innate immunity and mediate host responses (Lebeer et al., 2010; Díaz-Garrido et al., 2021).

Maintaining the proper balance of immune responses at mucosal surfaces is critical for maintaining homeostasis and successfully clearing pathogens. Epithelial cells have been identified as key players in the development of elaborate immune responses that discriminate between non-pathogenic and pathogenic microorganisms. In this regard, intestinal epithelial cells contribute to delaying and dampening infections by initiating the development of an immune response and attracting immune cells to the infectious site (Pellon et al., 2020). Among intestinal epithelial cells, enterocytes are the most abundant cells and represent approximately 90% of the total number. To study absorption and immune responses there are different *in vitro* models of cell lines: Caco-2, HT-29, and T-84. The remaining 10% of the cells consist of mucus-producing goblet cells, enteroendocrine cells, antimicrobial peptide-producing Paneth cells and others (Jochems et al., 2018).

In vitro and *in vivo* experiments with intestinal epithelial cells have demonstrated that EVs released by *E. coli*, *L. casei*, *L. paracasei*, *P. freudenreichii*, and *L. rhamnosus* can modulate NFκB levels (Cañas et al., 2018; Bäuerl et al., 2020; Choi et al., 2020; Vargoorani et al., 2020; Tong et al., 2021). NF-κB is a family of transcription factors and has an essential role in a variety of aspects related with human health including the development

of both innate and adaptive immunity. EVs from *L. paracasei* and *P. freudenreichii* decreased NF-κB levels in LPS-induced inflammation in HT-29 cell line (Choi et al., 2020; Rodovalho et al., 2020). At the same time, *L. rhamnosus* EVs had the same effect in an *in vivo* model of dextran sulfate sodium-induced colitis in mice (Tong et al., 2021). On the other hand, EVs from *E. coli* and *L. casei* increased NF-κB levels *per se* in Caco-2 and HT-29 cell lines (Cañas et al., 2018; Bäuerl et al., 2020). This opposite modulation of NFκB levels, in the presence or absence of LPS, was also observed for pro-inflammatory cytokines like IL-8 in both Caco-2 and HT-29 cell lines, and in *ex vivo* human colonic explant (Fábrega et al., 2016; Choi et al., 2020; Vargoorani et al., 2020).

On the contrary, in the presence or absence of LPS, *L. casei* and *L. paracasei* EVs always increase the levels of anti-inflammatory cytokines like IL-10. The inhibition of the NF-κB pathway and the increase of IL-10 by EVs have been extensively reported for probiotic bacteria in both *in vitro* and *in vivo* models of infection and/or inflammation (Liu et al., 2017; Bhardwaj et al., 2020). Moreover, Fábrega and colleagues demonstrated in an *in vivo* model of dextran sulfate sodium-induced colitis in mice that *E. coli* Nissle 1917 EVs decreased COX-2 and iNOS mRNA levels that encode important inducible enzymes for the synthesis of prostaglandins and nitric oxide, respectively. This decrease in COX-2 and iNOS levels leads to inflammation and tissue damage, and correlated with the reduced expression of the pro-inflammatory cytokines TNF-and IFN-γ, lower colon inflammation and tissue damage in EV-treated mice (Fábrega et al., 2016, 2017). This evidence suggests that EVs could mediate, at least in part, the beneficial effect of probiotics against infectious diseases.

With regard to immune cells, EVs from different species increase *per se* the levels of pro-inflammatory cytokines like TNF-alpha and IL-6 (Fábrega et al., 2016; Hu et al., 2020; Gu et al., 2021; Morishita et al., 2021) and, at the same time, increase the level of anti-inflammatory cytokines like IL-10 and IL-22 produced by macrophages, DCs and peripheral blood mononuclear cells (PBMC) (López et al., 2012; Al-Nedawi et al., 2015; Fábrega et al., 2016; Hu et al., 2020). In agreement with this effect, it has been reported that different probiotic bacteria stimulate pro-inflammatory and/or anti-inflammatory cytokines in different immune cells (Ren et al., 2016; Cristofori et al., 2021).

Modulation of the immune system by bacterial EVs has also been studied against pathogens in *in vitro* models. EVs from *L. rhamnosus* GG and *L. reuteri* DSM 17938 decreased inflammatory mediators like IFN-γ and IL-17A in *S. aureus*-stimulated human PBMC (Mata Forsberg et al., 2019), while EVs from the probiotic strain *E. coli* Nissle 1917 improved the antibacterial activity of macrophages against three bacterial pathogenic strains of *E. coli*, *S. typhimurium*, and *S. aureus* (Hu et al., 2020).

Regarding macrophage differentiation, *L. plantarum* APsulloc 331261 EVs induced monocyte-to-macrophage transition and polarization to M2b in human THP-1 (Kim et al., 2020). M2b, a subtype of M2 macrophages, has attracted increasing attention due to its strong immunoregulatory and anti-inflammatory effect (Wang et al., 2019). Probiotic bacteria are reported to have a beneficial effect on the host immune status through their ability to modulate macrophage polarization. Some probiotic strains are reported to activate macrophages to M1 phenotype to kill intracellular pathogens, while some other probiotics can induce M2 macrophages to exert an anti-inflammatory effect. Similarly, another strain of the same species (*L. plantarum* CLP-0611) also ameliorated colitis in mice by polarizing M1 to M2-like mouse peritoneal macrophages (Jang et al., 2014).

In line with the anti-inflammatory effects of bacterial EVs, *L. paracasei* and *L. reuteri* BBC3 EVs increased mRNA levels of TGF-β in a model of LPS-induced inflammation in human intestinal epithelial cells (HT-29) and jejunum tissues from chicken (Choi et al., 2020; Hu et al., 2020). TGF-β plays a critical role in the development of Treg cells (Zhao et al., 2017). At the same time, *B. bifidum* LMG13195 and *L. rhamnosus* JB-1 EVs incubation with human DCs induced differentiation to Treg cells and increased IL-10 levels (López et al., 2012), and *L. rhamnosus* EVs increased the number of Treg cells in Peyer's patch from mice (Al-Nedawi et al., 2015). While in some instances Treg cells appear to limit the efficiency of antiviral protective immunity, in other cases they reduce the level of tissue damage caused by a virus infection (Veiga-Parga et al., 2013).

Regarding adaptive immunity, vaccination with engineered EVs from the probiotic strain *E. coli* Nissle 1917 in mice increased the levels of IgG against a recombinant antigen comparable to the "gold standard" adjuvant (alum) (Rosenthal et al., 2014). This strong adjuvant capability of EVs from probiotic strains provides evidence that engineered EVs could be a useful platform for vaccines in humans. On the other hand, it is interesting to note that *L. johnsonii* N6.2 EVs are recognized by IgA and IgG from the plasma of individuals who had consumed the probiotic. In particular, the increase of IgA occurs as a result of a specific response to EV components: Sdp_SH3b2 and Sdp_SH3b6 (Harrison et al., 2021). Although the function of bacterial SH3b domains is not completely known, they are proposed to be cell wall binding domains in prokaryotes. In a previous work, the authors had shown that *L. johnsonii* N6.2 increased circulating levels of IgA (Marcial et al., 2017). Moreover, it has been demonstrated that *L. sakei* EVs enhanced IgA production by murine Peyer's patch cells (Yamasaki-Yashiki et al., 2019). A similar study found that commensal bacteria increase the serum levels of IgA, providing a protective effect against polymicrobial sepsis (Wilmore et al., 2018). Therefore, serum IgA concentrations depend on the interaction with the gut microbiota and these effects could be mediated, at least in part, by EVs.

It is interesting to note that *L. plantarum* KCTC 11401BP EVs decreased IL-6 levels, protected cell viability of human epidermal keratinocytes (HaCaT) incubated with *S. aureus* EVs and reduced skin inflammation in *S. aureus* EV-induced atopic dermatitis in mice (Kim et al., 2018). Moreover, *L. plantarum* EVs increased IL-10 and granulocyte Macrophage Colony-Stimulating Factor (GM-CSF) levels in *ex vivo* human skin cultures (Kim et al., 2020). These findings suggest that oral administration of bacteria could have a preventive effect on skin inflammation and these effects could be mediated by EVs. As mentioned below in Section "Uptake and Transport," *L. rhamnosus* JB-1 EVs appeared in

blood after oral consumption and consequently the presence of EVs in the bloodstream could in part explain the benefit of probiotics in extraintestinal tissues and organs (Stentz et al., 2018; Champagne-Jorgensen et al., 2021a).

Composition

Throughout the years, it has been shown that the supernatant from probiotic bacteria exert beneficial effects in both *in vitro* and *in vivo* models (De Marco et al., 2018; Mantziari et al., 2020). For instance, the culture supernatant from *L. rhamnosus* GG induces resistance to *Escherichia coli* K1 infection by enhancing intestinal defense in neonatal rats (He et al., 2017). In recent years, with the discovery of EVs from probiotics, we can speculate that at least part of these beneficial effects could be mediated by EV components.

As far as we know, there are differences in EV metabolite, nucleic acid and protein content compared with that of the bacterial cell (Briaud and Carroll, 2020). The relative abundance of certain components suggests not only a possible sorting mechanism to package EV cargo, but also a special biological role for EVs (Kim et al., 2018; Huang et al., 2021). For example, EVs from *L. rhamnosus* GG contain high levels of tryptophan metabolites that lead to an improved barrier function (Gu et al., 2021).

In the last few years, "omics" approaches, such as proteomics, transcriptomics and metabolomics, have enabled a comprehensive characterization of probiotics and their EVs, allowing us to gain a deeper understanding of their mechanisms of action (Cunningham et al., 2021). Proteomic analyses showed that EVs from *Lacticaseibacillus* genus (including *L. casei* and *L. rhamnosus* species) contain p40 and p75, two proteins associated with probiotic effects (Domínguez Rubio et al., 2017; Dean et al., 2019; Gu et al., 2021). In particular, p40, when administered in early life, increased TGF-β levels in mice and consequently prevented intestinal inflammation in adulthood (Gu et al., 2021). These proteins, p40 and p75, are able to induce the phosphorylation of the epidermal growth factor receptor (EGFR), and thus have anti-apoptotic effects, as demonstrated in intestinal epithelial cells (Zhang et al., 2020). For p40, this effect was also observed in a murine model of colitis (Yan et al., 2011). EGFR activation can also be triggered by *L. casei* EVs, which expose p40 and p75 at the surface (Bäuerl et al., 2020). Intriguingly, EVs from *L. rhamnosus* GG were shown to have apoptotic effects in hepatic cancer cells by the intrinsic pathway of apoptosis (Behzadi et al., 2017). Therefore, apoptotic effects seem to depend on the dose of EVs and on the model used. On the other hand, p40 and p75 were able to prevent the disruption of tight junctions by protein kinase C (PKC)-dependent mechanisms in Caco-2 cell monolayers (Seth et al., 2008). Anti-apoptotic effects and protection of tight junctions in intestinal epithelial cells are related to an enhancement of intestinal epithelial integrity, a key factor in the maintenance of barrier function, the first line of defense. On the other hand, p40 was proven to increase IgA levels. As mentioned in Section "Innate and Adaptive Immunity," IgA further contributes to the protection of the host against infections (Ho et al., 2016; Wang and Jeffery, 2016).

It has been shown that EVs from probiotics contain proteins that could mediate pathogen inhibition, and in this way could possibly compete with pathogens for colonization in the intestine (Domínguez Rubio et al., 2017; Bajic et al., 2020; Bäuerl et al., 2020; Nishiyama et al., 2020). Proteomic analyses of EVs from three different lactobacilli strains showed that protein composition of EVs can be very different among species (Dean et al., 2019). Interestingly, antimicrobial bacteriocins are enriched in EVs from *L. acidophilus* ATCC 53544. These EVs can fuse with other bacteria and thus may constitute a useful platform for the delivery of antimicrobial compounds (Dean et al., 2020). On the other hand, it would be interesting to investigate the occurrence of moonlighting proteins in EVs. Moonlighting proteins are proteins that have different functions according to their cellular location (Wang and Jeffery, 2016; Jeffery, 2018). For example, glyceraldehyde-3-phosphate dehydrogenase (GAPDH), a well-known cytoplasmic metabolic protein, is exposed at the surface of the bacterial cell and performs adhesion functions. Further analyses are necessary to confirm the localization of these proteins within EVs to better understand their multiple functions.

Indeed, EV composition is relevant to understand their biological function, even in the context of infections. EVs from *L. crispatus* BC3 and *L. gasseri* BC12, but not EVs from other strains, were capable of protecting vaginal tissues from HIV-1 infection *ex vivo*, suggesting virus inhibition was due to the presence of specific components of EVs (Ñahui Palomino et al., 2019). Regarding immunomodulatory effects of EVs from probiotics, EVs from *Propionibacterium freudenreichii* contain surface-layer protein B (SlpB), which effectively mitigated NF-κB activation (Rodovalho et al., 2020).

Lipoteichoic acid (LTA) has been found on the surface of EVs from *L. gasseri* JCM 1131, *L. casei* BL23 and *L. rhamnosus* JB-1 (Shiraishi et al., 2018; Champagne-Jorgensen et al., 2021b). LTA is a ligand for TLR2 in a heterodimer with TLR6, and it seems to induce immune tolerance in intestinal epithelial cells (Lebeer et al., 2010). In agreement with this, EVs from *L. rhamnosus* JB-1 expose LTA, which was responsible for TLR-2 activation and increase of IL-10 production by bone marrow-derived DCs (Champagne-Jorgensen et al., 2021b). LTA from probiotics could play a role in attenuating infections. In this regard, it has been shown that *L. plantarum* LTA inhibits virus-induced inflammatory responses in porcine intestinal epithelial cells and reduced *Enterococcus faecalis* biofilm *in vitro* (Kim et al., 2017, 2020).

As mentioned before, peptidoglycan contained in EVs from Gram (+) and Gram (−) probiotics is also an important factor in the enhancement of innate immunity and the maintenance of intestinal homeostasis (Cañas et al., 2018; Morishita et al., 2021). In fact, EVs from *Bifidobacterium longum*, *Clostridium butyricum*, and *L. plantarum* WCFS1 have been proposed as a novel immunotherapy formulation that would be advantageous over bacterial lysates due to protection from degradation of bioactives within EVs (Morishita et al., 2021).

As aforesaid, EVs from the Gram (−) probiotic strain *E. coli* Nissle 1917 were shown to have a strong adjuvant capability. The authors ascribed this result to LPS, proteins and glycosyl

composition (Rosenthal et al., 2014). The presence of LPS and other MAMPs, such as flagellin and mannose, may be responsible for the strong immune response when applying these EVs as vaccine platforms.

Previous work has established that bacterial EVs contain DNA and RNA (Koeppen et al., 2016; Bitto et al., 2017; Li and Stanton, 2021). Regarding EVs from probiotics, little is known about their nucleic acid cargo. Even though DNA and RNA were found in EVs from *L. reuteri* BBC3 and *L. casei* BL23 (Domínguez Rubio et al., 2017; Hu et al., 2021), the characterization of nucleic acids from probiotics remains to be studied. Small RNA contained in EVs from probiotics might possibly regulate gene expression in host cells, as it is the case for EVs from pathogenic bacteria, and this interaction could have implications in preventing and treating infections (Lee, 2019; Munhoz da Rocha et al., 2020).

Extracellular vesicles from probiotics have shown to contain phage nucleic acids (Domínguez Rubio et al., 2017; Champagne-Jorgensen et al., 2021b; Gu et al., 2021) and phage proteins (Domínguez Rubio et al., 2017; Gu et al., 2021). EVs can even transmit phage receptors to phage-resistant bacteria, which in turn become phage-sensitive (Tzipilevich et al., 2017). Both phage nucleic acid and phage-receptors transmission would lead to a broadened phage host range with potential applications in the treatment of infections (Liu et al., 2018).

Uptake and Transport

The communication between bacteria and the host could in part occur through bacterial EVs and other soluble factors (postbiotics). EVs are able to transport diverse bioactive molecules to host cells and trigger different effects such as the modulation of immune responses. It is generally accepted that, due to their nanosize, bacterial EVs can overcome epithelial barriers and migrate long distances in the human body (Macion et al., 2021). In fact, bacterial EVs have been demonstrated to enter host cells by several routes, including clathrin, caveolin or lipid raft mediated endocytosis, and membrane fusion (O'Donoghue and Krachler, 2016). Even though much research in the last decades has focused on the study of uptake and transport of EVs released by pathogenic bacteria (Bielaszewska et al., 2017; Bitto et al., 2017), few researchers have addressed these issues for EVs released by non-pathogenic bacteria. However, in the last years there has been an increase in research trying to understand the way that EVs from probiotics are internalized by host cells, or even more, transported through the intestinal barrier and delivered to different tissues and organs.

Before being uptaken by intestinal cells, EVs must also diffuse through the mucus layer. In this regard, EVs from *E. coli* Nissle 1917 were able to diffuse through the mucus layer in the mucin-producer HT29-MTX cell line (Cañas et al., 2016). Although there is no direct evidence of EV diffusion through the mucus layer *in vivo*, this event can be assumed from the fact that EVs can reach the bloodstream after oral administration (Champagne-Jorgensen et al., 2021a).

Extracellular vesicles from probiotics were proven to be internalized by intestinal epithelial cells in several studies (Fábrega et al., 2016; Bajic et al., 2020; Domínguez Rubio et al., 2020; Champagne-Jorgensen et al., 2021b). Although there are several routes of entry for EVs from pathogens into epithelial cells, clathrin-mediated endocytosis has been the most widely reported route among EVs from probiotics so far. Inhibitors of clathrin-mediated endocytosis, such as chlorpromazine and the dynamin dynasore, blocked the uptake of EVs by intestinal cells cultivated *in vitro* (Cañas et al., 2016; Bajic et al., 2020; Champagne-Jorgensen et al., 2021b). Additionally, EVs from *L. rhamnosus* JB-1 were shown to be internalized by intestinal epithelial cells in an *in vivo* model within 2 h after oral consumption (Champagne-Jorgensen et al., 2021a). It is likely that EVs are internalized simultaneously by different endocytic pathways depending on their size (El-Sayed and Harashima, 2013).

With respect to intracellular trafficking, colocalization analyses showed that EVs from *E. coli* Nissle 1917 are present in early endosomes and, once inside the cell, EV peptidoglycan interacts with NOD1 that leads to the activation of the immune system (Cañas et al., 2016, 2018; Fernández-García et al., 2021). Moreover, EVs can also fuse with lysosomes (Cañas et al., 2016). On the other hand, it was demonstrated that EVs from a pathogenic *E. coli* strain can deliver toxins to other subcellular compartments including the cytosol, nucleus and mitochondria (Bielaszewska et al., 2017). Bacterial EVs can deliver DNA or RNA to host cells (Bitto et al., 2017; Lécrivain and Beckmann, 2020), and there is evidence that nucleic acid cargo of EVs from pathogens may enter the nucleus of eukaryotic host cells (Blenkiron et al., 2016; Bitto et al., 2017). Furthermore, EVs from pathogens contain small RNA that might regulate gene expression in host cells (Koeppen et al., 2016). Although little studied to date, these mechanisms may be also applicable to EVs from probiotics.

While a portion of EVs may act in intestinal cells, another portion is possibly transported through the intestinal epithelium, either by paracellular or transcellular transport, to finally reach extraintestinal tissues and organs (Jang et al., 2015; Stentz et al., 2018; Jones et al., 2020). Park et al. (2017) revealed EVs from intestinal bacteria reach the bloodstream in a mouse model, where blood EV diversity was directly linked to intestinal microbiota diversity. Regarding probiotics, a proportion of CFSE-labeled EVs from *Bacillus subtilis* were transported through a monolayer of polarized epithelial cells in a transwell system. Transcellular transport resulted in the detection of intact EVs in the lower chamber in 60–120 min (Domínguez Rubio et al., 2020). Alternatively, EVs could possibly be transported through the intestinal epithelium via DCs, goblet cells or M-cells. On the other hand, microbiota EV transport through the epithelium can occur by paracellular transport when the intestinal epithelial barrier integrity is compromised (Chronopoulos and Kalluri, 2020).

The transport of EVs across the intestinal epithelium implies that EVs could reach the lamina propria, where they are able to interact with immune cells. EV uptake by immune cells has been described in a few studies. *In vivo* studies showed that EVs from *L. rhamnosus* JB-1 were uptaken by DCs in the lamina propria (Champagne-Jorgensen et al., 2021b). This internalization was thought to occur via clathrin-mediated endocytosis, as it was prevented by dynasore, even though

phagocytosis cannot be ruled out since dynamin is required for this process. In another study, probiotic-derived EVs were uptaken by mouse macrophage-like and DCs via clathrin-mediated endocytosis and macropinocytosis, as demonstrated in the presence of endocytosis inhibitors (Morishita et al., 2021).

Different studies support EVs distribution and delivery to distal body sites. For example, EVs from *L. rhamnosus* JB-1 were present in the bloodstream of mice fed with the bacteria (Champagne-Jorgensen et al., 2021a), as demonstrated by the detection of DNA from prophages in EVs. What is more, oral administration of EVs from *L. plantarum* reduced skin inflammation in mice with *S. aureus* EV-induced atopic dermatitis (Kim et al., 2018). In humans, microbiota-derived EVs were able to reach urine. In fact, urine-EVs were proposed as a useful assessment method of microbiota profiles (Li et al., 2017). In another study, intraperitoneally injected EVs from *L. plantarum* increased brain-derived neurotrophic factor (BDNF) mRNA levels in the hippocampus of mice and produced antidepressant effects (Choi et al., 2019). This increase in gene expression in the brain suggests that EVs might possibly cross the brain blood barrier. Indeed, EV transport could be one of the reasons why probiotics consumption exerts not only local but also systemic effects, since it is likely that EVs are released by probiotics in the GIT after the consumption of these bacteria.

Other Biological Effects

As it can be inferred from probiotic beneficial effects, modulation of symptoms is one important factor that explains the clinical efficacy of probiotics in the treatment of infectious diseases. It is often observed that EVs mimic the effect of the parent bacteria. For example, *L. reuteri* DSM 17938 clinical efficacy has been demonstrated for the treatment of colic, diarrhea and constipation (Coccorullo et al., 2010; Chau et al., 2015; Dinleyici et al., 2015). Accordingly, EVs from this strain could reproduce the bacteria beneficial effects on gut motility in jejunum and colon explants from mice (West et al., 2020). Therefore, EV release could be one mechanism whereby probiotics mediate their beneficial effects.

In relation to stress and immunity, chronic stress leads to constantly high corticosteroid levels in blood, an impaired immune function, and an increased susceptibility to infections and other health disorders (Bae et al., 2019). At the same time, exposure to stress can cause a decrease in the expression of BDNF in humans, a molecule with antidepressant-like effects (Yang et al., 2015). Some probiotics were shown to be antidepressants in patients and animal models, and even though the gut–brain axis is involved in this effect, the mechanisms of action are not completely understood (Yong et al., 2020). EVs might come into play here. In this regard, EVs from *L. plantarum* KCTC 11401BP counteracted the decreased levels of BDNF mRNA in the hippocampus of corticosteroid treated mice and also blocked the decrease in the levels of BDNF mRNA in corticosteroid post-treated mice, which was further evidenced in mice antidepressant behavior (Choi et al., 2019). If the anti-depressant effects of EVs are proven, they could possibly participate in preventing and/or treating infections given that immune function may be impaired in patients with depression (Andersson et al., 2016).

DISCUSSION

Potential Use of Extracellular Vesicles

The use of EVs as delivery systems could provide several advantages including their nanosize, their biocompatibility in comparison to synthetic drug delivery systems (low toxicity), the ability to cross biological barriers, their ability to protect their cargo from unfavorable environmental conditions (pH, enzymes, oxidative stress) and the possibility of engineering parent cells to modify EV composition (**Figure 3**). There is still a huge gap between basic research and clinical trials as far as bacterial EVs are concerned.

Postbiotics are a novel clinical strategy to consider for the treatment of infections in absence of cells. For example, in diabetic foot ulcers, skin barrier is impaired and thus administration of live bacteria is not a safe approach (Nam et al., 2021). Here is where probiotic-derived EV administration could fall into place and replace probiotic beneficial effects like pathogen inhibition and immunomodulation.

To prevent infectious diseases, only Gram (−) pathogenic bacterial EVs have been used as vaccines up to now, showing to be safe and efficacious on several occasions, while others are under evaluation (Behrens et al., 2021). For example, there are clinically available EV-based vaccines against *Neisseria meningitidis*, a causative agent of meningitis. The development of EV-based vaccines is a promising field for the prevention of infections. However, the isolation of EVs from several pathogenic microorganisms for vaccine design may have limitations. For example, many pathogens like bacteria, fungi and parasites cannot be cultured in the laboratory (Li et al., 2014; Roig et al., 2018). In the case of viruses, which do not produce EVs, cell cultures are necessary for the design of EV-based vaccines (Shehata et al., 2019; Yang et al., 2021). In this line, vaccination with engineered EVs from probiotic bacteria could

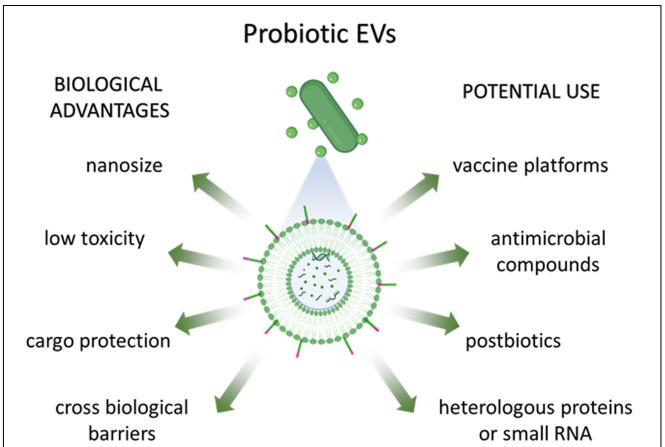

FIGURE 3 | Biological advantages and potential use of probiotic-derived EVs.

be a useful platform to express pathogen antigens to be used as vaccines without toxicity in humans. To our knowledge, *E. coli* Nissle 1917 was the only strain assessed for this application in an animal model (Rosenthal et al., 2014). Further studies comparing Gram (−) and Gram (+) probiotic EVs would be necessary to elucidate whether the presence of certain components like LPS or LTA on the surface is important for the enhancement of the immune response. It is important to highlight that different chemical composition of LPS and LTA induce differential inflammatory responses and this must be taken into account to enhance EV immunogenicity (Migale et al., 2015; Jastrząb et al., 2021).

On the other hand, to treat infectious diseases, genetic engineering could be exploited for pathogen inhibition by increasing the expression of antimicrobial peptides and further encapsulation in EVs (Dean et al., 2020). Bacteriocins are potent small antimicrobial peptides synthesized by certain bacteria that may be appointed as alternatives to traditional antibiotics (Gradisteanu Pircalabioru et al., 2021). Bacteriocins within EVs turn them into potential candidates against infections, including those caused by antimicrobial resistant pathogens. According to WHO, antimicrobial resistance continues to be a global health and development threat (World Health Organization, 2021). Indeed, an important advantage of probiotic administration is the reduction in the use of strong anti-inflammatory agents and/or antibiotics that can be unfavorable in the long term (Kasatpibal et al., 2017; Guo and Leung, 2020; Raheem et al., 2021). In this regard, the indiscriminate use of antimicrobials leads not only to the development of antimicrobial resistance in pathogens, but also to the loss of our microbiota. The latter increases the susceptibility to infections such as vaginal candidiasis (Xu et al., 2008). Administration of probiotic EVs could be used not only to treat and/or prevent infections, but also would decrease antimicrobial use.

By taking advantage of EV versatility, other genetic engineering approaches can be applied to modify EV cargo or surface for the delivery of drugs to target cells. Genetic engineering enables the overexpression of proteins or the synthesis of small RNA that could silence target host genes (Fantappiè et al., 2014; Koeppen et al., 2016). EV cargo could be protected from harsh environmental conditions and additionally surface molecules could direct EVs to target host cells. This strategy could be relevant for the delivery of two or more synergistic drugs and/or the delivery of compounds that have difficulties in crossing the cell membrane (Liu et al., 2018).

Missing Knowledge and Challenges

As documented in several studies, probiotic-derived EVs could be involved in the prevention and treatment of infectious diseases. However, the protective capacity of probiotic bacteria EVs against pathogen infections was only studied against one virus (HIV-1) and a few bacteria (*S. aureus, S. typhimurium* and *E. coli*) (Mata Forsberg et al., 2019; Ñahui Palomino et al., 2019; Hu et al., 2020). Therefore, there is still no information on its beneficial effect against fungal and parasitic infections.

To date, there are many unknowns regarding the use of probiotics EVs as pharmaceutical agents. Current challenges are the lack of standardized and cost-effective methods for EV isolation, purification, characterization and upscale processing (Gurunathan et al., 2021). Unlike human EV markers, specific bacterial EV markers remain mostly unidentified (Ñahui Palomino et al., 2021). Identifying these molecular markers could not only optimize current characterization techniques, but also improve our understanding about EV physiology and future possible biomedical applications. For example, the probiotic *B. subtilis* produced *S. aureus* intestinal decolonization by inhibiting the pathogen quorum-sensing, and thereby produced a general decolonization (including the nose) (Piewngam and Otto, 2020). It would be interesting to study if probiotic EV components can mediate the inhibition of quorum-sensing among pathogenic bacteria. Even more, advances in the understanding of the role of EVs in inter-kingdom communication will almost certainly provide valuable insights into the development of novel therapies against pathogens.

Regarding the use of probiotic bacteria to create engineered EVs with vaccination purposes, the expression of antigenic proteins from non-culturable eukaryotic pathogens (fungi and parasites) has some limitations related to bacterial ability to make post-translational modifications. In this case, expression of antigens in eukaryotic probiotic organisms like yeasts would be a better and low cost option.

One alternative to administering isolated EVs that remains to be evaluated is whether it would be more advantageous to administer functional food with probiotics as a platform for EV delivery. As far as we know, EVs are constantly secreted by metabolically active bacteria (Brown et al., 2015; Liu et al., 2018). In a bacterial culture, EV release can vary depending on the growth conditions, including pH, oxygen presence, and agitation rate (Müller et al., 2021). For example, at pH 5 *L. plantarum* released a smaller number of EVs than at pH 7. On the other hand, there is recent evidence that *L. rhamnosus* JB-1 EVs can reach the bloodstream of mice after oral administration of the probiotic (Champagne-Jorgensen et al., 2021a). This outcome strongly suggests *in situ* EV release in the GIT. Whole cells would resist better than EVs to conditions during storage and transit through the GIT. In the case of spore-producing probiotics (e.g., *B. subtilis*), spore administration would be a cost-effective option. In this way, problems concerning EV stability would be avoided. Another strategy to consider is the microencapsulation of probiotics contained in food matrices to improve their viability during storage and in the GIT (Qi et al., 2020). Besides, if the encapsulating agent is mucoadhesive, a longer residence time in the GIT may allow a sustained release of EVs over time (Yao et al., 2020). Another microparticle-based delivery system could be a particle with coupled EVs on the surface to achieve high concentrations of EVs, maximizing EV effects as demonstrated in *in vitro* models (Kuhn et al., 2020).

CONCLUSION

The new era of postbiotics has brought a new point of view on the beneficial effects of probiotics. Probiotic-derived EVs could be mediating, at least in part, the beneficial effects of

probiotics against infectious diseases via: inhibition of pathogens, enhancement of epithelial barrier function and modulation of the immune system. Remarkably, EVs can reach the bloodstream and consequently be delivered to extraintestinal organs, where probiotics were shown to have beneficial effects. Future studies should be focused on the characterization of EV active components and their interaction with the host. Novel EV-based technologies are promising for the design of therapies and/or vaccines against infections. Moreover, probiotics contained in food matrices could be used as EV-releasing devices in the GIT with potential applications in the functional food industry.

AUTHOR CONTRIBUTIONS

APDR and CLD designed the idea, collected literature data, created the tables and figures, and wrote the manuscript. MP and OP reviewed and approved the final version of the manuscript. All authors contributed to the article and approved the submitted version.

FUNDING

This research was supported by CONICET, Agencia Nacional de Promoción Científica y Tecnológica (PICT 2017-1683) and Universidad de Buenos Aires (UBACyT20020150100079BA to OP and UBACYT 20020170100591BA to MP).

ACKNOWLEDGMENTS

We are grateful to Sergio I. Nemirovsky for his collaboration. All figures were partially created with BioRender.com.

REFERENCES

Agostinis, C., Mangogna, A., Bossi, F., Ricci, G., Kishore, U., and Bulla, R. (2019). Uterine immunity and microbiota: a shifting paradigm. *Front. Immunol.* 10:2387. doi: 10.3389/fimmu.2019.02387

Ahlawat, S., Asha, and Sharma, K. K. (2021). Gut–organ axis: a microbial outreach and networking. *Lett. Appl. Microbiol.* 72, 636–668. doi: 10.1111/lam.13333

Aljutaily, T., Huarte, E., Martinez-Monteagudo, S., Gonzalez-Hernandez, J. L., Rovai, M., and Sergeev, I. N. (2020). Probiotic-enriched milk and dairy products increase gut microbiota diversity: a comparative study. *Nutr. Res.* 82, 25–33. doi: 10.1016/j.nutres.2020.06.017

Al-Nedawi, K., Mian, M. F., Hossain, N., Karimi, K., Mao, Y. K., Forsythe, P., et al. (2015). Gut commensal microvesicles reproduce parent bacterial signals to host immune and enteric nervous systems. *FASEB J.* 29, 684–695. doi: 10.1096/fj.14-259721

Alvarez, C. S., Badia, J., Bosch, M., Giménez, R., and Baldomà, L. (2016). Outer membrane vesicles and soluble factors released by probiotic *Escherichia coli* Nissle 1917 and commensal ECOR63 enhance barrier function by regulating expression of tight junction proteins in intestinal epithelial cells. *Front. Microbiol.* 7:1981. doi: 10.3389/fmicb.2016.01981

Alvarez, C. S., Giménez, R., Cañas, M. A., Vera, R., Díaz-Garrido, N., Badia, J., et al. (2019). Extracellular vesicles and soluble factors secreted by *Escherichia coli* Nissle 1917 and ECOR63 protect against enteropathogenic E. *coli*-induced intestinal epithelial barrier dysfunction. *BMC Microbiol.* 19:166. doi: 10.1186/s12866-019-1534-3

Anaya-Loyola, M. A., Enciso-Moreno, J. A., López-Ramos, J. E., García-Marín, G., Orozco Álvarez, M. Y., Vega-García, A. M., et al. (2019). *Bacillus coagulans* GBI-30, 6068 decreases upper respiratory and gastrointestinal tract symptoms in healthy Mexican scholar-aged children by modulating immune-related proteins. *Food Res. Int.* 125:108567. doi: 10.1016/j.foodres.2019.108567

Andersson, N. W., Goodwin, R. D., Okkels, N., Gustafsson, L. N., Taha, F., Cole, S. W., et al. (2016). Depression and the risk of severe infections: prospective analyses on a nationwide representative sample. *Int. J. Epidemiol.* 45, 131–139. doi: 10.1093/ije/dyv333

Aryayev, M. L., Senkivska, L. I., Bredeleva, N. K., and Talashova, I. V. (2018). Prophylaxis of acute respiratory infections via improving the immune system in late preterm newborns with E. coli strain Nissle 1917: a controlled pilot trial. *Pilot Feasibility Stud.* 4:79. doi: 10.1186/s40814-018-0271-y

Bae, Y. S., Shin, E. C., Bae, Y. S., and Van Eden, W. (2019). Editorial: stress and immunity. *Front. Immunol.* 10:245. doi: 10.3389/fimmu.2019.00245

Bajic, S. S., Cañas, M. A., Tolinacki, M., Badia, J., Sánchez, B., Golic, N., et al. (2020). Proteomic profile of extracellular vesicles released by *Lactiplantibacillus plantarum* BGAN8 and their internalization by non-polarized HT29 cell line. *Sci. Rep.* 10:21829. doi: 10.1038/s41598-020-78920-z

Banfi, D., Moro, E., Bosi, A., Bistoletti, M., Cerantola, S., Crema, F., et al. (2021). Impact of microbial metabolites on microbiota–gut–brain axis in inflammatory bowel disease. *Int. J. Mol. Sci.* 22:1623. doi: 10.3390/ijms22041623

Barbara, G., Barbaro, M. R., Fuschi, D., Palombo, M., Falangone, F., Cremon, C., et al. (2021). Inflammatory and microbiota-related regulation of the intestinal epithelial barrier. *Front. Nutr.* 8:718356. doi: 10.3389/fnut.2021.718356

Bäuerl, C., Coll-Marqués, J. M., Tarazona-González, C., and Pérez-Martínez, G. (2020). *Lactobacillus casei* extracellular vesicles stimulate EGFR pathway likely due to the presence of proteins P40 and P75 bound to their surface. *Sci. Rep.* 10:19237. doi: 10.1038/s41598-020-75930-9

Behrens, F., Funk-Hilsdorf, T. C., Kuebler, W. M., and Simmons, S. (2021). Bacterial membrane vesicles in pneumonia: from mediators of virulence to innovative vaccine candidates. *Int. J. Mol. Sci.* 22:3858. doi: 10.3390/ijms22083858

Behzadi, E., Mahmoodzadeh Hosseini, H., and Imani Fooladi, A. A. (2017). The inhibitory impacts of *Lactobacillus rhamnosus* GG-derived extracellular vesicles on the growth of hepatic cancer cells. *Microb. Pathog.* 110, 1–6. doi: 10.1016/j.micpath.2017.06.016

Bhardwaj, R., Singh, B. P., Sandhu, N., Singh, N., Kaur, R., Rokana, N., et al. (2020). Probiotic mediated NF-κB regulation for prospective management of type 2 diabetes. *Mol. Biol. Rep.* 47, 2301–2313. doi: 10.1007/s11033-020-05254-4

Bielaszewska, M., Rüter, C., Bauwens, A., Greune, L., Jarosch, K. A., Steil, D., et al. (2017). Host cell interactions of outer membrane vesicle-associated virulence factors of enterohemorrhagic *Escherichia coli* O157: intracellular delivery, trafficking and mechanisms of cell injury. *PLoS Pathog.* 13:e1006159. doi: 10.1371/journal.ppat.1006159

Binda, S., Hill, C., Johansen, E., Obis, D., Pot, B., Sanders, M. E., et al. (2020). Criteria to qualify microorganisms as "probiotic" in foods and dietary supplements. *Front. Microbiol.* 11:1662. doi: 10.3389/fmicb.2020.01662

Bitto, N. J., Chapman, R., Pidot, S., Costin, A., Lo, C., Choi, J., et al. (2017). Bacterial membrane vesicles transport their DNA cargo into host cells. *Sci. Rep.* 7:7072. doi: 10.1038/s41598-017-07288-4

Blenkiron, C., Simonov, D., Muthukaruppan, A., Tsai, P., Dauros, P., Green, S., et al. (2016). Uropathogenic *Escherichia coli* releases extracellular vesicles that are associated with RNA. *PLoS One* 11:e0160440. doi: 10.1371/journal.pone.0160440

Briaud, P., and Carroll, R. K. (2020). Extracellular vesicle biogenesis and functions in gram-positive bacteria. *Infect. Immun.* 88:e00433-20. doi: 10.1128/IAI.00433-20

Brown, L., Wolf, J. M., Prados-Rosales, R., and Casadevall, A. (2015). Through the wall: extracellular vesicles in Gram-positive bacteria, mycobacteria and fungi. *Nat. Rev. Microbiol.* 13, 620–630. doi: 10.1038/nrmicro3480

Cañas, M. A., Fábrega, M. J., Giménez, R., Badia, J., and Baldomà, L. (2018). Outer membrane vesicles from probiotic and commensal *escherichia coli* activate NOD1-mediated immune responses in intestinal epithelial cells. *Front. Microbiol.* 9:498. doi: 10.3389/fmicb.2018.00498

Cañas, M. A., Giménez, R., Fábrega, M. J., Toloza, L., Baldomà, L., and Badia, J. (2016). Outer membrane vesicles from the probiotic *Escherichia coli* Nissle 1917 and the commensal ECOR12 enter intestinal epithelial cells via clathrin-dependent endocytosis and elicit differential effects on DNA damage. *PLoS One* 11:e0160374. doi: 10.1371/journal.pone.0160374

Cao, E. Y., and Mortha, A. (2020). "Eukaryome: emerging field with profound translational potential," in *Eukaryome Impact on Human Intestine Homeostasis and Mucosal Immunology*, ed. N. Gullen (Cham: Springer). doi: 10.1007/978-3-030-44826-4

Champagne-Jorgensen, K., Jose, T. A., Stanisz, A. M., Mian, M. F., Hynes, A. P., and Bienenstock, J. (2021a). Bacterial membrane vesicles and phages in blood after consumption of *Lacticaseibacillus rhamnosus* JB-1. *Gut Microbes* 13:1993583. doi: 10.1080/19490976.2021.1993583

Champagne-Jorgensen, K., Mian, M. F., McVey Neufeld, K. A., Stanisz, A. M., and Bienenstock, J. (2021b). Membrane vesicles of *Lacticaseibacillus rhamnosus* JB-1 contain immunomodulatory lipoteichoic acid and are endocytosed by intestinal epithelial cells. *Sci. Rep.* 11:13756. doi: 10.1038/s41598-021-93311-8

Chang, H. Y., Chen, J. H., Chang, J. H., Lin, H. C., Lin, C. Y., and Peng, C. C. (2017). Multiple strains probiotics appear to be the most effective probiotics in the prevention of necrotizing *Enterocolitis* and mortality: an updated meta-analysis. *PLoS One* 12:e0171579. doi: 10.1371/journal.pone.0171579

Chau, K., Lau, E., Greenberg, S., Jacobson, S., Yazdani-Brojeni, P., Verma, N., et al. (2015). Probiotics for infantile colic: a randomized, double-blind, placebo-controlled trial investigating *Lactobacillus reuteri* DSM 17938. *J. Pediatr.* 166, 74–78.e1. doi: 10.1016/j.jpeds.2014.09.020

Chee, W. J. Y., Chew, S. Y., and Than, L. T. L. (2020). Vaginal microbiota and the potential of *Lactobacillus* derivatives in maintaining vaginal health. *Microb. Cell Fact.* 19, 1–24. doi: 10.1186/s12934-020-01464-4

Choi, J. H., Mo Moon, C., Shin, T.-S., Kim, E. K., Mcdowell, A., Jo, M.-K., et al. (2020). Experimental & Molecular Medicine *Lactobacillus paracasei*-derived extracellular vesicles attenuate the intestinal inflammatory response by augmenting the endoplasmic reticulum stress pathway. *Exp. Mol. Med.* 52, 423–437. doi: 10.1038/s12276-019-0359-3

Choi, J., Kim, Y. K., and Han, P. L. (2019). Extracellular vesicles derived from *Lactobacillus plantarum* increase BDNF expression in cultured hippocampal neurons and produce antidepressant-like effects in mice. *Exp. Neurobiol.* 28, 158–171. doi: 10.5607/en.2019.28.2.158

Chronopoulos, A., and Kalluri, R. (2020). Emerging role of bacterial extracellular vesicles in cancer. *Oncogene* 39, 6951–6960. doi: 10.1038/s41388-020-01509-3

Coccorullo, P., Strisciuglio, C., Martinelli, M., Miele, E., Greco, L., and Staiano, A. (2010). *Lactobacillus reuteri* (DSM 17938) in infants with functional chronic constipation: a double-blind, randomized, placebo-controlled study. *J. Pediatr.* 157, 598–602. doi: 10.1016/j.jpeds.2010.04.066

Collado, M. C., Vinderola, G., and Salminen, S. (2019). Postbiotics: facts and open questions. A position paper on the need for a consensus definition. *Benef. Microbes* 10, 711–719. doi: 10.3920/BM2019.0015

Cristofori, F., Dargenio, V. N., Dargenio, C., Miniello, V. L., Barone, M., and Francavilla, R. (2021). Anti-inflammatory and immunomodulatory effects of probiotics in gut inflammation: a door to the body. *Front. Immunol.* 12:578386. doi: 10.3389/fimmu.2021.578386

Cui, Y., Luo, L., Wang, X., Lu, Y., Yi, Y., Shan, Y., et al. (2021). Mining, heterologous expression, purification, antibactericidal mechanism, and application of bacteriocins: a review. *Compr. Rev. Food Sci. Food Saf.* 20, 863–899. doi: 10.1111/1541-4337.12658

Cunningham, M., Azcarate-Peril, M. A., Barnard, A., Benoit, V., Grimaldi, R., Guyonnet, D., et al. (2021). Shaping the future of probiotics and prebiotics. *Trends Microbiol.* 29, 667–685. doi: 10.1016/j.tim.2021.01.003

De Marco, S., Sichetti, M., Muradyan, D., Piccioni, M., Traina, G., Pagiotti, R., et al. (2018). Probiotic cell-free supernatants exhibited anti-inflammatory and antioxidant activity on human gut epithelial cells and macrophages stimulated with LPS. *Evid. Based Complement. Alternat. Med.* 2018:1756308. doi: 10.1155/2018/1756308

de Melo Pereira, G. V., de Oliveira Coelho, B., Magalhães Júnior, A. I., Thomaz-Soccol, V., and Soccol, C. R. (2018). How to select a probiotic? A review and update of methods and criteria. *Biotechnol. Adv.* 36, 2060–2076. doi: 10.1016/j.biotechadv.2018.09.003

Dean, S. N., Leary, D. H., Sullivan, C. J., Oh, E., and Walper, S. A. (2019). Isolation and characterization of *Lactobacillus*-derived membrane vesicles. *Sci. Rep.* 9:877. doi: 10.1038/s41598-018-37120-6

Dean, S. N., Rimmer, M. A., Turner, K. B., Phillips, D. A., Caruana, J. C., Hervey, W. J., et al. (2020). *Lactobacillus acidophilus* membrane vesicles as a vehicle of bacteriocin delivery. *Front. Microbiol.* 11:710. doi: 10.3389/fmicb.2020.00710

Demmelmair, H., Jiménez, E., Collado, M. C., Salminen, S., and McGuire, M. K. (2020). Maternal and perinatal factors associated with the human milk microbiome. *Curr. Dev. Nutr.* 4, 1–14. doi: 10.1093/cdn/nzaa027

Díaz-Garrido, N., Badia, J., and Baldomà, L. (2021). Microbiota-derived extracellular vesicles in interkingdom communication in the gut. *J. Extracell. Vesicles* 10:e12161. doi: 10.1002/jev2.12161

Dicks, L. M. T., and Grobbelaar, M. J. (2021). Double-barrel shotgun: probiotic lactic acid bacteria with antiviral properties modified to serve as vaccines. *Microorganisms* 9:1565. doi: 10.3390/microorganisms9081565

Ding, R., Goh, W. R., Wu, R., Yue, X., Luo, X., Khine, W. W. T., et al. (2019). Revisit gut microbiota and its impact on human health and disease. *J. Food Drug Anal.* 27, 623–631. doi: 10.1016/j.jfda.2018.12.012

Dinleyici, E. C., Dalgic, N., Guven, S., Metin, O., Yasa, O., Kurugol, Z., et al. (2015). *Lactobacillus reuteri* DSM 17938 shortens acute infectious diarrhea in a pediatric outpatient setting. *J. Pediatr. (Rio. J.)* 91, 392–396. doi: 10.1016/j.jped.2014.10.009

Domínguez Rubio, A. P., Martínez, J. H., Casillas, D. C. M., Leskow, F. C., Piuri, M., and Pérez, O. E. (2017). *Lactobacillus casei* BL23 produces microvesicles carrying proteins that have been associated with its probiotic effect. *Front. Microbiol.* 8:1783. doi: 10.3389/fmicb.2017.01783

Domínguez Rubio, A. P., Martínez, J., Palavecino, M., Fuentes, F., López, C. M. S., Marcilla, A., et al. (2020). Transcytosis of *Bacillus subtilis* extracellular vesicles through an in vitro intestinal epithelial cell model. *Sci. Rep.* 10:3120. doi: 10.1038/s41598-020-60077-4

El-Sayed, A., and Harashima, H. (2013). Endocytosis of gene delivery vectors: from clathrin-dependent to lipid raft-mediated endocytosis. *Mol. Ther.* 21, 1118–1130. doi: 10.1038/mt.2013.54

Fábrega, M. J., Aguilera, L., Giménez, R., Varela, E., Cañas, M. A., Antolín, M., et al. (2016). Activation of immune and defense responses in the intestinal mucosa by outer membrane vesicles of commensal and probiotic *Escherichia coli* strains. *Front. Microbiol.* 7:705. doi: 10.3389/fmicb.2016.00705

Fábrega, M. J., Rodríguez-Nogales, A., Garrido-Mesa, J., Algieri, F., Badía, J., Giménez, R., et al. (2017). Intestinal anti-inflammatory effects of outer membrane vesicles from *Escherichia coli* Nissle 1917 in DSS-experimental colitis in mice. *Front. Microbiol.* 8:1274. doi: 10.3389/fmicb.2017.01274

Fantappiè, L., de Santis, M., Chiarot, E., Carboni, F., Bensi, G., Jousson, O., et al. (2014). Antibody-mediated immunity induced by engineered *Escherichia coli* OMVs carrying heterologous antigens in their lumen. *J. Extracell. Vesicles* 3, 24015. doi: 10.3402/jev.v3.24015

FAO/WHO (2002). *Guidelines for the Evaluation of Probiotics in Food. Working Gr, 1–11. Working Group Report on Drafting Guidelines for the Evaluation of Probiotics in Food*. Geneva: World Health Organization.

Fernández-García, V., González-Ramos, S., Martín-Sanz, P., del Portillo, F. G., Laparra, J. M., and Boscá, L. (2021). NOD1 in the interplay between microbiota and gastrointestinal immune adaptations. *Pharmacol. Res.* 171:105775. doi: 10.1016/j.phrs.2021.105775

Fleming, D., Kesey, J., Rumbaugh, K., and Dissanaike, S. (2016). Comparing the survivability of *Lactobacillus* species in various probiotic delivery vehicles. *JPEN J. Parenter. Enteral Nutr.* 41, 1411–1413. doi: 10.1177/0148607116672266

Francavilla, R., Lionetti, E., Castellaneta, S., Ciruzzi, F., Indrio, F., Masciale, A., et al. (2012). Randomised clinical trial: *Lactobacillus reuteri* DSM 17938 vs. placebo in children with acute diarrhoea-a double-blind study. *Aliment. Pharmacol. Ther. Randomised* 36, 363–369. doi: 10.1111/j.1365-2036.2012.05180.x

Fusco, A., Savio, V., Donniacuo, M., Perfetto, B., and Donnarumma, G. (2021). Antimicrobial peptides human beta-defensin-2 and -3 protect the gut during *Candida albicans* infections enhancing the intestinal barrier integrity: in vitro study. *Front. Cell. Infect. Microbiol.* 11:666900. doi: 10.3389/fcimb.2021.666900

Gareau, M. G., Sherman, P. M., and Walker, W. A. (2010). Probiotics and the gut microbiota in intestinal health and disease. *Nat. Rev. Gastroenterol. Hepatol.* 7, 503–514. doi: 10.1038/nrgastro.2010.117

Gaspar, C., Donders, G. G., Palmeira-de-Oliveira, R., Queiroz, J. A., Tomaz, C., Martinez-de-Oliveira, J., et al. (2018). Bacteriocin production of the probiotic *Lactobacillus acidophilus* KS400. *AMB Express* 8:153. doi: 10.1186/s13568-018-0679-z

Ghosh, T., Beniwal, A., Semwal, A., and Navani, N. K. (2019). Mechanistic insights into probiotic properties of lactic acid bacteria associated with ethnic fermented dairy products. *Front. Microbiol.* 10:502. doi: 10.3389/fmicb.2019.00502

Gradisteanu Pircalabioru, G., Popa, L. I., Marutescu, L., Gheorghe, I., Popa, M., Czobor Barbu, I., et al. (2021). Bacteriocins in the era of antibiotic resistance: rising to the challenge. *Pharmaceutics* 13, 1–15. doi: 10.3390/pharmaceutics13020196

Grand View Research (2021). *Probiotics Dietary Supplements Market Size, Share & Trends Analysis Report*. Available online at: https://www.researchandmarkets.com/reports/3972861/probiotics-market-size-share-and-trends-analysis (accessed February 2, 2022).

Gu, Z., Li, F., Liu, Y., Jiang, M., Zhang, L., He, L., et al. (2021). Exosome-like nanoparticles from *Lactobacillus rhamnosus* GG protect against alcohol-associated liver disease through intestinal aryl hydrocarbon receptor in mice. *Hepatol. Commun.* 5, 846–864. doi: 10.1002/hep4.1679

Guo, C. G., and Leung, W. K. (2020). Potential strategies in the prevention of nonsteroidal anti-inflammatory drugs-associated adverse effects in the lower gastrointestinal tract. *Gut Liver* 14, 179–187. doi: 10.5009/gnl19201

Gurunathan, S., Kang, M. H., Qasim, M., Khan, K., and Kim, J. H. (2021). Biogenesis, membrane trafficking, functions, and next generation nanotherapeutics medicine of extracellular vesicles. *Int. J. Nanomedicine* 16, 3357–3383. doi: 10.2147/IJN.S310357

Hansson, G. C. (2020). Mucins and the microbiome. *Annu. Rev. Biochem.* 89, 769–793. doi: 10.1146/annurev-biochem-011520-105053

Harrison, N. A., Gardner, C. L., da Silva, D. R., Gonzalez, C. F., and Lorca, G. L. (2021). Identification of biomarkers for systemic distribution of nanovesicles from *Lactobacillus johnsonii* N6.2. *Front. Immunol.* 12:723433. doi: 10.3389/fimmu.2021.723433

Hassan, M. U., Nayab, H., Rehman, T. U., Williamson, M. P., Haq, K. U., Shafi, N., et al. (2020). Characterisation of bacteriocins produced by *Lactobacillus* spp. isolated from the traditional Pakistani yoghurt and their antimicrobial activity against common foodborne pathogens. *Biomed Res. Int.* 2020:8281623. doi: 10.1155/2020/8281623

He, X., Zeng, Q., Puthiyakunnon, S., Zeng, Z., Yang, W., Qiu, J., et al. (2017). *Lactobacillus rhamnosus* GG supernatant enhance neonatal resistance to systemic *Escherichia coli* K1 infection by accelerating development of intestinal defense. *Sci. Rep.* 7:43305. doi: 10.1038/srep43305

Higgins, J., Thomas, J., Chandler, J., Cumpston, M., Li, T., Page, M., et al. (2019). *Cochrane Handbook for Systematic Reviews of Interventions*, Second Edn. Hoboken, NJ: John Wiley & Sons.

Hill, C., Guarner, F., Reid, G., Gibson, G. R., Merenstein, D. J., Pot, B., et al. (2014). The International Scientific Association for Probiotics and Prebiotics consensus statement on the scope and appropriate use of the term probiotic. *Nat. Rev. Gastroenterol. Hepatol.* 11, 506–514. doi: 10.1038/nrgastro.2014.66

Hills, R. D., Pontefract, B. A., Mishcon, H. R., Black, C. A., Sutton, S. C., and Theberge, C. R. (2019). Gut microbiome: profound implications for diet and disease. *Nutrients* 11, 1–40. doi: 10.3390/nu11071613

Ho, M., Chang, Y. Y., Chang, W. C., Lin, H. C., Wang, M. H., Lin, W. C., et al. (2016). Oral *Lactobacillus rhamnosus* GR-1 and *Lactobacillus reuteri* RC-14 to reduce Group B *Streptococcus* colonization in pregnant women: a randomized controlled trial. *Taiwan. J. Obstet. Gynecol.* 55, 515–518. doi: 10.1016/j.tjog.2016.06.003

Hu, R., Lin, H., Li, J., Zhao, Y., Wang, M., Sun, X., et al. (2020). Probiotic *Escherichia coli* Nissle 1917-derived outer membrane vesicles enhance immunomodulation and antimicrobial activity in RAW264.7 macrophages. *BMC Microbiol.* 20:268. doi: 10.1186/s12866-020-01953-x

Hu, R., Lin, H., Wang, M., Zhao, Y., Liu, H., Min, Y., et al. (2021). *Lactobacillus reuteri*-derived extracellular vesicles maintain intestinal immune homeostasis against lipopolysaccharide-induced inflammatory responses in broilers. *J. Anim. Sci. Biotechnol.* 12, 1–18. doi: 10.1186/s40104-020-00532-4

Huang, F., Teng, K., Liu, Y., Cao, Y., Wang, T., Ma, C., et al. (2021). Bacteriocins: potential for human health. *Oxid. Med. Cell. Longev.* 2021:5518825. doi: 10.1155/2021/5518825

Invernici, M. M., Salvador, S. L., Silva, P. H. F., Soares, M. S. M., Casarin, R., Palioto, D. B., et al. (2018). Effects of *Bifidobacterium* probiotic on the treatment of chronic periodontitis: a randomized clinical trial. *J. Clin. Periodontol.* 45, 1198–1210. doi: 10.1111/jcpe.12995

Invernizzi, R., Lloyd, C. M., and Molyneaux, P. L. (2020). Respiratory microbiome and epithelial interactions shape immunity in the lungs. *Immunology* 160, 171–182. doi: 10.1111/imm.13195

Jang, S. C., Kim, S. R., Yoon, Y. J., Park, K. S., Kim, J. H., Lee, J., et al. (2015). In vivo kinetic biodistribution of nano-sized outer membrane vesicles derived from bacteria. *Small* 11, 456–461. doi: 10.1002/smll.201401803

Jang, S. E., Han, M. J., Kim, S. Y., and Kim, D. H. (2014). *Lactobacillus plantarum* CLP-0611 ameliorates colitis in mice by polarizing M1 to M2-like macrophages. *Int. Immunopharmacol.* 21, 186–192. doi: 10.1016/j.intimp.2014.04.021

Jastrząb, R., Graczyk, D., and Siedlecki, P. (2021). Molecular and cellular mechanisms influenced by postbiotics. *Int. J. Mol. Sci.* 22:13475. doi: 10.3390/ijms222413475

Jeffery, C. (2018). Intracellular proteins moonlighting as bacterial adhesion factors. *AIMS Microbiol.* 4, 362–376. doi: 10.3934/microbiol.2018.2.362

Jochems, P. G. M., Garssen, J., Van Keulen, A. M., Masereeuw, R., and Jeurink, P. V. (2018). Evaluating human intestinal cell lines for studying dietary protein absorption. *Nutrients* 10, 1–15. doi: 10.3390/nu10030322

Jones, E. J., Booth, C., Fonseca, S., Parker, A., Cross, K., Miquel-Clopés, A., et al. (2020). The uptake, trafficking, and Biodistribution of *Bacteroides* thetaiotaomicron generated outer membrane vesicles. *Front. Microbiol.* 11:57. doi: 10.3389/fmicb.2020.00057

Joseph, R. J., Ser, H. L., Kuai, Y. H., Tan, L. T. H., Arasoo, V. J. T., Letchumanan, V., et al. (2021). Finding a balance in the vaginal microbiome: how do we treat and prevent the occurrence of bacterial vaginosis? *Antibiotics* 10, 1–39. doi: 10.3390/antibiotics10060719

Kaparakis-Liaskos, M., and Kufer, T. A. (2020). in *Bacterial Membrane Vesicles Biogenesis, Functions and Applications*, eds M. Kaparakis-Liaskos and T. A. Kufer, Cham: Springer. doi: 10.1007/978-3-030-36331-4_4

Kasatpibal, N., Whitney, J. D., Saokaew, S., Kengkla, K., Heitkemper, M. M., and Apisarnthanarak, A. (2017). Effectiveness of probiotic, prebiotic, and synbiotic therapies in reducing postoperative complications: a systematic review and network meta-analysis. *Clin. Infect. Dis.* 64, S153–S160. doi: 10.1093/cid/cix114

Kim, K. W., Kang, S. S., Woo, S. J., Park, O. J., Ahn, K. B., Song, K. D., et al. (2017). Lipoteichoic acid of probiotic *Lactobacillus plantarum* attenuates poly I: C-induced IL-8 production in porcine intestinal epithelial cells. *Front. Microbiol.* 8:1827. doi: 10.3389/fmicb.2017.01827

Kim, M. H., Choi, S. J., Choi, H. I., Choi, J. P., Park, H. K., Kim, E. K., et al. (2018). *Lactobacillus plantarum*-derived extracellular vesicles protect atopic dermatitis induced by *Staphylococcus aureus*-derived Extracellular Vesicles. *Allergy Asthma Immunol. Res.* 10, 516–532. doi: 10.4168/aair.2018.10.5.516

Kim, W., Lee, E. J., Bae, I. H., Myoung, K., Kim, S. T., Park, P. J., et al. (2020). *Lactobacillus plantarum*-derived extracellular vesicles induce anti-inflammatory M2 macrophage polarization in vitro. *J. Extracell. Vesicles* 9, 314–319. doi: 10.1080/20013078.2020.1793514

Koeppen, K., Hampton, T. H., Jarek, M., Scharfe, M., Gerber, S. A., Mielcarz, D. W., et al. (2016). A novel mechanism of host-pathogen interaction through sRNA in bacterial outer membrane vesicles. *PLoS Pathog.* 12:e1005672. doi: 10.1371/journal.ppat.1005672

König, J., Wells, J., Cani, P. D., García-Ródenas, C. L., MacDonald, T., Mercenier, A., et al. (2016). Human intestinal barrier function in health and disease. *Clin. Transl. Gastroenterol.* 7:e196. doi: 10.1038/ctg.2016.54

Kotzampassi, K., Stavrou, G., Damoraki, G., Georgitsi, M., Basdanis, G., Tsaousi, G., et al. (2015). A four-probiotics regimen reduces postoperative complications after colorectal surgery: a randomized, double-blind, placebo-controlled study. *World J. Surg.* 39, 2776–2783. doi: 10.1007/s00268-015-3071-z

Kuhn, T., Koch, M., and Fuhrmann, G. (2020). Probiomimetics—novel *Lactobacillus* -mimicking microparticles show anti-inflammatory and barrier-protecting effects in gastrointestinal models. *Small* 16:2003158. doi: 10.1002/smll.202003158

Laue, C., Papazova, E., Liesegang, A., Pannenbeckers, A., Arendarski, P., Linnerth, B., et al. (2018). Effect of a yoghurt drink containing *Lactobacillus* strains on bacterial vaginosis in women - a double-blind, randomised, controlled clinical pilot trial. *Benef. Microbes* 9, 35–50. doi: 10.3920/BM2017.0018

Lazou Ahrén, I., Hillman, M., Arvidsson Nordström, E., Larsson, N., and Martinsson Niskanen, T. (2021). Fewer community-acquired colds with daily consumption of *Lactiplantibacillus plantarum* HEAL9 and *Lacticaseibacillus paracasei* 8700:2. A randomized, placebo-controlled clinical trial. *J. Nutr. Nutr. Immunol.* 151, 214–222. doi: 10.1093/jn/nxaa353

Lebeer, S., Vanderleyden, J., and De Keersmaecker, S. C. J. (2010). Host interactions of probiotic bacterial surface molecules: comparison with commensals and pathogens. *Nat. Rev. Microbiol.* 8, 171–184. doi: 10.1038/nrmicro2297

Lécrivain, A. L., and Beckmann, B. M. (2020). Bacterial RNA in extracellular vesicles: a new regulator of host-pathogen interactions? *Biochim. Biophys. Acta Gene Regul. Mech.* 1863:194519. doi: 10.1016/j.bbagrm.2020.194519

Lee, H. J. (2019). Microbe-host communication by small RNAs in extracellular vesicles: vehicles for transkingdom RNA transportation. *Int. J. Mol. Sci.* 20:1487. doi: 10.3390/ijms20061487

Lener, T., Gimona, M., Aigner, L., Börger, V., Buzas, E., Camussi, G., et al. (2015). Applying extracellular vesicles based therapeutics in clinical trials – an ISEV position paper. *J. Extracell. Vesicles* 4:30087. doi: 10.3402/jev.v4.30087

Li, L., Mendis, N., Trigui, H., Oliver, J. D., and Faucher, S. P. (2014). The importance of the viable but non-culturable state in human bacterial pathogens. *Front. Microbiol.* 5:258. doi: 10.3389/fmicb.2014.00258

Li, M., Lee, K., Hsu, M., Nau, G., Mylonakis, E., and Ramratnam, B. (2017). *Lactobacillus*-derived extracellular vesicles enhance host immune responses against vancomycin-resistant enterococci. *BMC Microbiol.* 17:66. doi: 10.1186/s12866-017-0977-7

Li, Z., and Stanton, B. A. (2021). Transfer RNA-derived fragments, the underappreciated regulatory small RNAs in microbial pathogenesis. *Front. Microbiol.* 12:687632. doi: 10.3389/fmicb.2021.687632

Liu, Q., Yu, Z., Tian, F., Zhao, J., Zhang, H., Zhai, Q., et al. (2020). Surface components and metabolites of probiotics for regulation of intestinal epithelial barrier. *Microb. Cell Fact.* 19:23. doi: 10.1186/s12934-020-1289-4

Liu, T., Zhang, L., Joo, D., and Sun, S. C. (2017). NF-κB signaling in inflammation. *Signal Transduct. Target. Ther.* 2:17023. doi: 10.1038/sigtrans.2017.23

Liu, Y., Defourny, K. A. Y., Smid, E. J., and Abee, T. (2018). Gram-positive bacterial extracellular vesicles and their impact on health and disease. *Front. Microbiol.* 9:1502. doi: 10.3389/fmicb.2018.01502

Loonen, L. M., Stolte, E. H., Jaklofsky, M. T., Meijerink, M., Dekker, J., van Baarlen, P., et al. (2014). REG3γ-deficient mice have altered mucus distribution and increased mucosal inflammatory responses to the microbiota and enteric pathogens in the ileum. *Mucosal Immunol.* 7, 939–947. doi: 10.1038/mi.2013.109

Lopes, E. G., Moreira, D. A., Gullón, P., Gullón, B., Cardelle-Cobas, A., and Tavaria, F. K. (2017). Topical application of probiotics in skin: adhesion, antimicrobial and antibiofilm in vitro assays. *J. Appl. Microbiol.* 122, 450–461. doi: 10.1111/jam.13349

López, P., González-Rodríguez, I., Sánchez, B., Gueimonde, M., Margolles, A., and Suárez, A. (2012). Treg-inducing membrane vesicles from *Bifidobacterium bifidum* LMG13195 as potential adjuvants in immunotherapy. *Vaccine* 30, 825–829. doi: 10.1016/j.vaccine.2011.11.115

Macion, A., Wyszyńska, A., and Godlewska, R. (2021). Delivery of toxins and effectors by bacterial membrane vesicles. *Toxins (Basel)* 13:845. doi: 10.3390/toxins13120845

Maguire, M., and Maguire, G. (2019). Gut dysbiosis, leaky gut, and intestinal epithelial proliferation in neurological disorders: towards the development of a new therapeutic using amino acids, prebiotics, probiotics, and postbiotics. *Rev. Neurosci.* 30, 179–201. doi: 10.1515/revneuro-2018-0024

Maldonado-Lobón, J. A., Díaz-López, M. A., Carputo, R., Duarte, P., Díaz-Ropero, M. P., Valero, A. D., et al. (2015). *Lactobacillus fermentum* CECT 5716 reduces *Staphylococcus* load in the breastmilk of lactating mothers suffering breast pain: a randomized controlled trial. *Breastfeed. Med.* 10, 425–432. doi: 10.1089/bfm.2015.0070

Mantziari, A., Salminen, S., Szajewska, H., and Malagón-Rojas, J. N. (2020). Postbiotics against pathogens commonly involved in pediatric infectious diseases. *Microorganisms* 8, 1–22. doi: 10.3390/microorganisms8101510

Marcial, G. E., Ford, A. L., Haller, M. J., Gezan, S. A., Harrison, N. A., Cai, D., et al. (2017). *Lactobacillus johnsonii* N6.2 modulates the host immune responses: a double-blind, randomized trial in healthy adults. *Front. Immunol.* 8:655. doi: 10.3389/fimmu.2017.00655

Mata Forsberg, M., Björkander, S., Pang, Y., Lundqvist, L., Ndi, M., Ott, M., et al. (2019). Extracellular membrane vesicles from Lactobacilli dampen IFN-γ responses in a monocyte-dependent manner. *Sci. Rep.* 9:17109. doi: 10.1038/s41598-019-53576-6

McGuire, M. A., and McGuire, M. K. (2017). "Prebiotics and probiotics in human milk," in *Prebiotics and Probiotics in Human Milk*, eds M. K. Mcguire, M. A. McGuire, and L. Bode (Amsterdam: Elsevier), 463–468. doi: 10.1016/B978-0-12-802725-7.00017-8

Migale, R., Herbert, B. R., Lee, Y. S., Sykes, L., Waddington, S. N., Peebles, D., et al. (2015). Specific lipopolysaccharide serotypes induce differential maternal and neonatal inflammatory responses in a murine model of preterm labor. *Am. J. Pathol.* 185, 2390–2401. doi: 10.1016/j.ajpath.2015.05.015

Morishita, M., Horita, M., Higuchi, A., Marui, M., Katsumi, H., and Yamamoto, A. (2021). Characterizing different probiotic-derived extracellular vesicles as a novel adjuvant for immunotherapy. *Mol. Pharm.* 18, 1080–1092. doi: 10.1021/acs.molpharmaceut.0c01011

Müller, L., Kuhn, T., Koch, M., and Fuhrmann, G. (2021). Stimulation of probiotic bacteria induces release of membrane vesicles with augmented anti-inflammatory activity. *ACS Appl. Bio Mater.* 4, 3739–3748. doi: 10.1021/acsabm.0c01136

Munhoz da Rocha, I. F., Amatuzzi, R. F., Lucena, A. C. R., Faoro, H., and Alves, L. R. (2020). Cross-Kingdom extracellular vesicles EV-RNA communication as a mechanism for host–pathogen interaction. *Front. Cell. Infect. Microbiol.* 10:593160. doi: 10.3389/fcimb.2020.593160

Ñahui Palomino, R. A., Vanpouille, C., Costantini, P. E., and Margolis, L. (2021). Microbiota–host communications: bacterial extracellular vesicles as a common language. *PLoS Pathog.* 17:e1009508. doi: 10.1371/journal.ppat.1009508

Ñahui Palomino, R. A., Vanpouille, C., Laghi, L., Parolin, C., Melikov, K., Backlund, P., et al. (2019). Extracellular vesicles from symbiotic vaginal lactobacilli inhibit HIV-1 infection of human tissues. *Nat. Commun.* 10:5656. doi: 10.1038/s41467-019-13468-9

Nam, Y., Kim, J., Baek, J., and Kim, W. (2021). Improvement of cutaneous wound healing via topical application of heat-killed *Lactococcus chungangensis* CAU 1447 on diabetic mice. *Nutrients* 13:2666. doi: 10.3390/nu13082666

Nishiyama, K., Takaki, T., Sugiyama, M., Fukuda, I., Aiso, M., Mukai, T., et al. (2020). Extracellular vesicles produced by *Bifidobacterium longum* export mucin-binding proteins. *Appl. Environ. Microbiol.* 86:e01464-20. doi: 10.1128/AEM.01464-20

Nougayrède, J.-P., Chagneau, C., Motta, J.-P., Bossuet-Greif, N., Belloy, M., Taieb, F., et al. (2021). A toxic friend: genotoxic and mutagenic activity of the probiotic strain *Escherichia coli* Nissle 1917. *mSphere* 6:e0062421. doi: 10.1128/mSphere.00624-21

O'Donoghue, E. J., and Krachler, A. M. (2016). Mechanisms of outer membrane vesicle entry into host cells. *Cell. Microbiol.* 18, 1508–1517. doi: 10.1111/cmi.12655

Olier, M., Marcq, I., Salvador-Cartier, C., Secher, T., Dobrindt, U., Boury, M., et al. (2012). Genotoxicity of *escherichia coli* nissle 1917 strain cannot be dissociated from its probiotic activity. *Gut Microbes* 3, 501–509. doi: 10.4161/gmic.21737

Olivares, M., Albrecht, S., De Palma, G., Ferrer, M. D., Castillejo, G., Schols, H. A., et al. (2015). Human milk composition differs in healthy mothers and mothers with celiac disease. *Eur. J. Nutr.* 54, 119–128. doi: 10.1007/s00394-014-0692-1

Panigrahi, P., Parida, S., Nanda, N. C., Satpathy, R., Pradhan, L., Chandel, D. S., et al. (2017). A randomized synbiotic trial to prevent sepsis among infants in rural India. *Nature* 548, 407–412. doi: 10.1038/nature23480

Park, D. H., Kim, J. W., Park, H.-J., and Hahm, D.-H. (2021). Comparative analysis of the microbiome across the gut–skin axis in atopic dermatitis. *Int. J. Mol. Sci.* 22:4228. doi: 10.3390/ijms22084228

Park, J. Y., Choi, J., Lee, Y., Lee, J. E., Lee, E. H., Kwon, H. J., et al. (2017). Metagenome analysis of bodily microbiota in a mouse model of Alzheimer disease using bacteria-derived membrane vesicles in blood. *Exp. Neurobiol.* 26, 369–379. doi: 10.5607/en.2017.26.6.369

Passali, D., Passali, G. C., Vesperini, E., Cocca, S., Visconti, I. C., Ralli, M., et al. (2019). The efficacy and tolerability of *Streptococcus salivarius* 24SMB and *Streptococcus oralis* 89a administered as nasal spray in the treatment of recurrent upper respiratory tract infections in children. *Eur. Rev. Med. Pharmacol. Sci.* 23, 67–72. doi: 10.26355/eurrev_201903_17352

Pellon, A., Sadeghi Nasab, S. D., and Moyes, D. L. (2020). New insights in *Candida albicans* innate immunity at the mucosa: toxins, epithelium, metabolism, and beyond. *Front. Cell. Infect. Microbiol.* 10:81. doi: 10.3389/fcimb.2020.00081

Peral, M. C., Huaman Martinez, M. A., and Valdez, J. C. (2009). Bacteriotherapy with *Lactobacillus plantarum* in burns. *Int. Wound J.* 6, 73–81. doi: 10.1111/j.1742-481X.2008.00577.x

Piewngam, P., and Otto, M. (2020). Probiotics to prevent *Staphylococcus aureus* disease? *Gut Microbes* 11, 94–101. doi: 10.1080/19490976.2019.1591137

Plaza-Diaz, J., Ruiz-Ojeda, F. J., Gil-Campos, M., and Gil, A. (2019). Mechanisms of action of probiotics. *Adv. Nutr.* 10, S49–S66. doi: 10.1093/advances/nmy063

Qi, X., Simsek, S., Ohm, J. B., Chen, B., and Rao, J. (2020). Viability of: *Lactobacillus rhamnosus* GG microencapsulated in alginate/chitosan hydrogel particles during storage and simulated gastrointestinal digestion: role of chitosan molecular weight. *Soft Matter* 16, 1877–1887. doi: 10.1039/c9sm02387a

Raheem, A., Liang, L., Zhang, G., and Cui, S. (2021). Modulatory effects of probiotics during pathogenic infections with emphasis on immune regulation. *Front. Immunol.* 12:616713. doi: 10.3389/fimmu.2021.616713

Rajilić-Stojanović, M. (2013). Function of the microbiota. *Best Pract. Res. Clin. Gastroenterol.* 27, 5–16. doi: 10.1016/j.bpg.2013.03.006

Ren, C., Zhang, Q., de Haan, B. J., Zhang, H., Faas, M. M., and de Vos, P. (2016). Identification of TLR2/TLR6 signalling lactic acid bacteria for supporting immune regulation. *Sci. Rep.* 6:34561. doi: 10.1038/srep34561

Riley, L. W., and Blanton, R. E. (2018). Advances in molecular epidemiology of infectious diseases: definitions, approaches, and scope of the field. *Microbiol. Spectr.* 6, 1–12. doi: 10.1128/microbiolspec.ame-0001-2018

Rodovalho, V. D. R., da Luz, B. S. R., Rabah, H., do Carmo, F. L. R., Folador, E. L., Nicolas, A., et al. (2020). Extracellular vesicles produced by the probiotic *Propionibacterium freudenreichii* CIRM-BIA 129 mitigate inflammation by modulating the NF-κB pathway. *Front. Microbiol.* 11:1544. doi: 10.3389/fmicb.2020.01544

Roig, J., Saiz, M. L., Galiano, A., Trelis, M., Cantalapiedra, F., Monteagudo, C., et al. (2018). Extracellular vesicles from the helminth *Fasciola hepatica* prevent DSS-induced acute ulcerative colitis in a T-lymphocyte independent mode. *Front. Microbiol.* 9:1036. doi: 10.3389/fmicb.2018.01036

Rosenthal, J. A., Huang, C., Doody, A. M., Leung, T., Mineta, K., Feng, D. D., et al. (2014). Mechanistic insight into the Th1-biased immune response to recombinant subunit vaccines delivered by probiotic bacteria-derived outer membrane vesicles. *PLoS One* 9:e112802. doi: 10.1371/journal.pone.0112802

Russo, R., Superti, F., Karadja, E., and De Seta, F. (2019). Randomised clinical trial in women with recurrent vulvovaginal *Candidiasis*: efficacy of probiotics and lactoferrin as maintenance treatment. *Mycoses* 62, 328–335. doi: 10.1111/myc.12883

Salminen, S., Collado, M. C., Endo, A., Hill, C., Lebeer, S., Quigley, E. M. M., et al. (2021). The international scientific association of probiotics and prebiotics (ISAPP) consensus statement on the definition and scope of postbiotics. *Nat. Rev. Gastroenterol. Hepatol.* 18, 649–667. doi: 10.1038/s41575-021-00440-6

Sanders, M. E., Benson, A., Lebeer, S., Merenstein, D. J., and Klaenhammer, T. R. (2018). Shared mechanisms among probiotic taxa: implications for general probiotic claims. *Curr. Opin. Biotechnol.* 49, 207–216. doi: 10.1016/j.copbio.2017.09.007

Santos, P., and Almeida, F. (2021). Exosome-based vaccines: history, current state, and clinical trials. *Front. Immunol.* 12:711565. doi: 10.3389/fimmu.2021.711565

Santos, T. T., Maria, R., Santos, D., Acurcio, L. B., Henrique, S., Sandes, C., et al. (2020). Differential immune response of *Lactobacillus plantarum* 286 against *Salmonella typhimurium* infection in conventional and germ-free mice. *Adv. Exp. Med. Biol.* 1323, 1–17. doi: 10.1007/5584_2020_544

Sassone-Corsi, M., and Raffatellu, M. (2016). No vacancy: how beneficial microbes cooperate with immunity to provide colonization resistance to pathogens. *J. Immunol.* 176, 139–148. doi: 10.1016/j.physbeh.2017.03.040

Seth, A., Yan, F., Polk, D. B., and Rao, R. K. (2008). Probiotics ameliorate the hydrogen peroxide-induced epithelial barrier disruption by a PKC- And MAP kinase-dependent mechanism. *Am. J. Physiol. Gastrointest. Liver Physiol.* 294, 1060–1069. doi: 10.1152/ajpgi.00202.2007

Sgibnev, A., and Kremleva, E. (2020). Probiotics in addition to metronidazole for treatment *Trichomonas vaginalis* in the presence of BV: a randomized, placebo-controlled, double-blind study. *Eur. J. Clin. Microbiol. Infect. Dis.* 39, 345–351. doi: 10.1007/s10096-019-03731-8

Shafaghi, A., Pourkazemi, A., Khosravani, M., Fakhrie Asl, S., Amir Maafi, A., Atrkar Roshan, Z., et al. (2016). The effect of probiotic plus prebiotic supplementation on the tolerance and efficacy of *Helicobacter* pylori eradication quadruple therapy: a randomized prospective double blind controlled trial. *Middle East J. Dig. Dis.* 8, 179–188. doi: 10.15171/mejdd.2016.30

Sharifi-Rad, J., Rodrigues, C. F., Stojanović, Z., Radić, S.-R., Dimitrijević, M. D., Aleksić, A. A., et al. (2020). Probiotics: versatile bioactive components in promoting human health. *Medicina (B. Aires)* 56, 433. doi: 10.3390/medicina56090433

Shehata, M. M., Mostafa, A., Teubner, L., Mahmoud, S. H., Kandeil, A., Elshesheny, R., et al. (2019). Bacterial outer membrane vesicles (OMVs)-based dual vaccine for influenza a H1N1 virus and MERS-CoV. *Vaccines* 7, 1–13. doi: 10.3390/vaccines7020046

Shi, X., Zhang, J., Mo, L., Shi, J., Qin, M., and Huang, X. (2019). Efficacy and safety of probiotics in eradicating *Helicobacter* pylori: a network meta-analysis. *Medicine (Baltimore)* 98:e15180. doi: 10.1097/MD.0000000000015180

Shin, D. Y., Yi, D. Y., Jo, S., Lee, Y. M., Kim, J. H., Kim, W., et al. (2020). Effect of a new *Lactobacillus plantarum* product, LRCC5310, on clinical symptoms and virus reduction in children with rotaviral enteritis. *Medicine (Baltimore)* 99:e22192. doi: 10.1097/MD.0000000000022192

Shiraishi, T., Yokota, S., Sato, Y., Ito, T., Fukiya, S., Yamamoto, S., et al. (2018). Lipoteichoic acids are embedded in cell walls during logarithmic phase, but exposed on membrane vesicles in *Lactobacillus gasseri* JCM 1131 T. *Benef. Microbes* 9, 653–662. doi: 10.3920/BM2017.0124

Silvia Ventimiglia, M., Jimena Valeff, N., Pozo Albán, M., Manuel Paturlanne, J., Juriol, L., Quadrana, F., et al. (2021). Probiotic *Lactobacillus kefiri* prevents endotoxin-induced preterm birth and stillbirth in mice. *Reproduction* 161, 657–667. doi: 10.1530/REP-20-0642

Singh, T. P., Kaur, G., Kapila, S., and Malik, R. K. (2017). Antagonistic activity of *Lactobacillus reuteri* strains on the adhesion characteristics of selected pathogens. *Front. Microbiol.* 8:486. doi: 10.3389/fmicb.2017.00486

Sokol, H. (2019). Definition and roles of the gut microbiota. *Rev. Prat.* 69, 776–782.

Spacova, I., De Boeck, I., Bron, P. A., Delputte, P., and Lebeer, S. (2021). Topical microbial therapeutics against respiratory viral infections. *Trends Mol. Med.* 27, 538–553. doi: 10.1016/j.molmed.2021.03.009

Stapleton, A. E., Au-Yeung, M., Hooton, T. M., Fredricks, D. N., Roberts, P. L., Czaja, C. A., et al. (2011). Randomized, placebo-controlled phase 2 trial of a *Lactobacillus crispatus* probiotic given intravaginally for prevention of recurrent urinary tract infection. *Clin. Infect. Dis.* 52, 1212–1217. doi: 10.1093/cid/cir183

Stavropoulou, E., and Bezirtzoglou, E. (2020). Probiotics in medicine: a long debate. *Front. Immunol.* 11:2192. doi: 10.3389/fimmu.2020.02192

Stentz, R., Carvalho, A. L., Jones, E. J., and Carding, S. R. (2018). Fantastic voyage: the journey of intestinal microbiota-derived microvesicles through the body. *Biochem. Soc. Trans.* 46, 1021–1027. doi: 10.1042/BST20180114

Su, G. L., Ko, C. W., Bercik, P., Falck-Ytter, Y., Sultan, S., Weizman, A. V., et al. (2020). AGA clinical practice guidelines on the role of probiotics in the management of gastrointestinal disorders. *Gastroenterology* 159, 697–705. doi: 10.1053/j.gastro.2020.05.059

Surendran Nair, M., Amalaradjou, M. A., and Venkitanarayanan, K. (2017). *Antivirulence Properties of Probiotics in Combating Microbial Pathogenesis*. Amsterdam: Elsevier Ltd. doi: 10.1016/bs.aambs.2016.12.001

Takiishi, T., Fenero, C. I. M., and Câmara, N. O. S. (2017). Intestinal barrier and gut microbiota: shaping our immune responses throughout life. *Tissue Barriers* 5:e1373208. doi: 10.1080/21688370.2017.1373208

Tamayo, C. (2008). Clinical research on probiotics: the interface between science and regulation. *Clin. Infect. Dis.* 46, S101–S103. doi: 10.1086/523332

Tang, N., Luo, Z.-C., Zhang, L., Zheng, T., Fan, P., Tao, Y., et al. (2020). The association between gestational diabetes and microbiota in placenta and cord blood. *Front. Endocrinol. (Lausanne)* 11:550319. doi: 10.3389/fendo.2020.550319

Théry, C., Witwer, K. W., Aikawa, E., Alcaraz, M. J., Anderson, J. D., Andriantsitohaina, R., et al. (2018). Minimal information for studies of extracellular vesicles 2018 (MISEV2018): a position statement of the International Society for Extracellular Vesicles and update of the MISEV2014 guidelines. *J. Extracell. Vesicles* 7:1535750. doi: 10.1080/20013078.2018.1535750

Tong, L., Zhang, X., Hao, H., Liu, Q., Zhou, Z., Liang, X., et al. (2021). *Lactobacillus rhamnosus* GG derived extracellular vesicles modulate gut microbiota and

attenuate inflammatory in DSS-induced colitis mice. *Nutrients* 13:3319. doi: 10.3390/nu13103319

Tsubura, S., Mizunuma, H., Ishikawa, S., Oyake, I., Okabayashi, M., Katoh, K., et al. (2009). The effect of *Bacillus subtilis* mouth rinsing in patients with periodontitis. *Eur. J. Clin. Microbiol. Infect. Dis.* 28, 1353–1356. doi: 10.1007/s10096-009-0790-9

Tuo, Y., Song, X., Song, Y., Liu, W., Tang, Y., Gao, Y., et al. (2018). Screening probiotics from *Lactobacillus* strains according to their abilities to inhibit pathogen adhesion and induction of pro-inflammatory cytokine IL-8. *J. Dairy Sci.* 101, 4822–4829. doi: 10.3168/jds.2017-13654

Tzipilevich, E., Habusha, M., and Ben-Yehuda, S. (2017). Acquisition of phage sensitivity by bacteria through exchange of phage receptors. *Cell* 168, 186–199.e12. doi: 10.1016/j.cell.2016.12.003

van Zyl, W. F., Deane, S. M., and Dicks, L. M. T. (2019). Bacteriocin production and adhesion properties as mechanisms for the anti-listerial activity of *Lactobacillus plantarum* 423 and *Enterococcus mundtii* ST4SA. *Benef. Microbes* 10, 329–349. doi: 10.3920/BM2018.0141

van Zyl, W. F., Deane, S. M., and Dicks, L. M. T. (2020). Molecular insights into probiotic mechanisms of action employed against intestinal pathogenic bacteria. *Gut Microbes* 12:1831339. doi: 10.1080/19490976.2020.1831339

Vargoorani, M. E., Modarressi, M. H., Vaziri, F., Motevaseli, E., and Siadat, S. D. (2020). Stimulatory effects of *Lactobacillus casei* derived extracellular vesicles on toll-like receptor 9 gene expression and cytokine profile in human intestinal epithelial cells. *J. Diabetes Metab. Disord.* 19, 223–231. doi: 10.1007/s40200-020-00495-3

Veiga-Parga, T., Sehrawat, S., and Rouse, B. T. (2013). Role of regulatory T cells during virus infection. *Immunol. Rev.* 255, 182–196. doi: 10.1111/imr.12085

Vinderola, G., and Pérez-Marc, G. (2021). Fermented foods and probiotics for children. The importance of knowing their microbiological differences. *Arch. Argent. Pediatr.* 119, 56–61. doi: 10.5546/AAP.2021.ENG.56

Vladareanu, R., Mihu, D., Mitran, M., Mehedintu, C., Boiangiu, A., Manolache, M., et al. (2018). Abstracts *Lactobacillus plantarum* new evidence on oral L . *plantarum* P17630 product in women with history of recurrent vulvovaginal *Exopolysaccharide* from *Lactobacillus plantarum* LRCC5310 offers protection against rotavirus-induced diarrhea and regulates. *Eur. Rev. Med. Pharmacol. Sci.* 22, 262–267. doi: 10.26355/eurrev_201801_14128

Wahlund, C. J. E., Güclüler, G., Hiltbrunner, S., Veerman, R. E., Näslund, T. I., and Gabrielsson, S. (2017). Exosomes from antigen-pulsed dendritic cells induce stronger antigen-specific immune responses than microvesicles in vivo. *Sci. Rep.* 7:17095. doi: 10.1038/s41598-017-16609-6

Wang, L., Zhang, S., Wu, H., Rong, X., and Guo, J. (2019). M2b macrophage polarization and its roles in diseases. *J. Leukoc. Biol.* 106, 345–358. doi: 10.1002/JLB.3RU1018-378RR

Wang, W., and Jeffery, C. J. (2016). An analysis of surface proteomics results reveals novel candidates for intracellular/surface moonlighting proteins in bacteria. *Mol. Biosyst.* 12, 1420–1431. doi: 10.1039/c5mb00550g

Wegh, C. A. M., Geerlings, S. Y., Knol, J., Roeselers, G., and Belzer, C. (2019). Postbiotics and their potential applications in early life nutrition and beyond. *Int. J. Mol. Sci.* 20:4673. doi: 10.3390/ijms20194673

West, C. L., Stanisz, A. M., Mao, Y. K., Champagne-Jorgensen, K., Bienenstock, J., and Kunze, W. A. (2020). Microvesicles from *Lactobacillus reuteri* (DSM-17938) completely reproduce modulation of gut motility by bacteria in mice. *PLoS One* 15:e0225481. doi: 10.1371/journal.pone.0225481

Wilmore, J. R., Gaudette, B. T., Gomez Atria, D., Hashemi, T., Jones, D. D., Gardner, C. A., et al. (2018). Commensal microbes induce serum IgA responses that protect against polymicrobial sepsis. *Cell Host Microbe* 23, 302–311.e3. doi: 10.1016/j.chom.2018.01.005

World Health Organization (2021). *World Health Statistics 2021: Monitoring Health for the SDGs, Sustainable Development Goals*. Available online at: https://reliefweb.int/report/world/world-health-statistics-2021-monitoring-health-sdgs (accessed December 30, 2021).

Xia, X., Chen, J., Xia, J., Wang, B., Liu, H., Yang, L., et al. (2018). Role of probiotics in the treatment of minimal hepatic encephalopathy in patients with HBV-induced liver cirrhosis. *J. Int. Med. Res.* 46, 3596–3604. doi: 10.1177/0300060518776064

Xu, J., Schwartz, K., Bartoces, M., Monsur, J., Severson, R. K., and Sobel, J. D. (2008). Effect of antibiotics on vulvovaginal Candidiasis: a MetroNet study. *J. Am. Board Fam. Med.* 21, 261–268. doi: 10.3122/jabfm.2008.04.070169

Yamasaki-Yashiki, S., Miyoshi, Y., Nakayama, T., Kunisawa, J., and Katakura, Y. (2019). IgA-enhancing effects of membrane vesicles derived from *Lactobacillus sakei* subsp. sakei NBRC15893. *Biosci. Microbiota Food Heal.* 38, 23–29. doi: 10.12938/bmfh.18-015

Yan, F., Cao, H., Cover, T. L., Washington, M. K., Shi, Y., Liu, L. S., et al. (2011). Colon-specific delivery of a probiotic-derived soluble protein ameliorates intestinal inflammation in mice through an EGFR-dependent mechanism. *J. Clin. Invest.* 121, 2242–2253. doi: 10.1172/JCI44031

Yang, L., Zhao, Y., Wang, Y., Liu, L., Zhang, X., Li, B., et al. (2015). The effects of psychological stress on depression. *Curr. Neuropharmacol.* 13, 494–504. doi: 10.2174/1570159x1304150831150507

Yang, Z., Hua, L., Yang, M., Liu, S. Q., Shen, J., Li, W., et al. (2021). RBD-modified bacterial vesicles elicited potential protective immunity against SARS-CoV-2. *Nano Lett.* 21, 5920–5930. doi: 10.1021/acs.nanolett.1c00680

Yao, M., Xie, J., Du, H., McClements, D. J., Xiao, H., and Li, L. (2020). Progress in microencapsulation of probiotics: a review. *Compr. Rev. Food Sci. Food Saf.* 19, 857–874. doi: 10.1111/1541-4337.12532

Yong, S. J., Tong, T., Chew, J., and Lim, W. L. (2020). Antidepressive mechanisms of probiotics and their therapeutic potential. *Front. Neurosci.* 13:1361. doi: 10.3389/fnins.2019.01361

Zhang, G., Huang, X., Xiu, H., Sun, Y., Chen, J., Cheng, G., et al. (2020). Extracellular vesicles: natural liver-accumulating drug delivery vehicles for the treatment of liver diseases. *J. Extracell. Vesicles* 10:e12030. doi: 10.1002/jev2.12030

Zhao, M., Zhang, H., Liu, X., Jiang, Y., Ren, L., and Hu, X. (2017). The effect of TGF-β on treg cells in adverse pregnancy outcome upon *Toxoplasma gondii* infection. *Front. Microbiol.* 8:901. doi: 10.3389/fmicb.2017.00901

Zhao, W., Liu, Y., Kwok, L. Y., Cai, T., and Zhang, W. (2020). The immune regulatory role of *Lactobacillus acidophilus*: an updated meta-analysis of randomized controlled trials. *Food Biosci.* 36:100656. doi: 10.1016/j.fbio.2020.100656

Zhao, W., Peng, C., Sakandar, H. A., Kwok, L. Y., and Zhang, W. (2021). Meta-analysis: randomized trials of *Lactobacillus plantarum* on immune regulation over the last decades. *Front. Immunol.* 12:643420. doi: 10.3389/fimmu.2021.643420

Zommiti, M., Feuilloley, M. G. J., and Connil, N. (2020). Update of probiotics in human world: a nonstop source of benefactions till the end of time. *Microorganisms* 8, 1–33. doi: 10.3390/microorganisms8121907

Conflict of Interest: The authors declare that the research was conducted in the absence of any commercial or financial relationships that could be construed as a potential conflict of interest.

Publisher's Note: All claims expressed in this article are solely those of the authors and do not necessarily represent those of their affiliated organizations, or those of the publisher, the editors and the reviewers. Any product that may be evaluated in this article, or claim that may be made by its manufacturer, is not guaranteed or endorsed by the publisher.

frontiers | Frontiers in Microbiology

ORIGINAL RESEARCH
published: 25 April 2022
doi: 10.3389/fmicb.2022.803688

Exploring the Therapeutic Potentials of Exopolysaccharides Derived From Lactic Acid Bacteria and Bifidobacteria: Antioxidant, Antitumor, and Periodontal Regeneration

Maha A. Khalil[1,2]*, *Fatma I. Sonbol*[3], *Lamiaa A. Al-Madboly*[3], *Tamer A. Aboshady*[4,5], *Abeer S. Alqurashi*[1] and *Sameh S. Ali*[2,6]*

[1] Biology Department, College of Science, Taif University, Taif, Saudi Arabia, [2] Botany and Microbiology Department, Faculty of Science, Tanta University, Tanta, Egypt, [3] Pharmaceutical Microbiology Department, Faculty of Pharmacy, Tanta University, Tanta, Egypt, [4] Periodontology, Oral Medicine, Diagnosis and Radiology Department, Faculty of Dentistry, Tanta University, Tanta, Egypt, [5] Oral and Maxillofacial Surgery and Diagnostic Sciences, Faculty of Dentistry, Taif University, Taif, Saudi Arabia, [6] Biofuels Institute, School of the Environment and Safety Engineering, Jiangsu University, Zhenjiang, China

OPEN ACCESS

Edited by:
Sabina Górska,
Hirszfeld Institute of Immunology and Experimental Therapy (PAS), Poland

Reviewed by:
Junling Shi,
Northwestern Polytechnical University, China
Babak Haghshenas,
Kermanshah University of Medical Sciences, Iran

***Correspondence:**
Maha A. Khalil
maha.ak@tu.edu.sa;
maha.khalil@science.tanta.edu.eg
Sameh S. Ali
samh@ujs.edu.cn;
samh_samir@science.tanta.edu.eg

Specialty section:
This article was submitted to Food Microbiology, a section of the journal Frontiers in Microbiology

Received: 28 October 2021
Accepted: 16 February 2022
Published: 25 April 2022

Citation:
Khalil MA, Sonbol FI, Al-Madboly LA, Aboshady TA, Alqurashi AS and Ali SS (2022) Exploring the Therapeutic Potentials of Exopolysaccharides Derived From Lactic Acid Bacteria and Bifidobacteria: Antioxidant, Antitumor, and Periodontal Regeneration. Front. Microbiol. 13:803688. doi: 10.3389/fmicb.2022.803688

The metabolites of lactic acid bacteria (LAB) and bifidobacteria (Bb) have recently received a lot of attention due to their ability to protect interactions in blood and tissues, as well as their biodegradability and biocompatibility in human tissue. Exopolysaccharides (EPS) derived from bacteria have a long history of use in therapeutic and other industrial applications with no adverse effects. In this regard, EPSs were isolated and characterized from LAB and Bb culture supernatants to determine their antioxidant, antitumor, and periodontal regeneration properties. The antioxidant capacity of the EPSs varied with concentration (0.625–20 mg/ml). The highest antioxidant activity was found in LAB: *Streptococcus thermophiles* DSM 24731-EPS_1, *Lactobacillus delbrueckii* ssp. *bulgaricus* DSM 20081^T-EPS_5, *Limosilactobacillus fermentum* DSM 20049-EPS_6, and Bb; *Bifidobacterium longum* ssp. *longum* DSM 200707-EPS_{10}. Human breast cancer cells (MCF7), human colon cancer cells (CaCo2), human liver cancer cells (HepG2), and human embryonic kidney 293 (HEK 293) cells were used as controls to assess the antitumor properties of the selected EPSs. According to the 3-(4,5-dimethylthiazol-2-yl)-2,5-diphenyltetrazolium-bromide (MTT) assay, EPS_5 had the highest cytotoxicity against MCF7, CaCo2, and HepG2, with IC_{50} values of 7.91, 10.69, and 9.12 mg/ml, respectively. Lactate dehydrogenase (LDH) activity was significantly higher in cell lines treated with EPS_5-IC_{50} values compared to other EPSs-IC_{50} values ($p < 0.05$). Real time (RT)-PCR results showed that EPS_5 treatment increased *Bax*, *Caspase 8*, *Caspase 3*, and *p53* gene expression. The expression of the *BCL2*, *MCL1*, and *Vimentin* genes, on the other hand, was reduced. The MTT test was used to examine the effect of EPS_5 on the viability of human periodontal ligament fibroblast cells (hPDLFCs),

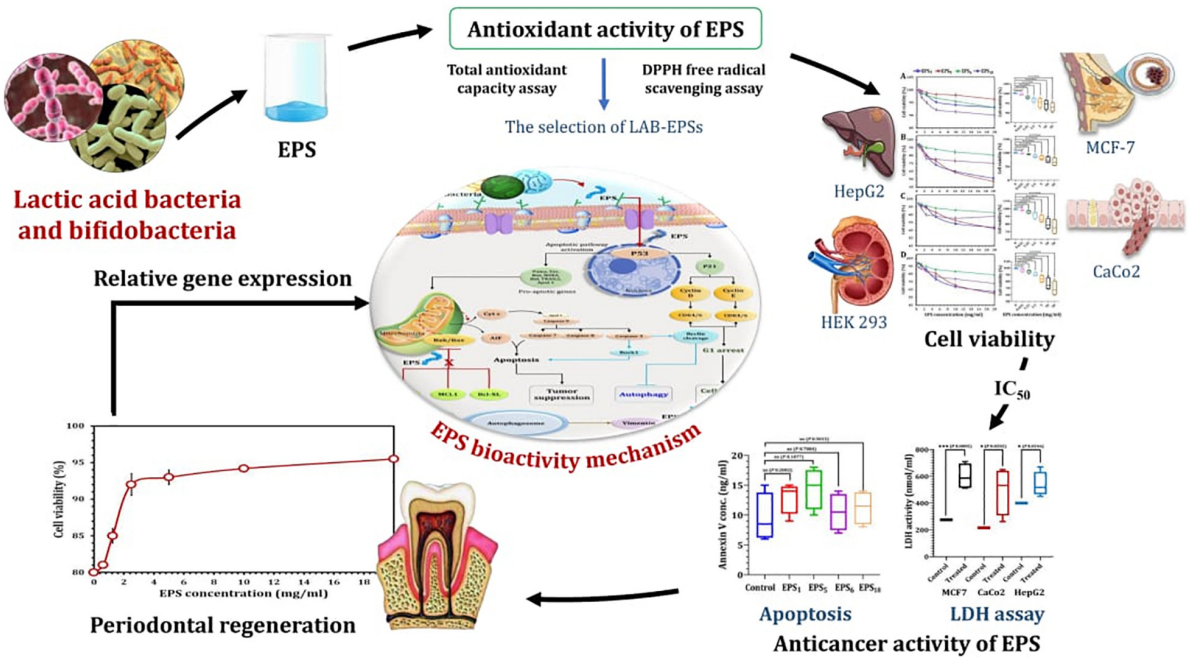

GRAPHICAL ABSTRACT | Therapeutic applications of exopolysaccharides derived from lactic acid bacteria and bifidobacteria.

and it was discovered that EPS_5 increased hPDLFC viability. According to high-performance liquid chromatography (HPLC) analysis, galactose made up 12.5% of EPS_5. The findings of this study pave the way for the use of EPS, which hold great promise for a variety of therapeutic purposes such as antioxidant, antitumor, and periodontal regeneration.

Keywords: lactic acid bacteria, bifidobacteria, exopolysaccharide, RT-PCR, MCF7, CaCo2, HepG2, therapeutic agent

INTRODUCTION

Bacteria are recognized for their ability to produce a wide variety of polysaccharides. These polysaccharides may either be tightly attached to the cell surface as capsular polysaccharides (CPS) or they can be released as exopolysaccharides (EPSs). Many bacterial taxa, particularly lactic acid bacteria (LAB) and bifidobacteria (Bb), produce a wide range of carbohydrate polymers during fermentation (Sanalibaba and Cakmak, 2016). LAB are generally considered as safe microorganisms (GRAS—generally recognized as safe) and also capable of creating EPSs with many different structures without any health risks (Surayot et al., 2014). LAB refers to Gram-positive bacteria that are often isolated from fermented natural products and are extensively employed in industrial operations. LAB and their metabolic products have been shown to enhance immunity, gastro-intestinal function, resistance to obesity, antioxidant activity, and blood glucose and cholesterol levels (Mathur et al., 2020; Wang et al., 2020). Additionally, they also have potential health benefits such as anticancer activity (Tukenmez et al., 2019), immunostimulatory activity (Adebayo-Tayo et al., 2018), antibiofilm activity (Lakra et al., 2020), and antiviral activity (Biliavska et al., 2019).

Exopolysaccharides have garnered significant interest in recent years owing to their potential pharmacological and biomedical uses (Barcelos et al., 2019). EPSs are classified into two categories: homopolysaccharides (HoPs) are composed entirely of single monosaccharides, heteropolysaccharides (HePs) are composed of a polymer chain of monomer units composed of two or more monosaccharides (Mende et al., 2016). High-molecular-mass polysaccharides exhibit a variety of chemical properties, including molecular weights, charges, side chains, and rigidity (Sanalibaba and Cakmak, 2016; Wang et al., 2020). Simultaneously, the growth conditions used to produce probiotic bacteria alter the chemical structure of EPS (Zannini et al., 2016). Additionally, experiments have demonstrated that the composition and structure of EPSs are strain-dependent (Li C. et al., 2014). Due to their chemical properties, including molecular structures, chain linkage, and molecular mass, EPS exhibit anticancer activity with minimal side effects. As a result, EPS with a diverse chemical structure and property profile may

be advantageous in a variety of therapeutic applications (Wang et al., 2014; Hussain et al., 2017; Lin et al., 2018).

Concerns have grown about the safety and toxicity of synthetic antioxidants, but researchers face a difficult task in identifying natural antioxidants that are safe for human health (Adebayo-Tayo and Fashogbon, 2020). It has recently been demonstrated that LAB EPS have antioxidant properties and could be used as potential antioxidants (El-Adawi et al., 2012; Adebayo-Tayo et al., 2018). *Lactobacillus helveticus* MB2-1 EPS has significant antioxidant and anticancer activity in colon cancer cells (Li W. et al., 2014; Li et al., 2015). Adebayo-Tayo and Fashogbon (2020) confirmed that EPS activity has pharmacological and nutraceutical applications in wild-type and mutant *Lactobacillus delbrueckii*. Furthermore, Joo Seo et al. (2015) established that purified *Lactiplantibacillus plantarum* YML009-EPS had high antioxidant activity. *Lactobacillus acidophilus*, *Lactobacillus gasseri*, *Lactiplantibacillus plantarum*, and *Lacticaseibacillus rhamnosus* were reported to have anticancer and antioxidant properties (Sungur et al., 2017; Adesulu-Dahunsi et al., 2018). The antioxidant activity of EPS extracted from fermented milk of *L. delbrueckii* ssp. *bulgaricus* SRFM-1 has been demonstrated to be acceptable (Tang et al., 2017). Additionally, EPS extracted from *L. plantarum* ZDY2013 was shown to have increased antioxidant activity following sulfonation (Zhang et al., 2016).

Periodontal diseases are noteworthy as a global "hidden" epidemic in terms of disease burden and socioeconomic consequences. Periodontal disease is caused by bacteria that live in the gingiva and on the tooth and is characterized by inflammation and destruction of the oral supporting tissue. If the biofilm is not removed from the periodontal pocket, it may induce an immune response and inflammation in other periodontal tissues, resulting in progressive periodontitis. Periodontitis left untreated may result in further bone loss and, eventually, tooth loss (Nasajpour et al., 2018). While dental scaling and open-flap surgery are effective at removing biofilms and regulating inflammation in order to prevent disease development, they are ineffective at regenerating periodontal tissue (Iviglia et al., 2019). The identification of naturally occurring biomaterials with multiple functions may hold enormous promise for periodontal repair and regeneration, as well as serve as a springboard for future research.

At the moment, researchers are investigating low-risk cancer medications, and one of their areas of interest is the antitumor properties of LAB (Norouzi et al., 2018). Cancer is a term that refers to the uncontrolled proliferation of abnormal cells that have the ability to invade and damage surrounding tissue. According to the Global Cancer Center, cancer has surpassed heart disease as the leading cause of death (Bray et al., 2018). Surgical excision, radiation, and medication therapy are all considered traditional cancer therapies (Qin, 2015). Drug therapy can have a detrimental effect on normal organs and tissues, including the bone marrow, kidneys, and oral mucosa, as well as impair normal metabolism. Additionally, these three approaches may result in inflammation and subsequent lymphedema following therapy (Hu et al., 2017; Adebayo-Tayo and Fashogbon, 2020). As a result of their affordability, availability, and lack of adverse effects, people prefer complementary and alternative medications (Liu et al., 2019). As a result, there is an increasing need for targeted therapies capable of successfully treating cancer while having a negligible effect on normal tissues or at the very least acting as adjuvants to reduce clinical doses and increase the potency of conventional chemotherapy agents (Liu et al., 2021).

Lactobacilli are anticancer agents because they can induce apoptosis in cancerous cells, differentiate them, and bind to genotoxic substances (Wu et al., 2021). Due to the fact that LAB EPS inhibits the growth of a variety of tumor cells, including those from the stomach, liver, and breast, it may be used as a complementary or alternative cancer treatment. These agents have a variety of antitumor effects, including cell cycle arrest and inducing apoptosis, as well as antimutagenic, antioxidative, antiangiogenesis, and anti-inflammatory properties (Nazir et al., 2018; Milner et al., 2021; Wu et al., 2021). Additionally, EPS has a wide range of effects, including decreasing tumor-promoting enzyme activity, increasing immune response, forming host-supporting metabolites and resistant pathogens, and limiting cell proliferation by inhibiting cancer cell spread *via* apoptosis (Liu et al., 2021). Apoptosis (programmed cell death) occurs at the molecular level *via* two distinct mechanisms, intrinsic and extrinsic (Śliżewska et al., 2021). The *BCl2* family of pro- and anti-apoptotic proteins regulates intrinsic or mitochondrial pathways. Exogenous apoptosis, alternatively referred to as the cytoplasmic route, is mediated by the death receptor Fas, a member of the tumor necrosis factor family (Zhao et al., 2019). Numerous publications have demonstrated that EPSs possess a variety of biologically active properties, including antioxidant, immune-stimulating, and anticancer properties (El-Adawi et al., 2012; El-Deeb et al., 2018; Angelin and Kavitha, 2020). In this regard, EPSs from the marine bacterium *L. plantarum* 70810 have shown an anti-proliferative effect on a hepatocellular cancer cell line (HepG2) (Yahya et al., 2019). Rajoka et al. (2018) investigated the bioactivity of the cell-free culture supernatant (CFCS) of *Lactobacillus* strains *Lactobacillus casei* SR1, *L. casei* SR2, and *Lactobacillus paracasei* SR4 obtained from human breast milk. They revealed that the CFCSs exhibited adequate anticancer effects on cervical cancer (HeLa) cells by upregulating the apoptotic genes *BAX*, *BAD*, *Caspase 3*, *Caspase 8*, and *Caspase 9* and downregulating the *BCl2* gene expression.

In terms of EPS's unique properties and potential effects, we hypothesized that it has a profound effect on periodontal repair and regeneration, as well as on cancer cell growth inhibition and apoptosis induction. To address this issue, we assessed the EPS's cytotoxicity against breast cancer (MCF7), colon cancer (CaCo2), human liver cancer cells (HepG2), and human embryonic kidney 293 (HEK 293) cells (control), as well as its antioxidant capacity. Additionally, using a variety of cancer cell lines, the current research examined their effect on apoptosis-related gene expression. Additionally, the effect of EPS on the survival of human periodontal ligament fibroblast cells (hPDLFCs) *in vitro* was investigated.

Numerous research were performed recently to characterize and comprehend the biotechnological application of EPS produced from LAB and Bb. However, the tremendous therapeutic potential of EPS, particularly in periodontal healing and regeneration, is still unknown. Due to the wide range

of uses for EPS and the rising demand for biopolymers, it is vital to develop new EPS produced from LAB. To our knowledge, the multifunctional therapeutic applications of EPS produced by *L. delbrueckii* ssp. *bulgaricus* DSM 20081^T have been emphasized for the first time. Under this scope, this work aims to look into the antioxidant, antitumor, and periodontal regeneration properties of EPSs derived using LAB and Bb culture supernatants. As a result, EPSs derived from *L. delbrueckii* ssp. *bulgaricus* DSM 20081^T may be a promising candidate for a variety of therapeutic applications.

MATERIALS AND METHODS

Cell Culture

On Dulbecco's Modified Eagle Medium (DMEM), non-cancerous HEK 293 cells were grown. CaCo2 and HepG2 cells were grown in DMEM; MCF7 cells were grown in Rosewell Park Memorial Institute (RPMI) medium. All cells were cultured in a medium containing 2 mM L-glutamine, 10% fetal bovine serum (FBS), and 1% penicillin–streptomycin combination. The cultures were incubated at 37°C for 24 h in a humidified environment containing 5% CO_2 and 95% air.

Bacterial Strains

Lactic Acid Bacteria

Lactic acid bacteria (n = 9) including *Streptococcus thermophiles* DSM 24731, *Lactobacillus lactis* ssp. *cremoris* DSM 20069^T, *Lacticaseibacillus casei* DSM 27537, *Lactobacillus delbrueckii* ssp. *bulgaricus* DSM 20080, *Lactobacillus delbrueckii* ssp. *bulgaricus* DSM 20081^T, *Limosilactobacillus fermentum* DSM 20049, *Lactobacillus acidophilus* DSM 20079^T, *Lactobacillus rhamnosus* DSM 20021, and *Lactobacillus plantarum* ssp. *plantarum* DSM 20174 were kindly obtained from the culture collection of the Faculty of Agriculture Ain Shams University and the Faculty of Science Tanta University (El-Adawi et al., 2012). LAB strains were grown in De Man–Rogosa–Sharpe (MRS, Biokar Diagnostics, Beauvais, France) broth [10.0 g/l peptone, 8.0 g/l meat extract, 4.0 g/l yeast extract, 20.0 g/l D (+)-glucose, 2.0 g/l dipotassium hydrogen phosphate, 5 g/l sodium acetate trihydrate, 2.0 g/l triammonium citrate, 0.2 g/l magnesium sulfate heptahydrate, 0.05 g/l manganous sulfate tetrahydrate, final pH 6.2] at 37°C for 24 h anaerobically. However, *Streptococcus thermophilus*, was cultured on M17 agar media and incubated at 37°C under aerobic and anaerobic conditions.

Bifidobacterial Strain

Bifidobacterium longum ssp. *longum* DSM 200707 was provided from Kafr El-Sheik University. *Bifidobacterium* was grown in MRS medium supplemented with l-cysteine at 0.5 g/l (MRSc) at 37°C in anaerobic environment.

Extraction of Crude Exopolysaccharides

The experimental setup for extracting EPS from a variety of LAB is depicted in **Figure 1**. Centrifugation at 4°C, 10,000 rpm, for approximately 20 min was used to remove bacteria from overnight cultures (Bajpai et al., 2016). The supernatant was collected and diluted with 14% trichloroacetic acid (1:1), followed by centrifugation (10,000 rpm at 4°C for 20 min) to remove the proteins. The clear supernatant was collected and concentrated using a rotary evaporator. The EPS was precipitated by adding double the amount of absolute cold ethanol and maintaining it at 4°C for 24 h, followed by 20 min of centrifugation at 4°C, 10,000 rpm. After dilution with deionized water, the residue was dialyzed for 48 h. The solution was concentrated and lyophilized to obtain dry powdered crude EPS (mg/l). The total carbohydrate content (%) of crude EPS was determined using the phenol-sulfuric acid method, using glucose (2 mg/ml) as a standard (Dubois et al., 1956). Approximately 0.5 ml of EPS solution (100 mg/ml) was combined with 0.5 ml of phenol 6% (v/v) in a test tube. A mixed solution of concentrated sulfuric acid (2.5 ml) was added to the test tube. After 10 min, the mixture was kept in a water bath (30°C) for 20 min, and the absorbance (Abs) at 490 nm was determined using a spectrophotometer. By substituting Abs into the standard curve, the carbohydrate content was determined. Simultaneously, the protein content of EPS was determined using Bradford method (Bradford, 1976). Protein reagent (2.5 ml, 50 ml containing 2.0 mg/ml Coomassie Brilliant Blue G-250 in 95% ethanol and 100 ml 85% phosphoric acid) was added to the polysaccharide solution (0.5 ml, 2 mg/ml). Abs at 595 nm was determined using a spectrophotometer following agitation. The protein content was determined by substituting Abs into a standard curve.

Antioxidant Activity of Crude Exopolysaccharides

The 1,1-diphenyl-2-pyridyl-hydrazine (DPPH) assay was used to investigate the antioxidant activity of EPSs (Kao and Chen, 2006) and the total antioxidant capacity (TAC) (Dilna et al., 2015), as shown in **Figure 1**.

1,1-Diphenyl-2-Pyridyl-Hydrazine Free Radical Scavenging Assay

The ability of EPS to scavenge DPPH radicals was determined using the procedures described by Kao and Chen (2006). Five millimeters of 0.02 methanolic DPPH radical solution was added to 5 ml of various EPS concentrations (0.625–20 mg/ml). For 30 min, the reaction mixture was kept in a darkroom. The Abs of the mixture was determined spectrophotometrically at 517 nm using a Spectrophotometer UV-visible 2401PC (Shimadzu, Japan). Three times for each measurement, the means and standard deviations (SD) were computed. The following equation was used to determine the capacity to scavenge the DPPH radical:

$$\text{Free radical scavenging\%} = [1 - (\text{Ac} - \text{As})/\text{Ac}] \times 100.$$

Ac, Absorbance of control (all reagents except the checked substance is replaced by distilled water).

As, Absorbance of the sample/standard.

Ascorbic acid has traditionally been utilized as a free radical scavenger.

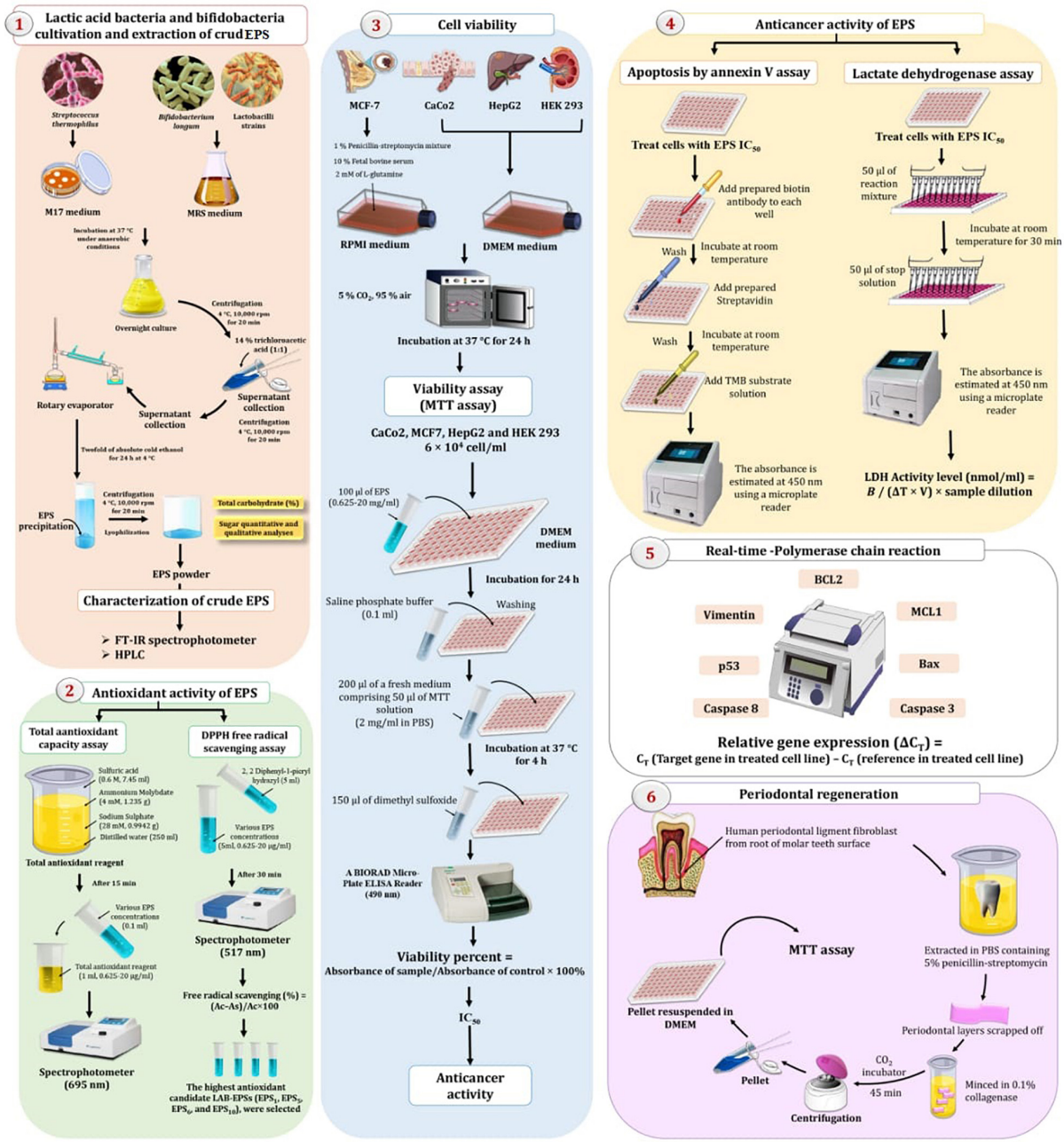

Figure 1 | Experimental setup for extraction and characterization of exopolysaccharides (EPS) by lactic acid bacteria (LAB) and bifidobacteria (Bb) exploring their therapeutic potentials.

Total Antioxidant Capacity Assay

The TAC of the EPS samples was determined as described by Dilna et al. (2015). To make the TAC reagent, mix 7.45 ml sulfuric acid (0.6 M), 1.235 g ammonium molybdate (4 mM), and 0.9942 g sodium sulfate (28 mM) in 250 ml distilled water. After 15 min, 0.1 ml of various EPS concentrations (0.625–20 mg/ml) were dissolved in 1 ml of total antioxidant reagent, and the Abs at 695 nm was measured with a spectrophotometer. Ascorbic acid served as a control substance. Additionally, the most antioxidant-potent candidate EPSs (EPS_1, EPS_5, EPS_6, and EPS_{10}) were chosen for future investigation.

Cytotoxicity Assay

The 3-(4,5-dimethylthiazol-2-yl)-2,5-diphenyltetrazolium-bromide (MTT) test was used to assess cytotoxicity (Sigma Aldrich, St. Louis, MO, United States), as previously described by Manivasagan et al. (2013) and Khalil et al. (2022). The cells (100 µl, MCF7, CaCo2, and HepG2) were seeded at a

density of 6×10^4 cells/ml in 96-well microplates and treated with EPS_1, EPS_5, EPS_6, and EPS_{10} at various concentrations (0.625–20 mg/ml). The optical density of the formazan solution was determined using a BIORAD Micro-Plate ELISA Reader at 490 nm. Additionally, to ensure that the extracted EPSs are safe for normal cells, their inhibitory effects on the normal HEK 293 cell line were determined. Because MTT decreases only in metabolically active cells, activity is a proxy for cell viability. The EPS extracts were tested in triplicate on the five cell lines, and the viability of the cells was estimated using the following equation: Viability % = Absorbance of sample/Absorbance of control × 100. According to El-Deeb et al. (2018) and Khalil et al. (2022), the IC_{50} values for EPS were calculated using the graphpad prism 9 program and indicate a 50% reduction in growth when compared to control cells (untreated cells).

Antitumor Activity

The annexin V test and the amount of lactate dehydrogenase (LDH) leaking out of the cell were used to determine the antitumor activity of EPSs (Gurunathan et al., 2013), as represented in **Figure 1**.

Apoptosis Assessment

According to the manufacturer's instructions, all cell lines exhibited apoptosis as determined by a human Annexin V platinum ELISA (eBioscience BMS252/BMS252TEN; Thermo Fisher Scientific, Waltham, MA, United States). For 24 h in a humidified incubator at 37°C and 5% CO_2, cell lines were grown in 96-well flat-bottom culture plates with the IC_{50} concentrations of EPS_1, EPS_5, EPS_6, and EPS_{10}. This assay is based on the fact that human Annexin V present in the sample or standard will bind to the Microwell Plate coating antibodies. As a result, a biotin-conjugated anti-human Annexin V antibody was added, which specifically recognizes the human Annexin V captured by the first antibody. Following incubation, all unbound biotin-conjugated anti-human Annexin V antibody was removed during the washing step. Streptavidin horseradish peroxidase (HRP) was used, which reacts with an anti-human Annexin V antibody conjugated to biotin. It is possible to create a colored substance that is proportional to the amount of human Annexin V in the sample or standard. After adding acid to terminate the reaction, the Abs at 450 nm is measured using a microplate reader. For the standard curve preparation, seven human Annexin V standard dilutions and seven human Annexin V sample concentrations were calculated.

Lactate Dehydrogenase Assay

The amount of LDH leaking out of EPS-treated cell lines was used to determine the plasma membrane integrity (Gurunathan et al., 2013). The cells were exposed to various EPSs at their IC_{50} concentrations for 24 h. LDH activity was determined in the culture after 3 h of incubation under standard conditions (K726-500) according to the manufacturer's instructions (Biovision, Mountain View, CA, United States). The quantification of LDH is based on the color change caused by the reduction of NAD to NADH by 450 nm of LDH using a microplate reader. The activity of LDH was determined according to the following equations; LDH Activity level (nmol/ml) = $\mathbf{B}/(\Delta T \times \mathbf{V}) \times$ sample dilution; where $\boldsymbol{B}$ is the amount of NADH produced from ΔT (T2 - T1), **T1** is the time of first reading (A1) (in min), **T2** is the time of second reading (A2) (in min), and **V** is the volume of pretreated sample added into the reaction well (in ml).

Characterization of Crude LAB-EPS_5

Fourier transform infrared (FT-IR) spectroscopy was used to determine the major structural groups of the selected EPS_5. The KBr technique was used to determine the EPS spectrum. Polysaccharide samples were crushed into KBr pellets at a sample ratio of 1:100. The infrared Fourier transform spectra were acquired using a Bruker Tensor 27 instrument with a resolution of 4 cm^{-1} in the range 4,000–400 cm^{-1} (Fontana et al., 2015). The monosaccharide content of EPS_5 was determined using high-performance liquid chromatography (HPLC) as described by Yang et al. (2012). Briefly, the rehydrated EPS_1 and EPS_5 samples were derivatized with 1-phenyl-3-methyl-5-pyrazolone and analyzed by HPLC using a four-unit pump (Agilent Technologies, Wilmington, DE, United States) and a Shim-Pak VPODS column (4.6 × 150 mm) with Abs monitoring at 245 nm. An integrator was used to compare different sugar standards to the EPS sample's retention time.

Gene Expression Analysis

RNA was isolated from all cancer cell lines using a MagJET RNA purification kit, either untreated (negative control) or 24 h after treatment with EPS_5 IC_{50}. The quality and quantity of extracted RNAs were determined using 1% agarose gel electrophoresis and Nanodrop (Thermo Fisher Scientific, Inc., Wilmington, DE, United States). Quantitative real-time (qRT)-PCR was performed according to the manufacturer's protocol using the Sybr Green Supermix RT-PCR kit, forward and reverse primers for each gene (**Supplementary Table 1**), and SYBR green PCR master mixture. The genes *BCL2*, *MCL1*, *Bax*, *Caspase 3*, *Caspase 8*, *Vimentin*, and *p53* were normalized with the housekeeping gene (GAPDH) and expressed about untreated cells. Following amplification, the obtained data were analyzed using the formula for relative gene expression (Winner et al., 1999; Livak and Schmittgen, 2001).

Determination of the Proliferative Effect

Human periodontal ligament fibroblast cells (hPDLFCs) were extracted and grown according to Arslan and Kantarcioglu (2019). The Clinical Study Ethics Committee of Taif University accepted the research on an ethical basis. To examine the impact of various EPS_5 concentrations on viability, hPDLFCs were plated of 1×10^4 cells/well in 96-well plates, and viability was assessed using the MTT assay.

Statistical Analysis

Minitab statistical software (17.1.0.0, Minitab Inc., Chicago, IL, United States) and GraphPad Prism version were used to interpret and process the data (9.0.0). To assess LDH activity and relative gene expression, the means of the groups were compared using an unpaired *t*-test. However, ANOVA single factor was used to analyze the synthesis of crude EPS by different

probiotic bacterial strains and antioxidant activities of EPS. All measurements are presented as means ± SD. The one-way ANOVA test for variance was used to compare two or more groups, and the Tukey test was used for multiple comparisons. A p-value less than 0.05 was considered significant.

RESULTS

Table 1 depicts the production of EPSs by LAB and Bb, as well as their carbohydrate and protein contents. The amount of EPS produced by various bacterial strains varied significantly ($p < 0.05$). The EPS derived from bacteria ranged from 174.9 to 295.4 mg/l. *L. delbrueckii* ssp. *bulgaricus* DSM 20081^T produced the most EPS (EPS_5, 295.4 ± 9.7), while *L. plantarum* DSM 20174 produced the least (EPS_9, 174.9 ± 5.2). The carbohydrate and protein content of crude EPS varied with strain ($p < 0.05$). The total carbohydrate content ranged from 85.0 to 96.7%, while the protein content ranged from 3.3 to 9.3%. The average carbohydrate level for EPS_5 is significantly higher (96.7 ± 0.3%) than for the other strains ($p < 0.05$). Furthermore, in the final lyophilized crude EPS samples, *S. thermophiles* DSM 24731-EPS_1 had the lowest concentration of protein contamination.

As shown in **Tables 2**, **3**, the antioxidant capabilities of crude EPSs from 10 bacterial strains were evaluated *in vitro* by evaluating the activity of radical scavengers (DPPH and TAC, respectively). The DPPH free radical scavenging potential of various EPS concentrations increased significantly concentration-dependently ($p < 0.05$) (**Table 2**). At 20 mg/ml, the capacity of EPS to scavenge DPPH radicals ranged from 33.3% to 77.0%. *S. thermophiles* DSM 24731-EPS_1 had the highest scavenging rate of all strains, at 77%, followed by *L. delbrueckii* ssp. *bulgaricus* DSM 20081^T-EPS_5, *B. longum* DSM 200707-EPS_{10}, and *L. fermentum* DSM 20049-EPS_6. *L. acidophilus* DSMZ 20079^T-EPS_7 had the least amount of scavenging activity (**Table 2**). The ability of a non-enzymatic antioxidant defense mechanism is represented by TAC. **Table 3** shows that the antioxidant capacity ranged between 0.75 and 2.5%; the highest rate of inhibition was 2.5% for *L. delbrueckii* ssp. *bulgaricus* DSM 20081^T-EPS_5, followed by *S. thermophiles* DSM 24731-EPS_1, *L. fermentum* DSM 20049-EPS_6, and *B. longum* ssp. *longum* DSM 200707-EPS_{10}, all of which had comparable degrading capabilities, and *L. acidophilus* DSM 20079 ^{T}-EPS_7 had the lowest rate of inhibition at 23.95%. Because EPS_1, EPS_5, EPS_6, and EPS_{10} exhibited significantly greater antioxidant activity than other EPSs tested, they were chosen for subsequent assays in this study.

TABLE 1 | Production of crude EPS by different LAB and Bb strains.

EPS	EPS yield (mg/l)	Total carbohydrates content (%)	Protein content (%)
Streptococcus thermophilus DSM 24731-EPS_1	240.0 ± 3.3^a	93.0 ± 0.4^a	3.3 ± 0.1^a
Lactobacillus lactis ssp. *cremoris* DSM 20069^T-EPS_2	189.72 ± 3.4^b	89.1 ± 0.08^b	7.4 ± 0.2^b
Lacticaseibacillus casei DSM 27537-EPS_3	245.6 ± 3.2^a	85.0 ± 0.1^c	9.3 ± 0.2^c
Lactobacillus delbrueckii ssp. *bulgaricus* DSM 20080-EPS_4	222.4 ± 7.1^c	93.1 ± 0.3^a	8.3 ± 0.3^d
Lactobacillus delbrueckii ssp. *bulgaricus* DSM 20081^T-EPS_5	295.4 ± 9.7^d	96.7 ± 0.3^d	4.3 ± 0.2^e
Limosilactobacillus fermentum DSM 20049-EPS_6	255.3 ± 4.3^e	95.1 ± 0.1^e	6.1 ± 0.2^f
Lactobacillus acidophilus DSM 20079^T-EPS_7	213. 4 ± 4.2^c	91.4 ± 0.4^f	7.3 ± 0.1^b
Lacticaseibacillus rhamnosus DSM 20021-EPS_8	214.5 ± 4.1^c	92.1 ± 0.4^f	5.5 ± 0.2^g
Lactiplantibacillus plantarum ssp. *plantarum* DSM 20174-EPS_9	174.9 ± 5.2^f	87.5 ± 0.2^g	6.6 ± 0.1^h
Bifidobacterium longum ssp. *longum* DSM 200707-EPS_{10}	260. 3 ± 7.1^e	94.1 ± 0.4^a	5.7 ± 0.1^g

EPS, exopolysaccharide.
Means in the same column followed by different letters are significantly different at $p < 0.05$.

TABLE 2 | Antioxidant activities (%) of EPS derived from LAB and Bb using DPPH radical scavenging assay.

EPS	DPPH scavenging rate (%) for different concentrations (mg/ml) of bacterial EPS					
	0.625	1.25	2.5	5.0	10.0	20
S. thermophilus DSM 24731-EPS_1	0.00 ± 0.00^a	14.3 ± 1.3^a	31.3 ± 1.2^a	41.8 ± 1.36^a	56.4 ± 2.78^a	77.0 ± 3.87^a
L. lactis ssp. *cremoris* DSM 20069^T-EPS_2	0.00 ± 0.00^a	10 ± 0.5^b	18.0 ± 0.8b	24.4 ± 1.3^b	27.6 ± 1.78^b	34.5 ± 1.98^b
L. casei DSM 27537-EPS_3	10.05 ± 0.98^b	11.04 ± 0.98^b	12.0 ± 1.34^c	19.0 ± 1.98^c	25.5 ± 1.4^c	35.5 ± 1.8^b
L. delbrueckii ssp. *bulgaricus* DSM 20080-EPS_4	17.10 ± 1.20^c	33.2 ± 2.78^c	37.8 ± 2.01^d	48.5 ± 2.67^d	50.4 ± 2.3^a	56.3 ± 2.2^c
L. delbrueckii ssp. *bulgaricus* DSM 20081^T-EPS_5	10.02 ± 2.13^b	17.15 ± 2.67^a	22.4 ± 1.43^e	44.1 ± 2.54^{ad}	65.0 ± 3.87^d	75.2 ± 2.67^a
L. fermentum DSM 20049-EPS_6	16.04 ± 0.43^c	17.06 ± 2.5^a	18.0 ± 0.78^b	29.1 ± 1.7^e	55.1 ± 1.5^a	60.2 ± 2.00^c
L. acidophilus DSM 20079^T-EPS_7	14.03 ± 0.92^d	17.08 ± 2.54^a	23.0 ± 2.5^e	30.0 ± 2.02^e	33.0 ± 1.9^e	33.3 ± 2.45^b
L. rhamnosus DSM 20021-EPS_8	10.02 ± 0.98^b	11.01 ± 1.67^b	12.0 ± 2.1^e	19.1 ± 1.78^c	25.5 ± 2.3^{bc}	35.5 ± 2.02^b
L. plantarum ssp. *plantarum* DSM 20174-EPS_9	13.10 ± 0.78^d	14.06 ± 2.99^a	21.6 ± 2.0^e	24.02 ± 2.88^b	35.2 ± 2.65^e	50.4 ± 2.78^d
B. longum ssp. *longum* DSM 200707-EPS_{10}	14.5 ± 2.24^{cd}	23.04 ± 2.67^d	31.4 ± 1.34^a	42.0 ± 1.98^a	54.0 ± 3.87^a	65.3 ± 2.99^e

EPS, exopolysaccharide; DPPH, 2, 2 diphenyl-1-picrylhydrazyl.
Each result is three times the mean ± SD. Means in the same column followed by different letters are significantly different at $p < 0.05$.

TABLE 3 | Antioxidant activities (%) of EPS derived from LAB and Bb using total antioxidant capacity (TAC) scavenging assay.

EPS	Total antioxidant capacity (%) for different concentrations (mg/ml) of bacterial EPS					
	0.625	1.25	2.5	5	10	20
S. thermophilus DSM 24731-EPS_1	0.41 ± 0.1^{a}	0.75 ± 0.3^{a}	0.82 ± 0.5^{a}	0.87 ± 0.1^{a}	1.42 ± 0.1^{a}	2.1 ± 0.2^{a}
L. lactis ssp. *cremoris* DSM 20069^{T}-EPS_2	0.2 ± 0.1^{b}	0.3 ± 0.1^{b}	0.52 ± 0.1^{a}	0.64 ± 0.1^{b}	0.8 ± 0.1^{b}	1.0 ± 0.1^{b}
L. casei DSM 27537-EPS_3	0.3 ± 0.2^{ab}	0.42 ± 0.1^{ab}	0.63 ± 0.2^{a}	$0.73 \pm 0.1a^{b}$	0.85 ± 0.2^{b}	1.3 ± 0.1^{c}
L. delbrueckii ssp. *bulgaricus* DSM 20080-EPS_4	0.37 ± 0.2^{ab}	0.4 ± 0.3^{ab}	0.55 ± 0.1^{a}	$0.65 \pm 0.2a^{b}$	0.73 ± 0.3^{b}	0.8 ± 0.1^{b}
L. delbrueckii ssp. *bulgaricus* DSM 20081^{T}-EPS_5	1.21 ± 0.1^{c}	1.47 ± 0.2^{c}	1.64 ± 0.1^{b}	1.75 ± 0.3^{c}	1.8 ± 0.2^{c}	2.5 ± 0.1^{d}
L. fermentum DSM 20049-EPS_6	1.1 ± 0.1^{c}	1.3 ± 0.2^{c}	1.5 ± 0.2^{b}	1.62 ± 0.3^{c}	1.73 ± 0.1^{c}	1.87 ± 0.3^{a}
L. acidophilus DSM 20079^{T}-EPS_7	0.23 ± 0.1^{ab}	0.35 ± 0.1^{ab}	0.45 ± 0.2^{a}	0.5 ± 0.2^{b}	0.64 ± 0.3^{b}	0.75 ± 0.2^{b}
L. rhamnosus DSM 20021-EPS_8	0.1 ± 0.1^{b}	0.21 ± 0.1^{b}	0.47 ± 0.1^{a}	0.6 ± 0.2^{ab}	0.8 ± 0.3^{b}	0.9 ± 0.2^{b}
L. plantarum ssp. *plantarum* DSM 20174-EPS_9	0.3 ± 0.2^{ab}	0.4 ± 0.2^{ab}	0.6 ± 0.1^{a}	0.73 ± 0.1^{ab}	0.9 ± 0.1^{b}	1.23 ± 0.1^{c}
B. longum ssp. *longum* DSM 200707-EPS_{10}	0.5 ± 0.2^{a}	0.8 ± 0.2^{a}	1.1 ± 0.2^{b}	1.4 ± 0.1^{c}	1.55 ± 0.3^{ac}	1.73 ± 0.2^{a}

EPS, exopolysaccharide.
Means in the same column followed by different letters are significantly different at $p < 0.05$.

As illustrated in **Figure 2**, MCF7, CaCo2, and HepG2 cells all responded differently to the MTT cytotoxicity experiment. All of the EPSs inhibited cells in a concentration-dependent manner, with varying effects on various cell lines. After 24 h of treatment with the highest doses (20 mg/ml) of EPS_1, EPS_5, EPS_6, and EPS_{10}, the viability percentages for HEK 293 cells were 93.07, 96.3, 93.05, and 90.07 mg/ml, respectively (**Figure 2A**); MCF7 cells were 55.9, 52.1, 85.52, and 75.01 mg/ml, respectively (**Figure 2B**); CaCo2 cells were 68.69, 67.0, and 87.59 mg/ml, respectively (**Figure 2C**) and HepG2 cells were 62.0, 59.5, 83.86, and 72.66 mg/ml, respectively (**Figure 2D**). As indicated in **Figure 2A**, the impact of the chosen EPSs on viability (%) of HEK 293 cells showed that at 0.625 mg/ml (98.9%), the viability rate of HEK 293 cells was not significantly different ($p = 0.1340$). When the growth rate of HEK 293 cells was compared to that of cells treated with EPS at doses of 0.125 mg/ml ($p = 0.0027$), 2.5 mg/ml ($p = 0.0021$), 5 mg/ml ($p = 0.0090$), 10 mg/ml ($p = 0.0037$), and 20 mg/ml ($p = 0.0012$), a significant difference was observed. At 20 mg/ml, MCF7 viability decreased by more than 30% as compared to control viability, a significant difference of $p = 0.0066$. On the other hand, at EPSs concentrations of 0.625 ($p = 0.1340$), the MCF7 viability rate was not significantly different (**Figure 2B**). A significant difference was detected when the CaCo2 viability% of the control was compared to cells treated with EPSs concentrations of 5 mg/ml ($p = 0.0022$), 10 mg/ml ($p = 0.0019$), and 20 mg/ml ($p = 0.0038$) (**Figure 2C**). When the HepG2 viability% of the control was compared to cells treated with EPSs doses of 2.5 mg/ml ($p = 0.0007$) and 5 mg/ml ($p = 0.0010$), a very significant difference was seen (**Figure 2D**). Generally, according to the obtained data for EPS_1 and EPS_5, the extract's potency was in the order MCF7 > HepG2 > CaCo2 at various concentrations; however, EPS_6 and EPS_{10} had a strong inhibitory rate in the order HepG2 > MCF7 > CaCo2. Furthermore, EPSs were found to have a minimal cytotoxic effect on HEK 293 cells. According to the findings, EPS greatly reduced the viability of different cancer cells while having no impact on normal cells.

As shown in **Figure 3**, the IC_{50} values of EPS_1, EPS_5, EPS_6, and EPS_{10}, for MCF7 cells were 8.06, 7.91, 22.97, and 12.36 mg/ml, respectively; for CaCo2, they were 10.69, 11.22, 25.85, and 15.23 mg/ml, respectively; and for HepG2 cells, they were 9.12, 9.37, 20.40, and 12.54 mg/ml, respectively. EPS_5 had the most active components and exhibited the highest cytotoxicity with the lowest IC_{50} values on MCF7, CaCo2, and HepG2 (7.91, 10.69, and 9.12 mg/ml, respectively). EPS_6, on the other hand, had the highest IC_{50} values against MCF7, CaCo2, and HepG2 at 12.36, 15.23, and 12.54 mg/ml, respectively. It is worth noting that untreated control cells retained a high viability. While EPS decreased the viability of normal HEK 293, their IC_{50} values of 29.26–85.7 mg/ml were significantly greater than those of cancerous cells (**Figure 3**). These results demonstrated that different EPSs may have a significant influence on EPS biological activities and that the inhibitory feature differed with human cell strains and produced severe cytotoxicity at large doses.

Annexin V has been shown to attach to apoptotic phosphatidylserine-releasing cells and decrease their pro-coagulant and pro-inflammatory activity. The obtained results showed that cellular apoptosis was triggered in MCF7, CaCo2, and HepG2-treated cells following the IC_{50} value treatment of the selected crude EPSs, as shown in **Figure 4**. In MCF7, CaCo2, and HepG2 cells treated with EPS_5-IC_{50} values, the greatest Annexin V quantities (18.4, 10.28, and 16.30 ng/ml, respectively) were observed in comparison to other EPS treatments. On the other hand, apoptosis assays after EPS_6 treatment revealed that total endogenous Annexin V levels were low in a variety of cancer cells, suggesting that EPS_6 is an ineffective anticancer agent. Generally, the total endogenous Annexin V levels in cells treated with various EPSs indicated that the concentrations of Annexin V were not significantly different ($p = 0.2002$, 0.1077, 0.7084, and 0.5011) in cells treated with EPS_1, EPS_5, EPS_6, and EPS_{10} compared to control cells (untreated) (**Figure 4**).

The quantity of LDH released, a soluble cytoplasmic enzyme, was utilized to determine the degree of degradation and leakage in cell membranes impacted by the IC_{50} of EPS_1, EPS_5, EPS_6, and EPS_{10} (**Figure 5**). Regarding MCF7, LDH activity in EPS_1 and EPS_5-treated cells significantly increased by 2.36 and 2.58 times, respectively, related to the control (untreated) MCF7 cells ($p < 0.0001$) as illustrated in **Figure 5**.

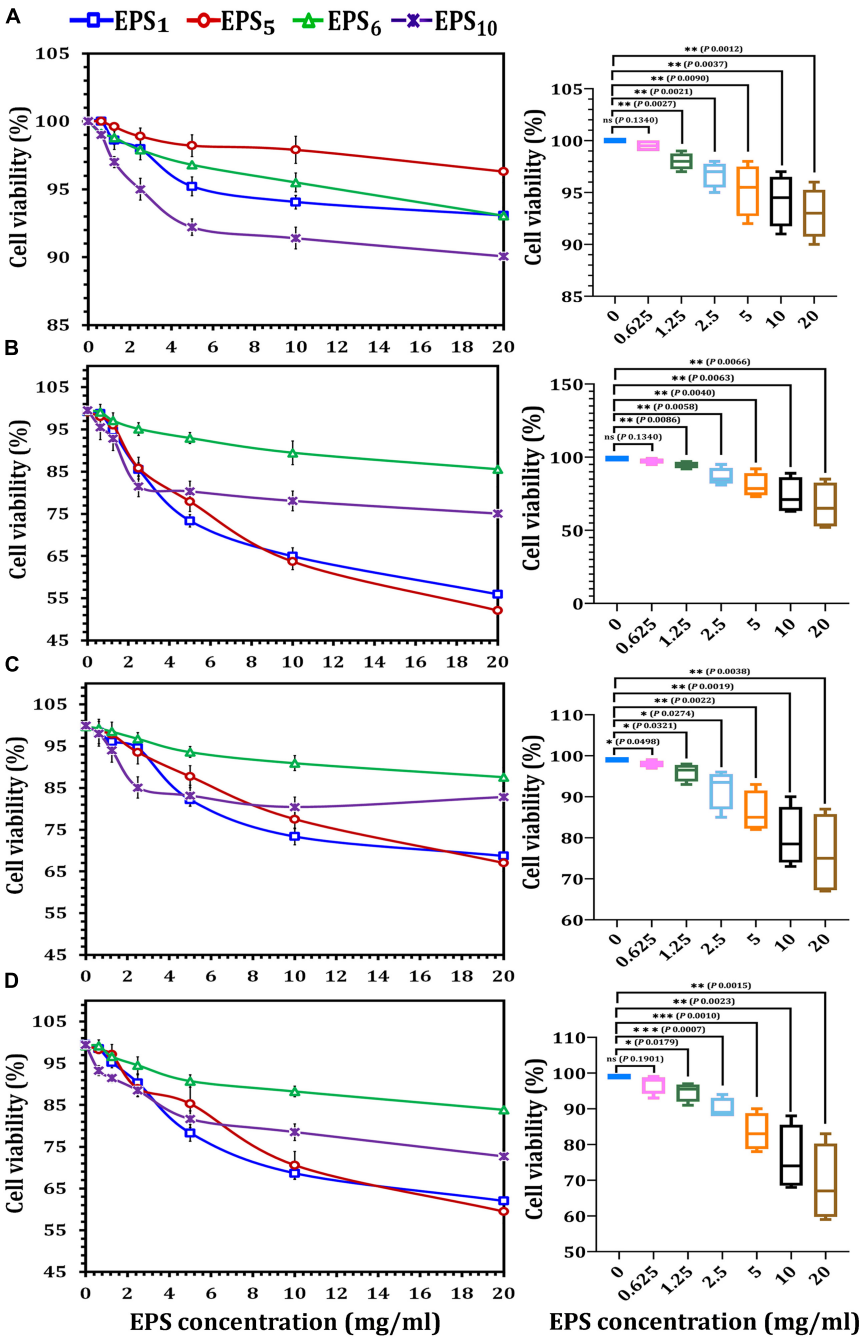

Figure 2 | Cytotoxicity assessments of exopolysaccharides on different cancer cell lines using MTT assay. **(A)** On HEK293 cell line, **(B)** on MCF7 cell line, **(C)** on CaCo2 cell line, and **(D)** on HepG2 cell line. EPS_1, EPS derived from *S. thermophilus* DSM 24731; EPS_5, EPS derived from *L. delbrueckii* ssp. *bulgaricus* DSMZ 20081^T; EPS_6, EPS extracted from *L. fermentum* DSMZ 20049, and EPS_{10}, EPS derived from *B. longum* ssp. *longum* DSMZ 200707.

Furthermore, in the case of CaCo2, LDH activity increased by 2.85- and 3.02-fold, respectively, in the cells treated with IC_{50} values of each EPS_1 and EPS_5 relative to the untreated CaCo2 cells. LDH activity was highest (670 nmol/ml) in HepG2 cells treated with EPS_5. As illustrated in **Figure 5**, EPS_5 had a considerably higher LDH activity than EPS_1 (p = 0.0001), followed by EPS_{10} and EPS_6. In comparison to the control cell, LDH leakage concentrations in MCF7 cells treated with various EPSs varied significantly (p = 0.0202). In general, EPS_5 demonstrated significant antitumor activity in the three types of cell lines analyzed in our research, based on the data obtained on the antitumor abilities of the tested EPSs. As a result, EPS_5 will be further characterized and used in the following biological applications.

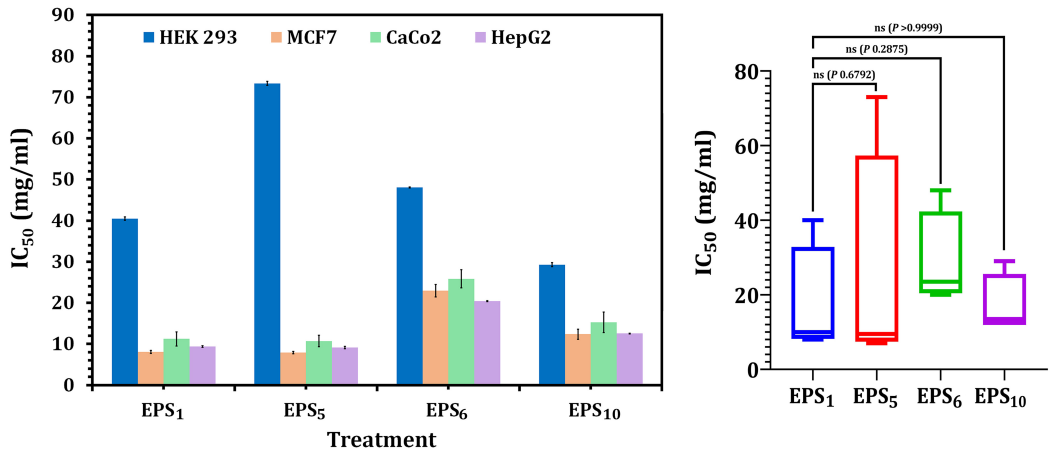

Figure 3 | Cytotoxicity of EPSs against HEK293, MCF7, CaCo2, and HepG2 using MTT assay. EPS_1, EPS derived from *S. thermophilus* DSM 24731; EPS_5, EPS derived from *L. delbrueckii* ssp. *bulgaricus* DSMZ 20081^T; EPS_6, EPS extracted from *L. fermentum* DSMZ 20049, and EPS_{10}, EPS derived from *B. longum* ssp. *longum* DSMZ 200707.

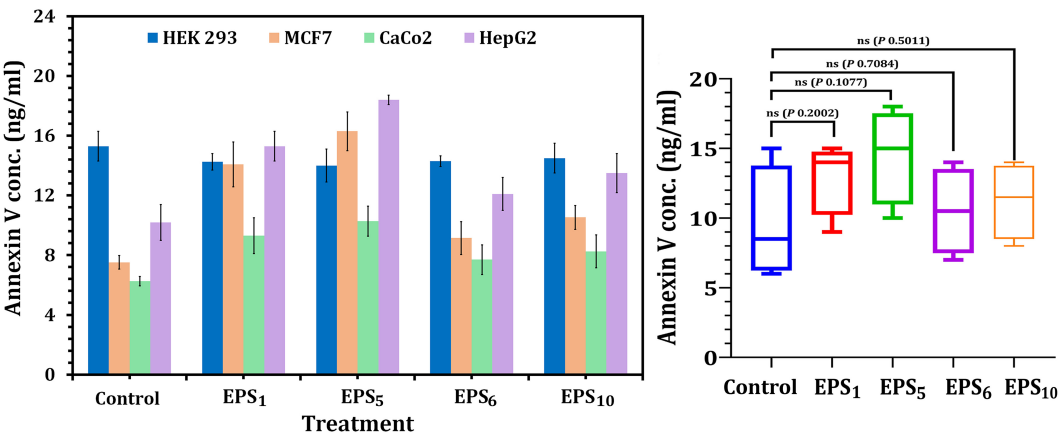

Figure 4 | Apoptosis assessment using annexin V ELISA kit on cancer cell lines. EPS_1, EPS derived from *S. thermophilus* DSM 24731; EPS_5, EPS derived from *L. delbrueckii* ssp. *bulgaricus* DSMZ 20081^T; EPS_6, EPS extracted from *L. fermentum* DSMZ 20049, and EPS_{10}, EPS derived from *B. longum* ssp. *longum* DSMZ 200707.

Fourier transform infrared analysis showed a variation in the functional groups formed in EPS_5, as shown in **Figure 6**. There were eight absorbance bands in the FT-IR spectrum of EPS_5; 3410, 2931, 2502, 1650, 1381, 1136, 872, 620, and 530 cm^{-1}. **Table 4** displays the retention period, area under the curve, and monosaccharide composition of EPS_5 samples as measured by HPLC. The EPS samples' sugar content varied substantially ($p < 0.05$). EPS_5 included a high concentration of sugars such as rhamnose, mannose, ribose, glucose, and galactose. The sugar concentrations in EPS_5 varied from 1.7938 to 38.8584 mg/100 g, with galactose being the greatest concentration. The ratio of ribose, rhamnose, glucose, mannose, and galactose in EPS_5 was 1:2.7:7.4:5.1:12.5. Consequently, the EPS_5 samples were heteropolysaccharides based on their sugar content.

For 24 h, we used quantitative real-time PCR to determine the mRNA levels of apoptotic and cell cycle-related genes in response to the IC_{50}-EPS_5 value (**Figure 7**). The data of gene expression revealed that EPS_5 with IC_{50} value was significantly upregulated *Bax* gene expression in CaCo2 cells ($p = 0.0065$) compared with that in control (**Figure 7A**). However, a marked reduction in expression of the *BCL2* and *MCL1* ($p = 0.0001$) genes were observed in treated CaCo2 cells (**Figure 7A**). Additionally, the results indicated that EPS_5 administration increased the expression of apoptotic genes *Caspase 3* and *Caspase 8*. The most significant upregulation of the *p53* gene was detected in CaCo2 cells treated with IC_{50}-EPS_5 ($p = 0.0001$). In comparison, the least significant upregulation of the *Bax* gene was found in MCF7 cells treated with the same concentration of EPS_5 ($p = 0.0002$) (**Figure 7B**). Additionally, in the treated MCF7 cells, *BCl2*, *MCL1*, and *Vimentin* genes observed a downregulation at their expression level ($p < 0.0001$). However, the *Caspase 3*, *Caspase 8*, and *Bax* genes recorded upregulation of expression (**Figure 7B**). As demonstrated in **Figure 7C**, *BCL2* expression was strongly downregulated in treated HepG2 cells, as has been the

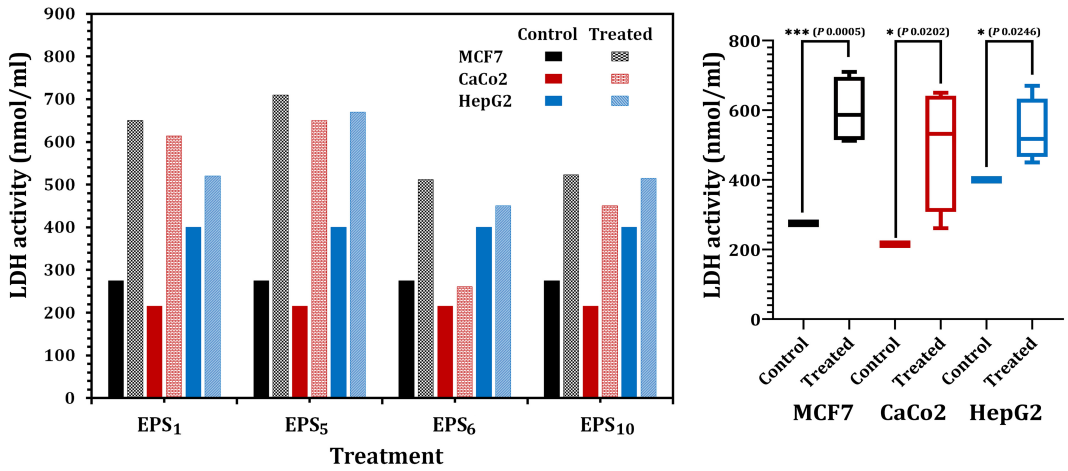

Figure 5 | Lactate dehydrogenase (LDH) activity in MCF7, CaCo2, and HepG2 treated with different EPSs. EPS_1, EPS derived from *S. thermophilus* DSM 24731; EPS_5, EPS derived from *L. delbrueckii* ssp. *bulgaricus* DSMZ 20081^T; EPS_6, EPS extracted from *L. fermentum* DSMZ 20049, and EPS_{10}, EPS derived from *B. longum* ssp. *longum* DSMZ 200707.

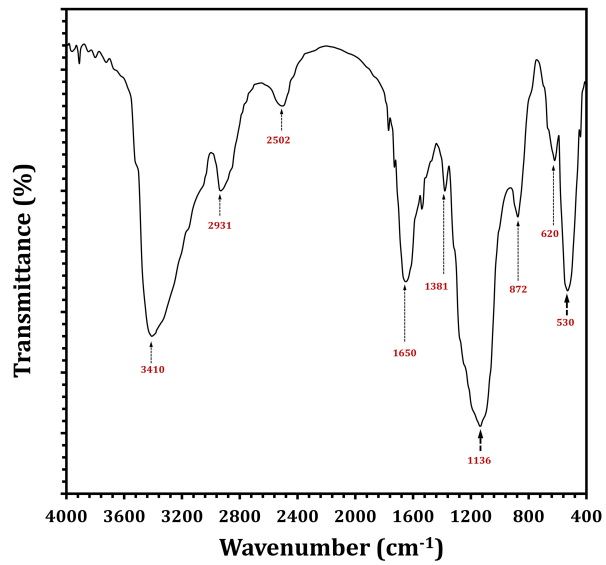

Figure 6 | FTIR spectra of *L. delbrueckii* ssp. *bulgaricus* DSM 20081^T-derived EPS_5.

TABLE 4 | Determination of monosaccharide composition of *L. delbrueckii* ssp. *bulgaricus* DSM 20081^T-EPS_5 using HPLC.

Monosaccharides	EPS_5	
	RT	Area under curve
Ribose	8.788	1.6
Rhamnose	13.66	1.06
Glucose	16.067	1.34
Mannose	17.092	4.81
Galactose	18.058	6.52

RT, retention time.

case with *MCL1* and *Vimentin* expression, dramatically lowering the levels of the studied genes relative to control (p = 0.0001). EPS_5, on the other hand, resulted in a significant increase in the expression of p53 (12.04) as compared to the control (p = 0.0001) but had no influence on *Bax* expression.

Cultured hPDLFCs were successfully extracted from healthy molar teeth (**Figure 8**). After 24 h of co-incubation with various concentrations of crude EPS_5, cell viability was determined using the MTT assay. As illustrated in **Figure 9**, the viability of hPDLFCs was significantly increased following exposure to crude EPS. When hPDLFCs were treated with EPSs at a concentration of 0.625 mg/ml, the viability rate was not significantly different from that of untreated cells (p = 0.1583). When the viability percent of untreated hPDLFCs was compared to cells treated with 2.5 mg/ml (p = 0.0003) and 5 mg/ml (p = 0.0003) EPSs, a significant difference (p = 0.0001) was observed (**Figure 9**).

DISCUSSION

In this study, LAB (n = 9) and Bb (n = 1) were used to extract EPS, and their EPS yield was determined. The EPS obtained demonstrated a high degree of concentration- and strain-dependent variation (p < 0.05). When compared to other tested strains, *L. delbrueckii* ssp. *bulgaricus* DSM 20081^T produced the most EPS (295.49 ± 0.7). Tukenmez et al. (2019) reported that *L. delbrueckii* ssp. *bulgaricus* B3 produced the highest amount of EPS (449.0 ± 0.4 mg/l). According to Sungur et al. (2017), two strains of *L. gasseri* produced 242 and 255 mg/l of EPS. *Bifidobacterium bifidum* WBIN03 produced EPS at a concentration of 241.20 mg/l, whereas *L. plantarum* R315 produced EPS at a concentration of 290.17 mg/l (Li S. et al., 2014).

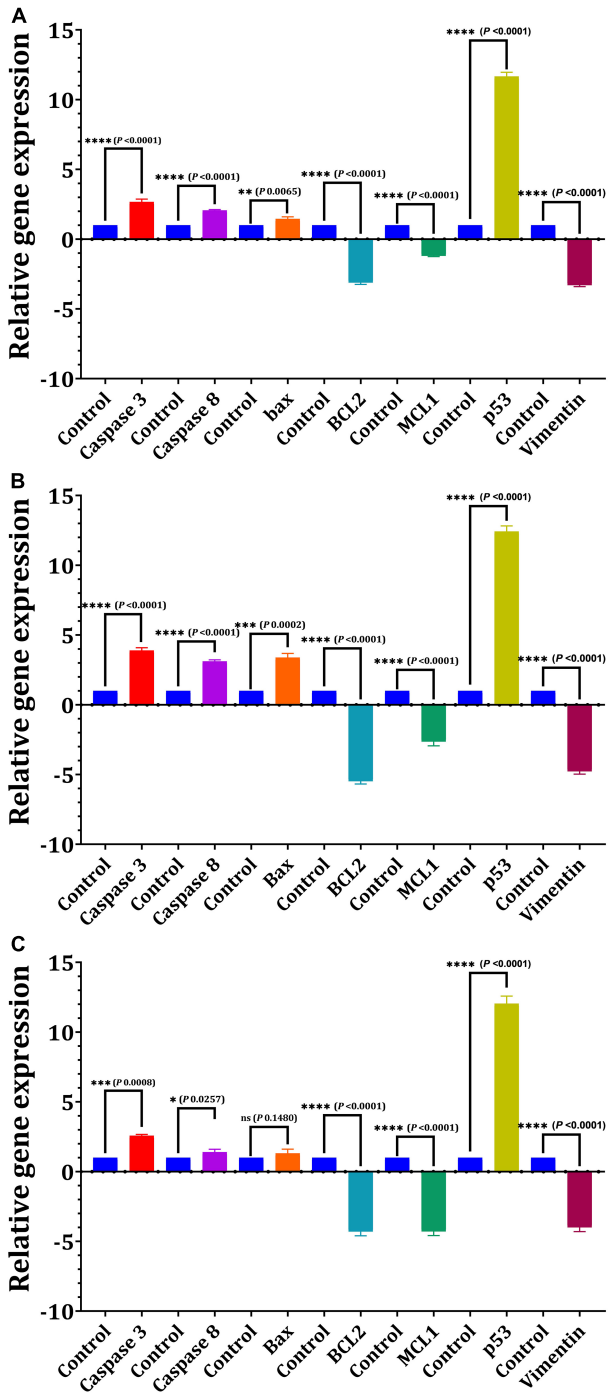

Figure 7 | Effect of *L. delbrueckii* subsp. *bulgaricus* DSM 20081^T-EPS$_5$ on the relative expression of genes linked to apoptosis in different cell lines. **(A)** MCF7, **(B)** CaCo2, **(C)** HepG2.

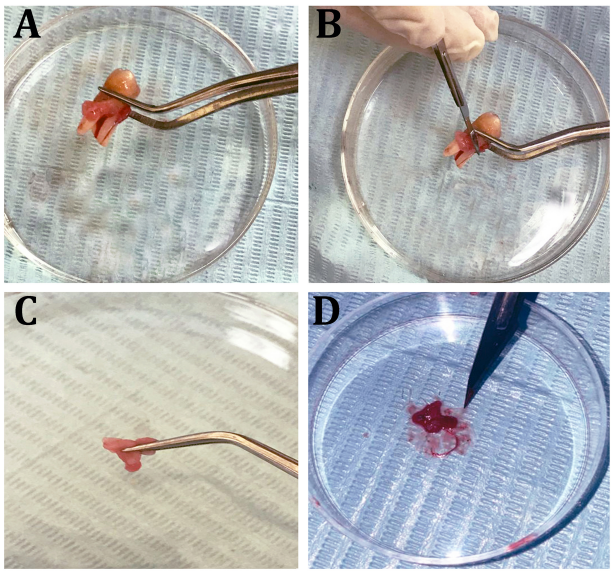

Figure 8 | Isolation steps of human periodontal ligament fibroblast cells (hPDLF). **(A)** Healthy molar tooth, **(B)** scraping periodontal layers, **(C,D)** mincing of the periodontal membrane.

Reactive oxygen species (ROS) and oxygen-centered free radicals are byproducts of a number of metabolic and physiological processes in the body (Thibessard et al., 2004). Increased levels of ROS degrade proteins, DNA, and lipids, causing additional tissue damage and organ dysfunction. This causes serious side effects in humans, such as carcinoma, arteriosclerosis, osteoarthritis, and neurodegeneration (Li C. et al., 2014). Antioxidants are substances that prevent or postpone oxidation. Tumor cells produce ROS as a result of increased metabolic activity and a variety of other tumorigenic processes, which promotes tumor cell proliferation and survival, mesenchymal migration and penetration, genetic mutations, and angiogenesis. Antioxidant-based therapy that reduces ROS generation may be used to delay or even prevent tumor development (Liou and Storz, 2010; Gurunathan et al., 2013). Numerous research have been conducted on EPS derived from probiotic bacteria, which may possess antioxidant activities (Adebayo-Tayo and Fashogbon, 2020; Wu et al., 2021). According to our findings, the radical scavenging capacity of EPS$_1$ (77%) and EPS$_5$ (75.2%) significantly contributes to antioxidant activity. Adebayo-Tayo and Fashogbon (2020) evaluate the antioxidant activity of EPS produced by wild type EPSWLD *L. delbrueckii* ssp. *bulgaricus* and mutant EPSMLD *L. delbrueckii* ssp. *bulgaricus* using the DPPH system and other biological tests. The antioxidant potential of EPSWLD and EPSMLD was found to be between 1.21 and 1.80% and between 0.41 and 1.42% for their DPPH-scavenging capacities (37.5–73.4% *vs.* 37.5–65.6%, respectively). El-Adawi et al. (2012) reported that extracellular extracts of *B. longum* and *L. plantarum* had a DPPH scavenging capacity of 89.8 and 89.8%, respectively. The entire culture of *L. delbrueckii* ssp. *bulgaricus* DSM 20081^T possessed the highest DPPH radical scavenging activity. According to Li S. et al. (2014), *B. bifidum* WBIN03 (B-EPS) and *L. plantarum* R315 (L-EPS) both had a high DPPH scavenging potential that increased with EPS concentration. Clearly, 70 mg/ml EPSs had a high DPPH scavenging potential when they compared the DPPH

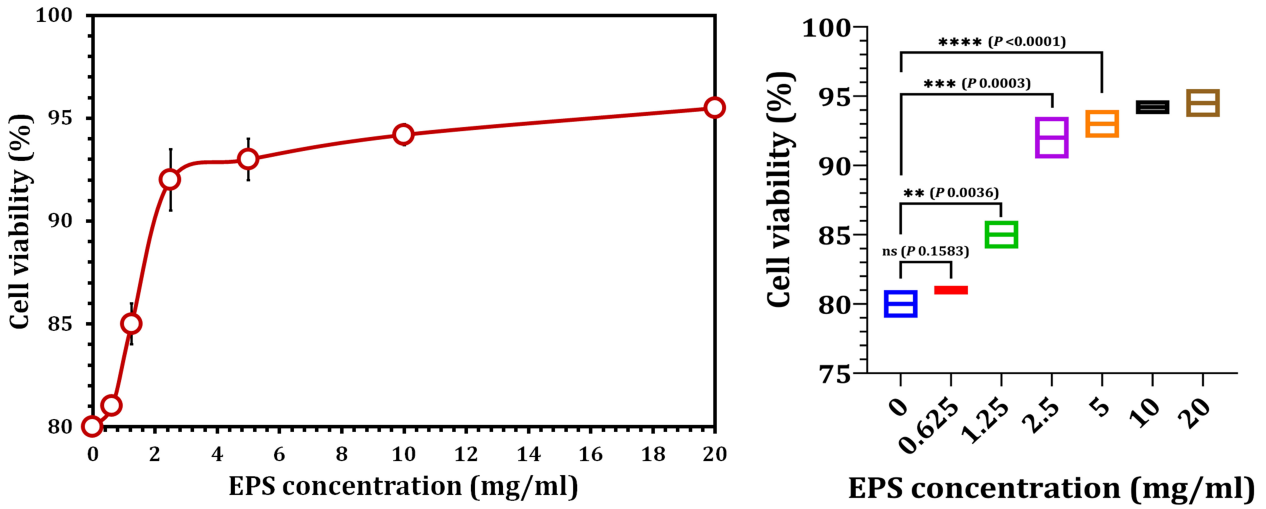

Figure 9 | The effect of crude EPS_5 derived from *L. delbrueckii* ssp. *bulgaricus* DSM 20081^T on cell viability in hPDLF cells using MTT assay.

scavenging behavior of different concentrations of B-EPS (30 mg/ml, 94.4%) and L-EPS (70 mg/ml, 94.49%). Recent research has revealed that the antioxidant ability of EPS is affected by a number of factors, including molecular weight, monosaccharide composition, monosaccharide molar ratio, and glycoside bonding (Wu et al., 2021). As a result, the significant antioxidant activity of EPS could be attributed to its chemical groups, which include the hydroxyl group, carbon-free radicals, and the sulfated group (Wang et al., 2015).

Cancer is a disease that causes uncontrollable cell proliferation, resulting in organ damage and, eventually, death. The death toll from various types of cancer is steadily rising year after year. Current chemo and radiation therapy for cancer patients harms both tumor and normal cells (El Ghany et al., 2015; Zhang et al., 2017). The current research aims to produce antitumor agents that have fewer side effects than currently available synthetic pharmaceuticals. As a result, the antitumor properties of EPS are being investigated as a potential cancer treatment in this study. The cytotoxicity of EPSs against human breast, colon, and liver cancer cells was determined, as well as their role in apoptotic gene expression. The majority of anti-cancer medications have been shown to be cytotoxic to healthy cells, highlighting the critical need for safe alternatives in biomedicine (Zhang et al., 2017). Mohanta et al. (2017) demonstrated that the MTT test is one of the most advanced methods for determining the cytotoxic effects of cancerous cells. It is based on the reduction of MTT into formazan by mitochondrial succinate dehydrogenase in the mitochondria of metabolically active cells. The results of the cytotoxicity tests in this experiment revealed that treatment with EPSs elicited different cellular responses depending on the cause of cell death and the sensitivity of the treatment. Specifically, the IC_{50} values for EPSs on normal mammalian cells (HEK 293) ranged from 85.7 to 29.68 mg/ml. Nami et al. (2015) found that *Enterococcus lactis* IW5 secretions had no negative effects on normal cells, with 95% of the cells developing normally. Furthermore, a dosage of 2–5 mg/ml of new purified EPS *L. acidophilus* 20079 in healthy mammalian cells was shown to have a selectivity index of 1.96–51.3 for destroying cancerous cells (El-Deeb et al., 2018).

Exopolysaccharides from *L. plantarum* has not been found to be harmful in normal fibroblast cells L929 until a concentration of 50 mg/ml is reached (Ismail and Nampoothiri, 2013). The viability percentage of L929 is greater than 60 after treatment with 40 mg/ml EPS from *L. paracasei* and *Lactobacillus brevis* on L929 and HT29. On the other hand, HT29 has a survival rate of less than 20% (Mojibi et al., 2019). Based on the multiple cancerous cell death pathways and related sensitivity to treatment, we can assume that cytotoxicity experiments revealed the presence of non-identical cellular responses to EPS treatment. EPS_5 had the most active components and exhibited the lowest IC_{50} values on MCF7, CaCo2, and HepG2 (7.91, 10.69, and 9.12 mg/ml, respectively, $p < 0.05$). Vidhyalakshmi and Vallinachiyar (2013) demonstrated that EPS derived from *Bacillus* sp. has a high potential for cytotoxicity against MCF7 cells at low concentrations while having no effect on normal cells. Additionally, Liu et al. (2011) found that *L. casei* 01 EPS inhibited HT29 growth at doses ranging from 5 to 100 μg/ml. *L. fermentum* extracts inhibited colon cancer cell growth while enhancing non-cancerous colon cell growth (Kahouli et al., 2015). Their findings on cancer cells suggest that the presence of propionate and butyrate may contribute to the probiotic bacteria's selectivity, as histone deacetylase inhibitors (HDACs) stimulate proliferation in healthy colon cells but kill cancer cells (Kahouli et al., 2015). Nami et al. (2015) reported that the *E. lactis* IW5 byproducts reduced the viability of several types of cancer cells, including HeLa, MCF7, AGS, and HT-29, and that the primary mechanism underlying this effect was the activation of apoptosis in cancer cells.

Annexin V analysis revealed a decrease in the percentage of viable cells in all investigated cell lines with increased EPSs concentrations. A rise in the concentration of Annexin V in treated cells indicates that EPS induces apoptosis. The

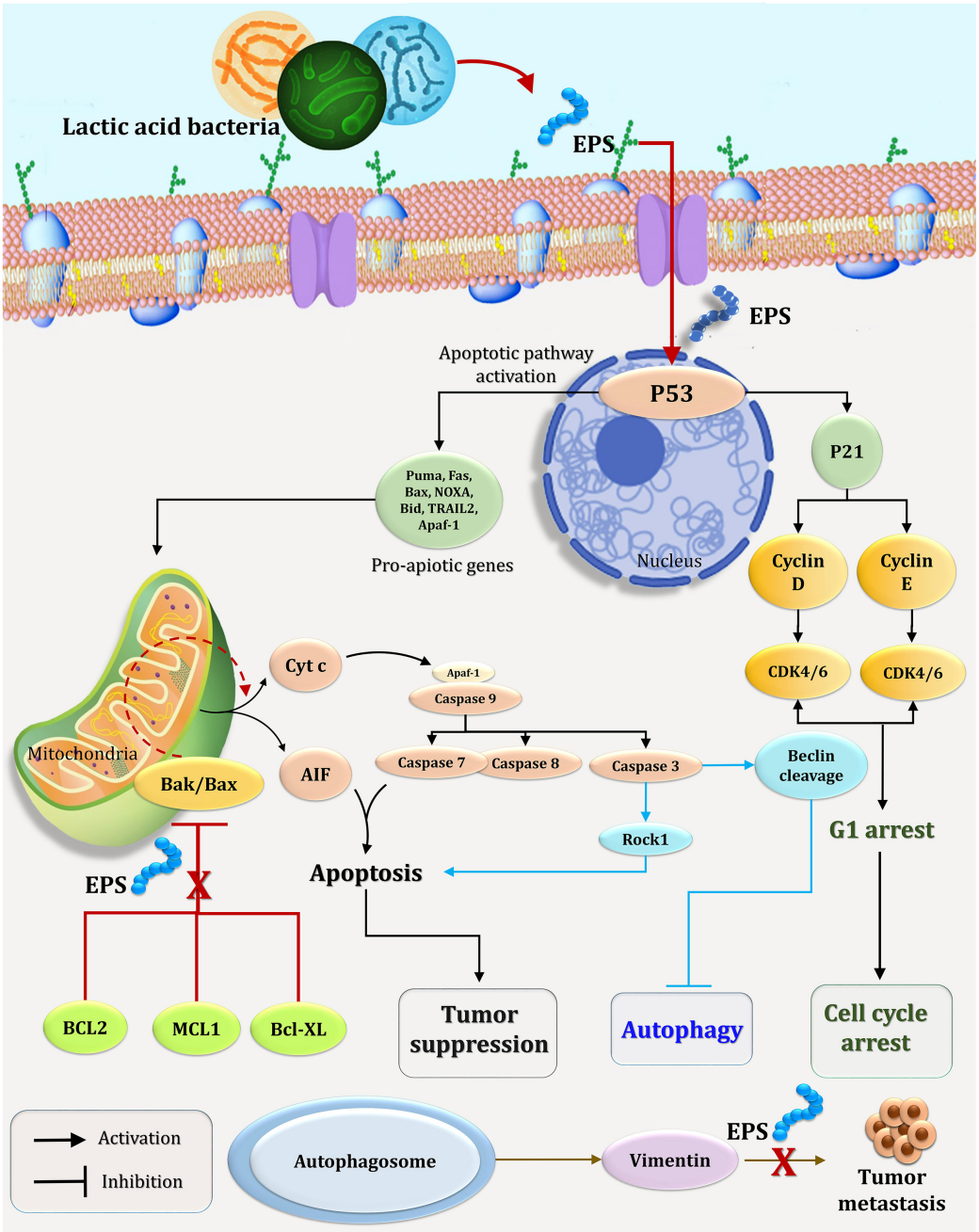

Figure 10 | A possible mechanism for EPS_5's effect on the cell cycle and apoptosis in cancer cells.

investigation revealed that treatment with the IC_{50} of EPS_5 resulted in a significantly increased number of apoptotic cells (18.4, 10.28, and 16.3 ng/ml) on MCF7, CaCo2, and HepG2, respectively, followed by treatment with EPS_1, whereas treatment with the IC_{50} of EPS_6 resulted in a significantly decreased number of apoptotic cells. Apoptosis is primarily defined by changes in the morphology and biochemistry of the cells. EPS of *L. paracasei* and *L. brevis* inhibited the proliferation of HT29 cancer cells (Mojibi et al., 2019). When anti-proliferative activity and cell growth are compared 24 h after treatment with *L. paracasei* or *L. brevis* EPS at a concentration of 40 mg/ml, anti-proliferative activity and cell death increase from 36 to 80% and from 40 to 90%, respectively. *S. thermophilus* CH9-EPS-3a demonstrated greater anticancer activity *in vitro* against human liver cancer HepG2 cells, and the antitumor efficacy of EPS's-3a was associated with cell apoptosis in HepG2 cells (Liu et al., 2019). Normal cells possess significantly fewer anti-proliferative and inhibitory properties than cancerous cells. Increased LDH

leakage into the culture supernatant is also indicative of EPS-induced membrane damage (Deepak et al., 2016). LDH activity was found to be significantly greater in cancer cells treated with EPS_5 than in cancer cells treated with EPS_1 ($p = 0.0001$), followed by EPS_{10} and EPS_6, confirming disruption of the plasma membrane and subsequent LDH dispersion into extracellular space (Fotakis and Timbrell, 2006).

It has been demonstrated that EPSs perform a variety of bioactive functions, and as a result, these functions are typically influenced positively by the EPS's physicochemical properties (Wang et al., 2014; Li et al., 2016). This indicates a distinction between the functional groups defined in EPS_5 when discussing FT-IR results. The strongest bands in the 3,410 cm^{-1} region are indicative of the presence of the EPS_5 hydroxyl-stretching vibration (Abdhul et al., 2014). The bands at 2,931 cm^{-1} are produced by CH_2 stretching vibrations, whereas the bands at 1,650 cm^{-1} are produced by –OH bending vibrations. Absorption at 1,381 cm^{-1} may be due to symmetric CH_3 bending. At 1,136 cm^{-1}, vibrations stretching the glycosidic bond (C–O–C) were responsible for the strong absorption (Adebayo-Tayo and Fashogbon, 2020). Additionally, strong infrared absorptions at 872 cm^{-1} indicated that EPS_5 was β-anomeric (Pan and Mei, 2010). The monosaccharide of EPS_5 was investigated using HPLC. The EPS_5 is primarily composed of various sugars with molecular ratios 1:2.7:7.4:5.1:12.5, reflecting ribose:rhamnose:glucose:mannose:galactose, respectively.

The most critical biochemical process that occurs during early apoptosis is phosphatidylserine translocation. Several biochemical pathways converge during apoptosis, resulting in the activation of a family of cysteine-dependent aspartate-directed proteases (caspases). Although caspase-dependent or caspase-independent mechanisms can regulate apoptosis, the latter is more prevalent because the majority of cells initiate apoptosis *via* caspase activation (Gamal-Eldeen et al., 2009). We investigated the effect of *L. delbrueckii* ssp. *bulgaricus* DSMZ 20081^T-EPS_5 on apoptotic marker gene expression in MCF7, CaCo2, and HepG2 cells as a result of the antitumor data obtained. The relative expression of the apoptotic genes *Bax*, *BCL2*, *Caspase 3*, *Caspase 8*, and *MCL1* was determined in this experiment. Board proteins, such as *BCL2*, regulate both cell damage and proliferation. *BCL2* family proteins are required for mitochondria-mediated apoptosis, as they maintain the mitochondrial membrane's integrity (Aouacheria et al., 2017).

The mechanism by which polysaccharides induce apoptosis in cancerous cells was investigated using BCL2 family proteins such as *BCL2*, which inhibits apoptosis, and *Bax*, which induces apoptosis. The results of the gene expression analysis indicated that EPS_5 increased *Bax* gene expression in the cell lines examined. However, cells treated with EPS_5 showed a significant decrease in *BCL2* gene expression. Numerous studies have shown that tumor cells treated with LAB EPS expressed significantly less *BCL2*. Tukenmez et al. (2019) found that *L. delbrueckii* ssp. *bulgaricus* B3-EPS inhibited time-dependent proliferation and induced apoptosis by increasing *Bax*, *Caspase 3*, and *Caspase 9* expression and decreasing *BCL2* and *Survivin* expression. Cell-bound exopolysaccharides (cb-EPS) derived from *L. acidophilus* 606 inhibited the growth of colon cancer cells HT-29 by activating the *Bax* gene (Yang et al., 2007). Additionally, the *MCL1* gene, a member of the *BCL2* family of anti-apoptotic proteins that promotes apoptosis activation *via* mitochondrial pathways in C32 melanoma cells, inhibits apoptosis in a variety of cancers *Bak* and *Bax* pro-apoptotic proteins (Beberok et al., 2020). Caspases are involved in the regulation of the majority of molecules involved in cell death. Caspases involved in apoptosis can be classified as initiators (*Caspases 2*, *8*, *9*, and *10*) or effectors (*Caspases 3*, *6*, and *7*) (Wang et al., 2016).

Given the critical role of *Caspase 3* in apoptosis and the fact that many well-characterized breast cancer cell lines have altered *Caspase 3* expression, RT-PCR was performed using *Caspase 3*-specific primers in treated MCF7 cells. *Caspase 3* was significantly overexpressed in treated MCF7 cells compared to other cancer cells tested, according to our findings. *Caspase 3* activity was detected in response to a variety of apoptotic factors, including chemotherapeutic agents, radiotherapy, and cytokines. Selective *Caspase 3* inhibition, on the other hand, is associated with cell death inhibition. It has been postulated that a lack of *Caspase 3* expression allows apoptosis-resistant breast cancer cells to respond to apoptotic stimuli like chemotherapy and radiotherapy. Several findings have significant clinical implications for using *Caspase 3* as a disease marker for breast cancer as well as a potential therapeutic target (Devarajan et al., 2002). Northern blot analysis was used to confirm the absence of *Caspase 3* expression in breast cancer cells. *Caspase 3* mRNA levels in breast cancer cells were 10- to 50-fold lower than in normal breast tissue. In drug-sensitive MCF7 cells, *Caspase 3* mRNA was truncated by a 125-bp transcript deletion. Additionally, it was established that drug-resistant (MCF7/DOX) MCF7 cells derived from continuous MCF7 cell culture had a maximum *Caspase 3* transcript duration in the presence of doxorubicin (Devarajan et al., 2002). The significant increases in *Caspase 8* and *Caspase 3* genes in treated cells in our results are consistent with Chang et al. (2013). *Caspase 3* was expected to be an adequate death protease catalyzing protein breakdown. *Caspase 8* is found at the apex of an apoptotic cascade, where it causes proteolytic activation of members of the downstream caspase family, which contributes to apoptosis (Chang et al., 2013). Two pathways triggered the initiator: the first is regulated by *Caspase 8*. It includes the insertion of cell death ligands, which then activates *Caspase 8* and *Caspase 3*, and the later involves apoptosis mediated by *Caspase 9* mitochondria (Karpel-Massler et al., 2017).

The *p53* tumor suppressor can also regulate pro-apoptotic genes related to both intrinsic and extrinsic pathways (Chipuk et al., 2003). El-Deeb et al. (2018) observed that after treating CaCo2 cells with *L. acidophilus* LA-EPS-20079 EPS, *p53* gene expressions increased. EPS_5 increased the level of *p53* transcript in the tested CaCo2 cell line, implying that a *p53*-dependent pathway is active in the apoptotic mechanism of CaCo2 cells. To maintain cellular integrity and tolerance to stress, normal mesenchymal cells produce *Vimentin*, a protein belonging to the intermediate filament (IF) family (Chipuk et al., 2003). *Vimentin* aberrant overexpression has been linked to a higher level of aggressiveness in cancer cells, including melanoma, breast

cancer, gastrointestinal cancers, and nervous system tumors. *Vimentin* overexpression in cancer is linked to increased tumor development, invasion, and a bad prognosis; nevertheless, the function of *Vimentin* in the development of cancer is still unknown. To our knowledge, no research on the effect of EPS on *Vimentin* gene expression regulation in MCF7 has been conducted. McInroy and Määttä (2007) demonstrated that silencing *Vimentin* expression inhibits the migration and invasion of colon and breast cancer cell lines. They demonstrated that downregulation of *Vimentin* expression impairs migration in both scratch wound experiments and invasion studies using collagen-coated cell culture inserts.

Recent research has established the efficacy of polysaccharides in inducing apoptosis in cancer cells by focusing on signaling molecules (Alwarsamy et al., 2016). As illustrated in **Figure 10**, polysaccharides exert their antitumor activity *via* two distinct mechanisms: the *BCL2*-regulated (also known as intrinsic, mitochondrial, or stress) pathway, which is activated by cytokine deprivation, ER stress, or DNA damage, and the death receptor (also known as extrinsic) pathway, which is activated by ligation of members of the tumor necrosis factor receptor (TNFR) family bearing an intracellular death domain (Green, 2005; Czabotar et al., 2014; Zhang et al., 2017). Overexpression of the pro-apoptotic *BH3*-only members (*BIM*, *PUMA*, *BID*, *BMF*, *BAD*, *BIK*, *NOXA*, and *HRK*) of the *BCL2* protein family, which are members of the pro-apoptotic *BH3*-only subfamily, promotes cell death through the *BCL2*-regulated apoptotic pathway. The *BH3*-only proteins interact with and block pro-survival *BCL2* proteins (*BCL2*, *BCLXL*, *MCL1*, *BCLW*, and *A1/BFL1*), hence activating the cell death effectors *BAX* and *BAK* (the pro-apoptotic multi-BH domain members of the *BCL2* family that may also contain *BOK*) (Ke et al., 2015; Llambi et al., 2016). Certain *BH3*-only proteins have been shown to directly activate *BAX/BAK* (Green, 2005; Youle and Strasser, 2008). When *BAX*/*BAK* is activated, the mitochondrial outer membrane (MOMP) is permeabilized, triggering the activation of a cascade of aspartate-specific cysteine proteases (Zhang et al., 2007) and its activator APAF-1 (Cecconi et al., 1998) that dismantle cells (**Figure 10**). In comparison, the downregulation system induces apoptosis by binding and activating *Procaspase-8* at ligated death receptors in the plasma membrane *via* the adaptors FADD and, in rare cases, TRADD. In so-called type 1 cells, activation of *Caspase 8* followed by activation of effector caspases (*Caspases 3* and *7*) is sufficient to successfully induce apoptosis (e.g., thymocytes). On the other hand, effective cell death in so-called type 2 cells (e.g., hepatocytes) requires caspase cascade amplification *via* crossover activation of the *BCL2*-regulated apoptotic pathway, which is accomplished through *Caspase 8*-mediated proteolytic activation of the normally inert *BH3*-only protein BID (**Figure 10**; Zhang et al., 2007, 2017; Fan et al., 2014).

Human periodontal ligament fibroblast cells (hPDLFCs) are one of several cell types involved in periodontal tissue regeneration (Son et al., 2019). In addition, few studies have been published on the effect of EPSs on the viability of hPDLFCs. In conclusion, EPS_5 derived from *L. delbrueckii* ssp. *bulgaricus* DSM 20081^T exhibits a range of bioactivities including antioxidant, antitumor, and proliferative properties, thereby establishing it as a possible natural agent for the development of novel periodontal healing and regeneration strategies. Furthermore, because of its extraordinary cytotoxic effect at the IC_{50} value in cancer cells, EPS_5 could be used in medical research as a potential antitumor agent. As a result, the potential for EPS to replace chemotherapeutic medications in the future must be considered alongside their safety and public health issues. Overall, the LAB EPS has significant therapeutic potential, most notably in the antioxidant, antitumor, and periodontal regeneration fields. However, additional research is necessary to fully understand EPS_5's mechanism of action in periodontal healing and tissue restoration.

DATA AVAILABILITY STATEMENT

The original contributions presented in the study are included in the article/**Supplementary Material**, further inquiries can be directed to the corresponding author/s.

ETHICS STATEMENT

The studies involving human participants were reviewed and approved by College of Dentistry, Taif University, Taif, Saudi Arabia, Dentistry Clinics Hospitals Ethical Committee Centers. The patients/participants provided their written informed consent to participate in this study.

AUTHOR CONTRIBUTIONS

MK: conceptualization, methodology, formal analysis, data curation, and writing—review and editing. FS: conceptualization, validation, and visualization. LA-M and AA: methodology and investigation. TA: methodology and writing—review and editing. SA: statistical analysis, formal analysis, data curation, and writing—review and editing. All authors contributed to the article and approved the submitted version.

FUNDING

This study was supported by Taif University Researchers Supporting Project Number (TURSP-2020/95), Taif, Saudi Arabia. This investigation was also funded by Research Project Funds from Tanta University (Tu-03-13-04).

SUPPLEMENTARY MATERIAL

The Supplementary Material for this article can be found online at: https://www.frontiersin.org/articles/10.3389/fmicb.2022.803688/full#supplementary-material

REFERENCES

Abdhul, K., Ganesh, J., Lee, M., Shanmughapriya, S., Kanagavel, M., Anbarasu, K., et al. (2014). Antioxidant activity of exopolysaccharide from probiotic strain *Enterococcus faecum* (BDU7) from Ngari. *Int. J. Biol. Macromol.* 70, 450–454. doi: 10.1016/j.ijbiomac.2014.07.026

Adebayo-Tayo, B., and Fashogbon, R. (2020). In vitro antioxidant, antibacterial, in vivo immunomodulatory, antitumor and hematological potential of exopolysaccharide produced by wild type and mutant *Lactobacillus delbureckii* subsp. *bulgaricus*. *Heliyon* 6:e03268. doi: 10.1016/j.heliyon.2020.e03268

Adebayo-Tayo, B., Ishola, R., and Oyewunmi, T. (2018). Characterization, antioxidant and immunomodulatory potential on exopolysaccharide produced by wild type and mutant *Weissella confusa* strains. *Biotechnol. Rep.* 19:e00271 doi: 10.1016/j.btre.2018.e00271

Adesulu-Dahunsi, A. T., Sanni, A. I., and Jeyaram, K. (2018). Production, characterization and in vitro antioxidant activities of exopolysaccharide from *Weissella cibaria* GA44. *LWT* 87, 432–442. doi: 10.1016/j.lwt.2017.09.013

Alwarsamy, M., Gooneratne, R., and Ravichandran, R. (2016). Effect of fucoidanfrom *Turbinaria conoides* on human lung adenocarcinoma epithelial (A549) cells. *Carbohydr. Polym.* 152, 207–213. doi: 10.1016/j.carbpol.2016.06.112

Angelin, J., and Kavitha, M. (2020). Exopolysaccharides from probiotic bacteria and their health potential. *Int. J. Biol. Macromol.* 162, 853–865. doi: 10.1016/j.ijbiomac.2020.06.190

Aouacheria, A., Baghdiguian, S., Lamb, H. M., Huska, J. D., Pineda, F. J., and Hardwick, J. M. (2017). Connecting mitochondrial dynamics and life-or-death events via Bcl-2 family proteins. *Neurochem. Int.* 109, 141–161. doi: 10.1016/j.neuint.2017.04.009

Arslan, Y. E., and Kantarcioglu, I. (2019). *Salvadora persica* extract-laden jellyfish collagen hybrid constructs for periodontal tissue regeneration. *J. Turk. Chem. Soc. Sec. A Chem.* 6, 51–62 doi: 10.18596/jotcsa.484936

Bajpai, V. K., Majumder, V., Rather, I. A., and Kim, K. (2016). Extraction, isolation and purification of exopolysaccharide from lactic acid bacteria using ethanol precipitation method. *Bangladesh J. Pharmacol.* 11, 573–576. doi: 10.3329/bjp.v11i3.27170

Barcelos, M. C. S., Vespermann, K. A. C., Pelissari, F. M., and Molına, G. (2019). Current status of biotechnological production and applications of microbial exopolysaccharides. *Crit. Rev. Food Sci. Nutr.* 60, 1475–1495. doi: 10.1080/10408398.2019.1575791

Beberok, A., Rok, J., Rzepka, Z., Marciniec, K., Boryczka, S., and Wrześniok, D. (2020). The role of MITF and Mcl-1 proteins in the antiproliferative and proapoptotic effect of ciprofloxacin in amelanotic melanoma cells: in silico and in vitro study. *Toxicol. In Vitro* 66:104884 doi: 10.1016/j.tiv.2020.104884

Biliavska, L., Pankivskay, P., Povnitsa, O., and Zagorodnya, S. (2019). Antiviral activity of exopolysaccharides produced by lactic acid bacteria of the genera *Pediococcus*, *Leuconostoc* and *Lactobacillus* against human adenovirus type 5. *Medicina* 55, 519–531. doi: 10.3390/medicina55090519

Bradford, M. M. (1976). A rapid and sensitive method for the quantitation of microgram quantities of protein utilizing the principle of proteindye binding. *Anal. Biochem.* 72, 248–254.

Bray, F., Ferlay, J., Soerjomataram, I., Siegel, R. L., Torre, L. A., and Jemal, A. (2018). Global cancer statistics 2018: GLOBOCAN estimates of incidence and mortality worldwide for 36 cancers in 185 countries. *CA Cancer J. Clin.* 68, 394–424. doi: 10.3322/caac.21492

Cecconi, F., Alvarez-Bolado, G., Meyer, B. I., Roth, K. A., and Gruss, P. (1998). Apaf-1 (CED-4 homologue) regulates programmed cell death in mammalian development. *Cell* 94, 727–737. doi: 10.1016/s0092-8674(00)81732-8

Chang, C. J., Lin, J. F., Chang, H. H., Lee, G. A., and Hung, C. F. (2013). Lutein protects against methotrexate-induced and reactive oxygen species-mediated apoptotic cell injury of IEC-6 cells. *PLoS One* 8:e72553. doi: 10.1371/journal.pone.0072553

Chipuk, J. E., Maurer, U., Green, D. R., and Schuler, M. (2003). Pharmacologic activation of p53 elicits Bax-dependent apoptosis in the absence of transcription. *Cancer Cell* 4, 371–381. doi: 10.1016/s1535-6108(03)00272-1

Czabotar, P. E., Lessene, G., Strasser, A., and Adams, J. M. (2014). Control of apoptosis by the BCL-2 protein family: implications for physiology and therapy. *Nat. Rev. Mol. Cell Biol.* 15, 49–63. doi: 10.1038/nrm3722

Deepak, V., Ramachandran, S., Balahmar, R. M., Pandian, S. R. K., Sivasubramaniam, S. D., Nellaiah, H., et al. (2016). In vitro evaluation of anticancer properties of exopolysaccharides from *Lactobacillus acidophilus* in colon cancer cell lines. *In Vitro Cell Dev. Biol. Anim.* 52, 163–173. doi: 10.1007/s11626-015-9970-3

Devarajan, E., Sahin, A. A., Chen, J. S., Krishnamurthy, R. R., Aggarwal, N., Brun, A. M., et al. (2002). Down-regulation of caspase 3 in breast cancer: a possible mechanism for chemoresistance. *Oncogene* 21, 8843–8851. doi: 10.1038/sj.onc.1206044

Dilna, S. V., Surya, H., Aswathy, R. G., Varsha, K. K., Sakthikumar, D. N., Pandey, A., et al. (2015). Characterization of an exopolysaccharide with potential health-benefit properties from a probiotic *Lactobacillus plantarum* RJF4. *LWT Food Sci. Technol.* 64, 1179–1186 doi: 10.1016/j.lwt.2015.07.040

Dubois, M., Gilles, K. A., Hamilton, J. K., Pebers, P. A., and Smith, F. (1956). Colorimetric method for determination of sugar and related substances. *Anal. Chem.* 28, 350–356. doi: 10.1021/ac60111a017

El-Adawi, H. I., Khalil, M. A., El-Sheekh, M. M., EL-Deeb, N. M., and Hussein, M. Z. (2012). Cytotoxicity assay and antioxidant activities of the lactic acid bacterial strains. *Afr. J. Microb. Res.* 6, 1700–1712. doi: 10.4014/jmb.1301.01032

El-Deeb, N. M., Yassin, A. M., Al-Madboly, L. A., and El-Hawiet, A. (2018). A novel purified *Lactobacillus acidophilus* 20079 exopolysaccharide, LA-EPS-20079, molecularly regulates both apoptotic and NF-κB inflammatory pathways in human colon cancer. *Microb. Cell Fact.* 17:29. doi: 10.1186/s12934-018-0877-z

El Ghany, K. A., Hamouda, R., Elhafez, E. A., Mahrous, H., Salem-Bekhit, M., and Hamza, H. A. (2015). A potential role of *Lactobacillus acidophilus* LA1 and its exopolysaccharides on cancer cells in male albino mice. *Biotechnol. Biotechnol. Equip.* 29, 977–983. doi: 10.1080/13102818.2015.1050455

Fan, Y., Lin, M., Luo, A., Chun, Z., and Luo, A. (2014). Characterization and antitumor activity of a polysaccharide from *Sarcodia ceylonensis*. *Molecules* 19, 10863–10876. doi: 10.3390/molecules190810863

Fontana, C., Li, S., and Yang, Z., (2015). Structural studies of the exopolysaccharide from *Lactobacillus plantarum* C88 using NMR spectroscopy and the program CASPER. *Carbohydr. Res.* 402, 7–94. doi: 10.1016/j.carres.2014.09.003

Fotakis, G., and Timbrell, A. (2006). In vitro cytotoxicity assays: comparison of LDH, neutral red, MTT and protein assay in hepatoma cell lines following exposure to cadmium chloride. *Toxicol. Lett.* 5, 171–177. doi: 10.1016/j.toxlet.2005.07.001

Gamal-Eldeen, A. M., Ahmed, E. F., and Abo-Zeid, M. A. (2009). In vitro cancer chemopreventive properties of polysaccharide extract from the brown alga, *Sargassum latifolium*. *Food Chem. Toxicol.* 47, 1378–1384 doi: 10.1016/j.fct.2009.03.016

Green, D. R. (2005). Apoptotic pathways: ten minutes to dead. *Cell* 121, 671–674. doi: 10.1016/j.cell.2005.05.019

Gurunathan, S., Han, J. W., Eppakayala, V., Jeyaraj, M., and Kim, J. H. (2013). Cytotoxicity of biologically synthesized silver nanoparticles in MDA-MB-231 human breast cancer cells. *Biomed. Res. Int.* 2013:535796. doi: 10.1155/2013/535796

Hu, Y. Q., Zhang, S., Xu, Z., Lv, Z. S., Liu, M. L., and Feng, L. S. (2017). 4-Quinolone hybrids and their antibacterial activities. *Eur. J. Med. Chem.* 141, 335–345. doi: 10.1016/j.ejmech.2017.09.05

Hussain, A., Zia, K. M., Tabasum, S., Noreen, A., Ali, M., Iqbal, R., et al. (2017). Blends and composites of exopolysaccharides; properties and applications: a review. *Int. J. Biol. Macromol.* 94, 10–27. doi: 10.1016/j.ijbiomac.2016.09.104

Ismail, B., and Nampoothiri, K. M. (2013). Exposition of antitumour activity of a chemically characterized exopolysaccharide from a probiotic *Lactobacillus plantarum* MTCC 9510. *Biologia* 68, 1041–1047. doi: 10.2478/s11756-013-0275-2

Iviglia, G., Kargozar, S., and Baino, F. (2019). Biomaterials, current strategies, and novel nanotechnological approaches for periodontal regeneration. *J. Funct. Biomater.* 10, 1–3. doi: 10.3390/jfb10010003

Joo Seo, B., Bajpai, V., Rather, I., and Park, Y. (2015). Partially purified exopolysaccharide from *Lactobacillus plantarum* YML009 with total phenolic content, antioxidant and free radical scavenging efficacy. *Ind. J. Pharm. Educ. Res.* 49, 282–292. doi: 10.5530/ijper.49.4.6

Kahouli, I., Malhotra, M., Alaoui-Jamaliand, M., Prakash S. (2015). In-vitro characterization of the anticancer activity of the probiotic bacterium

Lactobacillus fermentum NCIMB 5221 and potential against colorectal Cancer. *Cancer Sci. Ther.* 7, 224–235.

Kao, T. H., and Chen, B. H. (2006). Functional components in soybean cake and their effects on antioxidant activity. *J. Agric. Food Chem.* 54, 7544–7555. doi: 10.1021/jf061586x

Karpel-Massler, G., Ishida, C. T., Bianchetti, E., Shu, C., Perez-Lorenzo, R., Horst, B., et al. (2017). Inhibition of mitochondrial matrix chaperones and anti-apoptotic Bcl-2 family proteins empower antitumor therapeutic responses. *Cancer Res.* 77, 3513–3526. doi: 10.1158/0008-5472.CAN-16-3424

Ke, F., Grabow, S., Kelly, G. L., Lin, A., O'Reilly, L. A., and Strasser, A. (2015). Impact of the combined loss of BOK, BAX and BAK on the hematopoietic system is slightly more severe than compound loss of BAX and BAK. *Cell Death Dis.* 6:e1938. doi: 10.1038/cddis.2015.304

Khalil, M. A., El-Shanshoury, A.-E. R. R., Alghamdi, M. A., Alsalmi, F. A., Mohamed, S. F., Sun, J., et al. (2022). Biosynthesis of silver nanoparticles by Marine actinobacterium *Nocardiopsis dassonvillei* and exploring their therapeutic potentials. *Front. Microbiol.* 12:705673. doi: 10.3389/fmicb.2021.705673

Lakra, A. K., Domdi, L., Tilwani, Y. M., and Arul, V. (2020). Physicochemical and functional characterization of mannan exopolysaccharide from *Weissella confusa* MD1 with bioactivities. *Int. J. Biol. Macromol.* 143, 797–805. doi: 10.1016/j.ijbiomac.2019.09.139

Li, C., Li, W., Chen, X., Feng, M., Rui, X., Jiang, M., et al. (2014). Microbiological, physicochemical and rheological properties of fermented soymilk produced with exopolysaccharide (EPS) producing lactic acid bacteria strains. *LWT Food Sci. Technol.* 57, 477–485.

Li, C., Li, Z., Wang, Y., and Liu, H. (2016). Gold nanoparticles promote proliferation of human periodontal ligament stem cells and have limited effects on cells differentiation. *J. Nanomater.* 2016:1431836. doi: 10.1155/2016/1431836

Li, S., Huang, R., Shah, N. P., Tao, X., Xiong, Y., and Wei, H. (2014). Antioxidant and antibacterial activities of exopolysaccharides from *Bifidobacterium bifidum* WBIN03 and *Lactobacillus plantarum* R315. *J. Dairy Sci.* 97, 7334–7343 doi: 10.3168/jds.2014-7912

Li, W., Ji, J., Chen, X., Jiang, M., Rui, X., and Dong, M. (2014). Structural elucidation and antioxidant activities of exopolysaccharides from *Lactobacillus helveticus* MB2-1. *Carbohydr. Polym.* 102, 351–359. doi: 10.1016/j.carbpol.2013.11.053

Li, W. Tang, W., Ji, J., Xia, X., Rui, X., Chen, X. et al. (2015). Characterization of a novel polysaccharide with anti-colon cancer activity from *Lactobacillus helveticus* MB2-1. *Carbohydr. Res.* 411, 6–14. doi: 10.1016/j.carres.2014.12.014

Lin, X., Xia, Y., Wang, G., Yang, Y., Xiong, Z., Lv, F., et al. (2018). Lactic acid bacteria with antioxidant activities alleviating oxidized oil induced hepatic injury in mice. *Front. Microbiol.* 9:2684. doi: 10.3389/fmicb.2018.02684

Liou, G. Y., and Storz, P. (2010). Reactive oxygen species in cancer. *Free Radic. Res.* 44, 479–496. doi: 10.3109/10715761003667554

Liu, C., Zheng, J., Ou, X., and Han, Y. (2021). Anti-cancer substances and safety of lactic acid bacteria in clinical treatment. *Front. Microbiol.* 12:722052. doi: 10.3389/fmicb.2021.722052

Liu, C.-T., Chu, F.-J., Chou, C.-C., and Yu, R.-C. (2011). Antiproliferative and anticytotoxic effects of cell fractions and exopolysaccharides from *Lactobacillus casei* 01. *Mutat. Res.* 721, 157–162. doi: 10.1016/j.mrgentox.2011.01.005

Liu, J., Ren, Z., Fan, L., Wei, J., Tang, X., Xu, X., et al. (2019). Design, synthesis, biological evaluation, structure-activity relationship, and toxicity of clinafloxacin-azole conjugates as novel antitubercular agents. *Bioorganic Med. Chem.* 27, 175–187. doi: 10.1016/j.bmc.2018.11.035

Livak, K., and Schmittgen, D. (2001). Analysis of relative gene expression data using real time quantitative PCR and the 2 method. *Methods* 25, 402–408. doi: 10.1006/meth.2001.1262

Llambi, F., Wang, Y. M., Victor, B., Yang, M., Schneider, D. M., Gingras, S., et al. (2016). BOK is a noncanonical BCL-2 family effector of apoptosis regulated by ER-associated degradation. *Cell* 165, 421–433. doi: 10.1016/j.cell.2016.02.026

Manivasagan, P, Venkatesan, J, Senthikumar, K, Sivakumar, K, and Kim, S. K. (2013). Biosynthesis, antimicrobial and cytotoxic effect of silver nanoparticles using a novel *Nocardiopsis* sp. MBRC-1. *Biomed. Res. Int.* 2013:287638. doi: 10.1155/2013/287638

Mathur, H., Beresford, T. P., and Cotter, P. D. (2020). Health benefits of lactic acid bacteria (LAB) fermentates. *Nutrients* 12:1679. doi: 10.3390/nu12061679

McInroy, L., and Määttä, A. (2007). Down-regulation of vimentin expression inhibits carcinoma cell migration and adhesion. *Biochem. Biophys. Res. Commun.* 360, 109–114. doi: 10.1016/j.bbrc.2007.06.036

Mende, S., Rohm, H., and Jaros, D. (2016). Influence of exopolysaccharides on the structure, texture, stability and sensory properties of yoghurt and related products. *Int. Dairy J.* 52, 57–71. doi: 10.1016/j.idairyj.2015.08.002

Milner, E., Stevens, B., An, M., Lam, V., Ainsworth, M., Dihle, P., et al. (2021). Utilizing probiotics for the prevention and treatment of gastrointestinal diseases. *Front. Microbiol.* 12:689958. doi: 10.3389/fmicb.2021.689958

Mohanta, Y. K., Panda, S. K., Bastia, A. K., and Mohanta, T. K. (2017). Biosynthesis of silver nanoparticles from *Protium serratum* and investigation of their potential impacts on food safety and control. *Front. Microbiol.* 8:626. doi: 10.3389/fmicb.2017.00626

Mojibi, P., Tafvizi, F., and Bikhof Torbati, M. (2019). Cell-bound exopolysaccharide extract from indigenous probiotic bacteria induce apoptosis in HT–29 cell-line. *Iran. J. Pathol.* 14, 41–51. doi: 10.30699/ijp.14.1.41

Nami, Y., Haghshenas, B., Haghshenas, M., Abdullah, N., and Khosroushahi, A. (2015). The prophylactic effect of probiotic *Enterococcus lactis* IW5 against different human cancer cells front. *Microbiology* 6:1317. doi: 10.3389/fmicb.2015.01317

Nasajpour, A., Ansari, S., Rinoldi, C., Rad, A. S. Aghaloo, T., Shin, S. R., et al. (2018). A multifunctional polymeric periodontal membrane with osteogenic and antibacterial characteristics. *Adv. Funct. Mater.* 28, 1703437–1703445. doi: 10.1002/adfm.201703437

Nazir, Y., Hussain, S. A., Abdul Hamid, A., and Song, Y. (2018). Probiotics and their potential preventive and therapeutic role for cancer, high serum cholesterol, and allergic and HIV diseases. *Biomed. Res. Int.* 2018, 1–17. doi: 10.1155/2018/3428437

Norouzi, Z., Salimi, A., Halabian, R., and Fahimi, H. (2018). Nisin, a potent bacteriocin and anti-bacterial peptide, attenuates expression of metastatic genes in colorectal cancer cell lines. *Microb. Pathog.* 123, 183–189. doi: 10.1016/j.micpath.2018.07.006

Pan, D., and Mei, X. (2010). Antioxidant activity of an exopolysaccharide purified from *Lactococcus lactis* subsp. *lactis* 12. *Carbohydr. Polym.* 80, 908–914 doi: 10.1016/j.carbpol.2010.01.005

Qin, J.-Y. (2015). Current situation and prospect of human cancer prevention and control. *Sci. Technol. Rev.* 33:125

Rajoka, M. R. S., Zhao, H., Lu, Y., Lian, Z., Li, N., Hussain, N., et al. (2018). Anticancer potential against cervix cancer (HeLa) cell line of probiotic *Lactobacillus casei* and *Lactobacillus paracasei* strains isolated from human breast milk. *Food Funct.* 9, 2705–2715. doi: 10.1039/c8fo00547h

Sanalibaba, P., and Cakmak, G. A. (2016). Exopolysaccharides production by lactic acid bacteria. *Appl. Micro. Open Access* 2:1000115. doi: 10.4172/2471-9315.1000115

Śliżewska, K., Markowiak-Kopeæ, P., and Śliżewska, W. (2021). The role of probiotics in cancer prevention. *Cancers* 13:20. doi: 10.3390/cancers13010020

Son, H., Jeon, M., Choi, H. J., Lee, H. S., Kim, I. H., Kang, C. M., et al. (2019). Decellularized human periodontal ligament for periodontium regeneration. *PLoS One* 14:e0221236 doi: 10.1371/journal.pone.0221236

Sungur, T., Aslim, B., Karaaslan, C., and Aktas, B. (2017). Anaerobe impact of exopolysaccharides (EPSs) of *Lactobacillus gasseri* strains isolated from human vagina on cervical tumor cells (HeLa) *Anaerobe* 47, 137–144. doi: 10.1016/j.anaerobe.2017.05.013

Surayot, U., Wang, J., Seesuriyachan, P., Kuntiya, A., Tabarsa, M., Lee, Y., et al. (2014). Exopolysaccharides from lactic acid bacteria: structural analysis, molecular weight effect on immunomodulation. *Int. J. Biol. Macromol.* 68, 233–240. doi: 10.1016/j.ijbiomac.2014.05.005

Tang, W., Dong, M., Wang, W., Han, S., Rui, X., Chen, X., et al. (2017). Structural characterization and antioxidant property of released exopolysaccharides from *Lactobacillus delbrueckii* ssp. *bulgaricus* SRFM-1. *Carbohydr. Polym.* 173, 654–664. doi: 10.1016/j.carbpol.2017.06.039

Thibessard, A., Borges, F., Fernandez, A., Gintz, B., Decaris, B., and LeblondBourget, N. (2004). Identification of *Streptococcus thermophilus* CNRZ368 genes involved in defense against superoxide stress. *Appl. Environ. Microbiol.* 70, 2220–2229. doi: 10.1128/aem.70.4.2220-2229.2004

Tukenmez, U., Aktas, B, Aslim, B., and Yavuz, S. (2019). The relationship between the structural characteristics of lactobacilli-EPS and its ability to induce

apoptosis in colon cancer cells *in vitro*. *Sci. Rep.* 9:8268. doi: 10.1038/s41598-019-44753-8

Vidhyalakshmi, R., and Vallinachiyar, C. (2013). Apoptosis of human breast cancer cells (MCF-7) induced by polysaccharides produced by bacteria. *J. Cancer Sci. Ther.* 5, 31–34.

Wang, G., Si, Q., Yang, S., Jiao, T., Zhu, H., Tian, P., et al. (2020). Lactic acid bacteria reduce diabetes symptoms in mice by alleviating gut microbiota dysbiosis and inflammation in different manners. *Food Funct.* 11, 5898–5914. doi: 10.1039/C9FO02761K

Wang, J., Hu, S., Nie, S, Yu, Q., and Xie, M. (2016). Reviews on mechanisms of in vitro antioxidant activity of polysaccharides. *Oxid. Med. Cell Longev.* 2016, 1–13. doi: 10.1155/2016/5692852

Wang, J., Zhao, X., Yang, Y., Zhao, A., and Yang, Z. (2015). Characterization and bioactivities of an exopolysaccharide produced by *Lactobacillus plantarum* YW32. *Int. J. Biolog. Macromole* 74, 119–126. doi: 10.1016/j.ijbiomac.2014.12.006

Wang, K., Li, W., Rui, X., Chen, X., Jiang, M., and Dong, M. (2014). Characterization of a novel exopolysaccharide with antitumor activity from *Lactobacillus plantarum* 70810. *Int. J. Biol. Macromol.* 63, 133–139. doi: 10.1016/j.ijbiomac.2013.10.036

Winner, J., Jung, C. K., Shackel, I., and Williams, P. M. (1999). Development and validation of real-time quantitative reverse transcriptase-polymerase chain reaction for monitoring gene expression in cardiac myocytes in vitro. *Anal Biochem.* 270, 41–49. doi: 10.1006/abio.1999.4085

Wu, J., Zhang, Y., Ye, L., and Wang, C. (2021). The anti-cancer effects and mechanisms of lactic acid bacteria exopolysaccharides *in vitro*: a review. *Carbohydr. Polym.* 253:117308. doi: 10.1016/j.carbpol.2020.117308

Yahya, S. M. M., Abdelnasser, S. M., Hamed, A. R., El Sayed, O. H., and Asker, M. S. (2019). Newly isolated marine bacterial exopolysaccharides enhance antitumor activity in HepG2 cells via affecting key apoptotic factors and activating toll like receptors. *Mol. Biol. Rep.* 46, 6231–6241. doi: 10.1007/s11033-019-05061-6

Yang, C. M., Cao, G. T., Ferket, P. R., Liu, T. T., Zhou, L., Zhang, L., et al. (2012). Effects of probiotic, *Clostridium butyricum*, on growth performance, immune function, and cecal microflora in broiler chickens. *Poult. Sci.* 91, 2121–2129. doi: 10.3382/ps.2011-02131

Yang, P., Peairs, J. J., Tano, R., Zhang, N., Tyrell, N., and Jaffe, G. J. (2007). Caspase-8–mediated apoptosis in human RPE cells. *IVOS* 48, 3341–3349. doi: 10.1167/iovs.06-1340

Youle, R. J., and Strasser, A. (2008). The BCL-2 protein family: opposing activities that mediate cell death. *Nat. Rev. Mol. Cell Biol.* 9, 47–59. doi: 10.1038/nrm2308

Zannini, E., Waters, D. M., Coffey, A., and Arendt, E. K. (2016). Production, properties, and industrial food application of lactic acid bacteria-derived exopolysaccharides. *Appl. Microbiol. Biotechnol.* 100, 1121–1135. doi: 10.1007/s00253-015-7172-2

Zhang, F., Shi, J.-J., Thakur, K., Hu, F., Zhang, J.-G., and Wei, Z.-J. (2017). Anti-cancerous potential of polysaccharide fractions extracted from peony seed dreg on various human cancer cell lines via cell cycle arrest and apoptosis. *Front. Pharmacol.* 8:102. doi: 10.3389/fphar.2017.00102

Zhang, M., Cui, S. W., Cheung, P. C. K., and Wang, Q. (2007). Antitumor polysaccharides from mushrooms: a review on their isolation process, structural characteristics and antitumor activity. *Trends Food Sci. Technol.* 18, 4–19. doi: 10.1016/j.tifs.2006.07.013

Zhang, Z., Liu, Z., Tao, X., and Wei, H. (2016).Characterization and sulfated modification of an exopolysaccharide from *Lactobacillus plantarum* ZDY2013 and its biological activities. *Carbohydr. Polym.* 153, 25–33. doi: 10.1016/j.carbpol.2016.07.084

Zhao, H., Xu, X., Lei, S., Shao, D., Jiang, C., Shi, J., et al. (2019). Iturin A-like lipopeptides from *Bacillus subtilis* trigger apoptosis, paraptosis, andautophagy in Caco-2 cells. *J. Cell. Physiol.* 234, 6414–6427. doi: 10.1002/jcp.27377

Conflict of Interest: The authors declare that the research was conducted in the absence of any commercial or financial relationships that could be construed as a potential conflict of interest.

Publisher's Note: All claims expressed in this article are solely those of the authors and do not necessarily represent those of their affiliated organizations, or those of the publisher, the editors and the reviewers. Any product that may be evaluated in this article, or claim that may be made by its manufacturer, is not guaranteed or endorsed by the publisher.

frontiers | Frontiers in Microbiology

ORIGINAL RESEARCH
published: 29 April 2022
doi: 10.3389/fmicb.2022.817591

The Probiotic Strain *Bifidobacterium animalis* ssp. *lactis* HY8002 Potentially Improves the Mucosal Integrity of an Altered Intestinal Microbial Environment

Joo Yun Kim, So-Jung Bang, Ju-Yeon Kim, Eun Jung Choi, Keon Heo, Jae-Jung Shim and Jung-Lyoul Lee*

R & BD Center, hy Co., Ltd., Yongin-si, South Korea

Intestinal microbiota mediate the development and regulation of the intestinal immune system either directly or indirectly. Particularly, *Bifidobacterium* spp. play an important role in regulating the intestinal immunity and intestinal barrier. We demonstrated that *Bifidobacterium animalis* ssp. *lactis* HY8002, selected from eight *Bifidobacterium* strains by *in vitro* experimentation, had exceptional resistance to digestive tract conditions and high adhesion to intestinal epithelial cells and a positive effect on immunoglobulin A (IgA) secretion by Peyer's patch cells. Moreover, HY8002 restored the expression of tight junction-related genes, initially reduced by lipopolysaccharide treatment, to normal levels in human intestinal epithelial cells. Notably, HY8002 restored kanamycin-induced reduction in Peyer's patch cell numbers, serum and fecal IgA levels, and zonula occludens 1 and Toll-like receptor 2 levels in the mouse small intestine. In addition, HY8002 restores microbiome composition disturbed by kanamycin, and these microbiome changes have been found to correlate with TLR2 levels in the small intestine. Moreover, the ability of HY8002 to enhance IgA in Peyer's patch cells and ZO-1 levels in intestinal epithelial cells was significantly inhibited by a TLR2 blocking antibody, which suggests that the HY8002 improve intestinal barrier function *via* TLR2. Finally, whole-genome sequencing of HY8002 revealed that it did not possess any known virulence factors. Therefore, HY8002 is a promising, functional probiotic supplement to improve intestinal barrier function by improving intestinal immunity and microbiota balance.

Keywords: intestinal microbiome, Peyer's patches, IgA, tight junctions, dysbiosis, antibiotics—immune effect

OPEN ACCESS

Edited by:
Martin Schwarzer, Academy of Sciences of the Czech Republic (ASCR), Czechia

Reviewed by:
Julia M. Green-Johnson, Ontario Tech University, Canada
Jiri Hrdy, Charles University, Czechia

****Correspondence:***
Keon Heo
gunny@hy.co.kr

Specialty section:
This article was submitted to Food Microbiology, a section of the journal Frontiers in Microbiology

Received: *18 November 2021*
Accepted: *11 April 2022*
Published: *29 April 2022*

Citation:
Kim JY, Bang S-J, Kim J-Y, Choi EJ, Heo K, Shim J-J and Lee J-L (2022) The Probiotic Strain Bifidobacterium animalis ssp. lactis HY8002 Potentially Improves the Mucosal Integrity of an Altered Intestinal Microbial Environment. Front. Microbiol. 13:817591. doi: 10.3389/fmicb.2022.817591

INTRODUCTION

The mucosal immune system protects the body from foreign substances, such as pathogens and food allergens, and is closely associated with homeostasis (Brandtzaeg et al., 1999; Holmgren and Czerkinsky, 2005; Levit et al., 2017). In particular, mucosal immunity plays a crucial role in protecting intestinal mucosa, which has a large surface area that is exposed to the

external environment. Therefore, the mucosal-associated lymphoid tissue (MALT) forms a large area of the intestinal lymphoid tissue and consists of Peyer's patches, lamina propria, and mesenteric lymph nodes (Hansen and Sams, 2018; Park et al., 2020). Peyer's patches can be induced to secrete immunoglobulin A (IgA) to the mucosal surface; they play the most important role as an intestinal immune barrier (Fagarasan and Honjo, 2003; Cerutti and Rescigno, 2008; Macpherson et al., 2008; Hara et al., 2019). The IgA immunoglobulin accounts for nearly 80% of all the antibodies produced in the mucosal tissues and prevents the absorption of antigens at mucosal surfaces by attaching to bacteria or viruses (Macpherson et al., 2000; Cerutti and Rescigno, 2008; Kim et al., 2016). It is the first line of defense and ensures both immune exclusion and neutralization of the translocated bacteria. Thus, it is an important regulator of bacteria-induced inflammation and preserves the integrity of the intestinal barrier (Cunningham-Rundles, 2001; Macpherson et al., 2001; Boullier et al., 2009; Park et al., 2020). Intercellular movement of molecules in the intestine is regulated by complex interactions among numerous proteins in tight junctions, which connect intestinal epithelial cells. Therefore, tight junctions play an important role in maintaining the integrity of the intestinal epithelial barrier (Suzuki, 2013; Feng et al., 2019). Proteins, such as zona occludens 1 (ZO-1) and occludin (OCLN), that constitute tight junctions are selectively regulated by protein kinase C and have also been reported to be associated with Toll-like receptors (TLRs; Stuart and Nigam, 1995; Cario et al., 2004; Gu et al., 2016). The TLR family of receptors regulate the immune system by recognizing and discriminating between foreign pathogens and endogenous molecules. Previously, TLRs were known to be involved in innate immunity alone; however, studies have found that they play a key role in linking innate and acquired immunities. While 10 functional TLRs have been discovered in humans, research on each of their function and any related diseases is ongoing (El-Zayat et al., 2019).

Bifidobacterium spp. are gut microbes that play an important role in promoting a favorable intestinal ecosystem, and they exhibit immunomodulatory effects in both animals and humans (Hill et al., 2017; Shang et al., 2020). Studies have found that some *Bifidobacterium* spp. coexist beneficially with commensal microbes in the gut and have positive effects on the immune system (Routy et al., 2018; Bonfrate et al., 2020; Shang et al., 2020). These positive effects are attributable to interactions between specific molecules expressed by the *Bifidobacterium* spp. and pattern recognition receptors, such as TLRs, present on intestinal epithelial and immune cells (Meng et al., 2016; Ruiz et al., 2017; Shang et al., 2020). However, not all *Bifidobacterium* spp. exhibit identical immunoregulatory activities; rather, various strains of a single species may exhibit different immunoregulatory characteristics (Medina et al., 2007; Menard et al., 2008; Ruiz et al., 2017).

Broad-spectrum antibiotics promote intestinal bacterial imbalance, called gut dysbiosis, by dramatically reducing the diversity and taxonomic richness of the gut microbiota (Antonopoulos et al., 2009; Rea et al., 2011; Liu et al., 2020). Gut dysbiosis impairs the integrity of the intestinal barrier by inhibiting tight junction-related protein synthesis in intestinal epithelial cells and IgA secretion in Peyer's patches (Maruya et al., 2013; Kim et al., 2016; Feng et al., 2019). Disrupting this integrity can ultimately lead to and exacerbate gastrointestinal diseases and systemic immune and metabolic disorders (Carding et al., 2015; Feng et al., 2019; Ferreira et al., 2020). Of note, probiotics and prebiotics are being proposed as emerging dietary supplements that can prevent and improve gut dysbiosis by regulating the composition of the gut microbiota (Lee et al., 2006; Liu et al., 2020; Shi et al., 2020).

Several studies have attempted to use *Bifidobacterium* spp. to prevent and alleviate intestinal dysbiosis and dysbiosis-associated diseases (Medina et al., 2007; Meng et al., 2016; Lee et al., 2019; Invernici et al., 2020). However, most of these studies have only validated the mechanism of action and disease improvement properties of the bifidobacterial strains. They have not evaluated the characteristics or the potential of the strains as probiotics. Therefore, in this study, we selected bifidobacterial strains that exhibited high potential as probiotics, had high cell viability in simulated digestive tract conditions, and had good adherence ability with the intestinal epithelial cells. In addition, we selected a strain that could substantially induce IgA secretion in Peyer's patch cells and promote the expression of tight junction-related genes in the intestinal epithelial cells. Eventually, the effect of this strain on intestinal integrity and microbiota restoration was measured in a mouse model with a kanamycin-induced disturbed intestinal microbial environment.

MATERIALS AND METHODS

Preparation of the Bifidobacterial Strains

Bifidobacterium (*B*) *breve* HY3016, *B. breve* HY8921, *Bifidobacterium longum* HY3090, *B. longum* HY3181, *B. longum* HY8805, *Bifidobacterium animalis* ssp. *lactis* HY8002, *B. animalis* ssp. *lactis* HY8901, and *Bifidobacterium infantis* HY8941 were isolated from the feces of only breastfed infants and stored in a seed cell library at Hy Co., Ltd. (Yongin, South Korea). The well-known probiotic *B. animalis* ssp. *lactis* BB12 (ATCC 27536) was used as a reference strain for our *in vitro* experiments (Jungersen et al., 2014). All strains were anaerobically cultured in a blood glucose liver (BL) medium (KisanBio, Seoul, South Korea) at 37°C for 18 h and passaged twice before the experiment. Thereafter, the cultured cells were centrifuged at 4,000 × *g* at 4°C for 5 min and washed twice with saline. Subsequently, the cell pellets were resuspended in saline or phosphate-buffered saline (PBS) for *in vitro* and *in vivo* experiments.

Evaluation of Strain Viability in Simulated Gastrointestinal Tract Conditions

The probiotic potential of bifidobacterial strains were evaluated by measuring their survival rate in physiological conditions similar to those of the human gastrointestinal tract (GIT). This experiment was performed as previously reported (Kim et al., 2021). Briefly, 5 ml of the culture suspensions (1.0×10^9 CFU/ml in saline) was poured into 50 ml conical tubes. Following this, 26 μl of 0.3 M $CaCl_2$ solution and 4 ml of 6.55 mg/ml α-amylase solution were added to each suspension.

The physiological conditions of the oral cavity were simulated by adding 1 M NaOH to adjust the pH of the suspensions to 7.0, followed by incubation at 37°C for 2 min. Subsequently, the conditions of the gastric tract were simulated by adding 6 µl of 0.3 mol/L $CaCl_2$, 694 µl water, and 9.1 ml of 0.07 mg/ml pepsin to the above mixture. The pH was adjusted to 3 by adding 1 M HCl to the mixture and incubating it at 37°C with continuous shaking for 2 h. Eventually, the intestinal conditions were simulated by adding 40 µl of 0.3 M $CaCl_2$, 1.31 ml of distilled water, 2.5 ml of 160 mM bile extract, and 16 ml of 22 mg/ml pancreatic solution to the mixture. The pH of the mixture was adjusted to 7.0 using 1 M NaOH and incubated at 37°C for 2 h. Aliquots of the mixture were collected at the end of each digestive step and subsequently determined the cell viabilities using BL agar plates (Difco, Sparks, MD, United States).

Determination of Bifidobacterial Adhesion to Intestinal Epithelial Cells

The ability of *Bifidobacterium* strains to adhere to the human intestinal epithelial cells was evaluated by slightly modifying previously reported methods (Shang et al., 2020; Kim et al., 2021). For this purpose, the human colorectal adenocarcinoma cell line Caco-2 was purchased from the American Type Culture Collection (Manassas VA, United States) and was cultured in a Modified Eagle Medium (MEM; Thermo Fisher, Waltham, MA, United States) supplemented with 10% heat-inactivated fetal bovine serum (FBS) at 37°C and 5% carbon dioxide (CO_2). Subsequently, 1.0×10^5 Caco-2 cells/well were inoculated in a 24-well plate, and the medium was replaced with FBS-free MEM once the cells grew to a 100% confluency. The *Bifidobacterium* strains (test and reference strains) were diluted in PBS, inoculated at 1.0×10^8 CFU/ml of Caco-2 cells/well, and incubated in 5% CO_2 at 37°C for 2 h. Post-incubation, the cells were washed four times with PBS and separated from the plate by treatment with 0.05% trypsin–EDTA (Sigma-Aldrich, St. Louis, MO, United States) for 5 min. The Caco-2 cell count was obtained using an automated cell counter (Bio-Rad Laboratories, Hercules, CA, United States) and the cell viability of the *Bifidobacterium* spp. was estimated using BL agar plates.

Animals

Six-week-old specific pathogen-free male BALB/c mice were purchased from DooYeol Biotech (Seoul, South Korea) and maintained in a testing facility at Hy Co., Ltd. for 1 week before experiments were initiated. Animals were housed under controlled conditions: 23 ± 2°C temperature, 50 ± 5% humidity, and a 12-h light/dark cycle (7 AM to 7 PM). The mice were fed with sterile AIN-93G (Dyets, Bethlehem, Palestine), and a UV sterilizer and an autoclave were used to sterilize the breeding materials before use. No abnormalities that could possibly affect the experimental outcomes were found in the mice.

Ethics Approval Statement

The animal study was reviewed and approved by the Institutional Animal Care and Use Committee of hy Co., Ltd. (approval number: AEC-2021-00008-Y).

Isolation of Peyer's Patch Cells and Analysis of IgA Production

The BALB/c mice were sacrificed by CO_2 overdose and their small intestines were removed. Thereafter, Peyer's patches were separated using 4 µm micro-scissors. These patches were transferred to an RPMI 1640 medium (Thermo Fisher) supplemented with 1% antibiotic–antimycotic (Thermo Fisher) and were subsequently disrupted by a sterile 100 µm mesh to isolate Peyer's patch cells. The dissociated cells were aspirated, washed twice with Hank's balanced salt solution (Sigma-Aldrich), suspended in 10% RPMI 1640 medium, and eventually inoculated in a 96-well plate at a concentration of 1.0×10^6 cells/well. Thereafter, 1.0×10^8 CFU/ml/well of the *Bifidobacterium* strains were incubated at 37°C for 48 h to induce IgA secretion by Peyer's patch cells. Lipopolysaccharide (LPS) was used as a positive control for the induction of IgA secretion (Kim et al., 2016; Park et al., 2020). Subsequently, the plates were centrifuged and the levels of IgA secreted into the medium were estimated using a mouse IgA ELISA kit (Abcam, Cambridge, United Kingdom).

Analysis of Tight Junction-Related Gene Expression in CaCo-2 Cells

The expression of the tight junction-related genes, such as *ZO-1* and *OCLN*, was determined by quantitative PCR (qPCR), as follows. Caco-2 cells were cultured to 100% confluency in six-well plates. Next, *Bifidobacterium* strains were resuspended in an antibiotic-free MEM supplemented with 1 µg/ml LPS and incubated with Caco-2 cells at 37°C in a humidified incubator with 5% CO_2 for 24 h. The Caco-2 cells cultured in MEM without microbial inoculation were designated as the control group. Post-incubation, total RNA was extracted from the CaCo-2 cells using the TRIzol reagent (Sigma-Aldrich) according to the manufacturer's instructions. Subsequently, cDNA was synthesized using a reverse transcription kit (Qiagen, Hilden, Germany). The mRNA levels were measured using TaqMan Universal PCR Master Mix (Applied Biosystems, Foster, CA, United States) and the QuantStudio 6 Real-Time PCR System (Applied Biosystems). The TaqMan probes used to measure the mRNA expression levels are presented in **Table 1**. The mRNA expression of glyceraldehyde-3-phosphate dehydrogenase (GAPDH) was used to normalize the expression levels of each target gene (Kozera and Rapacz, 2013).

Design and Treatment for Animal Experiments

Seven-week-old male BALB/c mice were divided into four groups ($n = 8$ per group): normal group (N), 1,000 mg/kg/day

TABLE 1 | TaqMan probes for human genes.

Gene name	TaqMan® probe ID	Dye	Manufacturer
Human GAPDH (*GAPDH*)	Hs02786624_g1	FAM	Thermo Fisher Scientific
Human Zonula occludens 1 (*ZO-1*)	Hs01551861_m1	FAM	
Human occludin (*OCLN*)	Hs05465837_g1	VIC	

kanamycin administration group (C), kanamycin with 1.0×10^8 CFU/kg/day HY8002 administration group (8002L), and kanamycin with 1.0×10^9 CFU/kg/day HY8002 administration group (8002H). To induce intestinal dysbiosis, kanamycin was orally administered to all mice except the N group for 7 consecutive days. On the other hand, mice in the normal group were administered with only physiological saline (0.9% NaC). After kanamycin treatment, HY8002 suspended in physiological saline was orally administered to the HY8002L and HY8002H groups for 4 weeks, and only physiological saline was administered to the N and C groups during the same period (**Figure 1**). No animals died or exhibited any abnormal characteristics during the experiment. Food intake and body weight of the mice were measured once per week until the mice were sacrificed.

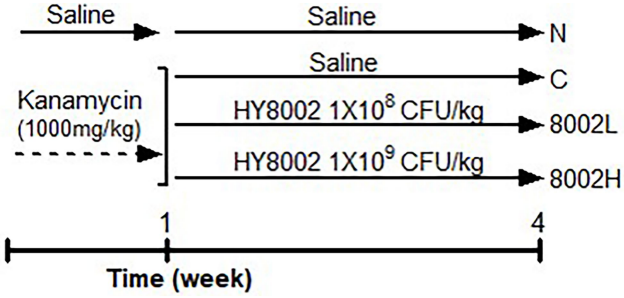

FIGURE 1 | Timeline and treatments of the animal experiments. N, normal group; C, kanamycin administration group; 8002L, kanamycin with 1.0×10^8 CFU/kg/day HY8002 administration group; 8002H, kanamycin with 1.0×10^9 CFU/kg/day HY8002 administration group.

Total Cell Count of Peyer's Patches and Measurement of Intestinal IgA Levels

Post-treatment, mice were euthanized by CO_2 overdose and their small intestines and cecum were dissected. Peyer's patch cells were isolated from the dissected small intestine using the method specified in Animals section. Subsequently, the total cell count was determined using an automatic cell counter (Bio-Rad). Upon isolating Peyer's patches, the remaining small intestines were stored at −80°C for mRNA analysis. Additionally, feces from the isolated cecum were collected, and the secreted IgA levels were measured using a mouse IgA ELISA kit (Abcam).

Measurement of Plasma Immunoglobulins and Cytokines

Before the mice were sacrificed, their blood was isolated from the abdominal vein using a syringe and isolated the plasma using EDTA tubes (BD, Franklin Lakes, NJ, United States). Thereafter, the blood immunoglobulin (such as IgA, IgG2a, and IgE) concentration in the isolated plasma (Kim et al., 2016; Park et al., 2020) was determined using an ELISA kit (Abcam) according to the manufacturer's instructions. The levels of pro-inflammatory cytokines tumor necrosis factor alpha (TNF-α), interleukin 1beta (IL-1β) and interferon gamma (IFN-γ), and anti-inflammatory cytokine Interleukin 10 (IL-10) in plasma were measured using the Multiplex Cytokine Assay Kit (Mouse Luminex Discovery Assay, R&D systems, Minneapolis, MN, United States).

Measurement of mRNA Levels in the Intestinal Tissue

The mRNA levels of ZO-1, OCLN, TLR2, and TLR4 were measured by qPCR. Briefly, total RNA was extracted from the small intestine tissues using the AllPrep RNA mini kit (QIAGEN Sciences Inc., Germantown, MD, United States) as per the manufacturer's instructions. Subsequently, cDNA synthesis and qPCR were performed as described in Analysis of Tight Junction-Related Gene Expression in CaCo-2 Cells section. The TaqMan probes used to measure mRNA levels in the tissues of the small intestine are presented in **Table 2**.

TABLE 2 | TaqMan probes for mouse genes.

Gene name	TaqMan® probe ID	Dye	Manufacturer
Mouse GAPDH (*GAPDH*)	Mm99999915_g1	FAM	Thermo Fisher Scientific
Mouse Zonula occludens-1 (*ZO-1*)	Mm01320638_m1	FAM	
Mouse occludin (*OCLN*)	Mm00500912_m1	FAM	
Mouse Toll-like receptor 2 (*TLR2*)	Mm01213946_g1	FAM	
Mouse Toll-like receptor 4 (*TLR4*)	Mm00445273_m1	FAM	

Fecal Microbiota Analysis

The feces (0.3 g per mouse) of four different mice were randomly collected from each group prior to sacrificing the animals for gut flora analysis. Total DNA was isolated from the feces, and the microbiota composition was verified by 16S rDNA sequencing using a next-generation sequencing platform (Illumina, San Diego, CA, United States). The universal primer pairs used for the sequencing were as follows: V3-F: 5′-TCGTCGGCA GCGTC AGATGTGTATAAGAGAC AGCCTACGGGNG GCWGCAG-3′ and V4-R: 5′-GTCTCGTGGGCTC GGAGATGT GTATAAGA GACAGGACTACHV GGGTATCTAATCC-3′. Next, DNA extraction, 16S rDNA sequencing, and bioinformatics analysis were performed at Macrogen (Seoul, South Korea). The operational taxonomic units were aligned with the NCBI 16S microbial database, and all the taxonomic information was compiled using the BLAST+ database (v. 2.9.0; Lee et al., 2021). The Chao1 and PD_whole tree indices were analyzed using the QIIME program (Magoc and Salzberg, 2011). Any significant differences in genus levels between groups were analyzed by conducting Linear discriminant analysis Effect Size online.[1] Correlation analyses were conducted and visualized using the FactoMineR package (available online: https://www.r-project.org accessed on September 10, 2021).

[1]http://huttenhower.sph.harvard.edu/galaxy

Spearman's correlation analysis was performed to analyze the results statistically by using FactoMineR (Lee et al., 2021).

Safety Evaluation by Whole-Genome Sequencing

Gelatinase, hyaluronidase, aggregation substance, enterococcal surface protein, cytolysin, enterotoxin, non-hemolytic enterotoxin, hemolysin, cereulide, serine protease, and transposon-related enzymes are well-established as potential virulence factors of microorganisms (Di Cagno et al., 2013; Kim et al., 2021). Analysis of whether HY8002 expressed the genes pertaining to these enzymes was done by performing whole-genome sequencing and bioinformatics analyses in Chunlab (Chunlab Inc., Seoul, South Korea). All datasets have been deposited in NCBI GeneBank with the accession number PRJNA819830.

Statistical Analyses

Statistical results for our *in vitro* and *in vivo* experiments are expressed as mean ± SEM at the 95% confidence limit. Data were statistically compared by one-way ANOVA and a *post-hoc* Tukey test. All statistical analyses were performed using GraphPad Prism v5 (San Diego, CA, United States).

RESULTS

Survival Rate of Bifidobacterial Strains Under Simulated Gastrointestinal Tract Conditions

Upon measuring the survival rate of the *Bifidobacterium* strains under simulated GIT conditions, the artificial saliva treatment was observed to have less effect on bacterial survival compared with the other two digestive juices. In fact, HY8002 exhibited a significantly higher gastric survival rate than the reference strain BB12, whereas HY3016 and HY8921 had survival rates that were similar to that of the reference strain. In contrast, HY3090 and HY8805 strains displayed relatively low resistance to intestinal conditions. Moreover, HY3181, HY8901, and HY8941 had a lower survival rate than BB12 under the simulated GIT conditions (**Figure 2A**).

Ability of Bifidobacterial Strains to Adhere to Caco-2 Cells

The *in vitro* test performed to estimate the ability of the bifidobacterial strains to adhere to the intestinal cells revealed that approximately 18 HY8002 cells adhered to the Caco-2 cells for 2 h. On the contrary, approximately only 10 BB12 adhered to the Caco-2 cells. Furthermore, HY3090, HY3181, HY8805, and HY8941 exhibited very low rates of adhesion to CaCo-2 cells, whereas HY3016 and HY8921 had adhesion rates similar to that of BB12. Therefore, HY8002 was validated to display the highest ability to adhere to intestinal epithelial cells among all the tested strains, including the reference strain (**Figure 2B**).

Effects of Bifidobacterial Strains on Immunoglobulin A Production *in vitro*

To predict the effect of *Bifidobacterium* strains on intestinal immune regulation, the levels of IgA produced by Peyer's patch cells were measured. Barring HY3081, HY8805, and HY8941, most strains were found to enhance IgA secretion in these cells. Notably, HY8002 was observed to significantly induce higher IgA secretion than the reference strain. Nonetheless, no strains induced higher IgA secretion than the positive control LPS (**Figure 3**).

Effects of Bifidobacterial Strains on Tight Junction-Related Gene Expression in Caco-2 Cells

The strains HY3016, HY3090, HY8002, and HY8921 were selected to determine the effect of bifidobacterial strains on tight junction-related gene expression in intestinal epithelial cells. This was because these strains remarkably induced IgA secretion and had substantial cell viability under GIT conditions. Moreover, they

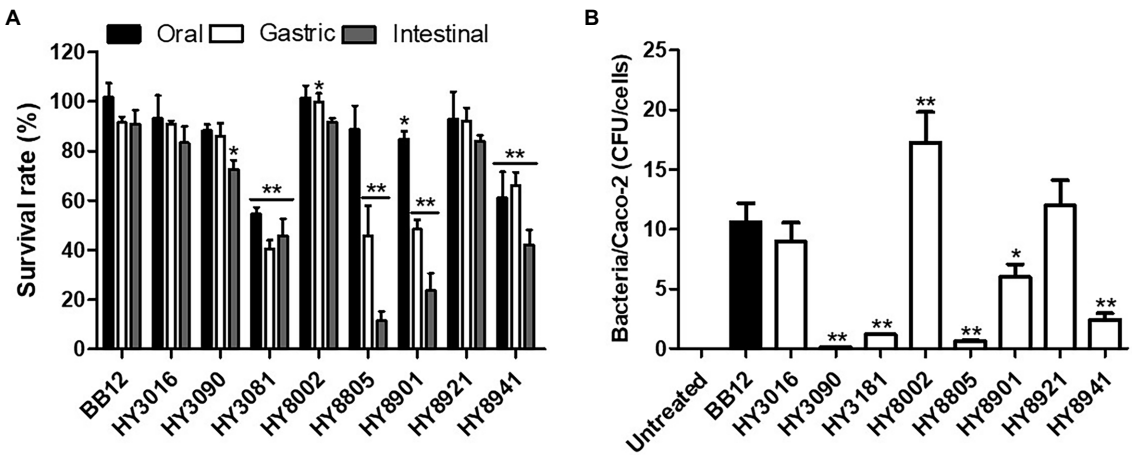

FIGURE 2 | (A) Survival rate of bifidobacterial strains in simulated gastrointestinal tract conditions. **(B)** The number of bacterial cells attached to one Caco-2 cell under co-culture conditions. "Bacteria/Caco-2 cells" indicates bacterial colony-forming units (CFU) per Caco-2 cell. Data are represented as mean ± SEM of three independent experiments. $^{*}p < 0.05$ and $^{**}p < 0.01$ as compared with BB12.

exhibited superior or similar magnitude of adherence to Caco-2 cells than the reference strain. While LPS treatment significantly reduced the mRNA levels of ZO-1 and OCLN in Caco-2 cells, HY8002 and HY8921 considerably restored the mRNA levels of ZO-1 (**Figure 4A**). However, the mRNA levels of OCLN were increased only in the HY8002 treated groups (**Figure 4B**).

Effect of HY8002 on the Food Intake, Body Weight, and Spleen Indices of Mice

Since HY8002 had the highest cell viability under GIT conditions and the most adherence to Caco-2 cells and induced the highest IgA secretion among all the bifidobacterial strains, a follow-up experiment was conducted to investigate its effect on intestinal integrity. For this purpose, a kanamycin-treated mouse model was used, and high kanamycin concentration was observed to slightly reduce the mouse body weight (**Figure 5A**). However, HY8002 administration restored this weight loss; nonetheless, there was no significant difference between all the groups. Moreover, no significant difference in food intake was observed between the normal group, the kanamycin-treated control group, and the HY8002 administered groups (**Figure 5B**). Although the weight of the mouse spleen decreased in the kanamycin-treated group and increased in the HY8002 treated groups, this difference was statistically insignificant (**Figure 5C**).

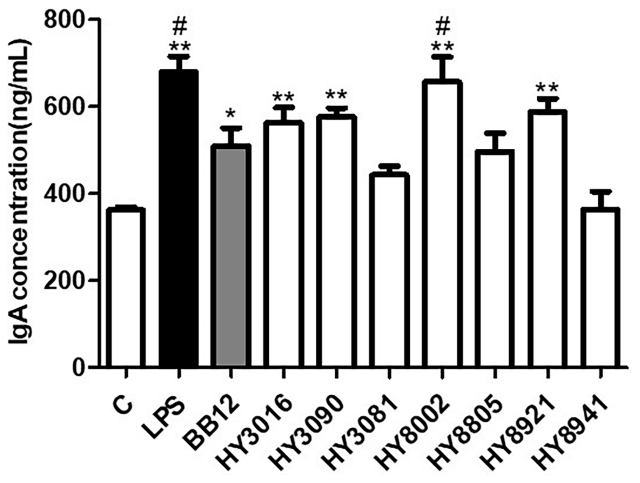

FIGURE 3 | Effect of *Bifidobacterium* strains on immunoglobulin A (IgA) production by Peyer's patch cells. Lipopolysaccharide was used as the positive control for induction of IgA secretion. The IgA concentration in the culture media was determined by ELISA. Each value is expressed as the means ± SEM of three independent experiments. $^{*}p < 0.05$ and $^{**}p < 0.01$ in comparison with the untreated control. $^{\#}p < 0.05$ compared with BB12 treated.

Effects of HY8002 on the Composition of Peyer's Patches in the Small Intestine

As shown in **Figure 6A**, the number of Peyer's patches in kanamycin-treated mice was significantly lower than that in normal mice. On the other hand, HY8002 administration was verified to increase the number of Peyer's patches to a value similar to that observed in the normal group. The same trend was observed for the total number of Peyer's patch cells (**Figure 6B**). However, no difference in the number of Peyer's patches and the total number of Peyer's patch cells between the 8002L and the 8002H groups was observed.

Effects of HY8002 on *in vivo* Immunoglobulin and Cytokine Production

Studies have reported that high-dose antibiotics treatment weakens the intestinal mucosal barrier by decreasing intestinal IgA levels. It also reduces plasma IgA and IgG2a levels and increases IgE levels, causing systemic immune dysfunction (Sudo et al., 2002; Kim et al., 2016). While kanamycin significantly decreased the plasma IgA levels, HY8002 administration recovered these levels to those in the untreated mice (**Figure 7A**). The same trend was observed for fecal IgA levels (**Figure 7D**). These effects

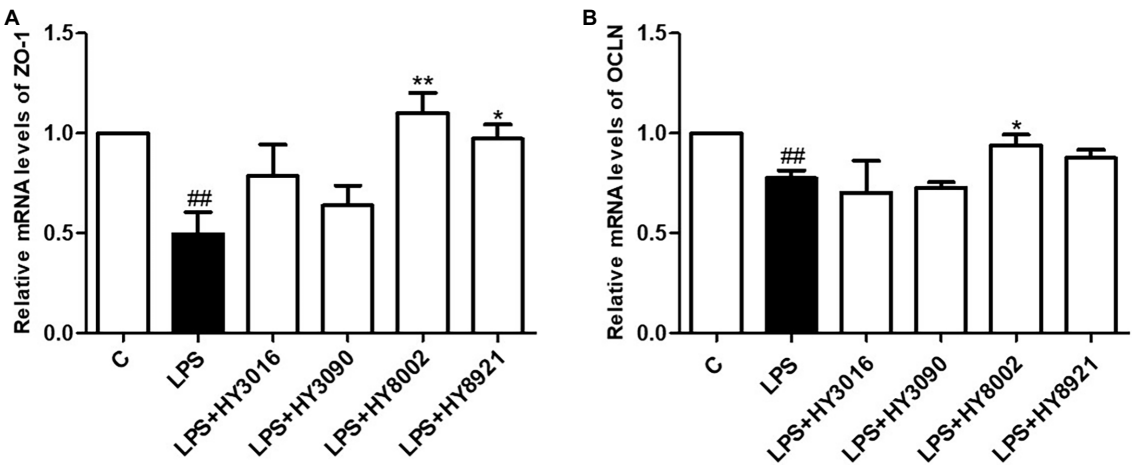

FIGURE 4 | Effect of *Bifidobacterium* strains on **(A)** zonula occludens-1 mRNA expression **(B)** and occludin mRNA expression in lipopolysaccharide (LPS)-treated Caco-2 cells. Each value is expressed as the mean ± SEM of three independent experiments. $^{*}p < 0.05$ and $^{**}p < 0.01$ compared with LPS-treated. $^{\#\#}p < 0.01$ compared with untreated control.

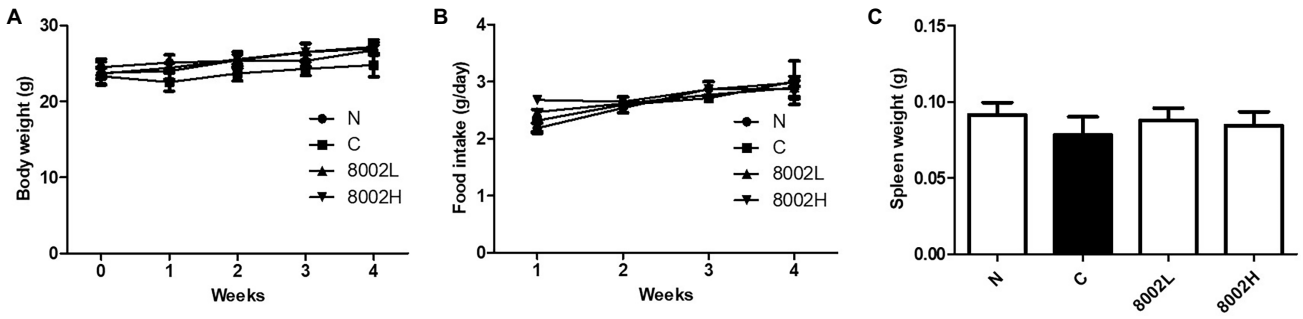

FIGURE 5 | Effect of HY8002 administration on **(A)** body weight, **(B)** food intake, and **(C)** spleen tissue mass in the kanamycin-treated mice. The results are expressed as the mean ± SEM. N, normal group ($n = 8$); C, kanamycin administration group ($n = 8$); 8002L, kanamycin with 1.0×10^8 CFU/kg/day HY8002 administration group ($n = 8$); 8002H, kanamycin with 1.0×10^9 CFU/kg/day HY8002 administration group ($n = 8$).

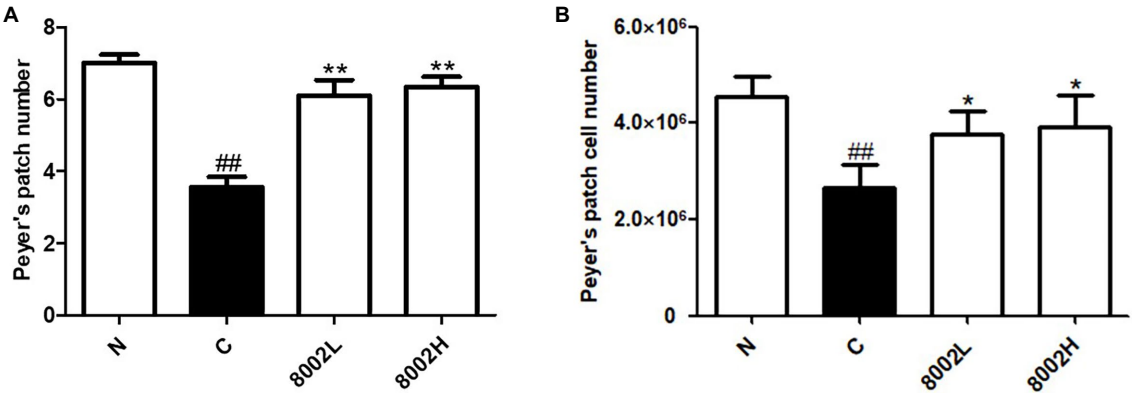

FIGURE 6 | Effect of HY8002 administration on the composition of Peyer's patch structures, including **(A)** number of Peyer's patches and **(B)** total number of Peyer's patch cells in kanamycin-treated mice. The results are expressed as the mean ± SEM. $^*p < 0.05$ and $^{**}p < 0.01$ compared with kanamycin-treated control groups. $^{\#\#}p < 0.01$ compared with normal groups. N, normal group ($n = 8$); C, kanamycin administration group ($n = 8$); 8002L, kanamycin with 1.0×10^8 CFU/kg/day HY8002 administration group ($n = 8$); 8002H, kanamycin with 1.0×10^9 CFU/kg/day HY8002 administration group ($n = 8$).

exhibited a HY8002 dose-dependent trend. Additionally, the plasma IgE levels in the control group were significantly higher than those in the normal group, even 3 weeks post the final kanamycin administration. However, this elevation was significantly suppressed in the HY8002 groups (**Figure 7B**). On the other hand, there were no significant differences in IgG2a levels among all the treatment groups (**Figure 7C**). Cytokines may positively or negatively affect intestinal epithelial barrier integrity and may originate from innate or adaptive immune cells or from the intestinal epithelial cells (Andrews et al., 2018). Blockade of the inflammatory cytokines TNF-α and IL-1β has been studied as a target for the treatment of inflammatory bowel disease (IBD) and ulcerative colitis (UC; Pizarro et al., 2021). IL-10 is an anti-inflammatory cytokine known to have a positive role in maintaining intestinal immune homeostasis, and it is known that intestinal inflammation occurs spontaneously in mice lacking the *IL-10* gene (Alfen et al., 2018). IFN-γ is an immunoregulatory cytokine involved in regulating macrophage activation and T helper cell differentiation. Levels of IFNγ are often elevated locally and systemically in chronic inflammatory diseases, including IBD, resulting in disruption of intestinal barrier function accompanied by decreased expression of the tight junction molecules ZO-1 and occluding (Smyth et al., 2011). Concentrations of TNF-α and IL-1β in plasma were measured at similar levels of all groups including the kanamycin-treated group (**Supplementary Figures 1A,B**). IFN-γ increased in the kanamycin group and tended to decreased in the HY8002 administration group (**Supplementary Figure 1C**). In contrast, plasma IL-10 levels tended to decrease in the kanamycin administration group and to increase in the HY8002 administration group (**Supplementary Figure 1D**). However, there was no statistical significance in IFN-γ and IL-10 levels between all treatment groups.

Effects of HY8002 on mRNA Levels of Tight Junction-Related Genes and Toll-Like Receptor Genes in the Small Intestine

The mRNA levels of the tight junction gene *ZO-1* and the genes encoding the pattern recognition receptors TLR2 and TLR4 were significantly decreased by kanamycin treatment in the mouse small intestine (**Figures 8A–D**). However, the mRNA

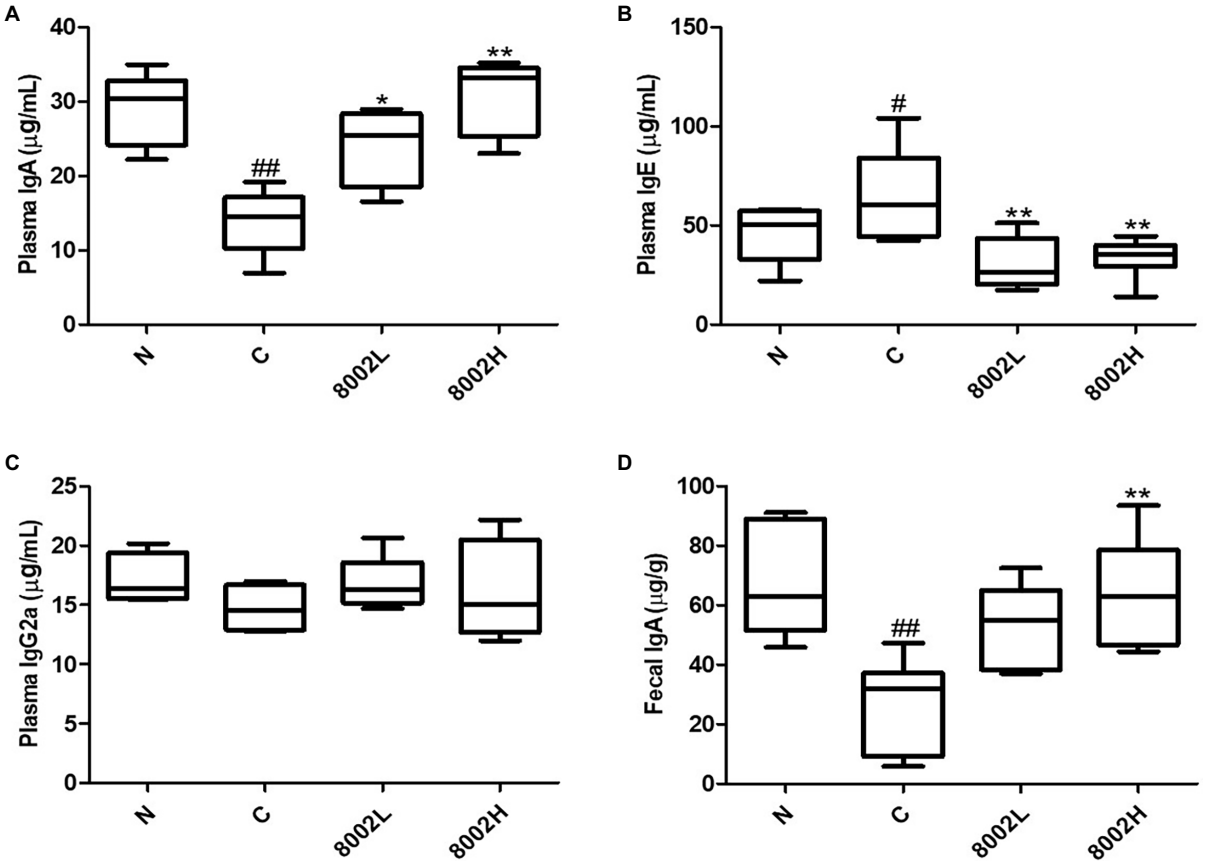

FIGURE 7 | Effect of HY8002 administration on plasma **(A)** IgA, **(B)** IgE, **(C)** IgG2a, and **(D)** fecal IgA in kanamycin-treated mice. The results are expressed as Box and Whisker Plots (median with minimum to maximum values). $^{*}p < 0.05$ and $^{**}p < 0.01$ compared with kanamycin-treated control groups. $^{\#}p < 0.05$ and $^{\#\#}p < 0.01$ compared with normal groups. N, normal group ($n = 8$); C, kanamycin administration group ($n = 8$); 8002L, kanamycin with 1.0×10^8 CFU/kg/day HY8002 administration group ($n = 8$); 8002H, kanamycin with 1.0×10^9 CFU/kg/day HY8002 administration group ($n = 8$).

levels of OCLN were not significantly reduced (**Figure 8B**). Notably, the mRNA level of ZO-1 was significantly upregulated in the 8002H group and the mRNA level of TLR2 was significantly upregulated in both the 8002L and 8002H groups (**Figures 8A,C**). In contrast, the mRNA levels of TLR4 were unaffected by HY8002 administration (**Figure 8D**).

Effect of HY8002 on Intestinal Microbial Diversity and Microbial Profiles in Kanamycin-Treated Mice

The effect of HY8002 on the intestinal environment was investigated by analyzing the differences in the intestinal microbial composition in each treatment group and comparing these differences within a specific microbial taxon. As shown in **Figure 9A**, Firmicutes comprised 28.1% and 35.5% of the total intestinal microbiome in the normal and control groups, respectively. Additionally, they amounted to 18.7% and 24.2% in the 8002L and 8002H groups, respectively. In contrast, kanamycin did not alter the percentage of Bacteroidetes in the microbiome (64% in the normal group and 63% in the control group). Proteobacteria were lower in number in the control, 8002L, and 8002H groups than in the normal group. Actinobacteria (the phylum that includes the *Bifidobacterium* spp.) were significantly decreased by kanamycin treatment; however, their numbers increased in a dose-dependent manner following HY8002 treatment. The α-diversity index, an indicator of microbial diversity within a group, was substantially lowered upon kanamycin treatment but was significantly improved upon HY8002 administration (**Figures 9B,C**). Notably, the Cho1 index was higher in the 8002H group than that in the 8002L group (**Figure 9C**). The linear discriminant analysis (LDA) scores for differentially enriched taxa post-kanamycin and HY8002 treatments are presented in **Figure 9D**. While the relative abundance of the *Oscillibacter* genus was significantly decreased in the control group, high-dose HY8002 administration significantly restored this abundance (**Supplementary Figure 2A**). In contrast, the relative abundances of the *Clostridium* and *Blautia* genera were significantly higher in the control group than that in the normal group. Moreover, HY8002 administration (at all doses) restored these levels to those in the normal group (**Supplementary Figures 2B,C**). Eventually, a Spearman correlation analysis between the mucosal integrity-related indicators of the intestine (e.g., intestinal immunity and tight junctions) and the genus-level taxa that contributed

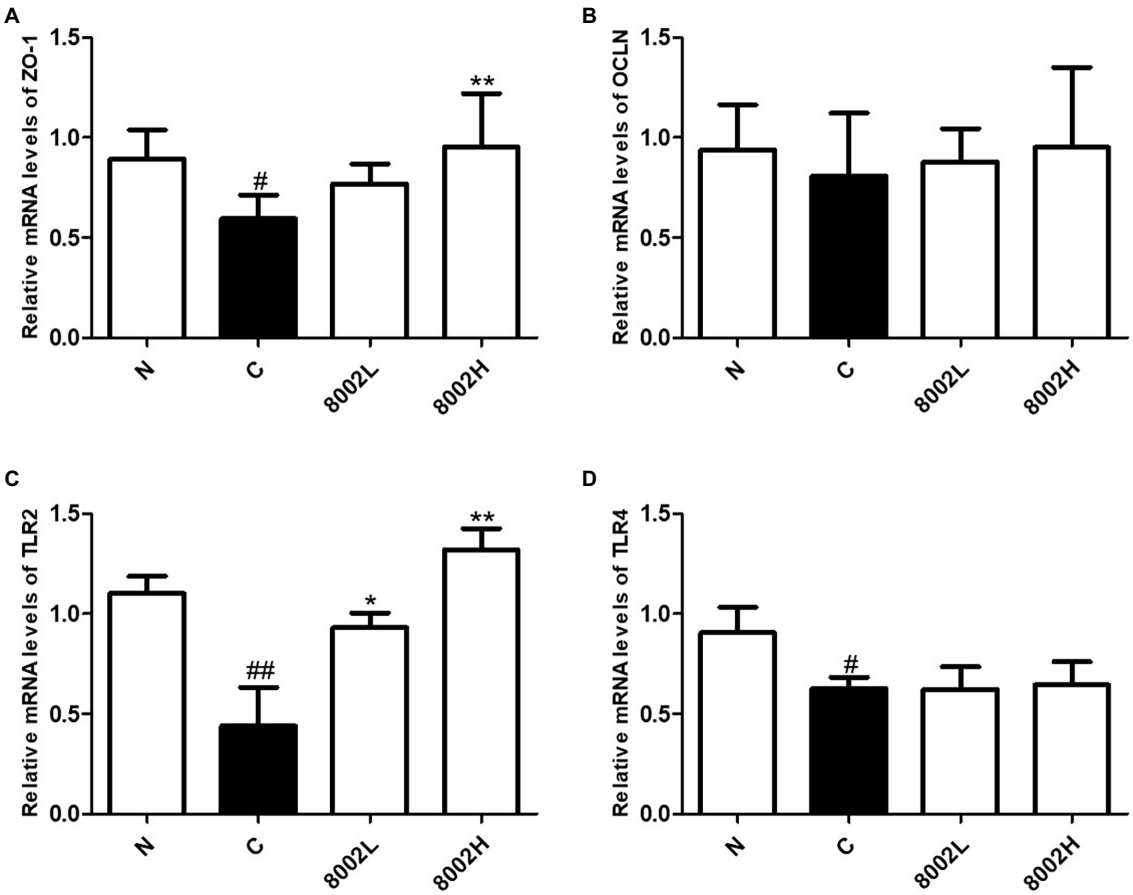

FIGURE 8 | The mRNA levels of **(A)** ZO-1, **(B)** occludin, **(C)** TLR2, and **(D)** TLR4 in small intestine. Data are represented as mean ± SEM. $^{*}p < 0.05$ and $^{**}p < 0.01$ compared with kanamycin-treated control groups. $^{\#}p < 0.01$ and $^{\#\#}p < 0.01$ compared with normal groups. N, normal group ($n = 8$); C, kanamycin administration group ($n = 8$); 8002L, kanamycin with 1.0×10^8 CFU/kg/day HY8002 administration group ($n = 8$); 8002H, kanamycin with 1.0×10^9 CFU/kg/day HY8002 administration group ($n = 8$).

the most to the LDA (except for *Bifidobacterium* spp.; **Figure 9E**) was performed. The *Lachnoclostridium* and *Oscillibacter* genera were observed to be positively correlated with the ZO-1 and TLR2 mRNA levels and IgA secretion in the small intestine. On the contrary, the *Beduini*, *Longibaculum*, *Ruthenibacterium*, *Erysipelatoclostridium*, *Clostridium*, and *Blautia* genera were negatively correlated with the ZO-1 and TLR2 mRNA levels and IgA secretion in the small intestine. The *Enterococcus* and *Terrisporobacter* genera had positive and negative correlations with ZO-1 expression, respectively.

Effects of Toll-Like Receptors on HY8002-Induced IgA Secretion and *ZO-1* Expression

In the above *in vivo* experiment, it was confirmed that administration of HY8002 restored the levels of TLRs, especially TLR2, which were reduced by kanamycin treatment. It was also found that the intestinal microbiota affected by kanamycin and/or HY8002 correlated with IgA secretion and ZO-1 and TLR2 levels in small intestine. Therefore, whether HY8002 directly affects IgA secretion and ZO-1 levels through TLR signaling was investigated using blocking antibodies. After treatment with 0.1 μg/ml of TLR2 and TLR4 blocking antibodies (InvivoGen, San Diego, CA, United States) to Peyer's patch cells isolated from the BALB/c mouse small intestine, the degree of IgA secretion by HY8002 was measured. As a result, IgA secretion was significantly reduced by the TLR2 antibody. In contrast, IgA secretion by LPS was decreased by TLR4 blockade (**Figure 10A**). As a result of confirming the mRNA change of the tight junction molecules by HY8002 in Caco-2 cells pretreated with TLR2 and TLR4 blocking antibody, ZO-1 was significantly reduced by TLR2 blocking. The mRNA levels of OCLN tended to be slightly decreased by TLR2 and TLR4 blockade, but there was no statistical significance (**Figure 10B**).

Biological Safety Assessment of HY8002 Based on Whole-Genome Sequencing

The total length of the HY8002 chromosomal DNA was 1,944,140 bp with 60.5% GC content and 1,563 predicted open

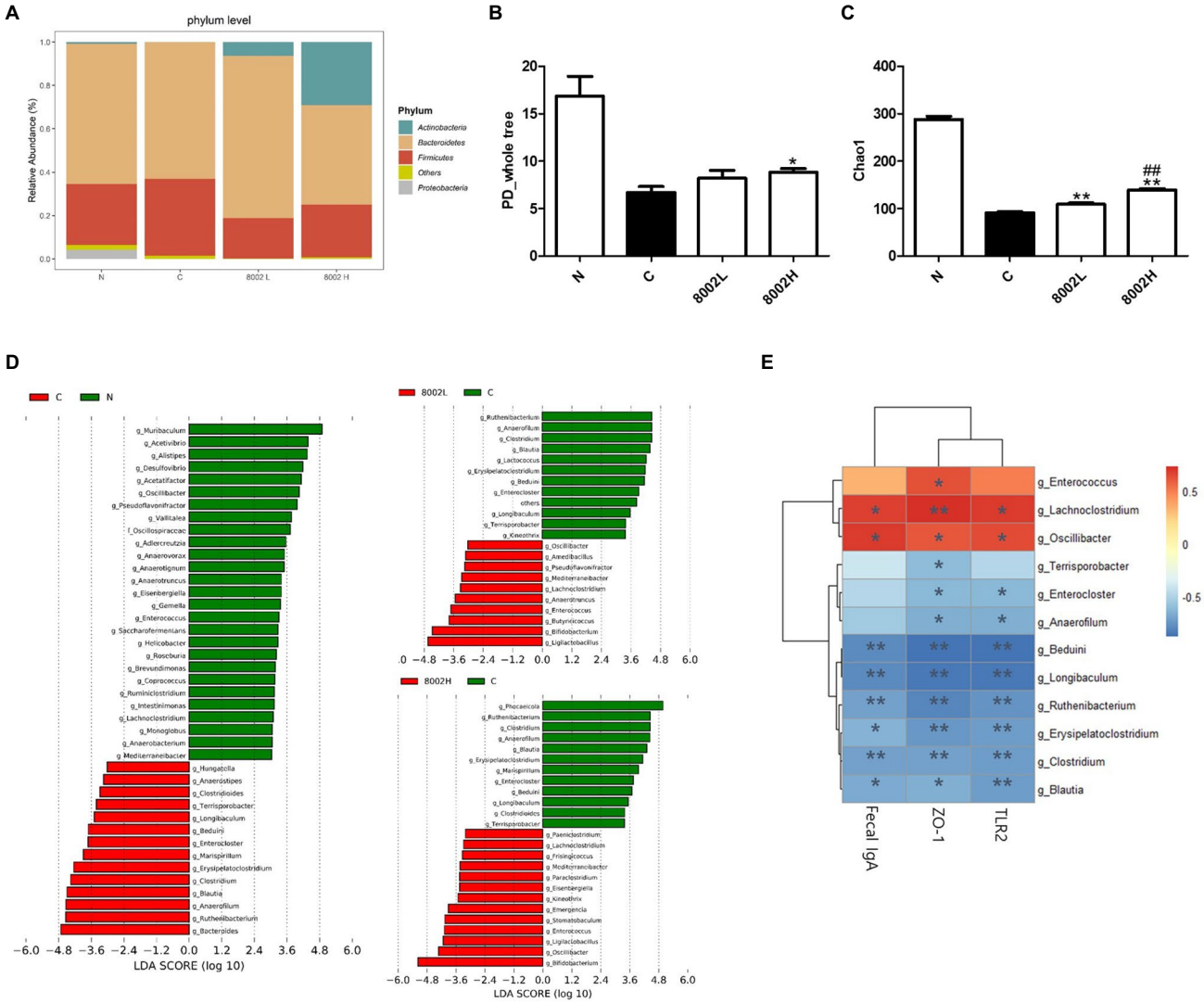

FIGURE 9 | Effect of HY8002 administration on the composition of bacterial taxa in mouse feces. **(A)** Relative abundance of phylum level in each treatment group. The α-diversity of each group: **(B)** PD_whole tree index and **(C)** Chao1 index. **(D)** Histogram of the linear discriminant analysis (LDA) scores for differentially abundant taxa following kanamycin treatment. **(E)** Correlation between bacterial genus-level taxa and measured intestinal integrity-related factors. Statistical analysis was conducted by the spearman correlation analysis. Data are represented as mean ± SEM. $^{*}p < 0.05$ and $^{**}p < 0.01$. $^{\#\#}p < 0.01$ compared with 8002L groups. N, normal group ($n = 4$); C, kanamycin administration group ($n = 4$); 8002L, kanamycin with 1.0×10^8 CFU/kg/day HY8002 administration group ($n = 4$); 8002H, kanamycin with 1.0×10^9 CFU/kg/day HY8002 administration group ($n = 4$).

reading frames. Additionally, genome annotation identified the major genes to be *beta-galactosidase*, *beta-cylosidase*, and *gamma-glutamylcysteine synthetase* involved in glycoside degradation, carbohydrate metabolism, and glutathione synthesis, respectively (**Supplementary Figure 3**). A phylogenetic tree was constructed based on the average nucleotide identity value, and HY8002 was confirmed to be similar to bifidobacterial probiotic strains, such as *Bifidobacterium animalis* ssp. *lactis* DSM10140 (Ehrmann et al., 2003), *Bifidobacterium animalis* ssp. *lactis* V9 (Sun et al., 2010), and *Bifidobacterium animalis* ssp. *lactis* B420 (Stahl and Barrangou, 2012; **Supplementary Figure 4**). In addition, it was established that HY8002 expressed no commonly known virulence genes (data not shown).

DISCUSSION

Scientific evidence that symbiotic and probiotic bacteria play an important role in maintaining and promoting gut homeostasis and intestinal epithelial barrier function is steadily increasing (Lee et al., 2019; Invernici et al., 2020; Ojima et al., 2020; Al-Sadi et al., 2021). Recently, studies have indicated that the intestinal tight junction barrier and immune response are therapeutic targets for the management of several diseases (Lee et al., 2018; Zeisel et al., 2019; Sun and Zhou, 2020). Of note, among the various probiotic bacteria reported to date, *Bifidobacterium* spp. are among the most widely used probiotic bacteria. They colonize the human intestine approximately first

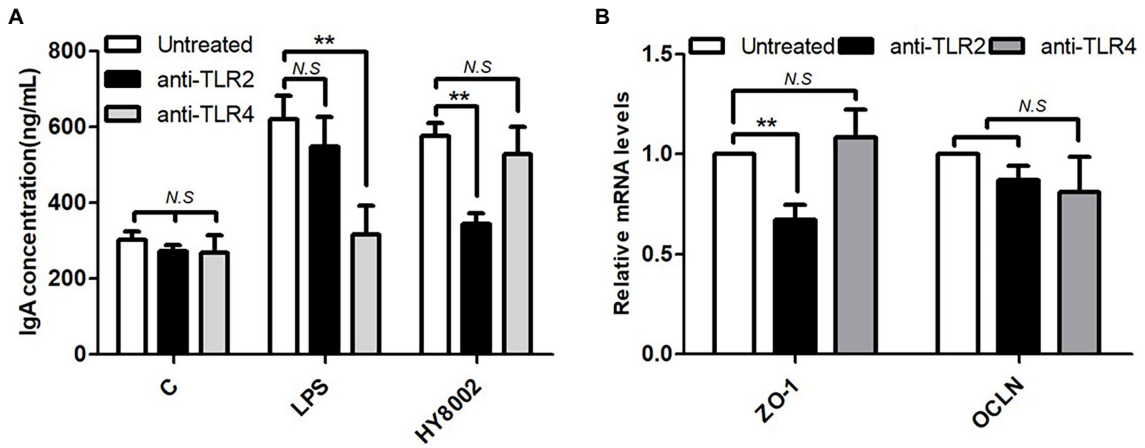

FIGURE 10 | Effect of TLR2 and TLR4 blockade by antibodies on **(A)** IgA production levels in Peyer's patch cells stimulated with HY8002 and **(B)** the mRNA levels of tight junction molecules in HY8002 treated Caco-2 cells. Data are represented as mean ± SEM. $^{**}p < 0.01$ compared with antibody untreated groups.

and account for approximately 80% of the gut microbiota of breastfed infants (Al-Sadi et al., 2021). Their health-promoting activities range from modulating the host immune response, strengthening the intestinal barrier, inhibiting pathogenic bacteria, and maintaining gut homeostasis by building a healthy microbiome. Studies have demonstrated *Bifidobacterium* spp. to be innate and essential members of the human gut, necessary for maintaining the integrity of the intestinal epithelial barrier (Lee et al., 2019; Invernici et al., 2020; Ojima et al., 2020; Shang et al., 2020; Al-Sadi et al., 2021). A recent study reported that gut microbiome profiles of patients with ulcerative colitis exhibited a significant reduction in *Bifidobacterium* spp. (Duranti et al., 2016). However, the beneficial effects of the *Bifidobacterium* genus in the treatment of various diseases remains a controversy (Al-Sadi et al., 2021). This is because there is a gap in scientific knowledge regarding which *Bifidobacterium* spp. is responsible for strengthening the intestinal barrier and which spp. or strain has the greatest effect. There is also a report that the effect of Bifidobacterium on immunomodulation differs depending on the strain, not the species (Medina et al., 2007).

In this study, our primary aim was to identify specific *Bifidobacterium* strains that preserve intestinal integrity by enhancing intestinal mucosal immunity and tight junction barrier function and evaluate their potential as probiotics. The secondary goal was to analyze the effects of the selected *Bifidobacterium* strains on the total intestinal microbiota and to analyze the correlation between the microorganisms involved in maintaining intestinal integrity. To this end, we evaluated the digestion resistance and IgA promoting activity of various bifidobacterial strains isolated from the feces of infants. Additionally, we measured the effect of these strains on upregulating the gene expression of *ZO-1* and *OCLN in vitro*. Consequently, we selected HY8002 for subsequent experiments and determined its *in vivo* effect on antibiotics-disrupted intestinal mucosal immunity (IgA production), tight junctions (ZO-1, OCLN, and TLR2), and intestinal microbiome (fecal microbiota by 16s sequencing analysis).

Although many *Bifidobacterium* strains are used as probiotics, all strains are not probiotics; rather, only strains with gastrointestinal stability and biosafety can be proposed as probiotics (Izquierdo et al., 2008; George Kerry et al., 2018). In fact, the ability to survive in the gastrointestinal tract and attach to the intestinal epithelium is one of the key criteria for probiotic strain selection (Shang et al., 2020; Kim et al., 2021). Orally ingested probiotics reach the intestines through stressful environments, such as saliva, gastric juice, and bile fluids. Therefore, an effective probiotic strain must have high a resistance to digestive conditions and the ability to adhere to the intestine epithelium (Shang et al., 2020). We simulated conditions of the GIT and determined that HY8002 exhibited very high cell viability, particularly in the gastric environment. Moreover, it displayed better digestive stability than the reference BB12 strain (Jungersen et al., 2014) a well-known commercial probiotic strain (**Figure 2A**). Furthermore, HY8002 adhered well to Caco-2 cells, a human intestinal epithelial cell line (**Figure 2B**). Additionally, we validated the genetic safety of this strain through whole-genome sequencing (**Supplementary Figure 3**).

The gastrointestinal tract is the most common entry point for infectious agents, including pathogenic bacteria and viruses, from the mucosal surfaces. The IgA immunoglobulin is a key factor at the forefront of mucosal tissue immunity, including that of the intestine, and serves as a standard for evaluating mucosal immunity (Cunningham-Rundles, 2001; Boullier et al., 2009; Park et al., 2020). Recent studies have confirmed that high-dose broad-spectrum antibiotics reduce IgA secretion because of the death of commensal strains, including intestinal probiotics. This decreases the defense against certain pathogenic bacteria, such as *Pseudomonas aeruginosa* and *Clostridium difficile* (Dzunkova et al., 2016; Robak et al., 2018). Our *in vitro* test determined that HY8002 induced the highest IgA secretion among the five *Bifidobacterium* strains (including BB12) that increased IgA secretion by Peyer's patch cells (**Figure 3**). In addition, our

animal experiments confirmed that HY8002 restores the number of Peyer's patches, total cell count of Peyer's patches, and the IgA levels decreased by kanamycin treatment (**Figures 6, 7A,D**). Remarkably, HY8002 significantly reduced the IgE levels increased by kanamycin, suggesting that it modulates the antibiotics-induced TH1/TH2 immune imbalance (**Figure 7B**). Although previous reports have stated that probiotics regulate systemic TH1/TH2 balance (Kim et al., 2016), the overall immunomodulatory effect of HY8002, excluding intestinal immunity, could not be deduced from this study and further studies are needed.

IgA plays a role in the front-line defense of the intestinal mucosa, whereas tight junctions play a role in maintaining a protective barrier in the posterior region in intestinal epithelium (Suzuki, 2013; Gu et al., 2016; Kim et al., 2016; Feng et al., 2019). Tight junction complexes have been predicted to be affected by TLRs, particularly by TLR2 that regulates *ZO-1* gene expression (Cario et al., 2004). Some probiotic strains of the *Lactobacillus* and *Bifidobacterium* genera increase the expression of tight junction-related genes (Kim et al., 2016; Al-Sadi et al., 2021); however, not all probiotic strains improve tight junction-related gene expression (Sultana et al., 2013). In our study, HY8002 significantly increased the mRNA levels of ZO-1 and OCLN reduced by LPS in Caco-2 cells (**Figures 4A,B**). It also restored the mRNA expression of ZO-1 to normal levels in the small intestine of kanamycin-treated mice (**Figure 8A**). While kanamycin or HY8002 treatment did not cause a significant change in the mRNA levels of OCLN, these levels were higher in the HY8002 treatment groups than those in the control group (**Figure 8B**). In addition, we observed that the mRNA levels of TLR2 and TLR4 in the mouse small intestine were significantly decreased upon kanamycin treatment. However, HY8002 administration restored the mRNA levels of TLR2 but not those of TLR4 (**Figures 8B,C**). Thus, we inferred that HY8002 has a positive effect on the expression of tight junction-related genes in the intestinal epithelial cells by particularly increasing the gene expression of *ZO-1*, related to TLR2. When TLR2 signaling was blocked with a blocking antibody, IgA secretion in Peyer's patch cells and *ZO-1* expression in intestinal epithelial cells by HY8002 were significantly reduced. These results demonstrates that HY8002 enhances the intestinal immune response and tight junctions through TLR2 signaling (**Figures 10A,B**). This observation concurred with that of a recent study wherein a specific strain of *Bifidobacterium bifidum* relieved dextran sulfate sodium-induced colitis by strengthening the tight junction of intestinal epithelial cells through TLR2 signaling (Al-Sadi et al., 2021).

The microbiome plays a pivotal role in the development and maintenance of the mammalian immune system. The GIT has a total area of 400 m^2 and along with an epithelial barrier forms a part of the human body that is greatly affected by the microbiome. It has a complex, open, and integrated ecology that is the most exposed to the external environment (Lazar et al., 2018). Therefore, the intestinal microbiome regulates the intestinal immune response and tight junctions either directly or indirectly. Studies have reported that the strengthening effect that probiotics and prebiotics have on the intestinal mucosa is because of changes in the intestinal microbiome (Duranti et al., 2016; Shi et al., 2020). However, some conflicting reports claim that that the effects some probiotics have on relieving intestinal mucosal inflammation are not correlated with changes in the intestinal microbiome (Ojima et al., 2020). In this study, we demonstrated that in addition to significantly reducing the α-diversity of the mouse gut microbiota, antibiotics also altered the proportions of several microbial genera in the intestine. Notably, HY8002 reversed some of these microbiome changes (**Figures 9B–D**); it restored the proportion of *Oscillibacter* genus that was sharply decreased by kanamycin treatment. In contrast, the intestinal abundances of the *Clostridium* and *Blautia* genera were greatly increased by kanamycin and decreased by HY8002. Recently, studies have reported that *Oscillibacter* are reduced in gastric cancer and Crohn's disease, whereas *Blautia* are associated with diarrhea and rheumatoid arthritis (Zhai et al., 2019; Ojima et al., 2020). The bacterial genus *Clostridium* includes multiple pathogenic strains and is well associated with enteritis and antibiotic-induced diarrhea (Rea et al., 2011; Dzunkova et al., 2016; Shao et al., 2020). We found that the *Oscillibacter* genus was positively correlated with intestinal IgA secretion and ZO-1 and TLR2 levels. In contrast, the *Clostridium* and *Blautia* genera had a negative correlation with IgA secretion and ZO-1 and TLR2 levels (**Figure 9E**). The correlation between the abundance of *Oscillibacter* and *Blautia* and intestinal TLR2 levels was first revealed in our study. From these results, it can be inferred that HY8002 itself not only strengthens the immune response and tight junction of the intestinal mucosa through TLR2 signaling, but also improves intestinal integrity by affecting the intestinal microbiome. Therefore, we confirmed that the bifidobacterial strain HY8002 exhibits excellent abilities to enhance intestinal immunity and strengthen the intestinal barrier. Moreover, it can improve the intestinal microbiota composition and has a high potential as a probiotic. Currently, we are planning a clinical trial to validate the effect of HY8002 on intestinal and systemic immune imbalance. Nevertheless, the limitation of this study is that the secretion of antimicrobial peptides, such as Reg3b and defensins that affects the homeostasis of the intestinal microbiota and the effect of HY8002 on individual immune cells present in Peyer's patch were not confirmed. Therefore, further studies are needed to investigate the effect of HY8002 on the activation of immune cells, such as T cells and B cells, in MALT and the secretion of antimicrobial peptides from the intestinal epithelium.

CONCLUSION

This study validated the potential of *Bifidobacterium animalis* ssp. *lactis* HY8002 as a probiotic to help maintain intestinal integrity. *In vitro*, it displayed a positive tolerance toward simulated digestive tract conditions, adhered well with the intestinal epithelium, and induced high IgA secretion by

Peyer's patch cells. *In vivo*, it restored tight junctions, enhanced systemic and intestinal IgA secretion, and improved the intestinal microbiota balance. In addition, HY8002 was genetically verified as a non-virulent or a safe strain. These results indicate that HY8002 can be used as a beneficial probiotic strain in animals and humans because of its protective effect on intestinal integrity. It is evident that HY8002 is greatly promising for the maintenance of a healthy physiological state, as it enhances the immunity and adhesion margins of the intestinal mucosa. However, further studies are needed to elucidate the molecular communication mechanisms between HY8002 and the host immune system and their effects on the gut microbiome.

DATA AVAILABILITY STATEMENT

The datasets presented in this study can be found in online repositories. The names of the repository/repositories and accession number(s) can be found in the article/ **Supplementary Material**.

ETHICS STATEMENT

The animal study was reviewed and approved by the Institutional Animal Care and Use Committee of hy Co., Ltd. (approval number: AEC-2021-00008-Y).

AUTHOR CONTRIBUTIONS

JK, KH, and J-LL contributed to conception and design of the study. JK and S-JB organized the database. J-YK performed the statistical analysis. JK wrote the first draft of the manuscript. JK, EC, and J-YK wrote sections of the manuscript. All authors contributed to the article and approved the submitted version.

SUPPLEMENTARY MATERIAL

The Supplementary Material for this article can be found online at: https://www.frontiersin.org/articles/10.3389/fmicb.2022.817591/full#supplementary-material

REFERENCES

Alfen, J. S., Larghi, P., Facciotti, F., Gagliani, N., Bosotti, R., Paroni, M., et al. (2018). Intestinal IFN-gamma-producing type 1 regulatory T cells coexpress CCR5 and programmed cell death protein 1 and downregulate IL-10 in the inflamed guts of patients with inflammatory bowel disease. *J. Allergy Clin. Immunol.* 142:1537.e1538–1547.e1538. doi: 10.1016/j.jaci.2017.12.984

Al-Sadi, R., Dharmaprakash, V., Nighot, P., Guo, S., Nighot, M., Do, T., et al. (2021). Bifidobacterium bifidum enhances the intestinal epithelial tight junction barrier and protects against intestinal inflammation by targeting the toll-like receptor-2 pathway in an NF-kappaB-independent manner. *Int. J. Mol. Sci.* 22. doi: 10.3390/ijms22158070

Andrews, C., Mclean, M. H., and Durum, S. K. (2018). Cytokine tuning of intestinal epithelial function. *Front. Immunol.* 9:1270. doi: 10.3389/fimmu.2018.01270

Antonopoulos, D. A., Huse, S. M., Morrison, H. G., Schmidt, T. M., Sogin, M. L., and Young, V. B. (2009). Reproducible community dynamics of the gastrointestinal microbiota following antibiotic perturbation. *Infect. Immun.* 77, 2367–2375. doi: 10.1128/IAI.01520-08

Bonfrate, L., Di Palo, D. M., Celano, G., Albert, A., Vitellio, P., De Angelis, M., et al. (2020). Effects of Bifidobacterium longum BB536 and lactobacillus rhamnosus HN001 in IBS patients. *Eur. J. Clin. Investig.* 50:e13201. doi: 10.1111/eci.13201

Boullier, S., Tanguy, M., Kadaoui, K. A., Caubet, C., Sansonetti, P., Corthesy, B., et al. (2009). Secretory IgA-mediated neutralization of Shigella flexneri prevents intestinal tissue destruction by down-regulating inflammatory circuits. *J. Immunol.* 183, 5879–5885. doi: 10.4049/jimmunol.0901838

Brandtzaeg, P., Baekkevold, E. S., Farstad, I. N., Jahnsen, F. L., Johansen, F. E., Nilsen, E. M., et al. (1999). Regional specialization in the mucosal immune system: what happens in the microcompartments? *Immunol. Today* 20, 141–151. doi: 10.1016/S0167-5699(98)01413-3

Carding, S., Verbeke, K., Vipond, D. T., Corfe, B. M., and Owen, L. J. (2015). Dysbiosis of the gut microbiota in disease. *Microb. Ecol. Health Dis.* 26:26191. doi: 10.3402/mehd.v26.26191

Cario, E., Gerken, G., and Podolsky, D. K. (2004). Toll-like receptor 2 enhances ZO-1-associated intestinal epithelial barrier integrity via protein kinase C. *Gastroenterology* 127, 224–238. doi: 10.1053/j.gastro.2004.04.015

Cerutti, A., and Rescigno, M. (2008). The biology of intestinal immunoglobulin A responses. *Immunity* 28, 740–750. doi: 10.1016/j.immuni.2008.05.001

Cunningham-Rundles, C. (2001). Physiology of IgA and IgA deficiency. *J. Clin. Immunol.* 21, 303–309. doi: 10.1023/A:1012241117984

Di Cagno, R., Coda, R., De Angelis, M., and Gobbetti, M. (2013). Exploitation of vegetables and fruits through lactic acid fermentation. *Food Microbiol.* 33, 1–10. doi: 10.1016/j.fm.2012.09.003

Duranti, S., Gaiani, F., Mancabelli, L., Milani, C., Grandi, A., Bolchi, A., et al. (2016). Elucidating the gut microbiome of ulcerative colitis: bifidobacteria as novel microbial biomarkers. *FEMS Microbiol. Ecol.* 92. doi: 10.1093/femsec/fiw191

Dzunkova, M., Moya, A., Vazquez-Castellanos, J. F., Artacho, A., Chen, X., Kelly, C., et al. (2016). Active and secretory IgA-coated bacterial fractions elucidate dysbiosis in Clostridium difficile infection. *mSphere* 1, e00101–e00116. doi: 10.1128/mSphere.00101-16

Ehrmann, M. A., Korakli, M., and Vogel, R. F. (2003). Identification of the gene for beta-fructofuranosidase of Bifidobacterium lactis DSM10140(T) and characterization of the enzyme expressed in Escherichia coli. *Curr. Microbiol.* 46, 391–397. doi: 10.1007/s00284-002-3908-1

El-Zayat, S. R., Sibaii, H., and Mannaa, F. A. (2019). Toll-like receptors activation, signaling, and targeting: an overview. *Bull. Natl. Res. Cent.* 43. doi: 10.1186/s42269-019-0227-2

Fagarasan, S., and Honjo, T. (2003). Intestinal IgA synthesis: regulation of front-line body defences. *Nat. Rev. Immunol.* 3, 63–72. doi: 10.1038/nri982

Feng, Y., Huang, Y., Wang, Y., Wang, P., Song, H., and Wang, F. (2019). Antibiotics induced intestinal tight junction barrier dysfunction is associated with microbiota dysbiosis, activated NLRP3 inflammasome and autophagy. *PLoS One* 14:e0218384. doi: 10.1371/journal.pone.0218384

Ferreira, C., Viana, S. D., and Reis, F. (2020). Gut microbiota Dysbiosis-immune Hyperresponse-inflammation triad in coronavirus disease 2019 (COVID-19): impact of pharmacological and Nutraceutical approaches. *Microorganisms* 8. doi: 10.3390/microorganisms8101514

George Kerry, R., Patra, J. K., Gouda, S., Park, Y., Shin, H. S., and Das, G. (2018). Benefaction of probiotics for human health: a review. *J. Food Drug Anal.* 26, 927–939. doi: 10.1016/j.jfda.2018.01.002

Gu, M. J., Song, S. K., Lee, I. K., Ko, S., Han, S. E., Bae, S., et al. (2016). Barrier protection via toll-like receptor 2 signaling in porcine intestinal epithelial cells damaged by deoxynivalnol. *Vet. Res.* 47:25. doi: 10.1186/s13567-016-0309-1

Hansen, N. W., and Sams, A. (2018). The microbiotic highway to health-new perspective on food structure, gut microbiota, and host inflammation. *Nutrients* 10. doi: 10.3390/nu10111590

Hara, S., Sasaki, T., Satoh-Takayama, N., Kanaya, T., Kato, T., Takikawa, Y., et al. (2019). Dietary antigens induce germinal center responses in Peyer's

patches and antigen-specific IgA production. *Front. Immunol.* 10:2432. doi: 10.3389/fimmu.2019.02432

Hill, C. J., Lynch, D. B., Murphy, K., Ulaszewska, M., Jeffery, I. B., O'shea, C. A., et al. (2017). Evolution of gut microbiota composition from birth to 24 weeks in the INFANTMET cohort. *Microbiome* 5:4. doi: 10.1186/s40168-016-0213-y

Holmgren, J., and Czerkinsky, C. (2005). Mucosal immunity and vaccines. *Nat. Med.* 11, S45–S53. doi: 10.1038/nm1213

Invernici, M. M., Furlaneto, F. A. C., Salvador, S. L., Ouwehand, A. C., Salminen, S., Mantziari, A., et al. (2020). Bifidobacterium animalis subsp lactis HN019 presents antimicrobial potential against periodontopathogens and modulates the immunological response of oral mucosa in periodontitis patients. *PLoS One* 15:e0238425. doi: 10.1371/journal.pone.0238425

Izquierdo, E., Medina, M., Ennahar, S., Marchioni, E., and Sanz, Y. (2008). Resistance to simulated gastrointestinal conditions and adhesion to mucus as probiotic criteria for Bifidobacterium longum strains. *Curr. Microbiol.* 56, 613–618. doi: 10.1007/s00284-008-9135-7

Jungersen, M., Wind, A., Johansen, E., Christensen, J. E., Stuer-Lauridsen, B., and Eskesen, D. (2014). The science behind the probiotic strain Bifidobacterium animalis subsp. lactis BB-12((R)). *Microorganisms* 2, 92–110. doi: 10.3390/microorganisms2020092

Kim, J.-Y., Choi, E.-J., Lee, J.-H., Yoo, M.-S., Heo, K., Shim, J.-J., et al. (2021). Probiotic potential of a novel vitamin B2-overproducing lactobacillus plantarum strain, HY7715, isolated from Kimchi. *Appl. Sci.* 11:5765. doi: 10.3390/app11135765

Kim, S. H., Jeung, W., Choi, I. D., Jeong, J. W., Lee, D. E., Huh, C. S., et al. (2016). Lactic acid bacteria improves Peyer's patch cell-mediated immunoglobulin A and tight-junction expression in a destructed gut microbial environment. *J. Microbiol. Biotechnol.* 26, 1035–1045. doi: 10.4014/jmb.1512.12002

Kozera, B., and Rapacz, M. (2013). Reference genes in real-time PCR. *J. Appl. Genet.* 54, 391–406. doi: 10.1007/s13353-013-0173-x

Lazar, V., Ditu, L. M., Pircalabioru, G. G., Gheorghe, I., Curutiu, C., Holban, A. M., et al. (2018). Aspects of gut microbiota and immune system interactions in infectious diseases, immunopathology, and cancer. *Front. Immunol.* 9:1830. doi: 10.3389/fimmu.2018.01830

Lee, H. C., Jenner, A. M., Low, C. S., and Lee, Y. K. (2006). Effect of tea phenolics and their aromatic fecal bacterial metabolites on intestinal microbiota. *Res. Microbiol.* 157, 876–884. doi: 10.1016/j.resmic.2006.07.004

Lee, K., Kim, J., Park, S.-D., Shim, J.-J., and Lee, J.-L. (2021). Lactobacillus plantarum HY7715 ameliorates sarcopenia by improving skeletal muscle mass and function in aged Balb/c mice. *Int. J. Mol. Sci.* 22:10023. doi: 10.3390/ijms221810023

Lee, H. J., Lee, K. E., Kim, J. K., and Kim, D. H. (2019). Suppression of gut dysbiosis by Bifidobacterium longum alleviates cognitive decline in 5XFAD transgenic and aged mice. *Sci. Rep.* 9:11814. doi: 10.1038/s41598-019-48342-7

Lee, B., Moon, K. M., and Kim, C. Y. (2018). Tight junction in the intestinal epithelium: its association with diseases and regulation by phytochemicals. *J Immunol Res* 2018, 1–11. doi: 10.1155/2018/2645465

Levit, R., De Giori, G. S., de Moreno de LeBlanc, A., and LeBlanc, J. G. (2017). Evaluation of the effect of soymilk fermented by a riboflavin-producing lactobacillus plantarum strain in a murine model of colitis. *Benefic. Microbes* 8, 65–72. doi: 10.3920/BM2016.0063

Liu, L., Liu, Z., Li, H., Cao, Z., Li, W., Song, Z., et al. (2020). Naturally occurring TPE-CA maintains gut microbiota and bile acids homeostasis via FXR signaling modulation of the liver-gut Axis. *Front. Pharmacol.* 11:12. doi: 10.3389/fphar.2020.00012

Macpherson, A. J., Gatto, D., Sainsbury, E., Harriman, G. R., Hengartner, H., and Zinkernagel, R. M. (2000). A primitive T cell-independent mechanism of intestinal mucosal IgA responses to commensal bacteria. *Science* 288, 2222–2226. doi: 10.1126/science.288.5474.2222

Macpherson, A. J., Hunziker, L., Mccoy, K., and Lamarre, A. (2001). IgA responses in the intestinal mucosa against pathogenic and non-pathogenic microorganisms. *Microbes Infect.* 3, 1021–1035. doi: 10.1016/S1286-4579(01)01460-5

Macpherson, A. J., Mccoy, K. D., Johansen, F. E., and Brandtzaeg, P. (2008). The immune geography of IgA induction and function. *Mucosal Immunol.* 1, 11–22. doi: 10.1038/mi.2007.6

Magoc, T., and Salzberg, S. L. (2011). FLASH: fast length adjustment of short reads to improve genome assemblies. *Bioinformatics* 27, 2957–2963. doi: 10.1093/bioinformatics/btr507

Maruya, M., Kawamoto, S., Kato, L. M., and Fagarasan, S. (2013). Impaired selection of IgA and intestinal dysbiosis associated with PD-1-deficiency. *Gut Microbes* 4, 165–171. doi: 10.4161/gmic.23595

Medina, M., Izquierdo, E., Ennahar, S., and Sanz, Y. (2007). Differential immunomodulatory properties of Bifidobacterium logum strains: relevance to probiotic selection and clinical applications. *Clin. Exp. Immunol.* 150, 531–538. doi: 10.1111/j.1365-2249.2007.03522.x

Menard, O., Butel, M. J., Gaboriau-Routhiau, V., and Waligora-Dupriet, A. J. (2008). Gnotobiotic mouse immune response induced by Bifidobacterium sp. strains isolated from infants. *Appl. Environ. Microbiol.* 74, 660–666. doi: 10.1128/AEM.01261-07

Meng, D., Zhu, W., Ganguli, K., Shi, H. N., and Walker, W. A. (2016). Anti-inflammatory effects of Bifidobacterium longum subsp infantis secretions on fetal human enterocytes are mediated by TLR-4 receptors. *Am. J. Physiol. Gastrointest. Liver Physiol.* 311, G744–G753. doi: 10.1152/ajpgi.00090.2016

Ojima, M. N., Gotoh, A., Takada, H., Odamaki, T., Xiao, J. Z., Katoh, T., et al. (2020). Bifidobacterium bifidum suppresses gut inflammation caused by repeated antibiotic disturbance without recovering gut microbiome diversity in mice. *Front. Microbiol.* 11:1349. doi: 10.3389/fmicb.2020.01349

Park, D. H., Han, B., Shin, M. S., and Hwang, G. S. (2020). Enhanced intestinal immune response in mice after oral administration of Korea red ginseng-derived polysaccharide. *Polymers* 12. doi: 10.3390/polym12102186

Pizarro, T. T., Dinarello, C. A., and Cominelli, F. (2021). Editorial: cytokines and intestinal mucosal immunity. *Front. Immunol.* 12:698693. doi: 10.3389/fimmu.2021.698693

Rea, M. C., Dobson, A., O'sullivan, O., Crispie, F., Fouhy, F., Cotter, P. D., et al. (2011). Effect of broad- and narrow-spectrum antimicrobials on Clostridium difficile and microbial diversity in a model of the distal colon. *Proc. Natl. Acad. Sci. U. S. A.* 108 (Suppl. 1), 4639–4644. doi: 10.1073/pnas.1001224107

Robak, O. H., Heimesaat, M. M., Kruglov, A. A., Prepens, S., Ninnemann, J., Gutbier, B., et al. (2018). Antibiotic treatment-induced secondary IgA deficiency enhances susceptibility to *Pseudomonas aeruginosa* pneumonia. *J. Clin. Invest.* 128, 3535–3545. doi: 10.1172/JCI97065

Routy, B., Gopalakrishnan, V., Daillere, R., Zitvogel, L., Wargo, J. A., and Kroemer, G. (2018). The gut microbiota influences anticancer immunosurveillance and general health. *Nat. Rev. Clin. Oncol.* 15, 382–396. doi: 10.1038/s41571-018-0006-2

Ruiz, L., Delgado, S., Ruas-Madiedo, P., Sanchez, B., and Margolles, A. (2017). Bifidobacteria and their molecular communication with the immune system. *Front. Microbiol.* 8:2345. doi: 10.3389/fmicb.2017.02345

Shang, J., Wan, F., Zhao, L., Meng, X., and Li, B. (2020). Potential Immunomodulatory activity of a selected strain Bifidobacterium bifidum H3-R2 as evidenced in vitro and in immunosuppressed mice. *Front. Microbiol.* 11:2089. doi: 10.3389/fmicb.2020.02089

Shao, H., Zhang, C., Xiao, N., and Tan, Z. (2020). Gut microbiota characteristics in mice with antibiotic-associated diarrhea. *BMC Microbiol.* 20:313. doi: 10.1186/s12866-020-01999-x

Shi, T., Bian, X., Yao, Z., Wang, Y., Gao, W., and Guo, C. (2020). Quercetin improves gut dysbiosis in antibiotic-treated mice. *Food Funct.* 11, 8003–8013. doi: 10.1039/D0FO01439G

Smyth, D., Phan, V., Wang, A., and Mckay, D. M. (2011). Interferon-gamma-induced increases in intestinal epithelial macromolecular permeability requires the Src kinase Fyn. *Lab. Investig.* 91, 764–777. doi: 10.1038/labinvest.2010.208

Stahl, B., and Barrangou, R. (2012). Complete genome sequences of probiotic strains Bifidobacterium animalis subsp. lactis B420 and bi-07. *J. Bacteriol.* 194, 4131–4132. doi: 10.1128/JB.00766-12

Stuart, R. O., and Nigam, S. K. (1995). Regulated assembly of tight junctions by protein kinase C. *Proc. Natl. Acad. Sci. U. S. A.* 92, 6072–6076. doi: 10.1073/pnas.92.13.6072

Sudo, N., Yu, X. N., Aiba, Y., Oyama, N., Sonoda, J., Koga, Y., et al. (2002). An oral introduction of intestinal bacteria prevents the development of a long-term Th2-skewed immunological memory induced by neonatal antibiotic treatment in mice. *Clin. Exp. Allergy* 32, 1112–1116. doi: 10.1046/j.1365-2222.2002.01430.x

Sultana, R., Mcbain, A. J., and O'Neill, C. A. (2013). Strain-dependent augmentation of tight-junction barrier function in human primary epidermal keratinocytes

by lactobacillus and Bifidobacterium lysates. *Appl. Environ. Microbiol.* 79, 4887–4894. doi: 10.1128/AEM.00982-13

Sun, Z., Chen, X., Wang, J., Gao, P., Zhou, Z., Ren, Y., et al. (2010). Complete genome sequence of probiotic Bifidobacterium animalis subsp. lactis strain V9. *J. Bacteriol.* 192, 4080–4081. doi: 10.1128/JB.00369-10

Sun, S., and Zhou, J. (2020). Phase separation as a therapeutic target in tight junction-associated human diseases. *Acta Pharmacol. Sin.* 41, 1310–1313. doi: 10.1038/s41401-020-0470-y

Suzuki, T. (2013). Regulation of intestinal epithelial permeability by tight junctions. *Cell. Mol. Life Sci.* 70, 631–659. doi: 10.1007/s00018-012-1070-x

Zeisel, M. B., Dhawan, P., and Baumert, T. F. (2019). Tight junction proteins in gastrointestinal and liver disease. *Gut* 68, 547–561. doi: 10.1136/gutjnl-2018-316906

Zhai, Q., Qu, D., Feng, S., Yu, Y., Yu, L., Tian, F., et al. (2019). Oral supplementation of Lead-intolerant intestinal microbes protects against lead (Pb) toxicity in mice. *Front. Microbiol.* 10:3161. doi: 10.3389/fmicb.2019.03161

Conflict of Interest: JK, S-JB, J-YK, EC, KH, J-JS, and J-LL are employed by hy Company Limited (hy Co., Ltd.).

frontiers | Frontiers in Microbiology

ORIGINAL RESEARCH
published: 11 May 2022
doi: 10.3389/fmicb.2022.863315

The Improvement of Semen Quality by Dietary Fiber Intake Is Positively Related With Gut Microbiota and SCFA in a Boar Model

Yan Lin[1,2*†], *Ke Wang*[1,2†], *Lianqiang Che*[1,2], *Zhengfeng Fang*[1,2], *Shengyu Xu*[1,2], *Bin Feng*[1,2], *Yong Zhuo*[1,2], *Jian Li*[1,2], *Caimei Wu*[1,2], *Junjie Zhang*[3], *Haoyu Xiong*[1,2], *Chenglong Yu*[1,2] *and De Wu*[1,2]

[1] *Key Laboratory of Animal Disease-Resistance Nutrition and Feed Science, Institute of Animal Nutrition, Sichuan Agricultural University, Chengdu, China,* [2] *Key Laboratory of Animal Disease-Resistance Nutrition, Ministry of Education, Chengdu, China,* [3] *College of Life Science, Sichuan Agricultural University, Ya'an, China*

OPEN ACCESS

Edited by:
Sabina Górska,
Polish Academy of Sciences, Poland

Reviewed by:
Tarique Hussain,
Nuclear Institute for Agriculture and Biology, Pakistan
Bi E. Tan,
Hunan Agricultural University, China

***Correspondence:**
Yan Lin
linyan936@163.com

[†] *These authors have contributed equally to this work*

Specialty section:
This article was submitted to Food Microbiology, a section of the journal Frontiers in Microbiology

Received: *27 January 2022*
Accepted: *11 April 2022*
Published: *11 May 2022*

Citation:
Lin Y, Wang K, Che L, Fang Z, Xu S, Feng B, Zhuo Y, Li J, Wu C, Zhang J, Xiong H, Yu C and Wu D (2022) The Improvement of Semen Quality by Dietary Fiber Intake Is Positively Related With Gut Microbiota and SCFA in a Boar Model. Front. Microbiol. 13:863315. doi: 10.3389/fmicb.2022.863315

Although fiber-rich diets have been positively associated with sperm quality, there have not been any studies that have examined the effects of dietary fiber and its metabolites on sperm quality in young or pre-pubescent animals. In this study, we aimed to explore the effect of dietary fiber supplementation on semen quality and the underlying mechanisms in a boar model. Sixty purebred Yorkshire weaning boars were randomly divided into the four groups (T1–T4). Groups T1, T2, and T3 boars were fed diets with different levels of fiber until reaching 160 days of age and were then fed the same diet, while group T4 boars were fed a basal diet supplemented with butyrate and probiotics. Compared with T1 boars, sperm motility and effective sperm number were significantly higher among T3 boars. Meanwhile, at 240 days of age, the acetic acid and total short-chain fatty acid (SCFA) contents in the sera of T3 and T4 boars were significantly higher than those in T1 boars. The abundance of microbiota in T2 and T3 boars was significantly higher than that in T1 boars ($P < 0.01$). Moreover, dietary fiber supplementation increased "beneficial gut microbes" such as *UCG-005*, *Rumenococcus*, *Rikenellaceae_RC9_gut_group* and *Lactobacillus* and decreased the relative abundance of "harmful microbes" such as *Clostridium_sensu_stricto_1*, *Romboutsia* and *Turicibacter*. Collectively, the findings of this study indicate that dietary fiber supplementation improves gut microbiota and promotes SCFA production, thereby enhancing spermatogenesis and semen quality. Moreover, the effects of dietary fiber are superior to those of derived metabolites.

Keywords: dietary fiber, growing boar, semen quality, gut microbiota, short-chain fatty acid

INTRODUCTION

In recent years, dietary fiber has played an increasingly important role in the treatment of diabetes, obesity, colon cancer and other diseases by regulating the diversity and composition of intestinal flora. Dietary fiber intake has been reported to enhance the reproductive performance of pregnant women (Tomsett et al., 2020), rats (Lin et al., 2012), and sows (Zhou et al., 2017). However, a few studies conducted on males have shown that dietary fiber either has some beneficial effect on

testosterone secretion and semen quality or no effect at all. Dorgan et al. (1996) found that plasma total testosterone and sex hormone-binding globulin levels were 13 and 15% higher, respectively, in the high-fat and low-fiber groups than in the low-fat and high-fiber groups in healthy men. Moreover, men with low-fat and high-fiber intake were reported to have reduced serum and urine androgen levels (Wang et al., 2005). Furthermore, studies in rabbits have shown that the addition of dietary fiber improves semen quality (Pascual et al., 2016). Thus, the findings of these studies have either directly or indirectly revealed that dietary fiber can have an important influence on reproductive hormone secretion and semen quality in male animals.

The intestine is the largest habitat for microorganisms and the composition and structure of the diet, especially fiber intake, has an important impact on the composition of intestinal flora (Mändar et al., 2015). Animals fed complex carbohydrate diets have a high abundance and diversity of gut flora. Inulin, composed of fructooligosaccharides, has been shown to increase the abundance of *Bifidobacteria* and reduce the number of total anaerobic bacteria and *Clostridium* in feces (Tian et al., 2017). Hermes et al. revealed that pectin in high-fiber diets is fermented by gut microbes, which increases short-chain fatty acid (SCFA) content and decreases intestinal pH. This inhibits the colonization and growth of certain pathogens and increases the number of beneficial bacteria (Hermes et al., 2009). Wu et al. (2018) fed weaned male piglets with different fiber sources and found that cellulose significantly increased the abundance of *Lactobacillus*, while xylan significantly increased the abundance of *Bifidobacterium*. This indicates that dietary fiber can regulate the structure of intestinal flora and that dietary fiber from different sources operates through various actions.

In addition to their associations with metabolic disorders, it is also well-established that components of the gut microbiota contribute to the regulation of reproductive hormone secretion (Hussain et al., 2021). For example, it has been demonstrated that dietary supplementation with probiotic *Lactobacillus reuteri* can increase and restore testosterone levels in aging mice; by using a testicular injury model, it was found that *Lactobacillus plantarum* TW1-1 has a regulatory effect on intestinal microbiota and can effectively ameliorate di(2-ethylhexyl) phthlate (DEHP)-induced testicular injury (Tian et al., 2019). Furthermore, exogenous supplementation with lactic acid, bacteria and bifidobacteria has been shown to enhance sperm motility and reduce the extent of sperm DNA fragmentation in asthenozoospermic human males (Valcarce et al., 2017), whereas in mice and broilers, probiotic supplementation enhances semen quality and sperm motility (Dardmeh et al., 2017; Inatomi and Otomaru, 2018). The aforementioned studies, thus, provide convincing evidence that gut flora has an important influence on the quality of semen in both the humans and animals. However, whether an intake of dietary fiber affects the composition of the gut microbiota and semen quality in young male animals still remains to be conclusively established.

Dietary fiber alters intestinal microorganisms, accompanied by changes in SCFAs. The major SCFAs in the colon and caecum of humans and pigs are acetic acid, propionic acid and butyric acid. Hermes et al. (2009) found that dietary fiber supplementation increased intestinal SCFA concentrations in 35-day-old piglets. Maternal fiber intake not only affected the production of SCFAs in sow feces, but also influenced the concentrations of SCFAs in the neonatal colon (Li et al., 2019a). In addition to providing energy, SCFAs are involved in regulating reproductive performance (Lin et al., 2014). Moreover, adding glyceride butyrate to the diet of cocks can improve sperm volume, sperm motility, sperm concentration and reduce abnormal sperm rates (Alhaj et al., 2018). Interestingly, exposing germ-free (GF) mice to *Clostridium tyrobutyricum* (CBUT), which secretes high levels of butyrate, increased their serum levels of gonadotropins [luteinising hormone (LH) and follicle-stimulating hormone (FSH)] (Al-Asmakh et al., 2014). Meanwhile, butyrate supplementation in suckling goat kids improved reproductive tract development and the total and daily gain by improving their antioxidant status (Mohamed et al., 2020). Therefore, we speculated that butyric acid, an important component of SCFAs, may play a role in regulating male reproduction.

We hypothesized that dietary fiber has beneficial effects on boar reproduction by inducing SCFAs production and regulating gut microbiota. Specifically, our objectives were to examine the effects and underlying mechanism of different levels of dietary fiber and their metabolites on semen quality in growing boars to provide a theoretical basis for dietary fiber applications in adolescent and immature male animals.

MATERIALS AND METHODS

Experimental Design and Animals Used

All the animal procedures used in this study were approved by the Animal Care and Use Committee of Sichuan Agricultural University (SAU-ANI-2020-117). Sixty weaned purebred Yorkshire boars with similar weights were selected and randomly divided into the four groups: T1, T2, T3, and T4 ($n = 15$ each). The T1 group was fed a basic diet, whereas those in the groups T2 and T3 were fed diets containing different levels of dietary fiber; the T4 group was fed a basic diet supplemented with probiotics and tributyrin. The basic diets for each stage of growth for the boars were prepared according to the recommendations of the Nutrient Requirement of Swine from the National Research Council (NRC) (2012) and the nutrition levels are shown in **Table 1**. The supplementary fibers used were inulin and cellulose. In each stage, the amount of tributyrin (Perstorp, Shanghai Chemical Products Trading Corporation, Ltd, China) was added at a concentration of 0.6 g/kg of diet and *Lactobacillus* and *Bifidobacterium* cultures [3×10^8 colony-forming unit (CFU)/g] were both added at 1 g/kg of diet. The growing boars received these diets until they reached an age of 160 days and then all the groups were fed the same diet. During the experimental period, the boars were provided with food and water *ad libitum* and their initial and final body weights were recorded.

To determine the beneficial effects of dietary fiber supplementation during the growing period, we assessed the quality of adult boar semen. At 210 days of age, the boars

TABLE 1 | Calculated nutrient levels of diets.

Nutrient composition	0–30 d				31–60 d				61–130 d				131–330 d
	T1	T2	T3	T4	T1	T2	T3	T4	T1	T2	T3	T4	All
DE (Mcal/kg)	3.54	3.54	3.54	3.54	3.45	3.45	3.45	3.45	3.37	3.37	3.37	3.37	3.37
CP (%)	18.81	18.81	18.81	18.81	15.68	15.68	15.68	15.68	15.52	15.52	15.52	15.52	15.52
CF (%)	1.60	1.89	2.19	1.60	2.19	2.57	2.95	2.19	2.38	2.65	3.12	2.38	2.73
Ca (%)	0.81	0.81	0.81	0.81	0.68	0.68	0.68	0.68	0.84	0.84	0.84	0.84	0.82
AP (%)	0.48	0.48	0.48	0.48	0.34	0.34	0.34	0.34	0.32	0.32	0.32	0.32	0.33
ADF (%)	8.38	9.30	10.28	8.38	14.99	16.27	17.52	14.99	15.82	16.44	17.94	15.82	16.98
NDF (%)	2.80	2.98	3.19	2.80	5.83	6.13	6.42	5.83	6.01	6.16	6.50	6.01	6.36
SDF (%)	1.72	1.84	2.09	1.72	1.76	2.43	2.84	1.76	1.82	2.72	3.28	1.82	1.96
IDF (%)	8.25	9.63	10.88	8.25	10.92	12.75	14.84	10.92	11.57	14.17	17.11	11.57	12.85
TDF (%)	9.97	11.47	12.97	9.97	12.68	15.18	17.68	12.68	13.39	16.89	20.39	13.39	14.81

T1, basal diet; T2, T3, basal diet supplemented with different fiber level; T4, basal diet supplemented with probiotics and butyrate. SDF, soluble fiber; IDF, insoluble fiber; TDF, total dietary fiber.

were trained to mount an artificial sows and semen was collected using the massage method from day 240 to day 330. After collection, semen volume, sperm concentration, and sperm motility were assessed according to previously reported methods (Ren et al., 2015). To minimize the effects of individual differences, eight ejaculations per boar were used to estimate sperm production. For microbiota analysis, we also collected fecal samples by massaging the rectum of boars to stimulate defaecation. The samples were immediately stored at −80°C until used for subsequent analyses.

Growth Performance and Testicular Development

The daily feed intake of each boar was recorded, boars were weighed and the feed conversion ratio (F/G) was calculated based on body weight and feed intake. Each boar was scored for diarrhea at 08:00, 12:00, and 16:00 every day during the 0–30 days of the experiment. The diarrhea index was calculated as the sum of diarrhea scores of pigs per pen/(the number of pigs per pen × total days) (Le Floc'h et al., 2014). In addition, to assess the effect of dietary fiber supplementation on testis development, we measured the long and short testicular diameters on both the sides of each boar at 4-week intervals to determine testicular volume.

Sexual Desire and Sperm Quality

The ejaculation response time and ejaculation duration of boars were measured (Louis et al., 1994). The sperm motility rate, sperm density and sperm motility characteristics of the filtered semen were determined using a computer-assisted sperm analysis (CASA) (Minitube, Tiefenbach, Germany) system. The total sperm count and effective sperm count per ejaculation were calculated using the formula described by Ren et al., 2015.

Short-Chain Fatty Acid Measurement

The feces and serum of the boars were collected on the 120th and 240th day of the experiment, respectively. The SCFA content was determined by using a CP-3800 gas chromatography (Varian Incorporation, Walnut Creek, California, USA) according to the method described by Zhou et al., 2017.

Bacterial Community Analysis

We adopted 16S rDNA sequencing technology to determine the microbial composition of feces collected on the 75th day of boar growth. Thirty-two fresh fecal samples collected from eight boars from the each treatment group were used to evaluate their respective microflora communities. Microbial community genomic DNA was extracted from the fecal samples using the E.Z.N.A.® Soil DNA Kit (Omega Bio-tek, Norcross, Georgia, USA) according to the manufacturer's instructions, with concentrations and purities of the isolated DNA being determined using a NanoDrop 2000 UV-Vis spectrophotometer (Thermo Fisher Scientific, Wilmington, USA). Using this DNA as a template, we amplified the V3–V4 hypervariable region of the bacterial 16S rRNA gene *via* an ABI GeneAmp® 9700 PCR Thermocycler (ABI, California, USA) using primer pair

TABLE 2 | Effect of dietary fiber and metabolites on diarrhea and growth performance of boars.

Items	T1	T2	T3	T4	*P*-value
Diarrhea index					
0–14 d	0.34 ± 0.07	0.25 ± 0.05	0.16 ± 0.04	0.20 ± 0.05	0.096
15–30 d	0.30 ± 0.10	0.30 ± 0.08	0.20 ± 0.07	0.25 ± 0.09	0.818
0–30 d	0.32 ± 0.07	0.27 ± 0.05	0.18 ± 0.05	0.22 ± 0.06	0.153
Average daily gain, g					
0–130 d	844.2 ± 21.2	839.6 ± 32	836.1 ± 30	860.3 ± 28.5	0.586
131–260 d	687.8 ± 25.8	649.9 ± 35.7	688.1 ± 24.3	685.0 ± 17.1	0.394
Average daily feed intake, g					
0–130 d	1.75 ± 0.04	1.75 ± 0.12	1.71 ± 0.09	1.78 ± 0.02	0.322
131–260 d	2.60 ± 0.04	2.58 ± 0.04	2.59 ± 0.06	2.60 ± 0.03	0.922
Feed conversion ratio					
0–130 d	2.07 ± 0.05	2.09 ± 0.10	2.04 ± 0.08	2.10 ± 0.07	0.322

T1, basal diet; T2, T3, basal diet supplemented with different fiber level; T4, basal diet supple mented with probiotics and butyrate. Values are means and SEMs, n = 15 per group.

338F (5′-ACTCCTACGGGAGGCAGCAG-3′) and 806R (5′-GGACTACHVGGGTWTCTAAT-3′). The purified amplicons were pooled in equimolar amounts and paired-end sequenced on an Illumina MiSeq PE300 platform/NovaSeq PE250 platform (Illumina, San Diego, California, USA) according to the standard protocols recommended by Majorbio Bio-Pharm Technology Corporation Ltd. (Shanghai, China).

The raw 16S rRNA gene sequencing reads, thus, obtained were demultiplexed, quality-filtered using fastp version 0.20.0 (Chen et al., 2018) and merged using FLASH version 1.2.7 (Magoč and Salzberg, 2011). Operational taxonomic units (OTUs) with a 97% similarity cutoff were clustered using UPARSE version 7.1 (Edgar, 2013) and chimeric sequences were identified and removed. The taxonomy of the representative sequence of each OTU was analyzed using RDP Classifier version 2.2 (Wang et al., 2007) against the 16S rRNA database (Silva v138) with a confidence threshold of 0.7. The Spearman's correlation analysis was used to assess the relationship between sperm quality and microorganisms.

Statistical Analysis

Collected data were analyzed using the one-way ANOVA procedure of the Statistical Product and Service Solutions (SAS) statistical software (version 9.4; SAS Institute Incorporation, Cary, North Carolina, USA), followed by a generalized linear model (GLM) analysis. Values are expressed as mean ± SEM, with differences being considered statistically significant at $P < 0.05$ and a value of $0.05 \leq P < 0.10$ being indicative of a "tendency."

RESULTS

Growth Performance and Diarrhea

As shown in **Table 2**, the diarrhea indices of the T2, T3, and T4 groups were lower than those of the group T1 at all the stages, but the differences were not statistically significant ($P > 0.05$). Compared with the T1 boars, the diarrhea index of the T3 boars on days 0 to 14 showed a decreasing trend ($P < 0.1$). During the same period, the average daily feed intake of T4 boars was found to be significantly higher than that of the T3 boars ($P < 0.05$). However, the differences were not significant throughout the experimental period. Similarly, we detected no significant differences in the average daily gain or feed conversion ratio ($P > 0.05$).

Testicular Development

As shown in **Figure 1**, although the testicular volumes of the T3 and T4 groups on days 225 and day 260 were 11–18 and 13–14% higher than those in the T1 group, respectively, there was no significant difference in the testis volume of boars among the groups at each stage ($P > 0.05$).

Sexual Desire of Boars

As shown in **Table 3**, compared with the T1 group, the sexual desire of boars in the T4 group showed an increasing trend, although the difference was not statistically significant ($P = 0.120$). There was no significant difference in the ejaculation reaction time or duration among treatments ($P > 0.05$).

Semen Quality of Boars

Notably, we detected significantly higher sperm motility in T3 boars during weeks 1–4 compared to T1 boars ($P < 0.05$); however, the proportion of immobile spermatozoa in T3 boars was lower than that in T1 boars (**Table 4**). Furthermore, T4 boars were found to have significantly higher sperm linear, oscillation, and forward ratios than group T1 boars ($P < 0.01$). There was no difference in the total sperm count per ejaculation during weeks 1–4 (**Table 4**). However, during weeks 5–8, there were marginally significant increase in sperm motility in T3 and T4 boars ($P = 0.057$; **Table 5**). In addition, during the entire assessed period (weeks 1–8), the motility of T3 boar sperm was significantly higher than that in the T1 and T2 boars ($P < 0.05$) and the effective sperm count per ejaculation showed an increasing trend ($P = 0.068$; **Table 6**). In addition, the sperm linear and oscillation ratios of T4 boars were significantly higher than those in T1 boars ($P < 0.05$).

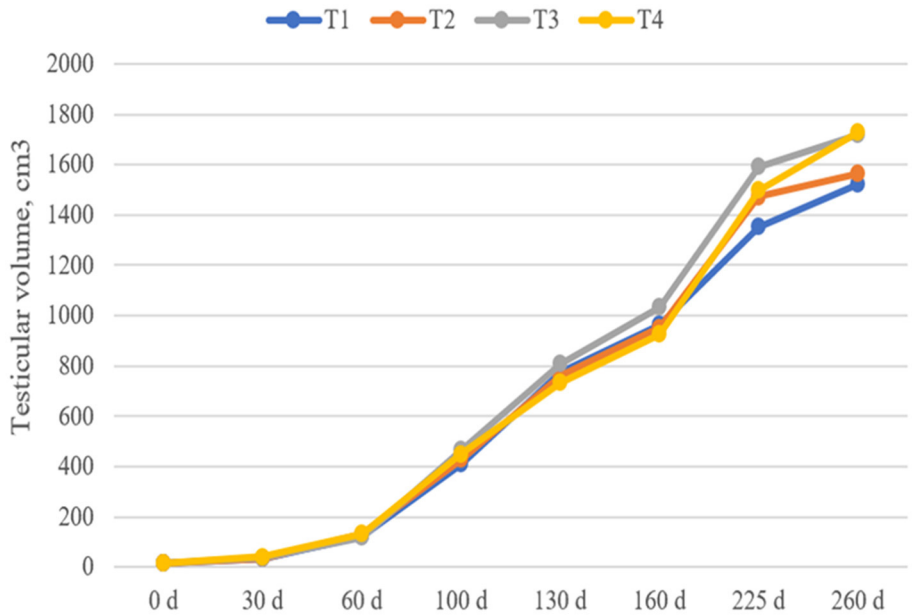

FIGURE 1 | Effect of dietary fiber and metabolites on boar testicle volume. T1, basal diet; T2, T3, basal diet supplemented with different dietary fiber level; T4, basal diet supplemented with probiotics and butyrate. Values are means and SEMs, $n = 15$ per group.

TABLE 3 | Effect of dietary fiber and metabolites on libido of boars.

Items	T1	T2	T3	T4	*P*-value
Libido score, s	3.42 ± 0.33	3.04 ± 0.45	3.24 ± 0.35	2.33 ± 0.33	0.120
Ejaculation reaction time, s	116.54 ± 37.56	115.23 ± 28.19	120.15 ± 40.11	78.69 ± 18.67	0.832
Duration of ejaculation, s	343.76 ± 68.82	375.66 ± 35.87	340.56 ± 13.23	483.91 ± 72.43	0.209

T1, basal diet; T2, T3, basal diet supplemented with different fiber level; T4, basal diet supplemented with probiotics and butyrate. Values are means and SEMs, n = 6 per group.

TABLE 4 | Effect of dietary fiber and metabolites on semen quality of boars (1–4 weeks).

Items	T1	T2	T3	T4	*P*-value
Semen volume (mL)	84.65 ± 6.96	93.90 ± 6.83	97.35 ± 7.22	96.47 ± 10.06	0.951
Sperm density, $\times 10^8$ spz/mL	1.55 ± 0.11	1.53 ± 0.07	1.49 ± 0.12	1.47 ± 0.13	0.311
Sperm motility, %	87.38 ± 2.09	91.90 ± 1.27	94.46 ± 0.83	90.21 ± 2.53	0.028
Total sperm count/ejaculation, $\times 10^8$ spz	131.20 ± 10.11	143.67 ± 12.26	145.05 ± 9.37	141.80 ± 11.39	0.402
Effective sperm count/ejaculation, $\times 10^8$ spz	114.64 ± 6.16	132.03 ± 7.35	137.02 ± 8.24	127.92 ± 12.37	0.109
Immobile ratio, %	12.62 ± 2.09	8.10 ± 1.27	6.25 ± 1.06	9.79 ± 2.53	0.056
Linear ratio, %	33.16 ± 1.54^{a}	33.24 ± 0.93^{a}	30.69 ± 1.34^{a}	39.00 ± 2.34^{b}	0.005
Oscillation ratio, %	46.53 ± 1.23^{a}	46.59 ± 0.75^{a}	44.55 ± 1.07^{a}	51.20 ± 1.88^{b}	0.005
Forward ratio, %	70.57 ± 1.42^{ab}	71.01 ± 0.87^{ab}	68.33 ± 1.26^{a}	75.31 ± 1.83^{b}	0.009

T1, basal diet; T2, T3, basal diet supplemented with different fiber level; T4, basal diet supplemented with probiotics and butyrate. Values are means and SEMs, n = 6 per group. Data with different letters are significantly different ($p < 0.05$).

Short-Chain Fatty Acids in Feces and Serum of Boars

Analyses of the fecal contents of 120-day-old boars in each group revealed no significant difference in SCFA levels ($P > 0.05$; **Table 7**). However, we detected significantly higher concentrations of acetic acid and total SCFAs in the sera of 240-day-old boars from the groups T3 and T4 compared with those in T1 boars ($P < 0.05$). Furthermore, serum butyrate

TABLE 5 | Effect of dietary fiber and metabolites on semen quality of boars (5–8 weeks).

Items	T1	T2	T3	T4	*P*-value
Semen volume (mL)	113.70 ± 4.02	114.72 ± 5.68	125.60 ± 4.45	127.61 ± 6.73	0.174
Sperm density, $\times 10^8$ spz/mL	1.98 ± 0.09	1.90 ± 0.08	1.86 ± 0.09	1.80 ± 0.15	0.264
Sperm motility, %	91.10 ± 1.70	94.16 ± 1.61	95.28 ± 0.74	95.95 ± 1.37	0.057
Total sperm count/ejaculation, $x10^8$ spz	225.39 ± 8.14	219.35 ± 9.75	233.61 ± 11.24	219.48 ± 7.48	0.162
Effective sperm count/ejaculation, $\times 10^8$ spz	211.57 ± 6.73^a	199.07 ± 8.33^a	222.58 ± 10.05^b	220.59 ± 8.27^{ab}	0.148
Immobile ratio, %	5.84 ± 1.70	8.90 ± 1.61	4.72 ± 0.74	4.05 ± 1.37	0.059
Linear ratio, %	33.96 ± 0.99	32.81 ± 1.56	35.44 ± 1.37	36.00 ± 1.64	0.406
Oscillation ratio, %	47.17 ± 0.79	46.25 ± 1.25	48.35 ± 1.09	48.80 ± 1.31	0.406
Forward ratio, %	71.80 ± 0.89	70.16 ± 1.45	72.74 ± 1.13	73.20 ± 1.61	0.357

T1, basal diet; T2, T3, basal diet supplemented with different fiber level; T4, basal diet supplemented with probiotics and butyrate. Values are means and SEMs, n = 6 per group. Data with different letters are significantly different ($p < 0.05$).

TABLE 6 | Effect of dietary fiber and metabolites on semen quality of boars (1–8 weeks).

Items	T1	T2	T3	T4	*P*-value
Semen volume (mL)	99.17 ± 8.86	104.31 ± 6.36	116.47 ± 7.47	110.04 ± 7.58	0.414
Sperm density, $\times 10^8$ spz/mL	1.65 ± 0.09	1.67 ± 0.08	1.57 ± 0.09	1.64 ± 0.15	0.180
Sperm motility, %	90.22 ± 1.62^a	91.53 ± 0.64^{ab}	94.89 ± 1.37^b	92.84 ± 1.71^{ab}	0.026
Total sperm count/ejaculation, $\times 10^8$ spz	163.63 ± 7.05	174.20 ± 9.16	182.00 ± 11.13	180.46 ± 9.38	0.142
Effective sperm count/ejaculation, $\times 10^8$ spz	147.63 ± 6.78	159.44 ± 11.06	173.89 ± 9.35	167.54 ± 12.31	0.068
Immobile ratio, %	9.78 ± 0.52^b	8.47 ± 0.70^b	5.47 ± 0.64^a	7.16 ± 0.59^{ab}	0.049
Linear ratio, %	33.50 ± 0.97^a	33.04 ± 0.87^a	33.13 ± 1.02^a	37.62 ± 1.48^b	0.018
Oscillation ratio, %	46.80 ± 0.78^a	46.43 ± 0.70^a	46.50 ± 0.82^a	50.10 ± 1.18^b	0.018
Forward ratio, %	71.09 ± 0.90^{ab}	70.62 ± 0.81^a	70.59 ± 0.91^a	74.35 ± 1.23^b	0.037

T1, basal diet; T2, T3, basal diet supplemented with different fiber level; T4, basal diet supplemented with probiotics and butyrate. Values are means and SEMs, n = 6 per group. Data with different letters are significantly different ($p < 0.05$).

TABLE 7 | Effect of dietary fiber and metabolites on short-chain fatty acids (SCFAs) concentrations of boars.

Items	T1	T2	T3	T4	*P*-value
Feces in 120 Days					
Acetate, mg/g	2.99 ± 0.14	3.37 ± 0.28	3.68 ± 0.39	4.02 ± 0.47	0.233
Propionate, mg/g	2.02 ± 0.12	2.46 ± 0.30	2.41 ± 0.27	2.36 ± 0.16	0.574
Isobutyric acid	0.26 ± 0.01	0.37 ± 0.06	0.35 ± 0.05	0.38 ± 0.04	0.336
Butyrate, mg/g	1.44 ± 0.11	1.82 ± 0.28	1.80 ± 0.29	1.86 ± 0.12	0.055
Isovaleric acid, mg/g	0.45 ± 0.02	0.71 ± 0.13	0.65 ± 0.11	0.73 ± 0.10	0.062
Valeric acid, mg/g	0.38 ± 0.02	0.68 ± 0.18	0.52 ± 0.1	0.51 ± 0.05	0.318
Total SCFAs, mg/g	7.54 ± 0.35	9.03 ± 1.14	9.41 ± 0.86	9.86 ± 0.88	0.075
Serum in 240 days					
Acetate, μmol/L	446.1 ± 49.3^a	586.1 ± 22.0^{ab}	687.3 ± 47.5^b	660.8 ± 67.3^b	0.014
Propionate, μmol/L	92.2 ± 6.1	87.79 ± 5.1	124.3 ± 20.4	101.1 ± 12.4	0.219
Butyrate, μmol/L	61.3 ± 13.7^a	93.62 ± 10.7^a	216.7 ± 39.7^b	157.3 ± 27.9^{ab}	0.003
Total SCFAs, μmol/L	599.7 ± 64.9^a	767.6 ± 30.9^{ab}	1028.0 ± 102.8^b	919.1 ± 95.6^b	0.008

T1, basal diet; T2, T3, basal diet supplemented with different fiber level; T4, basal diet supplemented with probiotics and butyrate. Values are means and SEMs, n = 6 per group. Data with different letters are significantly different ($p < 0.05$).

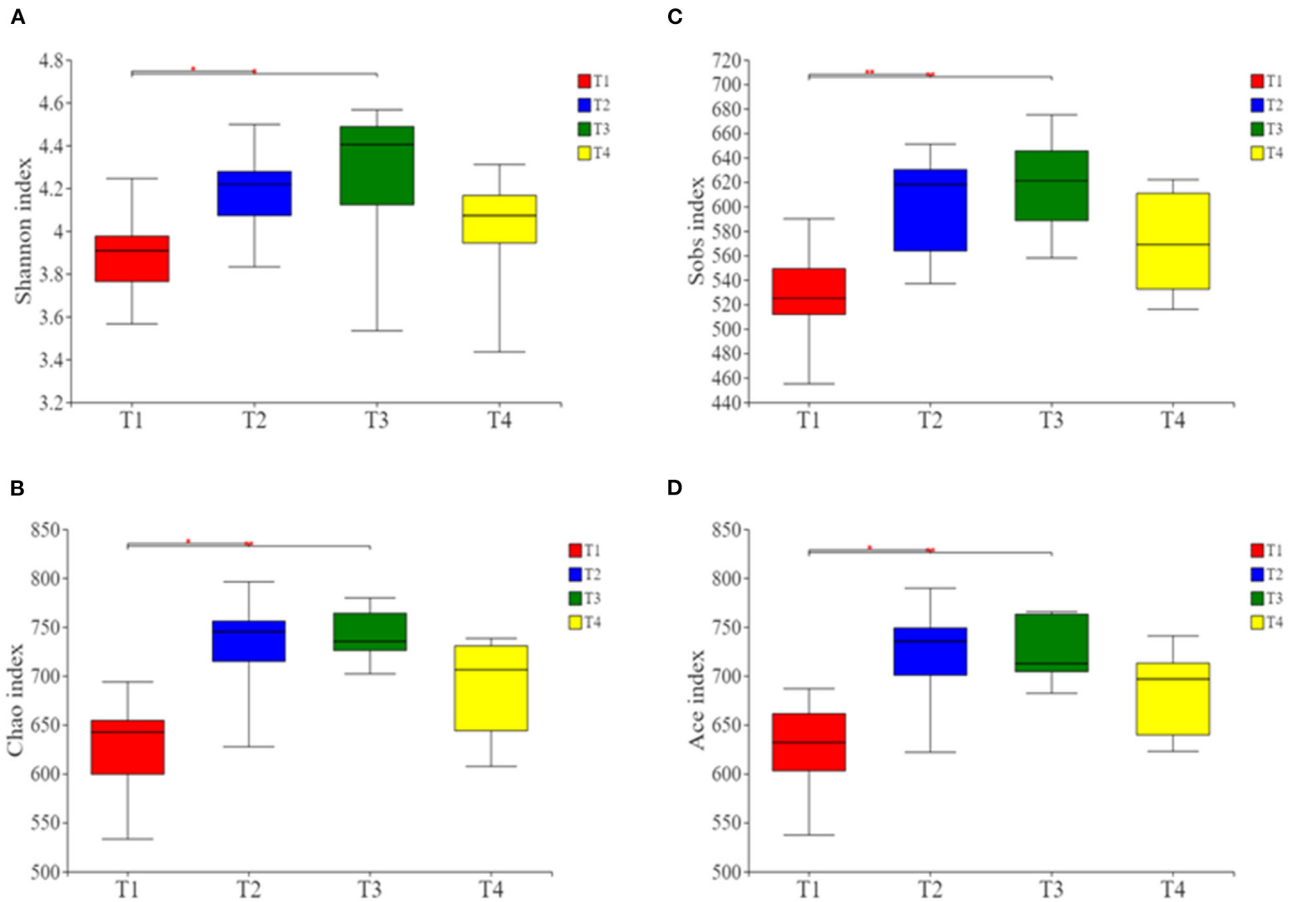

FIGURE 2 | Alpha-diversity analysis of gut microbial community structure in each group. **(A)** Shannon index. **(B)** Chao index. **(C)** Sobs index. **(D)** Ace index. Red represents the T1 group, blue represents the T2 group, green represents the T3 group and yellow represents the T4 group. *$p < 0.05$, and **$p < 0.01$.

contents in T3 boars were significantly higher than those in the T1 and T2 boars ($P < 0.05$). However, no significant difference was observed among the groups with respect to propionic acid concentrations ($P > 0.05$).

Overview of 16S rRNA Sequencing Data

To examine the effect of dietary fiber on the gut microbiota, stool samples were collected for 16S rRNA sequencing. A total of 1,400,127 sequences, with an average sequence length of 413 bp and 579,184,699 bases, were obtained from the 31 stool samples.

Analysis of Microbial Diversity and Community Composition

Alpha- and beta-diversity analyses revealed that compared with group T1 boars, the Shannon, Ace, Chao, and Sobs indices were significantly higher in T2 and T3 boars ($P < 0.01$; **Figures 2A–D**). This indicates that there were higher levels of microbial richness and diversity in the guts of boars fed a fiber-supplemented diet. Comparatively, boars fed with diets supplemented with butyrate and probiotic bacteria showed slight increase in gut microbiota diversity, indicating that the effects of metabolite supplementation are somewhat inferior to fiber supplementation.

To gain insight into the effects of dietary supplementation on gut microbiota composition, we analyzed changes in bacterial community composition at the phylum, order, and genus levels (**Figures 3A–F**). Briefly, at the phylum level (**Figures 3A,E**), we established that *Firmicutes*, *Bacteroidetes* and *Actinobacteriota* were the three dominant phyla in all the four groups and that the abundance of *Cyanobacteria* in the guts of T3 boars (0.51%) was higher than that of T1 boars (0.190%). At the order level (**Figure 3B**), the abundances of *Clostridiales* and *Erysipelotrichales* in T3 boars were lower than those in T1 boars ($P < 0.05$), while the abundance of *Oscillospirales* was significantly higher than in T1 and T4 boars ($P < 0.01$). At the genus level (**Figures 3D,F**), the abundances of *Clostridium*_sensu_stricto_1, *Romboutsia* and *Turicibacter* were lower in T3 boars than in T1 boars ($P < 0.05$), while the abundances of UCG-005, *Ruminococcus*, *Rikenellaceae*_RC9_gut_group and *Lactobacillus* were higher in T3 boars ($P < 0.05$). Notably, the abundances of *Lactobacillus* increased in response to fiber and metabolite supplementation

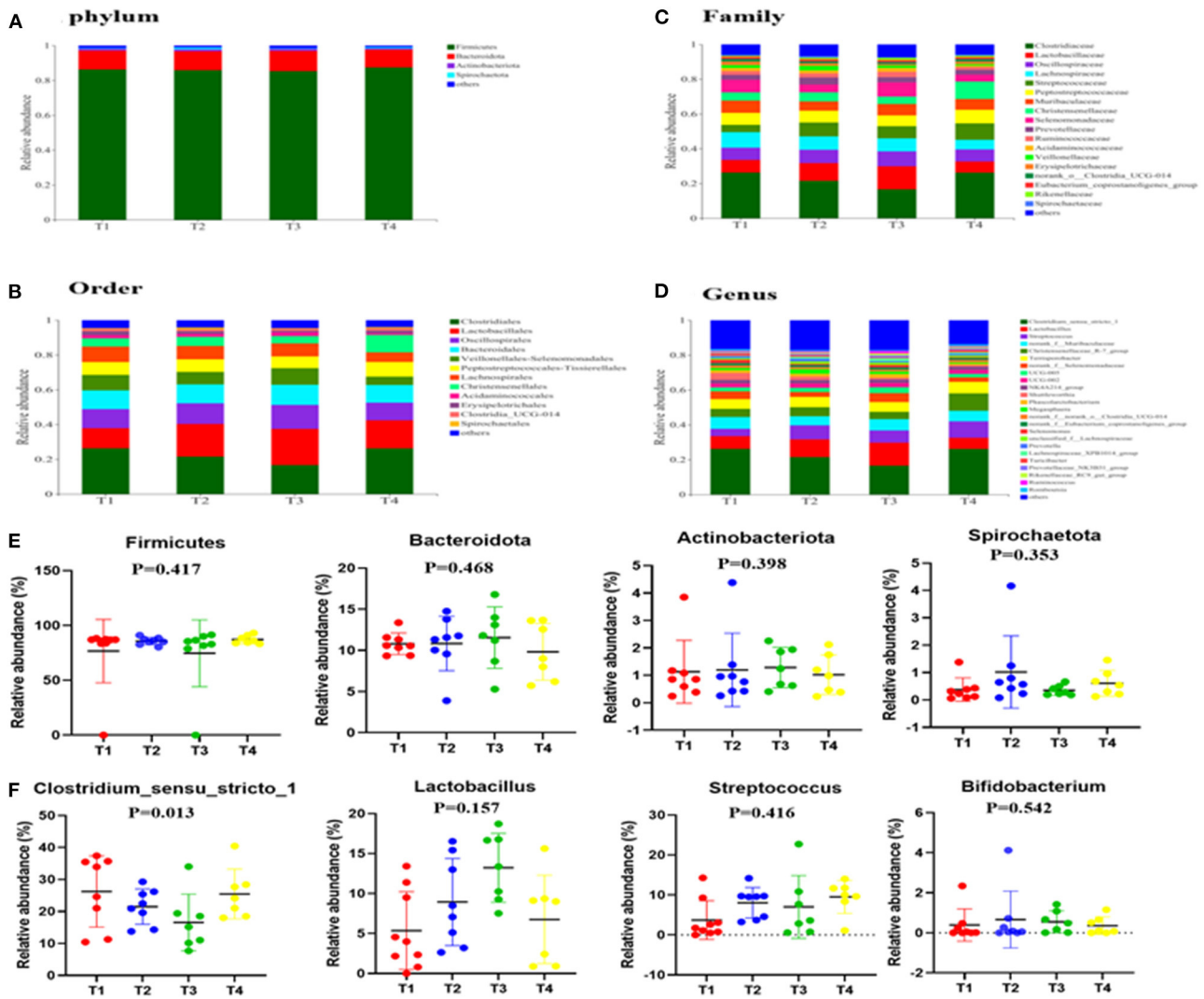

FIGURE 3 | Effects of dietary fiber on fecal microbial composition. **(A,E)** The relative amounts of microbiota in feces at the phylum level. **(B)** The relative amounts of microbiota in feces at the order level. **(C)** The relative amounts of microbiota in feces at the family level. **(D,F)** The relative amounts of microbiota in feces at the genus level. Data were expressed as the mean ± SEM.

($P > 0.01$), thereby providing evidence that dietary fiber has a potentially significant effect on gut microbiota composition.

Differential Analysis of Gut Microbiota Changed by Dietary Fiber and Metabolites Supplementation

To further screen for significant differences in the gut microbiota, differential analysis and linear discriminant analysis effect size (LEfSe) analysis were conducted. As shown in **Figure 4**, 213 taxa among the four groups were identified. The results indicate that the dominant bacteria in the T1 group were Erysipelotrichales, RF39, and *Romboutsia*; those in the T2 group were *Acetitomaculum*; those in the T3 group were Cyanobacteria, Desulfuromonadia, Oscillospirales, Burkholderiales, and Rikenellaceae; and in the T4 group was *Clostridia*.

Relationships Between Sperm Quality and Intestinal Microbiota

The Spearman's correlation analysis was used to study the relationship between environmental factors and microbial species richness and to study the relationship between environmental factors and species. At the phylum level, Firmicutes and Cyanobacteria were negatively correlated with the sperm forward ratio and Spirochaetota (**Figure 5A**), Proteobacteria, Firmicutes, and Cyanobacteria were negatively correlated with the sperm oscillation ratio. At the genus level (**Figure 5B**), *Bacillus Candidatus_Soleaferrea* and *dgA-11gut_group* were positively correlated with sperm

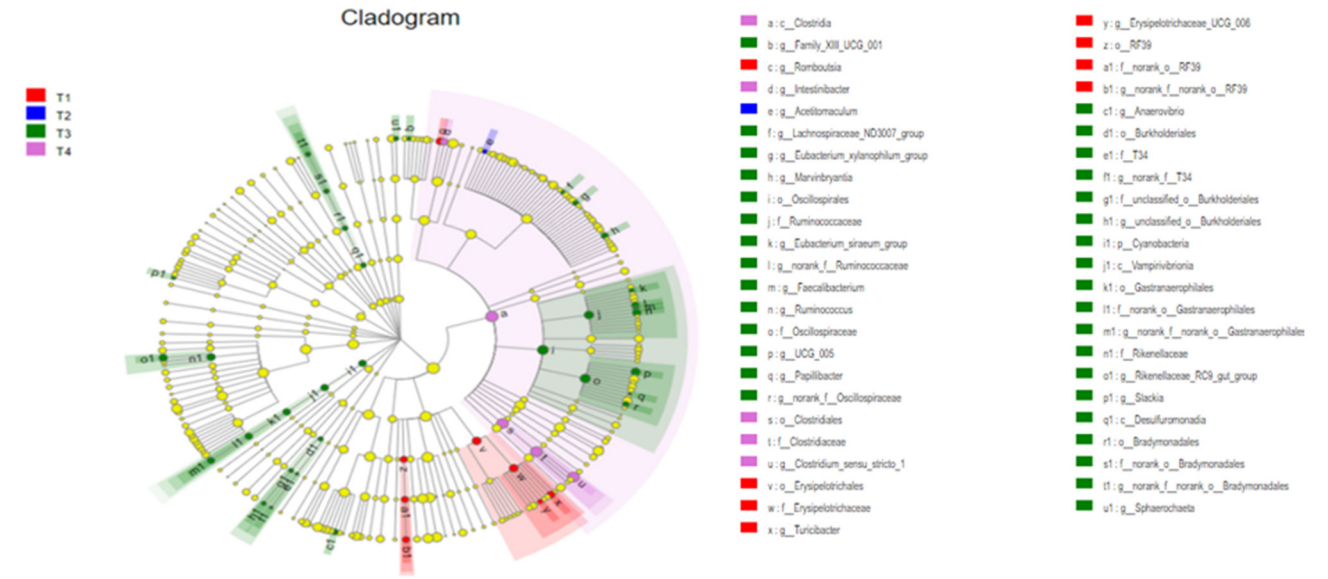

FIGURE 4 | The differently abundant taxa identified using linear discriminant analysis effect size (LEfSe) analysis. The LEfSe cladogram shows the most differentially abundant taxa among the groups. Taxa enriched in the T1 group are red, taxa enriched in the T2 group are blue, taxa enriched in the T3 group are green and taxa enriched in the T4 group are purple. The size of each dot is proportional to its effect size.

motility and *Bacillus* was positively correlated with sperm motility, oscillation ratio and linear ratio. Furthermore, *Mogibacterium*, Erysipelotrichaceae_UCG-006 and norank_f_norank_o_RF39 were negatively correlated with sperm motility. The *Lachnospiraceae_ND3007_group*, *Ruminococcus*, *Marvinbryantia*, and *Eubacterium_xylanophilum_group* were negatively correlated with the sperm oscillation ratio.

DISCUSSION

In this study, dietary fiber supplementation had no significant effect on the average daily gain, average daily feed intake and feed conversion ratio of Yorkshire boars at each growth stage. Although dietary fiber and metabolites tended to reduce the rate of early diarrhea, they had no significant effect on growth performance throughout the study period. This finding is supported by Batson et al. (2021), who demonstrated that piglets fed different fiber source had no change in growth performance, but pigs fed added cellulose had increased fecal DM. In addition, these findings suggest that DF treatment could reduce the diarrhea rate in piglets, which is consistent with the findings of Shang et al. (2021). The results of this study showed that the testes exhibited temporal and spatial changes with the development of growing boars.

Few studies have examined the effects of fiber on testicular development. In this study, we also established that dietary fiber supplementation was associated with the temporal and spatial changes in the testicular development of growing boars. On day 260, the testicular volumes of group T3 and T4 boars increased by 13–14% compared to the control group boars, but were not significant. Our previous studies have shown that maternal fiber intake can increase the number of spermatogonial stem cells in postnatal boars (Lin et al., 2019), indicating that appropriate dietary fiber levels may promote testicular development; however, this needs to be verified by further studies.

The sperm motility and effective sperm viability of boars in the T3 group increased significantly after supplementation with dietary fiber, while the sperm linear ratio and forward ratio increased significantly after the addition of tributyrin and probiotics. This suggests that dietary fiber and metabolite supplementation before sexual maturation have an important effect on spermatogenesis and sperm quality in adult boars. Very few studies have demonstrated the direct effect of fiber on sperm quality. Braga et al. (2012) observed that a diet comprising cereals and vegetables was positively associated with man sperm quality. Male rabbits fed a diet enriched with soluble fiber had less sperm abnormalities and higher percentages of normal and motile spermatozoa (Pascual et al., 2016). Moreover, study on women showed that partially hydrolysed guar gum supplementation helped to improve gut dysbiosis and pregnancy success in women with infertility (Komiya et al., 2020). Consistently, dietary fiber supplementation has been shown to improve the reproductive performance of sows (Li et al., 2019b). Collectively, these foregoing findings provide convincing evidence to indicate that dietary fiber supplementation has potentially beneficial effects on the reproductive performance of both the male and female boars.

Short-chain fatty acids are the main metabolites generated from the microbial fermentation of dietary fiber in the gut. In this study, total SCFAs, acetate and butyrate significantly increased after dietary fiber or metabolite supplementation.

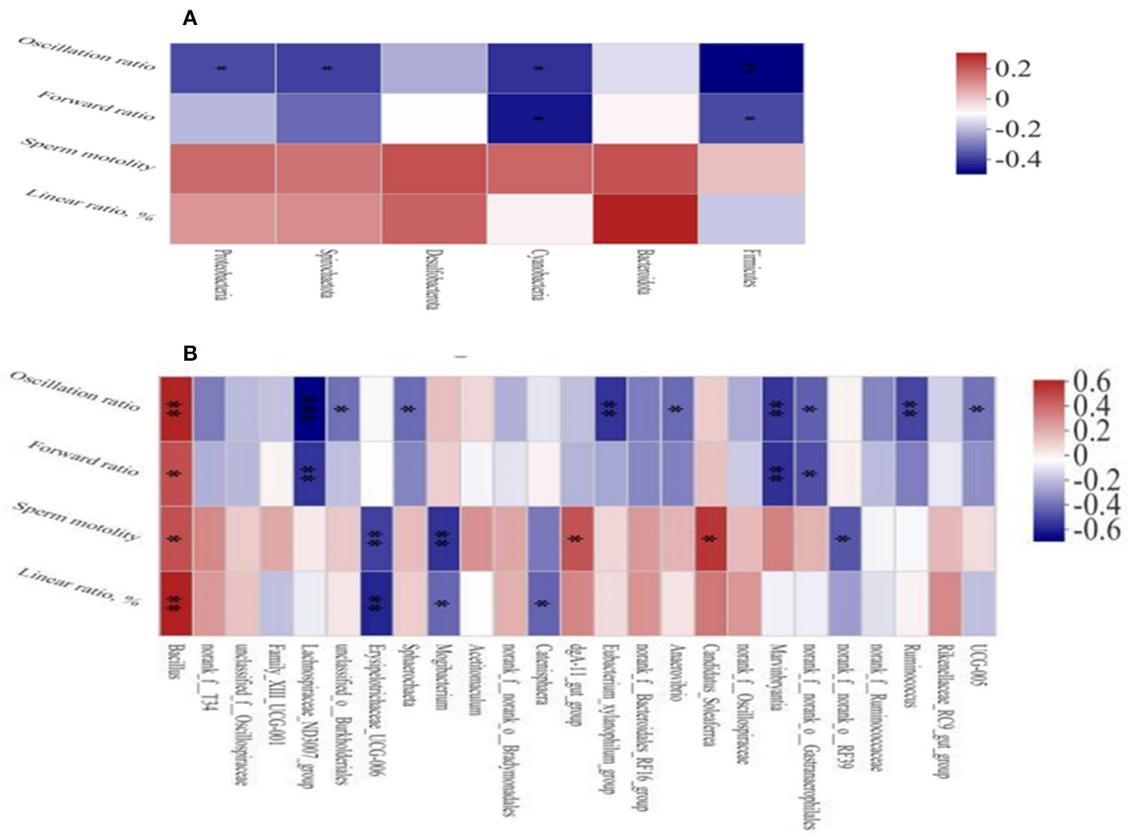

FIGURE 5 | Heat map of correlation analysis between sperm quality and intestinal microbiota at the phylum **(A)** and genus **(B)** level. Spearman's diagram showed that the ordinate was environmental factor information and the abscess was species information. The value corresponding to the middle heat map was the Spearman's correlation coefficient r, which was between −1 and 1. $r < 0$ is negative correlation and $r > 0$ is positive correlation. $^{*}p < 0.05$, $^{**}p < 0.01$, and $^{***}p < 0.001$.

Butyrate is one of the main metabolites in the intestinal microbial fermentation of dietary fiber. In addition, previous studies have established that supplementing the diets of adult roosters with sodium butyrate can improve semen volume and sperm motility by enhancing antioxidant capacity and testosterone hormone secretion (Alhaj et al., 2018). Butyric acid, which acts as a potent inhibitor of histone deacetylase (HDAC), has been reported to be involved in modulating sperm movement (Parab et al., 2015) and is a key regulator of the transcriptional program during the meiotic-to-post-meiotic transition in spermatogenesis (Yin et al., 2021). Furthermore, butyrate plays an important role in the redox balance (Lin et al., 2014), which is very important for spermatogenesis (Sênos and Jones, 2021). In addition, SCFAs have been found to exert notable immune and anti-inflammatory effects. In mice, butyrate was shown to promote the secretion of regulatory T cells (Tregs), interleukin-18 (IL-18) and the production of interleukin-10 (IL-10) in intestinal epithelial cells (Singh et al., 2014). SCFAs have also been demonstrated to activate NLRP3 inflammasome and decrease the inflammatory response in the gut (Macia et al., 2015). In this study, we observed that although butyrate supplementation promoted increase in the concentrations of total SCFAs, acetate and butyrate in group T4 boars, the levels were lower than those recorded in T3 boars, which indicate that the beneficial effects of butyric acid supplementation are less pronounced than diets supplemented with fiber. An increasing number of studies have shown that probiotics play a very important role in regulating body health and reproduction. Rats supplemented with a prebiotic, mannan-oligosaccharides (MOS), showed higher concentrations of testosterone and increased spermatozoa relative scores of the testicles (Rodrigues et al., 2021). Furthermore, supplementation of a probiotic with a prebiotic improved the quality/quantity of spermatozoa in infertile patients (Maretti and Cavallini, 2017). From the abovementioned results, it can be concluded that dietary fiber supplementation has beneficial effects on spermatogenesis and the actions of butyrate, *Lactobacillus*, and Bifidobacterium supply are inferior to those of dietary fiber.

It has been reported that the gut microbiota thrives on fiber-rich diets and, thus, the addition of fiber (or metabolites) to diets has a great effect on microbiota composition in humans and animals (Li et al., 2019b). In this study, the relative abundance of *Clostridium_sensu_stricto_1* decreased, whereas that of *Lactobacillus* tended to increase with the addition of dietary fiber. A previous study showed that high-purity insoluble dietary fiber supplementation affected the proliferation of key bacteria, such as *Lactobacillus* and Peptostreptococcaceae and

then affected the synthesis of SCFAs in mice (Lyu et al., 2022). Dietary fiber supplementation increased the abundance of *UCG-005* in sows (Yu et al., 2020) and *Lactobacillus* in rats (Hua et al., 2021) and decreased the abundance of *Turicibacter i*n sows (Yu et al., 2021). Consequently, the addition of fiber to diets would appear to contribute to maintaining and enhancing the balance of intestinal bacterial numbers and diversity.

Moreover, the effects of *Lactobacillus* and *Bifidobacterium* supplementation on flora composition and abundance were inferior to those of dietary fiber supplementation. Study has shown that supplementation with a mixed prebiotic blend elicited the most abundant changes in microbiota, fermentative end products and immunoglobulin A (IgA) in dogs (Panasevich et al., 2021). However, there is limited study on the effect of dietary fiber supplementation on the microbiota composition in male animals. A high-fat diet induces intestinal flora disorders, resulting in testicular dysfunction and decreased spermatogenesis (Ding et al., 2020). In addition to this, *Lactobacillus* species significantly reversed testicular damage induced by gamma irradiation in rats (Changizi et al., 2021). *Lactobacillus casei* and *Lactobacillus coagulans* supplementation have protective effects against CCl_4-induced testicular toxicity, thereby increasing the rate of spermatogenesis in rats (Keshtmand et al., 2021). Meanwhile, probiotic supplementation has been reported to exert beneficial effects on semen quality (Tomaiuolo et al., 2020). A 6-week long period of supplementation with *Lactobacillus* and *Bifidobacterium* in asthenozoospermic males increased sperm motility and reduced the rate of sperm DNA fragmentation (Valcarce et al., 2017). Moreover, a 6-month long treatment with daily administration of *Lactobacillus paracasei*, arabinogalactan, fructo-oligosaccharides and L-glutamine had a positive effect on sperm count and motility (Maretti and Cavallini, 2017). Furthermore, fecal microbiota transplantation (FMT) from alginate oligosaccharide (AOS)-dosed animals improved mouse sperm quality and spermatogenesis after busulfan treatment (Zhang et al., 2021). As mentioned above, dietary fiber and metabolites affect microbiota composition, diversity and sperm quality; therefore, it seems that gut microbiota might also be involved in the beneficial effects of dietary fiber on spermatogenesis.

Due to the lack of study on the results so far, the effect of microbiota on spermatogenesis is still unclear. In this study, we found that there was significantly correlation between the microbiota and sperm motility and oscillation ratio. Study has shown that glyphosate-induced gut microbiota dysbiosis changes the relative abundance of the phyla Bacteroidetes and Firmicutes and reduces sperm motility, while increasing the sperm malformation ratio in rats (Liu et al., 2022). With the increase in the genera *Bacteroides* and *Prevotella*, semen production decreased after the intake of a high-fat diet (Ding et al., 2020). *Lactobacillus* seemed to play a beneficial role in semen quality as *Lactobacillus* supplementation in rats increased the rate of spermatogenesis, which was accompanied by significant increase in the testicular spermiogenesis index (Keshtmand et al., 2021). Collectively, these findings reveal strong correlations between gut microbiota and spermatogenesis. To the best of our knowledge, this study is the first study to report that supplementing pig diets with fiber prior to sexual maturity could represent an effective strategy for enhancing spermatogenesis and sperm motility by improving the balance of the gut microbiota and promoting SCFA production. Further study is necessary to reveal the respective roles of the microbiota and SCFAs in male reproduction.

CONCLUSION

In summary, we demonstrated that fiber supplementation in boar diets prior to their sexual maturity improves semen quality by favorably modifying gut microbiota composition and promoting the production of SCFAs. Moreover, the effects of dietary fiber were superior to those obtained by diets supplemented with dietary fiber metabolites. Our findings indicate that dietary fiber supplementation prior to puberty should be considered a potential nutrition-centered approach for improving animal reproduction and that of humans.

DATA AVAILABILITY STATEMENT

The original contributions presented in the study are publicly available. This data can be found at: https://www.ncbi.nlm.nih.gov/bioproject/, PRJNA814434.

ETHICS STATEMENT

The animal study was reviewed and approved by Animal Care and Use Committee of Sichuan Agricultural University (SAU-ANI-2020- 117).

AUTHOR CONTRIBUTIONS

DW and YL conceived and designed the study. YL, HX, KW, LC, ZF, SX, and CY performed the experiments and analyzed the data. BF, JL, YZ, and CW contributed to the laboratory analysis. YL and JZ wrote and edited the original draft. All authors have read and agreed to the published version of the manuscript.

FUNDING

This study was funded by the National Key R&D Program of China (2018YFD0501002), the National Natural Science Foundation of China (Grant No. 035Z2060), and the Sichuan Pig Innovation Team (sccxtd-2022-08).

SUPPLEMENTARY MATERIAL

The Supplementary Material for this article can be found online at: https://www.frontiersin.org/articles/10.3389/fmicb.2022.863315/full#supplementary-material

REFERENCES

Al-Asmakh, M., Stukenborg, J. B., Reda, A., Anuar, F., Strand, M. L., and Hedin, L. (2014). The gut microbiota and developmental programming of the testis in mice. *PLoS ONE* 9, e103809. doi: 10.1371/journal.pone.0103809

Alhaj, H. W., Li, Z., Shan, T., Dai, P., Zhu, P., Li, Y., et al. (2018). Effects of dietary sodium butyrate on reproduction in adult breeder roosters. *Anim. Reprod. Sci.* 196, 111–119. doi: 10.1016/j.anireprosci.2018.07.002

Batson, K. L., Neujahr, A. C., Burkey, T., Fernando, S. C., Tokach, M. D., Woodworth, J. C., et al. (2021). Effect of fiber source and crude protein level on nursery pig performance and fecal microbial communities. *J. Anim. Sci.* 99, skab34. doi: 10.1093/jas/skab343

Braga, D. P., Halpern, G., Figueira, R. C., Setti, A. S., and Iaconelli, A. Jr, Borges, E. Jr. (2012). Food intake and social habits in male patients and its relationship to intracytoplasmic sperm injection outcomes. *Fertil. Steril.* 97, 53–59. doi: 10.1016/j.fertnstert.2011.10.011

Changizi, V., Azadbakht, O., Ghanavati, R., Behrouj, H., Motevaseli, E., and Khanzadeh, P. (2021). Effect of lactobacillus species on apoptosis-related genes BCL2, BAX, and caspase 3 in the testes of gamma-irradiated rats. *Rev. Assoc. Med. Bras.* 67, 1581–1585. doi: 10.1590/1806-9282.20210634

Chen, S., Zhou, Y., Chen, Y., and Gu, J. (2018). fastp: an ultra-fast all-in-one FASTQ preprocessor. *Bioinformatics* 34, i884–i890. doi: 10.1093/bioinformatics/bty560

Dardmeh, F., Alipour, H., Gazerani, P., van der Horst, G., Brandsborg, E., and Nielsen, H. I. (2017). *Lactobacillus rhamnosus* PB01 (DSM 14870) supplementation affects markers of sperm kinematic parameters in a diet-induced obesity mice model. *PloS ONE* 12, e0185964. doi: 10.1371/journal.pone.0185964

Ding, N., Zhang, X., Zhang, X. D., Jing, J., Liu, S. S., Mu, Y. P., et al. (2020). Impairment of spermatogenesis and sperm motility by the high-fat diet-induced dysbiosis of gut microbes. *Gut* 69, 1608–1619. doi: 10.1136/gutjnl-2019-319127

Dorgan, J. F., Judd, J. T., Longcope, C., Brown, C., Schatzkin, A., Clevidence, B. A., et al. (1996). Effects of dietary fat and fiber on plasma and urine androgens and estrogens in men: a controlled feeding study. *Am. J. Clin. Nutr.* 64, 850–855. doi: 10.1093/ajcn/64.6.850

Edgar, R. C. (2013). UPARSE: highly accurate OTU sequences from microbial amplicon reads. *Nat. Methods* 10, 996–998. doi: 10.1038/nmeth.2604

Hermes, R. G., Molist, F., Ywazaki, M., Gomez,de, Segura, A., Gasa, J., et al. (2009). Effect of dietary level of protein and fiber on the productive performance and health status of piglets. *J. Anim. Sci.* 87, 3569–3577. doi: 10.2527/jas.2008-1241

Hua, M., Liu, Z., Sha, J., Li, S., Dong, L., and Sun, Y. (2021). Effects of ginseng soluble dietary fiber on serum antioxidant status, immune factor levels and cecal health in healthy rats. *Food Chem.* 365, 130641. doi: 10.1016/j.foodchem.2021.130641

Hussain, T., Murtaza, G., Kalhoro, D. H., Kalhoro, M. S., Metwally, E., Chughtai, M. I., et al. (2021). Relationship between gut microbiota and host-metabolism: emphasis on hormones related to reproductive function. *Anim. Nutr.* 7, 1–10. doi: 10.1016/j.aninu.2020.11.005

Inatomi, T., and Otomaru, K. (2018). Effect of dietary probiotics on the semen traits and antioxidative activity of male broiler breeders. *Sci. Rep.* 8, 5874. doi: 10.1038/s41598-018-24345-8

Keshtmand, Z., Akbaribazm, M., Bagheri, Y., and Oliaei, R. (2021). The ameliorative effects of *Lactobacillus coagulans* and *Lactobacillus casei* probiotics on CCl4-induced testicular toxicity based on biochemical, histological and molecular analyses in rat. *Andrologia* 53, e13908. doi: 10.1111/and.13908

Komiya, S., Naito, Y., Okada, H., Matsuo, Y., Hirota, K., Takagi, T., et al. (2020). Characterizing the gut microbiota in females with infertility and preliminary results of a water-soluble dietary fiber intervention study. *J. Clin. Biochem. Nutr.* 67, 105–111. doi: 10.3164/jcbn.20-53

Le Floc'h, N., Knudsen, C., Gidenne, T., Montagne, L., Merlot, E., and Zemb, O. (2014). Impact of feed restriction on health, digestion and faecal microbiota of growing pigs housed in good or poor hygiene conditions. *Animal* 8, 1632–1642. doi: 10.1017/S1751731114001608

Li, Y., Liu, H., Zhang, L., Yang, Y., Lin, Y., Zhuo, Y., et al. (2019a). Maternal dietary fiber composition during gestation induces changes in offspring antioxidative capacity, inflammatory response, and gut microbiota in a sow model. *Int. J. Mol. Sci.* 21, 31. doi: 10.3390/ijms21010031

Li, Y., Zhang, L., Liu, H., Yang, Y., He, J., Cao, M., et al. (2019b). Effects of the ratio of insoluble fiber to soluble fiber in gestation diets on sow performance and offspring intestinal development. *Animals* 9, 422. doi: 10.3390/ani9070422

Lin, Y., Fang, Z. F., Che, L. Q., Xu, S. Y., Wu, D., Wu, C. M., et al. (2014). Use of sodium butyrate as an alternative to dietary fiber: effects on the embryonic development and anti-oxidative capacity of rats. *PLoS ONE* 9, e97838. doi: 10.1371/journal.pone.0097838

Lin, Y., Han, X. F., Fang, Z. F., Che, L. Q., Wu, D., Wu, X. Q., et al. (2012). The beneficial effect of fiber supplementation in high- or low-fat diets on fetal development and antioxidant defense capacity in the rat. *Eur. J. Nutr.* 51, 19–27. doi: 10.1007/s00394-011-0185-4

Lin, Y., Li, L., Li, Y., Wang, K., Wei, D., Xu, S., et al. (2019). Interpretation of fiber supplementation on offspring testicular development in a pregnant sow model from a proteomics perspective. *Int. J. Mol. Sci.* 20, 4549. doi: 10.3390/ijms20184549

Liu, J. B., Chen, K., Li, Z. F., Wang, Z. Y., and Wang, L. (2022). Glyphosate-induced gut microbiota dysbiosis facilitates male reproductive toxicity in rats. *Sci. Total Environ.* 805, 150368. doi: 10.1016/j.scitotenv.2021.150368

Louis, G. F., Lewis, A. J., Weldon, W. C., Ermer, P. M., Miller, P. S., Kittok, R. J., et al. (1994). The effect of energy and protein intakes on boar libido, semen characteristics, and plasma hormone concentrations. *J. Anim. Sci.* 72, 2051–2060. doi: 10.2527/1994.7282051x

Lyu, B., Wang, Y., Fu, H., Li, J., Yang, X., Shen, Y., et al. (2022). Intake of high-purity insoluble dietary fiber from okara for the amelioration of colonic environment disturbance caused by acute ulcerative colitis. *Food Funct.* 13, 213–226. doi: 10.1039/D1FO02264D

Macia, L., Tan, J.,Vieira, A. T., Leach, K., Stanley, D., Luong, S., et al. (2015). Metabolite-sensing receptors GPR43 and GPR109A facilitate dietary fibre-induced gut homeostasis through regulation of the inflammasome. *Nat. Commun.* 6, 6734. doi: 10.1038/ncomms7734

Magoč, T., and Salzberg, S. L. (2011). FLASH: fast length adjustment of short reads to improve genome assemblies. *Bioinformatics* 27, 2957–2963. doi: 10.1093/bioinformatics/btr507

Mändar, R., Punab, M., Borovkova, N., Lapp, E., Kiiker, R., Korrovits, P., et al. (2015). Complementary seminovaginal microbiome in couples. *Res. Microbiol.* 166, 440–447. doi: 10.1016/j.resmic.2015.03.009

Maretti, C., and Cavallini, G. (2017). The association of a probiotic with a prebiotic (Flortec, Bracco) to improve the quality/quantity of spermatozoa in infertile patients with idiopathic oligoasthenoteratospermia: a pilot study. *Andrology* 17, 439–444. doi: 10.1111/andr.12336

Mohamed, M. Y., Saba, F. E., Gomaa, A. A. A. I., Desoky, A. L. I., Almwafy, A. A., AbdEl-Salam, O. M., et al. (2020). Reproductive tract development and histomorphometric analysis of testes in neonatal zaraibi kids raised on milk replacer supplemented with sodium butyrate. *J. Anim. Physiol. Anim. Nutr.* 104, 812–822. doi: 10.1111/jpn.13334

Panasevich, M. R., Daristotle, L., Quesnell, R., Reinhart, G. A., and Frantz, N. Z. (2021). Altered fecal microbiota, IgA, and fermentative end-products in adult dogs fed prebiotics and a nonviable *Lactobacillus acidophilus*. *J. Anim. Sci.* 99, skab347. doi: 10.1093/jas/skab347

Parab, S., Shetty, O., Gaonkar, R., Balasinor, N., Khole, V., and Parte, P. (2015). HDAC6 deacetylates alpha tubulin in sperm and modulates sperm motility in holtzman rat. *Cell Tissue Res.* 359, 665–678. doi: 10.1007/s00441-014-2039-x

Pascual, J. J., Marco-Jiménez, F., Martínez-Paredes, E., Ródenas, L., Fabre, C., Juvero, M. A., et al. (2016). Feeding programs promoting daily feed intake stability in rabbit males reduce sperm abnormalities and improve fertility. *Theriogenology* 86, 730–737. doi: 10.1016/j.theriogenology.2016.02.026

Ren, B., Cheng, X., Wu, D., Xu, S. Y., Che, L. Q., Fang, Z. F., et al. (2015). Effect of different amino acid patterns on semen quality of boars fed with low-protein diets. *Anim. Reprod. Sci.* 161, 96–103. doi: 10.1016/j.anireprosci.2015.08.010

Rodrigues, L. E., Kishibe, M. M., Keller, R., Caetano, H. R. D. S., Rufino, M. N., Sanches, O. C., et al. (2021). Prebiotics mannan-oligosaccharides accelerate sexual maturity in rats: a randomized preclinical study. *Vet. World* 14, 1210–1219. doi: 10.14202/vetworld.2021.1210-1219

Sênos, D. R., and Jones, D. L. (2021). Redox signaling as a modulator of germline stem cell behavior: implications for regenerative medicine. *Free Radic. Biol. Med.* 166, 67–72. doi: 10.1016/j.freeradbiomed.2021.02.001

Shang, Q., Liu, H., Wu, D., Mahfuz, S., and Piao, X. (2021). Source of fiber influences growth, immune responses, gut barrier function and

microbiota in weaned piglets fed antibiotic-free diets. *Anim. Nutr.* 7, 315–325. doi: 10.1016/j.aninu.2020.12.008

Singh, N., Gurav, A., Sivaprakasam, S., Brady, E., Padia, R., Shi, H., et al. (2014). Activation of Gpr109a, receptor for niacin and the commensal metabolite butyrate, suppresses colonic inflammation and carcinogenesis. *Immunity* 40, 128–139. doi: 10.1016/j.immuni.2013.12.007

Tian, G., Wu, X., Chen, D., Yu, B., and He, J. (2017). Adaptation of gut microbiome to different dietary non-starch polysaccharide fractions in a porcine model. *Mol. Nutr. Food Res.* 61, 1700012. doi: 10.1002/mnfr.201700012

Tian, X., YU, Z., Feng, P., Ye, Z., Li, R., Liu, J., et al. (2019). *Lactobacillus plantarum* TW1-1 alleviates diethylhexylphthalate-induced testicular damage in mice by modulating gut microbiota and decreasing inflammation. *Front. Cell Infect. Microbiol.* 9, 221. doi: 10.3389/fcimb.2019.00221

Tomaiuolo, R., Veneruso, I., Cariati, F., and D'Argenio, V. (2020). Microbiota and human reproduction: the case of male infertility. *High Throughput* 9, 10. doi: 10.3390/ht9020010

Tomsett, K. I., Barrett, H. L., Dekker, E. E., Callaway, L. K., McIntyre, D. H., and Dekker, N. M. (2020). Dietary fiber intake alters gut microbiota composition but does not improve gut wall barrier function in women with future hypertensive disorders of pregnancy. *Nutrients* 12, 3862. doi: 10.3390/nu12123862

Valcarce, D. G., Genovés, S., Riesco, M. F., Martorell, P., Herráez, M. P., Ramón, D., et al. (2017). Probiotic administration improves sperm quality in asthenozoospermic human donors. *Benef. Microbes* 8, 193–206. doi: 10.3920/BM2016.0122

Wang, C., Catlin, D. H., Starcevic, B., Heber, D., Ambler, C., Berman, N., et al. (2005). Low-fat high-fiber diet decreased serum and urine androgens in men. *J. Clin. Endocrinol. Metab.* 90, 3550–3559 doi: 10.1210/jc.2004-1530

Wang, Q., Garrity, G. M., Tiedje, J. M., and Cole, J. R. (2007). Naive bayesian classifier for rapid assignment of rRNA sequences into the new bacterial taxonomy. *Appl. Environ. Microbiol.* 73, 5261–5267. doi: 10.1128/AEM.00062-07

Wu, X., Chen, D, Yu, B., Luo, Y., Zheng, P., Mao, X., et al. (2018). Effect of different dietary non-starch fiber fractions on growth performance, nutrient digestibility, and intestinal development in weaned pigs. *Nutrition* 51–52, 20–28. doi: 10.1016/j.nut.2018.01.011

Yin, H., Kang, Z., Zhang, Y., Gong, Y., Liu, M., Xue, Y., et al. (2021). HDAC3 controls male fertility through enzyme-independent transcriptional regulation at the meiotic exit of spermatogenesis. *Nucleic Acids Res.* 49, 5106–5123. doi: 10.1093/nar/gkab313

Yu, M., Gao, T., Liu, Z., and Diao, X. (2020). Effects of dietary supplementation with high fiber (stevia residue) on the fecal flora of pregnant sows. *Animals* 10, 2247. doi: 10.3390/ani10122247

Yu, X., Fu, C., Cui, Z., Chen, G., Xu, Y., and Yang, C. (2021). Inulin and isomalto-oligosaccharide alleviate constipation and improve reproductive performance by modulating motility-related hormones, short-chain fatty acids, and feces microflora in pregnant sows. *J. Anim. Sci.* 99, skab257. doi: 10.1093/jas/skab257

Zhang, P., Feng, Y., Li, L., Ge, W., Yu, S., Hao, Y., et al. (2021). Improvement in sperm quality and spermatogenesis following faecal microbiota transplantation from alginate oligosaccharide dosed mice. *Gut* 70, 222–225. doi: 10.1136/gutjnl-2020-320992

Zhou, P., Zhao, Y., Zhang, P., Li, Y., Gui, T.,Wang, J., et al. (2017). Microbial mechanistic insight into the role of inulin in improving maternal health in a pregnant sow model. *Front. Microbiol.* 8, 2242. doi: 10.3389/fmicb.2017.02242

Conflict of Interest: The authors declare that the research was conducted in the absence of any commercial or financial relationships that could be construed as a potential conflict of interest.

Publisher's Note: All claims expressed in this article are solely those of the authors and do not necessarily represent those of their affiliated organizations, or those of the publisher, the editors and the reviewers. Any product that may be evaluated in this article, or claim that may be made by its manufacturer, is not guaranteed or endorsed by the publisher.

Advantages of publishing in Frontiers

OPEN ACCESS
Articles are free to read for greatest visibility and readership

FAST PUBLICATION
Around 90 days from submission to decision

HIGH QUALITY PEER-REVIEW
Rigorous, collaborative, and constructive peer-review

TRANSPARENT PEER-REVIEW
Editors and reviewers acknowledged by name on published articles

Frontiers
Avenue du Tribunal-Fédéral 34
1005 Lausanne | Switzerland

Visit us: www.frontiersin.org
Contact us: frontiersin.org/about/contact

REPRODUCIBILITY OF RESEARCH
Support open data and methods to enhance research reproducibility

DIGITAL PUBLISHING
Articles designed for optimal readership across devices

FOLLOW US
@frontiersin

IMPACT METRICS
Advanced article metrics track visibility across digital media

EXTENSIVE PROMOTION
Marketing and promotion of impactful research

LOOP RESEARCH NETWORK
Our network increases your article's readership